A RELIABLE POTABLE WATER PURIFICATION SYSTEM USING NANOMATERIAL-INCORPORATED MATRIX FOR HOUSEHOLDS IN CKDu PREVALENT AREAS

Madhusha Ishanthi Sudasinghe

158051P

Degree of Doctor of Philosophy

Department of Civil Engineering

University of Moratuwa

Sri Lanka

November 2021

A RELIABLE POTABLE WATER PURIFICATION SYSTEM USING NANOMATERIAL-INCORPORATED MATRIX FOR HOUSEHOLDS IN CKDu PREVALENT AREAS

Madhusha Ishanthi Sudasinghe

158051P

Thesis submitted in partial fulfilment of the requirement for the Degree Doctor of Philosophy in Civil Engineering

Department of Civil Engineering

University of Moratuwa

Sri Lanka

November 2021

DECLARATION

I declare that this is my own work, and this thesis does not incorporate without acknowledgement any material previously submitted for a Degree or Diploma in any other university or institute of higher learning and to the best of my knowledge and belief, it does not contain any material previously published or written by another person except where the acknowledgement is made in the text.

Also, I hereby grant to the University of Moratuwa the non-exclusive right to reproduce and distribute my thesis, in whole or in part in print, electronic or other media. I retain the right to use this content in whole or part in future works (such as articles or books).

Signature of the candidate: UOM Verified Signature Date: 15.11.2021

Madhusha I. Sudasinghe

The above candidate has carried out research for PhD thesis under my supervision.

Name of the supervisor: Prof. M. W. Jayaweera

UOM Verified Signature

Signature of the supervisor: Date: 15.11.2021.

Name of the co-supervisor: Prof. J. M. A. Manatunge

UOM Verified Signature

Signature of the co-supervisor: Date: 15.11.2021

Name of the co-supervisor: Prof. W. B. Gunawardana

UOM Verified Signature

Signature of the co-supervisor: Date: 15.11.2021

ABSTRACT

Chronic kidney disease of unknown aetiology (CKDu) in Sri Lanka is a national concerning health hazard as those affected face high mortality rates per year. One hypothesis on the disease pathogenesis is long-term exposure to fluoride, hardness, and cadmium in drinking water and their synergic effects, which causes nephrotoxic health hazards. Removal of fluoride, hardness, and cadmium is paramount in providing safe drinking water to the community in CKDu areas. However, available water treatment technologies in such areas do not offer an appropriate solution to drinking water issues. Hence, there are prerequisite to developing a reliable water purification unit to provide safe drinking water. This study investigated the best combination of materials to remove fluoride, hardness, cadmium, and faecal coliform in water to develop a reliable water purification unit to protect the community health and enhance their well-being.

Firstly, nephrotoxic risk factors in drinking water, their threshold levels, and the level of components required to remove complying with the required drinking water guideline values were evaluated. Water samples collected reported hardness in the range of 111.73 ± 1.41 – 680.33 ± 1.53 mg/L as $CaCO_3$ and fluoride 0.72 ± 0.03 mg/L and 2.84 ± 0.05 mg/L. The cadmium concentrations reported below the detection limit of 0.025 mg/L. Literature reported that fluoride (0.1–13.7 mg/L) and hardness (63.6–1921.0 mg/L) concentrations in water are very high. Fluoride concentrations in most CKDu prevalent areas exceed the drinking water guideline value (1.5 mg/L). The World Health Organisation does not declare a health concern permissible value to hardness in water. The cadmium level was reported in trace level in potable water less than the permissible drinking water guideline value (0.003 mg/L). Nephrotoxic drinking water guideline values should be declared for CKDu prevalent areas to control the spreading of nephrotoxic health hazards. In non-CKDu prevalent areas, potable water hardness values were often reported below the level of 120.0 mg/L and fluoride around 0.2 mg/L. Hence, potable water consumption with a fluoride level of around 0.2 mg/L, hardness 120.0 mg/L and cadmium 0.003 mg/L will control the occurrence of CKDu.

Available water treatment technologies introduced in CKDu prevalent areas were evaluated to identify their effectiveness in removing fluoride, hardness, and cadmium. Reverse osmosis, two-layer and seven-layer filter units have been introduced, treating potable water as a short-term

solution for the disease. The reverse osmosis unit removes most of the ions in water, retaining beneficial ions less in hardness 4.0–20.0 mg/L, high in fluoride 0.29–5.5 mg/L for human intake. The other two filters (two-layer and seven-layer filter units) do not remove fluoride and hardness effectively and add more ions into treated water due to the leachability in some minerals in the media. Treated water does not meet the required drinking water guideline values, highlighting a new requirement for water treatment units.

The risk assessment for RO treated water was conducted to identify non-carcinogenic health effects in long term consumption. Hazard's quotient values of different age categories did not exceed the value one (1 > HQ) for a short duration of water consumption. Children (Age category 1-9 years) are highly vulnerable to non-carcinogenic health hazards, and their HQ value exceeded one (HQ > 1) within a short period for fluoride (80 days), calcium (1,440 days), magnesium (2,160 days), and cadmium (360 days) before other age categories. HI mean values with higher concentrations elaborated that multicomponent concentration combinations bring adverse health effects on females in 1–9 and 10–19 years of age categories and males after 20 years of age. With mixture of component, age category 1–9 years exceeded HI>1 within 2 weeks for higher concentrations of the mixture, age category 10–19 years within one month, age category 2–90 years withing three months. The higher concentration value of components makes people vulnerable for adverse health hazard within short period of exposure. Long-run consumption of RO water causes non-carcinogenic health effects. Hence, developing a new water treatment unit is of utmost importance to provide safe drinking water.

The modified fly ash (Zeolite) (ZEOL), MgO loaded alumina (MOMA), silver oxide nanoparticle + graphene oxide composite (SONPs + GO) proposes the best combination of materials to remove hardness, fluoride, and faecal coliform in potable water after conducting batch and fixed-bed column studies. The fluoride (Q = 18.76 mg/g) and hardness (Q = 263.16 mg/g) experimental data aligned with the Langmuir model for batch studies. The fluoride and hardness data corroborated with the Thomas model for fixed-bed column studies. The length of unused bed values was calculated as 1.62 cm, 1.00 cm, and 0.81 cm for ZEOL, MOMA, and SONPs + GO when each material's breakthrough points were considered the maximum allowable concentration. The height of the ZEOL bed required to remove hardness for three months of service period was calculated as 29.09 cm with the mass of adsorbent 2.63 Kg, 18.86 cm adsorbent bed height including the mass of 1.37 Kg of MOMA, and 6.48 cm with the mass

of 1.09 Kg of SONPs + GO. The cost of 1.0 L of treated water production was approximately Rs. 8.80 and the total cost for 10.0 L of water (daily consumption of a family) was estimated at Rs. 88.00. If a family of five household members consumes water for three months, the cost of treated water production was calculated as Rs. 7,920.00 (monthly cost Rs. 2,640.00). The best combination of multi-layer materials is a promising water treatment unit to remove fluoride, hardness, and faecal coliform in drinking water. Therefore, the fabrication of a multi-layer home filter unit using ZEOL, MOMA, and SONPs + GO is recommended to provide safe, clean potable water for the community in CKDu prevalent areas.

Keywords: Adsorption, Faecal coliform, Fluoride, hardness, isotherms, kinetics, nanomaterial, risk assessment

ACKNOWLEDGEMENT

First, I extend my deepest gratitude and admiration to my supervisors, Prof. M. W. Jayaweera, Prof. J. M. A. Manatunge, and Prof. W. B. Gunawardana Environmental Engineering Division, Department of Civil Engineering, University of Moratuwa for their excellent supervision, generous help, indispensable guidance throughout the study, valuable time, energy, and sincere effort extended to train me as a researcher.

A special appreciation to the Senate Research Committee (SRC), the University of Moratuwa, for graciously awarding the research fellowship and providing the necessary research funds to undertake this research study.

I want to extend my sincere gratitude to the former heads and the present Head/ Department of Civil Engineering, University of Moratuwa, for providing me with a valuable opportunity to conduct the research along with all the necessary facilities to carry out research activities within a conducive environment.

I am very grateful to the former heads and the present head, academic staff, Department of Materials Science and Engineering, University of Moratuwa for providing me with the necessary laboratory facilities, workshop facilities and other essential facilities available in the Department.

I am genuinely thankful to Mr E. K. Zoysa, Mrs N. S. Gunathilake, Mr Justin Silva, Mr D. Bandara, academic support and non-academic staff members in the Environmental Engineering Division, Department of Civil Engineering and Mr M. T. M. R. Jayaweera, Mr M. A. P. C. Gunawardana, and Mr R. R. P. Perera, non-academic staff, Department of Materials Science and Engineering, University of Moratuwa for their generous and amicable support during the laboratory analysis and other research activities.

My special thanks to Ms P. D. N. Sigera for being an assistive partner in my research life and supporting me to accomplish all laboratory activities with standard quality.

I want to extend my sincere gratitude to Ms T. Wimalarathna, Ms G. Dhanushika, Ms S. Gunawardana, Dr A. Witharana and my colleagues in the Environmental Engineering Division, for ensuring my research journey was blissful, joyous, and filled with affection and care.

Finally, I am grateful to my loving husband for his patience and support through my research endeavours and day to day activities, standing by me through thick and thin, sharing my thoughts, giving me courage, and always bringing positive vibes into my heart to complete the research study. I should thank my dearest mother, brothers, and family members who always shower me with love, affection, care, and inspiration, which tremendously helped me complete my studies successfully.

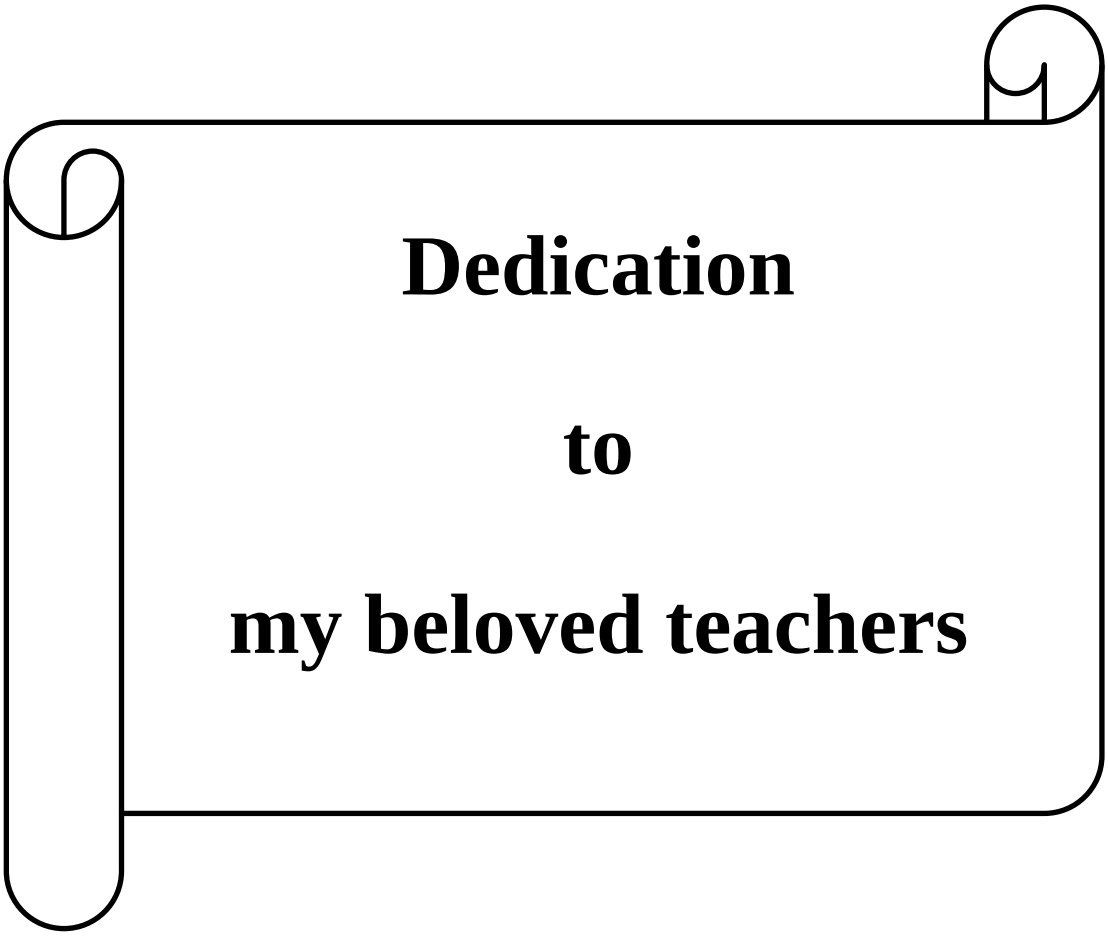
Dedication
to
my beloved teachers

TABLE OF CONTENT

LIST OF FIGURES

LIST OF TABLES

LIST OF ABBREVIATION

CKDu	- Chronic kidney disease of unknown aetiology
CKD	- Chronic Kidney Disease
WHO	- World health organisation
RO	- Reverse Osmosis
HQ	- Hazard quotient
MEN	- Mesoamerican nephropathy
BEN	- Balkan endemic nephropathy
CIN	- Chronic interstitial nephropathy
GFR	- Glomerular filtration rate
NCP	- North central province
CAN	- Chronic agrochemical nephrology
CINAC	- Chronic interstitial nephritis of agricultural communities
CKDmfo	- CKD of multifactorial origin
NSAIDs	- Nonsteroidal anti-inflammatory drugs
DOC	- Dissolved organic carbon
Cd	- Cadmium
ROS	- Reactive oxygen species
O_2^-	- Superoxide anion
$ROO^\cdot$	- Peroxyl radicals
H_2O_2	- Hydrogen peroxide
$R\text{-}NO^\cdot$	- Peroxynitrite
$OH^\cdot$	- Hydroxyl radicals
$O^\cdot$	- Singlet oxygen
$(CH_3)_2AsOO^\cdot$	- Dimethyl peroxyl radicals

$(CH_3)_2As^{\cdot}$ - Dimethyl arsenic radicals

Ca - Calcium

Mg - Magnesium

F - Fluoride

SLS - Sri Lanka Standards

US EPA - United States Environmental Protection Agency

NPDWRs - National Secondary Drinking Water Regulations

MDP - Meta-phenylenediamine

TMC - Trimesoyl Chloride

nZVI - Nano zero valent iron

CFU - Colony forming unit

MTZ - Mass transfer zone

XRD - X-ray powder diffraction

ESEM - Environmental scanning electron microscope

EDAX - Energy Dispersive Spectroscopy

FT–IR - Fourier-transform infrared spectroscopy

USGS - United States Geological Survey

SMART - Specific, measurable, attainable, relevant, and time-bound

$CaCO_3$ - Calcium carbonate

ADD - Average daily dose

HI - Hazard index

C - Concentration

IR - Intake rate

ED - Exposure duration

BW - Body weight

AT	- Average time
ZEOL	- Zeolite
GO	- Graphene oxide
FeONs	- Iron oxide nanoparticles
MESA	- Mesoporous alumina
Al_2O_3	- Alumina
COMA	- Calcium oxide loaded mesoporous alumina
MOMA	- Magnesium oxide loaded mesoporous alumina
TiO_2	- Titanium dioxide
SONPs	- Silver oxide nanoparticles
MO	- Microorganism
ACS	- American chemical society
PEG	- Polyethylene glycol
DI	- Deionized
BET	- Brunauer-Emmett-Teller
IAST	- Ideal adsorption solution theory
EDTA	- Ethylenediaminetetraacetic acid
ICP-MS	- Inductively coupled plasma mass spectrometry
USA	- United states of America
MPN	- Most probable number
E. coli	- *Escherichia coli*
EOM	- Electronic optical microscopy
EBCT	- Empty bed contact time
BV	- Bed volume

H_{MTZ}	- Length of mass transfer zone
ANOVA	- Analysis of variance
O & M	- Operation and maintenance
NGO	- Non-governmental organization
NaF	- Sodium fluoride
$CaCO_3$	- Calcium carbonate
$MgCO_3$	- Magnesium carbonate
IS	- Inner sphere
OS	- Outer sphere
DNA	- Deoxyribonucleic acid
RNA	- Ribonucleic acid
NAOH	- Sodium hydroxide
HCl	- Hydrochloric acid
EDTA	- Ethylenediaminetetraacetic acid
BTC	- Breakthrough curve

CHAPTER 1

1. INTRODUCTION

1.1. Chronic kidney disease of unknown aetiology and risk on human health

Chronic kidney disease of unknown aetiology (CKDu) is a heterogeneous disorder that affects kidney structure and functions (Bandarage, 2013). CKDu has been identified in several countries such as Nicaragua, Mexico and other Central American countries, Sri Lanka, India, China, Australia, Argentina, and United Kingdom (Wijerathne et al., 2014). More than 16,000 people have been reported to have died of CKDu in Central America from 2005 to 2009 (Gorry, 2014). Since 2007, more than 1,500 people have undergone treatment for CKDu in Andra Pradesh, India (Chavkin, 2012). More than 35,000 patients have been found in Sri Lanka, while over 1,000 people have been reported dead (Bandarage, 2013). Several studies have found that CKDu in Sri Lanka doubles every 4–5 years, and currently, more than 150,000 people suffer from the disease.

Several factors suggested to cause CKDu, including fluoride and hardness (Sengupta 2013; Jayasumana et al., 2014; Dharma–wardana, 2018) cadmium (Wasana et al., 2016) have been implicated to be multifaceted causal factors. Fluoride is a common element in groundwater, as fluoride compounds arise naturally in rocks and soils. The fluoride concentration may be as high as 50.0 mg/L depending on the locality's geochemical properties (Barbier et al., 2010). The maximum guideline value for fluoride in drinking water specified by the World Health Organisation is 1.5 mg/L (WHO, 2017). Fluoride has interfered with and altered mitochondria abundant cells (Yang et al., 2015). The cells in the human kidney are rich in mitochondria (Barbier et al., 2010). It seems that fluoride links with CKDu since kidney diseases emerge where the fluoride level in groundwater is higher (Wasana et al., 2016; Dharma–wardana, 2018).

Fluoride and its interactions with other ions [hardness (hardness has been comprised mainly with calcium & magnesium) and cadmium)] have also been suggested as a triggering factor of the CKDu prevalent in Sri Lanka (Dissanayake and Chandrajith, 2017; Dharma–wardana, 2018). Fluoride has been found to have increased the severity of CKDu in the presence of hardness and cadmium (Wasana et al., 2016). Calcium (which causes hardness) activity has been identified as prominent in CKDu endemic areas, while fluoride has shown more affinity towards calcium ions (Chandrajith et al., 2011). The endemic fluorosis is more common in high calcium activity areas and with a higher content of fluoride. Chandrajith and co-workers have emphasized that high calcium activity triggered the damage instigated by fluoride, causing lesions on kidneys' tubular cells, leading to apoptosis. They have suggested that inorganic fluoride intake can cause substantial nephrotoxic damage on proximal tubular cells in the kidneys. However, this toxicity depends strongly on sodium and calcium activity (Chandrajith et al., 2011). Moreover, potable water with high fluoride and hardness levels have been highlighted to increase kidney damage causing end-stage renal failure (Wickramarathna et al., 2017). Thus, the combined effect of fluoride and hardness (Dharma–wardana, 2018) has received more attention because the interaction of fluoride with hardness increased the severity of nephrotoxic effects (Dharmawardana et al., 2014).

Cadmium has also been proposed as another triggering factor of CKDu (Dharma-wardana, 2018). People consume cadmium-contaminated groundwater for extended periods of more than 20 years; thus, they are vulnerable to cadmium-prone kidney diseases such as renal damage and renal complications (Barbier et al., 2010). Cadmium is non-biodegradable and has been found to have accumulated in the human body through the food chain (Peng et al., 2018). Even at trace levels, Cadmium has been highly toxic to human beings (Zhang et al., 2014; Carolin et al., 2018) (WHO drinking water guideline value for cadmium - 0.003 mg/L). Cadmium, together with hardness, has shown synergic effects on the incidence of CKDu in Sri Lanka (Jayathilaka et al., 2013; Wasana et al., 2016). The groundwater of CKDu prevalent areas has been reported to contain high hardness levels and cadmium (Jayathilaka et al., 2013). Therefore, a

triggering factor for CKDu has been suspected to be either cadmium or hardness or both, with cadmium and hardness interacting with each other (Wasana et al., 2016).

People who resided in CKDu prevalent areas depend on springs, reservoirs, irrigation canals, protected and unprotected dug wells pipe born water, and tube wells for their potable water (Chandrajith et al., 2011, Rango et al., 2014, Road development authority, Sri Lanka, 2014). Instead of nephrotoxic risk factors in potable water, causative pathogens of water-borne diseases (e.g., Salmonellosis and Shigellosis) have been recorded in most ground, and surface water sources in CKDu prevalent areas (Mahagamage & Manage, 2019). The surface and groundwater sources in CKDu prevalent Anuradhapura district have been flagged as contaminated with *Escherichia coli* (*E. coli*) bacteria (Mahagamage & Manage, 2017). *E. coli* bacteria have not been promulgated as one of the nephrotoxic risk factors, however, can be used as an indicator of pathogenic contamination of potable water and the possibility of an outbreak of water-borne diseases. Therefore, potable water provided for the people in the CKDu area should be free from *E. coli* bacteria following WHO drinking water guideline values (*E. coli* 0 CFU/100 mL) (WHO, 2017). The supply of safe and clean water (free from *E. coli*) for households in CKDu prevalent areas will ensure community health and safety by protecting people from water-borne diseases.

1.2. Problem statement

CKDu has been recognized as an environmentally induced and preventable occupational disease predominantly affected by male farmers in Sri Lanka (Wimalawansa, 2020). People affected by the disease have increased over the past two decades, with the death toll in Sri Lanka exceeding 90,000 (Wimalawansa, 2014). Several nephrotoxic risk factors such as fluoride, hardness, and cadmium in potable water have been proposed as possible causative factors for the disease (Dharma–wardana, 2018; Cooray et al., 2019). Thus, special attention should be paid to remove nephrotoxic risk factors in potable water responsible for CKDu.

Conventional water treatment technologies do not remove fluoride, hardness, and cadmium efficiently and effectively. Hence, different water filter units have been introduced in areas to provide safe potable water. However, numerous limitations and concerns related to available water filters, including their inferior quality and effectiveness in water treatment, have been corroborated by past studies. The observations of preliminary studies conducted by Sudasinghe et al. (2014) before the design of research questions revealed that reverse osmosis (RO) filters had been introduced by different governmental and non-governmental organisations in CKDu prevalent areas assuming that it would be a lasting solution. It is, however, reported that RO filters remove all macro-and micronutrients (including calcium and magnesium) that are considered essential elements for cellular processes such as proliferation, survival, and differentiation of cell growth in the human body (Arigony et al., 2013, Sudasinghe et al., 2014). Consumption of water with insufficient micronutrients may result in adverse health effects such as ailments impacting the central nervous system (Jacqmin et al., 1994; Sengupta, 2013), cardiovascular disease (Kohri et al., 1989, WHO, 2009, Gaurav et al., 2014), the formation of kidney stones, risks of gastric cancer (Yang, 1998), pre-term birth and low weight at birth (Melles & Kiss, 1992, Yang, et al., 2002), etc. Therefore, using RO treated water does not seem to be a long-term solution for the CKDu epidemic. Hence, the most cost-effective way is to identify the causal factor or factors of the disease and develop efficient and effective novel water treatment technologies to prevent the disease from spreading. Past studies have also highlighted the need for new technologies to remove nephrotoxic risk factors from potable water (Chandrajith et al., 2011; WHO, 2012). Hence, technology invention in removing nephrotoxic risk factors is a dire need to provide safe potable water to the CKDu-affected community and eliminate adverse health effects on the population. In this context, research and development needs to investigate the best combinations of different materials capable of removing nephrotoxic risk factors to control any further spreading of CKDu and new reported cases.

Recently, many researchers have studied the removal of water contaminants using different techniques such as coagulation and microfiltration (Da Conceição et al., 2015), precipitation (Jadhav et al., 2014), electrodialysis (Ergun et al., 2008), adsorption (Bhatnagar et al., 2011), ion exchange (Viswanathan et al., 2009), and membrane filtration (Camacho et al., 2013). Among the removal techniques mentioned above, adsorption using engineered materials has received considerable attention due to its effectiveness in removing water contaminants, high surface to volume ratio, high reactivity, cost, simplicity of design, and operations (Mohapatra et al., 2009; Bhatnagar et al., 2011). Among the engineered materials, nanomaterials and industrial by-products have received considerable attention in the recent past, especially its specific attributes such as the ability to remove water contaminants effectively, and the means to expedite the process at a low cost. Therefore, choosing the best combination of materials is the most important first step to develop a promising technology to remove fluoride, hardness, and cadmium concentrations to the levels that meet permissible drinking water guideline values.

Therefore, this study aims to investigate a combination of materials that can remove nephrotoxic risk factors in potable water to provide safe and clean water for households in the CKDu prevalent areas in Sri Lanka and elsewhere. Several cases have been reported that surface and groundwater sources in CKDu prevalent areas are contaminated with faecal matter leading to the outbreak of water-borne diseases. The multi-layered unit should remove pathogens causing water-borne diseases from potable water. The potable water provided for the community should be free from *E. coli*. The removal of causal factors in waterborne diseases ensures the community's water safety whilst avoiding water-borne diseases. Therefore, removing *E. coli* in potable water and the nephrotoxic risk factor is studied to provide clean and safe water for households using the multi-layered unit to protect people from water-borne diseases and CKDu.

1.3. Research questions

The following research questions are developed based on the problem statements discussed above:

1. Are nephrotoxic risk factors such as high fluoride levels, hardness and cadmium present in surface and groundwater consumed by people in CKDu prevalent areas? What are the concentration levels of fluoride, hardness and cadmium in surface and groundwater? Are fluoride, hardness and cadmium concentrations exceeding the permissible drinking water standard/guideline values? To what extent does the removal of fluoride, hardness and cadmium is required to provide safe potable water for people in CKDu prevalent areas?

2. Are the present treatment systems/technologies capable enough in removing nephrotoxic fluoride, hardness, and cadmium to permissible levels? If not, can these fluoride levels, hardness and cadmium be removed from potable water, and how can they be removed?

3. If the present water treatment systems do not remove nephrotoxic risk factors effectively, how could it affect the health of people who consume potable water from such treatment units available in CKDu prevalent areas? Can these fluoride, hardness, and cadmium bring up non-carcinogenic health hazards? How long do risk factors take to bring up non-carcinogenic health hazards?

4. Are engineered materials presently available to remove nephrotoxic risk factors and water-borne risk factors from potable water? If yes, what are the most suitable materials to remove fluoride, hardness, cadmium, and *E. coli*? Are the selected materials efficient enough to remove nephrotoxic and water-borne risk factors from water? Are the selected materials capable enough to be regenerated and reused repeatedly in several cycles during water treatment? If yes, what are the most suitable, different eluting agents used for the regeneration of materials?

Can a combination of materials in a multi-layered unit be developed to effectively remove fluoride, hardness, cadmium, and *E. coli* to levels below permissible standard/guideline values?

1.4. Research objectives

This study's overall objective is to supply safe and clean potable water for households in CKDu prevalent areas by investigating the best combination of materials in a multi-layered water purification unit to enhance the community's living standards in CKDu widespread areas. Thus, the specific objectives are;

1. to identify different nephrotoxic risk factors, their concentrations, threshold levels of nephrotoxicity, and the extent to which the removal is required in potable water

2. to evaluate the performance of commercially available domestic water purification techniques/systems/units to delineate their limitations and drawbacks

3. to assess the health risk of people who consume potable water from such commercially available units in CKDu prevalent areas, and

4. to investigate the applicability of the best combination of adsorbent materials in a multi-layered water purification unit capable of lessening the health impacts of selected nephrotoxic risk factors with ingestion of potable water in CKDu prevalent areas.

1.5. Outline of the thesis

This thesis covers the investigation of the best combination of materials to remove nephrotoxic risk factors in water to ensure safe potable water to communities in CKDu prevalent areas.

Chapter 1 provides a concise introduction to the research problem, the study's main objective and specific objectives, and the thesis's outline.

Chapter 2 gives background information for the research topic based on a comprehensive literature review. This chapter presents a detailed introduction to CKDu, possible etiologies, water treatment technologies available, and the procedure as to how to perform health risk assessments. Finally, modelling batch adsorption and column studies is introduced, including a brief description of model development theories that provide a basis for calculating kinetic adsorption parameters and fixed bed process parameters.

Chapter 3 explains the protocols developed concerning materials and methods such as experimental methods, road maps of the experimental designs, location map, instrumental and data analyses.

Chapter 4 illustrates the results described to each objective, observation, justification, and interpretation of experimental data. The section discusses different nephrotoxic risk factors in potable water, their concentrations, threshold levels, and the extent to which it is required to remove toxic constituents in water to meet drinking water guideline values. Secondly, the performance of commercially available domestic water purification techniques/systems/units and their limitations, drawbacks are presented. Thirdly, this chapter discusses the health risk of people who consume potable water from such commercially available RO units. Finally, it gives applicability of the best combination of material in multi-layer columns that can remove nephrotoxic risk factors in potable water and the conceptual design for the water purification system in future development.

Chapter 5 provides the main conclusions and recommendations of this research.

CHAPTER 2

2. LITERATURE REVIEW

2.1. Difference between CKD and CKDu

Chronic Kidney Disease (CKD) has been identified as a global public health problem. The symptoms of the disease have been ascertained as kidney damage with a decreased glomerular filtration rate (< 60.00 mL/min or 1.73 m^2), progressive disruption of kidney mass, reduction of the number of nephrons over time and irreversible sclerosis (Noble et al., 2014). Non-infectious diseases such as diabetes mellitus and hypertension are highly prevalent among CKD patients and indicates that CKD increases with these non-infectious diseases (Ene-Iordache et al., 2016). Diabetes mellitus and hypertension have been identified as significant CKD etiologies (Lovre et al., 2018). Hypertension has been reported to damage blood vessels and decrease blood flow to the kidneys. Moreover, high pressure has been found to increase nephrons' damage, leading to renal impairment (Judd and Calhoun, 2015).

The patients affected by CKDu do not have common non-infectious diseases such as diabetes mellitus and hypertension, obesity, or other risk factors associated with CKD (Athuraliya et al., 2011). The disease is prevalent among young, male agricultural workers farming under sweltering conditions. Intake of drinking water is limited during working hours at the farmland. The disease shows features of low-grade proteinuria and is mostly asymptomatic. However, the progressive decline of the glomerular filtration rate (Table 2.1) can be seen towards the latter stages of the disease (Levine et al., 2016). Histopathological findings of CKDu corroborates that CKDu patients are affected with tubular interstitial nephritis, including mononuclear cell infiltration, tubular atrophy, and glomerular sclerosis. The disease's clinical characteristics have been identified as tubular proteinuria: alpha-1 and beta-2 microglobulinuria and high urine neutrophil gelatinase-associated lipocalin level (Nanayakkara et al., 2012a). Many patients do not become

aware of the disease at the early stages, and available treatment options are peritoneal, hemodialysis, and finally, kidney transplantation.

2.2. Geographical distribution of CKDu

CKDu has emerged under different names in several countries (Table 2.1). Rural inhabitants in Latin American countries such as El Salvador (Peraza et al., 2012), Nicaragua (Laux et al., 2012), and Mexico (Gutiérrez-Amavizca et al., 2013) have experienced the effects of CKDu for many years. The disease is attributed to a progressive decline in glomerular filtration rate, low-grade proteinuria, an asymptomatic and renal tubulointerstitial disease (Levine et al., 2016). CKDu disease is prevalent in Latin American countries and has been called Mesoamerican nephropathy (MeN).

Table 2.1: Different stages of CKDu and treatment processes required

Stage of CKDu	Description of different stages	Creatinine clearance (GFR) (mL/min/1.73 m^2)	Treatment process
1	Kidney damage with normal or increased Glomerular Filtration Rate (GFR)	>90.00	Screening for CKDu risk reduction
2	Kidney damage with mildly impaired GFR	60.00–89.00	Diagnosis and treatment Slowing progression
3	Moderately impaired GFR (chronic renal failure)	30.00–59.00	Evaluating and treating complications, Kidney dialysis
4	Severely impaired GFR	15.00–29.00	Preparation for kidney replacement therapy
5	End-stage renal disease (uremia)	15.00	Replacement

Source: Chandrajith et al., 2011a

CKDu has also been reported in other countries such as Andra Pradesh in India, Sri Lanka, El-Minia Governorate in Egypt, and several Central American countries (Weaver et al., 2015). CKDu in the Srikakulam district of Andra Pradesh and other places in India has shown similarities to the observations of CKDu affected communities in Sri Lanka and Central American countries (Kumar et al., 2019). Balkan endemic nephropathy (BEN) has been localised for over 50 years in the Balkan Peninsula, affecting thousands of people in Serbia (Janković et al., 2013). In Tunisia, CKDu has been described as chronic interstitial nephropathy (CIN) (Gifford et al., 2017).

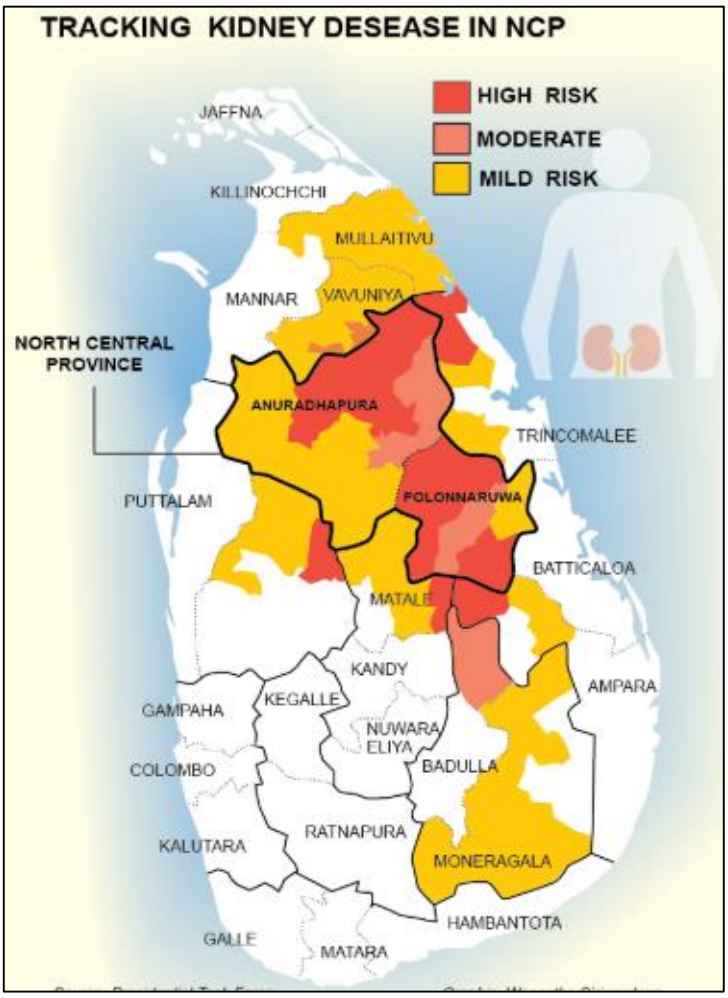

Figure 2.1: Distribution of CKDu prevalent areas in Sri Lanka

Source: Presidential Task Force, 2019

During the last two decades, the epidemic of CKDu among people in rural farming communities has increased mainly in the North Central Province (NCP) of Sri Lanka (Figure 2.1). The government and health authorities have declared the CKDu endemic disease to become a national concern. CKDu in Sri Lanka has been referred to using different names such as chronic agrochemical nephrology (CAN), chronic interstitial nephritis of agricultural communities (CINAC), and CKD caused multifactorial origin (CKDmfo) (Jayasinghe, 2014). Males from low socio-economic status and paddy farming workers are highly vulnerable to the CKDu more than women and children in the area (Bandara et al., 2011; Nanayakkara et al., 2012a). In Sri Lanka, more than 500,000 people have been estimated as affected, and around 20,000 fatalities have been recorded each year (Elledge et al., 2014). Several areas in Sri Lanka (Dehiattakandiya, Padaviya, Girandurukotte, Kabithigollawa, Medawachchiya, Medirigiriya, and Nikawewa) have been found affected with CKDu. There has also been an increase of reports of CKDu patients from other districts. However, researchers in the main domain have not found the exact causal factor for CKDu yet.

2.3. Proposed possible causal factors of CKDu

Different nephrotoxic risk factors have been suggested as causal factors of CKDu in Sri Lanka and other countries where CKDu is highly prevalent. The multifactorial origin of aetiology has been suggested, such as industrial related products, hydrogeochemical properties, biochemical parameters, and other several risk factors (Table 2.2 and 2.3).

Different multi-factors of CKDu have been predicted, including exposure to various environmental nephrotoxin, hydration/dehydration, nutritional status, genetic condition, snake bite, other diseases, and lifestyle behaviour (Levine et al., 2016). There is a knowledge gap in the possible causal factors and geographical distribution of CKDu. The causal factor of CKDu has been suggested to directly link with different drinking water contaminants (CSE, 2012). However, the evidence for the contamination of potable water as a potential cause of CKDu is inadequate (Table 2.3).

Table 2.2: Possible causal factors of CKDu in different countries

Country	Hypothesis about CKDu declared by scientists	References
Mesoamerican nephropathy Latin American countries	Heat stress and dehydration during heavy work in a hot climate	Roncal-Jimenez et al. (2015)
	Exposure to heavy metals (Lead, cadmium, arsenic, mercury, & uranium), agrochemicals, and nephrotoxic substances such as aristolochic acid	Correa-Rotter et al. (2015)
	Use of nonsteroidal anti-inflammatory drugs (NSAIDs) & the infectious diseases leptospirosis, hantavirus, & malaria (endemic in central America)	Correa-Rotter et al. (2015)
	pesticide exposure, alcohol consumption, non-steroidal anti-inflammatory drugs, and heat stress	González-Quiroz et al. (2018)
Balkan endemic nephropathy	Exposure to heavy metals (lead, cadmium, arsenic, mercury, and uranium); agrochemicals, and nephrotoxic substances such as aristolochic acid	Orantes et al. (2009)
	Nephrotoxic mycotoxins including ochratoxin A	Batuman (2006)
Chinese herbs nephropathy	Chinese herbs contaminated with the botanical nephrotoxin aristolochic acid	Batuman (2006) Thuy et al. (2012)
States of Andhra Pradesh, Odisha, Goa, and Maharashtra In India	Water-borne agrochemicals, silica, chemical flavours in betel nuts, and pesticides	Abraham et al. (2019)

Exposure to high concentrations of nephrotoxic elements/compounds such as fluoride, hardness, and heavy metals have been considered as elements causing functional and structural damage in kidney tissue (Sabolic, 2006). Agricultural practices and fertiliser, and other agrochemicals have also been considered as risk factors for CKDu (Jayathilake et al., 2013; Nanayakkara et al., 2012b). The intensive use of agrochemicals and contamination with seepage from irrigation or farming and industrial activities also increases the level of toxic constituents in water. Different toxic constituents have increased in water pollution due to the leachability of elements

from geological sources. Consumption of water contaminated with different toxic constituents has been implied as a significant causal factor for CKDu.

Table 2.3: Possible causal factors of CKDu in Sri Lanka

Hypothesis about CKDu declared by scientists	References
Excessive amounts of fluoride in drinking water and high use of low-quality aluminium utensils	Herath et al. (2005)
A deficient level of fluoride exposure over a longer period	Liu et al. (2005)
Myotoxins, ochratoxins, hard water, leptospirosis	Wanigasuriya et al. (2008)
Exposure to a high concentration of fluoride ions for a prolonged period	Heiri et al. (2009)
Fluoride in the combination of aluminium may produce alumino-fluoride complexes	Illeperuma et al. (2009)
Variability in the sodium and calcium in the groundwater and the calcium saturation factor in the presence of fluoride	Chandrajith et al. (2010)
Arsenic, cadmium, fluoride, and agrochemicals as potential causes of CKDu	Wanigasuriya et al. (2011), Wickramasinghe et al. (2011)
Develop secondary factors such as the variety of toxins, including snakebites, herbal toxins & chemicals, and immunological disorders	Athuraliya et al. (2011), Nanayakkara et al. (2012), Herath et al. (2012)
Toxin produce by microorganisms such as cyanobacteria and the presence of radionuclides introduced by inorganic fertiliser	Chandrajith et al. (2011)
Cyanobacteria growth, blooming and toxin production	Jayasekara et al. (2015)
The high content of fluoride in groundwater, artificial fertiliser, use of aluminium pots and toxin release from blue algae	Jayasumana et al. (2014)
Chronic exposure to low levels of cadmium, coupled with a deficiency of selenium and concurrent exposure to arsenic and pesticide	Jayathilake et al. (2013)

Glyphosate & nephrotoxic metals forming complexes with hard water	Jayasumana et al. (2015)
Prolonged consumption of drinking water with high ionicity and fertiliser runoff	Darmawardane et al. (2014)
Exposure to one or more environmental factors, together with lifestyle conditions, and a genetic predisposition	Levine et al. (2016)
Cumulative levels of heavy metals (Such as Cd)	Wanasinghe et al. (2018)
High concentrations of water hardness, fluoride, salinity, dissolved organic carbon (DOC), and the general alkaline nature of water	Cooray et al. (2019)
Coupled with heat stress, ionic interactions in groundwater, precipitation of calcium phosphate nanoparticles due to nano-bacteria	Dissanayaka & Chandrajith et al. (2019)
Fluoride in drinking water in combination with hardness	Balasooriya et al. (2019)

However, a specific causal factor caused for CKDu has not been investigated at present. Most hypotheses on CKDu have acknowledged fluoride, hardness, heavy metals (mainly cadmium) along with their combination effects as causal factors. The WHO in 2012 highlighted the effects of hardness to heavy metal toxicity through antagonistic mechanism and the influence of hardness to increase renal damage by cadmium. On the other hand, concentrations of fluoride, hardness, and cadmium reported in the literature, were not covered by all CKDu affected and non-affected areas in Sri Lanka. There was a lack of discussion in the research pertaining to the combined effects of fluoride, hardness, and cadmium. Few researchers recently reported (Wasana et al., 2017 and Dharma-wardana, 2017), synergistic fluoride effects, cadmium, and hardness in potable water. In the meantime, WHO has been recommended to implement measures to control farmers' exposure to nephrotoxic risk factors; therefore, it is essential to identify different nephrotoxic risk factors, their concentrations, and their threshold levels of nephrotoxicity, and the extent to which the removal is required in potable water.

2.4. Potential health risk due to the daily intake of nephrotoxic risk factors

2.4.1. Individual effects of nephrotoxic risk factors on human health

Human exposure to nephrotoxic risk factors such as fluoride, hardness, and cadmium can be entered into the human body through different pathways. The nephrotoxic constituent enters the human body through potable water. The gastrointestinal tract adsorbs these constituents and deposits in the skeleton and tissue and affects various illnesses relevant to the bone, such as osteoporosis and osteosclerosis (Jaishankar et al., 2014). The kidney is one of the human organs where tissue contains many mitochondria. In mitochondrial contained tissue, nephrotoxic risk factors produce reactive oxygen species. Production of reactive oxygen species (ROS) is brought detrimental health effects such as damages nephrons, glomeruli, and kidney tissue in the human body (Jarup, 2003) (Table 2.4). Nephrotoxic risk factors produce the reactive oxygen species such as Superoxide anion (O_2^-), Peroxyl radical (ROO^-), Hydrogen peroxide (H_2O_2), Peroxynitrite (R -$NO^\cdot$), Hydroxyl radicals (OH^-), Singlet oxygen (O^-), Dimethyl peroxyl radicals $(CH_3)_2AsOO^\cdot$), and Dimethyl arsenic radicals $(CH_3)_2As^\cdot$). These compounds act as cytotoxic agents, inspiring to damage the kidney tissue (Jarup, 2003).

Table 2.4: Nephrotoxic effects of nephrotoxic risk factors in potable water

Scenarios	Intestine	Mitochondria	Cytotoxicity at kidney
Nephrotoxic contaminant in potable water including Cadmium	Calcium absorption (20%) Magnesium absorption (25%)	Produce reactive oxygen species Superoxide anion ($O_2^\cdot$)	Inhibit the activity of antioxidant enzymes Superoxide dismutase Glutathione peroxidase Catalase
Complexation of Glyphosate with hard water and multiple heavy metals (Cadmium)	Paracellular pathway Transcellular pathway (Blaine et al., 2014) Fluoride (45%)	Peroxyl radical ($ROO^\cdot$) Hydrogen peroxide (H_2O_2)	Inhibit mitochondrial respiration and mitochondrial damage
Prolong use of excessively ionic water	Non-ionic diffusion of HF (Barbier et at., 2010)	Peroxy nitrite (R -$NO^\cdot$)	Lipid peroxidation and cell membrane damage Oxidative stress

Waterborne elements and variability in the sodium and calcium in the groundwater and the calcium be saturation factor in the presence of fluoride	Arsenide and arsenate (Methylation of Arsenic at the Cell) (Hirano et al., 2004) Glyphosate (2.5%) (Convert to Phosphate)	Hydroxyl radicals ($OH^{\cdot}$) Singlet oxygen ($O^{\cdot}$) Dimethyl peroxyl radicals ($(CH_3)_2AsOO^{\cdot}$) Dimethyl arsenic radicals ($(CH_3)_2As^{\cdot}$)	Programmed cell death (Apoptosis)

High production of ROS has been reported to diminish antioxidant enzymes such as Superoxide dismutase, Glutathione peroxidase, and Catalase, inhibit mitochondrial respiration and increase mitochondrial damage (Valko et al., 2005). The inhibition of mitochondrial activity increases oxidative stress on the cell membrane, promoting phospholipid membrane damage calling lipid peroxidation and cell death, leading to cell apoptosis.

2.4.2. Combined effects of nephrotoxic risk factors on human health

(a) Combined impact of fluoride and hardness

The disease patterns and hydro-geochemical factors show that Ca-hardness, Mg-hardness, and temporary hardness play a significant role rather than total hardness in the water (Dissanayake and Chandrajith, 2017). Hence, modification of chemical forms of fluoride and other trace elements in the presence of hardness may persist as a secondary factor for the disease's aetiology. The presence of high fluoride in water has been shown to increase high Ca^{2+} activity in groundwater (Chrandrajith et al., 2011a, 2011b), suggesting that CKDu may erupt in dry zone areas due to the combined effects of fluoride and hardness. One of the main elements present in hard water is magnesium, which does not play a significant role as a nephrotoxic risk factor (Dissanayake and Chandrajith, 2017). However, calcium plays a crucial role in the disease's causal factor (Dharma-wardana, 2017). Further investigations have been suggested to identify the synergistic effects of fluoride and harnesses in potable water (Wasana et al., 2017).

(b) The combined effect of fluoride and calcium

Acute and chronic exposures to elevated fluoride levels have shown fewer adverse effects on several Ca-dependent processes in human kidneys (Borke and Whiteford,1999). Long-term fluoride intakes have been suggested to produce high fluoride levels in human plasma. High fluoride in plasma affects Ca^{2+} homeostasis, influencing the plasma membrane's expression and endoplasmic reticular Ca^{2+} pump proteins (Borke and Whiteford, 1999). Fluoride has been found to make complexes with dietary calcium and iron and decrease solubility (Sauerheber, 2013). Then, individuals with higher blood calcium are more resistant to fluoride toxicity and henceforth, calcium acts as an antidote to fluoride toxicity. Apart from that, it has been found that high dissolved F^- in groundwater decreases Ca^{2+} ion concentrations in water of some areas in CKDu prevalent areas (Paranagama, 2014). Combination effects of fluoride and hardness further inferred that a study on synergic effects of fluoride and hardness needs to be implemented.

(c) The combined effect of fluoride and magnesium

The ion pairing of fluoride with magnesium in potable water has been proposed as one of the plausible factors of CKDu (Dharma-wardana, 2017). Magnesium has been found to activate more than 300 enzymes in the human body, while fluoride has shown inhibitory attributes (Strochkova and Zhavoronkov, 1983). However, few enzymes are activated by fluoride. The investigation of biochemical and geochemical interaction of magnesium and fluoride provides a path to identify their link to CKDu. Fluoride and magnesium ratio in groundwater, which people in CKDu affected areas consume, play a critical role as fluoride interferes with the human body's magnesium reactivity. Fluoride concentration has been found to pair totally with magnesium ion and produces MgF^+ (Wasana et al., 2017; Dharma-wardana, 2017). Fluoride pairing with magnesium has been investigated, showing more nephrotoxic than single fluoride (Wasana et al., 2017).

(d) The combined effect of fluoride and cadmium

People in CKDu prevalent areas are exposed to fluoride and cadmium through water. The toxic effects of fluoride have increased in the presence of cadmium at trace levels (Dharma-wardana, 2017). $(CdF)^+$ ion-pair has been shown as a "sodium-like" ion binding to the protein, transporting into cell plasma, and finally bringing cadmium and fluoride toxicity to human cells (Dharma-wardana, 2017). The combined toxicity of cadmium and fluoride is very strong, and they have shown to be three-times higher toxicity than the toxicity of cadmium and fluoride alone (Dharma-wardana, 2017; Zhang et al., 2017)). A strong positive correlation between fluoride in the presence of cadmium in potable water has been emphasised by the study conducted by Wasana et al. (2017). People who consumed spring water with low fluoride and cadmium levels have also been affected by CKDu (Wasana et al., 2015). The study on the disruption of kidney tissue in the rat confirmed that WHO permissible levels (Cadmium – 0.003 mg/L and Fluoride – 1.5 mg/L) of fluoride and cadmium in water bring nephrotoxic effects (Wasana et al., 2017). Past studies on cadmium and fluoride showed a strong synergistic effect on the kidney by cadmium and fluoride in potable water.

Past studies corroborated that fluoride, hardness alone, combined effects of fluoride, hardness, and cadmium increase the severity of CKDu. People consume water in CKDu affected areas contaminated with fluoride, hardness, and cadmium for their day-to-day requirements with or without treatment. They are exposed to nephrotoxic risk factors directly without knowing that they may be vulnerable to renal damage. Further, the literature corroborated that removing fluoride, hardness, and cadmium from potable water will ensure water safety in people living in CKDu affected areas if there is a health risk on people. Therefore, the detailed evaluation of fluoride, hardness, and cadmium concentrations in potable water compared to drinking water reference values for concentrations, and if removal is required, what is the extent to which removal is required, is of utmost importance before introducing removal techniques. Hence, drinking water guideline values were referred to identify the removal requirement.

2.5. Different drinking water guideline values for nephrotoxic risk factors

The primary purpose of drinking water guideline values is to protect people from adverse health risks. The World Health Organisation has provided drinking water guideline values to ensure drinking water safety for people. Water should be provided to all communities with accessible, safe, and adequate supplies (WHO, 2017). According to WHO guidelines, safe drinking water has been defined as drinking water that should not contain any significant health risk factor over a lifetime consumption and any sensitivities in the body at other ill-health conditions. Several institutes and countries have been established by drinking water guideline values (Table 2.5), for the purpose of developing risk management strategies to control hazardous water constituents.

Table 2.5: Different drinking water guideline values for nephrotoxic risk factors

Reference	Fluoride (mg/L)	Hardness as $CaCO_3$ (mg/L)	Calcium (mg/L)	Magnesium (mg/L)	Cadmium (mg/L)
WHO, 2017	1.50	None	None	None	0.003
Sri Lanka Standards (SLS 2148/20: NER No. 01: 2019)	1.00	250.00–600.00	100.00–240.00	30.00–150.00	0.005
US EPA National Secondary Drinking Water Regulations (USEPA, 1991)	2.00–4.00	None	None	None	0.005
Australian Water Quality Guidelines (2011)	1.50	None	None	None	0.002
Canadian Water Quality Guidelines (2011)	1.50	None	None	None	0.005
European Union Drinking Water Regulations (EUDWR, 2018)	0.80–1.50	None	None	None	0.005

Bureau of Indian Standards (IS10500:2012)	1.50	600.00	200.00	100.00	None
National water quality standards of China (NSPRC, 2006)	1.00	450.00	None	None	0.005
Drinking water quality standards Nepal (NDWQS, 2005)	0.50–1.50	500.00	200.00	None	0.003
Drinking water quality standards Bangladesh (BNWQS, 2009)	1.00–1.50	200.00–500.00	75.00	30.00	0.003
Drinking water quality standards Pakistan (NSDWQ, 2008)	1.50	500.00	None	None	0.01
Maximum contaminant concentration levels in the dialysis water (NSW, 2008)	0.20	35.00	2.00	4.00	0.001

Drinking water guideline values have been given for fluoride and cadmium by each guideline value considered in the study. The WHO, USEPA, Australian, Canadian, and European Union have not been provided with the guideline values for hardness, calcium, and magnesium. However, in countries in the Asian region, the drinking water guideline value for hardness has been declared. Hardness guideline values given by the Asian Region can be classified under "Very hard, > 180 mg/L hardness as $CaCO_3$" according to the hard water classification provided by the United States Geological Survey, 2012. In the Asian Region, hardness has become a main water quality parameter in potable water. Finally, hardness has been predicted as a national and international causal factor for CKDu. As the directing and coordinating authority in international health and promoting people's health at the country level, WHO keeps the world safe and serves the vulnerable, however, has not taken into consideration the hardness in the Asian region's potable water in the drinking water guideline values. Therefore, as a

CKDu affected country, Sri Lanka should take the initiative to revisit the drinking water guideline values and declared the most suitable guideline values, especially for CKDu affected areas and non-affected areas.

2.6. Water treatment technologies available in CKDu prevalent areas and their drawbacks

Conventional water treatment technologies do not remove nephrotoxic risk factors efficiently and effectively. Hence, Reverse Osmosis (RO) filters have been introduced in CKDu affected areas as a lasting solution.

The RO filter unit consists of various components such as inlet water line, pre-filters, RO membrane, post-filter, storage tank, and drain line. The filtration process could describe five stages responsible for removing different water constituents (Table 2.6). Sediment filter, carbon block filter, granular activated carbon, and post-carbon filters belong to pre-filtration processes. These components remove sand, clay, and silt mechanically and protect the RO membrane from chlorine.

Table 2.6: Different unit processes in the RO filter unit

RO filter components	Removal of different constituents in drinking water
Sediment filter (5 µ)	Sand particles, dust, dirt, floating matter
Granular activated carbon	Chlorine, taste, and odour particulate matter
Carbon block (1 µ)	Synthetic detergent, colour, odour, taste, antibacterial properties
RO membrane	Removal of inorganic solutes in water
Post carbon filter	Removal of taste and odour

The structural and transport properties of the RO membrane is varied across the membrane due to asymmetric porosity and the thickness of the membrane (Kesting, 1990). The dense layer thickness in the membrane has been found as 0.1–1.0 µm, highly porous (100–200 µm) with a thick layer (Kesting, 1990). Separation properties of the membrane depend on the chemical nature, size of the pores, and the membrane's

thickness. RO has often been composed of a thin film composite membrane. The components of the RO filter unit have been shown in Figure 2.2.

Figure 2.2: Different components in the RO filter unit

RO membrane comprises of a fully aromatic polyamide which has been formed by interfacial polymerisation of meta-phenylenediamine (MDP) and Trimesoyl Chloride (TMC) (Cadotte, 1980). RO membrane is negatively charged by acyl chloride groups, which are not fully converted to amide groups. It has recently been determined that the polyamide RO membrane consists of positive and negative fixed charges in the dense layer composite (Coronell et al., 2011).

RO membrane has been reported to be performing with four retention mechanisms. They are adsorption, size exclusion, charge interaction, and solute-diffusion models (Shen & Schäfer, 2014). The chemical properties such as solution concentration, pH, counter ions; operating parameters such as pressure and crossflow velocity; solute and

solute interaction, speciation, membrane characteristics, and fouling effects have been identified as attributes of RO membrane (Shen & Schäfer, 2014). Removal mechanisms of RO membrane and activated carbon are depicted in Figures 2.3 and 2.4, respectively.

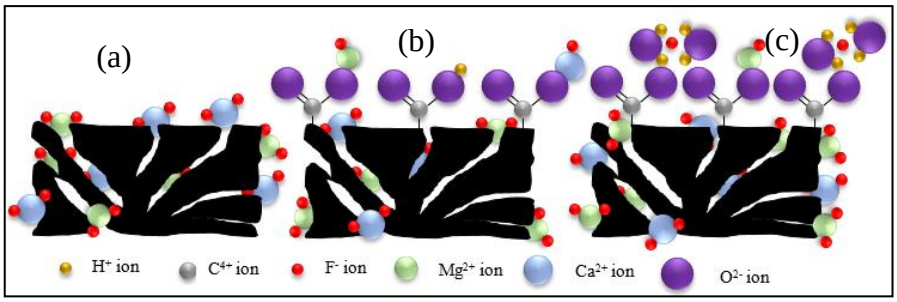

Figure 2.3: The schematic diagram of activated carbon in RO system consists of mesoporous, microporous and macroporous; a) Adsorption of calcium, magnesium, and fluoride ions on the surface of activated carbon, b) Adsorption of calcium, magnesium and fluoride ions on functional groups, c) Adsorption of hydrated fluoride on functional groups

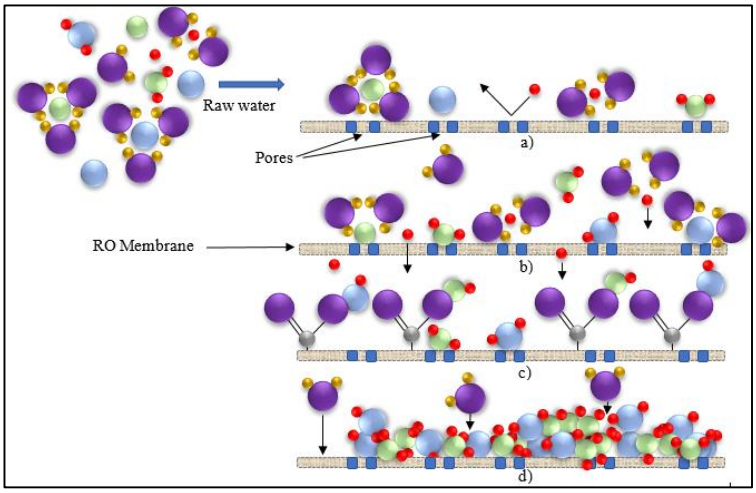

Figure 2.4: Schematic diagram of calcium, magnesium, and fluoride retention mechanisms of RO membrane; a) Size exclusion (Large ionic radii do not allow to permeate through the pores), b) Solute-diffusion (Reduce negative charge of the layer and allow the fluoride to diffuse), c) Charge interaction/ adsorption (Pores covered by counter functional groups) and d) Fouling effects (Act as a barrier to permeate)

Adsorption in the membrane filtration process refers to the interaction between membrane charges and the solute. Mainly, chemisorption and physisorption occur as non-electro statistic mechanisms. Physisorption occurs due to Van der Waals forces, which are reversible and weak. Chemisorption arises due to covalent chemical bonds, which are strong and irreversible (Arshadi et al., 2014). Cations in the solution adsorb to the negatively charged membrane. Anions also adsorb in terms of available positive charges on the RO membrane, as mentioned by Coronell et al., 2011. In some cases, cations have been reported on the assumption that it may modify the charge of the RO membrane and affect the anions adsorption indirectly or allow anions to be adsorbed on the membrane together with other ions as a complex (Shen & Schäfer, 2014).

Retention mechanisms of charge interaction refer to the charge repulsion or attraction between the charged RO membrane and the charged solutes in the solution. This mechanism has been suggested when the membrane's pore size is larger than the charged solutes' size (Shen & Schäfer, 2014). The solute charges have been varied according to the solution's chemical attributes, such as temperature, pH, ionic strength, and available ligands (Morel & Hering, 1993). The membrane charge has been observed to be determined by ionisable functional groups on the membrane surface (Childress & Elimelech, 1996). The functional groups on the surface dissociate. This process increases the charge repulsion between the polymer chains. The charge repulsion forcefully opens up the pores on the membrane's surface (Bragetta et al., 1997). The process promotes the permeation of water.

Size exclusion retention mechanism refers to any larger solute than the pore size of the membrane retained. Generally, small solutes have non-spherical and flexible shapes. In the size-exclusion model, it has been assumed that solutes are spheroids. The pores in the membrane are cylindrical capillaries (Shen & Schäfer, 2014). The adequate size of the solutes has been accounted for both ionic size and the hydration layer. The dissolve solutes in the solution have been observed surrounding water molecules; then, it increases the ions' size (Tansel et al., 2006). The hydration increases the retention of the solutes.

The solute-diffusion model has been described based on a three stepped chemical process: 1) solutes dissolve in the membrane, 2) solute diffuse through the membrane depending on the concentration gradient, and 3) solute enter the solution again after permeating through the membrane. The diffusion rate depends on the solute's solubility limit within the polymer matrix (Shen & Schäfer, 2014).

The RO plant's serious concern has been reported as a decrease in RO plant operation, maintenance, and management period due to the fouling of membrane with high alkaline water and higher mineral concentration (Cooray et al., 2019). However, it is reported that RO filters remove all minerals essential for human cell growth (Le & Nunes, 2016). Consumption of water with insufficient mineral levels may result in adverse health effects such as central nervous system related ailments (Jacqmin et al., 1994; Sengupta, 2013), cardiovascular disease (Kohri et al., 1989; WHO, 2009; Gaurav et al., 2014), kidney stones, risks of gastric cancer (Yang, 1998), pre-term birth and low weight at birth (Melles & Kiss, 1992; Yang et al., 2002), etc. The use of RO filters does not seem to be a long-term solution for drinking water treatment in the CKDu endemic areas due to (i) high capital cost, (ii) high operational and maintenance cost, (iii) lack of technical know-how in operational aspects, (iv) permeate being rich with nephrotoxic risk factors and (v) non-availability of essential mineral in permeate. Past studies have suggested that the most cost-effective way was to identify the aetiology of disease and develop effective new technologies to control the disease's outbreak (Chandrajith et al., 2010; Cooray et al., 2019).

Technology invention to remove nephrotoxic compounds for the provision of safe potable water to the CKDu affected community is a dire need at this juncture to eliminate the adverse health effects on the population in CKDu prevalent areas. However, the research conducted to find available water treatment technologies and their effectiveness in removing nephrotoxic risk factors was rarely reported in the literature. Although RO is the most prominent water treatment technology used in CKDu affected areas, very few studies have evaluated their performance at a shallow level. Therefore, the study on available water treatment technologies in CKDu affected areas

and evaluating their performance in removing nephrotoxic risk factors is a prerequisite to developing effective new technologies.

2.7. Different water treatment techniques to remove nephrotoxic risk factors in water

Various mechanisms such as membrane filtration (Camacho et al. 2013), coagulation and microfiltration (Da Conceicao et al. 2015), chemical precipitation (Jadhav et al. 2015), electrodialysis (Belkada et al., 2018), adsorption (Jayarathna et al. 2015; Jayaweera et al., 2019; Sudasinghe et al., 2019), and ion exchange (Robshaw et al., 2019) have been identified as removal techniques of different constituents in potable water. Membrane processes, at present, have become popular in the sector of water treatment and supply. Advantages of membrane technology have been identified as cost-effectiveness, operation flexibility, and high removal capacity (Lounici et al., 2004). Reverse osmosis and electrodialysis have shown practical application in inorganic contaminants removal from water (Belkada et al., 2018).

In drinking water treatment, coagulation is one of the pretreatment processes to control membrane fouling. Coagulation is popularised due to its advantages, such as i) removal of the particular matter and natural organic matter, ii) low cost, and iii) simple operation (Song et al., 2015). Particular matter and natural organic matter have been identified as the leading causes of membrane fouling. Membrane fouling is a significant challenge in the microfiltration of low cost, decentralised water treatment systems (Katalo et al., 2018). The use of alum, or ferric chloride has been investigated as effective coagulants in the pretreatment process to decrease membrane fouling in microfiltration (Zhang et al., 2015).

Chemical precipitation popularises as a water pretreatment method of high fluoride-containing water. The advantages of chemical precipitation have been found at low cost, the simple and widely used fluoride removal method (Wang et al., 2019). High fluoride-containing water show high acidity levels. Calcium ions can be used to precipitate

fluoride in water, and wastewater can be neutralised using lime or calcium salts (Wang et al., 2019).

Electrodialysis has been used to treat fluoride rich-water because the treatment method is simple and enables the avoidance of many defects of chemical processes. Several disadvantages can be found in electrodialysis compared to conventional water treatment. The electrodialysis process contains cations and anions exchange membrane with multiple electrodialysis cells, and the process permeates the ion through the membrane under the influence of electric potential. Anode attach anions in water, and they permeate through the positively charged membrane. The cation retains anions exchange membrane, which is negatively charged (Majewska-Nowak et al., 2015).

Ion exchange resin has been used in water treatment to exchange ions with other ions to remove contaminants in water (Kansara et al., 2016). Two categories of ion exchange resins can be identified as cation and anion exchange resins. Ion exchange softening plays a role in decontaminating water by eliminating the hardness level of water. The process instigates the removal of calcium and magnesium ions in water. Regeneration of ion exchange resin can be conducted after saturation of the resin's bed by calcium and magnesium. The cation exchange resin can regenerate using sulphuric or hydrochloric acid, and anion exchange resin has been regenerated by sodium hydroxide (Kansara et al., 2016). In past studies, advantages of ion exchange resin have been mentioned as cost-effectiveness, less energy requirement, higher shelf-life, and regeneration ability. Fouling effects due to calcium and other ions, adsorption of organic matter, non-ionized organic contamination, and contamination from bacterial growth have been highlighted as disadvantages of ion exchange resins.

Adsorption of water constituents using adsorbents is a widely used technique in removing toxic constituents in water. At the beginning of water treatment, the main target has been found to remove the taste and odour compound using adsorption. Later, the adsorption process's application was changed, and a range of organic substances and

inorganic ions have been removed from aqueous solutions using different adsorbents (Table 2.7, 2.8, 2.9 & 2.10).

The different adsorbents were chosen for adsorption, such as industrial by-products, natural adsorbents, and nanomaterials. Engineered adsorbents have been reported in many materials, including artificial zeolite, polymeric adsorbents, nanomaterials, oxidic adsorbents, and carbonaceous adsorbents. Materials remove nephrotoxic risk factors in water using different mechanisms such as adsorption/desorption, oxidation/reduction, ion exchange, complexation, precipitation, etc. (Bhatnagar et al., 2010). Different materials to remove hardness, fluoride, and faecal coliform will help increase the removal effectiveness of nephrotoxic and water-borne risk factors in potable water.

Engineered adsorbents show the highest adsorption capacities. These materials need to produce under strict quality control and have almost the same properties in each material. The adsorption process occurs on the surface of the adsorbent. Hence, the surface area of the adsorbent is of great importance for the increase of adsorption capacity. A high surface area is prominent with the high porosity of the materials. The high porosity increases larger internal surface areas due to pore walls. Larger pore systems with more refined pores increase the inner surface area. The fraction of larger pores is most vital as it increases fast adsorbate transport into the adsorption sites.

The surface chemistry of an adsorbent plays a crucial role in the chemisorption process. All properties found in nanomaterials are more vital to perform as an effective adsorbent. Nanomaterials have been reported to perform different removing mechanisms such as coagulation and precipitation, adsorption, oxidation/reduction, and ion exchange (Boparai et al., 2013; Wu et al., 2013). Removal mechanisms of nanomaterials are attributed to different characteristics such as high reactivity and high surface energy, high performance due to the large specific surface area (Sun et al., 2006; Cundy et al., 2008).

Adsorbents used in drinking water treatment should fulfil the required water quality standards, and treated water should comply with drinking water guideline values. The

consumption of treated water with nephrotoxic risk factors makes people vulnerable to adverse health effects. When an engineering adsorbent was selected to remove nephrotoxic risk factors, attention should be drawn to their attributes and removal effectiveness.

Table 2.7: Materials and their removal capacities and kinetics parameters in the removal of fluoride

Adsorbent	**F levels (mg/L)**	**pH**	**Contact time (Hours)**	**Adsorption capacity (mg/g)**	**References**
Alum sludge	5.00–35.00	6.00	4.00	5.39	Sujana et al. (1998)
Activated alumina	15.00–100.00	5.00–6.00	16.00–24.00	0.86 mmol/g	Ku & Chiou (2002)
Aluminum hydroxide	5.00–30.00	7.00	24.00	23.70	Shimelis et al. (2006)
Various grades of graphite	2.00–10.00	6.00–7.00	1.00	3.13	Karthikeyan & Elango (2008)
γ-Fe_2O_3	10.00 – 100.00	6.00–10.00	12.00	3.65	Jayarathna et al. (2015)
Chitosan_iron complex	50.00	3.00–10.00	1.00	2.34	Patnaik et al. (2016)
magneticFe_3O_4@Fe-Ti composite	4.00–200.00	3.00–11.00	1.00	41.80	Zhang et al. (2016)
α-Fe_2O_3 and Fe_3O_4	1.00–60.00	2.00–10.00	5.00 min	9.04	Dewagea et al. (2018)
CaO loaded mesoporous alumina	5.00–40.00	6.50	2.00	17.83	Jayaweera et al. (2019)
Iron oxide nanoparticles	1.00–20.00	6.50	1.00	10.75	Sudasinghe et al. (2019)

Table 2.8: Materials and their removal capacities and kinetics parameters in the removal of hardness

Adsorbents	Hardness levels (mg/L)	pH	Contact time (Hours)	Adsorption capacity (mg/g)	References
Modified Pumice Stones	25.00–150.00	6.00	3.30	62.30 – Ca^{2+} 56.11 – Mg^{2+}	Sepehr et al. (2013)
Phyllanthus emblica wood	92.17 Ca^{2+} 68.05 – Mg^{2+}	6.30	2.00	13.22 – Ca^{2+} 9.48 – Mg^{2+}	Kannan & Mani (2014)
Prepared Zeolite	1,000.00	–	1.00	200.00	Goud et al. (2015)
Cashew nutshell Activated Carbon	1,214.80	6.00	50.00 min	384.60	Rolence-China (2016)
Zeolite from Ethiopian kaolin	1,000.00	6.50	4.00	12.50 – Ca^{2+} 15.70 – Mg^{2+}	Aragaw & Ayalew (2018)
Kaolinite Smectite	1,000.00	5.00	2.50	32.10 – Ca^{2+} 122.90 – Mg^{2+}	Shenzhen et al. (2018)

Table 2.9: Materials and their removal capacities and kinetics parameters in the removal of cadmium

Adsorbents	Cadmium concentration (mg/L)	pH	Contact time (Hours)	Adsorption capacity (mg/g)	References
Coffee grounds	10.00–700.00	7.00	2.00	15.65	Azouaoua et al. (2010)
Activated carbon prepared from aguaje (*Mauritia flexuosa*) (AG) and olive fruit stones (*Olea europaea* L.) (OL)	10.00	5.00	24.00	26.33 AG 24.83 OL	Obregón-Valencia & Sun-Kou (2014)
Activated carbon	1.00	7.00	2.00	2.72	Al-Khaldi et al. (2013)
Carbon nanotube				1.66	

Carbon nanofiber				2.12	
Carbon fly ash				11.23	
Modified poly(ethylene terephthalate) fiber	120.00	6.70	1.00	18.87	Borzou et al. (2014)
Water treatment residuals	10.00–500.00	8.10	24.00	47.00	Elkhatib et al. (2016)
Chemically and thermally treated rice husk	20.00–100.00	6.00	72.00	28.27	Hoyos-Sánchez et al. (2017)
Biochar derived from lotus seedpods	40.00	6.90	48.00	31.69	Chen et al. (2018)
Coal fly ash-nZVI	5.00–200.00	8.50	5.00 min	120.00	Ma et al. (2018)

Table 2.10: Materials and their removal capacities and kinetics parameters in the removal of faecal coliform

Materials	***E. coli*/ coliform count (CFU/100 mL)**	**pH**	**Contact time (Hours)**	**Final *E. coli* (CFU/100 mL)**	**References**
Silver supported on natural Mexican zeolite	1.53×10^3	–	24.00	0.00	Rivera-Garza et al. (2000)
Nanostructured hexagonal cobalt dendrites	3.50×10^5	7.40	3.00	0.00	Panmand et al. (2014)
Fly ash geopolymer paste	1.53×10^4	7.90	8.00	0.00	Jo et al. (2015)
Graphene functionalized by 1,6-diamino hexane with silver nanoparticles	1.20×10^6	–	2.00	0.00	Abdelhalim et al. (2016)
Silver nanoparticles	4.10×10^4	–	15.00 min	0.00	Moustafa (2017)
Air-ozone micro-nanobubbles	2.40×10^5	7.00	–	100.00	Cruza & Flores (2017)

2.8. Summary of adsorbents used to remove fluoride, hardness, and cadmium in potable water in Sri Lanka

Effective and efficient technologies have been highlighted as a prerequisite by several past studies to remove nephrotoxic risk factors in potable water (Chandrajith et al., 2011; Wickramarathna et al., 2017). Although removing water contaminants using adsorbents is popular, applying different materials such as nanomaterials, industrial by-products, and natural adsorbents is limited in removing nephrotoxic risk factors CKDu prevalent areas in Sri Lanka. However, few studies in removing hardness, fluoride and cadmium from potable water using different materials were recorded in Table 2.11.

Table 2.11: Different materials employed to remove fluoride, hardness, and cadmium in potable water of CKDu prevalent areas in Sri Lanka

Adsorbent	Origin	Target risk factor (mg/L)	Adsorption capacity (mg/g)	References
Silver oxide nanoparticles	Nanomaterial	Faecal coliform	0 CFU/100 mL	This study Sudasinghe et al. (2018)
Iron oxide nanoparticles	Nanomaterials	Fluoride and calcium	Fluoride-10.75 Calcium - 9.86	This study Sudasinghe et al. (2019)
CaO loaded mesoporous alumina	Nanomaterials	Fluoride	17.83	This study Jayaweera et al. (2019)
Kaolinitic clay	Natural adsorbents	Fluoride	Not given	Jinadasa et al. (1988)
Turmeric, ginger, and curry leaves	Natural adsorbents	Fluoride	1.42	Paranagama (2014)
$\gamma - Fe2O3$	Nanomaterials	Fluoride	3.65	Jayarathna et al. (2015)
Rice husk, saw dust and bagasse	Natural adsorbents	Cadmium	Not given	Ambepitiya (2015)
Fly ash	Industrial by-product	Fluoride and hardness	Not given	Ranasinghe and Nanayakkara (2018)
Chicken bone char	Natural adsorbents	Fluoride	11.20	Herath et al. (2018)

Montmorillonite and hydroxyapatite	Nanocomposite	Fluoride	16.70	Fernando et al. (2019)
Coal fly ash	Industrial by-product	Fluoride	3.64	Pitawala et al. (2020)
Modified clay	Natural adsorbents	Hardness	Not given	Perera et al. (2020)

Most studies have employed natural adsorbents to remove fluoride, hardness, and cadmium in reducing the cost of water treatment. However, the adsorption capacity of most natural materials is substantially low. Hence, nanomaterials associated with industrial by-products in multi-layer units seem to be a suitable approach to removing nephrotoxic risk factors in water.

Alumina has been applied in several studies to remove fluoride in potable water. Mesoporous alumina has been reported to have a well-distributed pore structure with nano-scaled pores and a high surface area. However, MgO loaded alumina was not used in fluoride removal in potable water, and most applications were found to remove atmospheric carbon dioxide. ZEOL produced from fly ash (industrial solid waste) attribute more refined pore structure, low cost, easy accessibility to raw materials, and is rarely used for value-added produce. In adsorption processes in past studies, zeolite produced from fly ash was not used to remove hardness in potable water. The different applications of nZVI can be found in the literature on a vast scale due to their magnetic properties, high surface to area ratio, small size, and higher reactivity. However, the nZVI standalone application was found rarely in literature to remove cadmium in potable water. Nano silver oxide and graphene oxide have shown bacterial cell growth inhibitory effects separately, and most studies have used these two materials to remove faecal coliform in potable water. However, composite nano silver oxide and graphene oxide is rarely reported in the application as an antibacterial agent to remove *E. coli* in potable water.

2.9. Summary of the literature review

The exact aetiology for the CKDu has not been corroborated yet by scientists engaged in scientific studies, even though the outbreak of CKDu reaches its third decade (from 1990). Past studies have highlighted that disease originality is multifactorial and has a prominent direct link to potable water. Various water-related nephrotoxic risk factors [hydrogeochemical properties: fluoride and hardness, heavy metals (cadmium)] have been suggested as an aetiology of the disease by several studies from 2004 to date. Fluoride, hardness, and cadmium in groundwater, their associated distribution pattern, and synergic effects are given an insight in literature as prominent nephrotoxic risk factors. Fluoride and hardness exceed the permissible drinking water guideline values. Cadmium is reported as trace level in the groundwater, and its interaction with fluoride and hardness are ascertained in several studies, increasing the severity of the disease. Therefore, several studies have manifested the need for technology to remove excess levels of nephrotoxic risk factors from potable water in CKDu prevalence areas.

Water treatment technologies have been introduced in CKDu prevalence areas, with reverse osmosis (RO) water purification systems being the most popular option. Both CKDu affected and non-affected people consume treated water from available water filter units. People do not have a broad knowledge of the water filters' techniques and their water quality standards. Scientific evidence was not provided to show that water treated by water filters have complied with the required drinking water standards. Hence, it is necessary to evaluate the water purification systems' performance in the Sri Lankan market. Few studies are recorded in past studies about groundwater treatment using only RO systems and water quality analysis of RO treated water. However, extensive studies have not reported to what extent the RO system or other treatment units improve potable water quality and their long-term health effects on people. Hence, this study focused on analysing the performance of available water treatment technologies in CKDu prevalence areas and assessing people's vulnerability to expose non-carcinogenic health hazards to consume potable water treated by available technologies.

Recently, special attention has been given to preparing adsorbents from different materials to remove nephrotoxic risk factors from groundwater. Although several studies are recorded in literature, studies using nanomaterials and industrial by-products are limited in removing fluoride, hardness, and cadmium in potable water of CKDu areas. Few studies are reported in the literature related to nanomaterials and their removal to nephrotoxic risk factors. Zeolite produced from fly ash is not applied to remove hardness in potable water of CKDu affected areas. Fluoride removal using MgO loaded mesoporous alumina is not reported in CKDu affected areas. nZVI to remove cadmium, and silver oxide loaded graphene oxide composite to remove *E. coli* from potable water within CKDu prevalent areas is not explicitly recorded. Therefore, the study was designed to find the best-engineered materials (nanomaterials or industrial by-products) to remove fluoride, hardness, *E. coli* and cadmium from groundwater in CKDu prevalent areas. The multi-layered unit investigation to remove multi-solute in potable water in CKDu areas can be acknowledged as a novel approach in this study to design a home filter unit.

CHAPTER 3

3. RESEARCH METHODOLOGY

The chapter describes the experimental procedure of the research study as follows (Figure 3.1). Four hypotheses (related to nephrotoxicity) were considered during the study in terms of CKDu: i). cadmium alone as a possible nephrotoxic risk factor in potable water; ii). cadmium in the presence of hardness and fluoride; iii). fluoride alone; and iv). fluoride in the presence of hardness. One hypothesis (related to non-nephrotoxicity) was considered in terms of waterborne diseases: v) microbial contamination of potable water by faecal matter (removal of *E. coli* bacteria from potable water was studied because of the study was finally developed the home filter unit to provide safe drinking water).

- Identification of possible nephrotoxic risk factors in potable water by field studies and literature review and compare their concentration levels with drinking water guideline values
- Performance evaluation of available water purification systems used abundantly in CKDu prevalent areas
- Assessment of non-carcinogenic health risk due to ingestion of reverse osmosis treated water
- Investigation of the best combination of materials for a multi-layered water purification unit, synthesis of different materials to remove fluoride, hardness, cadmium and faecal coliform, characterization of materials using analytical techniques such as XRD, ESEM/EDAX, and FT–IR, batch experiments and fixed-bed column studies were described in detail.

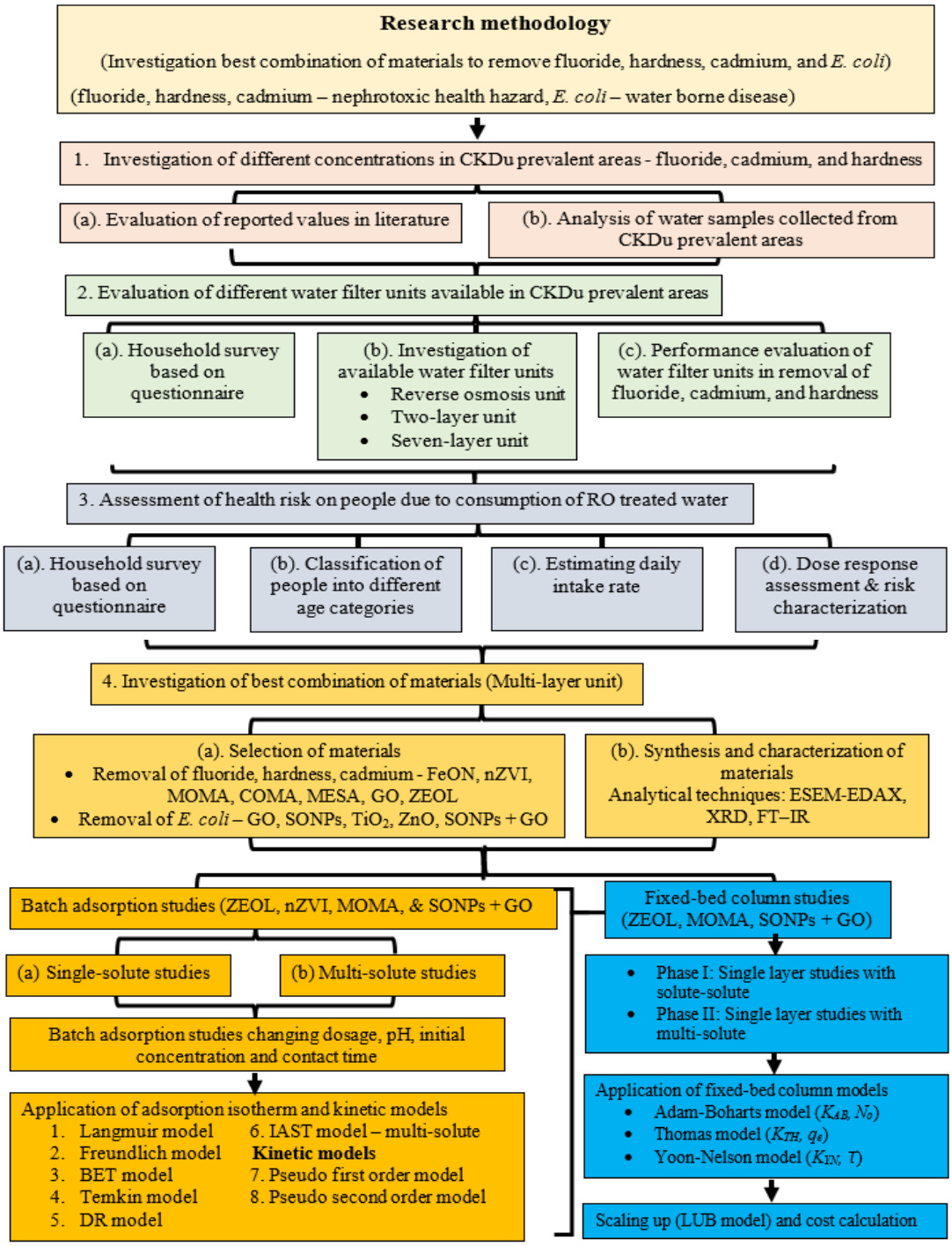

Figure 3.1: Schema for overall research methodology represented the main activities in each specific objective

3.1. Objective 01: To identify different nephrotoxic risk factors, their concentrations, threshold levels of nephrotoxicity, and the extent to which the removal is required in potable water

The study's overall objective is to investigate the multi-layers with different micro and nanomaterials to provide safe drinking water for people in CKDu prevalent areas. In past studies, it has been reported that the potable water consumed by people in CKDu prevalent areas comprise of different nephrotoxic risk factors (fluoride, hardness, and cadmium). Hence, objective 01 was designed to investigate concentrations of nephrotoxic risk factors in CKDu areas; to identify their levels in reference to drinking water guideline values and the extent to which the removal is required. Firstly, the concentrations of hardness, fluoride and cadmium were gathered from the literature. The potable water samples were collected and analyzed from the selected CKDu affected areas. The concentrations were compared with the drinking water reference values to identify the removal requirement.

3.1.1. Identification of possible nephrotoxic risk factors in potable water and their concentrations

Hydro-geochemical properties such as fluoride, hardness, and cadmium, have been postulated as possible causal factors for CKDu in Sri Lanka (Dharmawardana et al., 2014; Jayasumana et al., 2015; Rango et al., 2015; Wasana et al., 2016). Therefore, concentrations reported of water constituents (fluoride, hardness, and cadmium) that have been suspected as causal factors of CKDu were collected from a comprehensive literature review (Secondary data). Groundwater samples from 12 protected and four unprotected wells located in Wewelketiya Village, Rambewa, Anuradhapura district were analysed to identify fluoride, hardness, and cadmium concentrations under the preliminary studies (Primary data). All wells located in Wewelketiya Village were considered for the sampling analyses. The samples were collected in a pre-cleaned high-density polypropylene bottle and acidified with concentrated nitric acid. The standards sampling and analytical methods were applied throughout the study (APHA, 1997). The

data collected from the water sample analysis and the data reported in literature were interpreted to identify excess or deficiency of fluoride, hardness, and cadmium in potable water. The reported values for cadmium were considerably lower in number. A set of data for fluoride, hardness, and cadmium in CKDu prevalent and non-prevalent areas was analysed using descriptive statistics, percentile values and independence sample T-test. Null hypotheses ($H_o = 1$) were defined "Concentrations are significantly equal in CKDu and non-CKDu prevalent areas" and the opposite of the null hypothesis was considered as an alternative hypothesis ($H_1 \neq 1$). Statistical packages of social sciences (IBM®SPSS®25) and Microsoft excel 2016 were used to analyse descriptive statistics and the summarisation of data.

3.1.2. Identification of threshold levels of nephrotoxicity and the extent to which the removal is required in potable water

Drinking water permissible values were evaluated in different countries such as Australia, Canada, European Union, China, South Asian countries like India, Nepal, Bangladesh, Pakistan, and Sri Lanka. Drinking water guideline values of international institutions like USEPA and WHO were referred and compared to identify the threshold levels for nephrotoxic risk factors. WHO drinking water guideline values were chosen to compare fluoride, hardness, cadmium concentrations and *E. coli* values in potable water, WHO guideline values provide a scientific basis to derive national or regional standards for drinking water and describe reasonable minimum ion requirements in drinking water to protect consumers' health (WHO, 2017). Therefore, the WHO drinking water guideline values were used to compare nephrotoxic risk factors. Additionally, Sri Lankan drinking water standards were also considered because the standard values of Sri Lanka have been derived for the quality of drinking water in Sri Lankan conditions. General guidelines for classification of hard water [0.0 to 60.0 mg/L (milligrams per liter) as calcium carbonate as soft; 61.0 to 120.0 mg/L as moderately hard; 121.0 to 180.0 mg/L as hard; and more than 180.0 mg/L as very hard] derived by the United States Geological Survey (USGS, 2012) were considered to compare the hardness in groundwater.

3.1.3. Analytical methods used for nephrotoxic risk factors

The analytical methods used to analyse nephrotoxic (fluoride, hardness, and cadmium) and non-nephrotoxic (*E. coli*) risk factors throughout the study were described under section 3.1.3. Individual components were analysed using standard laboratory methods. Fluoride concentrations in water samples were analysed using Ion Chromatography (Metrohm, 930 Compact IC Flex, Switzerland) with a mobile phase of 3.2 mmol/L Na_2CO_3 + 1 mmol/L $NaHCO_3$ and a flow rate of 0.7 m L/min^{-1}. Hardness concentrations were analysed using the EDTA titrimetric method (USEPA Method No. 130.2). Cadmium concentration in the samples was analysed using Flame Atomic Absorption Spectroscopy (AAS: GBC 932 plus, Australia) with a minimum detection level of 0.25 mg/L of Cd and using Agilent® 7900 ICP-MS System, USA, with a minimum detection level of 0.001 mg/L of cadmium. Deionized water was used in all experiments. *E. coli* in water samples were analysed using multiple fermentation tube techniques (MPN method) (UNEP/WHO, 1986).

3.2. Objective 02: To evaluate the performance of commercially available domestic water purification techniques/systems/units to delineate their limitations and drawbacks

The nephrotoxic risk factors (fluoride and hardness) in potable water exceeded the drinking water guideline values (findings of objective 01). Different water filter units have been introduced in CKDu prevalent areas by government and non-governmental organizations to provide safe drinking water. A comprehensive study on available filter units, their types, removal mechanisms, removal effectiveness in removing nephrotoxic elements, overall performance, and O & M conditions were not conducted after introducing different water filter units. Therefore, objective 02 was designed to investigate the removal effectiveness of water filter units prominently used by people in CKDu prevalent areas. Firstly, water filter units were available commercially, and CKDu affected areas were identified. The water filter units introduced in CKDu affected areas were evaluated to identify their nephrotoxic risk factors' removal effectiveness.

3.2.1. Identification of commercially available domestic water purification systems

A survey with key informant interviews was conducted in the CKDu prevalent areas to identify the commercially available water purification systems. Several suppliers (10 businesses) were visited, and information (key informant interviews, focus group discussions, informal discussions were conducted) was collected relevant to such water purification systems. Suppliers/importers who retail domestic water purification systems to CKDu-affected areas were contacted to conduct key informant interviews to gather more information through leaflets, brochures, and other technical details about water treatment technologies. Several businesses that are the main dealers of water purification systems in CKDu prevalent areas were visited. Information on such products were obtained from brochures, leaflets, and manuals.

3.2.2. Identification of different water purification units in operation and abandoned

According to research justification, most CKDu prevalent areas depend on RO treated water for water consumption. No precise information was identified about different water treatment technologies available and water consumption pattern of people, their dependency on water treatment technologies, and the burden on finding clean water for drinking purposes all over the CKDu prevalent areas. As a preliminary study, a situation analysis was conducted using participatory rural appraisal tools (PRA) such as transect walks, field observations, focus group discussions and discussions with technical personnel in operation and maintenance (O & M) of commercial RO units. Moreover, a detailed household survey using a questionnaire (Appendix I) was conducted on randomly selected households (22 households from Thambalagollawa and 25 households from Palugasketuwewa) to identify different water purification units in operation and abandoned. Forty (40) domestic RO units installed were visited in Thambalagollawa and Palugasketuwewa at Anuradhapura district. The pros and cons of available water purification units, their present situation and people's perspectives on RO units were gathered and documented. Statistical packages of social sciences (IBM®

SPSS® 25) and Microsoft excel 2016 were used to analyse the descriptive statistics and summarise the data, respectively.

3.2.3. Chemical and physical characteristics of existing water purification units

The most popular and frequently used water treatment units in the Thambalagollawa and Palugasketuwewa in the Anuradhapura district were selected and studied in detail, their performance, adsorbent materials, and mechanisms of removal. Water filters are composed of different unit processes. Different components in unit processes of RO filters were studied by direct observations. The details of the unit processes and adsorbent materials used to fabricate the RO filters were reported in the literature. Hence, information on RO unit processes and their removal mechanisms were included in the literature review chapter (refer to section 2.6). The information relevant to two- and seven-layer filter units and their adsorbent materials used to remove water contaminants have not been reported in the literature in detail. Hence, the different adsorbents available in two- and seven-layer filters in CKDu prevalent areas were investigated through applying reverse engineering techniques such as dismantling the water purification units and analysing the materials consisted of the different layers. The samples of materials in two (top and bottom layers) and seven layers of two- and seven-layer filter units were ground separately to fine powder particles. The powdered particles were analysed using XRD, ESEM-EDAX, and FT–IR techniques to ascertain mineral composition in two and seven layers, elemental composition, surface morphology of materials in different layers, and their functional groups on the surface.

3.2.4. Removal of possible nephrotoxic risk factors by existing water purification units

The onset of monsoon seasons during a year in the Anuradhapura district was defined based on rainfall data. Rainfall data in the Anuradhapura district for a period of five years was obtained from the Department of Meteorology located in Sri Lanka (Figure 3.1). Twelve months in a year were divided into four distinctly different seasons. Different months during a year were demarcated as dry (March, May, and August,

Rainfall < 100 mm), extremely dry (June, and July, Rainfall < 50 mm), wet (January, February, April, and September, Rainfall > 100 mm), and extremely wet (October, November, December, Rainfall > 250 mm) months considering rainfall data.

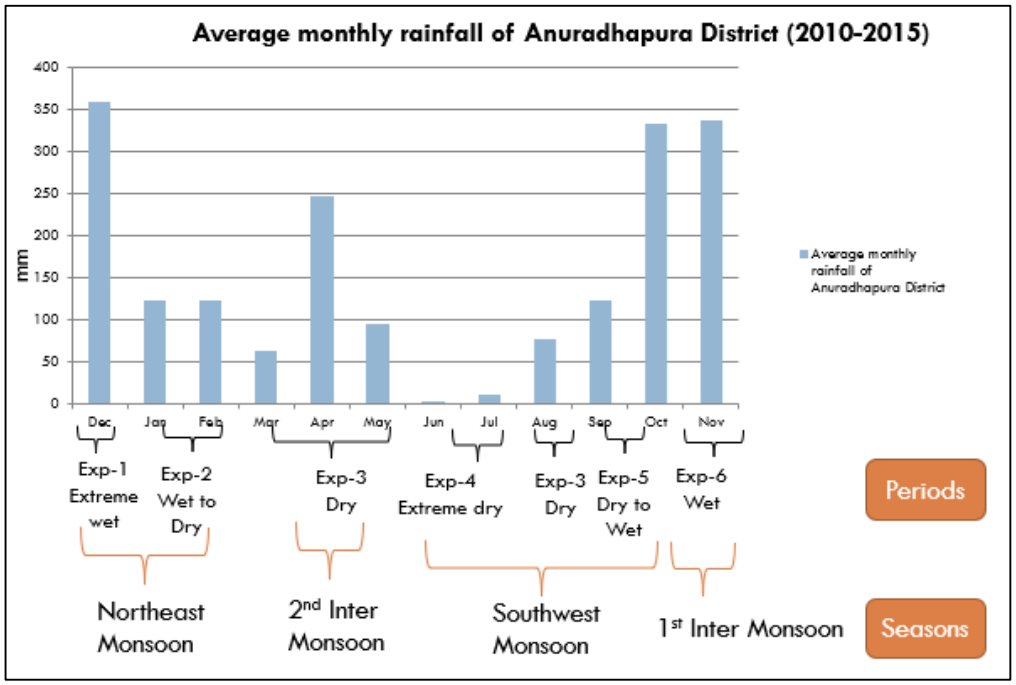

Figure 3.2: Rainfall distribution pattern in Anuradhapura district

Source: Department of Meteorology, Sri Lanka

Each season was subdivided into seven sections called “extreme wet, wet to dry, dry, extremely dry, dry, dry to wet and wet” based on the typical rainfall distribution pattern (Figure 3.2). Concentrations of fluoride, hardness, and cadmium were defined for each sub-period (Table 3.1). Fluoride (0.18–15.90 mg/L) and hardness (68.5–1921.0 mg/L) concentrations were decided according to the minimum and the maximum concentrations reported in CKDu prevalent areas. The cadmium concentration in CKDu prevalent areas was reported at trace levels. However, cadmium concentration was kept in feed water varied at 0.06–0.75 mg/L. The pH was maintained as 6.5–8.5 in the feed solution of filter units. The ambient temperature of 28ºC was assumed to be constant during the laboratory experiments. The laboratory experiments were conducted assuming that a person drinks 2.0 L of water per day, and a family in CKDu prevalent

areas consists of four members. The total drinking water requirement per day for a family was calculated as 8.0 L of treated water. The synthetic water sample of 8.0 L was fed into two-layer, and seven-layer filters. Both filters did not produce reject water. The RO unit was fed with 32.0 L of water considering the number of reject water and treated water volumes produced during the water treatment process according to the volume of feed water (ratio 4:1; feed: treated water).

Table 3.1: Different concentrations of nephrotoxic risk factors corresponding to different seasons

Periods in year	Fluoride (mg/L)	Hardness as $CaCO_3$ (mg/L)	Cadmium (mg/L)
Extreme Wet	0.50	100.00	0.06
Wet to Dry	3.00	500.00	0.10
Dry	7.00	1,000.00	0.50
Extreme Dry	15.00	1,500.00	0.75
Dry to Wet	5.00	750.00	0.25
Wet	2.00	300.00	0.10

A domestic RO (Rs. 53,000.00), a two-layer (Rs. 4,500.00), and seven-layer filter unit (Rs. 7,500.00) were purchased to conduct the laboratory experiments. Sodium chloride (ACS grade, high purity ≥ 99%, Sigma Aldrich), calcium carbonate (ACS grade, high purity ≥ 99%, Sigma Aldrich) and magnesium carbonate (ACS grade, high purity ≥ 99%, Sigma Aldrich), cadmium nitrate (ACS grade, high purity ≥ 99%, Sigma Aldrich) and distilled water were used to prepare the synthetic feed water samples (100.0 L in volume) at the laboratory. The feed water samples were passed through the RO, the two-layer, and the seven-layer water filters. Treated water samples were collected for time intervals defined for three (3) months until the filter units reached out of work. The treated water samples were analysed for fluoride, hardness, and cadmium to ascertain residual concentration in treated water. The removal effectiveness of each filter was investigated considering the reference levels of fluoride (< 0.2 mg/L) and hardness as $CaCO_3$ (< 120.0 mg/L (USGS), and cadmium (0.003 mg/L). One sample t-test was carried out to determine whether the experimental mean value of fluoride, hardness, and cadmium in the treated water is significantly different from the reference

levels considered in the study. The null hypothesis ($H_o = 1$, mean concentration values are equal to reference values; alternative hypothesis, $H_1 \neq 1$) of the study was considered to mean fluoride values, hardness, and cadmium equal to the reference levels considered.

3.2.5. Performance evaluation of existing water purification units

A multi-criteria analysis tool, including tangible key performance indicators, was performed to evaluate existing water treatment units (RO units, two-layer, and seven-layer filters) (Table 3.2). Indicators of performance evaluation were derived based on i) performance based on user responses at the questionnaire survey and direct observations and ii) performance based on the analytical experiments in the laboratory. Key performance indicators were formulated considering the SMART criteria, which stands for specific, measurable, attainable, relevant, and time-bound (Bovend'Eerdt et al., 2009). A checklist (Appendix II), including fourteen indicators, was designed to evaluate the performance of available water purification systems in CKDu prevalent areas. The first ten indicators were focused on technological suitability. The rest of the indicators were formulated to evaluate the filter units' removal effectiveness of possible nephrotoxic risk factors.

Table 3.2: List of key performance indicators in multi-criteria analysis

	Performance indicators	**RO unit**	**Clay water filter**	**Seven-layer filter**
	Performance-based on user response			
1	Does the filter unit treat water more than a daily requirement? (4 members x 2 L/day/person = 8 L/day)	-	-	-
2	Does the storage capacity of the filter provide treated water for several days?	-	-	-
3	Does the filter rate in the filters facilitate a supply of 0.25 L (1 cup) of treated water after emptying the storage tank?	-	-	-
4	Is the taste of the treated water palatable?	-	-	-

5	Is O & M easy to carry out? If yes, do you have enough technical know-how to conduct O & M?	-	-	-
6	Do filter media/ RO membrane have the properties of durability for the use of the long term?	-	-	-
7	Does slim layer formation on the surfaces of the filter unit occur while the filter unit is used?	-	-	-
8	Are facilities available for replacement of filter's parts enough to conduct O & M?	-	-	-
9	Are there any facilities available for the management of reject water?	-	-	-
10	Does clogging of the filter unit happen frequently, and the system gets often failed to operation?	-	-	-
	Performance-based on laboratory experiments			
11	Is treated water comply with 0.2 mg/L of fluoride?	-	-	-
12	Is treated water comply with 120 mg/L of hardness?	-	-	-
13	Is treated water comply with 0.003 mg/L of cadmium?	-	-	-
14	Is treated water comply with 0 CFU/100 mL of feacal coliform?	-	-	-

The limitations and drawbacks of filter units were ascertained to identify their inadequacy and incompetence capacity to treat CKDu prevalent areas' potable water. Scientific interpretation of what takes place inside these units was deduced, and the pros and cons of such units were identified further. Their effectiveness for long-term usage, people's perception of water quality produced by filters, and improvements to produce a new filter unit were studied in detail to determine future development requirements for a water filter unit.

3.3. Objective 03: To assess the health risk of people who consume potable water from such commercially available units in CKDu prevalent areas

CKDu affected and non-affected people consume RO treated water for daily water requirements. It was investigated that the RO filter unit removes beneficial micro and macronutrients in potable water. In some cases, high concentrations of nephrotoxic ions remained in the RO treated water during dry and arid seasons (refer to section 4.2.4). Unintentionally, people consume the RO treated water which contains higher concentrations of nephrotoxic elements. A risk assessment was not conducted previously to ascertain how RO treated water brings up non-carcinogenic health hazards to people in CKDu prevalent areas. Therefore, objective 03 was designed to investigate non-carcinogenic health hazards due to the RO treated water consumption using the risk assessment process. The components of risk analysis and management have been included; i) hazard identification (the source of danger), ii) exposure characterization (the type and form of hazard), iii) exposure assessment (the spatial and temporal extent of exposure), iv) risk characterization (the causal relationship between exposure and response) and v) risk management actions (actions to reduce or eliminate hazards).

3.3.1. Characterization of raw, treated and, rejected water in commercial RO unit

The removal effectiveness in removing fluoride and hardness was evaluated using a domestic RO filter unit in the laboratory experiment (refer to section 4.2.4). Different water quality parameters in commercial RO units in the Anuradhapura district were analyzed to investigate removal effectiveness. Water samples from RO units were collected from ten different locations during dry (six RO units) and wet spells (four RO units) (Two RO units were abandoned due to malfunctioned). The map in Figure 3.2 depicts ten different locations where RO water samples were collected. The sample collection during dry and wet seasons (Figure 3.2) was carried out to compare the variation of concentrations in dry and wet seasons and identify the removal effectiveness of RO filters during both seasons. The descriptive statistics of the water quality parameters were estimated to identify mean, minimum, and maximum values using

SPSS. Paired samples t-test was conducted to measure the significant difference in hardness, fluoride, calcium, magnesium, and cadmium during the dry and wet seasons before and after treatment. The mean values of hardness, fluoride, and cadmium before treatment are equal to the means values after treatment during the wet and dry season (null hypothesis $H_o = 1$, alternative hypothesis $H_1 \neq 1$, $p < 0.05$)

All water samples were analysed to determine water quality parameters, including hardness as $CaCO_3$ (mg/L)) [EDTA titrimetric method (USEPA Method No. 130.2)], alkalinity as $CaCO_3$ (mg/L) (2320, Alkalinity, APHA, 2017), total suspended solids (mg/L) (2540, Solid, APHA, 2017) fluoride (mg/L), (Ion Chromatography, Metrohm, 930 Compact IC Flex, Switzerland) with a mobile phase of 3.2 mmol/L Na_2CO_3 + 1 mmol/L $NaHCO_3$ and a flow rate of 0.7 mL/min), calcium (mg/L), and magnesium (mg/L) [EDTA titrimetric method (USEPA Method No. 130.2)], cadmium (mg/L) [Flame atomic absorption spectroscopy (AAS: GBC 932 plus, Australia)], pH (EUTECH pH 2700 meter, Thermo scientific eutech instruments, Netherlands), conductivity (Portable water quality meter pro-DSS, four-port, digital sampling system, Airmet Scientific, Australia) (µs/cm) and turbidity (NTU) (Portable water quality meter pro-DSS, four-port, digital sampling system, Airmet Scientific, Australia).

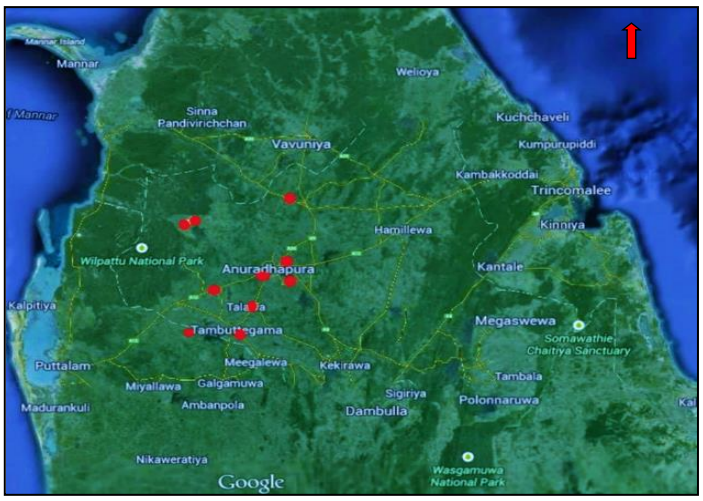

Figure 3.3: Locations of RO filter units selected for the study (Scale 1:20,000)

(Source: Google Map)

3.3.2. Health risk assessment - reactions nature of fluoride, calcium, magnesium (hardness), and cadmium in the human body

Types and nature of adverse health effects of fluoride, calcium, magnesium (hardness), and cadmium on humans were studied through a literature review. Reactions of different constituents in the human body from ingestion to kidney failure and fate of constituents in the human body were reviewed to identify how these constituents transfer to humans and how their mode of actions cause kidney failure. Schematic diagrams were then prepared to show how these nephrotoxic risk factors activated different organs in the human body.

3.3.3. Household survey for the assessment of exposure

A questionnaire survey (Appendix III) was conducted in Thambalagollawa Village, Anuradhapura District, in Sri Lanka. All information on demographic (family members, age, sex, occupation, income), geographic (water sources), lifestyle attributes, the number of RO units available in areas, consumption of RO treated water, and the way of exposure (ingestion) was collected. The daily intake of water, body weight of people, the average exposure time for the nephrotoxic risk factor, health-related information, and type of water usage were gathered during the questionnaire survey. The questionnaire survey was conducted with 22 households that depended on the RO treated water for their daily water requirements. Based on household samples, six groups of people such as 1–9, 10–19, 20–50, 51–70, 71–90, and 91<< years were categorized based on age distribution pattern to investigate their vulnerability non-carcinogenic health hazards. The average daily intake of drinking water and their body weight in kilograms for different age categories were considered for the risk assessment.

3.3.4. Health risk assessment due to the consumption of RO treated water

Health risk assessment due to water consumption treated by RO units was conducted following the method described in Figure 3.4. The main steps described in the USEPA

Guidelines for health risk assessment process were considered as follows (USEPA, 1992): for

- health hazard identification
- exposure assessment
- dose-response assessment and
- risk characterization

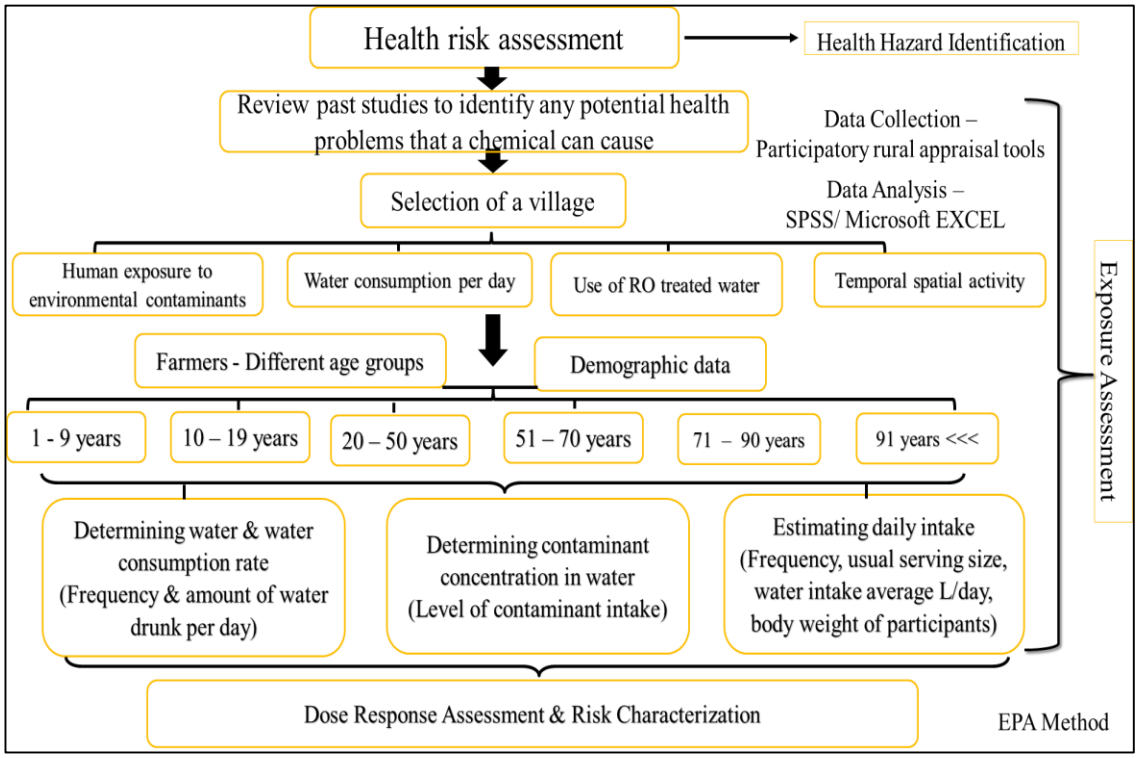

Figure 3.4: Steps followed for the risk assessment process for the consumption of RO treated water

Potential average dose ($AD_{potential}$) [Eq. (2)] was calculated using the concentrations data of RO treated water (the potential dose is simply the level of chemicals ingested), and health risk assessment was performed following the risk assessment process steps. The average values of RO treated water concentrations considered for fluoride, calcium,

magnesium (hardness), and cadmium illustrate in Table 3.3 based on the experimental results.

Table 3.3: Concentration of fluoride, calcium, magnesium (Hardness), and cadmium concentrations considered for the risk assessment

Scenario	Fluoride concentration in treated water (mg/L)	Calcium concentration in treated water (mg/L)	Magnesium concentration in treated water (mg/L)	Cadmium concentration in treated water (mg/L)
1	0.29	8.80	2.20	0.005
2	0.88	11.20	2.80	0.010
3	2.90	14.40	3.60	0.015
4	5.00	20.80	5.20	0.052

The average concentration value (*C*) of the fluoride, calcium, magnesium (Hardness), and cadmium were decided based on the results obtained from the laboratory experiments conducted using the domestic RO unit (refer to section 4.2.3) and characterization of commercial RO treated water (refer section 4.3.1). The intake rate (*IR*) of the process was considered a frequency of the event, such as cups of water consumed per day. The exposure duration was taken as an element in contact with the person ($t_2 - t_1$) (2 hours was considered exposure duration). The body weight (*BW*) of different age categories was estimated using the household survey, and average time (*AT*) was taken as one day to calculate the average potential daily dose.

$$AD_{(potential)} = \frac{\bar{C} \text{ X } \overline{IR} \text{ X EF X } ED}{(BW \text{ X } AT)} \quad (2)$$

where $AD_{(potential)}$ is the average daily potential dose (mg/kg/day), *C* is the average value for concentration (mg/L), *IR* is intake rate (L/day), EF - Exposure Frequency (days/Year), *ED* is exposure duration (day), *BW* is body weight (kg) and *AT* is time over which the dose is averaged (day).

The hazard quotient (HQ) [Eq. (3)] values for individual elements for hardness (calcium, magnesium), fluoride, and cadmium and hazard index (HI) values [Eq. (4)] the mixture of elements was calculated using actual health-based reference values. **HI, and HQ values greater than 1;** Exposure is the likelihood of adverse health effects or **HI and HQ values much lower than 1;** Exposure is unlikely to result in an adverse effect.

$$\text{Hazard quotient} = \frac{\text{Intake rate } (\text{mg}.\frac{\text{kg}}{\text{day}})}{\text{Reference level } (\text{mg}.\frac{\text{kg}}{\text{day}})} \quad (3)$$

$$\text{Hazard index of mixture contaminant} = \frac{\text{Intake Rate } (\frac{\text{mg.Kg}}{\text{day}})}{\text{Reference Level } (\frac{\text{mg.Kg}}{\text{day}})} \quad (4)$$

The descriptive statistics and analysis of variance (ANOVA) using the HQ and HI values were conducted for different age categories and concentrations values to identify the most vulnerable age category for non-carcinogenic health hazards and toxicity of the different concentration combinations. One-way ANOVA's null hypothesis has considered that mean HQ values of each age category are significantly equal ($H_o = 1$, $H_1 \neq 1$, $p<0.05$). One sample t-test was conducted to estimate the significant difference of the HQ, and HI values to identify values are either lower (HQ, HI < 1) or higher (HQ, HI > 1) than value HQ and HI value 1.

3.4. Objective 04: To investigate the applicability of the best combination of adsorbent materials in a multi-layered water purification unit capable of lessening the health impacts of selected nephrotoxic risk factors concerning ingestion of potable water in CKDu prevalent areas.

After identifying the requirement in removing nephrotoxic risk factors in potable water, different materials were chosen to remove hardness, fluoride, cadmium, and *E. coli* in the potable water. The materials selected were synthesised in the laboratory and characterised using different analytical techniques such as XRD, ESEM–EDAX, and FT–IR (See section 4.4.2). The batch adsorption studies were carried out using different materials to investigate their removal effectiveness. The experimental data best fitted to

adsorption isotherms and kinetics models. The best-performed materials were selected in removing hardness, fluoride, cadmium, and *E. coli*. The fixed-bed column studies (See section 4.4.3) were carried out i) single-layer with single-solute, ii) single-layer with multi-solute, to determine the adsorption behaviour. The experimental data were best fitted to adsorption isotherms and kinetics models. Finally, a multi-layered column (See section 4.4.8) was designed to remove hardness, fluoride, and faecal coliform in potable water. The design parameters and calculation of the cost of 1.0 L of treated water production were carried out.

3.4.1. Selection of different materials to remove nephrotoxic risk factors

Various materials such as modified fly ash [Zeolite (ZEOL)], graphene oxide (GO), iron oxide nanoparticles (FeONs), mesoporous Al_2O_3 (MESA), CaO loaded mesoporous alumina (COMA), MgO loaded mesoporous alumina (MOMA), nano-zerovalent iron (nZVI), titanium dioxide (TiO_2), nano silver oxide (SONPs), and SONPs + graphene oxide (GO) composite were synthesized in the laboratory. The potential for removing fluoride, hardness, cadmium, and *E. coli* were investigated to identify their long-term adsorption behaviour and disinfection potential, respectively. The adsorption potential of each material was evaluated under different scenarios in the presence of constituents of concern: (i) hardness alone; (ii) fluoride alone; (iii) fluoride in the presence of calcium; (v) cadmium alone; (vi) cadmium in the presence of calcium and (vii) faecal coliform. These scenarios were postulated in the experimental design combining the hypothesis considered for the study (fluoride, hardness, and cadmium are nephrotoxic risk factors; *E. coli* contribute to the water-borne diseases). The combinations of constituents such as fluoride, hardness, and cadmium have been suggested to exist of synergic effects, which increase the severity of the kidney damage (Wasana et al., 2017; Dharama-wardana, 2018). Therefore, materials that showed the best performance in removing fluoride, hardness, cadmium, and *E. coli* were chosen to investigate their long-term removal potential. The different materials such as modified fly ash (zeolite – ZEOL), graphene oxide (GO), nano iron oxide (FeONs), nano zerovalent iron (nZVI), mesoporous alumina (MESA), calcium oxide loaded mesoporous alumina (COMA), and magnesium

oxide loaded mesoporous alumina (MOMA) chosen to remove hardness, fluoride, and cadmium in potable water. The materials such as nano titanium dioxide (NTO), nano silver oxide (SONPs), and SONPs + GO were used to remove *E. coli* in potable water. These materials were synthesized and characterized in the laboratory. Adsorption studies were conducted to investigate their effectiveness in removing hardness, fluoride, cadmium, and *E. coli*. ZEOL (hardness), MOMA (fluoride), nZVI (cadmium), and SONPs + GO (*E. coli)* were investigated as the best-performed materials effectively and efficiently. Therefore, here onward, all laboratory experiments (synthesis and characterization of materials, desorption and regeneration studies, batch adsorption studies) were discussed based on the ZEOL, MOMA, nZVI, and SONPs + GO. For the purpose of comparison, analytical data of other material were used during the discussion.

3.4.2. Synthesis of selected materials

nZVI, MOMA, SNOPs + GO, and ZEOL were synthesized in the laboratory and characterised to investigate the removal potential of selected nephrotoxic risk factors. Materials were synthesised in the laboratory, and the synthesis processes are presented using schematic diagrams.

The materials used for the synthesis processes

High purity, Sigma Aldrich chemicals, and deionized water were used to synthesise each material. Iron(III) chloride hexahydrate, ACS reagent, 97.0-102.0%, ethanol, 99%, polyethyleneglycol MW- 20,000, sodium borohydride, ≥98.0%, stearic acid, analytical grade, 98.5%, aluminum nitrate nonahydrate, ACS reagent, ≥98%, triethanolamine, reagent grade, 98%, calcium nitrate tetrahydrate, ≥99.0%, magnesium nitrate hexahydrate, 99.9% trace metals basis, sodium nitrate, ACS reagent, ≥99.0%, sulfuric acid, ACS reagent, 95.0-98.0%, potassium permanganate, ACS reagent, ≥99.0%, hydrochloric acid, ACS reagent, 37%, hydrogen peroxide solution, ≥30%, for trace analysis, silver nitrate ACS reagent, ≥99.0%, sodium hydroxide ACS reagent, ≥97.0%, pellets, nitric acid ACS reagent, 70%.

(a) Synthesis of nano zero-valent iron (nZVI)

nZVI was synthesized in the laboratory using the method developed by Sun et al., 2006 with modification. The material used a 1:1 volume ratio of 0.2 M NaBH4 solution and 0.05 M $FeCl_3 \cdot 6H_2O$ under an oxygen-free environment. Anoxic conditions were maintained during the nZVI synthesis process; hence, N_2 was purged into the mixture. After the $NaBH_4$ solution (pH 11) was added completely, the slurry was vigorously mixed in the reactor for an additional 30 minutes. The iron particles were extracted from the slurry by centrifugation and washed with ethanol (~98 %) five times. The thin ethanol layer on the top of iron particles was maintained and stored in the refrigerator to preserve it from oxidation. Figure 3.5 & 3.6 depicts the flow chart and schematic diagram for the synthesis process of nZVI.

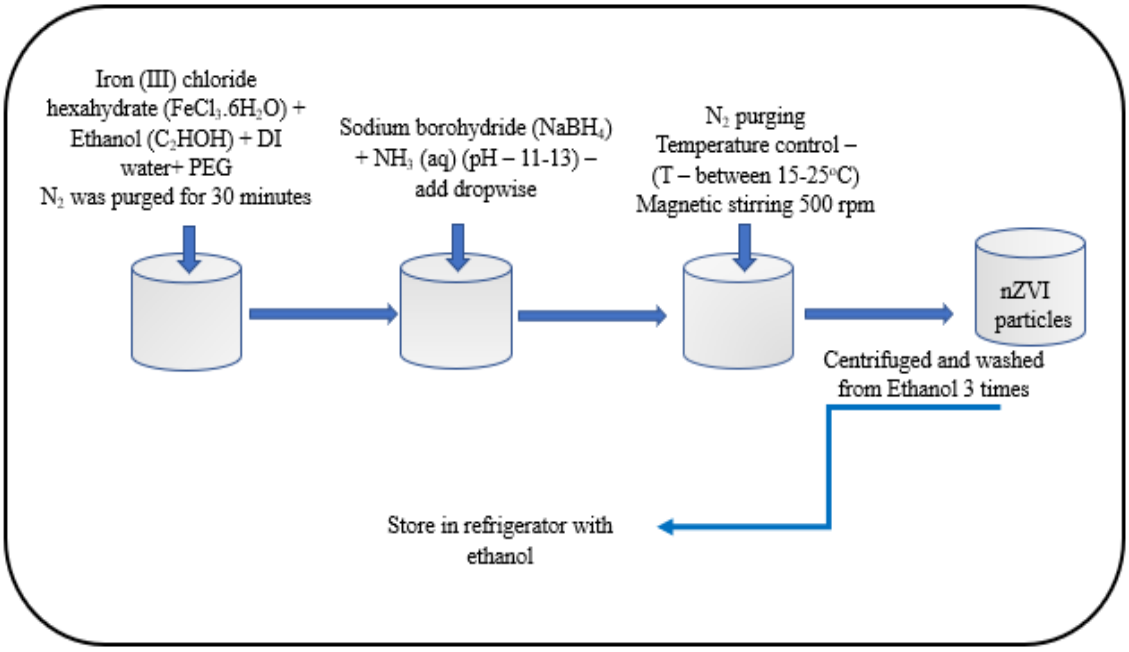

Figure 3.5: Schematic diagram for nZVI synthesis process

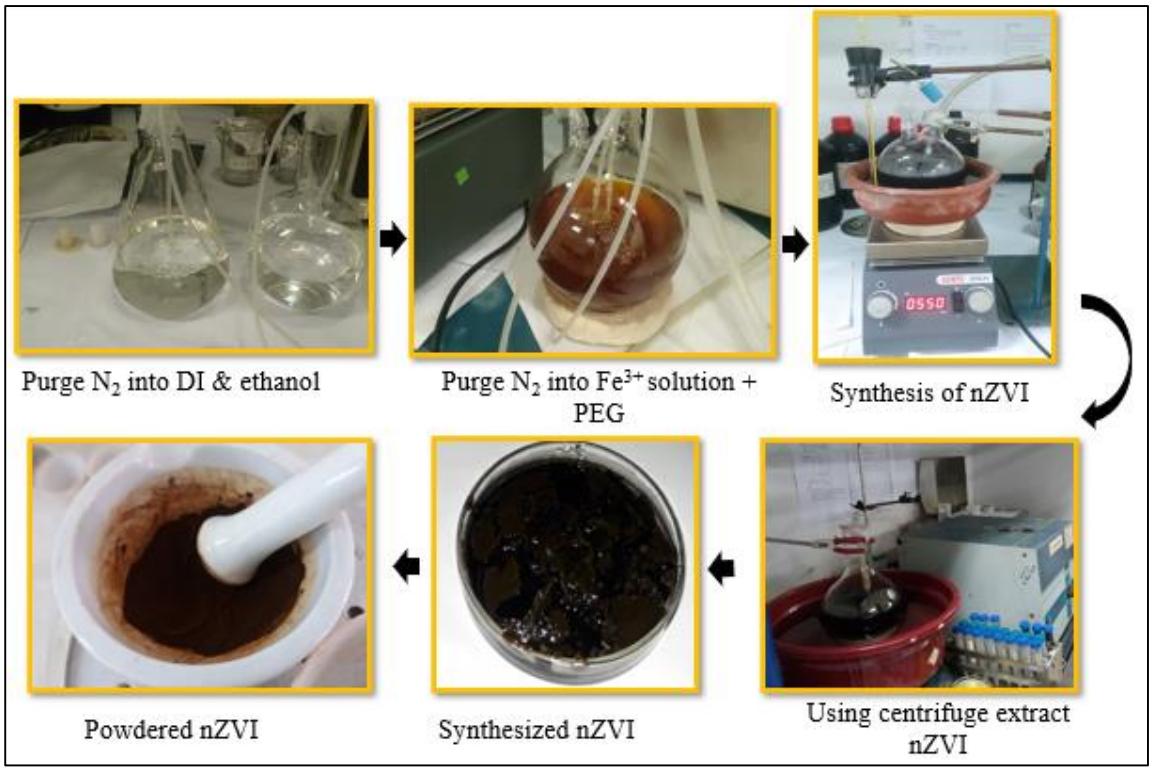

Figure 3.6: Steps for the nZVI synthesis process

(b) Synthesis of MgO loaded mesoporous alumina (MOMA)

Figures 3.7 & 3.8 illustrate the MOMA synthesis process using aluminium nitrate, stearic acid, and triethanolamine with modification of method followed by Dayananda et al. (2014) to synthesis CaO loaded mesoporous alumina. The ageing process in mixtures of chemicals in the middle of the synthesis process was the most crucial step to form mesoporous alumina (MESA). Then magnesium nitrate hexahydrate solution was introduced to the MESA and mechanically stirred for 24 hours. The calcination of the dried mixture was undergone at 550 ºC for 4 hours to obtain MOMA.

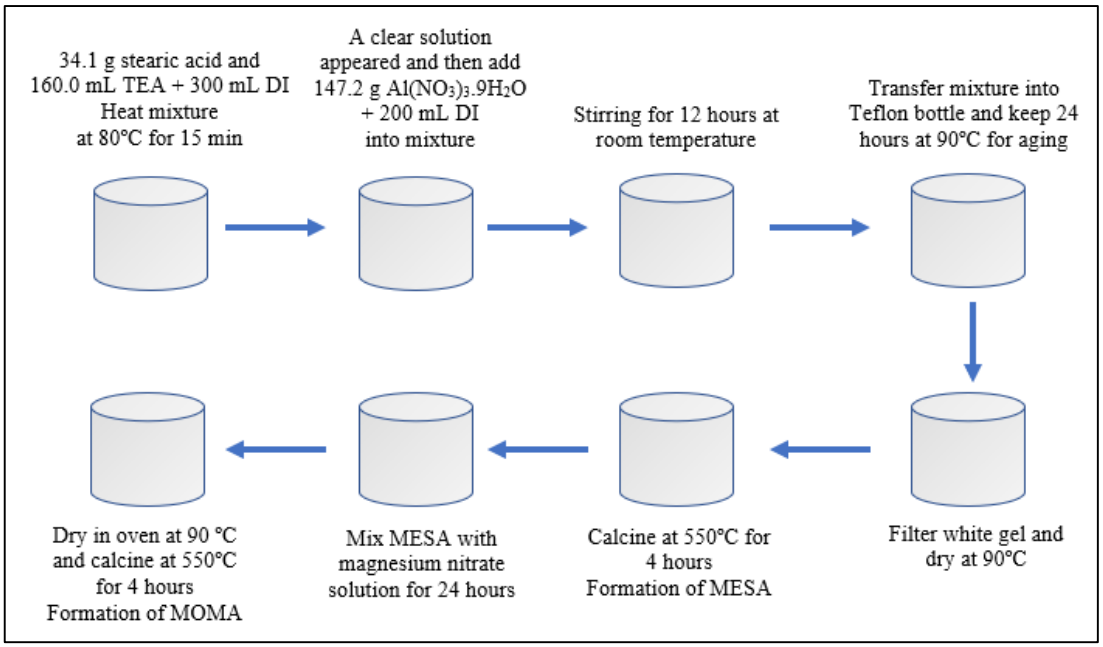

Figure 3.7: Schematic diagram of the MOMA synthesis process

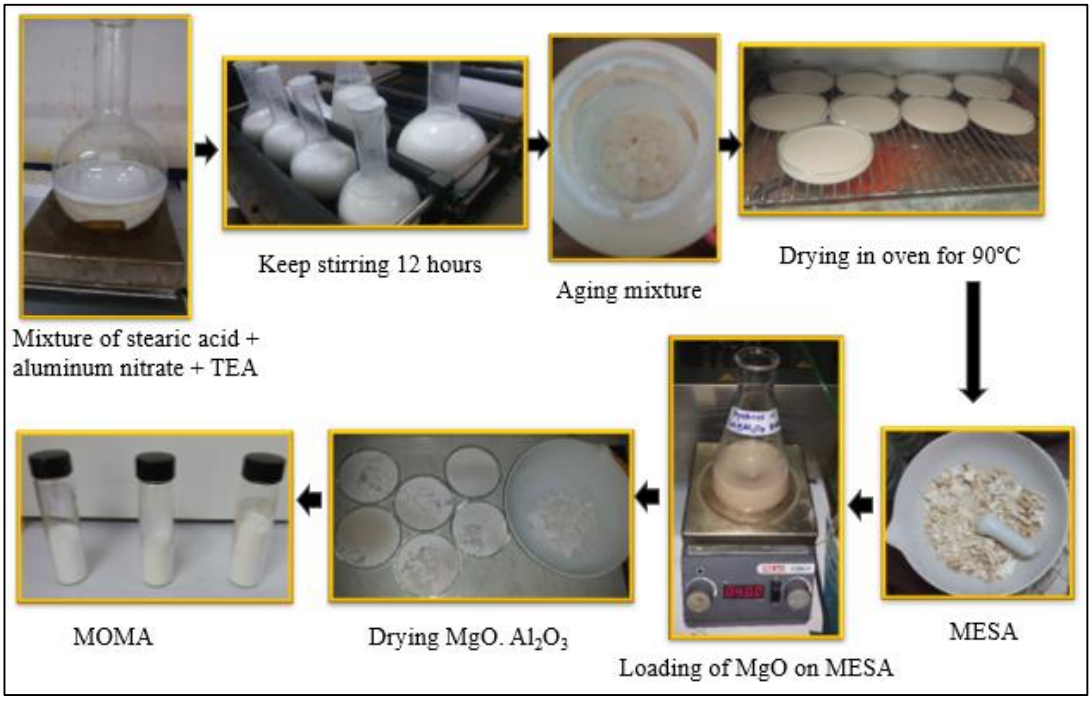

Figure 3.8: Steps for MOMA synthesis process

(c) Synthesis of graphene oxide using graphite flakes

The GO synthesis process's schematic diagrams using graphite flakes, $NaNO_3$, and sulphuric acid are presented in Figures 3.9 and 3.10. The improved Hummer's method published by Paulchamy et al., 2015, was used to synthesise GO with method modification. One of the most critical steps during the GO synthesis process was maintaining experimental temperature under 5 ºC. Otherwise, the reaction could cause an explosion while adding DI water to the mixture. Finally, the mixture's pH was adjusted to pH (pH 5.5–6.0) after washing with HCl and DI water, and brown coloured sol-gel was kept in an oven at 60 ºC for 24 hours to take dry powder of GO.

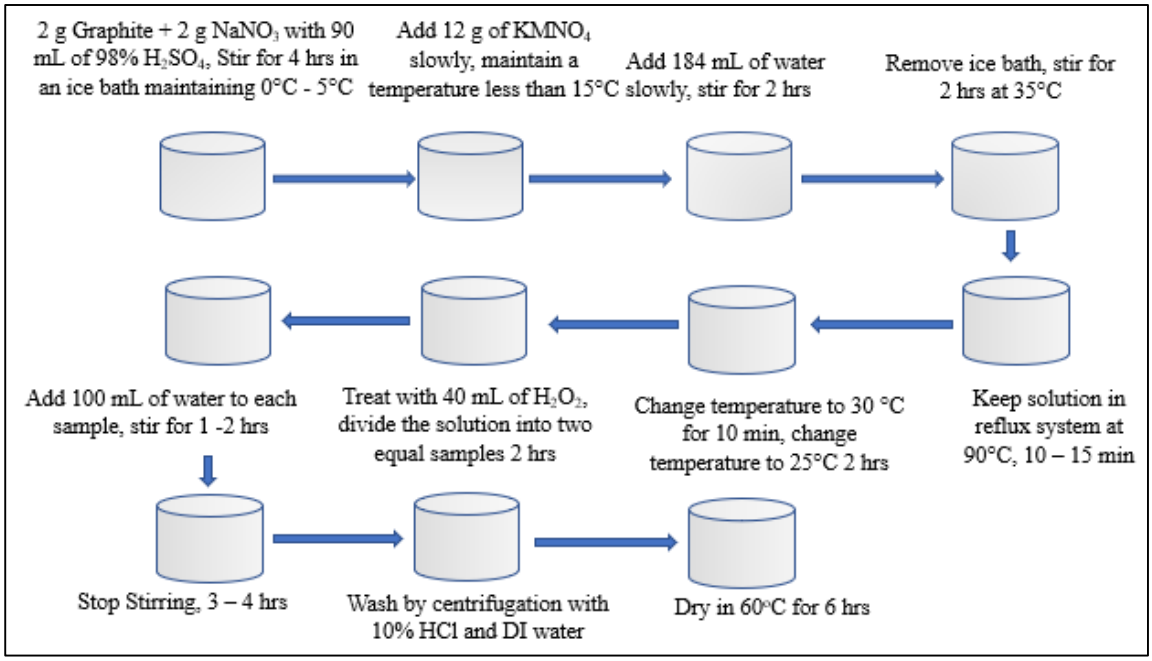

Figure 3.9: Schematic diagram of GO synthesis process

(d) Synthesis of silver oxide nanoparticles (SONPs) and SONPs + GO composite

The schematic diagrams of the synthesis process of SONPs in the laboratory illustrate in Figures 3.11 & 3.12. The synthesis process was simple, and the pH of the solution was maintained during the synthesis process. Controlling pH in the solution was a significant step that increases the formation of SONPs.

SONPs + GO composite was synthesized in 1:1, 1:2, 1:3; 2:1, and 3:1 ratio adding SONPs, GO, and 50 mL of methanol. The mixture of materials was constantly stirred on a magnetic stir for 24 hours. The mixtures were sonicated for two hours. The powder was washed and dried in an oven at 60 ºC. The batch experiments were performed with each SONPs + GO composite using 100.0 mL *E. coli* solution (1,800 CFU/100 mL) with 0.5 g of dosage for 24 hours contact time. After 24 hours, the MPN method was carried out to investigate the *E. coli* removal by different SONPs + GO ratios. The SONPs + GO in 2:1 ratio was identified as the best-performed composite. The material characterization, batch adsorption studies were discussed using the SONPs + GO in ratio 2:1.

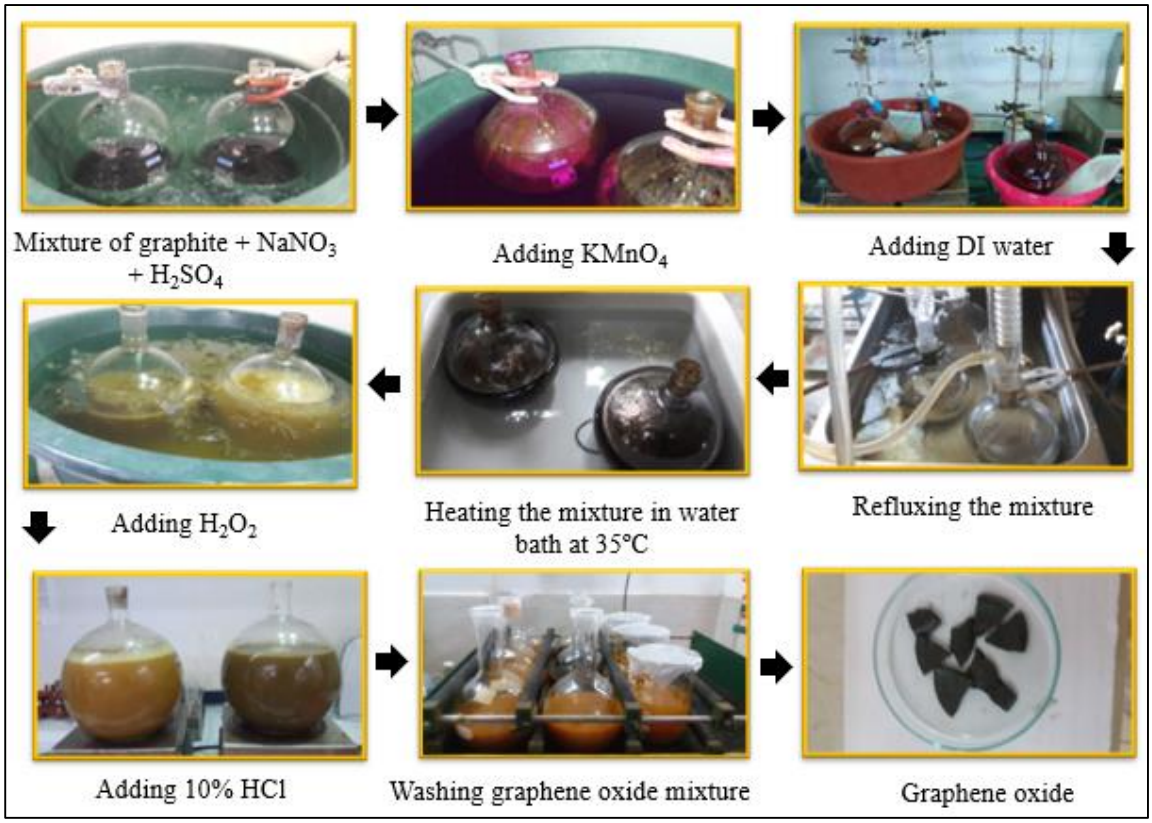

Figure 3.10: Steps for GO synthesis process

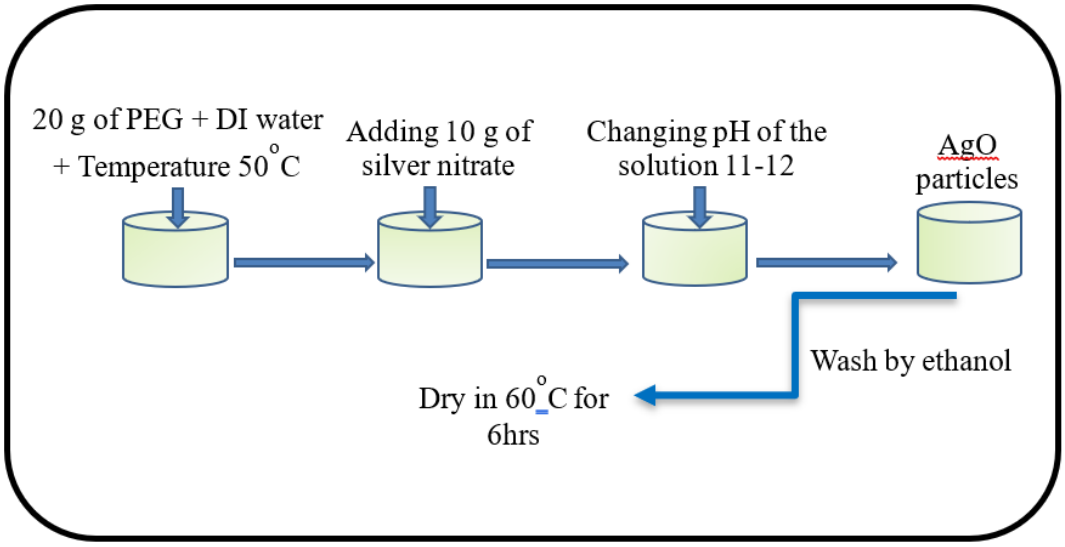

Figure 3.11: Schematic diagram for the process of SONPs synthesis

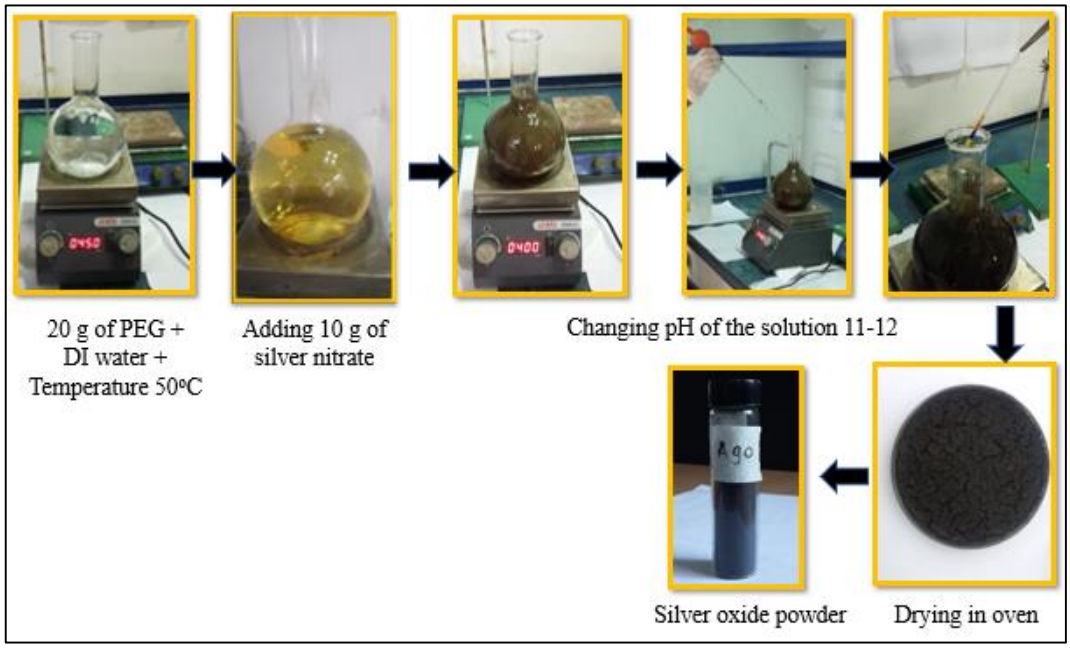

Figure 3.12: Steps for SONPs synthesis process

(e) Synthesis of modified fly ash [Zeolite (ZEOL)]

The schematic diagrams of the synthesis process of ZEOL from fly ash depict in Figures 3.13 & 3.14. The synthesis method of ZEOL published by Franus et al., 2014, was

followed with modification. The fly ash was collected from the coal power plant at Norochcholai. Fly ash is an industrial by-product used as a value-added product by transforming fly ash into ZEOL and removing hardness in potable water. The synthesis process was found as simple, however, time-consuming (96 hours). If the synthesis process can perform continuously, ZEOL can produce within four days. If the laboratory is furnished with a high-pressure autoclave, ZEOL can synthesize within 30 minutes. The time is taken to synthesis the process depends on the method followed to synthesize ZEOL. Proper maintenance of temperature and duration of refluxing was found as deterministic process parameters in ZEOL formation. Improper maintenance of temperature and refluxing time have increased the accumulation of solid and large-sized crumbs, challenging to crush as ZEOL powder.

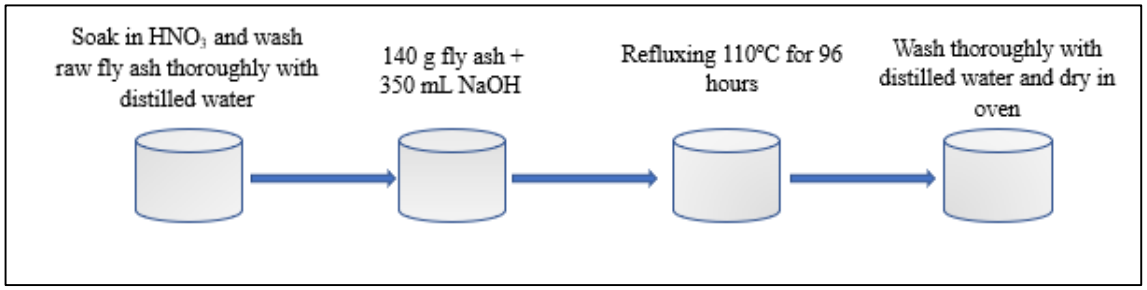

Figure 3.13: Schematic diagram for the synthesis process of ZEOL

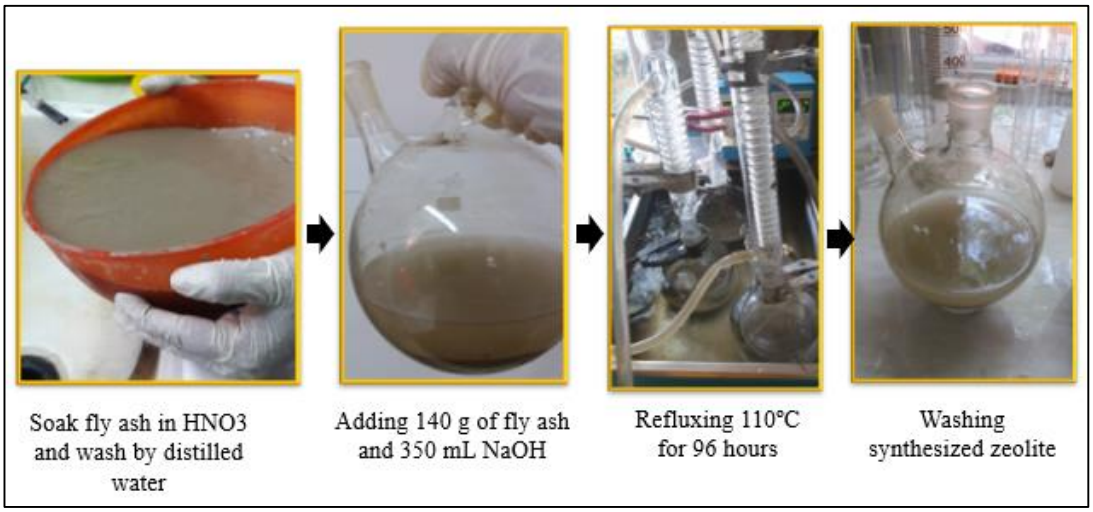

Figure 3.14: Steps for the ZEOL synthesis process

3.4.3. Characterisation of materials

Magnetic properties, surface oxidation, potential aggregation, and interaction with environmental elements of materials mainly depend on the adsorbent attributes such as particle size, shape, surface chemistry, surface charges, and bulk composition (Chekli et al., 2016). These properties change from time to time due to their reactive nature. Fine powder particles of nZVI, MOMA, GO, SONPs and ZEOL were characterized using ESEM-EDAX, XRD and FT–IR. The attributes of materials changed with time and storage conditions due to the reactive nature of materials. The description of analytical techniques and characteristics of materials measured were illustrated in Table 3.4.

Table 3.4: Different analytical techniques used to characterise materials

Analytical techniques	Characteristics of materials
Environmental Scanning Electron Microscopy (ESEM- Carl Zeiss, EVO 18, Secondary Electron Microscope, Germany) coupled with Energy-Dispersive X-ray Spectroscopy (EDAX Z1 analyser, USA)	Morphology of the material (size and shape) and surface elemental composition on the surface, were analysed before and after the batch adsorption experiments
X-ray Powder Diffraction (XRD-D8, ECO, Advance Bruker Diffractometer with filtered Cu Kα radiation, Germany), wavelength 1.54 Å, 10-80º range	Crystalline phase identification of each material
Fourier Transform-Infrared Spectroscopy (FT-IR, ALPHA Bruker, Germany) Adsorption mode in a spectral range of 400–4,000 cm^{-1} with KBr pellet	Identification of surface functional groups

3.4.4. Batch adsorption studies to remove nephrotoxic risk factors

Batch adsorption studies to determine the adsorption equilibrium state in single-solute and multi-solute conditions were conducted with the initial concentration of adsorbate, adsorbent dosage, contact time and solution pH. The experimental determination of a single-solute equilibrium state does not create interferences during the adsorption of other elements on the adsorbate's surface. The multi-solute equilibrium state produces interventions due to multi-elements in same system and multidimensional characteristics of equilibrium isotherms (Worch, 2012). Desorption and regeneration studies were carried out to investigate the reusable potential of the selected materials. The reusable potential of used adsorbents was studied by conducting batch studies on adsorption and desorption using the ZEOL, MOMA, nZVI, and SONPs + GO.

3.4.4.1. Single-solute studies

Single-solute batch experiments were carried out using different adsorbents to study the adsorption isotherms and kinetics (See Section 4.8.4). The adsorbent dosage, initial concentration, contact time, and solution pH were varied to determine optimum performance conditions in removing fluoride, hardness, and cadmium. Calcium represents a higher share in hardness compared to magnesium. Hence, during batch adsorption studies, only calcium ion was considered hard in water to avoid the study's complexity and minimise calcium and magnesium interference for the fluoride adsorption process. The contact time was one hour, the volume of the solution was 100 mL, the temperature was 28 ºC, the stirring speed was 150 rpm, and the initial solution pH was in the range of 5.5–6.5. The optimum adsorbent dosages in removing fluoride, hardness, and cadmium were determined using a range of adsorbent dosages with fixed initial concentrations. A series of batch experiments were then conducted to determine the isotherm and kinetic behaviour, the effect of the initial level, contact time, and solution pH in removing selected nephrotoxic risk factors. All other experimental conditions were maintained similarly to those in determining the optimum dosage.

In single-solute experiments, the adsorbed amount per unit mass of adsorbent in equilibrium (Q_e in mg/g) was calculated using a material balance equation (Eq. 5).

$$Q_e = (C_o - C_e) \times \frac{V}{M} \quad (5)$$

where C_o and C_e are initial and the equilibrium concentrations (mg/L), respectively, V is the volume of solution (L), and M is the mass of the adsorbent (g).

Experiment data were fitted to different mathematical models such as Langmuir [Eq. (6)], Freundlich [Eq. (8)], Brunauer-Emmett-Teller [Eq. (9)], Dubinin-Radushkevich [Eq. (10), (11) & (12)], and Temkin [Eq. (13) & (14)]. The experimental data were fitted to pseudo-first order [Eq. (15)] and pseudo second order [Eq. (16)] kinetic models.

(a) Effects of nZVI dosage, contact time, initial concentration, and solution pH

Single-solute batch-mode experiments were carried out using nZVI to study the cadmium and calcium removal effectiveness. The nZVI dosage was varied from 0.4 to 8.0 g/L to determine optimum dosage in removing cadmium and calcium with the volume of 100.0 mL each for a contact time of 1.0 hour, with the initial concentration of cadmium and calcium being 0.06 and 300.00 mg/L, maintaining the pH at 6.5, the temperature at 28 ºC, and the stirring speed of 150.0 rpm. The optimum nZVI dosage in removing cadmium and calcium were determined as 4.0 g-nZVI/L, respectively. Consequently, a series of batch experiments were conducted using optimum nZVI dosages of 4.0 g-nZVI/L and varying the initial concentrations of cadmium and calcium from 1.0–25.0 mg/L and 100.0–400.0 mg/L to determine the isotherm and kinetic behaviour. The cadmium and calcium solution's pH were changed from 3.0 to 10.0 to investigate removal effectiveness with solution pH change. All experiments were conducted in 100.0 mL, and other parameters were maintained the same as mentioned above, and experiments were replicated twice.

(b) Effects of MOMA dosage, contact time, initial concentration, and solution pH

Single-solute batch-mode experiments were carried out using MOMA to study the fluoride and calcium removal effectiveness. The MOMA dosage was varied from 0.2 to 5.2 g/L to determine optimum dosage in removing fluoride and calcium, with the volume of 100.0 mL, the contact time of 1 hour, the initial concentration of fluoride and calcium being 3.0 and 300.0 mg/L, the pH at 6.5, the temperature at 28 ºC, and the stirring speed of 150.0 rpm. The optimum MOMA dosage in removing fluoride and calcium were determined as 1.2 g- MOMA /L, respectively. A series of batch experiments were conducted using optimum MOMA dosages of 1.2 g- MOMA /L and varying the initial fluoride and calcium concentrations from 1.0–13.0 mg/L and 100.0–400.0 mg/L to determine the isotherm and kinetic behaviour. The pH of the fluoride and calcium solution was changed from 3.0 to 10.0 to investigate removal effectiveness. All experiments were conducted in 100.0 mL, and other parameters were maintained the same as mentioned above, and experiments were replicated twice.

(c) Effects of ZEOL dosage, contact time, initial concentration, and solution pH

Single-solute batch-mode experiments were carried out using ZEOL to study the hardness and fluoride removal effectiveness. The ZEOL dosage was varied from 4.0 to 32.0 g/L to determine optimum dosage in removing hardness and fluoride, with the volume of 100.0 mL, the contact time of 1.0 hour, the initial concentration of hardness and fluoride being 300.0 and 3.0 mg/L, maintaining the pH at 6.5, the temperature at 28 ºC, and the stirring speed of 150.0 rpm. The optimum ZEOL dosage in removing hardness and fluoride was 4.8 g- ZEOL /L, respectively. A series of batch experiments were conducted using optimum ZEOL dosages of 4.8 g- ZEOL /L and varying the initial concentrations of hardness and fluoride from 50.0–1,000.0 mg/L and 1.0–10.0 mg/L to determine the isotherm and kinetic behaviour. The hardness and fluoride solution's pH were changed from 3.0 to 10.0 to investigate removal effectiveness with solution pH change. All experiments were conducted in 100.0 mL, and other parameters were maintained the same as mentioned above, and experiments were replicated twice.

(d) Mathematical models in single-solute batch studies

The Langmuir model was used to study the removal mechanisms of the nephrotoxic risk factors. The amount of adsorbate per unit weight of adsorbent adsorbed was calculated for the equilibrium state. The model assumes that monolayer adsorption occurs with no interaction between adjacent adsorbed ions. The adsorbent surface is homogeneous with the same adsorption sites, and adsorbate ions tend to either adsorb or desorb. Langmuir model (Langmuir, 1918) is presented in Eq. 6:

$$\frac{1}{Q_e} = \frac{1}{Q_m} + \frac{1}{Q_m K_L C_e} \quad (6)$$

where C_e is the equilibrium concentration of adsorbate (mg/L), Q_e is the amount of adsorbate adsorbed per unit mass of adsorbent at equilibrium (mg/g), Q_m is maximum monolayer coverage capacity (mg/g), and K_L is Langmuir isotherm constant (L/mg). The Langmuir model's essential characteristics can be described using a dimensionless constant separation factor or equilibrium parameter, R_L shows in Eq. 7, where C_o is the initial concentration (mg/L), and K_L is Langmuir isotherm constant. R_L value reads the adsorption mechanisms, which is unfavorable ($R_L > 1$), linear ($R_L = 1$), favorable ($0 < R_L > 1$), or irreversible ($R_L = 0$) (Weber and Chakravorti 1974).

$$R_L = \frac{1}{[\,1 + (1 + K_L C_o)]} \quad (7)$$

Freundlich model was used to study the adsorption characteristics in removing nephrotoxic risk factors, assuming the heterogeneous surfaces where adsorbed ions form multi-layer and interact with each other. Freundlich model (Freundlich 1906) is given by Eq. 8:

$$\ln Q_e = ln\, K_f + \frac{1}{n}\,(ln\, C_e) \quad (8)$$

where K_f is the Freundlich isotherm constant (mg/g), n is the adsorption intensity, C_e is the equilibrium concentration of adsorbate (mg/L), and Q_e is the amount of adsorbate adsorbed per gram of the adsorbent at equilibrium (mg/g). The Freundlich constant (n)

describes the adsorption mechanism (when $2 < n < 10$, adsorption is favorable, between $1 < n < 2$ moderately difficult and $n < 1$ poor adsorption) (Kakavandi et al. 2013).

Brunauer-Emmett-Teller (BET) adsorption isotherm model describes that adsorption forms multilayers and no interaction among adsorbed ions. The BET model describes the adsorption of multiple ions in each site. Moreover, energetically homogeneous adsorption sites appear on the adsorbent's surface with no adsorbed ions interactions between neighbouring ions and the stasis of adsorbed ions. The BET model (Brunauer et al. 1938) is given by Eq. 9:

$$\left[\frac{C_e}{(C_s - C_e) \times Q_e}\right] = \left(\frac{K_B - 1}{K_B \times Q_o}\right) \times \frac{C_e}{C_s} + \frac{1}{(K_B Q_o)} \quad (9)$$

where C_e is the equilibrium concentration (mg/L), C_s is adsorbate monolayer saturation concentration (mg/L), Q_o is maximum adsorption capacity for forming single layers (mg/g), and K_B is BET adsorption isotherm constant (L/mg).

Dubinin-Radushkevich model was applied to describe the adsorption mechanism by Gaussian energy distribution onto a heterogeneous surface. The model distinguishes adsorption mechanisms such as chemisorption and physisorption (Dubinin, 1959). The model is given by Eq. 10:

$$ln\ Q_e = ln\ Q_d - B_D \varepsilon^2 \quad (10)$$

where Q_e is the amount of adsorbate on the adsorbent at equilibrium (mg/g), Q_d is theoretical isotherm saturation capacity (mg/g), B_D is Dubinin-Radushkevich constant (mol^2/kJ^2), ε - potential energy (Eq. 11). E is the Dubinin-Radushkevich isotherm constant (kJ/mol) (Eq. 12). Physisorption will occur if $E < 8$ kJ/mol, chemisorption will occur if $8 < E < 16$ kJ/mol and ion exchange are likely occurred if $E > 16$ kJ/mol.

$$\varepsilon = RT \ln \left[1 + \left(\frac{1}{C_e}\right)\right] \quad (11)$$

$$E = \frac{1}{\sqrt{2 B_D}} \quad (12)$$

Temkin isotherm model, which considers adsorbent-adsorbate interactions. The model assumes that all molecules' heat of adsorption in the layer decreases linearly rather than logarithmic with coverage. The equation describes the uniform distribution of binding energy. The Temkin model (Tempkin and Pyzhev, 1940) is given by Eqs. 13 and 14:

$$Q_e = \left(\frac{R_L}{b}\right) \ln A_T + \left(\frac{R_L}{b}\right) \ln C_e \quad (13)$$

$$B = \left(\frac{R_T}{b}\right) \quad (14)$$

where A_T is Temkin isotherm equilibrium binding constant (L/g), b is Temkin isotherm constant, R is the universal gas constant (8.314 J/mol/K), T is the temperature (K), and B is constant related to the heat of sorption (J/mol).

Kinetics parameters of adsorption were determined using Lagergren's pseudo-first-order model (Lagergren, 1898) (Eq, 15), which describes the intraparticle diffusion rate-limiting factor promoting the physical sorption or physisorption. The pseudo-second-order model (Eq. 16) assumed that the rate-limiting factor is chemical sorption or chemisorption, which involves valency forces by sharing or exchanging electrons between adsorbate and adsorbent (Ho and McKay, 1999). These two models represent the kinetics of adsorption processes that fit best either chemisorption or physisorption.

$$\left(Q_e - Q_t\right) = log\, Q_e - \left(\frac{K_1}{2.303}\right) t \quad (15)$$

$$\frac{t}{Q_t} = \frac{1}{\left[K_2 \left(Q_e\right)^2\right]} + \left(\frac{1}{Q_e}\right) t \quad (16)$$

where Q_e is the amount of adsorbate adsorbed on adsorbent (mg/g) at equilibrium, Q_t is the amount of adsorbate adsorbed on adsorbent (mg/g) at time t (minutes), K_1 is rate constant (min^{-1}) for pseudo-first-order kinetics, and K_2 is rate constant (gm/g/ min) for pseudo-second-order kinetics.

3.4.4.2. Multi-solute studies

The multi-solute experiments were carried out to investigate the competitive adsorption of different adsorbates in the multi-solute solution. Each experiment's calcium concentration with different materials was decided based on the calcium concentration range (50.0–1,000.0 mg/L), where the materials were best performed.

(a) Effects of nZVI dosage and initial concentration

The optimum adsorbent dosage to remove cadmium in calcium presence was investigated using a range of adsorbent dosages (0.4–8.0 g/L). The initial concentrations of selected nephrotoxic risk factors were kept constant (0.06 mg/L of cadmium and 300.63 mg/L of calcium). The contact time was two hours, the volume of 100.0 mL, the temperature of 28 ºC, the initial solution pH 5.5, and the stirring speed of 150.0 rpm was maintained. The initial concentration effects were determined using concentration combinations of cadmium (1.0–15.39 mg/L) and calcium (80.6–344.4 mg/L). Experimental data were fitted with the ideal adsorbed solution theory (IAST) [Eq. (19), (20), (21), and (22)].

(b) Effects of MOMA dosage and initial concentration

The optimum adsorbent dosage to remove fluoride in calcium presence was determined using a range of adsorbent dosages (0.3 – 10.0 g/L). The initial concentrations of selected nephrotoxic risk factors were constant (4.9 mg/L of fluoride and 304.0 mg/L of calcium). Simultaneously, the contact time was two hours, the volume of solution 100.0 mL, the temperature 28ºC, the initial solution pH 6.5, and the stirring speed 150.0 rpm were maintained. The effects of initial concentration were determined using concentration combinations of fluoride (1.4–13.3 mg/L) and calcium (100.0 – 1,000.0 mg/L). Fluoride and calcium concentration values were decided based on fluoride concentrations and hardness reported in the literature.

(c) Effects of ZEOL dosage and initial concentration

The optimum adsorbent dosage to remove hardness in fluoride presence was determined using a range of adsorbent dosages (4.0 – 32.0 g/L). The initial concentrations of selected nephrotoxic risk factors were kept constant (3.0 mg/L of fluoride and 500.0 mg/L of calcium). Simultaneously, the contact time was two hours, the volume of solution was 100.0 mL, the temperature was 28 ºC, the initial solution pH was 6.5, and the stirring speed was 150.0 rpm. The effects of initial concentration were determined using concentration combinations of fluoride (0.9–10.2 mg/L) and hardness (100.0 – 1,000.0 mg/L). Fluoride and hardness concentration values were decided based on different fluoride concentrations and hardness reported in the literature.

(d) Mathematical models adopted for multi-solute batch studies

The ideal adsorbed solution theory (IAST) was used to determine multi-solution adsorption using single-solute adsorption isotherm and kinetic parameters (Radke and Prausnitz, 1972). The adsorption data described by different isotherm models in single-solute studies can apply to the IAST model when the adsorbate is a multi-solute solution. The IAST considers the following conditions; the adsorbed phase is regarded as a two-dimensional layer, which is in equilibrium with the liquid phase, both the liquid phase and the adsorbed phase show ideal phase (no interaction occur between the adsorbate molecules), the adsorbent surface is accessible to all adsorbates in equal measure, to consider the adsorbed phase, the Gibbs fundamental equation is extended by the product of surface area as extensive variables, and spreading pressure as intensive variables. The required parameters were estimated using following a set of Eqs. 17, 18, 19, and 20:

$$\psi_i = \frac{Q_{m,\ i}}{n_i}\left[1 + b_i \left(C_i^0\right)^{n_i}\right] \tag{17}$$

$$\sum_{i=1}^{N} Z_i = \sum_{i=1}^{N} \frac{C_i b_i^{\frac{1}{ni}}}{\left[exp\left(\frac{n_i \psi}{Q_{m,\ i}}\right) - 1\right]^{\frac{1}{ni}}} = 1 \tag{18}$$

$$Q_T = \left[\sum_{i=1}^{N} \frac{Z_i}{Q_{m,\,i}\left[1 - \exp\left(-\frac{n_i \psi}{Q_{m,\,i}}\right)\right]} \right]^{-1} \quad (19)$$

$$Q_i = Z_i Q_T \quad (20)$$

where ψ_i is spreading pressure; $Q_{m,\,i}$ is adsorption capacities of adsorbates at equilibrium under single-solute study (mg/g); b_i is Langmuir isotherm constants for adsorbates under single-solute study (L/mg), and n_i is the value of the Freundlich exponent; C_i^o is the equilibrium concentration of component i that causes in single-solute adsorption; C_i is the equilibrium concentration of component i in the multi-adsorbate solution (mg/L); Z_i is the mole fraction of component i in the adsorbed phase; Q_T is total adsorbed amount during multi-solute adsorption (mg/g); Q_i is partial adsorption loading of each element in multi-solute adsorption (mg/g), respectively.

3.4.5. Inhibition of faecal coliform in potable water using nanomaterials

The diffusion pattern of SONPs through the nutrient agar was studied with the different SONPs dosages in a range of 0.1–1.2 g/L. A range of SONPs dosages that effectively inhibit bacterial growth was determined as a range of 0.004 to 4.000 g/L. Cotton pellets were used to place the different dosages of SONPs in the middle of the Petri dishes, which contained nutrient agar. Three replications were practised to increase the accuracy of the experiments. The diameters of the distribution zone were measured using a Vernier Caliper, and the mean values of the diameters were calculated. SONPs are challenging to use as individual material because small particles of SONPs can leach out from the filters. Impregnation of SONPs with GO was practised being avoided the leachability of SONPs from the media. The composite of SONPs and GO was synthesized, and the laboratory experiments were conducted to investigate the bacterial inhibition potential of SONPs + GO using the inhibition zone, well-diffusion method, and broth dilusion method (Figure 3.15).

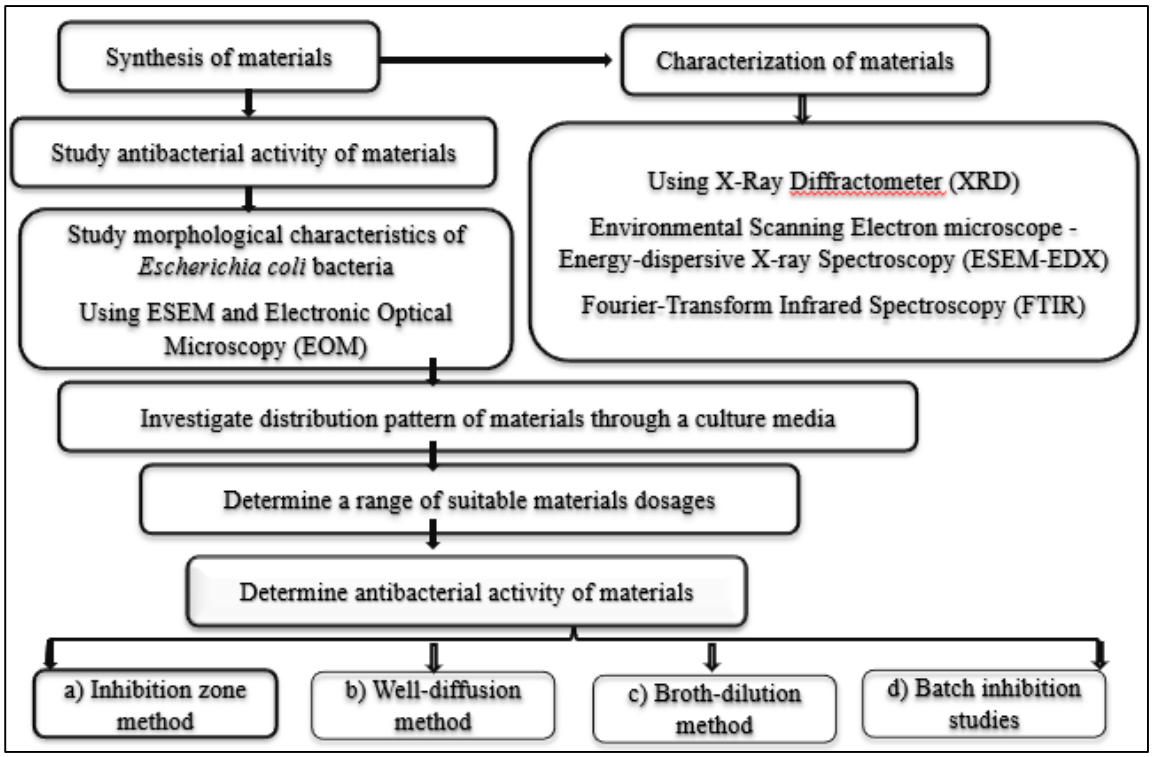

Figure 3.15: Road map for the laboratory experiments in removing *E. coli* in potable water

(a) Investigation of a range of suitable SONPs + GO dosage using the inhibition zone method

Suitable SONPs + GO dosage to inhibit the growth of *E. coli* bacteria was investigated using the inhibition zone method. Petri dishes with 10 mL of selective agar were prepared using the standard laboratory method. SONPs + GO dosage (0.001 g – 1.0 g) was added into the middle of each petri dish and observed the growth inhibition zone formation. The petri dishes were inoculated by *E. coli* suspension (3 X 10^4 CFU/100 mL) at the sterilized laboratory environment using the standard methods. Petri dishes which were contained SONPs + GO and *E. coli* bacteria were incubated at 44 ºC, and diameters of growth inhibition zone were measured using a Vernier calliper for different time series (1 hour to 120 hours) (Figure 4.39). Three replications were carried out, and the mean diameter was calculated. The data were statistically compared using t-test.

(b) Investigation of growth inhibition of *E coli* using the well-diffusion method

The disinfection potential of SONPs + GO was determined using the well-diffusion method with a range of SONPs + GO dosage from 0.02 to 0.08 g. Petri dishes were prepared with 10.0 mL of HiCrome *E. coli* selective culture media.

The volume (0.1 mL) of *E. coli* bacterial suspension (3 X 10^4 CFU/100 mL) was evenly distributed on the surface of semi-solidified culture media. With a diameter of 11.35 mm in size, Wells were dug in the middle of the petri dishes. A range of SONPs + GO dosages (0.02 g – 0.08 g) was placed in the well excavated at the middle of petri dishes and added few drops of the sterilized distilled water to enrich the dispersion of SONPs + GO particles through the culture media.

Petri dishes were incubated at 44 ºC, and the diameter of the inhibition zones was measured using a Vernier calliper for different time series (24 hours to 120 hours). The experiments were conducted with three replications, including control, and the mean value of the growth inhibition zone was calculated.

(c) Investigation of *E. coli* disinfection potential using broth-dilution (Optical density) method

The kinetics of bacterial growth inhibition was observed using the broth-dilution method with a range of SONPs + GO dosage (0.01 g – 0.09 g). Test tubes were prepared, adding 10.0 mL of MacConkey broth culture media, and sterilized to avoid contamination from wild microorganism species in the atmosphere. Range of SONPs + GO dosage was introduced, and at the same time, the volume (1.0 mL) of *E. coli* suspension (3 X 10^4 CFU/100 mL) was added into each test tubes. The series of experiments were conducted with three replications and the control. The sample's optical density was analyzed using wavelength 600 nm in UV/Vis spectrophotometer (UV-1900i, SHIMADZU, USA) for the time series of 1 to 120 hours. The growth inhibition of the bacteria was calculated using the equation: % of growth inhibition = $[(O_{Dc} – O_{dt})/O_{Dc}$ X 100]; where O_{Dc} and

O_{Dt} represent the optical density of control and test samples of SONPs + GO, respectively.

(d) Investigation of *E. coli* disinfection potential using batch studies

The SONPs and the GO composite were prepared at a 2:1 weight to weight ratio after identifying the disinfection potential of SONPs. The effects of SONPs and GO composite dosage to remove *E. coli* in water were determined by varying dosage from 0.4 g/L to 8. 0 g/L in 1,600.0 CFU/100.0 mL solution, pH of 6.5, contact time 24 hours, and 150 rpm stirring speed. After 24 hours, the filtered sample was inoculated to MacConkey broth culture media (MPN method) to determine the *E. coli* removal capacity of SONPs and GO composite. *E. coli* bacteria was used as an indicator organism to conduct the study. *E. coli* bacteria was extracted from MPN presumptive test's positive samples using Brilliance ^{TM} *E. coli*/coliform selective agar.

3.4.6. Desorption and regeneration studies

Batch adsorption-desorption studies were carried out to evaluate different adsorbents' desorption and regeneration potential in removing selected nephrotoxic risk factors. In this study, the optimum adsorbent dosages were introduced to the solution, which contained fluoride (3.0 mg/L, 1.2 g-MOMA/L), hardness (300.0 mg/L, 4.8 g-ZEOL/L), cadmium (0.06 mg/L, 4.0 g-nZVI/L) concentrations, and *E. coli* (1800 CFU/ 100 mL, 4.0 g-SONPs + GO/L) separately, the volume of the aqueous solution was taken as 100.0 mL, the contact time of two hours, the temperature at 28 ºC. The stirring speed was set at 150.0 rpm. Then, the aqueous solution was filtered and analysed for the residual concentration in the solution. The adsorbents used to adsorbate in the solution were collected, and the eluting agents were introduced to conduct the desorption studies. The desorption studies were conducted using adsorbate adsorbed adsorbents with three different eluting agents: 0.2 M Sodium hydroxide (NaOH) (pH 10), 0.001 M Hydrochloric acid (HCL) (pH 4), and 0.01 M Ethylenediamine tetra-acetic acid (*EDTA*) (pH 7). Different pH in eluting solution has been reported to enhancing the stripping efficiency of adsorbed ions on the surface of adsorbent (Lata et al., 2015). Hence,

eluting agents in three different pH values were chosen for regeneration studies. The EDTA was selected as an eluting agent due to its chelating properties and maintained neutral pH after dissolution in distilled water. The volumetric flasks with eluting solutions and the used adsorbent were shaken for one hour and then filtered. The filtered samples were analysed to determine the desorbed adsorbate concentrations. Then adsorbent was washed with the deionised water and dried in the oven at 60 ºC for 24 hours. After that, the adsorbate solution was introduced to the adsorbent and shaken for 2 hours. The ions leached out from the adsorbent were measured in the water samples and the eluting solutions. After the first cycle of adsorption-desorption experiments, the collected adsorbents were washed twice with deionised water following ethanol and dried at 60 ºC for 24 hours. The dried adsorbent was repeatedly used for several cycles of adsorption-desorption reactions. After determining the residual ion concentration, the number of ions adsorbed per unit mass and desorption efficiency were calculated using the Eqs. (21) and (22):

$$Q_e = Q_o + \frac{(C_i - C_e) \text{ X } V_a}{m_a} \tag{21}$$

$$\text{Desorption \%} = \frac{C_{ed} \text{ X } V_a}{Q_e \text{ X } m_a} \tag{22}$$

where Q_o is the initial amount of ion on the solid surface (mg/g), C_i and C_e are the initial and equilibrium ion concentrations in the solution (mg/L), respectively, m_a is the dry mass of the adsorbent (g), V_a is the volume of solution (L), C_{ed} is the volume of the regeneration solution (L), and Q_e is the ion concentrations loaded on the solid surface before desorption (mg/g). The values were compared statistically using paired sample t-test to identify significance difference in adsorption and desorption ability of eluting agents.

3.4.7. Fixed-bed column studies

The batch adsorption data cannot directly be applied to the fix-bed column performance. Isotherm data generated from batch studies are not accurately described the scale-up

process (Yaguba et al., 2015). Therefore, the fixed-bed column studies are needed to use materials selected from batch studies to identify fixed-bed performance. The fixed-bed column studies offer the opportunity to perform continuous adsorption processes and scale-up potential in the adsorption process. The schematic diagram (Figure 3.16) elaborates the steps followed in fixed-bed column studies.

3.4.7.1. Selection of materials for fixed-bed column studies

The different materials were tested (Table 3.5) in batch adsorption studies to identify best-performed materials in hardness, fluoride, and *E. coli* removal. ZEOL, MOMA, and SONPs + GO composite were selected based on batch studies investigating fixed-bed column performance.

These materials effectively remove hardness, fluoride, and *E. coli* in potable water, which meet the required drinking water guideline values. The optimum dosage of ZEOL in batch studies was identified as 4.0 g/L to remove 300.0 mg/L of hardness with pH 7, contact time 30 minutes. The percentage of hardness removal was reported as 95%, and residual hardness concentration was 96.0 mg/L. The adsorption capacity of ZEOL at equilibrium was calculated as 263.16 mg/g, and the most suitable eluting agents in the regeneration were found as HCl and NaOH. The optimum dosage of MOMA in batch studies was identified as 2.0 g/L to remove 3.0 mg/L of fluoride with pH 4.0, the contact time 40 minutes (Percentage of hardness removal 98% and the residual fluoride concentration 0.21 mg/L, adsorption capacity at equilibrium 18.76 mg/g, and most suitable eluting agents in the regeneration found as HCl and EDTA. The optimum dosage of SONPs + GO in batch studies were identified as 4.0 g/L to remove 1,800.0 CFU/100 mL of *E. coli* with pH 6.5, contact time more than 24 hours (Percentage of *E. coli* removal 100%), and most suitable eluting agents in the regeneration found as HCl. ZEOL, MOMA, and SONPs + GO performed better in removing hardness, fluoride, and *E. coli* than other materials (FeON, GO, MESA, COMA, nZVI, TiO_2) studied in the batch adsorption studies.

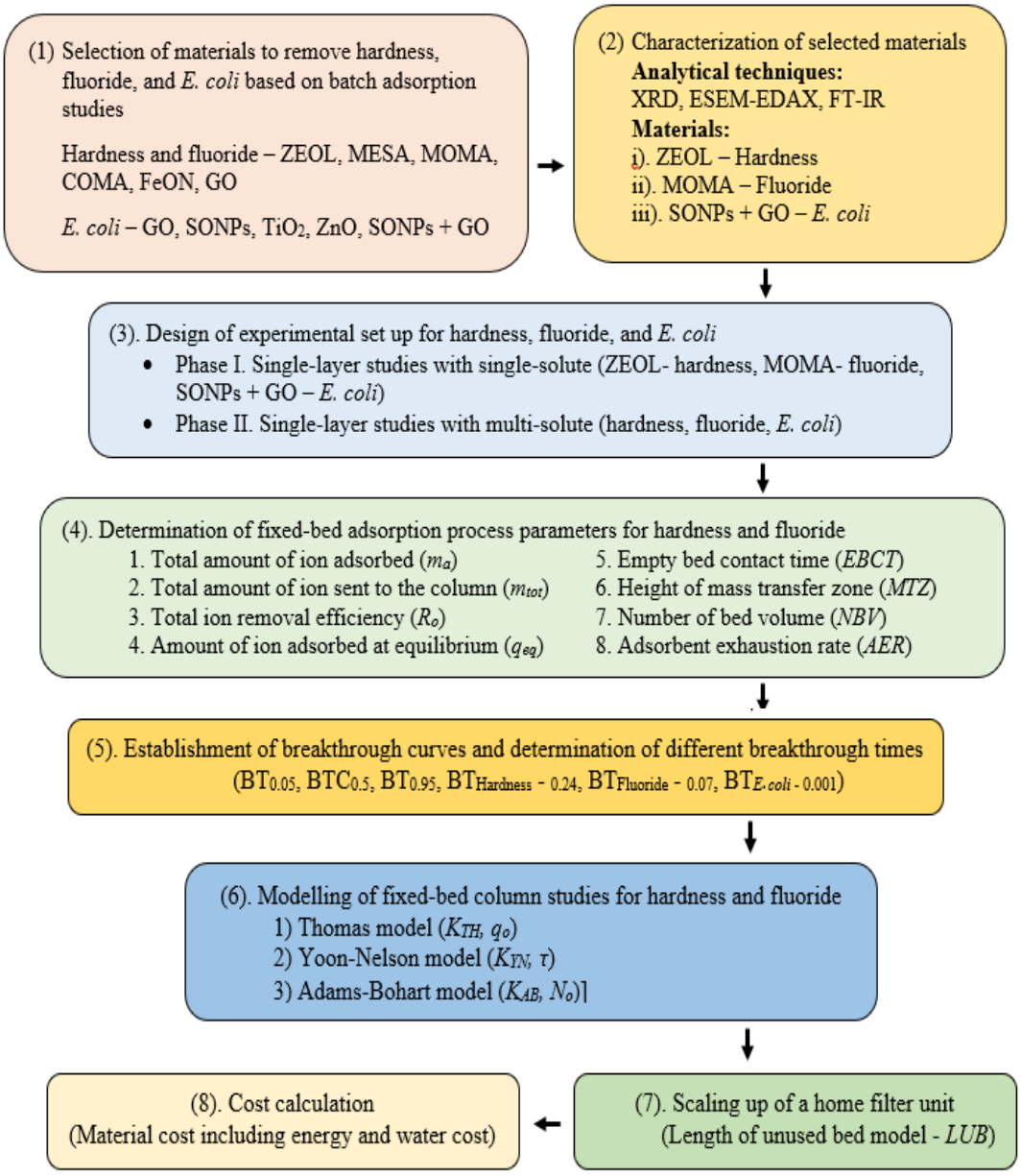

Figure 3.16: Schematic diagram for fixed bed column studies

Table 3.5: Materials selected for fixed-bed column studies

Constituent	Materials											Physio-chemical characteristics evaluated	Material selection criteria considered
	ZEOL	MESA	COMA	MOMA	FeON	nZVI	GO	SONPs	ZnO	TiO_2	SONPs+ GO		
Hardness	√	√	√	√	√	√	√	X	X	X	X	Dosage (g) Initial concentration (mg/L) Contact time (Minutes) pH of the solution	Maximum adsorption capacity (mg/g) based on Langmuir model (Langmuir, 1918)
Fluoride	√	√	√	√	√	X	√	X	X	X	X		
Cadmium	X	X	X	X	X	√	X	X	X	X	X		
E. coli	X	X	X	X	X	X	√	√	√	√	√	Batch studies Inhibition zone method Well-diffusion method Optical density method	Growth inhibition (%) Inhibition zone diameter (mm) [Chandraker et al. (2017)]

Therefore, fixed-bed column studies were carried out using ZEOL, MOMA, and SONPs + GO by changing the filter bed's heights and volumetric flow rates for scale-up as a home filter unit. Therefore, ZEOL, MOMA, and SONPs + GO were packed in columns separately for further evaluation. The materials were added from the top of the column and allowed to settle by gravity force.

The columns were packed with ZEOL, followed by a glass filter, glass wool, glass beads, and sand layers (Figure 3.17). The glass filter and glass wool were used to avoid the leaching of powdered materials with the treated solution. The glass beads were used to compact the bed, prevent the space of dead volume, and avoid the pressure developed inside the column. The sand was used to slow down the flow and avoid the pressure drop and channel formation through the bed. The sand was tested for the

removal of fluoride and hardness before being used in the column. The removal of fluoride and hardness by sand was negligence (<<0.001 mg/L).

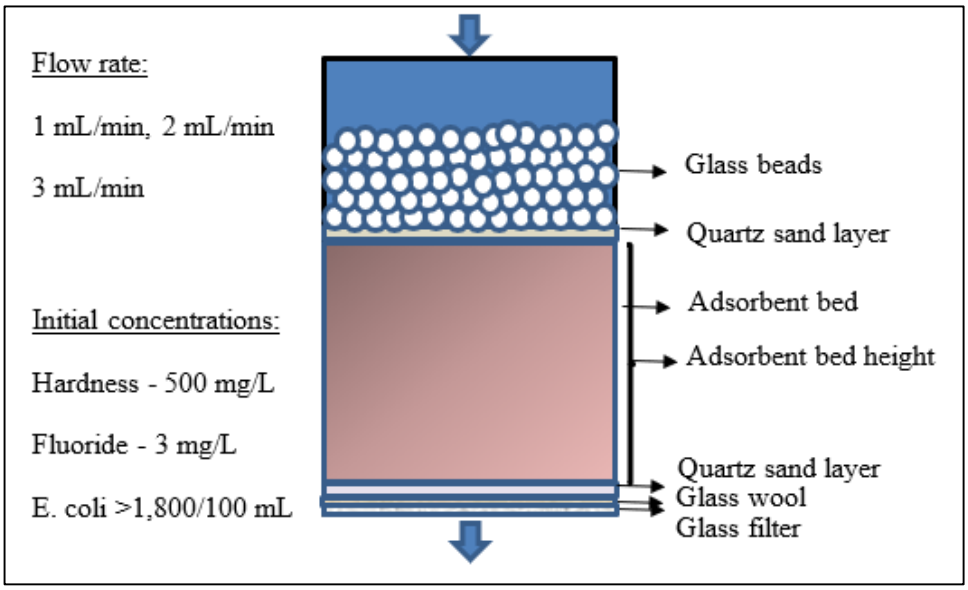

Figure 3.17: Order of composition in the fixed-bed column

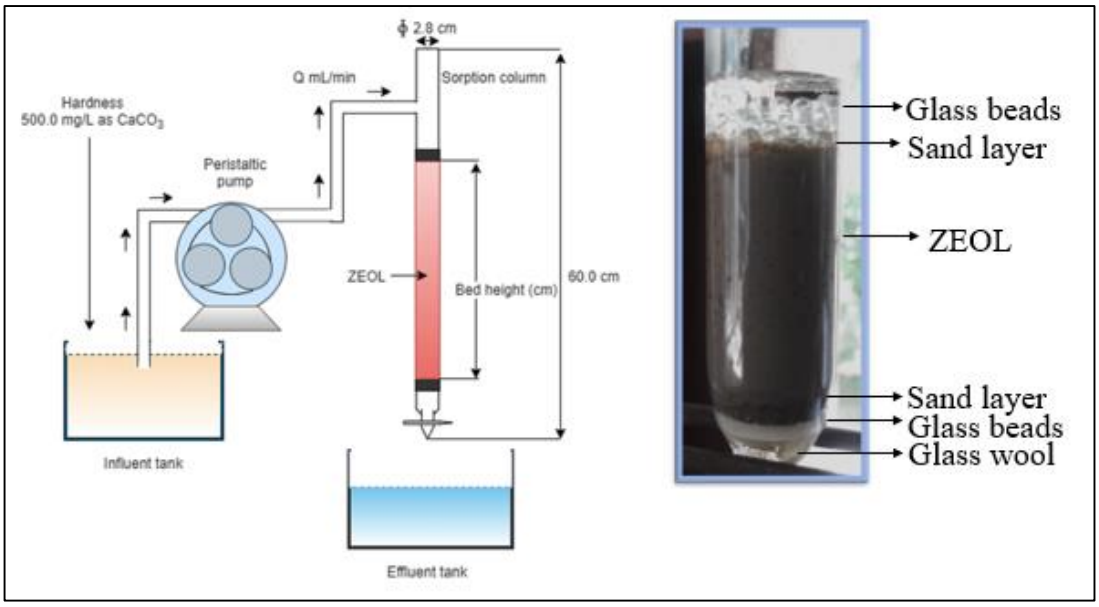

Figure 3.18: Experimental diagram and experimental setup: Phase 1 – ZEOL in single-layer studies with single-solute for hardness removal

The multi-layered column was designed to remove hardness first from potable water due to high hardness concentrations from a calcined crust on any surface. The formation of calcined coating over the surface of other layers such as MOMA and SONPS + GO will decrease their surface chemical and physical properties. Changes in chemical and physical properties on the material's surface decrease the removal effectiveness of selected materials in removing nephrotoxic risk factors in potable water.

MOMA was selected as the second layer in the multi-layered fixed-bed column to remove fluoride. MOMA did not facilitate hardness removal because it did not show hardness removal possibilities during batch adsorption studies. Fluoride adsorbed on MOMA's surface can produce calcium fluorite complexes with higher hardness concentration (exceeding the saturation index value 3.9 X 10^{-11} for CaF_2). The formation of calcium fluorite complexes covers the counter ions on MOMA's surface, decreasing effectiveness in removing fluoride. Therefore, MOMA was selected as the second layer in the multi-layered fixed-bed column to remove fluoride after removing a higher concentration of hardness in potable water.

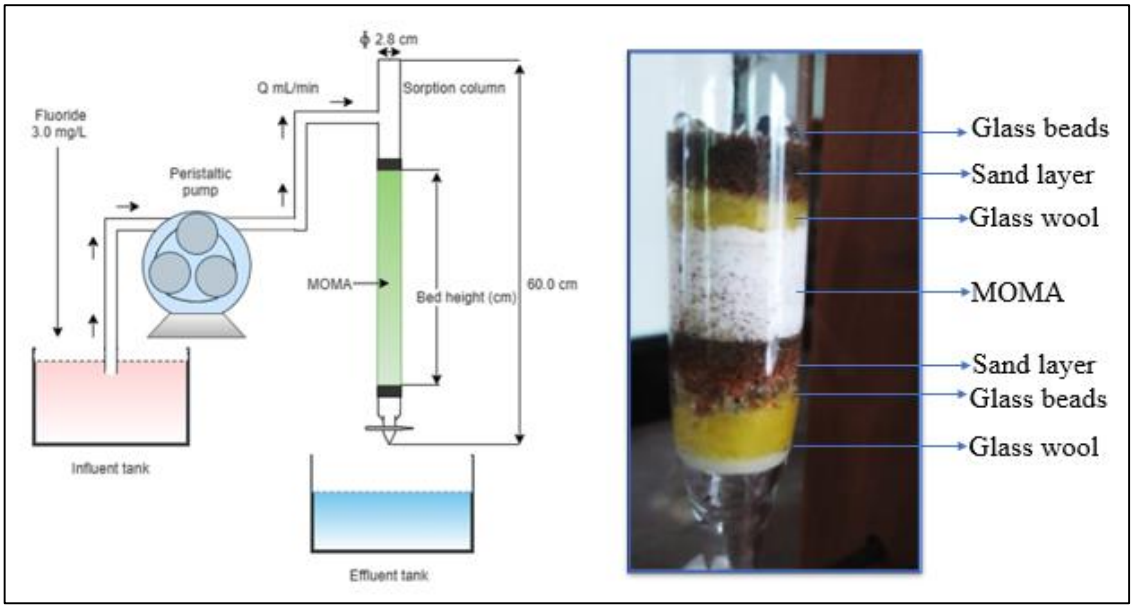

Figure 3.19: Experimental diagram and experimental setup: Phase 1 – MOMA in single-layer studies with single-solute for fluoride removal

Most people in CKDu prevalent areas often use groundwater as a potable water source. Contamination of groundwater with *E. coli* has accidentally occurred mainly in less moisture soil profiles in dry zone areas in Sri Lanka. However, surface water bodies, which people use as potable water sources, are probably contaminated with faecal matter. Hence, the consumption of contaminated water magnitudes vulnerability to outbreak the water-borne diseases. Therefore, the SONPs + GO layer, which has disinfection potential, was entailed in the multi-layered column to ensure water safety. SONPs + GO were selected as the third layer in the multi-layered fixed-bed column to remove *E. coli*. *E. coli* bacteria can be removed by ZEOL and MOMA mildly as they contained metal oxides such as CaO, MgO, and Al_2O_3 in their composition. Hence, the mass of SONPs + GO used in the layer can be reduced.

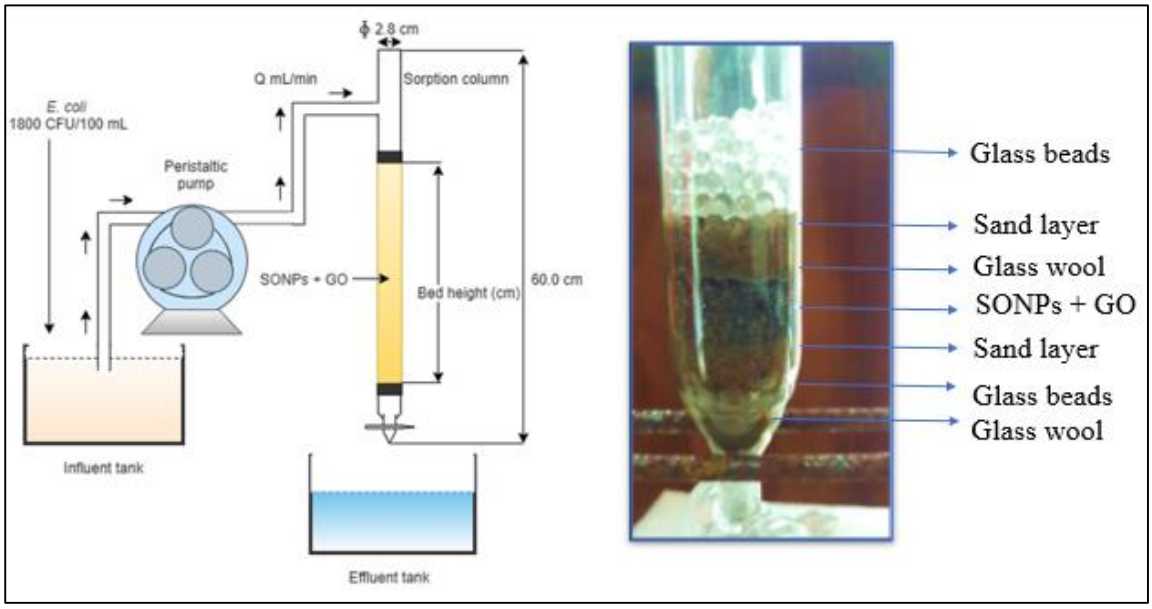

Figure 3.20: Experimental diagram and experimental setup: Phase 1 – SONPs + GO in single-layer studies with single-solute for *E. coli* removal

3.4.7.2. Fixed-bed column studies to remove nephrotoxic risk factors

Fixed bed columns (Figure 3.20) with ZEOL, MOMA, and SONPs + GO were prepared to determine the breakthrough time reference to best-performed bed height and flow

rate. Removal of hardness, fluoride, and *E. coli* was studied i) phase I - fixed-bed column studies for the single layer with single-solute, and ii) phase II - fixed-bed column studies for the single layer with multi-solute. The column bed heights (3.5, 4.5 and 5.5 cm of ZEOL, 1.0, 1.5 and 2.0 cm for MOMA and 0.5, 1.0 and 1.5 cm for SONPs + GO) and flow rates (1.0, 2.0 and 3.0 mL/min) of the solution were decided based on the optimum adsorbent dosages in respective batch adsorption studies. Bed heights of each fixed-bed column were decided based on the optimum dosage chosen during each material's batch adsorption studies. The effective bed contact time (EBCT) of ZEOL, MOMA, and SONs + GO were calculated using the mass of materials, bulk density of the materials and volumetric flow rate as 1.0 mL/min. The volumetric flow rate (1.16 mL/min–2.13 mL/min) required for fix-bed column studies was calculated using EBCT values and adsorber volume. The experiment's volumetric flow rates (1.0 mL/min, 2.0 mL/min, and 3.0 mL/min) were decided based on the calculated volumetric flow rates. The solution was fed into the columns by downflow direction using the peristaltic pump (MasterFlex, model 7553–79, Cole - Parmer Instruments, Canada, 6–600 RPM, 180 VDC, 0.1 HP). High purity ≥ 99%, Sigma Aldrich chemicals, and distilled water were used to prepare fixed-bed column studies solutions. The treated samples were collected at 2 hours' time intervals.

Phase I –Fixed-bed column for single-solute studies with a single layer

Fixed-bed studies were carried out to remove hardness, fluoride, and *E. coli* with nine glass columns with an internal diameter of 2.5 cm and 55.0 cm in height, as depicted in Figure 3.21. The column bed was soaked with distilled water to wash out excess particles and impurities. First, ZEOL fixed-bed columns were fed with hardness solution (500.0 mg/L) in bed height 3.5 cm and flow rates 1.0 mL/min, 2.0 mL/min, and 3.0 mL/min. The same experiments were followed, changing the ZEOL bed heights to 4.5 cm and 5.5 cm. Secondly, MOMA fixed-bed columns were fed with fluoride solution (3.0 mg/L) in bed height 1.0 cm and flow rates 1.0 mL/min, 2.0 mL/min, and 3.0 mL/min. The same experiments were followed, changing the MOMA bed heights to 1.5 cm and 2.0 cm.

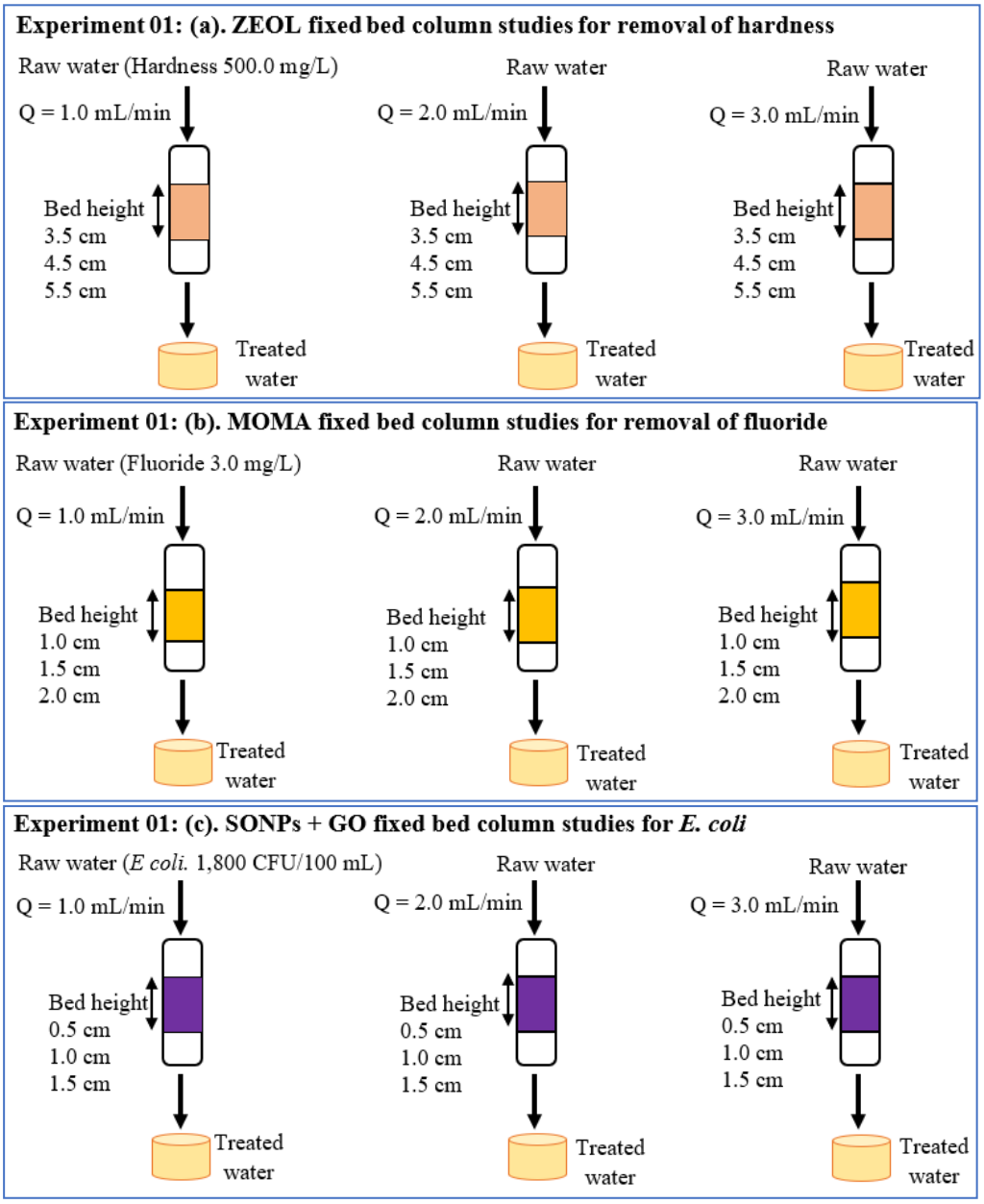

Figure 3.21: Phase I – The fixed-bed column for single-solute studies with a single layer

Thirdly, SONPs + GO fixed-bed columns were fed with *E. coli* solution (1,800.0 CFU/100 mL) in bed height 0.5 cm and flow rates 1.0 mL/min, 2.0 mL/min, and 3.0

mL/min. The same experiments were followed, changing the SONPs + GO bed heights to 1.0 cm and 1.5 cm. A single-solute solution with hardness, fluoride, and *E. coli* was fed into the individual column downward through the peristaltic pump at a uniform flow rate. The samples were collected for 2 hours at regular intervals. Concentrations of hardness as $CaCO_3$, fluoride, *E. coli*, and pH of the treated water were measured.

Phase II – Fixed-bed column for multi-solute studies with a single layer

Fixed bed studies were carried out to remove multi-solute with a single layer of ZEOL, MOMA and SONPs + GO (Figure 3.22). The bed heights and flow rate were selected based on the best-performed parameters in Experiment 01. The columns were packed with ZEOL (5.5 cm), MOMA (2.0 cm), and SONPs + GO (1.5 cm), followed by a glass filter, glass wool, glass beads, and sand layers. A multi-solute solution with hardness, fluoride, and *E. coli* was fed downward through the peristaltic pump at a uniform flow rate (1.0 mL/min) into the column with a defined bed height. The samples were collected for 2 hours at regular intervals. Concentrations of hardness as $CaCO_3$, fluoride, *E. coli*, and pH of the treated water were measured.

The experimental data C_t/C_o Vs time (t) was plotted in breakthrough curve to identify the breakthrough points of ZEOL, MOMA and SONPs + GO. The breakthrough time at $C_t/C_o = 0.24$ for hardness, $C_t/C_o = 0.07$ for fluoride, $C_t/C_o = 0.001$ for *E. coli*, $C_t/C_o = 0.05$, $C_t/C_o = 0.5$, and $C_t/C_o = 0.95$ were determined based on breakthrough curve. The breakthrough time for hardness was calculated as $C_t/C_o = 0.24$ dividing the initial hardness concentration (500.0 mg/L as $CaCO_3$) by the reference value (120.0 mg/L as $CaCO_3$) considered in the study. The breakthrough time for fluoride was calculated as $C_t/C_o = 0.07$ dividing the initial hardness concentration (3.0 mg/L) by fluoride reference value (0.2 mg/L). The breakthrough time for *E. coli* was calculated as $C_t/C_o = 0.001$ dividing the initial hardness concentration (1,800.0 CFU/ 100 mL) by the reference value (1.0 CFU/ 100 mL) considered in the study. The breakthrough curve in Figure 3.23 depicts how establish breakthrough curve using experimental data and determining the breakthrough time based on breakthrough curve.

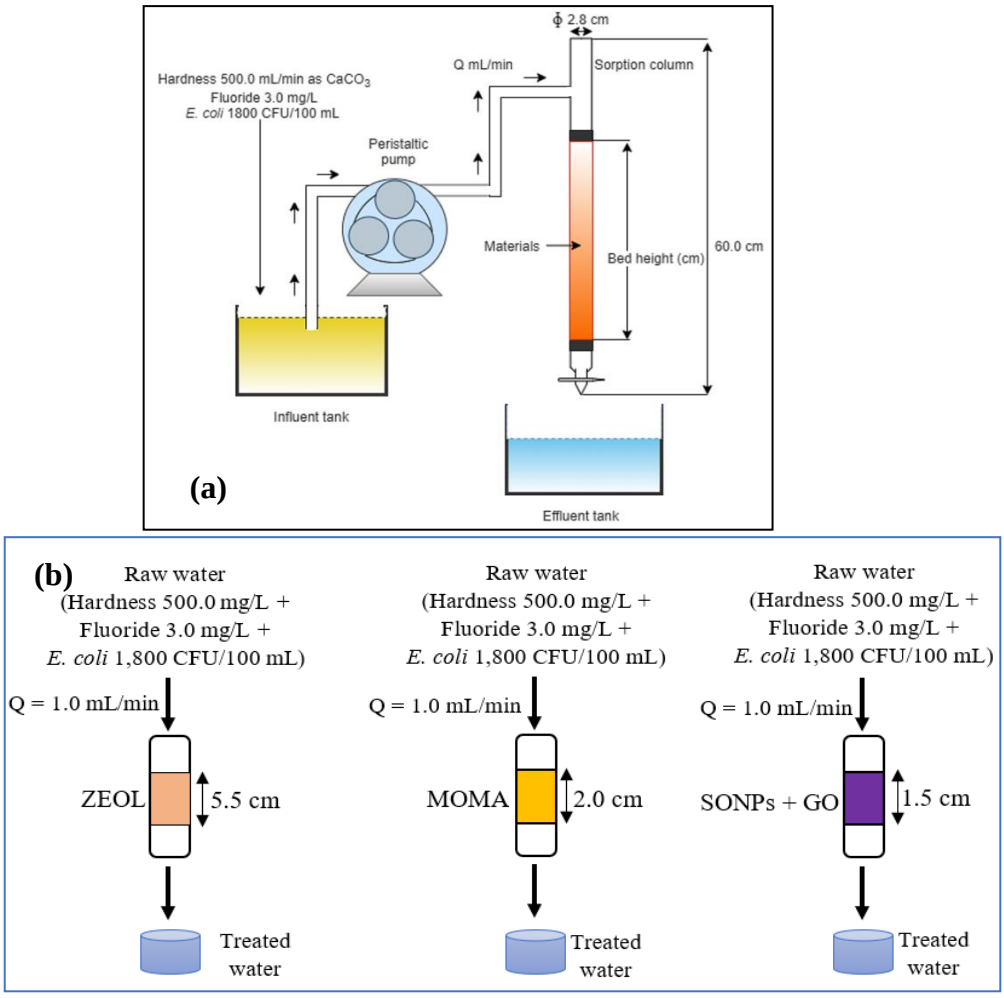

Figure 3.22: Phase II – (a) Experimental set up and (b) descriptive methodology of the fixed-bed column for multi-solute studies with a single layer

3.4.7.3. ZEOL, MOMA, and SONPs + GO characterization using the pycnometer method

The volume of materials used in the adsorber was measured using a pycnometer. The distilled water was used as the pycnometer liquid due to the application of distilled water is a more straightforward method to maintain a conventional glass pycnometer (Worch, 2012). The weight of an empty, dry pycnometer (m_{pyc}) was determined using the top loading balance (ACB 1500, Adam Equipment, Accuracy 0.01 g). About 1/3 of the

pycnometer volume was filled with material, and weight (m_1 - Pycnometer + dry material) was measured. The distilled water was added until the pycnometer drained the excess water, closed the lid, dried the pycnometer surface, and estimated the total weight (m_2 - Pycnometer + dry material + distilled water).

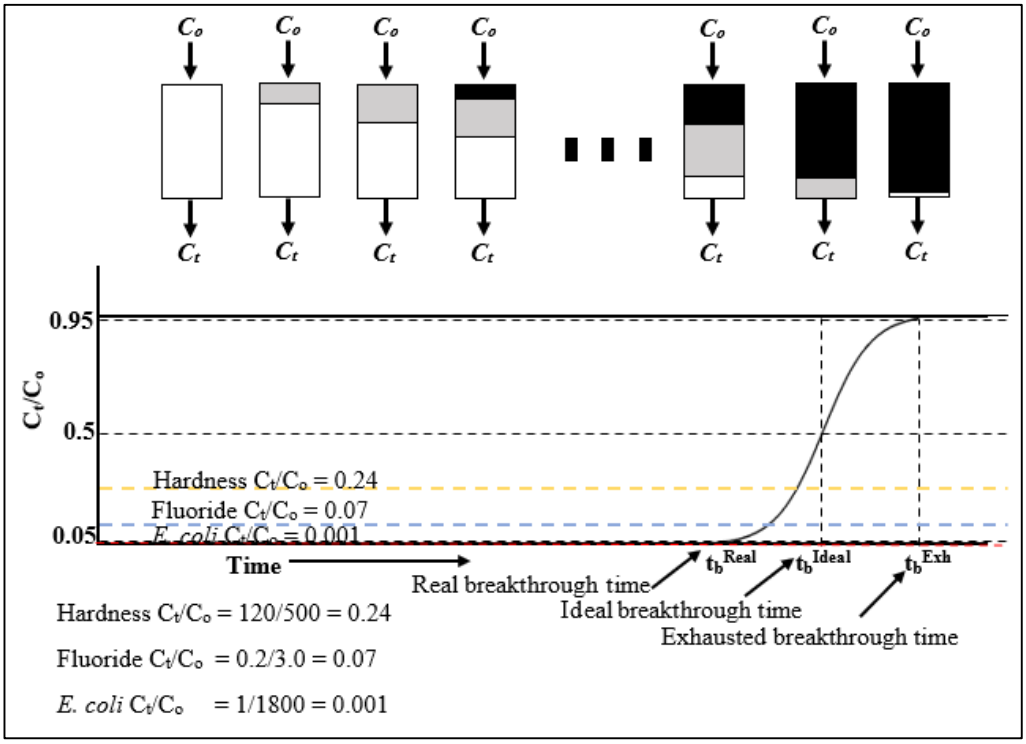

Figure 3.20: Establishment of breakthrough curves and determination of different breakthrough time

The distilled water in the upper part of the pycnometer was removed, and excess distilled water was well-drained. The pycnometer weight with the wet adsorbent (m_3 - Pycnometer + wet material) was measured. The pycnometer was filled with distilled water, dried the surface, and measured the pycnometer weight with distilled water (m_4 - Pycnometer + distilled water). Moreover, volumes of the empty pycnometer (V_1) and volume of dry material (V_2) were measured. Table 3.5 shows all measurement which was taken to determine the material characteristics of the fixed bed column.

Table 3.6: Measurement to determine the material characteristics using the pycnometer

Materials	Parameters	Sample 01	Sample 02	Sample 03	Mean
ZEOL	m_{pyc} (g)	8.18	8.15	8.19	8.17±0.02
	m_1 (g)	10.54	10.52	10.57	10.54±0.03
	m_2 (g)	25.17	24.65	25.23	25.02±0.32
	m_3 (g)	12.68	12.44	12.77	12.63±0.17
	m_4 (g)	23.72	23.65	23.97	23.78±0.17
	V_1 (mL)	16.00	16.00	16.00	16.00±0.00
	V_2 (mL)	3.77	3.77	3.77	3.77±0.00
MOMA	m_{pyc} (g)	8.18	8.10	8.18	8.15±0.04
	m_1 (g)	9.91	9.85	10.33	10.03±0.26
	m_2 (g)	25.03	24.80	25.37	25.07±0.28
	m_3 (g)	12.58	12.48	13.24	12.77±0.42
	m_4 (g)	23.55	23.52	23.60	23.55±0.04
	V_1 (mL)	16.00	16.00	16.00	16.00±2.37
	V_2 (mL)	3.77	3.77	3.77	3.77±0.00
SONPs+GO	m_{pyc} (g)	8.14	8.08	8.18	8.13±0.05
	m_1 (g)	12.49	12.44	12.59	12.51±0.08
	m_2 (g)	26.98	26.86	27.11	26.98±0.12
	m_3 (g)	15.11	14.99	15.15	15.08±0.08
	m_4 (g)	23.65	23.58	23.73	23.65±0.08
	V_1 (mL)	16.00	16.00	16.00	16.00±0.00
	V_2 (mL)	3.77	3.77	3.77	3.77±0.00

The pycnometer data were gathered with three replications to reduce the errors. Different parameters such as the mass of wet adsorbent (g), the volume of the wet

adsorbent (mL), particle density (g/cm^3), material density (g/cm^3), bulk density (g/cm^3), particle and bulk porosity were calculated for each adsorbent using the pycnometer data. The mean values of the data were considered for further calculations.

3.4.7.4. Calculation of fixed-bed column process parameters

As adsorbents are porous materials, the adsorbent bed and the bed's flow conditions can be characterised using different process parameters (Worch, 2012). The adsorbent bed is described using different parameters such as adsorbent volume, adsorbent mass, bed porosity, bed density, and material density (Eqs 23 – 48). Different symbols in equations are represented as m_{pyc} - the weight of the empty pycnometer, m_1 - the weight of pycnometer + material, m_2 - the weight of pycnometer + material + water, m_3 - the weight of pycnometer + wet adsorbent, m_4 - the weight of pycnometer filled with water, v_1 - the volume of the pycnometer, v_2 - the volume of adsorbent.

Mass of wet adsorbent (m_{wet})

$$m_{wet} = m_3 - m_{pyc} \tag{23}$$

The volume of the wet adsorbent (V_{wet})

The volume of wet adsorbent represents the sum of materials volume and pore volume.

$$V_{wet} = V_{pyc} - \frac{m_1 - m_{pyc}}{\rho_M} \tag{24}$$

Material density (ρ_M)

Material density represents the materials' true density and can calculate as the quotient of adsorbent mass and volume of the solid material without pores.

$$\rho_M = \frac{m_1 - m_{pyc}}{V_{pyc} - \frac{m_{wet} - (m_1 - m_{pyc})}{\rho_M}} \tag{25}$$

Bulk density (ρ_B)

Bulk density is used to characterise the mass/volume ratio in columns, and it has been defined as the ratio of the adsorbent mass and the total reactor volume filled with liquid and solid.

$$\rho_B = \frac{m_1 - m_{pyc}}{V_L + V_A} \quad (26)$$

Particle density (ρ_B)

Particle density refers to the apparent density and can be calculated as the ratio of adsorbent mass and adsorbent volume, including pores.

$$\rho_p = \frac{m_1 - m_{pyc}}{V_{wet}} \quad (27)$$

Particle porosity (ε_p)

This term referred to the internal porosity defined as the pore volume ratio and the adsorbent particle's volume.

$$\epsilon_p = 1 - \frac{\rho_p}{\rho_M} \quad (28)$$

Bulk porosity (ξ_B)

The term bulk porosity is the external void fraction and can calculate using the liquid-filled void volume ratio in the adsorbent particles and the reactor volume.

$$\epsilon_B = 1 - \frac{\rho_B}{\rho_p} \quad (29)$$

Adsorbent volume (V_R)

The adsorbent volume is calculated using the cross-sectional areas (A_R) and the adsorbent bed's height (h).

$$V_R = A_R h \quad (30)$$

Linear filter velocity (V_f)

V_f is the superficial velocity calculated as the quotient of the volumetric flow rate (Q) and the adsorber's cross-sectional area (A_R).

$$V_f = \frac{Q}{A_R} \quad (31)$$

Effective flow velocity (U_F)

The effective flow velocity can be calculated by dividing the volumetric flow rate (Q) by the cross-sectional area (A_R), which is available for water filtration. The parameter can calculate using the cross-sectional area and the bed porosity (ε_B)

$$U_f = \frac{Q}{A_R \varepsilon_B} = \frac{V_f}{\varepsilon_B} \quad (32)$$

Empty bed contact time (*EBCT*)

Empty bed contact time is referred to as the residence time for an empty reactor.

$$EBCT = \frac{Z\ X\ S}{Q} \quad \ldots\ldots\ldots\ldots\ldots\ldots \quad (33)$$

Z – Bed depth (cm)

S – Cross-sectional area of the adsorbent bed (cm^2)

Effective residence time (t_r)

The effective residence time is lower than the EBCT and is related to the effective flow velocity.

$$t_r = \frac{Z}{V_f} = \frac{hA_R\varepsilon_B}{Q} = \frac{V_R\varepsilon_B}{Q} = EBCT \times \varepsilon_B \quad (34)$$

Number of bed volume (*NBV*)

BV is the dimensionless parameter used to determine the throughput for the column bed size. BV refers to the number of bed volumes fed to the adsorber [V_{feed} = volumetric flow rate x time (t)].

$$NBV = \frac{Volume\ of\ water\ treated\ till\ breakthrough\ point}{volume\ of\ the\ adsorbent\ bed} \quad (35)$$

Specific throughput (*Vsp*)

Specific throughput is the normalised parameter that is used to describe the adsorber's runtime. The volume fed to the adsorber is considered relevant to the adsorbent mass. Hence, the unit of specific throughput is given as L of water treated per 1 Kg of the adsorbent.

$$V_{sp} = \frac{V_{Feed}}{m_A} = \frac{V\ X\ t}{m_A} = \frac{V\ X\ t}{V_R\ \rho_B} = \frac{t}{EBCT\rho_B} \quad (36)$$

The total adsorbed mass of adsorbent (Q_{total})

The area under the breakthrough curve represents the total mass of constituents adsorbed (mg) for the given initial concentration and the flow rate (pez-Cervantes et al., 2018).

The area under the breakthrough curve (A_1)

$$A_1 = \int_{t=0}^{t=t\ total} C\ \ X\ dt \quad (37)$$

$$A_2 = 0.95\ X\ C_o\ X\ t_{total} \quad (38)$$

C – Concentration difference (mg/L)

C_o – Initial concentration (mg/L)

t – Breakthrough time (Hours)

A_2 - rectangular area of the plot

The total amount of ions sent to the column (m_{total})

$$m_{total} = \frac{C_o\ Q\ t_{total}}{1000} \quad (39)$$

Total ion removal %

Total ion removal percentage can be calculated as the ratio of ion mass adsorbed to the total amount of ion sent to the adsorber bed.

$$R_o = \frac{m_a}{m_{total}}\ X\ 100\% \quad (40)$$

Amount of ion adsorbed at equilibrium (q_e)

$$q_{eq} = \frac{m_a}{X} \quad (41)$$

X – mass of adsorbent (mg)

Equilibrium ion concentration (C_e)

$$C_e = \frac{m_{total} - Q_{total}}{V_{ef}} \times 1000 \quad (42)$$

Height of the mass transfer zone (H_{MTZ})

$$MTZ = Z\ X\ \left[1 - \frac{t_b}{t_e}\right] \quad (43)$$

t_b – time of breakthrough point (Hours)

t_e – Time of exhausted point (Hours)

Adsorbent usage rate (g/L)

$$AER = \frac{Mass\ of\ adsorbent}{Volume\ of\ water\ treated\ till\ exhaustion\ point} \quad (44)$$

3.4.7.5. Application of mathematical models for fixed-bed column studies

Knowledge relevant to the breakthrough behaviour of ions that need to be removed is the essential precondition for fixed bed adsorber design. Different mathematical models are available to predict the breakthrough behaviour of the adsorbents in the column bed. The breakthrough behaviour of full-scale adsorbers can predict the basis in breakthrough curves, which were determined using lab-scale experiments. The lab-scale experiments using fixed-bed columns were conducted to remove nephrotoxic risk factors in potable water. The experimental data were fitted with different mathematical models to predict the breakthrough behaviour in different adsorbents.

(a). Adam-Boharts model

The model (Eq. 45, 46) describes the first part of the breakthrough period in the fixed-bed column (Priya and Radha, 2015). The equation describes the fundamental relationship between the fixed bed column's service time against different bed heights. This model is based on surface reaction theory (Kiran & Kaushik, 2008). It assumes that the adsorption rate is proportional to the fraction of adsorption capacity, which is left on the adsorbent's surface (Lehmann & Zouboulis, 2001).

$$ln\left(\frac{C_t}{C_o}\right) = K_{AB}\, C_o\, t - \frac{K_{AB}\, N_o\, Z}{U_o} \quad (45)$$

$$C = C_o \left[e^{K_{AB}\, C_o\, t - \frac{K_{AB}\, N_o\, Z}{U_o}}\right] \quad (46)$$

where K_{AB} is Adams-Bohart rate constant (L/mg.min); Z is bed depth (cm); N_o is maximum adsorption capacity per unit volume of adsorbent column (mg/L); U_o is linear velocity (cm/min); C_o is inlet concentration (mg/L) and C_t is concentration at time t (mg/L).

(b). Thomas model

Thomas model (Eq. 47, 48) is a simple and dynamic mathematical model used to predict the whole length of the breakthrough curve (Kumar et al., 2007). This model assumes a plug flow behaviour through the column bed following Langmuir's theory, second-order reversible kinetic model, and external and internal diffusion considered negligible (Chen et al., 2012).

$$ln\left(\frac{C_0}{C_t}-1\right) = \left(\frac{K_T\, Q_0\, m}{Q}\right) - K_T\, C_0\, t \quad (47)$$

$$C = \frac{C_o}{1+\left[e^{\frac{K_T\, q_o\, m}{Q} - K_T\, C_o\, t}\right]} \quad (48)$$

where k_T is Thomas rate constant (mL/min.mg), Q is the inlet flow rate (mL/min), q_0 is sorption capacity of the adsorbent per unit mass of the adsorbent (mg/g), m is mass of adsorbent (g), C_o is inlet concentration (mg/L), and C_t is outlet concentration (mg/L).

(c). Yoon-Nelson model

The Yoon-Nelson model (Eq. 49, 50) describes that the rate of the probability of adsorption decrease in each adsorbate is proportional to the probability of adsorbate breakthroughs and the likelihood of adsorbate adsorption (Yoon & Nelson, 1984).

$$ln\left(\frac{C_t}{C_o - C_t}\right) = K_{YN}\, t - K_{YN}\, \tau \quad (49)$$

$$C = \frac{C_o}{1+e^{\tau\, K_{YN} - K_{YN}\, t}} \quad (50)$$

Where K_{YN} is Yoon-Nelson rate constant (1/min), T is the time required for 50% breakthrough (min), C_o is inlet concentration (mg/L), and C_t is the concentration at time t (mg/L).

(d). Length of the unused bed (LUB) model

The LUB model has been used as a scale-up model (Collons, 1967; Lukchis, 1973), which describes the unused bed length at a breakthrough point characterizing breakthrough behaviour. The fraction of the adsorption capacity of the adsorbent bed remains unused if the fixed bed adsorption process is terminated at the point of breakthrough (Worch, 2012). The LUB model represents the length of the adsorbent bed, which is not saturated at the system's breakthrough point. The scale-up process concept describes the fact that the length of the new bed has not been varied with the overall length of the adsorbent bed as the breakthrough curve slope has not been changed throughout the curve (Moreno-Piraj´an et al., 2008).

The fraction of adsorption capacity has been found proportional to the distance between the point of the stoichiometric front (h_{st}) and the adsorbent bed height (h). The LUB model (Eq. 51) has been investigated as related to the rate of adsorption. The LUB is longer when the system's mass transfer process is slower (Worch, 2012). The experimental data of multilayer column studies (Experiment 03) were fitted to the LUB model below, and a scaling-up process was conducted for the desired breakthrough time.

$$LUB = \frac{t_{st} - t_b}{t_{st}}\ h \qquad (51)$$

Where t_{st} is the stoichiometric time (time at $C/C_o = 0.5$) (minutes), t_b is the breakthrough time (minutes), and υ_z is the zone velocity (cm/min).

The scaling-up process of the fixed bed column in removing hardness, fluoride, and *E, coli* using ZEOL, MOMA, and SONPs + GO was conducted, assuming the facts that drinking water supply a family with four members for six months. In the scale-up process, the zone velocity was calculated using equation (52), and the location of the stoichiometric front, h_{st}, was calculated using equation (53). The required adsorbent height to treat water for six months was determined by adding h_{st} and LUB [equation (54)]. Finally, the adsorbent mass required to treat water for six months was calculated for each adsorbent.

$$U_z = \frac{v_f\, c_o}{q_o\, \rho_B} \tag{52}$$

$$U_z = \frac{h_{st}}{t_b} \tag{53}$$

$$h = LUB + h_{st} \tag{54}$$

3.4.8. Design a home filter unit and cost calculations for 1.0 L of treated water production

The home filter design was carried out assuming that a family consists of 5 members and that each member consumes 2.0 L of water per day. Hence, the total water requirement for a family was considered as 10.0 L per day and potable water is supplied to a family for six months (4,320 hours). The mass of ZEOL, MOMA, and SONPs + GO required to treat potable water for six months were calculated using the LUB model results. The design of bed volume of ZEOL, MOMA, and SONPs + GO were calculated using the mass required and the bulk densities of the materials (ZEOL – 0.45 g/cm^3, MOMA – 0.36 g/cm^3, and SONPs + GO – 0.84 g/cm^3). The volumetric flow rate was calculated, considering that the water volume was treated for six months. The cross-sectional area and heights of the columns were calculated using 8.0 cm of the diameter, which was decided based on the functional requirement in filter operation and maintenance.

Each material's synthesized cost was calculated to determine the production cost of 1.0 L of potable water. The cost was calculated based on the column's specific output, representing the amount of water treated by 1.0 kg of the adsorbent. Cost components considered include the cost of chemicals used to synthesise the material, cost for reactivation of adsorbent, water and electricity cost incurred for the synthesis process.

CHAPTER 4

4. RESULTS AND DISCUSSIONS

4.1. Objective 01: To identify different nephrotoxic risk factors, their concentrations, threshold levels of nephrotoxicity, and the extent to which the removal is required in potable water

4.1.1. Nephrotoxic risk factors and their concentrations

A summary of different fluoride, hardness, and cadmium and their concentration values gathered during the literature review is included in APPENDIX IV. The data corroborated spatial and temporal variation with low to high distribution patterns at different CKDu endemic dry zone areas. The concentration distribution pattern depends on the geological formation of the underneath soil profile in the dry zone of Sri Lanka. The same argument was proclaimed by past studies (Chandrajith et al., 2011; Wickramarathna et al., 2017). The origin of most nephrotoxic risk factors ascertains as water related. People over 75% of CKDu prevalent areas consume groundwater which contains a higher fluoride concentration, hardness, and cadmium (Dissanayake, 2005). The low prevalence of CKDu occurred among the people who consumed water from natural springs, which contained low levels of fluoride, hardness, and cadmium (Jayasekara et al., 2015). Hence, the causative factor of CKDu could be suggested as nephrotoxic constituents in drinking water. Different authors have been postulated the same arguments in past studies (Chandrajith et al., 2011; Wickramarathna et al., 2017), but not thoroughly investigated and well established.

The results of water samples analysed during the study and reported values in the literature were corroborated that fluoride, hardness, and cadmium values in potable water exceed the drinking water guideline values. The minimum and maximum hardness values in water samples were analysed as 111.73 ± 1.41 mg/L as $CaCO_3$ and 680.33 ± 1.53 mg/L as $CaCO_3$. The minimum and the maximum values of hardness in literature have been reported as 10.00 ± 0.10 mg/L as $CaCO_3$ and 1921.00 ± 2.50 mg/L as $CaCO_3$,

respectively (Rango et al., 2015; Chandrajith et al., 2011b). The water samples' minimum and maximum fluoride values were examined as 0.72 ± 0.03 mg/L and 2.84 ± 0.05 mg/L. The minimum and maximum fluoride values in literature have been reported as 0.18 ± 0.01 mg/L and 13.70 ± 1.20 mg/L, respectively (Weragoda and Kawakami, 2017, Chandrajith et al., 2015; Chandrajith et al., 2012a). The minimum and maximum cadmium values in water samples analysed were examined as < 0.025 ± 0.01 and 0.0065 ± 0.01 mg/L. The literature's minimum and maximum cadmium values have been reported as < 0.00027 ± 0.01 mg/L and 0.034 ± 0.001 mg/L, respectively (Chandrajith et al., 2012; Wasana et al., 2016). The concentration values implied that potable water consumption by people in CKDu affected areas is vulnerable to adverse health effects, most likely with renal damage.

The literature's maximum hardness and fluoride values were more remarkable than the maximum hardness and fluoride levels in this study. The hardness and fluoride data published in the literature covers the different geological areas all over the dry zone where CKDu is endemic in Sri Lanka. Hence, hardness and fluoride concentration reported in the literature have been found to vary in considerably higher levels. The maximum hardness levels in both data sets are rested in the range of the “very hard (> 180.00 mg/L)” category according to USGS (United State Geological Survey) hard water classification. Minimum hardness found in analytical and reported data could be categorized under “moderately hard (61.00–120.00 mg/L)” and as “soft water (< 60.00 mg/L), respectively. Maximum fluoride values in analytical data and the literature exceeded the WHO drinking water guideline values (1.50 mg/L). The minimum fluoride level in the groundwater of Wewelketiya village exceeds the WHO recommended fluoride concentration of 0.60 mg/L for tropical countries (WHO, 2012). The minimum fluoride concentration in the reported value (0.18 mg/L) was observed as a lower prevalence of fluoride concentration in natural spring water (Jayasekara et al., 2015). These water sample results and levels reported in the literature indicate the prevalence of trace levels of cadmium in groundwater. However, cadmium reported values were very limited in past studies. The cadmium concentration was investigated very low (lower

than the detection limit of 0.025 mg/L in analytical samples. According to available data, in case, cadmium concentrations in potable water in CKDu prevalent areas exceed the WHO drinking water guideline value (0.003 mg/L).

4.1.2. Threshold levels of possible nephrotoxic risk factors and the extent to which removal is required

The literature's concentrations of nephrotoxic risk factors were compared with WHO drinking water guidelines (WHO, 2017) and Sri Lankan standards (SLS 614:2013) for drinking water. Fluoride, hardness, and cadmium in potable water led to severe kidney damage as their existing synergic effect. These molecules' toxic effects have been more pronounced present in potable water at higher concentrations (doubling the WHO maximum value). Wasana et al., 2017 stated that WHO maximum levels are also responsible for CKDu due to the synergic effects of hardness, fluoride, and cadmium.

The concentration values of hardness and fluoride in CKDu prevalent areas have exceeded the acceptable drinking water standard (95% of percentile value). Drinking water guideline values for hardness have not been declared by WHO drinking water guideline values and several other guideline values such as USEPA, Australian, Canadian, and European Union. However, several countries such as India, China, Nepal, Bangladesh, Pakistan, and Sri Lanka have been proposed hardness guideline values (Refer section 2.6). The taste threshold levels for hardness have been given as 100.0–300.0 mg/L by WHO (2012). Hardness level, which exceeds 500.0 mg/L, has been derived as a tolerable consumer level (WHO, 2017). However, WHO does not provide the health concern value for hardness in drinking water. The minimum and maximum Sri Lankan drinking water guideline values have been given for calcium and magnesium 100.0–240.0 mg/L and 30.0–150.0 mg/L, for hardness 250.0–600.0 mg/L, respectively. The minimum amount of 250.0 mg/L could be classified as “very hard” according to the general guideline of hard water classification derived by the USGS.

Hardness has been considered a significant etiological factor for many diseases such as cardiovascular problems, diabetes, reproductive failure, neural diseases, and renal

failure (Sengupta, 2013). Some studies said water hardness had increased the risk of atopic dermatitis among preschool children in Japan and the United Kingdom (Miyake et al., 2004). Atopic dermatitis is an inflammatory, chronically relapsing, non-contagious and pruritic skin disorder (Sengupta, 2013). Reproductive failure and stillbirth were found in India's hard water resources (Sengupta et al., 2010). Also, drinking water with magnesium and sulfate has caused a laxative effect with nearly 250.0 mg/L of hardness (Sengupta, 2013). Comstock, 1971, said that 0.0–200.0 mg/L of hardness might bring hypertensive disease, atherosclerotic heart disease (hardening arteries), and stroke-like cardiovascular disease.

In non-CKDu prevalent areas, hardness values were often reported below the level of 120.0 mg/L (Figure 4.1). The hardness concentrations reported in the water of CKDu prevalent areas were reported above the limit of 120.0 mg/L moderately hard water. Most people who consumed spring water contained low hardness (< 100.0 mg/L) levels. The lower hardness levels do not promote CKDu (Rango et al., 2015; Wasana et al., 2016). Hardness level > 100.0 mg/L has been reported to have a low buffering capacity and more corrosive effects in water distribution pipes (WHO, 2017).

According to Das, 1998, > 100.0 mg/L of hardness has been considered to cause several health effects such as cardiovascular disease, kidney stones, the risk of gastric cancer, and the possibility of the malformation of the central nervous system. Less than 75.0 mg/L of hardness has been reported to cause ischemic heart disease, which causes chest pain and heart attack. Past studies postulated that lower levels of hardness in potable water do not cause CKDu; however, lower levels of hardness cause non-nephrotoxic health hazards. The hardness distribution pattern in CKDu non-prevalent areas emphasized that the treated water's hardness concentration in CKDu prevalent areas should be less than 120.0 mg/L (moderately hard water). Therefore, the hardness level of 120.0 mg/L is expected to be maintained in the treated water throughout the study considering the USGS hard water classification.

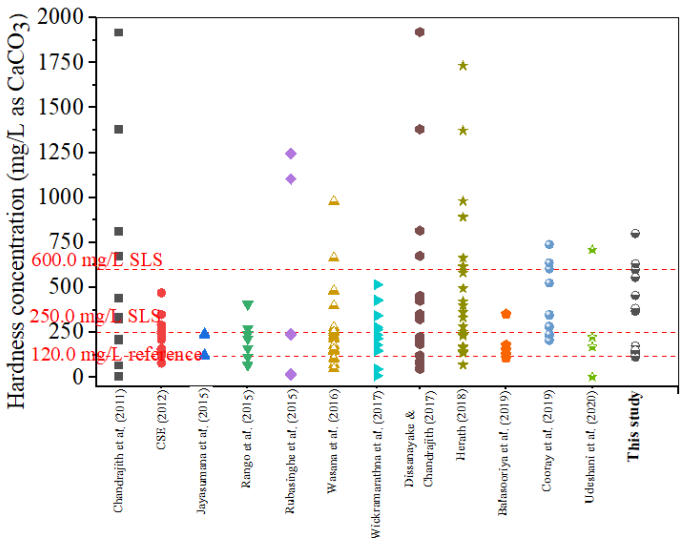

Figure 4.1: Distribution pattern of hardness concentration in CKDu non-prevalent areas (ten concentration points from the study and the rest were taken from the literature) (SLS and USGS represent the permissible hard water level of Sri Lankan drinking water standards and hard water classification of United States Geological Survey, respectively)

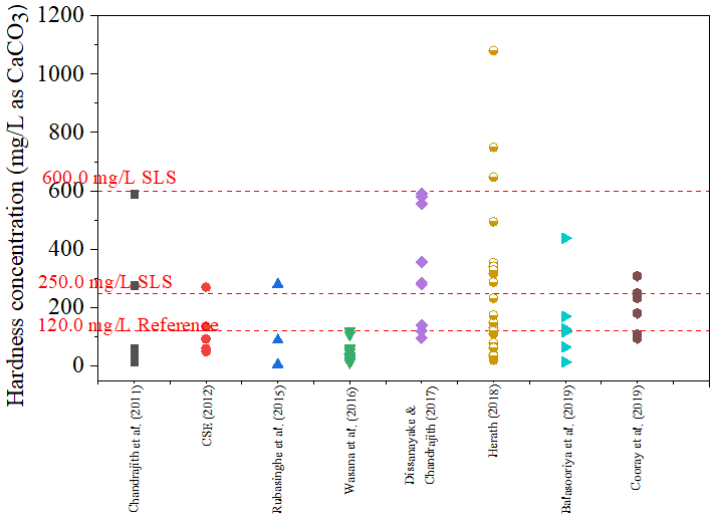

Figure 4.2: Distribution pattern of hardness concentration in CKDu prevalent areas (ten concentration's points from the study and the rest were taken from the literature)

The WHO health-based drinking water guideline value has been recommended as 1.5 mg/L for fluoride (Refer section 2.6). If water consumption is higher in any region, fluoride's guideline values are recommended to be decreased to lower than 1.5 mg/L (WHO, 2017). The required amount of fluoride in drinking water has been derived as 1.0 mg/L in the Sri Lankan drinking water standards (Refer section 2.6). WHO states that a level of 1.5 mg/L of fluoride in drinking water is not acceptable for NCP areas where hot and dry climates prevail (Warnakulasuriya et al., 1992). The high fluoride in water is not the only reason for CKDu. Nevertheless, it may have some relationship with the disease, as high fluoride content, can increase the severity of CKDu (Chandrajith et al., 2010). They further emphasized that the variation of sodium and calcium concentration in groundwater and precipitation of calcium with fluoride would be the causes of kidney disease (Sengupta et al., 2011).

Along with fluoride 1.5 mg/L, hardness 385.0 mg/L, and cadmium 0.006 mg/L have been reported to deteriorate the kidney in slow progress (Wasana et al., 2017). The fluoride values in CKDu non-prevalent areas show that the distribution pattern of fluoride concentrations was investigated below 1.0 mg/L. Fluoride values reported in the literature and analyzed in the study were scattered highly around 0.2 mg/L in CKDu non-affected areas (Figure 4.3). When people consume spring water with fluoride concentrations of about 0.18 mg/L, it has been reported that people are not affected by CKDu (Chandrajith et al., 2011; Rango et al., 2015). The provision of potable water with a fluoride level of around 0.2 mg/L will control the occurrence of CKDu.

The CKDu prevalent areas indicated higher fluoride concentration in potable water. Over 2.0 mg/L of fluoride in drinking water can cause renal damage in children. When fluoride content increases in drinking water, the degree of renal damage increases (Liu et al., 2005). 8.0–12.7 mg/L of fluoride in drinking water has shown to cause crippling skeletal fluorosis, on the other hand, 4.0 mg/L of fluoride can prevent the disease (Liang et al., 1997; WHO, 2012; Ayoob & Gupta, 2006). Fluoride with 4.0 mg/L has been found to have a higher incidence of hip fracture among women, than women using 1.0 mg/L (Sowers et al., 2005). People using less than 1.5 mg/L of fluoride has affected

human birth rate and possibly increased the risk of bone fractures (WHO, 2009). Consumption of less than 1.0 mg/L of fluoride has been reported to increase the risk of osteoporosis, reduced bone density, collapsed vertebrae in women and visible calcification of the aorta in men (Bernstein et al., 1996). According to Dissanayake (2005), 0 mg/L of fluoride has been found to limit growth and fertility; 0.0–0.5 mg/L causes dental caries; 0.5–1.5 mg/L promotes dental health; 1.5–4.0 mg/L increased dental fluorosis; 4.0–10.0 mg/L reported skeletal fluorosis; > 10.0 mg/L; results in crippling fluorosis (Dissanayake, 2005).

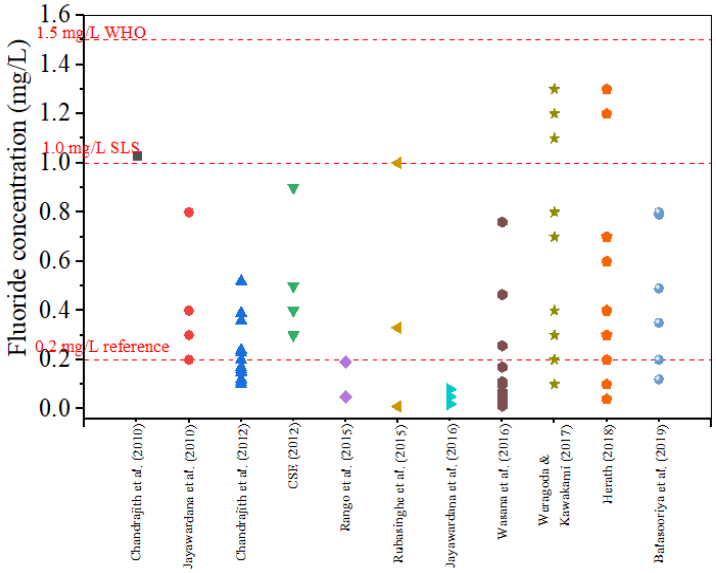

Figure 4.3: Distribution pattern of fluoride concentration in CKDu non-prevalent areas (ten concentration's points from the study and the rest were taken from the literature)

The consumption of lower fluoride concentrations of less than 1.0 mg/L causes adverse non-nephrotoxic health hazards to people. Moreover, fluoride in 0.5 mg/L in potable water may cause a possible risk in the occurrence of CKDu (Figure 4.4). Therefore, the study was designed to remove fluoride to the level of 0.2 mg/L to provide safe potable water for people affected with CKDu. The extent to which nephrotoxic risk factors required removing potable water was identified as hardness 120.0 mg/L, fluoride

0.2 mg/L, and cadmium 0.003 mg/L based on the drinking water standards. Fluoride and hardness in drinking water have been suggested to play a significant role in the occurrence of CKDu in several studies (Wasana et al., 2016; Wickramarathna et al., 2017, Cooray et al., 2019). Cadmium is also one of the causal factors of the disease (Wasana et al., 2016). Cadmium has been recognized as another well-known nephrotoxic risk factor that targets proximal tubular cells' damage by forming a Cd-metallothionein complex (Wickramarathna et al., 2017).

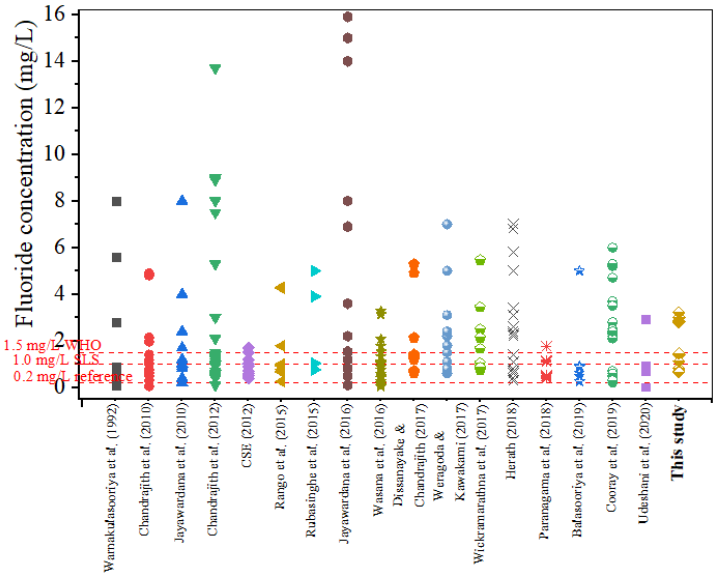

Figure 4.4: Distribution pattern of fluoride concentration in CKDu prevalent areas (ten concentration's points from the study and the rest were taken from the literature)

Cadmium concentration reported in CKDu prevalent areas had been determined as very low (Chandrajith et al., 2010; Jayasumana et al., 2015; Rango et al., 2015). Cadmium concentrations (95% of values) have not exceeded the Sri Lankan standards of 0.005 mg/L (WHO–0.003 mg/L). However, when people are exposed to trace levels of cadmium for a long time, it has been said that cadmium accumulates in the human body (Bandara et al., 2008). Cadmium in drinking water has been shown 10 to 30 years of biological lifestyle, leading to kidney tissue damage, binds cadmium to calcium active

site during the intestine's low calcium concentration (Chandrajith et al., 2011). It has been reported that cadmium brings adverse health effects on humans, such as severe bone malformation and kidney damage (Rango et al., 2015).

There is a significant difference in fluoride (CKDu area: mean 3.21 ± 3.13, non-CKDu: mean 0.43 ± 0.41; $p < 0.05$) and hardness (CKDu area: mean 306.27 ± 301.13, non-CKDu: mean 89.19 ± 85.99; $p < 0.05$) levels in the CKDu and non-CKDu prevalent areas. No significant difference was observed in cadmium levels in CKDu and non-CKDu prevalent areas ($p > 0.05$).

Fluoride, hardness, and cadmium have synergic effects, increasing the severity of kidney failure (Wasana et al., 2016; Dharma-wardana, 2018). The existence of fluoride, hardness, and cadmium in potable water provides insight into the occurrence of CKDu. Hence, removing these nephrotoxic risk factors from potable water appears to be of utmost importance to provide safe potable water. Most patients affected with CKDu have little kidney function (Wasana et al., 2016). If they drink water with a high concentration of fluoride and hardness, such constituents accumulate in the body organs and increase the severity of kidney failure. Therefore, they should be given water with a low concentration of such constituents; thus, the nephrotoxic reference values were considered were: 0.2 mg/L for fluoride and 120.0 mg/L for hardness.

Interaction of fluoride with a concentration of 0.2 mg/L with different water quality constituents including cation such as calcium, magnesium, sodium and potassium, iron, and anions such as nitrate, phosphate, sulphate, bicarbonate and carbonate, and further dissolved oxygen (DO), pH, temperature and alkalinity have been rarely reported in the literature. However, based on the pH of the medium, fluoride produces water-soluble complexes with cations such as Ca^{2+}, Mg^{2+}, Fe^{3+}, and Al^{3+}; these complexes can increase the severity of kidney failure (Illeperuma, 2009; Dharma-wardana, 2018). Further, fluoride forms binary pairs like $(FeF)^{2+}$, but those forms remain in solution at low concentrations (Dharma-wardana, 2018). Even at a low fluoride concentration in water (fluoride values had not been given), it remains as free fluoride due to low binding

affinity, and a small amount exists as cation complexes (Edmunds and Smedley, 2013). Therefore, a fluoride concentration of 0.2 mg/L appears not to produce complexes with cations in terms of the low binding affinity of fluoride. The interaction of fluoride at 0.2 mg/L with different water constituents has not been reported in past studies. However, several studies reported higher fluoride interactions with varying constituents of water, including cation, anion, pH, DO, temperature, and alkalinity. Therefore, further studies, including a series of laboratory experiments, are needed to clarify the interaction of fluoride at 0.2 mg/L with different water constituents.

The literature has reported the interaction of hardness at higher concentrations with different water quality constituents, including cation, anions, DO, pH, temperature, and alkalinity. However, the interaction of hardness at 120.0 mg/L as CaCO3 with different water constituents has not been reported in past studies. Therefore, further studies with different experimental series need to identify the interaction of hardness (120 mg/L as CaCO3) with other constituents.

The study's overall aim is to develop a multi-layered filter unit to remove nephrotoxic risk factors in potable water. Therefore, removing *E. coli* from potable water was incorporated into the study to protect people from water-borne diseases. *E. coli* in potable water indicates the risk of the possible outbreak of water-borne diseases. The ground and surface water are contaminated with faecal matter in CKDu affected areas (Mahagamage and Manage, 2017; 2019). However, *E. coli* has also been reported as occasionally harmful bacteria in human health (Van Elsas et al., 2011). People who resided in CKDu prevalent areas have been affected profoundly by water-borne diseases. The removal of bacteria originating from faecal matter is a prerequisite to ensure the community's water safety. *E. coli*, total coliform, faecal coliform, or pathogenic microorganisms caused for water-borne diseases have not been corroborated as nephrotoxic risk factors. However, removal of *E. coli* was considered in the study, which is focused on treating surface and groundwater using a portable multi-layered home filter unit.

Hence, the study was focused on assessing the performance of the water purification system available at present in CKDu prevalent areas if the community consume treated water from available water filter units.

4.1.3. Key findings of objective 01

- The high fluoride concentrations (> 0.2 mg/L) associated with high hardness (> 120.0 mg/L) concentrations are a significant hydrogeochemical attribute in groundwater at CKDu prevalent dry zone areas in Sri Lanka.
- The concentration levels of fluoride and hardness ions fluctuate well within a concise period (four weeks), illustrating an irregular distribution pattern of concentrations even in the nearest villages of CKDu prevalent.
- The excess or deficiency of fluoride and hardness levels in different CKDu prevalence and non-affected areas depend on groundwater's geochemical composition, mineralogical composition of the aquifer, seasonal variation of rainfall pattern, and excessive evaporation.
- Most fluoride (maximum 13.70 ± 1.20 mg/L) and hardness (maximum 1927.00 ± 2.50 mg/L) concentrations are greater than the permissible drinking water guideline values. The fluoride and hardness in deficient concentrations in spring water (fluoride 0.18 mg/L and hardness 60.00 mg/L) do not aggravate the occurrence of CKDu.
- There is a significant difference in fluoride (CKDu area: mean 3.21 ± 3.13, non-CKDu: mean 0.43 ± 0.41; $p < 0.05$) and hardness (CKDu area: mean 306.27 ± 301.13, non-CKDu: mean 89.19 ± 85.99; $p < 0.05$) levels in the CKDu and non-CKDu prevalent areas. No significant difference was observed in cadmium levels in CKDu and non-CKDu prevalent areas ($p > 0.05$).
- Cadmium concentrations reported and analyzed in groundwater do not exceed permissible drinking water guideline values (0.003 mg/L). The synergic effects of cadmium with fluoride and hardness increase the severity of the disease.

- Available drinking water guideline values are unsuitable for providing safe potable water for people in CKDu prevalent areas.
- Nephrotoxicity-related drinking water standards are not promulgated yet, even after three decades are passed in CKDu outbreak (CKDu patients were reported enormously in 1990 in Sri Lanka).

4.1.4. Limitations of the objective 01

- The data published about concentration levels of nephrotoxic risk factors is lacking in CKDu and non-CKDu prevalent areas. The broad picture of the nephrotoxic risk factor can be acquired when concentrations are available for all CKDu and non-CKDu affected areas.
- The field sampling and analysis of water quality parameters in this study were limited to two villages in the Anuradhapura district. Therefore, the study's sample size was limited to the groundwater sources available in the selected area. A limited number of groundwater sources were found in the area.
- The data relating to cadmium concentrations in potable water were not available to find in the literature. Cadmium concentrations in potable water have been reported in trace levels, and limited data were available to be referred.
- Most published data indicated that nephrotoxic risk factors are not acting alone, but several factors' combination effects were not addressed, covering all hypotheses in CKDu.
- Nephrotoxic reference levels for drinking water are not promulgated yet to identify the extent to which potable water needs to be treated, avoiding renal damage.

4.2. Objective 02: Performance evaluation of commercially available domestic water filter units to delineate their limitation and drawbacks

4.2.1. Different water filters in operation and abandoned in CKDu prevalent areas

The number of businesses in the water sector has introduced several water purification systems in the water market in Sri Lanka. Several filters are portable, and others have been designed to be fixed to a wall. The prices of water filters vary from Rs. 4,500.00 to more than Rs. 50,000.00 during the year 2017. The detailed information gathered about available water filter units in the market at CKDu prevalent areas and household surveys depict in Table 4.1. Water filters selected for the study are consist of different removal techniques such as media and membrane filtrations. Two-layer, seven-layer, PureiT, and gravity water filters can be categorised under media filtration, and the RO filter comes under membrane filtration. Capacity, lifetime, cost, adsorption matrixes, consistency, and purification processes are different in each of these water filters. The results confirmed that different water filter units had been introduced in CKDu prevalent areas to provide safe potable water for people. However, these filters' performance in removing nephrotoxic risk factors was not reported in past studies.

Table 4.1: Summary of different types of water purification systems

Model	Holding Capacity	Cost in 2020	Filtration techniques	Purification processes
 Reverse Osmosis filter unit	9.0 L	Rs. 40,000.00	Membrane filtration	Sédiment filter Granular activated carbon filter Block carbon filter RO membrane Post carbon filter

 The two-layer water filter unit	40.0 L	Rs. 6,000.00	Media filtration	1. Pulverised clay 2. Sifted rice husk 3. Impregnated with colloidal silver
 Seven-layer filter unit	14.0 L 16.0 L 24.0 L	Rs. 8,500.00	Media filtration	Micro ceramic filter dome Silver impregnated granulated activated carbon Ionic exchange resin Far infrared ball Silica sand Mineral sand Mineral stones
 PureiT filter unit	9.0 L	Rs. 11,000.00	Media filtration	1. Microfibre Filtre 2. Activated Carbon Filter 3. Germ kill Processor 4. Polisher
 Gravity water filter	25.0 L	Rs. 6,500.00	Membrane filtration	Unique 0.1µm Dual ceramic membrane cartridge Activated carbon Nano metal cluster media Media box

 Non-electric automatic ultrafiltration unit	75.0 L	Rs. 55,000.00	Membrane filtration	0.01µ Ultrafiltration membrane Sediment filter Silver impregnated activated carbon

4.2.2. Summary of household's survey

People who resided in both villages at Thambalagollawa and Palugasketuwewa strongly believe that potable water plays a significant role in the occurrence of CKDu. Household surveys helped to identify several water purification systems that are popularly used in CKDu prevalent areas (APPENDIX V). Most domestic RO units (9 units from Thambalagollawa and 23 units from Palugasketuwewa) are out of work. Earlier, most families have purchased domestic RO units with instalment payment for use in an individual household. Households in two villages have faced technical difficulties during the operation and maintenance of the RO units. Before the instalment covered the RO unit's full payment, several units were out of work due to scaling and clogging. Foulant precipitation and cake layer formation on the RO membrane could decrease water permeation compared to the virgin membrane (Xu et al., 2005). After clogging the RO filters, people abandoned domestic RO filters because they do not have the facilities to get Operation and Maintenance (O & M) done at the household level. The dealers claimed the full payment forcefully even after the RO system was failed to work. Leasing companies have filed several coat cases against farmers due to avoidance of the settlement of total payment. In case, people in Thambalagollawa and Palugasketuwewa were disappointed in the use of domestic RO filters for water treatment.

However, two domestic RO units in Palugasketuwewa out of 25 units worked as they conducted operation and maintenance (O & M) regularly (Table 4.2). However, they have faced several difficulties, such as scaling and clogging of sediment filters and RO membranes during the RO filter process in operation. Maintenance and replacement

of the filter and filter parts have been frequently employed within one to three months. O & M cost and frequent O & M are unbearable for people in two villages due to the high cost of filter accessories. People have been disappointed with the domestic RO filter unit due to an operation's failure within few (2–8) weeks. Another drawback of the RO filter is that the reject water consists of high concentrations of possible nephrotoxic constituents (Sudasinghe et al., 2014). The reject water is released into the environment without prior treatment, leading to significant soil and groundwater contamination (Nghiem et al., 2004; Sudasinghe et al., 2014).

Table 4.2: Water purification systems in operation and abandoned in CKDu prevalent areas

Village	Domestic RO unit	Commercial RO Unit	Two-layer filter	Seven-layer filter
Thambalagollawa	9	4	1	2
Palugasketuwewa	25	0	4	11

All domestic RO units available in Thambalagollawa have been abandoned. At present, most people in Thambalagollawa and Palugasketuwewa purchase RO treated water (Rs 4.00 – 10.00/ 1.0 L) for their consumption. People are fetching treated water from long distances using plastic containers for household consumption. Some people use water from natural springs or protected well located close to the area. Carrying water from far away has become a burden for people and enormously affected their livelihood activities. People in Palugasketuwewa seek support from the government to install a commercial RO system in their area.

The household survey provides an insight into the popularity of the RO unit in CKDu prevalent areas and the availability of different water filter units, and their contribution to protecting the people’s health from CKDu. (The summary of the results gathered from the questionnaire survey has provided in APPENDIX V. Questionnaire survey was conducted as the preliminary studies to establish the research problem).

4.2.3. Different components in the water filter units available in CKDu prevalent areas

The household survey results illustrated that a seven-layer, two-layer and RO unit was operated by households in CKDu prevalent areas to receive potable water. Among the three filter units, domestic and commercial RO units are the most popular filter units. Most people in the area depend on RO treated water for their daily water requirements (cooking and drinking). The two- and seven-layer filter units have been donated by various non-governmental organizations to few households in the area. These filters are employed either water storage appliances or re-filtered the RO treated water for drinking. Therefore, the different components in two- and seven-layer filters were illustrated to provide a broad picture of how different materials in both filters contribute to removing nephrotoxic risk factors in potable water. Information regarding RO units was included in the literature chapter (refer to section 2.6).

(a) Seven-layer filter unit

The filter unit consists of a micro-ceramic filter dome, activated carbon, mineral–sand, silica–sand, silver impregnated granular activated carbon, far-infrared balls, and minerals stones layers (Figure 4.5). Micro-ceramic filter dome contained Wollastonite ($CaSiO_3$), Anorthite ($CaAl_2Si_2O_8$ Feldspar mineral), 2-Thiohydantoin ($C_3H_4N_2OS$), and Lapacol ($C_{15}H_{14}O_3$). Lapachol (Souza et al., 2013) and 2-Thiohydantoin (Hady, 2012) are widely used as antimicrobial agents. Wollastonite employs to remove ammonia and phosphorus in potable water (Brooks et al., 2000), and anorthite acts as a good source that provides different micronutrients to water filtered (Kumanan et al., 2016).

ESEM-EDAX analysis [Figure 4.5(a_i) & (a_{ii})] of micro-ceramic filter dome also indicate that material consists of different elements such as aluminum (Al) (6.7%), potassium (K) (2.2%), silicon (Si) (35.6%), calcium (Ca) (9.5%), and oxygen (O) (46.0%). XRD spectrum confirms the presence of Ca, Al, and Si [Figure 4.6(a)]. FT–IR spectrum (Figure 4.7) shows different peaks at 535 cm^{-1}, 642 cm^{-1}, 915 cm^{-1}, 1,017 cm^{-1}, which assigned to Si–O– asymmetrical bending vibration, Al–O– coordination, Al–O–

Al is bending vibration, and in-plane Si–O–Si is stretching, respectively (Mu¨ller et al., 2014).

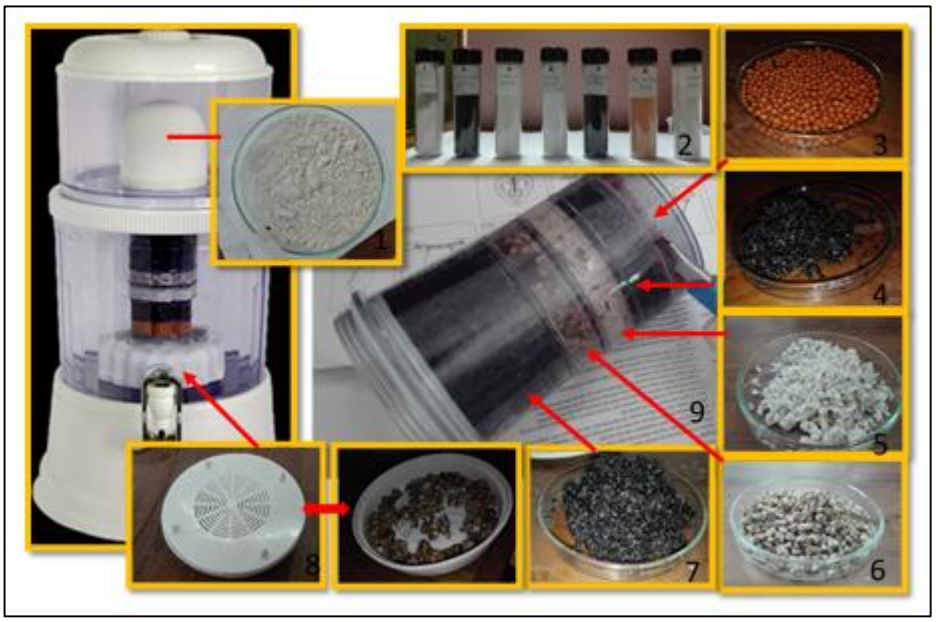

Figure 4.5: Structure of a seven-layer filter unit: 1. Ceramic dome, 2. The powdered clay filter unit, 3. Far infra-red ball, 4. Activated carbon, 5. Silica sand, 6. Mineral sand, 7. Silver impregnated granulated activated carbon, 8. Mineral filter -remineralisation unit, 9. Filter media unit and 10. Seven-layers filter unit

ESEM-EDAX analysis [Figure 4.5(b_i) & (b_{ii})] indicates the presence of carbon (C) (80.5%), O (15.7%), and Si (3.8%) on the surface of activated carbon. XRD patterns of the activated carbon layers [Figure 4.6(b)] show a peak at 26.6º, and different minerals in these layers were found as silicon dioxide, quartz, and a graphitic structure. FT–IR analysis (Figure 4.7) shows a broad peak at 1,300–1,000 cm^{-1}. The peaks are assigned to all carbon samples, with a mixed combination of –C–C–, –C=C–, –C–H stretches and –C–CH rocking vibrations (Mishra, 2016).

ESEM-EDAX analysis of mineral sand and mineral stones [Figure 4.5(c_i) & (c_{ii})] imply presence of oxygen (46.5%), silicon (28.6%), aluminum (12.2%), sodium (Na) (7.1%), calcium (3,4%), potassium (1.2%), and iron (Fe) (0.9%) on the mineral surface.

Mineral sand and mineral stones layers show similar XRD patterns [Figure 4.6(c) & (g)] and accounted that these two layers contained the same mineral type.

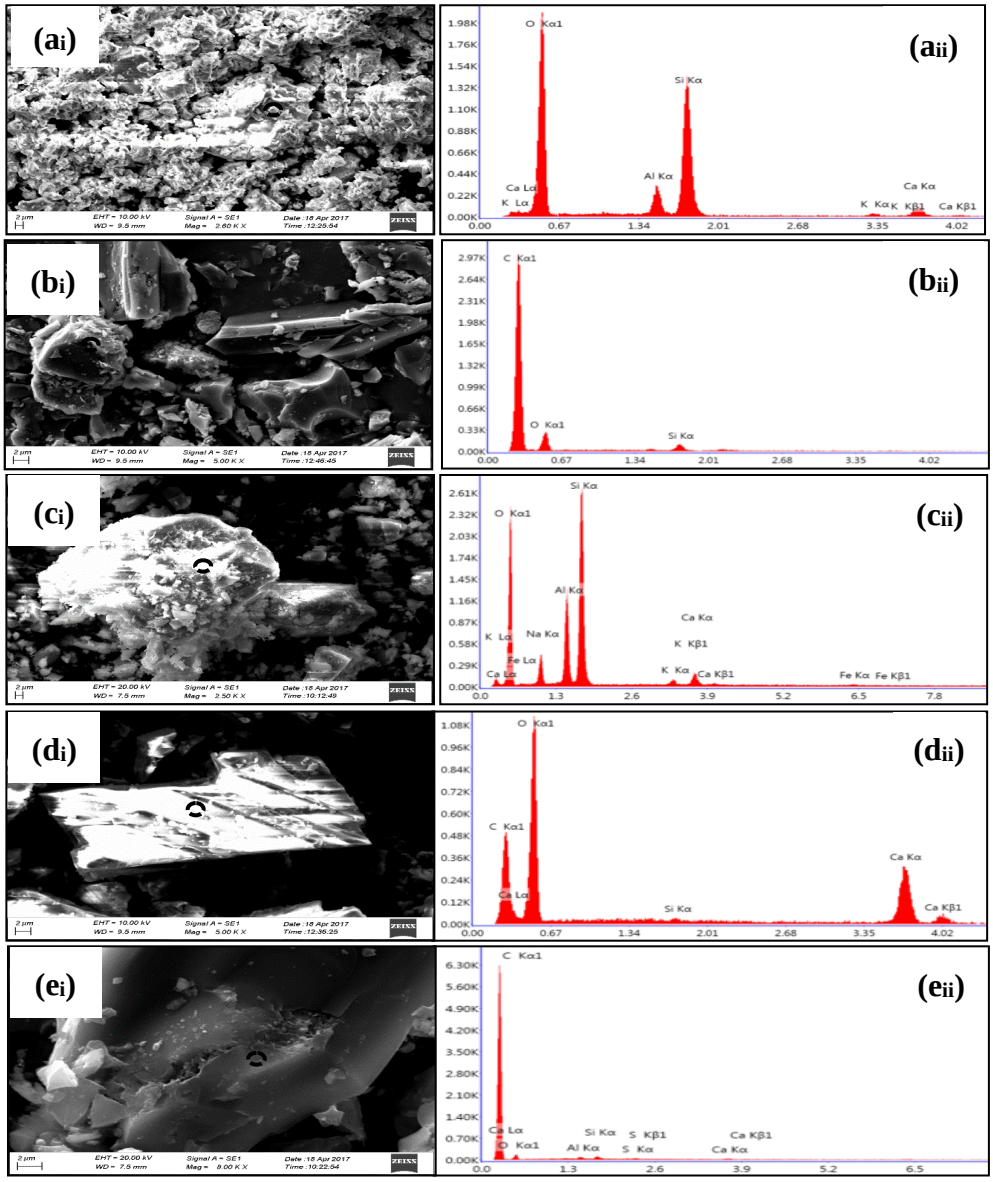

Figure 4.6: ESEM-EDAX analysis of different layers in seven-layer filter (a_i) & (a_{ii}) micro-ceramic filter dome, (b_i) & (b_{ii}) activated carbon and silver impregnated granular activated carbon, (c_i) & (c_{ii}) mineral sand, and minerals stones, (d_i) & (d_{ii}) silica sand, (e_i) & (e_{ii}) far-infrared balls

Two prominent peaks were found at 26.6º and 27.5º. Different crystalline phases can find in mineral sand and mineral stone layers such as Albite ($NaAlSi_3O_8$), Quartz (SiO_2), Magnesium carbon arsenide ($MgCAs_2$), Hexamethylene tetra selena fulvalene perfluoro tetra cyanoquinodi-methane ($C_{24}\ H_{12}\ F_4\ N_4\ Se_4$), Microcline ($KAlSi_3O_8$). FT–IR spectrum (Figure 4.7) illustrates peaks at 535 cm^{-1} due to Si–O– asymmetrical bending vibration, at 695 cm^{-1} due to Si–O– symmetrical bending vibration, at 775 cm^{-1} due to Si–O– symmetrical stretching vibration and at 1,037 cm^{-1} due to Si–O–Si symmetrical stretching vibration. The peaks at 3,695 cm^{-1}, 3,670 cm^{-1}, 3,650 $cm^{-1,}$ and 3,620 cm^{-1} confirm the availability of stretching vibration of inner surface –OH groups.

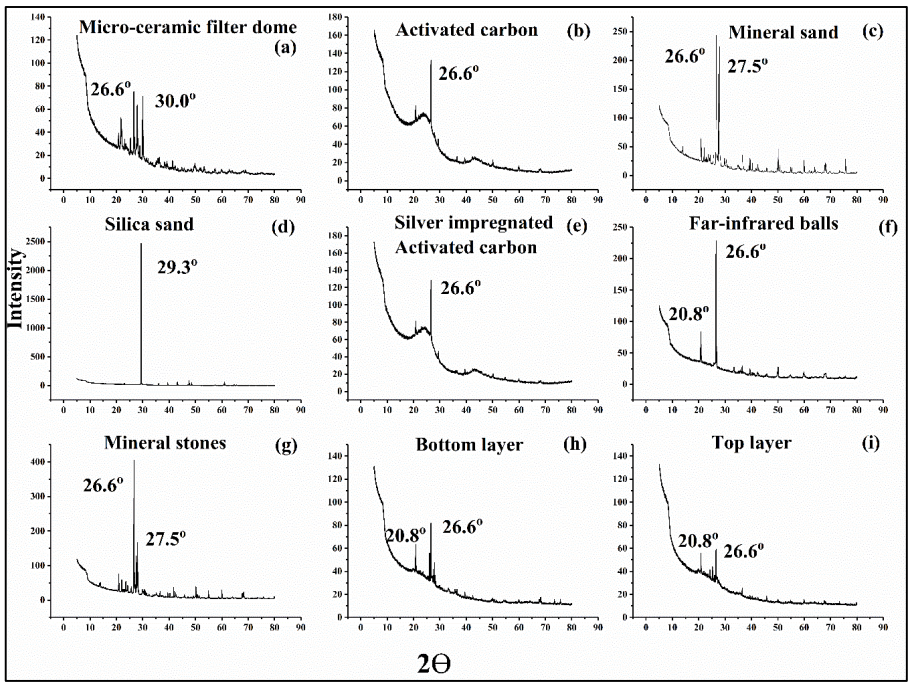

Figure 4.7: XRD analysis of the seven-layer and two-layer filter units

The ESEM-EDAX analysis of silica sand [Figure 4.5(d_i) & (d_{ii})] shows that the silica sand layer is mainly composed of O (48.2%), Ca (44.1%), C (7.3%), and Si (0.3%). The XRD pattern [Figure 4.6(d)] of the silica sand layer shows a prominent peak at 29.4º, and Ferro-gedrite ($Fe_5Al_4Si_6O_{22}(OH)_2$) is the leading mineral in the crystalline phase. FT–IR spectrum (Figure 4.7) indicates peaks at 1,395 cm^{-1} due to asymmetric

vibration of COO^{-} groups, at 872 cm^{-1} due to FeAl–OH vibration, at 738 cm^{-1} due to symmetric Si–O– vibration, at 642 cm^{-1} due to Al–O– coordination vibration, at 535 cm^{-1} due to Si–O– asymmetrical bending vibration (Sivakumar et al., 2012).

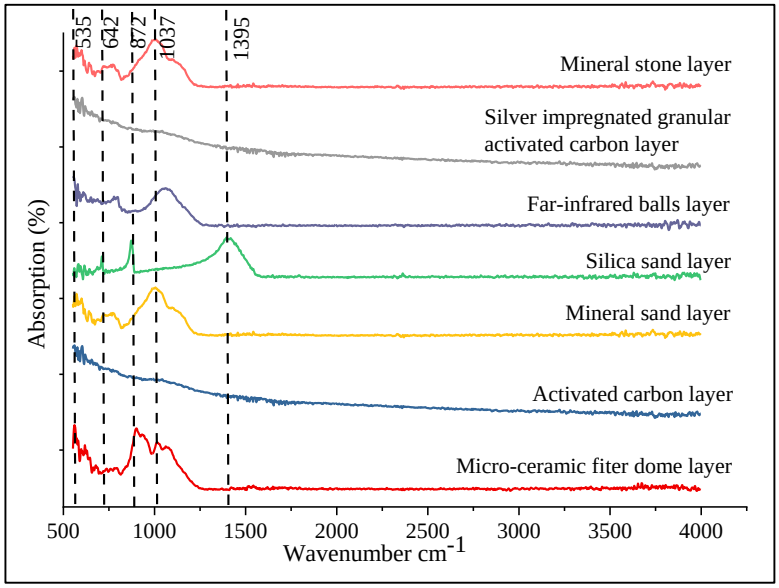

Figure 4.8: FT–IR analysis of the seven-layer filter unit

ESEM-EDAX analysis of far-infrared balls [Figure 4.5(e_i) & (e_{ii})] indicates presence of C (88.3%), O (10.3%), Si (0.6%), Al (0.5%), and sulphur (S) (0.2%). XRD pattern of far-infrared balls confirms the availability of different crystal phases such as [Figure 4.6(f)] di-chloroglyoxime ($C_2H_2Cl_2N_2O_2$), quartz (SiO_2), silicon dioxide (alpha–SiO_2), and 4–butyl 1, 2–di-phenylpyrazolidine 3, 5–dione ($C_{19}H_{20}N_2O_2$). The FT–IR (Figure 4.7) bands around 3,400–3,700 cm^{-1} are attributed to the Si–O–H and H–O–H molecules' stretching vibration. The peak at 1,055 cm^{-1} is assigned to stretching vibration of the symmetric Si–O–Si, and peaks at 789 cm^{-1}, 646 cm^{-1}, and the motion of silicon atoms was assigned to 610 cm^{-1}.

(b) Two-layer filter unit

The two-layer filter unit consists of top and bottom layers of clay mixture (Figure 4.8). ESEM-EDAX analysis [Figure 4.8(a)] of bottom layer indicate the availability of O

(45.8%), Si (31.9%) Al (20.7%), fluoride (f) (1.2%) and phosphorus (p) (0.4%). ESEM-EDAX analysis [Figure 4.8(b)] of the top layer corroborates that it is composed of different types of minerals calling silicon oxide (α–SiO_2), quartz (SiO_2), and gottardiite (natural zeolite).

Figure 4.9: Different components of clay water filter a) clay filter located with plumbing; b) a clay filter unit; c) the top layer of the filter unit and d) bottom layer of the filter unit

The XRD patterns of the bottom and top layers show that it is composed of albite ($NaAlSi_3O_8$), quartz (SiO_2), hydrogen aluminium silicate ($H_3(Al_3Si_{93})$, O_{192}) and derivatives of organic salicylic acid such as -2-hydroxybenzoic acid, 2-hydroxy-5-((2-nitrophenyl) azo), and 2-Hydroxy-5-((2-nitrophenyl) azo) salicylic acid ($C_{13}H_9N_3O_5$). The different peaks at 20.80°, 26.67° were attributed to quartz-type minerals [Figure

4.6(h) & (i)] and peaks at 27.52° and 27.95° for Albite, which were assigned to one of feldspar type minerals.

FT–IR (Figure 4.10) confirmed peaks at 650 – 1,200 cm^{-1} are due to the Si–O–Si bending and stretching vibration, respectively. The peak at 800 cm^{-1} is assigned to symmetric stretching of –Si–O (Mu¨ller et al., 2014), and 1087 cm^{-1} is due to the stretching vibration of symmetrical Si-O groups (Elhefnawy & Elabd, 2017). The broad peak at 3,451 cm^{-1} assigned to hydrogen-bonded –OH due to surface adsorbed water molecules, and the broad peak at around 1,632 cm^{-1} confirms further –OH bonding (Akl et al., 2013). The asymmetric stretching vibration around 2,375 cm^{-1} represents adsorbed $–CO_2$ molecules (Seiferth et al., 1999).

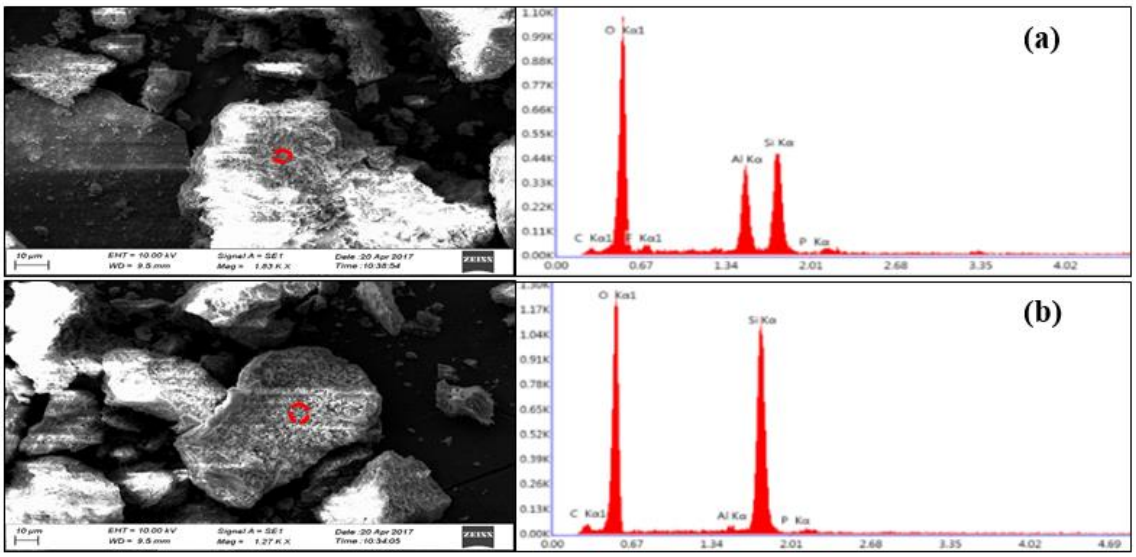

Figure 4.10: ESEM-EDAX analysis of clay filter (a) Bottom layer, and (b) Top layer

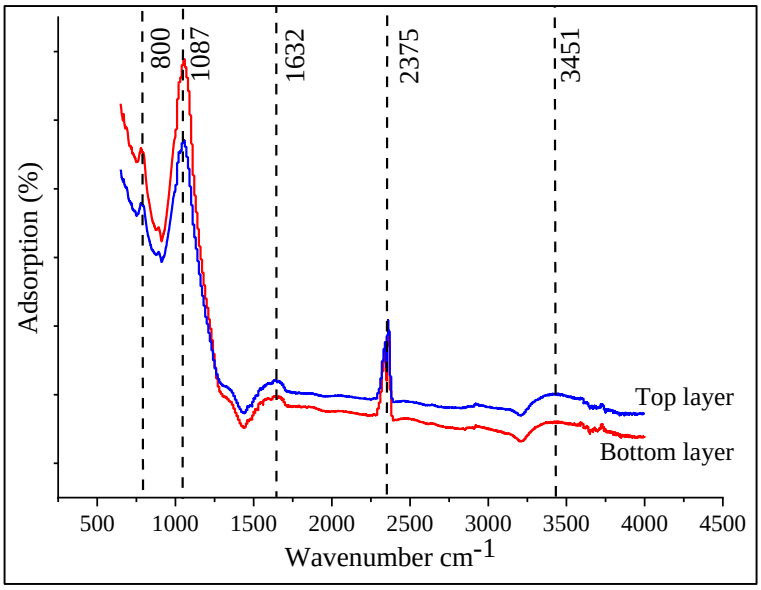

Figure 4.11: FT–IR analysis of the two-layer filter unit

The ESEM-EDAX, XRD, and FT–IR analysis results corroborated that the two-layer and seven-layer filters are composed of different mineral components. Different mineral components can treat potable water contained contaminants when the water passed through filter units. The acidic and alkaline salt in raw water taken from different surface and groundwater sources in CKDu prevalent areas may enhance the leaching of fluoride, calcium, magnesium, and other ions composed of minerals. Different conditions calling water temperature, macro and micronutrients and their concentrations in raw water, and percentages of elements present in minerals, can affect the mineral dissolution. The dissolution of minerals can increase the concentration levels of these elements in potable water. The results in removing fluoride and hardness using two- and seven-layer filter units indicated the dissolution of different elements from minerals composed in both filters.

4.2.4. Effectiveness of water filter units in removing hardness and fluoride

(a) Seven-layer filter unit

The experimental results (Figure 4.11) represent the removal effectiveness of the seven-layer filter in removing hardness during wet (two months) and extreme wet (one month)

seasons. It was observed that final hardness concentrations (in a range 312.0–357.0 mg/L) in treated water exceeded hardness values in the raw water (344.0 mg/L) after fifteen (15) days during the wet season. The hardness values (in the range 149.0–164.0 mg/L) in treated water were exceeded the raw water concentration (144.0 mg/L) throughout the extreme wet season. The hardness concentrations in the treated water do not comply with the reference value (120.0 mg/L) for hardness.

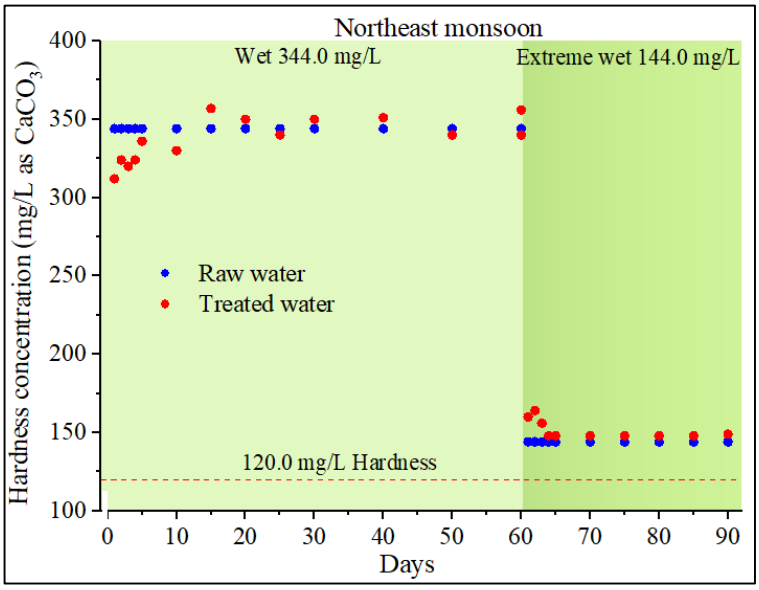

Figure 4.12: Removal effectiveness of the seven-layer filter unit in the removal of hardness

The results corroborated those different layers in a seven-layer filter unit composed of calcium and magnesium contained minerals [Wollastonite ($CaSiO_3$), Anorthite ($CaAl_2Si_2O_8$ Feldspar mineral), Magnesium carbon arsenide (MgCAs2)]. Weathering minerals consisting of different ions increases calcium and magnesium ions in treated water when the raw water passes through the filter unit. Besides that, a toxic heavy metal such as arsenic may be investigated in the treated water due to the effects of mineral weathering contained arsenic ion. The higher calcium and magnesium concentrations in the treated water corroborated further those dosages of activated carbon and other adsorbents in the filter unit cannot remove these elements from raw water contained high

hardness levels. Therefore, the treated water did not comply with the required drinking water standards considered in the study.

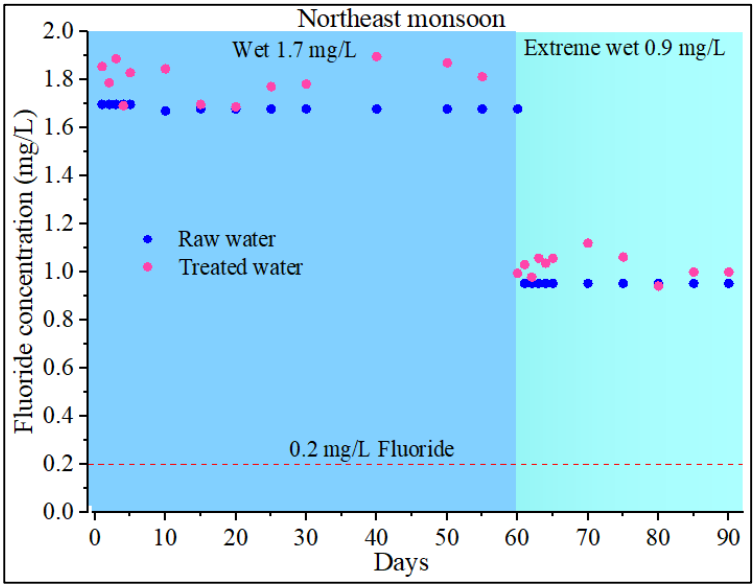

Figure 4.13: Removal effectiveness of seven-layer filter unit in the removal of fluoride

The experimental results illustrated in Figure 4.12 reveal the removal effectiveness of the seven-layer filter in removing fluoride during wet and extreme wet seasons. The final fluoride concentrations (in a range of 1.69–1.89 mg/L) in treated water exceeded fluoride values in the raw water (1.70 mg/L) even when the experiments started in the wet season. The fluoride values (in a range of 1.33–1.70 mg/L) in the treated water were surpassed the raw water concentration (0.90 mg/L) throughout the extreme wet season. The fluoride concentrations in the treated water do not comply with the reference value (0.20 mg/L) for fluoride considered in the study, WHO guideline (1.50 mg/L), and Sri Lankan standards (1.00 mg/L).

The results agreed that different layers in a seven-layer filter unit composed of fluoride contained minerals ($C_{24}H_{12}F_4N_4Se_4$). Mineral sand and mineral sandstones layers in seven-layer filter consist of fluoride contained minerals. Weathering minerals

consisting of fluoride increases fluoride concentrations in treated water when the raw water passes through the filter unit. The higher fluoride concentration in treated water corroborated those adsorbents in the filter unit do not remove fluoride from the raw water. Fluoride ions available in raw water and fluoride ions generated due to the dissolution of minerals in the filter contribute to the final fluoride concentration in the treated water.

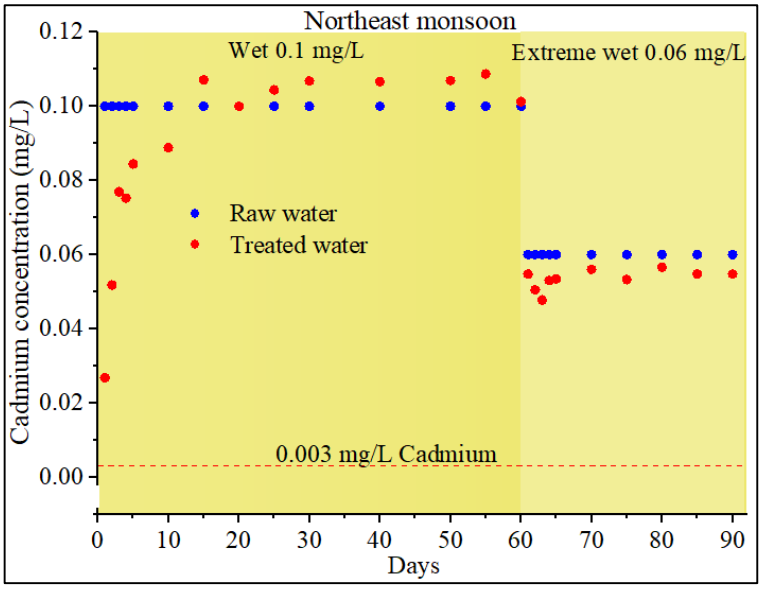

Figure 4.14: Removal effectiveness of seven-layer filter unit in the removal of cadmium

The experimental results shown in Figure 4.11 confirmed the removal effectiveness of the seven-layer filter in removing cadmium during wet and extreme wet seasons. The final cadmium concentrations (in a range of 0.03–0.11 mg/L) varied in treated water during the wet season. At the beginning of the experiment (for 15 days), the seven-layer filter unit removed cadmium (percentage of removal 73.2%–11.2%) in raw water considerably. Later, cadmium concentration in treated water exceeded cadmium values in the raw water (0.10 mg/L) during the wet season. The higher cadmium levels in the treated water may be due to cadmium adsorbed can detach from the surface of materials and react with fluoride ions in solution and ion-pair CdF^{+} which appears as “sodium-

like" ion (Wasana et al., 2017; Dharma-wardana, 2018). The removal of cadmium (in a range 0.04–0.05 mg/L) was observed during the extreme wet season due to cadmium ions and ions pair (CdF^+) attach to the active adsorption sites formed newly by leaching of calcium and magnesium ions from minerals contained in the seven-layer filter. However, the cadmium concentrations in the treated water do not comply with the reference value (0.003 mg/L) for cadmium considered by the study.

The results of one sample t-test illustrated that mean values of fluoride (1.44 ± 0.39), hardness (256.83 ± 96.26), and cadmium (0.07 ± 0.02) are significantly different (hardness: $t_{13.50}$, df 23, $p > 0.05$, fluoride: $t_{17.71}$, df 23, $p > 0.05$, cadmium: $t_{13.57}$, df 23, $p > 0.05$) from the reference levels considered in the study, values are not equal to the reference values (null hypothesis was rejected). Therefore, the treated water does not comply with the required drinking water standards considered in the study. The higher concentrations of fluoride and hardness decrease filter performance within a short duration. The study's key findings corroborated that the seven-layer filter unit is not effective in removing fluoride, cadmium, and hardness in potable water.

(b) Two-layer filter unit

The experimental results depicted in Figure 4.14 represent the removal effectiveness of the two-layer filter in removing hardness during wet (two months) and extreme wet (one month) seasons. The final hardness concentrations (in a range of 328.0–352.0 mg/L) in treated water exceeded hardness concentrations in the raw water (344.0 mg/L) after 25 days in the experiment during the wet season. The hardness concentrations (in a range 140.0–152.0 mg/L) in the treated water for the first two days during the extreme wet season were exceeded hardness concentration in the raw water (144.0 mg/L), and later final hardness concentrations in the treated water were observed less than the initial hardness concentrations in raw water. However, the hardness concentrations in treated water do not comply with the reference value (120.0 mg/L) for hardness considered in the study.

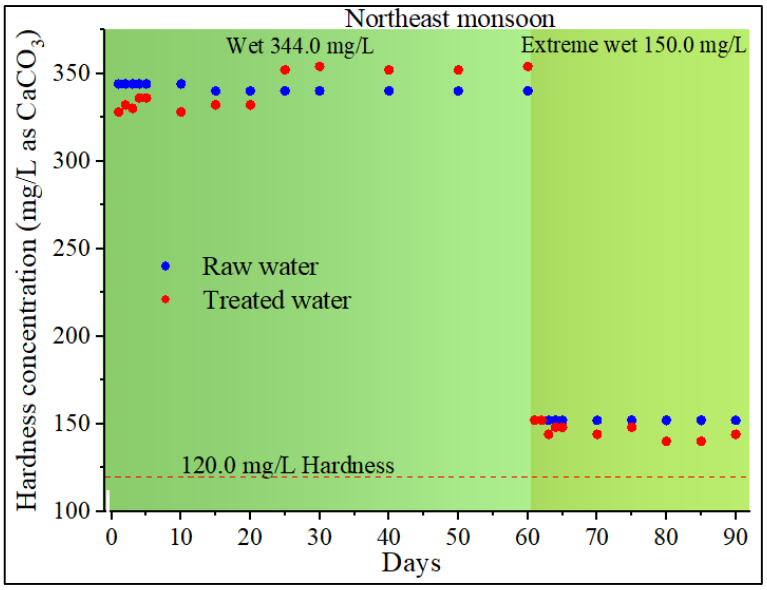

Figure 4.15: Removal effectiveness of two-layer filter unit in the removal of hardness

The results corroborated that top and bottom parts in a two-layer filter composed of calcium and magnesium contained minerals gottardiite (Natural zeolite) ($Na_3Mg_3Ca_5Al_{19}Si_{117}O_{272}$). Weathering of minerals consist of calcium and magnesium increasing ion concentrations in the water treated when raw water passes through the filter. The lower concentrations of hardness in the raw water were removed slightly during the extreme wet season. The higher calcium and magnesium concentrations in the treated water corroborated further that adsorbent in the filter unit cannot remove the higher levels of hardness from raw water.

The experimental results depicted in Figure 4.15 corroborates the fluoride removal effectiveness of the two-layer filter unit during the wet and extreme wet seasons. Initially, the treated water's fluoride concentrations were observed as 0.00 mg/L for five days and later, the concentrations gradually increased up to 1.33 mg/L during the wet season. The fluoride values exceeded the initial fluoride concentration in the raw water during wet (In a range of 1.16–1.70 mg/L) and the extreme wet season (0.90 mg/L). The fluoride concentrations in the treated water do not comply with the reference value (0.20 mg/L) for fluoride considered in the study, WHO guideline (1.50 mg/L), and Sri Lankan

standards (1.00 mg/L). The increment of fluoride concentrations during the extreme wet season may be observed as a detachment of fluoride adsorbed from different minerals in the top and bottom layers with the lower fluoride concentrations in raw water.

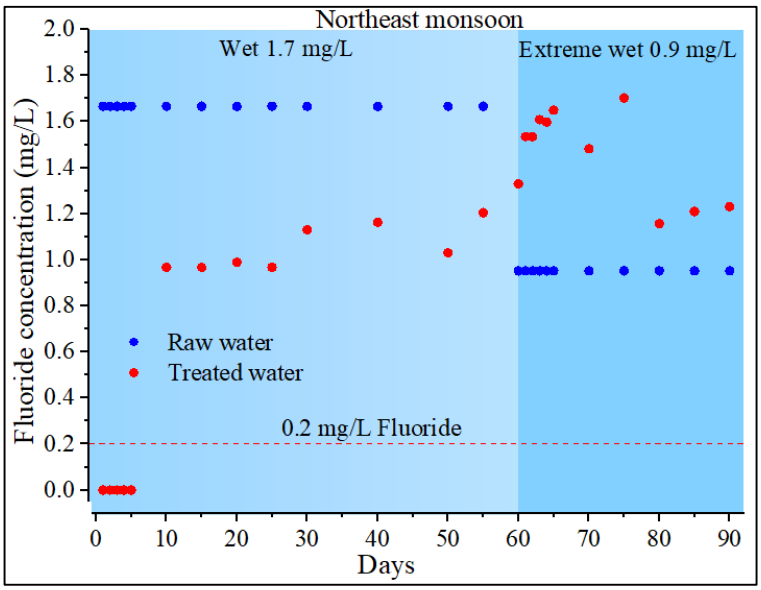

Figure 4.16: Removal effectiveness of two-layer filter unit in the removal of fluoride

Moreover, the raw water consists of a higher content of calcium, magnesium, and cadmium ions. These ions have been shown a high affinity towards fluoride ion (Sevonkaev & Matijević, 2009; Dharmawardhana et al., 2014) and investigated pairing effects for calcium, magnesium, and cadmium ions with fluoride as CaF^+, MgF^+, and CdF^+ (Wasana et al., 2017; Dharma-wardana, 2018). The paring effects of fluoride with cations in raw water may increase the fluoride concentrations in water treated during the extreme wet season. The two-layer filter unit is not effective in the removal of fluoride in potable water.

The experimental results shown in Figure 4.16 indicate the removal effectiveness of the two-layer filter in removing cadmium during wet and extreme wet seasons. The final cadmium concentrations varied in a range of 0.006–0.049 mg/L in treated water during

the wet season. The two-layer filter unit removed cadmium (percentage of removal during wet season varied 93%–30% and the extreme wet season 88%–63%) in the raw water considerably. The substantial removal of cadmium during the wet and extreme wet season may be investigated due to cadmium ions and ions pair (CdF^{+}) attached to the active adsorption sites formed newly by leaching calcium magnesium ions from minerals contained in the two-layer filter. However, the cadmium concentrations in the treated water do not comply with the reference value (0.003 mg/L) for cadmium considered by the study.

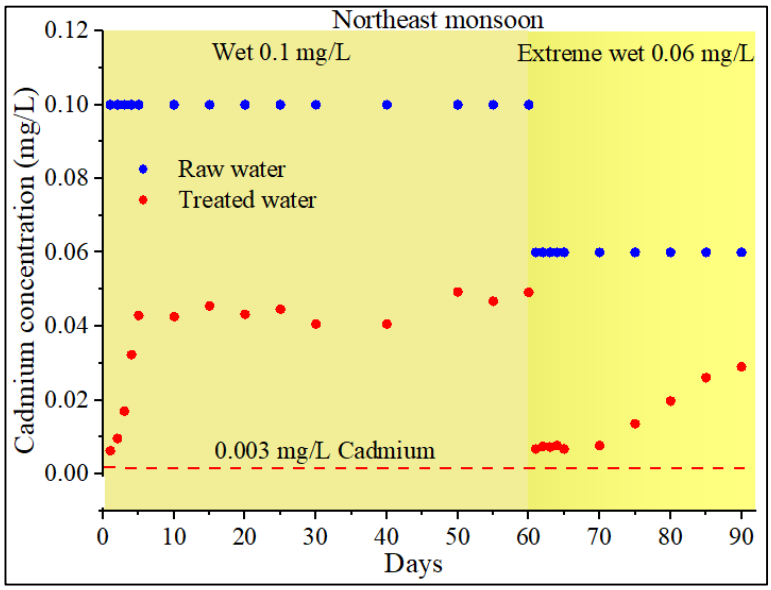

Figure 4.17: Removal effectiveness of two-layer filter unit in the removal of cadmium

The results of one sample t-test corroborated that mean values of fluoride (1.02 ± 0.58), hardness (260.29 ± 94.43), and cadmium (0.03 ± 0.02) are significantly different (hardness: $t_{12.91}$, df 23, $p > 0.05$, fluoride: $t_{8.59}$, df 23, $p > 0.05$, and cadmium: $t_{7.04}$, df 23, $p > 0.05$) from reference levels considered in the study, values are not equal to reference values (null hypothesis was rejected). The treated water does not comply with required drinking water standards considered for fluoride 0.20 mg/L, hardness 120.00 mg/L, and cadmium 0.003 mg/L in the study. The higher concentrations of fluoride and hardness

decrease filter performance within a short duration (one month). The two-layer filter unit is not effective in removing fluoride, cadmium, and hardness in potable water.

(c) RO filter unit

The experimental results depicted in Figure 4.17 corroborates the RO filter unit's hardness removal effectiveness during the different seasons. When the hardness concentrations in raw water (100.0–1,500.0 mg/L) were increased in different seasons, hardness as $CaCO_3$ in RO treated water increased gradually until the 180^{th} day. Hardness concentrations were observed significantly lower in treated water during extreme wet (8.0–11.0 mg/L), wet to dry (11.0–24.0 mg/L), dry (28.0–40.0 mg/L), and about 18 days of extreme dry (48.0–52.0 mg/L) seasons. In the latter part of the extreme dry season, hardness concentration (88.0–184.0 mg/L) in the treated water was gradually increased, exceeding the reference value for hardness (120.0 mg/L) in the study, significantly different from the reference value ($p > 0.05$). During the extreme dry season, hardness concentration fluctuated considerably even though the initial raw water concentration was the same throughout the season. Calcium and magnesium ions (consisting of hardness) may effectively retain granular activated carbon with specific chemical and morphological attributes such as acidic and basic functional groups and micropores and mesoporous structure (Liu et al., 2015). Besides that, the RO membrane's pore sizes have been reported to be within the range of 0.5–2.0 nm (Conidi et al., 2020). Hence, the RO membrane retains effectively high ionic radius calcium and magnesium in raw water even after detaching from the pre-activated carbon filter. The removal effectiveness of the RO filter unit in removing cadmium in potable water was not conducted due to the study's limitation (refer to section 4.2.7).

The RO filter with the lower hardness concentrations could remove hardness effectively for about six months if a RO filter was used at the beginning of extreme wet, wet and wet to dry seasons. Consumption of RO treated water during wet seasons with the lower hardness concentrations is not suitable as potable water as the treated water contained significantly lower concentrations of micronutrients in water (Hardness <<<

120.0 mg/L). However, if the RO filter was started to filter the potable water during the extreme dry season, the removal of hardness becomes less effective within three weeks.

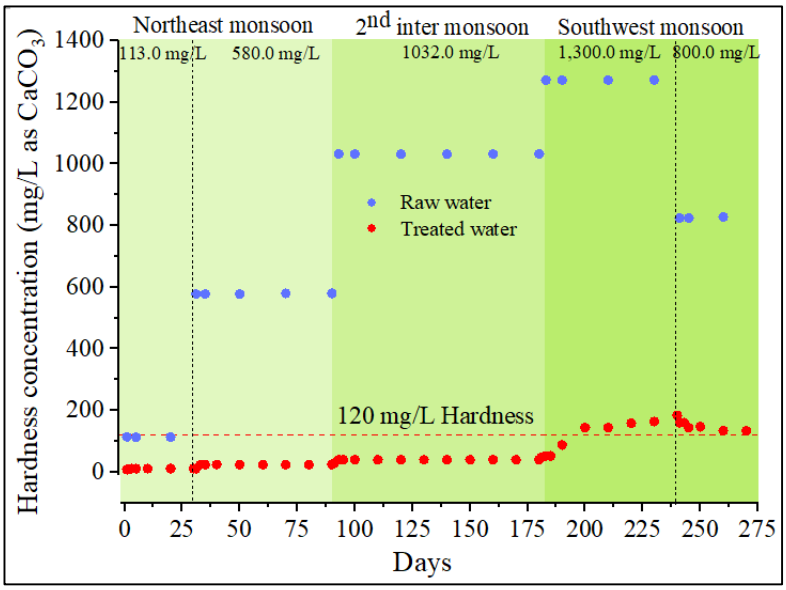

Figure 4.18: Removal effectiveness of RO filter unit in the removal of hardness

The laboratory experiments conducted using a domestic RO filter unit to remove fluoride are depicted in Figure 4.18. Fluoride concentrations in the RO treated water increased gradually when the fluoride concentrations increased in raw water from 0.5 mg/L to 16.0 mg/L. A more significant fluctuation of fluoride concentrations (0.15–1.68 mg/L) in RO treated water was observed during the extreme dry season as there was a higher concentration of fluoride in the raw water. The average fluoride concentration in the treated water was higher during the 2nd dry season (0.83 mg/L) than the 1st dry season (0.38 mg/L). The results showed that the removal capacity of the RO filter in removing fluoride was decreased after both extreme wet and wet to dry seasons (percentage of fluoride removal decreases from 100% to 88%). The polyamide thin-film RO membrane is charged negatively (Xu et al., 2005). Hence, the intensive removal of fluoride ions can be observed in terms of electrostatic repulsion of negatively charged fluoride ions in raw water by RO membrane (Radjenovic et al., 2008).

Fluoride concentration in the RO treated water after these two seasons [extreme wet (one month) and wet to dry (two months)] exceeded the reference value considered (0.2 mg/L) in the study. The RO filter with the lower fluoride concentrations could effectively remove fluoride for about five months if a RO filter was started to use at the beginning of extreme wet, wet and wet to dry seasons. Consumption of RO treated water during wet seasons with lower fluoride concentrations is suitable for people affected with CKDu. Nevertheless, if the RO filter was started to filter the potable water during the dry season, fluoride removal becomes less effective within one month. The mean value of fluoride (0.37 ± 0.36 mg/L) for one sample t-test nullified the null hypothesis of the study, corroborating that the mean value of fluoride is significantly varied from the reference value of fluoride 0.2 mg/L ($p > 0.05$). However, the raw water with the lower fluoride concentration meets the reference value for fluoride (0.20 mg/L). Therefore, the RO filter is most suitable to remove lower concentrations of fluoride in potable water.

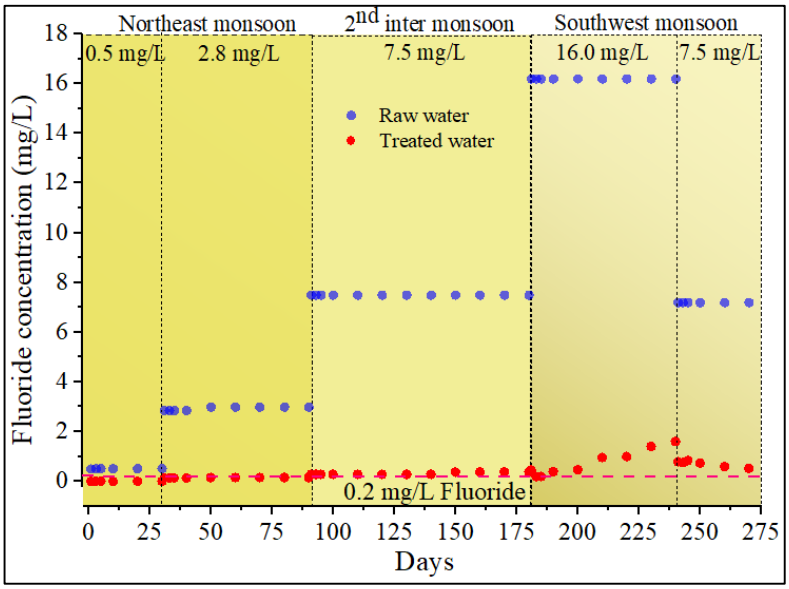

Figure 4.19: Removal effectiveness of RO filter unit in the removal of fluoride

The experimental results show that RO, two-layer, and seven-layer filter units are not suitable to provide safe potable water for people in CKDu prevalent areas. RO units remove many calcium and magnesium ions in the raw water and retain significantly

lower residual hardness concentrations in the RO treated water. Calcium and magnesium are macronutrients in the water, playing the most beneficial role in human health. Intake of low content of calcium and magnesium ion for the long run may bring adverse health effects. People in CKDu areas may receive low nutrients from foods due to the consumption of less nutritious food.

In some cases, people often have one meal per day which are not nutritionally balanced (findings of the household survey). Hence, the use of RO water, in the long run, seems not a suitable solution for the CKDu. RO treated water will make people vulnerable to different diseases, which brings up the lower content of beneficial macro and microelements in potable water for the long run.

The two-layer filter unit is most suitable for removing low ion concentrations in groundwater since the filter does not effectively remove high ion levels. The seven-layer filter unit is ineffective in removing fluoride and hardness in groundwater. The dissociation of clay and non-clay minerals in filter material has increased ion concentrations in the treated water. Thus, ion concentrations in the treated water exceed the acceptable drinking water standards. Hence, the seven-layer filter unit is not suitable to treat surface and groundwater in CKDu prevalent areas. The filter unit is appropriate to remove water with low ions concentration in non-CKDu affected areas.

4.2.5. Performance evaluation of the existing water purification units

The results of the performance evaluation of available water filter units in CKDu prevalent areas represent in Table 4.3. A domestic water filter unit used by households should provide daily potable water requirements for all family members. The water filter units' capacity implied that they satisfy households' daily potable water requirement (2.0 L per person/day). Poor taste characteristics of the RO treated water decreased the organoleptic properties of drinking water. People expressed their hatred for drinking such kind of water with poor taste. The water filter users do not have the proper technical know-how to conduct O & M activities. The high content of organic and

inorganic substances in CKDu prevalent areas' feed water increases scaling and clogging in the filter bed.

Table 4.3: Key performance indicators considered to evaluate the performance of water filters available in CKDu prevalent areas

	Performance indicators	RO unit	Two-Layer	Seven-layer
Performance-based on user response				
1	Does the filter unit treat water more than a daily requirement? (4 members x 2 L/day/person = 8 L/day)	Yes (92%)	No (80%)	No (76%)
2	Does the storage capacity of the filter provide treated water for several days?	No (90%)	Yes (100%)	No (74%)
3	Does the filter rate facilitate a supply of 0.25 L (1 cup) of treated water after emptying the storage tank?	Yes (92%)	No (71%)	No (96%)
4	Is the taste of the treated water palatable?	No (74%)	Yes (82%)	Yes (90%)
5	Is O & M easy to carry out? If yes, do you have enough technical know-how to conduct O & M?	No (96%)	Yes (80%)	Yes (74%)
6	Do filter media/ RO membranes have the properties of durability for the use of the long term?	No (97%)	No (52%)	No (76%)
7	Does slim layer formation on the surfaces of the filter unit occur while the filter unit is used?	Yes (52%)	Yes (75%)	Yes (87%)
8	Are facilities available for replacement of filter's parts enough to conduct O & M?	No (100%)	No (96%)	No (100%)
9	Are there any facilities available for the management of reject water?	No (96%)	Not applicable	Not applicable
10	Does clogging of the filter unit happen frequently, and the system gets often failed to operation?	Yes (94%)	No (100%)	Yes (90%)
Performance-based on laboratory experiments				
11	Is treated water comply with 0.2 mg/L of fluoride?	No (Exceeded)	No (Exceeded)	No (Exceeded)
12	Is treated water comply with 120 mg/L of hardness?	No (trace level of hardness)	No (Exceeded)	No (Exceeded)
13	Is treated water comply with 0.003 mg/L of cadmium?	Yes	No (Exceeded)	No (Exceeded)
14	Is treated water comply with 0 CFU/100 mL of feacal coliform?	Yes	Yes	yes

In many cases, after O & M requirements popped up frequently and the cost of regular O & M is elevated, people abandoned the domestic RO units and shifted to purchase treated water from commercial RO units (20%). The rest (10%) of people fetch water from spring well water far away from their residencies, and others (70%) depend on protected well (Public health officer has recommended water in a protected well suitable for drinking purposes) closed to their residencies. Two-layer and seven-layer filter units were not produced the required amount of potable water for daily household use (drinking and cooking). These filters have simple O & M activities that can handle by households. The monitoring programs were not conducted after introducing how these filter units performed in CKDu prevalent areas. The data regarding the performance evaluation of available filter units were not found in the literature. Hence, according to the research gap, performance evaluation of available water filter units in CKDu areas brings great understanding to investigate a multi-layer filter unit to remove nephrotoxic risk factors in potable water.

4.2.6. Key findings of objective 02

- Different water filters such as two-layer, seven-layer and RO filter units have been introduced to CKDu prevalent areas. RO filters are the most popular filter unit. The treated water produced from the commercial RO unit is purchased often by people in CKDu affected areas.
- Adsorbents in two- and seven-layer filter units consist of calcium, magnesium, and fluoride contained minerals. The dissolution of these minerals increases concentration levels in the treated water that exceeded the reference values of hardness (120.0 mg/L) and fluoride (0.2 mg/L) in drinking water.
- The two-layer filter unit is most suitable for removing low ion concentrations in groundwater since the filter does not effectively remove high ion levels. The seven-layer filter unit is ineffective in removing fluoride and hardness in groundwater.
- The RO unit removes essential micronutrients such as calcium and magnesium in raw water significantly. The calcium and magnesium concentrations that

remained in treated water were investigated as very low during extreme wet (8.0–11.0 mg/L), wet to dry (11.0–24.0 mg/L), and dry (28.0–40.0 mg/L) seasons. Long-term water intake with a trace level of beneficial ions brings up adverse health effects to people. CKDu affected and non-affected people consume RO treated water. They are vulnerable to other health hazards due to the lower intake of beneficial elements in drinking water for the long run.

- The domestic RO filter with lower fluoride (≤ 2.8 mg/L) and hardness (≤ 580.0 mg/L as $CaCO_3$) concentrations can effectively remove fluoride and hardness for about five and six months, respectively, if the filtration of RO filter was started at the beginning of extreme wet, wet and wet to dry seasons. However, if the RO filter was started to filter the potable water during dry (fluoride > 7.5 mg/L and hardness > 1,000.0 mg/L as $CaCO_3$) and extremely dry (fluoride ≥ 16.0 mg/L and hardness ≥ 1,300.0 mg/L as $CaCO_3$) seasons, the removal of fluoride and hardness becomes less effective within one month and three weeks, respectively.
- The mean values fluoride, hardness, and cadmium in treated water of RO, two-, and seven-layer filter units are significantly higher than the reference value of potable water for fluoride (0.2 mg/L), hardness (120.0 mg/L), and cadmium (0.003 mg/L) considered in the study ($p > 0.05$). The results corroborated that RO, two-, and seven-layer filter units are not suitable for providing safe potable water for people in CKDu prevalent areas.

4.2.7. Limitation of the study

- Names of entrepreneurs who introduced water filter units to CKDu affected areas were not maintained in the government office or office bearers in community-based organisations operated in the areas.
- The household survey was limited to the two villages in the Anuradhapura district. Hence, the limited number of different filter units introduced in CKDu areas were investigated during the household survey. All households had water filters that said different filter units had been introduced by governmental and non-governmental organizations in the area.

- Households abandoned most domestic RO units due to clogging and failure in operation. It was challenging to examine the domestic RO unit's operational data during the study, as most domestic RO units were abandoned.
- The minimum detection limit was limited to 0.25 mg/L in the analytical instrument (AAS) for cadmium. The instrument was the failure to operate in the middle of the RO unit studies. Hence, the cadmium removal effectiveness of the RO filter unit was not studied. To overcome the limitation commercial ICP-MS instrument was hired for the data analysis in the rest of the experiments. The cost and time taken for the sample analysed were limiting factors in the cadmium study.
- The study on the removal effectiveness of two- and seven-layer filter units was limited to the extreme wet and wet season. The treated water exceeds the reference values for fluoride and hardness with lower concentrations.

4.3. Objective 03: Assessment of health risk of people who consume potable water from such commercially available units in CKDu prevalent areas

4.3.1. Characterization of raw, treated and reject water in commercial RO

The results of the descriptive statistics on water quality parameters are present in Table 4.4 for commercial RO units. The result showed that raw water fed into commercial RO units during the wet season could classify under "hard" water while the rest of raw water samples comes under the "very hard" according to USGS hard water classification (USGS, 2012). The percentage of hardness removal by commercial RO unit ranged from 79 to 99%, representing a low concentration of hardness in treated water. Hardness concentration in treated water during the dry season (mean 28.00 ± 14.78) is significantly different compared to hardness concentration (8.00 ± 1.50) in the treated water during the wet season ($P < 0.05$), rejecting the null hypothesis. There is no significant correlation between hardness concentrations between raw and treated water, while raw (t = 0.11) and rejected water (t = 0.68) have weak, positive, and negative correlations, respectively, during wet and dry seasons. People consume water with a considerably low level of hardness during the wet season, leading to adverse health effects due to fewer macronutrients required for a healthy life. Past studies have reported that 0.0–200.0 mg/L of hardness may bring hypertensive disease, atherosclerotic heart disease (hardening arteries), and stroke-like all cardiovascular disease (Comstock, 1971). A study further said that less than 75.0 mg/L of hardness has been reported for risk of ischemic heart disease, which causes chest pain, heart attack, and this disease has been recorded to reduce the blood supply to the heart (Yang, 1998). According to past studies, either the high or low levels of hardness in the potable water seem to bring adverse health effects on a human differently. However, RO units remove high concentrated hardness in water, reporting a low amount in the treated water that discourages additional calcium and magnesium supply. The total alkalinity as $CaCO_3$ in the treated water complied with the Sri Lankan standards for potable water (200.0 mg/L). Total suspended solids values are considerably decreased compared to the Sri Lankan standards (25.0 mg/L).

Table 4.4: Water quality characteristics of raw, treated and rejected RO water

RO water characteristics	Wet season			Dry season		
	Minimum	Maximum	Mean	Minimum	Maximum	Mean
Hardness Raw (mg/L)	112.00	152.00	126.00 ± 17.74	176.00	800.00	493.33 ± 224.95
Hardness Treated (mg/L)	8.00	8.00	8.00 ± 0.00	8.00	80.00	36.00 ± 31.49
Hardness Rejected (mg/L)	136.00	224.00	176.00 ± 42.83	216.00	1,200.00	600.00 ± 345.17
Alkalinity as $CaCO_3$_Raw (mg/L)	700.00	1,700.00	1,025.00 ± 457.35	1,100.00	4,400.00	3,283.33 ± 1,137.39
Alkalinity as $CaCO_3$_Treated (mg/L)	100.00	200.00	150.00 ± 57.74	100.00	300.00	183.33 ± 75.28
Alkalinity as $CaCO_3$ Rejected (mg/L)	1,000.00	2,300.00	1,350.00 ± 635.09	1,100.00	5,100.00	3,883.33 ± 1,467.54
TSS Raw (mg/L)	3.00	11.00	5.50 ± 3.69	5.00	14.00	7.33 ± 3.39
TSS Treated (mg/L)	0.00	1.00	0.50 ± 0.58	0.00	15.00	5.00 ± 5.25
TSS Rejected (mg/L)	1.00	5.00	2.00 ± 2.00	2.00	28.00	8.83 ± 9.68
Fluoride Raw (mg/L)	0.65	0.80	0.71 ± 0.03	0.65	1.45	1.20 ± 0.29
Fluoride Treated (mg/L)	0.35	0.40	0.39 ± 0.03	0.25	0.55	0.42 ± 0.12
Fluoride Rejected (mg/L)	0.70	0.80	0.75 ± 0.04	0.70	2.40	1.41 ± 0.56
Calcium Raw (mg/L)	391.90	545.40	489.10 ± 72.54	33.10	690.90	341.07 ± 278.68
Calcium Treated (mg/L)	0.40	1.10	0.88 ± 0.32	1.30	4.30	2.42 ± 1.21
Calcium Rejected (mg/L)	516.40	988.80	820.60 ± 208.23	151.10	826.40	484.45 ± 248.57
Magnesium Raw (mg/L)	10.80	27.50	20.28 ± 7.89	13.50	218.20	124.65 ± 77.42
Magnesium Treated (mg/L)	0.20	2.40	0.90 ± 1.01	0.20	7.50	2.13 ± 2.70
Magnesium Rejected (mg/L)	24.40	59.40	34.43 ± 16.75	15.90	261.50	147.03±112.82
Cadmium Raw (mg/L)	ND	ND	ND	ND	ND	ND
Cadmium Treated (mg/L)	ND	ND	ND	ND	ND	ND

Cadmium Rejected (mg/L)	ND	ND	ND	ND	ND	ND
pH Raw	6.68	7.28	7.02 ± 0.29	7.13	7.46	7.31 ± 0.11
pH Treated	6.70	7.49	7.17 ± 0.36	6.91	7.56	7.29 ± 0.22
pH Rejected	6.78	7.27	7.05 ± 0.25	7.12	7.34	7.27 ± 0.08
Conductivity Raw (µs/cm)	392.00	505.00	424.25 ± 53.97	294.00	2,580.00	1,658.50 ± 880.78
Conductivity Treated (µs/cm)	27.90	58.60	42.50 ± 12.89	91.70	450.00	186.68 ± 135.12
Conductivity Rejected (µs/cm)	427.00	634.00	528.75 ± 84.55	395.00	3,290.00	1,996.00 ± 1,095.27
Turbidity Raw (NTU)	0.44	3.55	1.34 ± 1.48	0.38	1.74	0.91 ± 0.55
Turbidity Treated (NTU)	0.25	0.58	0.41 ± 0.14	0.23	11.05	2.14 ± 4.37
Turbidity Rejected (NTU)	0.45	2.36	0.97 ± 0.93	0.46	0.94	0.72 ± 0.17

The fluoride concentrations in RO treated water exceed the reference values for fluoride in the study (0.2 mg/L). Consumption of less than 1.0 mg/L of fluoride has been increased the risk of osteoporosis, reduced bone density, collapsed vertebrae in women and visible calcification of the aorta in men (Bernstein et al., 1996). According to Dissanayake (2005), different fluoride levels have been affected by severe fluorosis of skeletal in different ways, concluding the significance of sufficient fluoride intake that meets required drinking water guidelines. Percentages of fluoride ion removed were ranged between 38.5 to 80.8% in the commercial RO units. The fluoride removal percentages were reported less than the several studies conducted to remove fluoride using RO units. A study performed in the Ethiopian rift region showed that fluoride removal with RO membranes ranged between 94 to 99% (Assefa, 2006). Fluoride removal in brackish groundwater was performed with a low-pressure RO unit in a Senegal study, and 97 to 98.9% of fluoride rejection was observed (Diawara et al., 2011). A study conducted with a polyamide RO membrane in Chandrapur district, India, showed 95 to 98% fluoride removal from groundwater (Gedam et al., 2012). The fluoride concentration in treated water during the dry season (mean 0.45 ± 0.14) is not significantly different compared to the fluoride concentration (0.39 ± 0.03) in the treated

water during the wet season ($P > 0.05$). The result accepted the null hypothesis that "values of fluoride concentrations in treated water are equal during the dry and wet season" and rejected the alternative hypothesis. There is a weak and negative correlation (t = -0.246) between mean values of fluoride concentrations in treated water while raw (t = 0.132) and rejected water (t = 0.028) have weak and strong, positive correlation, respectively, during wet and dry seasons.

The results of calcium in RO treated water indicated that a low calcium ion content remained in the treated water compared to the calcium content in the raw water during wet and dry seasons. Calcium ion removal efficiencies ranged from 87 to 99.9% for RO units. Inadequate intake of calcium ions leads to adverse health effects such as osteoporosis, kidney stones, colorectal cancer, hypertension, coronary artery diseases, insulin resistance, and obesity (WHO, 2017). According to WHO, 2009, adequate calcium consumption has reduced elevated blood pressure in some people. That meant inadequate consumption may enhance the risk of elevated not only blood pressure but also increase the risk of osteoporosis, nephrolithiasis (Kidney stones), colorectal cancer, hypertension, stroke and coronary artery disease, insulin resistance and obesity (WHO, 2009) (Gaurav et al., 2014). The imbalance of calcium in the human body has been promoted hormonal changes in calcium and phosphorus metabolism (Kozisek, 2005) that could affect bone health and bone density (Bo¨hmer et al., 2000). In addition to that, low calcium intakes have been increased bone mass during the growth, reduce bone loss and fracture risk for adult age. Calcium has been recorded to be interacted with iron, zinc, magnesium and phosphorous in the intestine and reduce these minerals' absorption. The intake of sufficient amounts of dietary calcium has reduced cardiovascular risk (Allender et al., 1996). The long-term consumption of < 30.0 mg/L of calcium water has caused a higher risk of fracture in children (Kozisek, 2005), certain neurodegenerative diseases (Jacqmin et al., 1994), preterm birth and low weight at birth, some cancer type (colon cancer) (Yang et al., 2002). Intake calcium with 3.0 mg/L concentration has been recorded, leading to cardiovascular changes, high blood pressure, somatoform autonomic dysfunctions, headache, dizziness, and osteoporosis (Kozisek, 2005).

Calcium concentrations in treated water were well below this minimum requirement; hence, to protect consumers from different diseases in terms of inadequate calcium intake, a re-mineralization cartridge could introduce as the final stage in the RO treatment process. Calcium concentration in treated water during wet and dry seasons are strongly and positively ($t = 0.084$, $p > 0.05$) correlated, and there is a significant difference between calcium in the treated water during dry (mean 2.47 ± 1.32) and wet (mean 0.88 ± 0.32) seasons ($p < 0.05$). The average calcium concentration in treated water during the dry season is higher at 1.60 mg/L comparisons to the calcium concentration during the wet season with 95% confidence intervals (-3.72, 0.52).

The magnesium in RO treated water indicated that a low magnesium ion content remained in the treated water compared to the magnesium ion content in raw water during wet and dry seasons. The percentages of magnesium ion removal ranged between 91 to 99% during the dry and wet seasons. Inadequate intake of magnesium ions leads to different health hazards in human being such as endothelial dysfunction, increased vascular reactions, decreased insulin sensitivity, hypertension, coronary heart disease, type 2 diabetes mellitus, and metabolic syndrome (WHO, 2017).

Hypermagnesemia has been considered to cause renal insufficiency due to reduced excrete magnesium (Chandra et al., 2013). More than 30.0 mg/L of magnesium intake has been reported causing bowel habits like diarrhoea and rarely hypomagnesaemia (Ayoob & Gupta, 2006). A higher intake of magnesium changes bowel habits (Sengupta, 2013). The less than 10.0 mg/L magnesium has been increased the morbidity and mortality from cardiovascular disease, cardiac arrhythmias, pre-eclampsia (Kozisek, 2005) (WHO, 2009), a higher risk of neuronal motor disease (Iwami et al., 1994), pregnancy disorders (Preeclampsia) (Melles & Kiss, 1992) the risk of low birth weight (Yang et al., 2002), seizures, abnormal heart rate, muscle contraction and muscle twitching (Kohri et al., 1989) (Kozisek, 2005).

In addition to that, more than 7.3 mg/L magnesium has been reported to be an increased risk of sudden death in infants; 3.8 mg/L magnesium causes endothelial

dysfunction, decreased insulin sensitivity, hypertension, coronary heart disease, type 2 diabetes, mellitus metabolic syndrome (Kozisek, 2005). Magnesium concentrations in treated water were below this minimum required value. A re-mineralization cartridge could be introduced in the final stage of the treatment process. Magnesium concentration in treated water during wet and dry seasons are significantly and positively ($r = 0.939$, $p < 0.05$) correlated, and there is a significant difference between magnesium in the treated water during dry (mean 2.80 ± 3.22) and wet (mean 0.90 ± 1.00) seasons ($P < 0.05$). The average value of calcium in treated water during the dry season is higher at 1.90 mg/L comparisons to the calcium during the wet season, with 95% confidence intervals (-5.56, 1.76).

The cadmium values were not at detectable levels. The pH, conductivity, and turbidity in treated water during wet and dry seasons comply with the required Sri Lankan drinking water standards. However, CKDu affected and non-affected consume either treated water, partially treated water or raw water depending on their situation in the field or home. Therefore, people are exposed to different levels of nephrotoxic constituents, making possible people vulnerable to different stages of kidney impairment and other non-nephrotoxic health hazards.

4.3.1.1. The environmental concern of RO reject water

The concentration values of different water quality parameters remained in RO reject water depicts in Table 4.4. The reject water produced by RO contains a higher amount of water constituents, either beneficial or toxic to human beings. The RO reject water releases to the environment without any pretreatment, which can further contaminate soil and groundwater in surrounding areas where reject water is released.

High concentrated soil and water elements lead to bioaccumulation in terrestrial and aquatic fauna and flora, finally entering the human body through the food chain. Calcium and magnesium (hardness) are micronutrients in animal tissue. They could help maintain ionic balance, energy metabolism, DNA and RNA production, and neurological function in animal cells (Kozisek, 2005). Calcium has been investigated as

the main cation in skeletal tissue vertebrates, and invertebrates and magnesium are essential elements in chlorophyll in plants (Mallick et al., 2009). However, the study said the excess calcium and magnesium levels are more toxic to fish since the accumulation of excess calcium and magnesium in soft tissue brings adverse health effects (Mallick et al., 2009).

The beneficial effect of excess calcium in aquatic media has been ascertained as inhibition of the cadmium accumulation in animals' body tissue due to calcium competes and suppresses the cadmium absorption (Baldisserotto et al., 2005). Excess calcium concentration in water plays a vital role by inhibiting toxic metals accumulation in animal tissue, which transfers the human body through the food chain and cause kidney impairment. Elevated calcium concentration seems to be significantly decreased the acute toxicity of cadmium. It said that calcium concentration could affect the different cadmium transport pathways and affect the body's cadmium uptake process. The cadmium inhibiting process is crucial for CKDu affected areas as cadmium has been reported as one of the nephrotoxic constituents retained as chronic levels in soil, water, and food sources. In addition to that, calcium carbonate in water could neutralize the metal plume enter the groundwater table by precipitating the metals and increasing the pH of water (Sullivan et al., 2001; Koc et al., 2009). Therefore, an appropriate high concentration of calcium and magnesium ions in water is important for buffering process.

The low concentration of magnesium in water and soil may be why plants uptake more magnesium more than calcium in soil and water media. Plants growing is lagging when even one element of both minerals lacks in soil media. Calcium and magnesium accumulate in plants, primarily fruits, leaves, roots, buds, stem, and roots, reported in a high proportion of ions. With high concentrated calcium in leaves like to immobilize the sulphur, leading to sulphur deficiency in plants. Plants inhibit the growth in media contained a high concentration of calcium. High sodium concentration in soil encourages calcium leaching that damages the soil structure and may affect plants' sodium toxicity. With high pH values in the soil above 7.0, free or calcium iron has been

accumulated in the soil, leading to the low content of phosphorous plants because calcium produces insoluble Ca-P complexes with prosperity. Excess of soil calcium causes high soil pH, which could reduce the uptake of other cation nutrients. Excess magnesium is also increasing yellowing and brown spots on plants (Naddy et al., 2002). The high concentration of calcium, magnesium and sodium has beneficial behaviour and negative impacts on plants growth and nutrients uptakes and bioaccumulation of fauna and flora (Van Dam et al., 2010). Therefore, the balance of minerals in soil and water should be maintained to provide the proper environment for the plant's growth and wildlife. Discharge of toxic substances to the environment without treatment violates the environmental laws which follow in Sri Lanka. Hence, appropriate reject water treatment technologies need to be introduced for CKDu prevalent areas to further protect people from exposure to nephrotoxic constituents. RO technologies are the only option in water treatment in areas where people depended on their daily potable water requirements. Therefore, it is important to provide safe drinking water to people and protect soil and groundwater sources from contamination by excess RO reject water elements.

4.3.2. Types, forms of hazards, and nature of the reactions of fluoride, calcium, magnesium (hardness), and cadmium in the human body

The results of health hazard identification in terms of fluoride, calcium, magnesium (hardness) and cadmium illustrate using the schematic diagrams (Figures 4.20–4.23), representing fates of selected elements in the human body and their adverse health effects on different organs. Ingestion is the main pathway, where toxic contaminants enter the human body and then transmit to all organs, interfering with the different mechanisms.

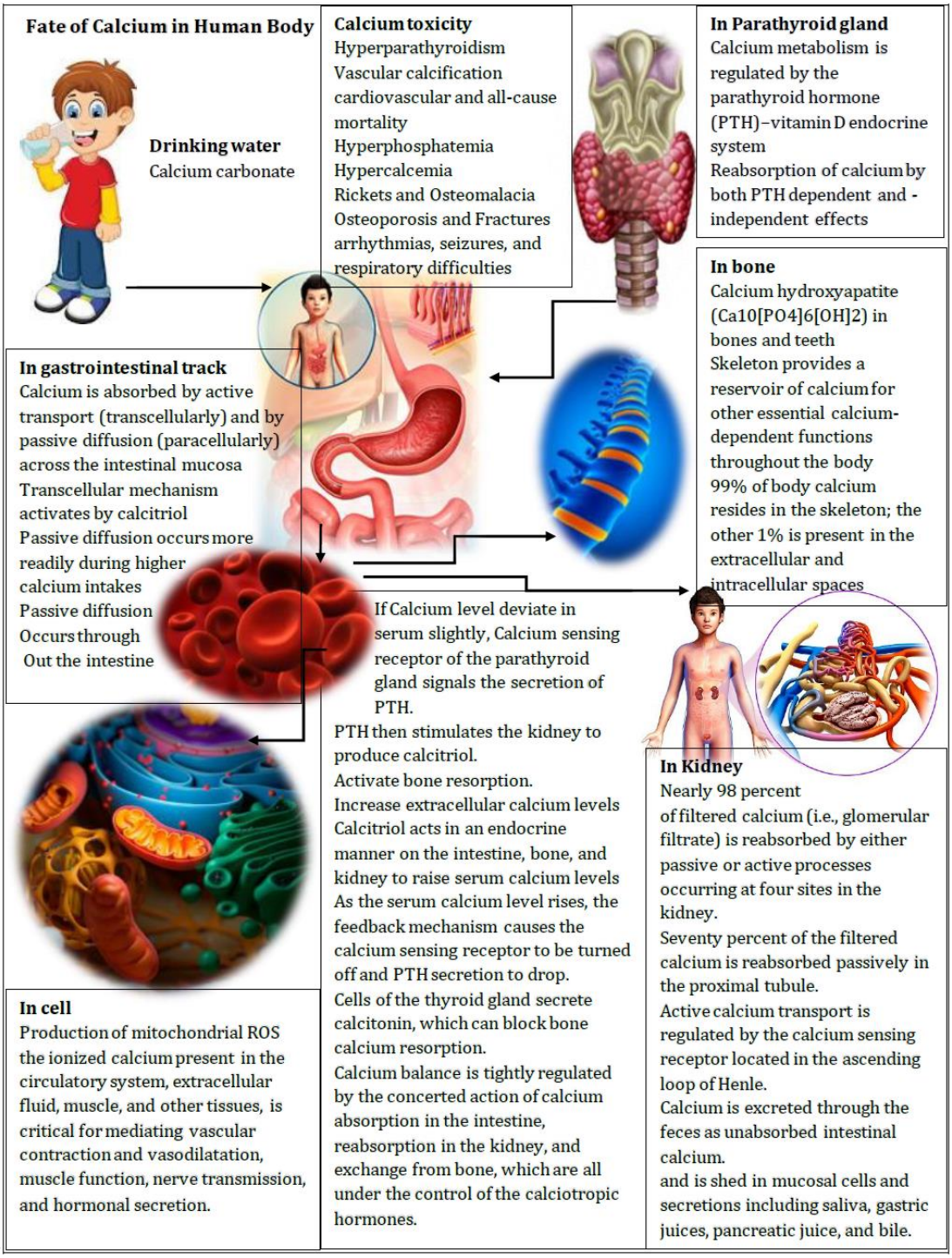

Figure 4.20: Nature of the calcium reaction in the human body

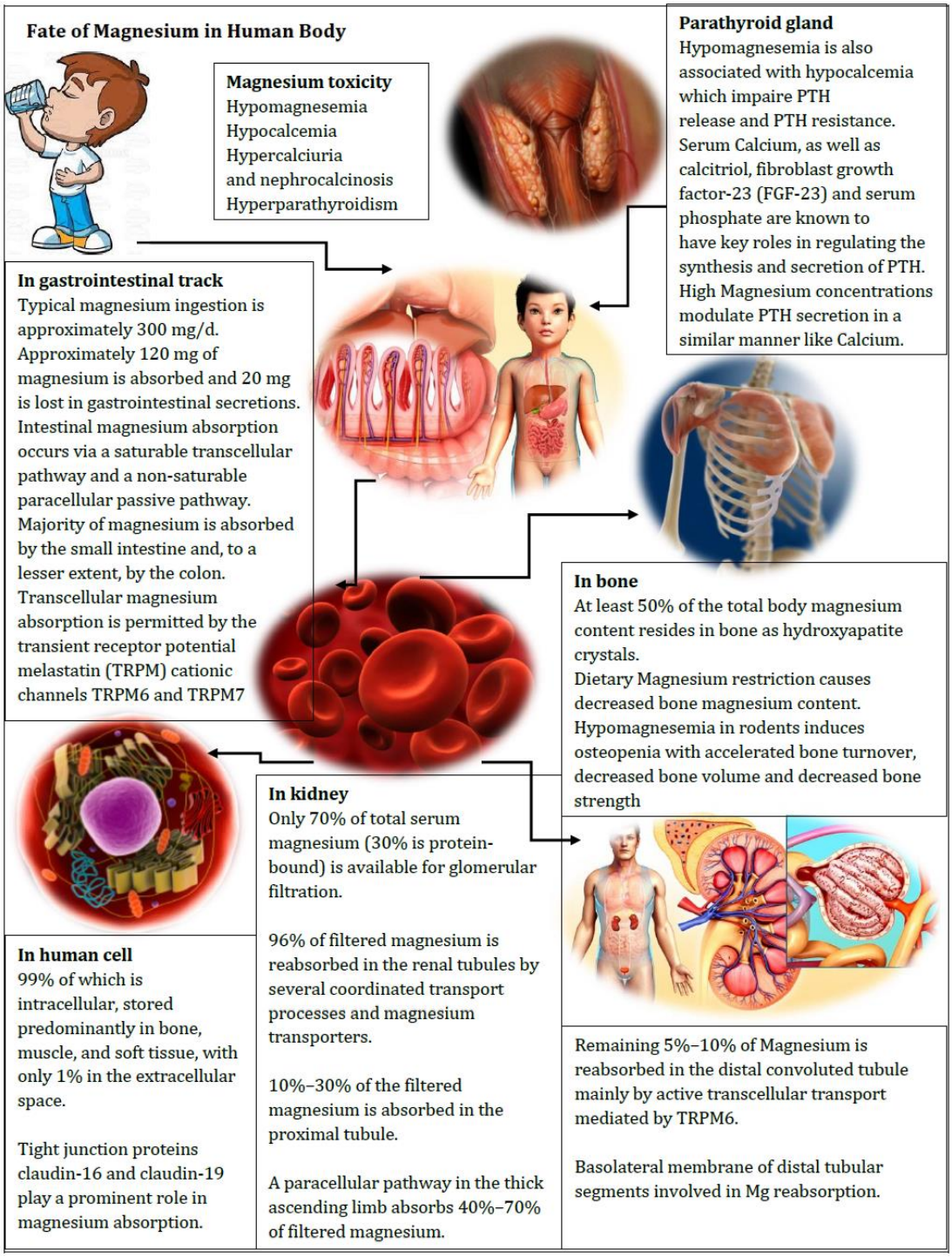

Figure 4.21: Nature of the magnesium reaction in the human body

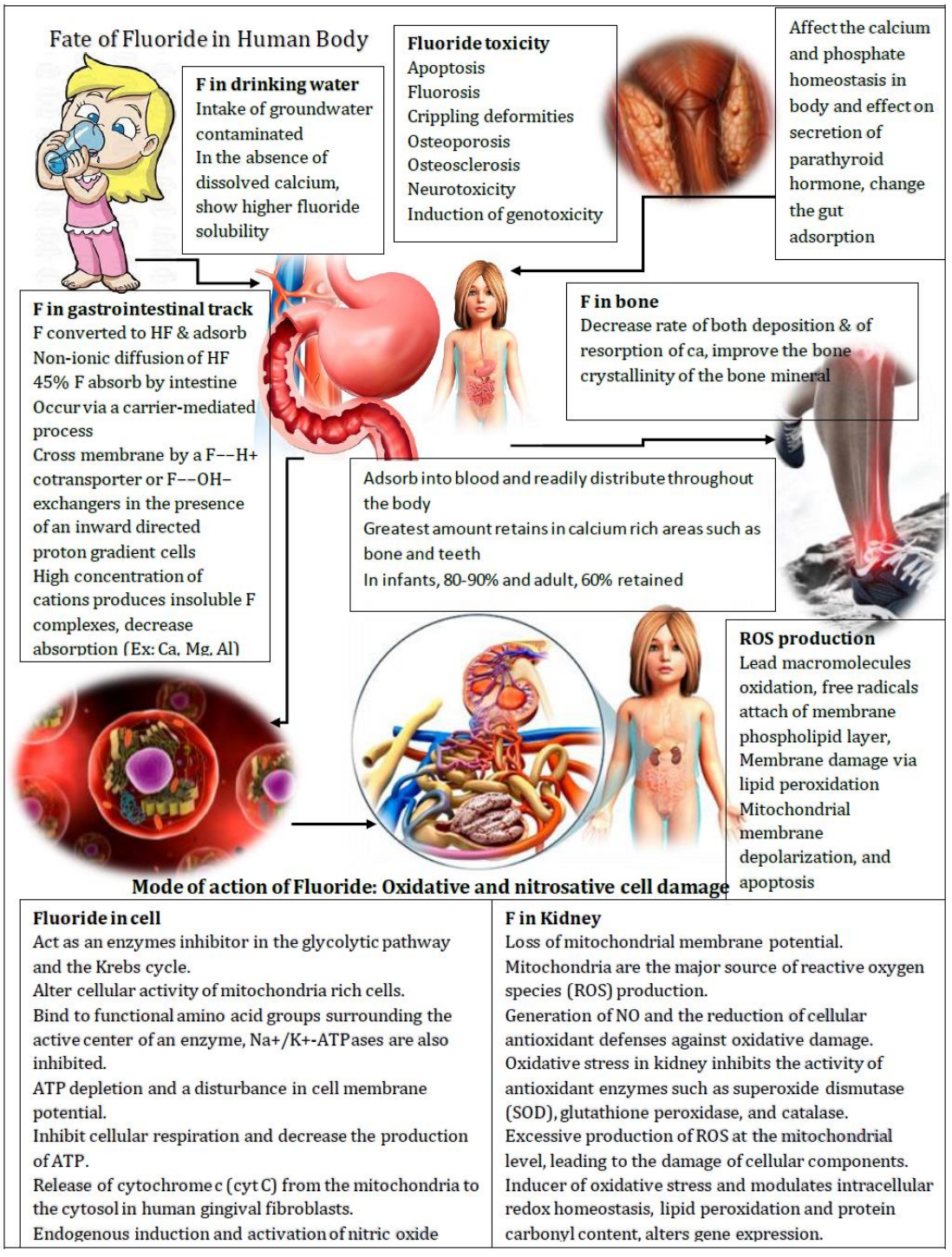

Figure 4.22: Nature of the fluoride reaction in the human body

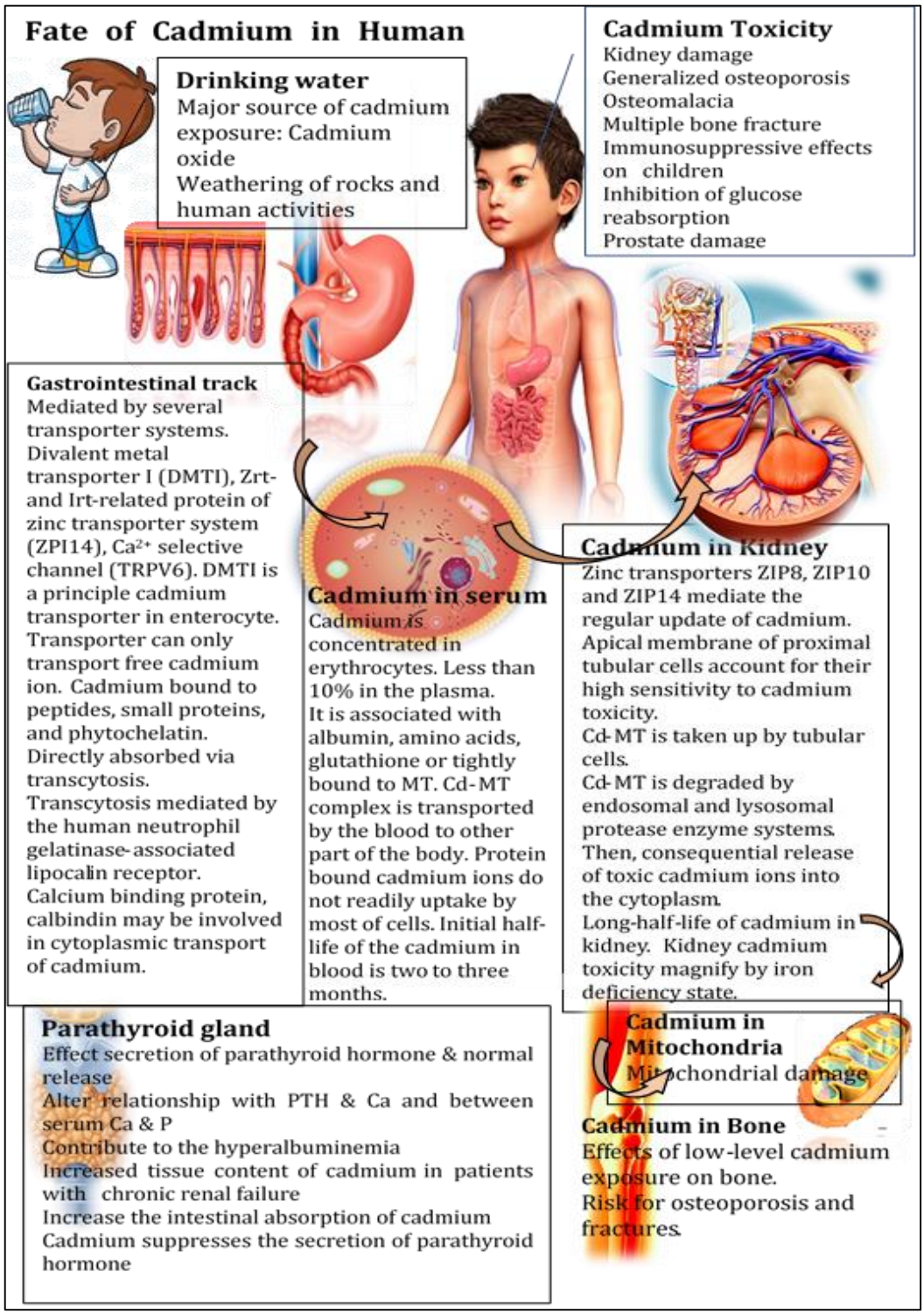

Figure 4.23: Nature of the cadmium reaction in the human body

4.3.3. Household survey for the assessment of exposure

The household survey results to gather information about daily water consumption and people's body weight in different age categories are presented in Table 4.5. Males in age category 21–91 years consumes a large amount of water per day, more significantly than females, as male farmers work in the field the whole day under the sun. Male body weight in each age category is higher than females' body weight in the same age categories. People (20%) in Thambalagollawa areas have purchased domestic RO units to protect themselves from CKDu. However, all domestic RO units are out of work at present due to early clogging of RO membrane with extreme high hard water [hardness as $CaCO_3$ > 180.0 mg/L in raw water (USGS)]. The domestic RO unit is not effective in removing nephrotoxic risk factors with high hardness levels in raw water. Therefore, at present, most (76%) people consume water from protected and unprotected garden wells located nearest to their residing places. Occasionally, they (24%) purchase treated water from commercial RO units if they have enough money to spend on commercially treated RO water. However, 88% of potable water sources consumed by people have proven to be unpalatable in taste due to its higher hardness levels.

Table 4.5: Average daily intake of drinking water and their body weight for different age categories (based on a household survey)

Age category (Years)	Ingestion of water (cups*/day)		Average body weight (Kg)	
	Male	Female	Male	Female
1–9	5.0 ± 0.5	4.0 ± 0.2	19.0 ± 0.2	18.0 ± 0.1
10–20	11.0 ± 1.2	8.0 ± 0.6	48.0 ± 0.3	46.0 ± 0.1
21–50	13.0 ± 0.9	9.0 ± 0.1	71.0 ± 0.5	59.0 ± 0.2
51–70	13.0 ± 1.3	9.0 ± 0.5	70.0 ± 0.3	59.0 ± 0.0
71–90	13.0 ± 0.6	9.0 ± 0.5	69.0 ± 0.1	55.0 ± 0.1
91 <	13.0 ± 0.2	9.0 ± 0.0	66.0 ± 0.1	52.0 ± 0.3

- One cup contained 250.0 mL of water

RO treated water increases the taste and colour of water, which increases the palatability of consumers. Generally, a family with four members consumes an average of 8.43 L of water per day, and their monthly consumption of water is approximately 260.0 L/month. The cost of water was calculated as Rs. 1,560.0/month, and the value can vary with their monthly water requirement. RO treated water cost is unbearable for most households (75%) in the farming community. Hence, they depend on potable water sources available to satisfy their daily water requirement and are vulnerable to the severe outbreak of kidney failure in the future. Therefore, the government should take the necessary action plan to provide safe drinking water for poor farming communities in CKDu affected areas. National water supply and drainage boards can involve establishing water supply schemes and provide safe water in areas where people suffer without clean drinking water for their daily consumption.

4.3.4. Health risk assessment due to the consumption of RO treated water

The HQ values calculated using average potential dosages and reference values/daily intake for fluoride, calcium, magnesium, and cadmium in different age categories are depicted in Table 4.6. Results showed that children in the age category 1–9 years are generally exposed to a higher risk than adults (male and female) in other age categories. Females in each age category are vulnerable to the non-carcinogenic health hazard greater than the male counterpart. The results of the ANOVA test conclude that the mean HQ values of fluoride (female - F = 1.727, R^2 – 0.96, $P > 0.05$; male - F = 1.607, R^2 – 0.98, $P > 0.05$) and cadmium (female - F = 0.322, R^2 – 0.95, $P > 0.05$; male - F = 0.159, R^2 – 0.97, $P > 0.05$) for male and female are not significantly different between each age categories (accept the null hypothesis; $H_o = 1$, $H_1 \neq 1$). But, the mean HQ values of calcium (female - F = 23.739, R^2 – 0.99, $P < 0.05$; male - F = 16.181, R^2 – 0.98, $P < 0.05$) and magnesium (female - F = 9.460, R^2 – 0.96, $P < 0.05$; male - F = 9.419, R^2 – 0.96, $P < 0.05$) for male and female are significantly different between each age categories (reject the null hypothesis; accept the alternative hypothesis; $H_o \neq 1$, $H_1 = 1$). Multiple comparisons [using post hoc test with Fisher's least significant difference (LSD)] of the mean values among each age category for fluoride, calcium, magnesium,

and cadmium corroborated that the mean of age category 1–9 years are significantly different from other age categories ($P < 0.05$). ANOVA results corroborated that a 1–9-year age category indicates higher vulnerability for non-carcinogenic health effects than other age categories. If people in age category 1–9 continue to drink RO water, they will be vulnerable for adverse health hazard in future; they are in risk more than other age categories. Therefore, it is a prerequisite to decrease RO treated water intake or improve the quality of RO treated water that meets the required drinking water guideline values or develops a new filter unit to provide safe drinking water.

Table 4.6: Mean hazard quotient (HQ) values for different age categories

Age (Years)	Fluoride Mean HQ		Calcium Mean HQ		Magnesium Mean HQ		Cadmium Mean HQ	
	Female	Male	Female	Male	Female	Male	Female	Male
1-9	0.1125 ± 0.1059	0.0995 ±0.0937	0.0009 ±0.0002	0.0009 ±0.0002	0.0005 ±0.0001	0.0006 ±0.0001	0.0446 ±0.0517	0.0422 ±0.0489
10-19	0.0484 ± 0.0456	0.0406 ±0.0382	0.0004 ±0.0001	0.0004 ±0.0001	0.0005 ±0.0001	0.0004 ±0.0001	0.0384 ±0.0445	0.0367 ±0.0427
20-50	0.0298 ± 0.0281	0.0305 ±0.0288	0.0003 ±0.0001	0.0004 ±0.0001	0.0005 ±0.0001	0.0003 ±0.0001	0.0245 ±0.0284	0.0294 ±0.0341
51-70	0.0298 ± 0.0281	0.0262 ±0.0228	0.0003 ±0.0001	0.0004 ±0.0001	0.0003 ±0.0001	0.0003 ±0.0001	0.0245 ±0.0284	0.0298 ±0.0346
71-90	0.0249 ± 0.0234	0.0242 ±0.0228	0.0002 ±0.0001	0.0002 ±0.0001	0.0003 ±0.0001	0.0002 ±0.0001	0.0204 ±0.0237	0.0232 ±0.0269
90<<<	0.0263 ± 0.0557	0.0252 ±0.0238	0.0003 ±0.0003	0.0003 ±0.0002	0.0003 ±0.0001	0.0002 ±0.0001	0.0216 ±0.0250	0.0243 ±0.0282

The results of the HQ values calculated for fluoride, calcium, magnesium, and cadmium in terms of different concentrations are illustrated in Table 4.7. Results corroborated those higher concentrations of nephrotoxic risk factors in RO treated water can increase risk than lower concentrations. The mean HQ values of males consuming RO treated water with high concentrations of calcium, magnesium, and cadmium excluding fluoride, result in higher vulnerability for non-carcinogenic health hazards

than females consuming the same. However, minimum, and maximum HQ values corroborated those females are highly vulnerable to greater adverse health effects than males in CKDu prevalent areas. The test results of the ANOVA estimated that the mean HQ values of fluoride (female - F = 5.679, R^2 – 0.98, $P < 0.05$; male - F = 6.296, R^2 – 0.96, $P < 0.05$), magnesium (female - F = 1.816, $P < 0.05$; male - F = 2.063, R^2 – 0.99, $P < 0.05$), and cadmium (female - F = 33.781, R^2 – 0.98, $P < 0.05$; male - F = 71.963, R^2 – 0.93, $P < 0.05$) are significantly different for male and female in term of different concentrations (reject the null hypothesis; accept the alternative hypothesis $H_o \neq 1$, $H_1 = 1$). The mean HQ values of calcium (female - F = 0.626, R^2 – 0.96, $P > 0.05$; male - F = 1.131, R^2 – 0.98, $P > 0.05$) for male and female are not significantly different between each concentration (accept the null hypothesis; reject the alternative hypothesis; $H_o = 1$, $H_1 \neq 1$). Multiple comparisons [using post hoc test with Fisher's least significant difference (LSD)] of the mean values among each concentration for fluoride, calcium, magnesium, and cadmium corroborated that means are not significantly different from one another ($P > 0.05$) for low concentrations. A significant difference in mean values was observed between higher and lower concentrations for each element ($P < 0.05$). The results corroborated that people exposed to higher concentrations of nephrotoxic risk factors are in risk of non-carcinogenic health hazards. Therefore, potable water quality protection and monitoring measures should be incorporated into CKDu affected areas, and new water treatment technologies should introduce safe drinking water to people.

The HI values of multiple concentration combinations for each age category of males and females are depicted in Table 4.8. The highest HI for multiple elements in the treated water was identified as 0.092 ± 0.118 of mixture 4 for females in the age category 1–9 years. Combined effects of fluoride, calcium, magnesium, and cadmium ions were determined higher for female consumers than males under the age categories 1–9 and 10–19 years. The test results of the ANOVA concluded that male and female HI values are strongly and significantly different in age category 1–9 years for mixture 1 (R^2 = 0.99, F = 765.85, $p < 0.05$), mixture 2 (R^2 = 1.0, F = 5,476.85, $p < 0.05$), mixture 3 (R^2 = 1.0, F = 6,445.87, $p < 0.05$), and mixture 4 (R^2 = 0.99, F = 1,609.63, $p < 0.05$),

and in age category 10–19 years for mixture 1 (R^2 = 0.99, F = 390.63, $p < 0.05$), mixture 2 (R^2 = 0.99, F = 383.16, $p < 0.05$), mixture 3 (R^2 = 0.99, F = 408.05, $p < 0.05$), and mixture 4 (R^2 = 0.98, F = 219.82, $p < 0.05$).

Table 4.7: Hazard quotient (HQ) values for different concentrations of nephrotoxic risk factors

Components	**Female**			**Male**		
Fluoride (mg/L)	**Mean HQ**	**Minimum**	**Maximum**	**Mean HQ**	**Minimum**	**Maximum**
0.29	0.0058 ± 0.0044	0.0032	0.0144	0.0053 ± 0.0037	0.0031	0.0127
0.88	0.0176 ± 0.0132	0.0097	0.0437	0.0159 ± 0.0113	0.0094	0.0386
2.90	0.0579 ± 0.0435	0.0318	0.1438	0.0525 ± 0.0374	0.0309	0.1272
5.00	0.0999 ± 0.0557	0.0549	0.2480	0.0905 ± 0.0645	0.0533	0.2193
Calcium (mg/L)						
8.80	0.0004 ± 0.0002	0.0002	0.0008	0.0004 ± 0.0002	0.0002	0.0008
11.20	0.0004 ± 0.0003	0.0002	0.0010	0.0005 ± 0.0003	0.0003	0.0010
14.40	0.0006 ± 0.0004	0.0003	0.0013	0.0006 ± 0.0004	0.0003	0.0013
20.80	0.0012 ± 0.0002	0.0003	0.0018	0.0012 ± 0.0002	0.0003	0.0016
Magnesium (mg/L)						
2.20	0.0003 ± 0.0002	0.0002	0.0005	0.0003 ± 0.0001	0.0002	0.0005
2.80	0.0004 ± 0.0001	0.0003	0.0005	0.0003 ± 0.0002	0.0002	0.0006
3.60	0.0005 ± 0.0001	0.0004	0.0006	0.0004 ± 0.0002	0.0002	0.0005
5.20	0.0003 ± 0.0002	0.0012	0.0019	0.0013 ± 0.0001	0.0003	0.0018
Cadmium (mg/L)						
0.005	0.0076 ± 0.0026	0.0053	0.0116	0.0080 ± 0.0019	0.0060	0.0110
0.005	0.0076 ± 0.0026	0.0053	0.0116	0.0080 ± 0.0019	0.0060	0.0110
0.015	0.0226 ± 0.0078	0.0159	0.0347	0.0241 ± 0.0057	0.0181	0.0329
0.052	0.0783 ± 0.0269	0.0552	0.1204	0.0836 ± 0.0198	0.0628	0.1140

HI values are greater for males than females in age categories after 20 years with the high concentration combinations in mixture 4. The test results of the ANOVA corroborated that mean HI values are significantly different from male compared to

female in each age category for mixture 4 (R^2 = 0.98, $p < 0.05$). The statistical test results of HI mean values with high concentrations (mixture 4) elaborated that multicomponent concentration combinations are likely to bring adverse health effects on female in 1–9 and 10–19 years of age categories and male after age 20 years. The occurrence of CKDu among male farmers in age category 30-60 years (Chandrajith et al., 2011) was further confirmed by the results.

Table 4.8: Hazard index for multiple elements in different concentration combinations

Age categories	**Concentration combinations**			
1–9 years	Mixture 1	Mixture 2	Mixture 3	Mixture 4
Male	0.006 ± 0.007	0.013 ± 0.018	0.041 ± 0.059	0.084 ± 0.105
Female	0.007 ± 0.007	0.014 ± 0.020	0.045 ± 0.068	0.092 ± 0.118
10–19 years				
Male	0.004 ± 0.004	0.007 ± 0.008	0.020 ± 0.025	0.047 ± 0.055
Female	0.004 ± 0.005	0.008 ± 0.009	0.023 ± 0.029	0.053 ± 0.061
20–50 years				
Male	0.003 ± 0.004	0.005 ± 0.006	0.016 ± 0.019	0.037 ± 0.043
Female	0.003 ± 0.003	0.005 ± 0.006	0.015 ± 0.018	0.033 ± 0.038
51–70 years				
Male	0.003 ± 0.004	0.004 ± 0.005	0.012 ± 0.015	0.029 ± 0.034
Female	0.003 ± 0.003	0.004 ± 0.005	0.012 ± 0.015	0.028 ± 0.032
71–90 years				
Male	0.002 ± 0.003	0.004 ± 0.005	0.012 ± 0.015	0.029 ± 0.034
Female	0.002 ± 0.003	0.004 ± 0.005	0.012 ± 0.015	0.028 ± 0.032
90<< years				
Male	0.003 ± 0.003	0.004 ± 0.005	0.013 ± 0.016	0.030 ± 0.035
Female	0.002 ± 0.003	0.004 ± 0.005	0.013 ± 0.016	0.029 ± 0.033

Note: The mixture represents HI in concentration combinations of multiple elements. Mixture 1 included HI in concentrations combinations of fluoride 0.29 mg/L, calcium 8.80 mg/L, magnesium 2.20 mg/L, and cadmium 0.005 mg/L; mixture 2 illustrated HI in concentrations combinations of fluoride 0.88 mg/L, calcium 11.20 mg/L, magnesium 2.80 mg/L, and cadmium 0.01 mg/L, mixture 3 represented HI in concentrations combinations of fluoride 2.90 mg/L, calcium 14.40 mg/L, magnesium 3.60 mg/L, and cadmium 0.015 mg/L, and mixture 4 included HI in concentrations combinations of fluoride 5.00 mg/L, calcium 20.80 mg/L, magnesium 5.20 mg/L, and cadmium 0.052 mg/L.

The non-carcinogenic health hazards may occur in male after 20 years due to male are exposure to high concentration of nephrotoxic risk factors at the field while drinking large quantity of water. However, all HQ and HI values calculated by the laboratory experiments were observed to be < 1 indicating no potential risk of non-carcinogenic health effects on consumers due to acute exposure to individual nephrotoxic risk factors. However, long term (chronic) exposure to low and high ionicity in RO treated water will adversely affect males and females living in CKDu prevalent areas.

People who consume RO treated water in the long run have shown vulnerability to significant health risks. The time is taken to exceed the HI value one (HI > 1) calculated considering the exposure time of each ion in lower concentrations. The results showed that children in the age category 1–9 years exceeded HI > 1 after 14 days of exposure to a high concentration's mixture [Table 4.9 (i) & (ii)]. All people exceed HI > 1 after exposure to nephrotoxic constituents for more than one year. Exposure to cadmium over 20 years, in the long run, causes renal damage (Bandara et al., 2008). Other age categories have taken a long duration to reach the hazardous of the age category 1–9 years. Children in the age category 1–9 years are a more vulnerable group for non-carcinogenic health hazards within a short period. The statistical analysis of the t-test verified the children in age category 1–9 is significantly vulnerable to non-carcinogenic health hazards than other age categories ($t_{3.6}$ - 29.8, $p < 0.05$). Age is identified as a deterministic parameter of the occurrence of non-carcinogenic health hazards. The

literature stated that people in the age category 40 to 60 years are affected by chronic renal failure (Bandara et al., 2008). Long-term exposure to nephrotoxic risk factors might make people in this age category vulnerable to the disease.

Table 4.9: (i) Exposure duration which exceeds hazard quotient value HQ > 1

	Exposure duration - 1 day				**2 weeks**				**1 month**			
	Mixture 1	**Mixture 2**	**Mixture 3**	**Mixture 4**	**Mixture 1**	**Mixture 2**	**Mixture 3**	**Mixture 4**	**Mixture 1**	**Mixture 2**	**Mixture 3**	**Mixture 4**
Age 1-9 years - HI values												
Male	0.01	0.01	0.04	0.08	0.09	0.18	0.57	1.17	0.19	0.38	1.22	2.51
Female	0.01	0.01	0.04	0.09	0.09	0.19	0.63	1.29	0.20	0.43	1.36	2.77
Age 10-19 years												
Male	0.01	0.01	0.02	0.05	0.05	0.09	0.29	0.66	0.11	0.20	0.61	1.42
Female	0.01	0.01	0.02	0.05	0.06	0.11	0.33	0.74	0.13	0.23	0.70	1.58
Age 20-50 years												
Male	0.01	0.01	0.02	0.04	0.04	0.07	0.22	0.52	0.09	0.15	0.47	1.10
Female	0.01	0.01	0.02	0.03	0.04	0.07	0.20	0.46	0.08	0.14	0.44	0.99
Age 51-70 years												
Male	0.01	0.01	0.01	0.03	0.04	0.06	0.17	0.41	0.09	0.12	0.37	0.87
Female	0.01	0.01	0.01	0.03	0.04	0.06	0.17	0.39	0.08	0.12	0.36	0.83
Age 71-90 years												
Male	0.01	0.01	0.01	0.03	0.03	0.06	0.17	0.41	0.07	0.12	0.37	0.87
Female	0.01	0.01	0.01	0.03	0.03	0.06	0.17	0.37	0.07	0.12	0.36	0.83
Age 90<< years												
Male	0.01	0.01	0.01	0.03	0.04	0.06	0.18	0.43	0.08	0.13	0.39	0.91
Female	0.01	0.01	0.01	0.03	0.03	0.06	0.18	0.41	0.07	0.12	0.38	0.88

Consumption of RO treated water, in the long run, could bring health hazards in future due to the intake of the lower mineral contained water, which affects severely for biological activities of the human body. The RO treated water is thirst-quenching, whereas consumers can adapt to negative taste characteristics of RO treated water.

Negative thirst characteristics and thirst-quenching could lead to less or excessive water consumption (Williams, 2012). Water content in the body is essential to the function of body parts (Popkin et al., 2010).

Table 4.10: (ii) Exposure duration which exceeds hazard quotient value HQ > 1

	3 months				6 months				12 months			
	Mixture 1	**Mixture 2**	**Mixture 3**	**Mixture 4**	**Mixture 1**	**Mixture 2**	**Mixture 3**	**Mixture 4**	**Mixture 1**	**Mixture 2**	**Mixture 3**	**Mixture 4**
Age 1-9 years												
Male	0.56	1.15	3.65	7.53	1.12	2.30	7.31	15.07	2.23	4.61	14.62	30.13
Female	0.61	1.28	4.07	8.32	1.22	2.56	8.14	16.63	2.45	5.11	16.27	33.26
Age 10-19 years												
Male	0.34	0.59	1.84	4.27	0.68	1.17	3.67	8.53	1.37	2.34	7.34	17.06
Female	0.39	0.68	2.10	4.75	0.77	1.35	4.19	9.50	1.55	2.70	8.39	19.01
Age 20-50 years												
Male	0.27	0.45	1.41	3.31	0.54	0.90	2.83	6.62	1.08	1.80	5.65	13.25
Female	0.24	0.42	1.31	2.98	0.49	0.85	2.61	5.96	0.97	1.69	5.22	11.92
Age 51-70 years												
Male	0.26	0.35	1.12	2.62	0.52	0.70	2.23	5.24	1.04	1.40	4.46	10.48
Female	0.24	0.35	1.09	2.48	0.49	0.70	2.18	4.97	0.97	1.40	4.36	9.94
Age 71-90 years												
Male	0.22	0.35	1.12	2.62	0.43	0.70	2.23	5.24	0.86	1.40	4.46	10.48
Female	0.20	0.35	1.09	2.48	0.40	0.70	2.18	4.97	0.79	1.40	4.36	9.94
Age 90<< years												
Male	0.23	0.38	1.16	2.74	0.45	0.76	2.32	5.47	0.90	1.51	4.64	10.94
Female	0.22	0.37	1.15	2.63	0.43	0.74	2.30	5.26	0.86	1.48	4.61	10.51

The results in Table 4.10 (i) and (ii) corroborated that HI values are substantially higher with higher concentration and lower concentration of RO-treated water among each age category. Those lower concentration values represent the concentration in RO treated water by the newly purchased RO system. The higher concentration values indicate concentration in treated water of RO system before failure to work. However, higher HI values (Table 4.10) indicated that people in CKDu affected areas are exposed to non-carcinogenic health hazards within a short period if they continue to drink RO-treated water. The HI values exceeded 1 (HI > 1) within a short period because the recommended daily dietary intake for fluoride (range in men and women: 1.4–3.4 mg/kg/day), calcium (range in men and women: 600–1,200 mg/kg/day), magnesium (range in men and women: 250–350 mg/kg/day), and cadmium (range in men and women: 0.03 mg/kg/day) have been calculated only for healthy people, but not CKDu affected people. However, the interaction of water constituents occurred only in high or medium concentrations. At low concentration levels, their toxicology is unlikely to occur. Under different conditions, water constituents act synergistically to cause higher toxicity in humans. The combined effects of a mixture of constituents are more significant than the single constituent. With nephrotoxic dietary intake levels, sometimes, the occurrence of non-carcinogenic health hazards may not be evident. However, people can affect with nephrotoxic health hazard due to intake of high content of water. Therefore, the nephrotoxic dietary intake levels need to establish to calculate HI values for RO treated water if people consume water for long period.

Excessive water consumption increases the extracellular and intracellular mineral excretion in the body fluid (Gropper & Smith, 2012). The imbalance of minerals in the human body changes the body's water levels, hormones, and enzyme activities (Williams, 2012). When the body absorbs low mineral water through the intestine, the body starts to add electrolytes to the water (Fabrizi, 2014). As a result, water takes electrolytes from the body reserves and enhances the electrolytes' dilution dissolved in the body water (Williams, 2012). The consumption of RO treated water, in the long run, increases the vulnerability of people to different health risks. Therefore, the provision of

safe drinking water is of the utmost importance to ensure the water safety of people in CKDu prevalent areas. Hence, it is necessary to develop new technology to remove the nephrotoxic risk factors in the water to avoid adverse health impacts.

4.3.5. Key findings of objective 3

- The percentage of hardness as $CaCO_3$ (dry season 28.00 ± 14.78 mg/L; wet season 8.00 ± 1.50 mg/L) fluoride (dry season 0.45 ± 0.14 mg/L; wet season 0.39 ± 0.03 mg/L), calcium (dry season 2.47 ± 1.32 mg/L; wet season mean 0.88 ± 0.32 mg/L), and magnesium (dry season 2.80 ± 3.22 mg/L; wet season mean 0.90 ± 1.00 mg/L) removal observed greater than 80% for each element in potable water treatment using commercial RO units. The very low concentrations of elements are remained in the treated water.
- The fluoride, calcium, and magnesium concentration in RO treated water during the dry season are not significantly different comparing to the concentration in the treated water during the wet season ($P > 0.05$), which corroborated "fluoride concentrations in treated water are equal during the dry and wet season" even though the fluoride concentration of raw water varied spatially and temporally.
- Most (76%) people consume water from protected and unprotected garden wells located nearest to their residing places. Occasionally, they (24%) purchase treated water from commercial RO units if they have enough money to spend on commercially treated RO water.
- However, essential elements required for people's good health remain in low concentration in RO treated water. The exposure to low macro and microelements for the long run due to RO treated water consumption brings non-carcinogenic health hazards to people in CKDu prevalent areas.
- The group of 1–9 years' age category indicates higher vulnerability for non-carcinogenic health effects than other age categories. HQ values of fluoride for males and females are not significantly different between other each age category. The HQ values of calcium and magnesium for males and females are significantly different between each age category.

- People exposed to higher concentrations values are most vulnerable to non-carcinogenic health hazards within short period.
- Multicomponent concentration combinations are likely to negatively affect females in 1–9 and 10–19 years of age categories and males after age 20 years.

4.3.6. Limitations of the study

- A limited number of RO units have been established in CKDu prevalent areas. Therefore, the sample size of the study in the characterization of RO treated water were limited. To avoid the limitation, all commercial RO units located in the selected villages were considered for the study.
- The sample size of the population was not enough to conduct the full-scale risk assessment process. The population size should be more than 400, but 134 males and females were included in this study. To avoid the limitation, all households living in Thambalagollawa village was accounted for the risk assessment process.
- Past studies of the risk assessment process for the mixture of components were limited.
- The health effects of fluoride, calcium, magnesium, and cadmium on the human body were not well established and rarely reported in the literature.

4.4. Objective 04: Investigation of applicability of the best combination of adsorbent material in multi-layered water purification unit capable of removing selected nephrotoxic risk factors in potable water for households in CKDu prevalent areas

This section describes how the multi-layered column was designed to remove fluoride, hardness, and faecal coliform in potable water. Firstly, different synthesis processes and characterisation of materials were discussed to show the potential ability to synthesise material with the available laboratory facilities. Secondly, results in batch adsorption studies for single and multi-solute, results of isotherm and kinetics models and process of desorption and regeneration were described to illustrate how these series of

experiments were supported to investigate the best combination of adsorbents materials for multi-layer units. Thirdly, fixed-bed column studies, results of different mathematical models, scaling up as home filter design, and cost of 1.0 L of water production were presented. All results were provided evidence for the feasibility and affordability of the best combination of adsorbents, removing selected nephrotoxic risk factors in water. Finally, the key findings of the study and limitations of the study needed were elaborated.

4.4.1. Characterisation of materials synthesized in the laboratory

The results of the XRD, ESEM-EDAX, and FT–IR analysis were illustrated separately to identify the morphological properties of the materials.

(a) XRD analysis of nZVI

X-ray diffraction (XRD) technique determines crystalline materials' phases, assesses the percentage of crystallinity, evaluates the purity of materials, and determines the unit cell dimension. XRD pattern of nZVI represents (Figure 4.24) by prominent peaks at 2Ɵ 44–45º, 65–66º, and 82–85º (Chekli et al., 2016). Prominent 2Ɵ peaks were weakened due to nZVI particles are covered by the amorphous phase of iron (Wang et al., 2009; Fang et al., 2011; Azzam et al., 2016). The peaks of nZVI (after five days of synthesis) 2Ɵ of 30.1º (220), 35.7º (311), 43.7º (400), 57.6º (511), and 63.1º (440) represent the existence of the iron oxide (Magnetite/maghemite). The aged nZVI (after 30 days of synthesis) consist of iron oxide/hydroxide peaks at 27.1(120), 31.7°(220), 35.7°(311), 43.7°(400), 57.6°(511), and 63.1°(440). Magnetite or/and maghemite and lepidocrocite are dominant ageing products of nZVI (Liu et al., 2015, Dong et al., 2016, & Gong et al., 2018).

The average particle size obtained from XRD data was 30.5 nm, confirming that a significant fraction of nZVI was within the nanoscale. The particle size of nanomaterials was calculated from the XRD spectrum using Scherrer Formula using Equation 55 (Patterson, 1939):

$$D=n\lambda/\beta cos\Theta \quad (55)$$

Where D is the crystalline size, n is a constant, λ is the X-ray radiation wavelength, β is the line width, and Θ is the diffraction angle.

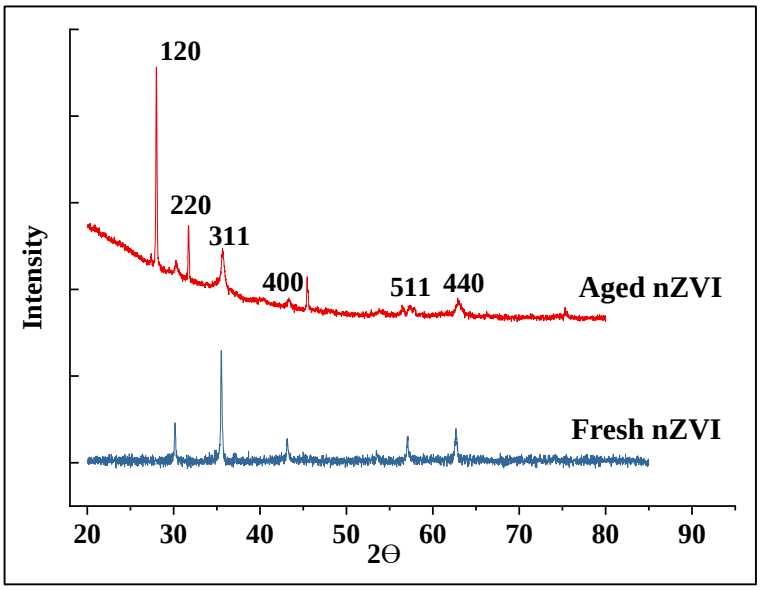

Figure 4.24: XRD analysis of nZVI

(b) ESEM-EDAX analysis of nZVI

ESEM-EDAX is surface analysis technique that determine surface morphology, aggregation state, the spatial distribution of the particles, and less frequently, the size determination. Figure 4.25 presents ESEM images of the nZVI particle, which appeared as a spherical shape and formed chain-like aggregate, attributed to the magnetic dipole interactions between adjacent particles and aggregation. These facts agree with Fu et al., 2015; Reddy et al., 2016; Dong et al., 2016.

The EDAX analysis (Figure 4.26) shows that surface was primarily comprised of iron (Fe) (62.7%), oxygen (O) (31.5%), and sodium (Na) (5.6%). EDAX analysis of cadmium and calcium adsorbed nZVI in single-solute studies confirm the presence of Fe (68.1%), O (29.0%), Cd (0.4%), and Ca (0.2%) adsorbed on the nZVI surface. The ESEM image of nZVI after adsorption (Figure 4.27) shows that the presence of flake-

like aggregates connected indicates agglomeration of nZVI due to the formation of different FeONs species adsorption.

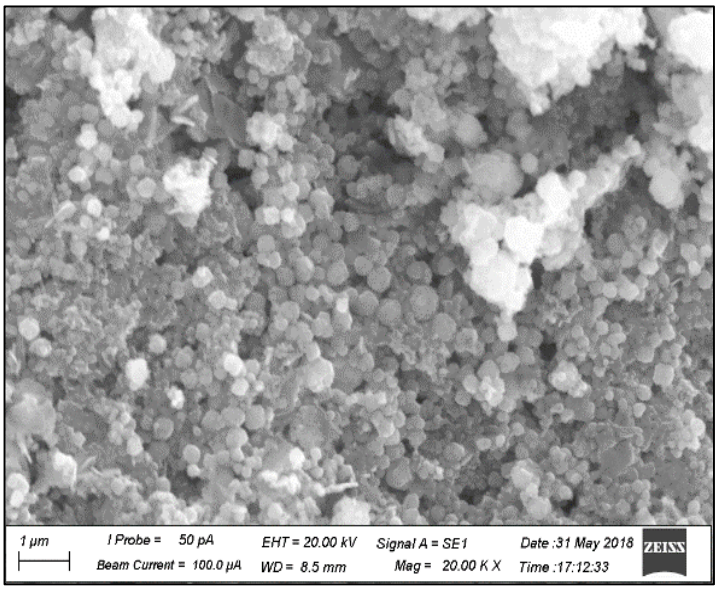

Figure 4.25: ESEM image of nZVI before adsorption

After adsorption of cadmium and calcium under multi-solute studies, nZVI shows spherical shape agglomerated particles with flocculent and flaky structure with some oxidised particles (Dong et al., 2016). ESEM image corroborated that the appearance of nZVI particles changed after the adsorption of cadmium and calcium ions. EDAX analysis (Figure 4.28) shows that the surface of nZVI was composed of Fe, O, Cd and Ca and no other impurities. The narrow peaks with high intensity confirmed the presence of crystalline structure (Lin et al., 2005; Azzam et al., 2016). EDAX analysis confirms that nZVI adsorb cadmium and calcium from potable water.

(c) FT–IR analysis of nZVI

The FT–IR spectrum of synthesized nZVI (Figure 4.29) showed broad bands around 1318 and 3395 cm^{-1}, which are attributed to O–H bending and O–H stretching due to surface adsorbed water, respectively, which suggests the formation of ferric oxyhydroxide (FeOOH) layer on nZVI (Singh et al., 2018, Azzam et al., 2016). The

narrowband around 585 cm^{-1} represented a typical characteristic peak at Fe-O vibrations of magnetite nanoparticles, indicating the occurrence of a certain degree of oxidation on the nZVI surface. The peak at 683 cm^{-1} represented a symmetric Fe-O stretching bond (Yin et al., 2012; Liu et al., 2015). The broad peak at 901 cm^{-1} is observed due to bending vibrations of O–Fe–O groups (Patnaik et al., 2015). The band at 1629 cm^{-1} is attributed to adsorbed water molecules deformation vibration (Mohapatra et al., 2010).

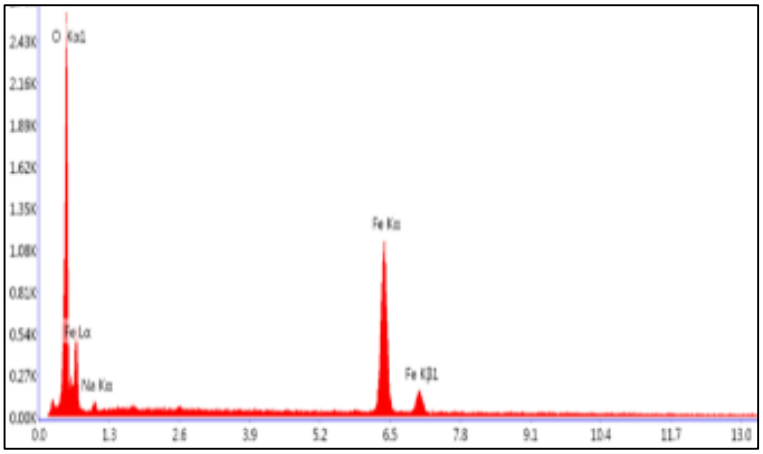

Figure 4.26: EDAX image of nZVI before adsorption (Note: EDAX was performed on the all-surface area)

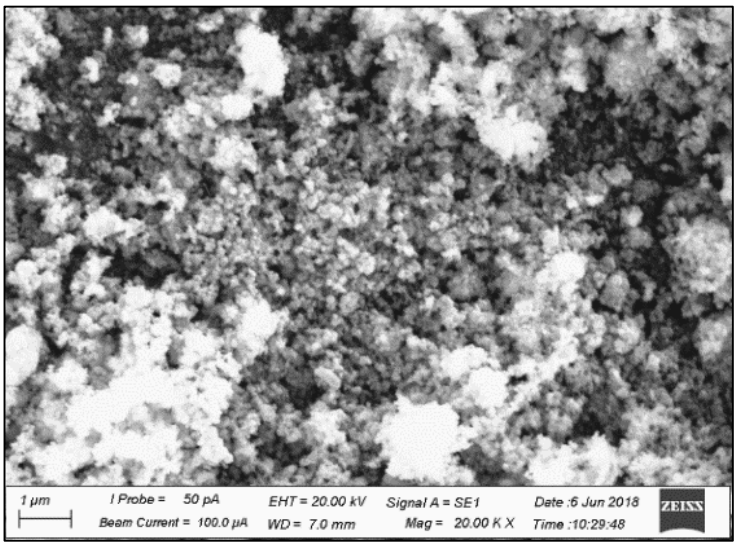

Figure 4.27: ESEM image of nZVI after adsorption

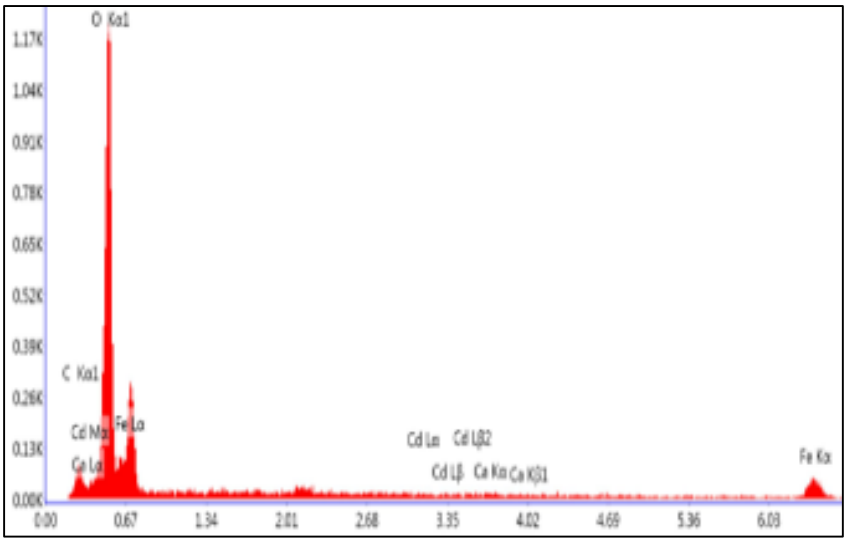

Figure 4.28: EDAX image of nZVI after adsorption (Note: EDAX was performed on all surface areas)

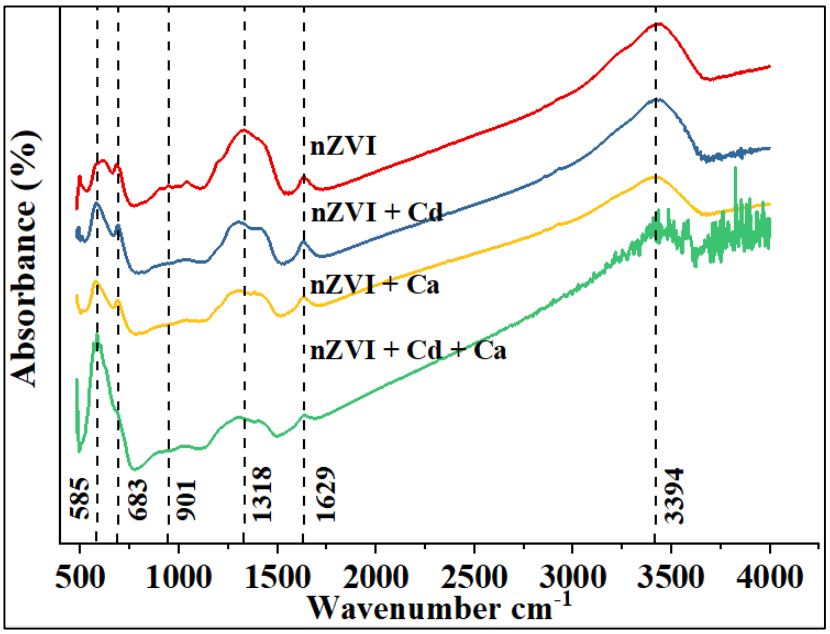

Figure 4.29: FT–IR analysis of nZVI

After the adsorption of cadmium and calcium, functional groups can be observed changing on the surface of nZVI, attributed with; new peaks were formed, peak disappeared, peaks shifted, peaks decreased, and the peaks increased. Peng et al., 2018

was highlighted the same observation for different materials. The brand at 3394 cm^{-1} shifted to 3415 cm^{-1}, 3384 cm^{-1}, and 3382 cm^{-1} and weaken. It may be attributed to the formation of surface functional groups such as ≡Fe–O–Cd^{+}, ≡$(Fe–O)_2$–Cd, ≡Fe–O–$Cd^{+}OH^{-}$, ≡Fe-O–Ca^{+} on the surface of nZVI. Boparai et al. (2013) & Ma et al. (2018) have been mentioned that ≡Fe–O–Cd^{+}, ≡$(Fe–O)_2$–Cd, ≡Fe–O–$Cd^{+}OH^{-}$, ≡Fe-O–Ca^{+} are formed in the removal of cadmium by nZVI around pH 8. After cadmium adsorption by nZVI pH of the solution reached 7.9 (pH value of the potential of zero charge - pH_{zpc}), which can enhance the formation of ≡Fe–O–Cd^{+}, ≡$(Fe–O)_2$–Cd, ≡Fe–O–$Cd^{+}OH^{-}$, ≡Fe-O–Ca^{+} increasing the cadmium removal capacity of nZVI.

(d) XRD analysis of MOMA

The characteristic peak at 11.1º (100) confirms the formation of the mesoporous structure of mesoporous alumina (Figure 4.30) (Camacho et al., 2010). The peak does not appear clearly in the spectrum because the sample is amorphous as their thermal treatment was carried out at a low temperature, 550ºC. However, the presence of aluminium and magnesium was confirmed by speciation given by the XRD information sheet, which indicated the formation of aluminum and magnesium oxides ($MgAl_2O_3$ – spinel phases, MgO cubic phases). The peaks at 33.7º (311), 45.7º (400), 60.6º (511), and 66.7º (440) are characterised by mesoporous Al_2O_3 (Dayananda et al., 2014). Diffraction 2Ɵ for magnesium oxide appeared at 111, 200, and 220 (Lesbani et al., 2016).

The XRD pattern of MOMA shows the poorly crystalline MgO and mesoporous alumina, which might be attributed to mesoporous alumina, with the higher MgO dispersion on the surface and hinder the growth of crystalline structure. The same behaviour has been observed by Li et al., 2015; Alemu et al., 2014, when MgO loaded into the surface of aluminium oxide. Broad peaks in the XRD spectrum are indicated the ultrafine nature of the crystalline (Adeno et al., 2015) and determined the amorphous nature of MOMA (Naik et al., 2010). The particle size of the crystalline was found to be 15.3 nm.

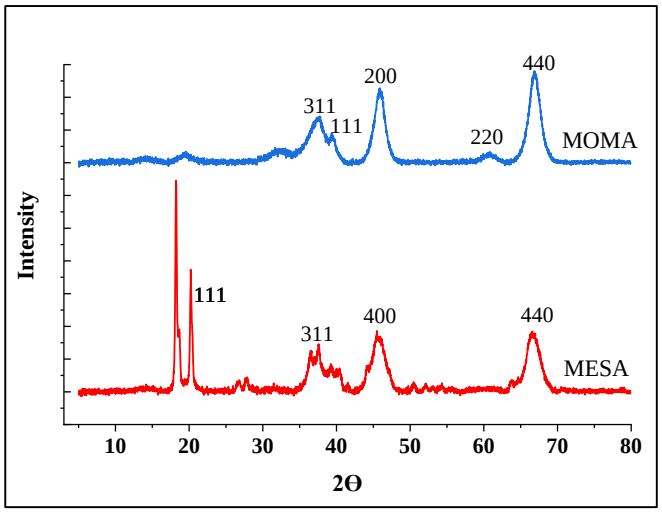

Figure 4.30: XRD analysis of MOMA and MESA

(e) ESEM-EDAX analysis of MOMA

Before MgO loaded into MESA, surface morphology manifests high porosity, a rough surface with a honeycomb-like structure (Figure 4.31) EDAX analysis of mesoporous alumina shows the presence of aluminium (56.4%) and oxygen (44.6%) (Figure 4.32) which indicates the presence of high content of aluminium and oxygen without impurities.

After MgO was loaded into the surface of MESA, MOMA (Figure 4.33) depicts a porous, large, and wormhole-like structure. EDAX analysis (Figure 4.34) proves that MOMA's surface consists of magnesium (2.61%), aluminium (50.41%), and oxygen (46.98%) without other impurities. EDAX analysis of MOMA confirmed that MgO had been loaded into the MESA surface (Figure 4.33). After adsorption of fluoride shows a flake-like structure with a smooth surface, it appeared to form aluminium, magnesium, and fluoride salts (Change et al., 2014). Few porous structures appeared disturbing the MOMA's surface morphology after fluoride adsorption (Figure 4.35). EDAX analysis confirms the presence of Al (44.6%), O (53.19%), Mg (0.8%), F (1.4%) (Figure 4.36).

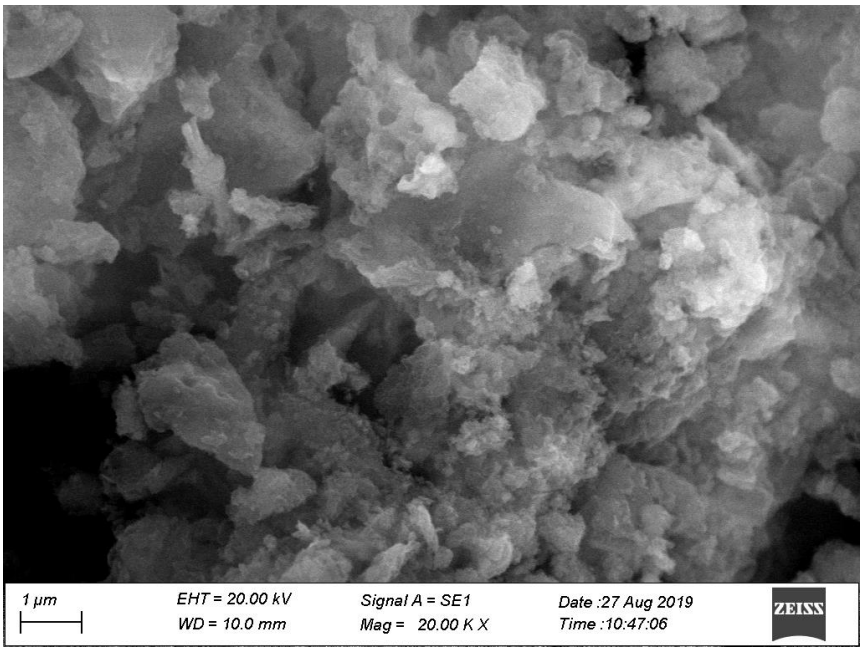

Figure 4.31: ESEM analysis of MESA

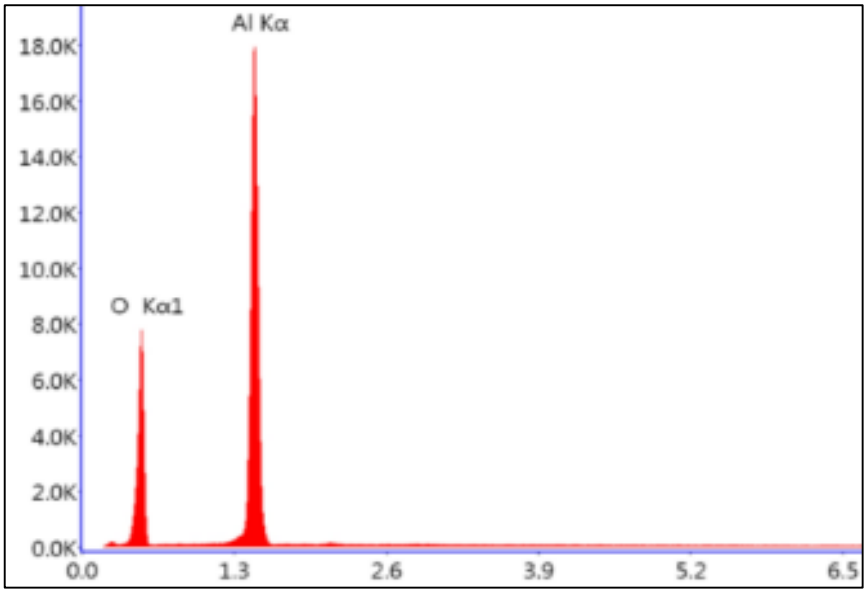

Figure 4.32: EDAX analysis of MESA

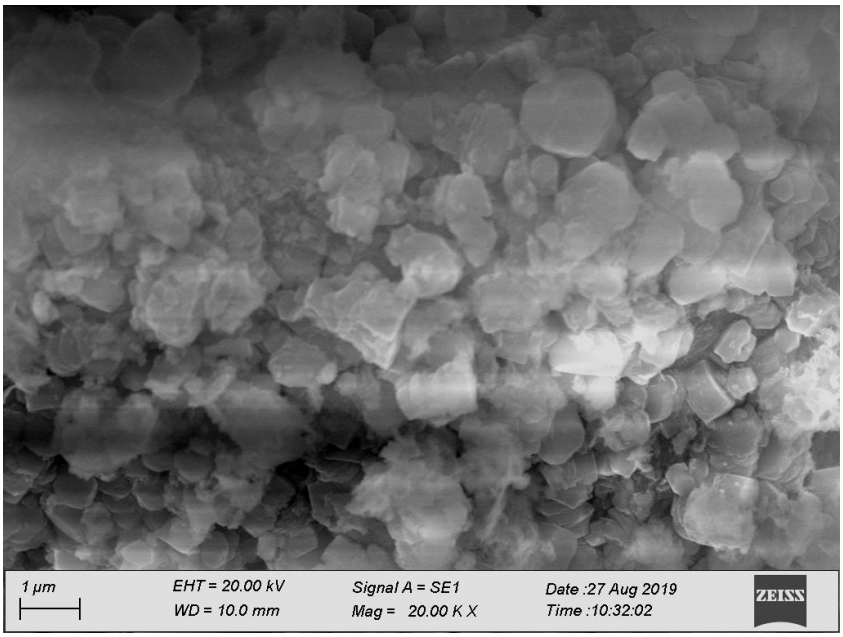

Figure 4.33: ESEM analysis of MOMA

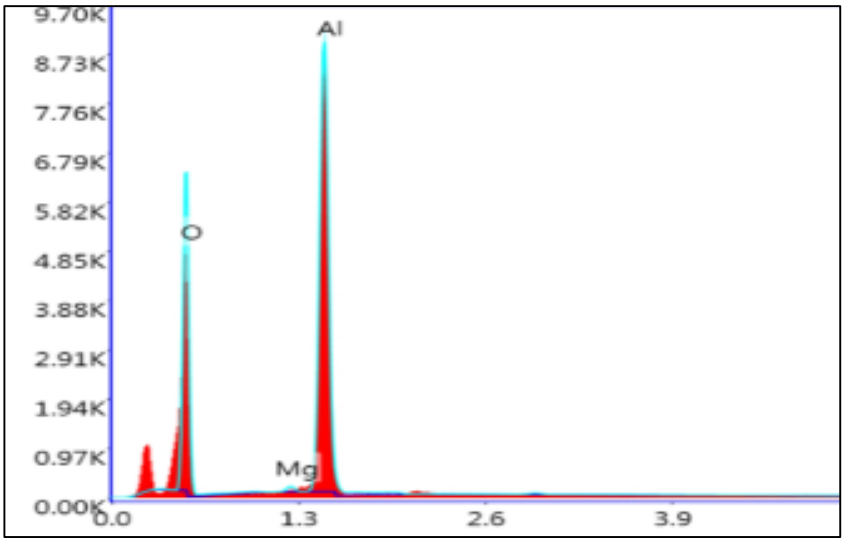

Figure 4.34: EDAX analysis of MOMA

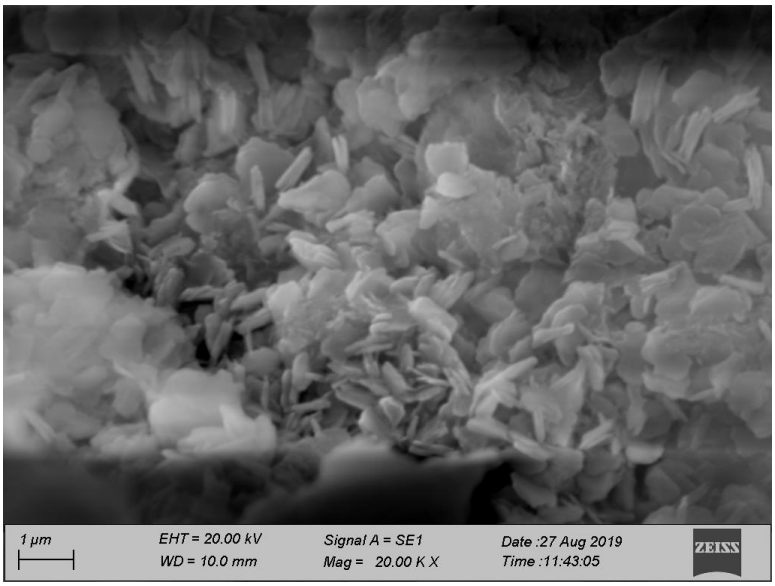

Figure 4.35: ESEM analysis of MOMA after fluoride adsorption

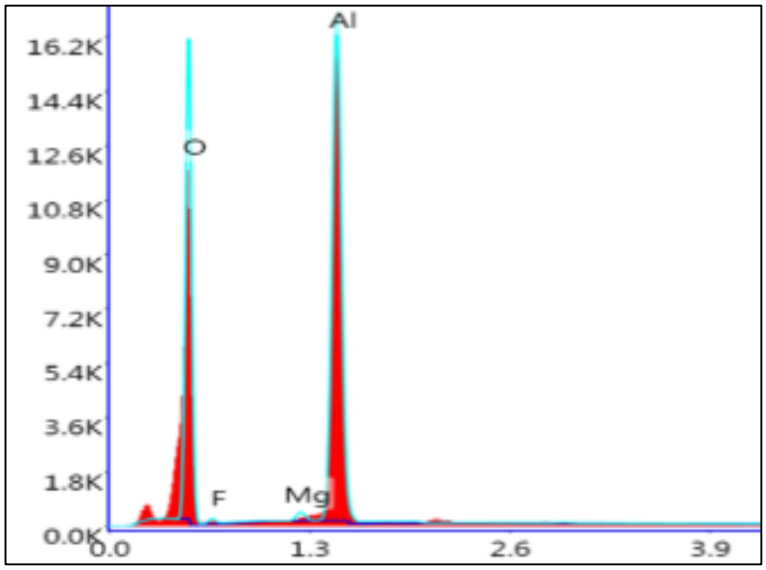

Figure 4.36: EDAX analysis of MOMA after fluoride adsorption

(f) FT–IR analysis of MOMA

FT–IR spectrum of Al_2O_3 and MOMA (Figure 4.37) showed that vibrational peaks at 668 cm^{-1} appeared due to functional groups of Al–O and 865 cm^{-1} symmetric bending of Al-O-H (Chang et al., 2014; Imtiaz et al., 2013). Peaks did not change remarkably

after the adsorption. The peaks appeared at 874 $cm^{-1,}$ and 1425 cm^{-1} were assigned to vibration Mg–O species (Marinković et al., 2015; Devi et al., 2014). O–H stretching vibration at 1629 cm^{-1} (Lesbani et al., 2016) and O–H bending vibration at 3459 cm^{-1} (Chang et al., 2014) were observed in all spectra. The O–H stretching peak at 1629 cm^{-1} and O–H bending vibration at 3459 cm^{-1} decreases gradually after the adsorption.

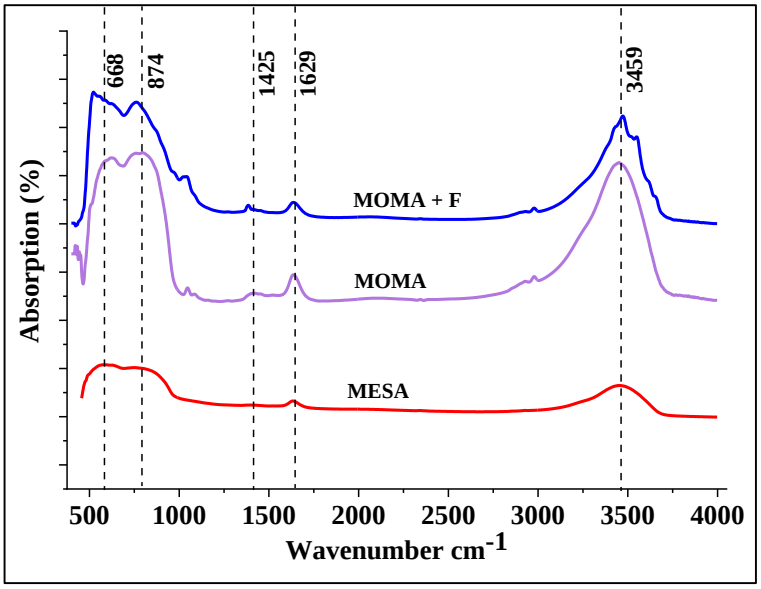

Figure 4.37: FT–IR analysis of MESA, MOMA, and MOMA + F

(g) XRD analysis of GO

XRD analysis was performed to determine the structure and the crystal phases of the GO (Figure 4.38). Graphite was exhibited high intense broad peaks at 26.4º (002) and 43.7º (100) due to pristine graphite. The sharp diffraction peak at 26.4º (002) was observed due to the highly organised layer structure (Thakur & Karak, 2012). The interlayer d-spacing of two planes were reported as 0.33 and 0.21 nm, respectively. The peak that appeared around 10–11º (001) was indicated 001 planes of dispersed GO with an interlayer spacing of 0.66 nm. The diffraction peak was shifted to the lower angle 9.9º (001) after the chemical oxidation and exfoliation of GO. The increased d-spacing in the 001 plane was due to the formation of oxygen-containing functional groups during the oxidation of graphite (Liu et al., 2016). The robust and broad peak at 23.9º represents the

amorphous phase of GO due to reduced graphene oxide. Wu et al. (2015) also have reported the same observation.

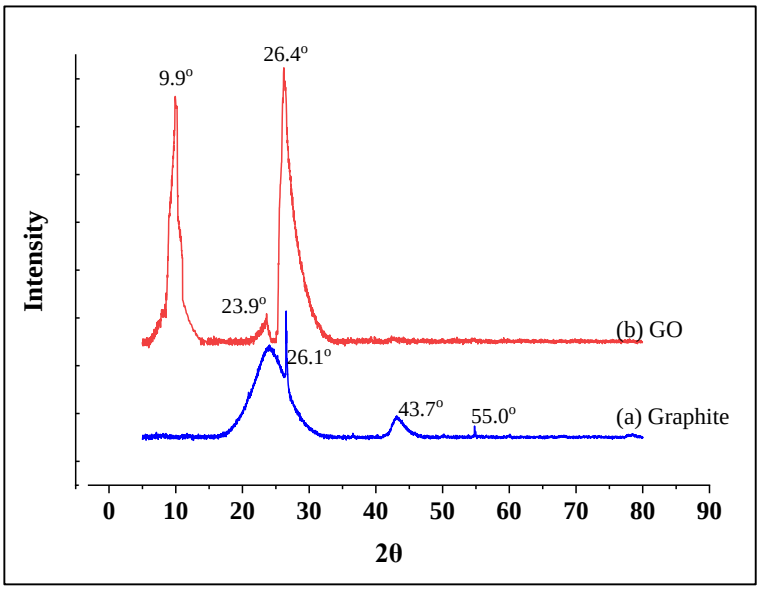

Figure 4.38: XRD analysis of GO

(h) ESEM-EDAX analysis of GO

ESEM image (Figure 4.39) shows that GO manifests with high porosity with micropores, layered structure, including kinked and wrinkled areas from edges. The GO surface appeared as a randomly aggregated, thin, furrowed sheet closely associated with each other and forming a disordered solid. The platelet-like, porous interlinked structure formed due to the exfoliation and restacking process of GO (Benjwal et al., 2015). These attributes, such as high porosity and layered structure of the GO, support profoundly impregnating other elements. The EDAX analysis (Figure 4.40) shows that the surface of GO was mainly composed of C (59.5%) and O (30.3%), with other elements such as Ca (0.9%) and Si (4.4%). The results indicated that graphite contains different other elements in its structure, except carbon and oxygen. The presence of these elements may bring beneficial effects on the removal of contaminants in potable water.

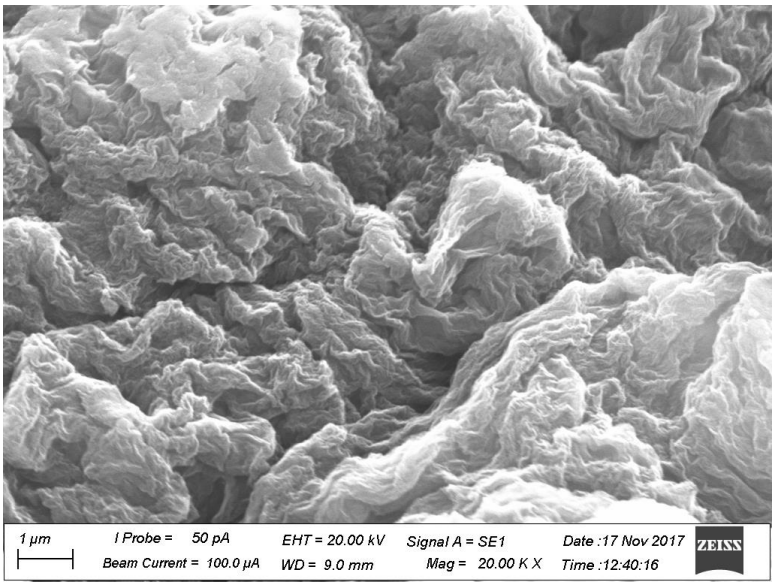

Figure 4.39: ESEM analysis of GO

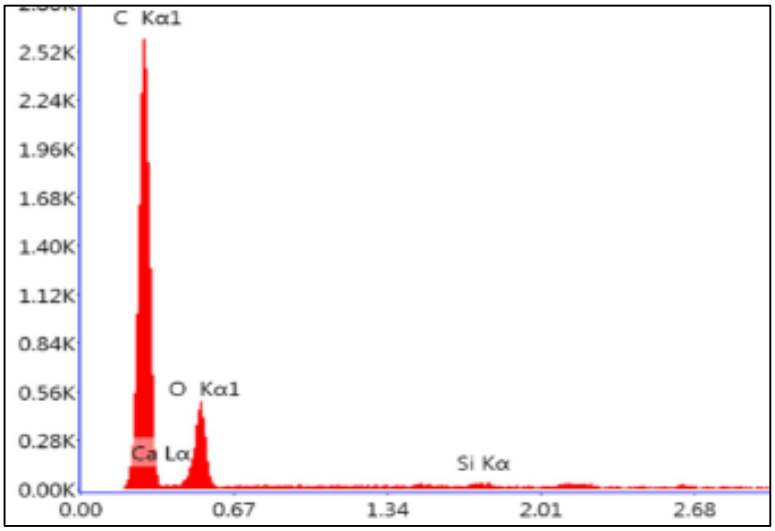

Figure 4.40: EDAX analysis of GO

(i) FT–IR analysis of GO

FT–IR spectrum of GO (Figure 4.41) was carried out in a range of 500–4,000 cm^{-1}. The broad peak at 3,450 cm^{-1} arises due to the stretching vibration of O–H groups (Loryuenyong et al., 2013). The small peaks at 1,854 cm^{-1} and 2,921 cm^{-1} are attributed

to the stretching vibration of the $–CH_2$ bond. The adsorption peak at 1,624 cm^{-1} can be assigned to the vibration of adsorbed water molecules (Loryuenyong et al., 2013) and C–C bonds (Singh et al., 2018). The small broad peak at 1,419 cm^{-1} can be attributed to –CO carboxylic groups (Bykkam et al., 2013). The vibration band at 1,229 cm^{-1} and 1,070 cm^{-1} is due to C–O–C epoxide groups (Singh et al., 2018; Loryuenyong et al., 2013). After the adsorption of fluoride and calcium, the functional groups were changed on the GO surface where new peaks were formed, peaks disappeared, peaks shifted, peaks decreased, and peaks increased.

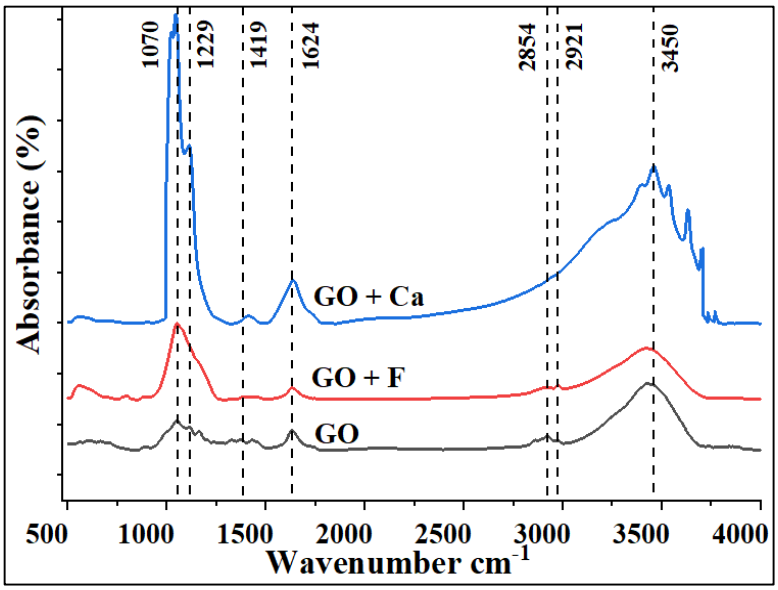

Figure 4.41: FT–IR analysis of GO

(j) XRD analysis of SONPs

Figure 4.42 shows the prominent peak at 38.2º, 44.4º, 64.5º, and 77.4º, which are attributed to the crystallographic planes of silver oxide nanoparticles in (111), (200), (220) and (311). The peak at 38.2º established crystalline silver formation, which has also been observed by Das et al. (2011) and Jalali et al. (2015). The average crystalline size of the particles was calculated as 64.2 nm. The method used to produce SONPs from nanosilver was successful in producing high purity SONPs with high crystallinity. Alkalinity pH maintained in the solution during the synthesis process may produce large

amounts of silver oxide nanoparticles. The same observation has been indicated by Yong et al. (2013).

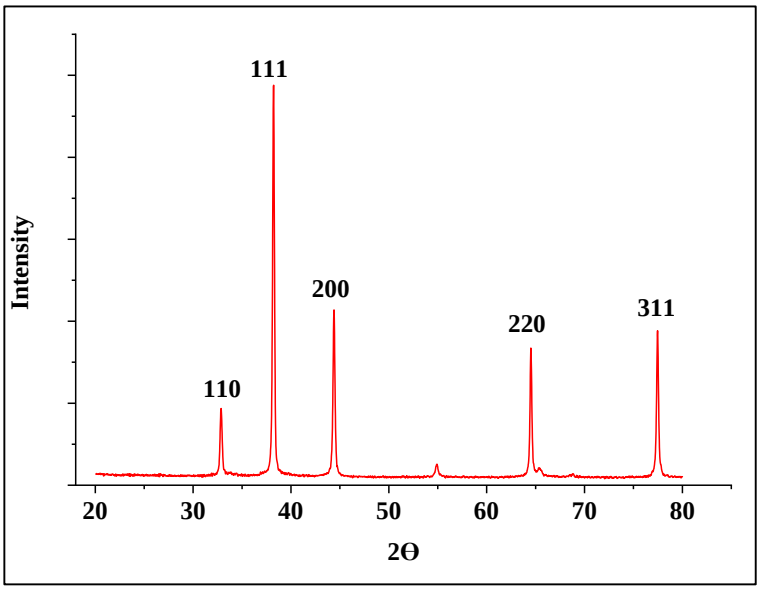

Figure 4.42: XRD analysis of SONPs

(k) ESEM-EDAX analysis of SONPs

ESEM image of SONPs (Figure 4.43) appeared to be a small spherical shape with smooth edges and confirmed that particle agglomeration has occurred due to chemical and magnetic interactions among particles. The small particles are mutually different in size and complied with the densest sphere packaging. The size of SONPs increases aggregation due to high surface reactivity. Aggregation decreases the production of SONPs in a small and uniform size. The aggregation of SONPs has also been observed by Devaraj et al. (2013). EDAX spectrum of SONPs shows that samples compost silver (89.97%) and oxygen (10.03%) (Figure 4.44).

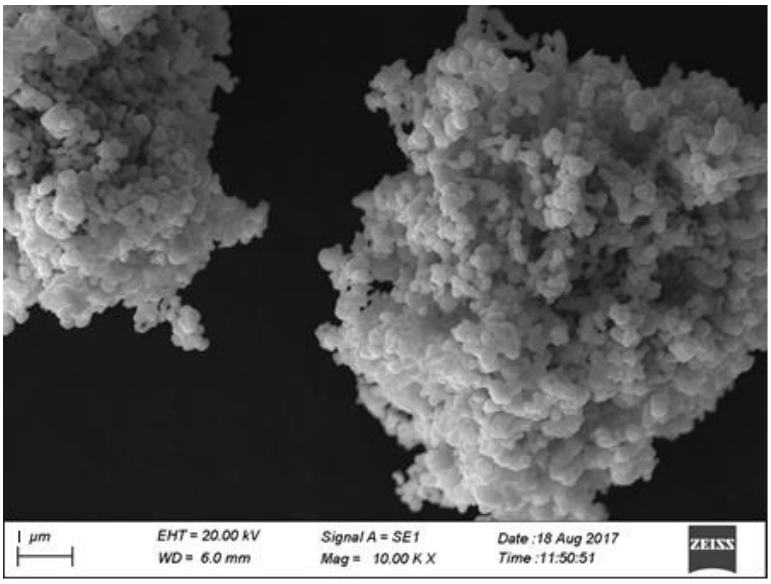

Figure 4.43: ESEM analysis of SONPs

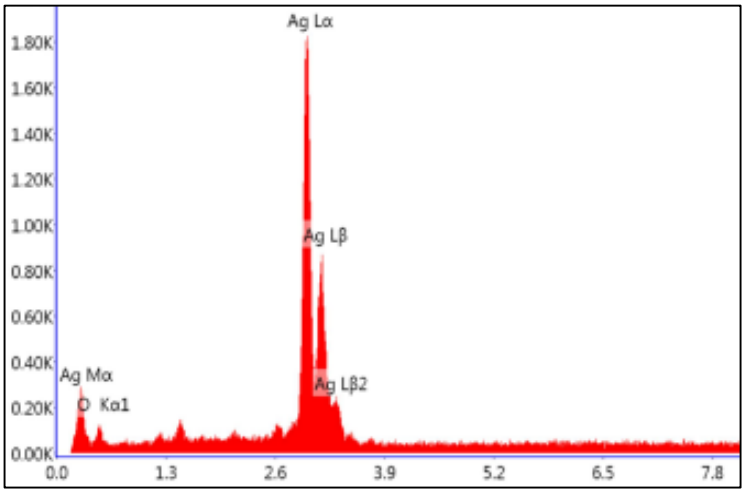

Figure 4.44: EDAX analysis of SONPs

(l) XRD analysis of SONPs + GO

XRD spectrum exhibited peaks related to both SONPs and GO composite with interlayer 1.65 nm (Figure 4.45). The slight shift of the peak position toward higher 2Θ values indicated intercalation of SONPs with GO sheets.

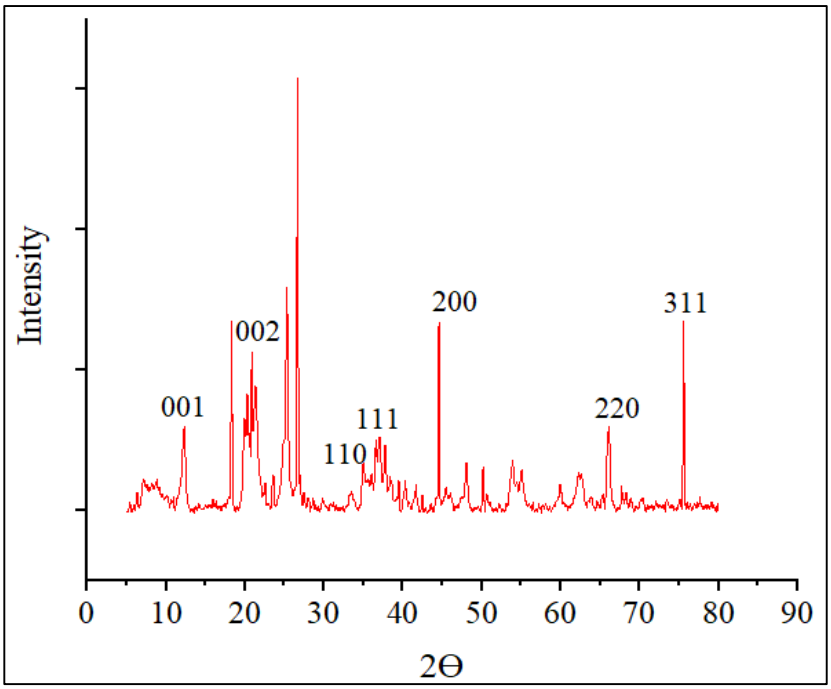

Figure 4.45: XRD analysis of SONPs + GO

(m) ESEM-EDAX analysis of SONPs + GO

ESEM analysis of SONPs + GO composite shows a circular flaky structure on the surface of GO (Figure 4.46). SONPs were unevenly distributed not only on the surface of GO but inside the layered structure of the GO. ESEM images confirm that SONPs adhere to the surface of GO. ESEM of GO after impregnation with silver oxide shows that there are aggregated flakes with a cluttered appearance, typical wrinkled, loose sponge-like structure, including a large surface area that causes folding of GO sheets. EDAX spectrum indicates the presence of carbon, silver, and oxygen in the SONPs + GO sample. The percentages of carbon (24.32%), silver (62.0%) and oxygen (13.69%) (Figure 4.47) on the surface corroborated that SONPs were loaded into the GO surface.

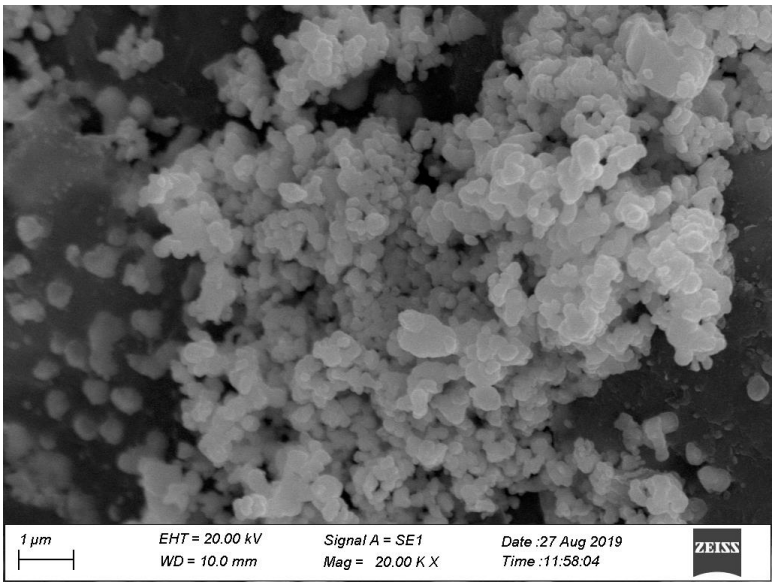

Figure 4.46: ESEM analysis of SONPs + GO

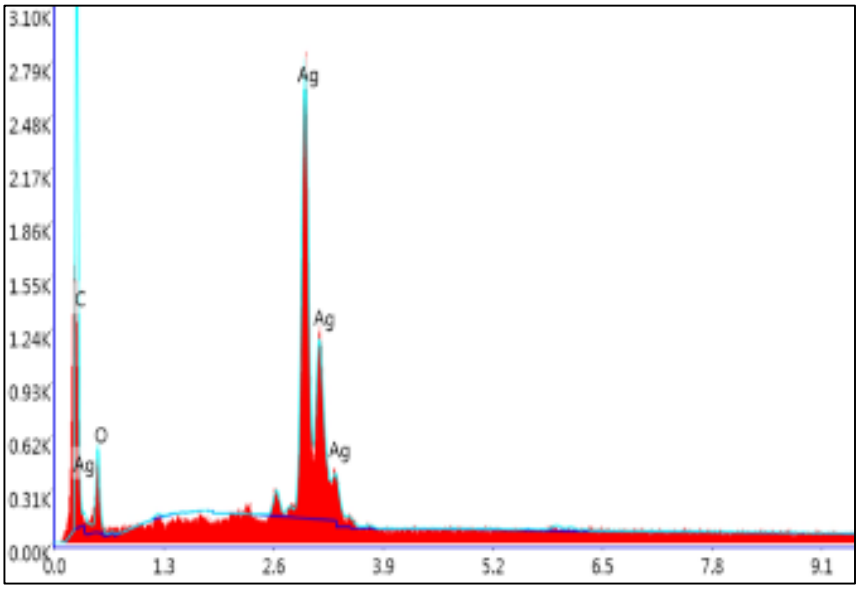

Figure 4.47: ESEM analysis of SONPs + GO

(n) FT–IR analysis of SONPs

FT–IR analysis of SONPs showed peaks (Figure 4.48) at the 3,394 cm^{-1}, 1,649 cm^{-1}, 1,370 cm^{-1}, and 883 cm^{-1}. Stretching and bending vibration of hydroxyl groups were

assigned to the peaks at 3,394 cm^{-1} and 1649 cm^{-1}, respectively. The O–H vibration was manifested in the surface adsorbed water, which promotes the formation of the hydroxide groups on the surface of SONPs. The broad peak at 1,370 cm^{-1} was attributed to stretching vibration N–H groups, which might be due to silver nitrate's chemical composition. FT–IR analysis SONPs + GO composite was manifested that new peaks at 1,229 cm^{-1} and 2,854 cm^{-1} were appeared due to vibration of C–O–C epoxide and $–CH_2$ groups, respectively.

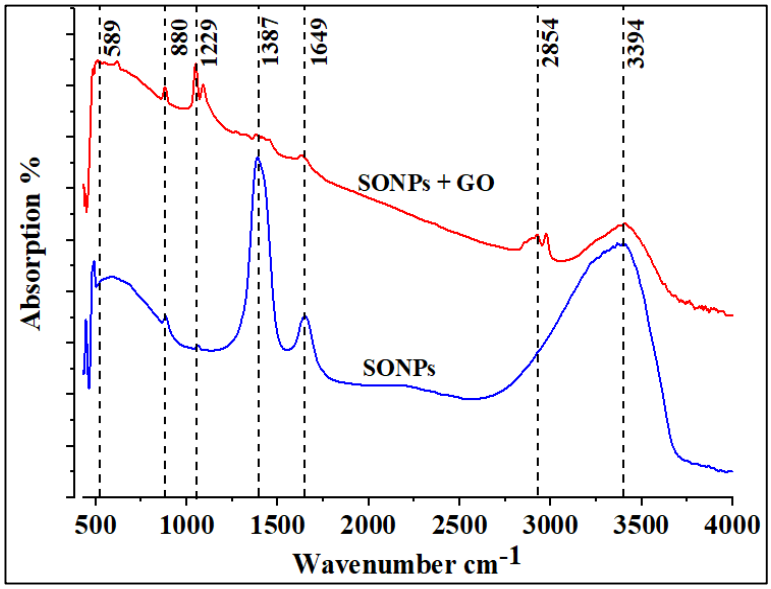

Figure 4.48: FT–IR analysis of SONPs, and SONPs + GO

(o) XRD analysis of ZEOL

Figure 4.49 shows the XRD pattern of modified fly ash and different mineral phases such as Mullite, Hematite, Magnetite, and α–Quartz, which is the main crystal phases in fly ash. XRD analysis of ZEOL showed that sodium aluminium silicate hydrate formed after the alkali treatment (Franus et al., 2014). Aluminium silicate hydrate consists of zeolites like structures such as fauzasite, NaP1, and chabazite (Cama et al., 2005).

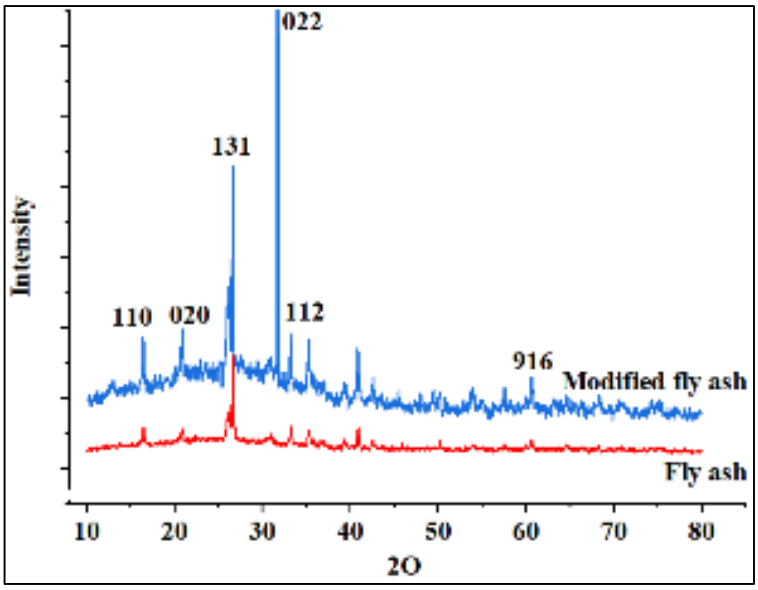

Figure 4.49: XRD analysis of ZEOL

(p) ESEM-EDAX analysis of ZEOL

The ESEM image of fly ash (Figure 4.50) indicates that particles before the alkali treatment are spherical with a smooth surface due to the alumino-silicate layer on the surface. EDAX analysis (Figure 4.51) confirms the availability of different elements on the surface of fly ash such as Si (23.5%), Al (14.6%), O (48.6%), Fe (7.2%), Ti (1.4%), Ca (1.2%), K (1.3%), P (0.8%), Mg (0.9%), and krypton (0.5%).

The ESEM analysis of fly ash after alkali treatment (ZEOL) (Figure 4.52) shows that spherical shapes of fly ash particles disappeared and became highly porous with the rough surface. The highly porous surface showed the formation of ZEOL on the surface of fly ash after hydrothermal treatment. The EDAX analysis of ZEOL shows the availability of different element on the surface such as Si (25.9%), O (45.8%), Al (12.3%), Na (6.5%), Fe (3.6%), Ca (2.8%), Ti (1.6%), K (0.9%), and Mg (0.6%). However, the peak intensity of a few elements has decreased (Figure 4.51). The high percentage of oxygen confirmed that ZEOL consists of aluminium oxide, silicon oxide, calcium oxide, magnesium oxide, sodium oxide, potassium oxide, and iron oxide.

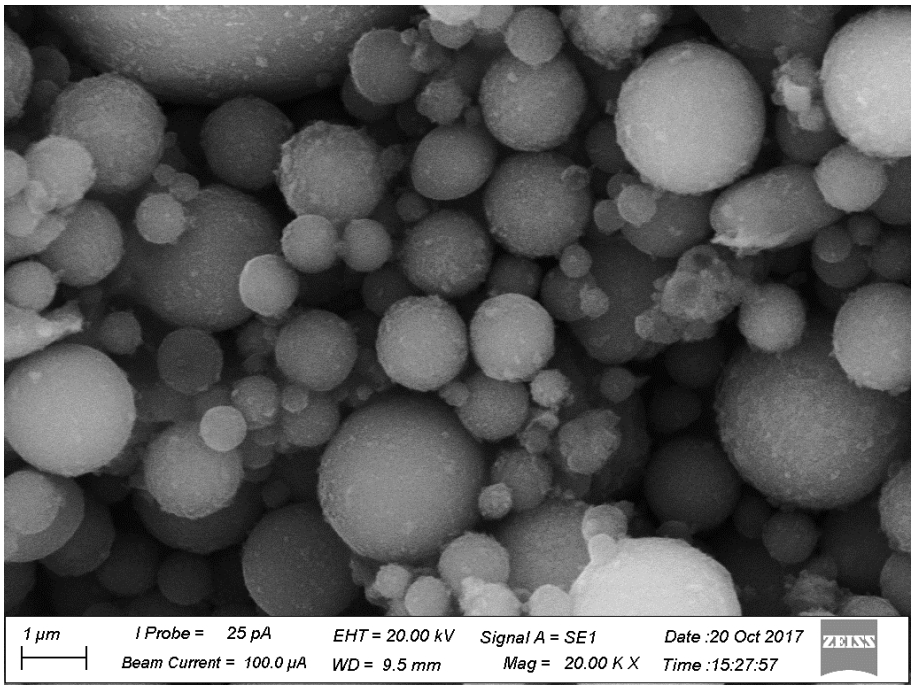

Figure 4.50: ESEM analysis of fly ash

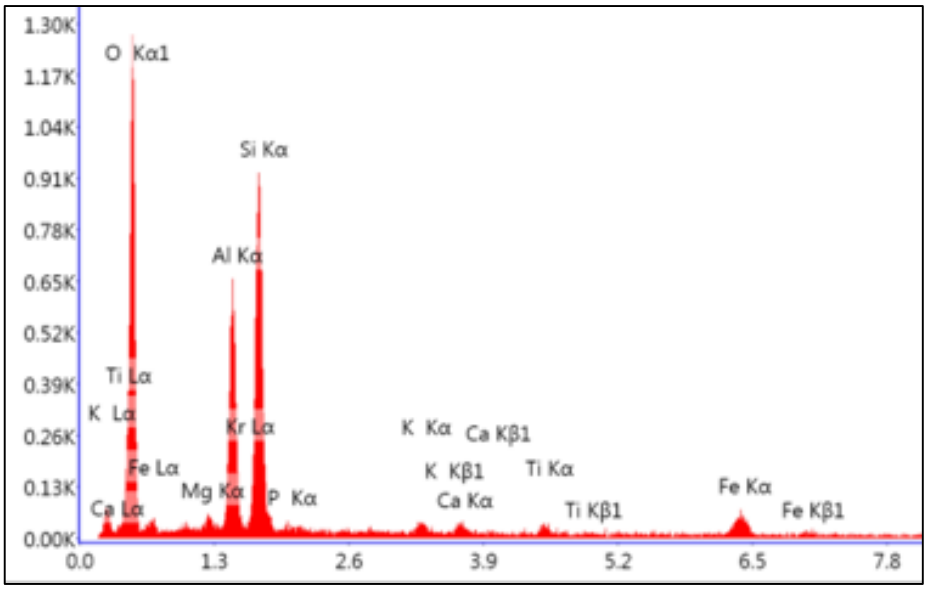

Figure 4.51: EDAX analysis of fly ash

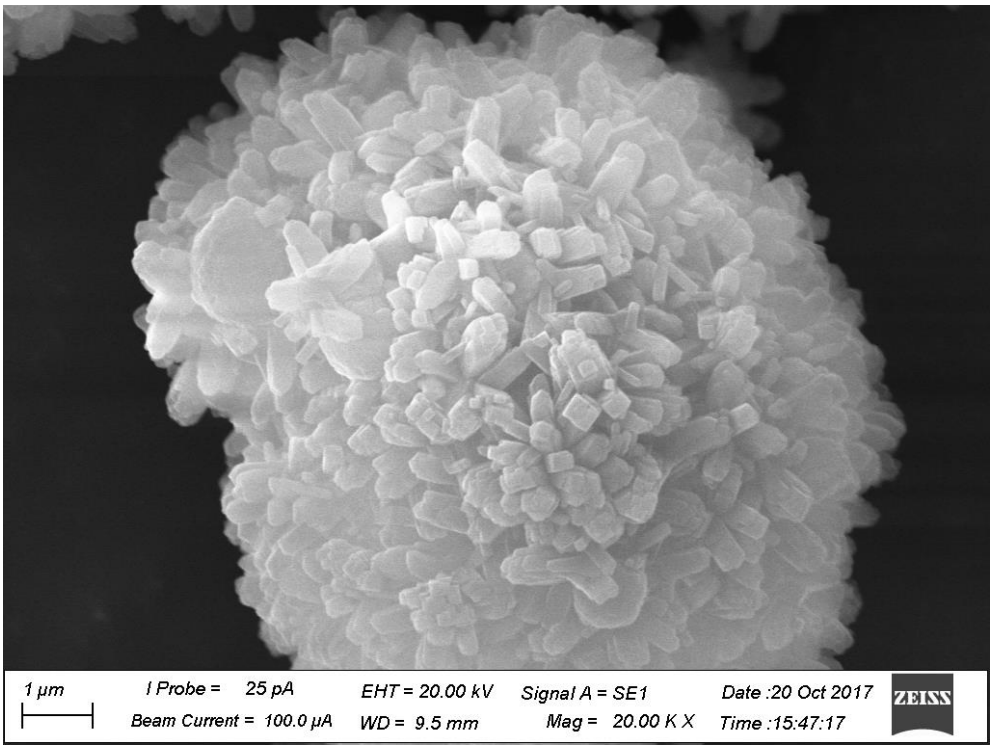

Figure 4.52: ESEM analysis of ZEOL

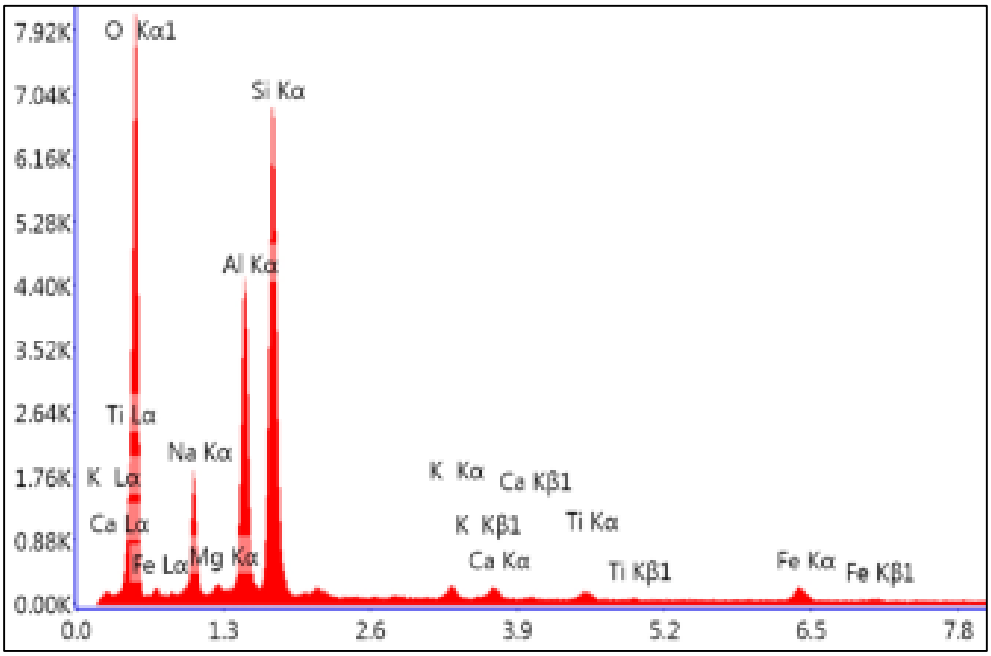

Figure 4.53: EDAX analysis of ZEOL

(q) FT–IR analysis of ZEOL

The FT–IR spectrum of modified fly ash and after adsorption (Figure 4.54) shows that the broad peak at 3,453 cm^{-1} is attributed to O–H groups and the small peak at 2,854 cm^{-1} represents vibration of aliphatic C–H groups. The peak at 479 cm^{-1} is assigned for O–Si–O bending vibration, and the peak at 788 cm^{-1} is attributed to symmetric vibration of Si–O–Si, which manifests the presence of mullite in the sample (Lin et al., 2016). The intensive peak at 1,023 cm^{-1} is assigned to the asymmetric stretching vibration of aluminium present in the tetrahedral silica framework.

After alkali treatment of fly ash to produce zeolite, the broad peak at 3,453 cm^{-1} is further broadened and show high intensity (Aragaw & Ayalew, 2019). After identifying morphological characteristics, removal mechanisms of selected materials were studied to determine adsorption behaviour in the water-solid interface.

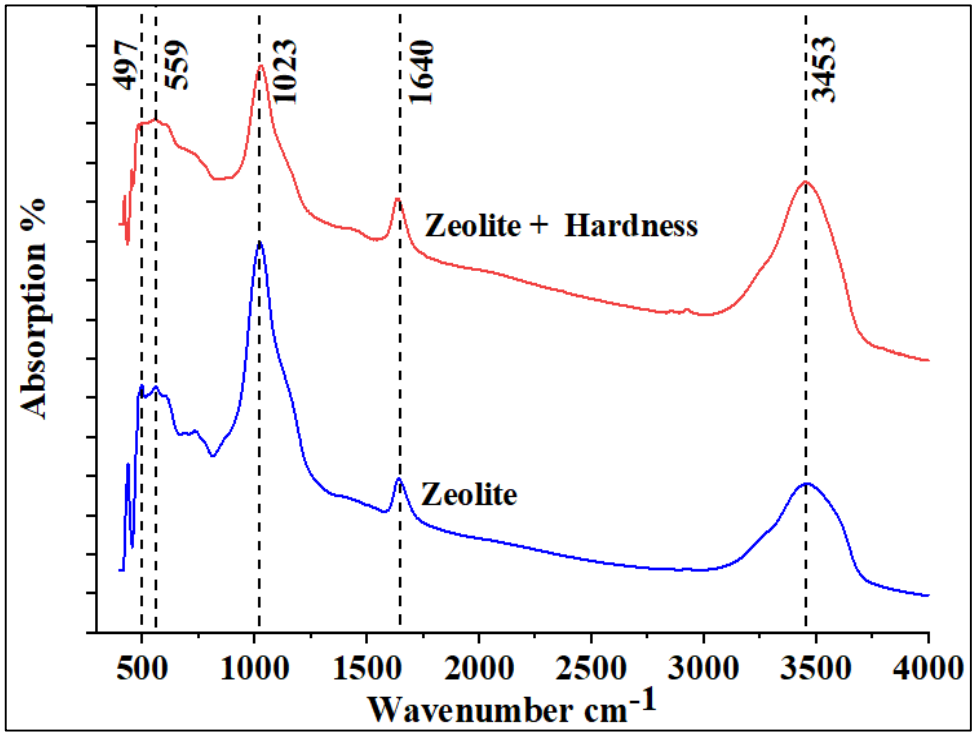

Figure 4.54: FT–IR analysis of ZEOL

4.4.2. Batch adsorption studies

The single-solute and multi-solute batch studies were presented under section 4.4.2, which describes the effectiveness of different materials in removing fluoride, hardness, cadmium, and faecal coliform in potable water. The effects of adsorbent dosage, initial concentration, contact time, and pH solution were discussed, removing nephrotoxic risk factors. The results of batch adsorption studies were accounted to choose the best-performed materials to fabricate a multi-layered home filter unit.

(i) Removal of cadmium by nano zero-valent iron

The nZVI dosage results in removing cadmium and calcium were presented varying nZVI dosage from 0.4 mg/L to 8.0 g/L in single-solute and multi-solute studies (Figure 4.55). Adsorption efficiency gradually increased in single-solute (Cadmium 13 ± 2%–58 ± 2%; Calcium 9 ± 1%–46 ± 1.5%) and multi-solute studies (Cadmium 48 ± 1.5% – 91 ± 1.8%; Calcium 14 ± 0.6% – 34 ± 1.0%) with the increase of nZVI loading. The adsorption capacity (Q_e mg/g) at the equilibrium of nZVI may be decreased due to the unsaturation/partial filling of sorption sites, increasing nZVI dosage. The amount of cadmium adsorbed remained constant after the equilibrium. The adsorbent dosage for individual cadmium and calcium removal was chosen as 4.0 g/L. Beyond 4.0 g/L, cadmium and calcium removal did not lead to significant improvement as the system reaches equilibrium (single-solute: $t_{-7.8}$, $P < 0.05$; multi-solute: $t_{-1.1}$, $P < 0.05$). A similar observation was illustrated by Boparai et al., 2013, and Azam et al., 2016. In multi-solute studies, the percentage of cadmium removal was drastically increased in calcium, which indicates that calcium affects the affinity of cadmium adsorption by nZVI. The different affinities of cadmium and calcium ions for the same active adsorption sites and different groups of functional sites for different adsorbates may increase cadmium's adsorption capacity in the presence of calcium (Boparai et al., 2013). Therefore, nZVI was a promising adsorbent to remove cadmium in CKDu prevalent areas as the treated water meet the required drinking water guideline values of 0.003 mg/L.

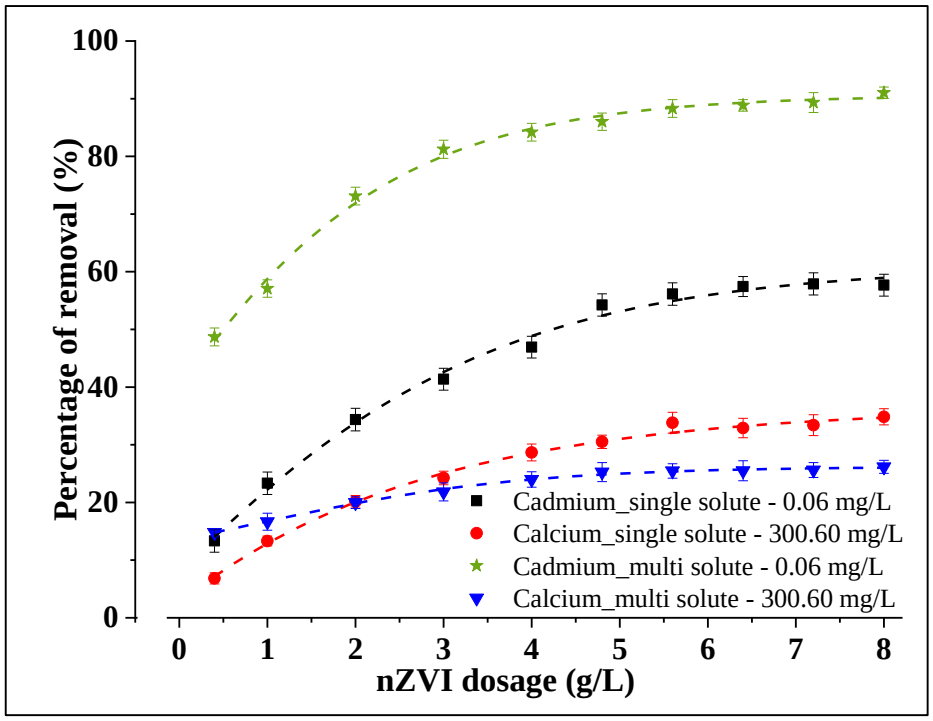

Figure 4.55: Percentage of cadmium removal without calcium and in the presence of calcium changing the nZVI dosage

The effect of pH (3–10) on the adsorption of cadmium and calcium on nZVI was first investigated by fixed nZVI dosage 4.0 g/L and initial cadmium (0.06 mg/L) and calcium (300.10 mg/L) concentrations (Figure 4.56). The removal percentage (25 ± 1.5%–99 ± 1.7%) of cadmium increased with an increase in the initial pH, and the removal rates did not vary above pH 5. Below pH 8.0, cadmium presents as Cd (II) ions, and above pH 8, various cadmium hydroxide species (i.e., $CdOH^{+}$, $Cd_2(OH)^{3+}$, $Cd(OH)_2$, $Cd(OH)^{3-}$ and $Cd(OH)_4^{2-}$) start to form (Ma et al., 2018). Consequently, cadmium hydroxide precipitation might have contributed to its removal from the solution at a pH greater than 8.0. Cd (II), Boparai et al. (2013) reported that cadmium removal increased with solution pH and reached a maximum at pH 8.0. At pH above 7.9, the nZVI surface reached the point of net negative charge (pH_{zpc}), making the surface electrostatically favourable for higher adsorption of cadmium (Boparai et al., 2013).

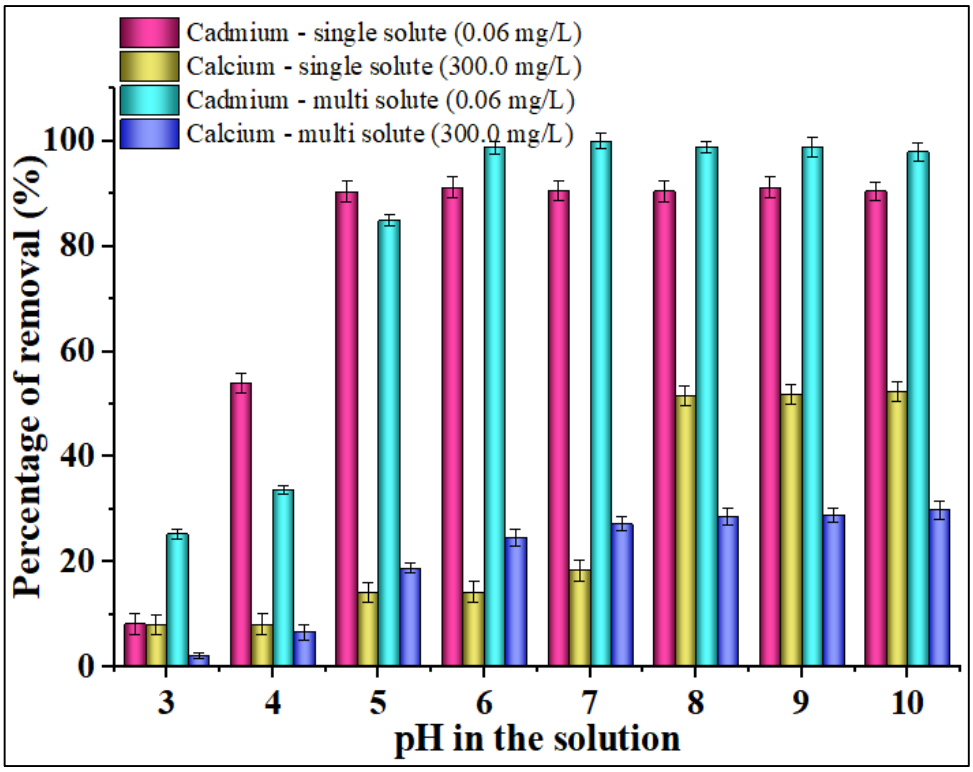

Figure 4.56: Percentage of cadmium and calcium removal changing pH in the solution

The effects of contact time on cadmium and calcium adsorption were determined within the contact time range from 0.5 to 40.0 minutes (Figure 4.57). The initial cadmium and calcium ions levels were kept at 0.062 mg/L and 310.75 mg/L, respectively. Percentage of cadmium and calcium removal was in the range of 39 ± 1.0%–98 ± 1.5% and 16 ± 1.7%–20 ± 2.0%, respectively. The adsorption capacity was increased when the contact time was increasing. Initially, cadmium and calcium's adsorption capacity increased rapidly due to the abundance of active adsorption sites (Peng et al., 2018; Azzam et al., 2016).

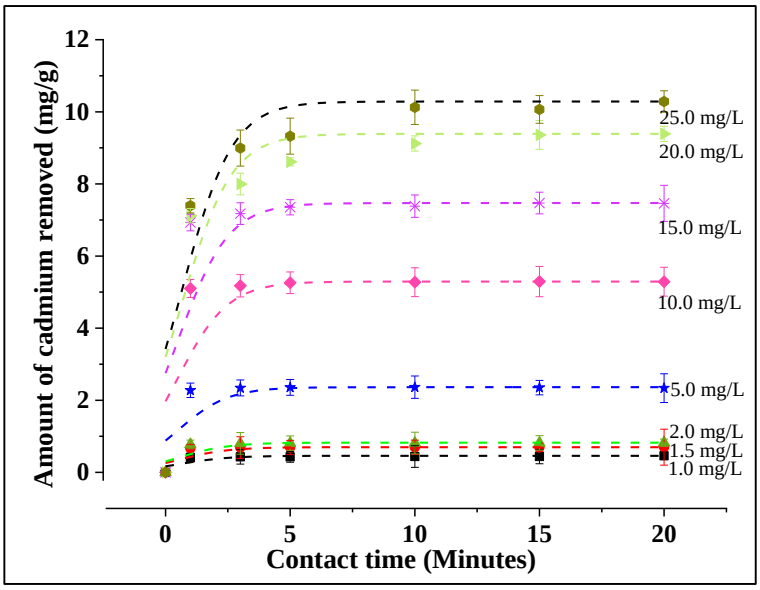

Figure 4.57: Percentage of cadmium removal changing the contact time

The effect of initial concentration on cadmium adsorption with a constant dosage of 4.0 g/ L of nZVI and initial cadmium concentration varying from 1.0 to 25.0 mg/ L was studied (Figure 4.58). When the initial cadmium concentration increased, the amount of cadmium adsorbed risen from 0.41 ± 0.21 to 10.28 ± 0.29 mg/g (88%–96%). The initial concentration effect was determined with a constant dosage of 4.0 g/L of nZVI by varying the calcium concentration from 100.0 to 400.0 mg/L. The amount of calcium adsorbed increased from 8.3 ± 0.13 to 16.31 ± 0.51 mg/g. Cadmium and calcium uptake increased while the initial concentrations were raised because the initial ion concentration in the solution facilitates the mass transfer between the solution and solid phases. The same observation has been reported by Peng et al., 2018, for a different system.

The multi-solute studies adsorption equilibria of cadmium and calcium by single-solute data were determined using the IAST model [Eq. (18), (19), (20) & (21)] (Table 4.10). The partial cadmium loading for corresponding combinations of cadmium and calcium was estimated to be between 17.39 ± 0.19–21.21 ± 0.17 mg/g of cadmium, and the partial calcium loading was 6.85 ± 0.15–8.35 ± 0.16 mg/g. The amount of cadmium

and calcium adsorbed in multi-solute studies corresponding to concentrations of single-solute studies was determined as 0.44 ± 0.11–8.78 ± 0.08 mg/g and 8.34 ± 0.12–14.53 ± 0.07 mg/g, respectively. The results showed that the total cadmium and calcium removal in mixture adsorption equilibria were gradually increased when cadmium and calcium concentration was increased in the system.

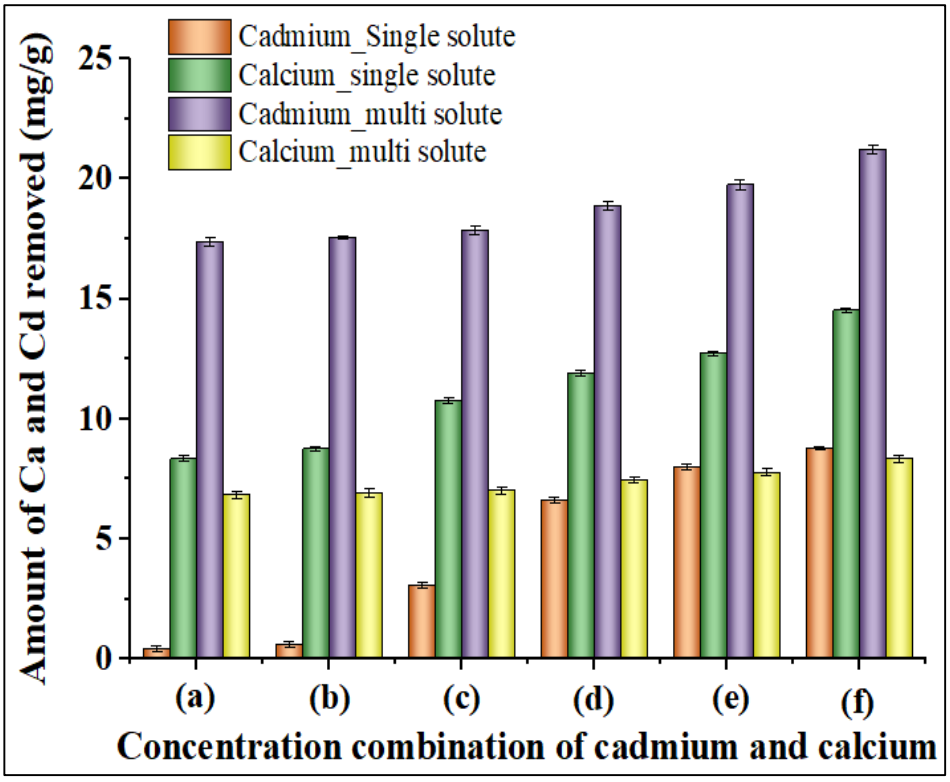

Figure 4.58: Cadmium and calcium removal using nZVI dosage 4.0 g/L using combinations of cadmium (mg/L) and calcium (mg/L) a). 1.0, 110.4 b). 1.5, 149.6 c). 4.9, 206.4 d). 15.39, 248.8 e). 20, 293.6 f). 24.75, 396.8

The increase of the spreading pressure is definite in the system; it increases the tendency of wetting the surface of the nZVI entirely by cadmium and calcium solution. The removal of cadmium by nZVI in the multi-solute studies increased compared to cadmium in the single-solute studies. The results implied that the cadmium's spreading pressure is lower than calcium, which enhances the tendency to wet the surface of nZVI by cadmium. The removal of calcium by nZVI in multi-solute studies was decreased

compared to the amount of calcium removal in the single-solute studies. The mole fraction of calcium adsorbed in multi-solute studies was lower than the mole fraction of calcium adsorbed in single-solute studies. Hence, the removal of cadmium might be increased more than calcium in the competitive adsorption system.

Table 4.11: Partial adsorption of cadmium and calcium during competitive adsorption in multi-solute studies

Concentration combinations (mg/L)		**Basis on mass balance equation**				**Based on IAST**			
		Single solute (Q_e) (mg/g)		**Multi-solute (Q_i) (mg/g)**		**Mole fraction (Z_i)**		**Spreading pressure (ψ) (N/m)**	
Cd	Ca	Cd	Ca	Cd	Ca	Cd	Ca	Cd	Ca
1.00	100.00	0.44 ± 0.11	8.34 ± 0.12	17.39 ± 0.19	6.85 ± 0.15	0.71	0.28	0.38	54.96
1.50	150.00	0.62 ± 0.11	8.76 ± 0.09	17.57 ± 0.08	6.92 ± 0.16	0.71	0.28	0.57	64.38
5.00	200.00	3.09 ± 0.12	10.76 ± 0.11	17.85 ± 0.17	7.03 ± 0.16	0.71	0.28	0.96	73.75
15.00	250.00	6.63 ± 0.11	11.93 ± 0.12	18.91 ± 0.18	7.45 ± 0.11	0.71	0.28	2.72	78.13
20.00	300.00	8.02 ± 0.12	12.74 ± 0.09	19.76 ± 0.19	7.78 ± 0.14	0.71	0.28	4.50	82.22
25.00	400.00	8.78 ± 0.08	14.53 ± 0.07	21.21 ± 0.17	8.35 ± 0.15	0.71	0.28	8.99	90.24

(ii) Removal of fluoride using MOMA

The results indicated that the percentage of fluoride removal in single and multi-solute studies sharply increased until MOMA dosage reached 2.0 g/L (Figure 4.59). The removal of fluoride after 2.0 g/L was almost the same since the system reached its equilibrium state ($t_{3.4}$, $P < 0.05$); MOMA particles subsequently upsurge unsaturated partial filling of adsorption sites, particles-particles interactions, and particle

agglomeration took place in the solution (Marinković et al., 2015; Prathibha et al., 2015). Therefore, the optimum dosages were chosen as 2.0 g/L; after 2.0 g/L, no substantial fluoride removal was observed.

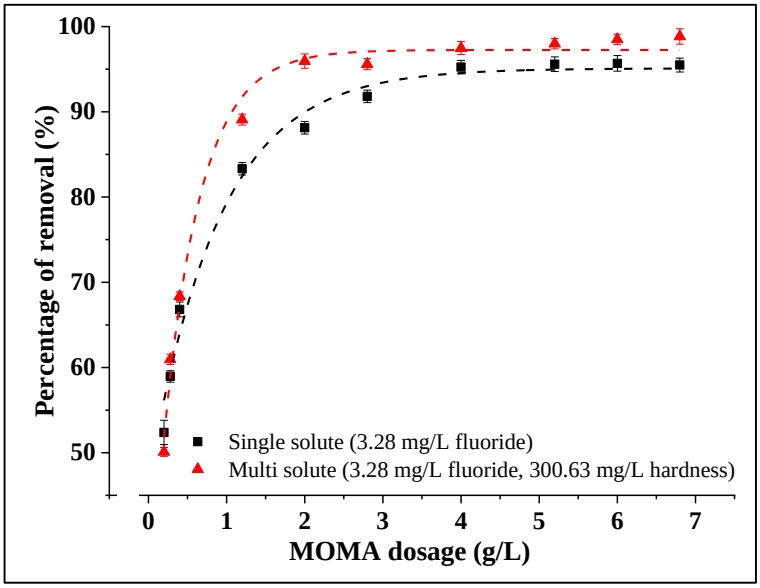

Figure 4.59: Removal of fluoride from potable water changing the adsorbent dosage

MOMA's adsorption capacity did not show a significant difference with pH varying between 3–10 (Figure 4.60). Low pH (pH 4) increased fluoride adsorbed by MOMA more than MESA and COMA. The results corroborated that MOMA's positive surface charges at the pH_{zpc} (pH – 4) show a high affinity towards fluoride. The same observation has been explained by Singh et al. (2018). MOMA demonstrated high interaction with fluoride more than the other adsorbents (98% of fluoride removal, 96% by COMA, 92% by FeON, 88% by MESA, 51% by GO), which may be due to surface functional groups such as Al–O and Mg–O enhance the affinity towards fluoride more than calcium ions. The water treated by MOMA complied with drinking water guideline values (0.2 mg/L) considered in the study. However, water treated with other materials did not meet 0.2 mg/L. Hence, the MOMA was chosen as one of the adsorbents in the

multilayer column and used for the rest of fluoride adsorption studies to identify their fluoride removal effectiveness.

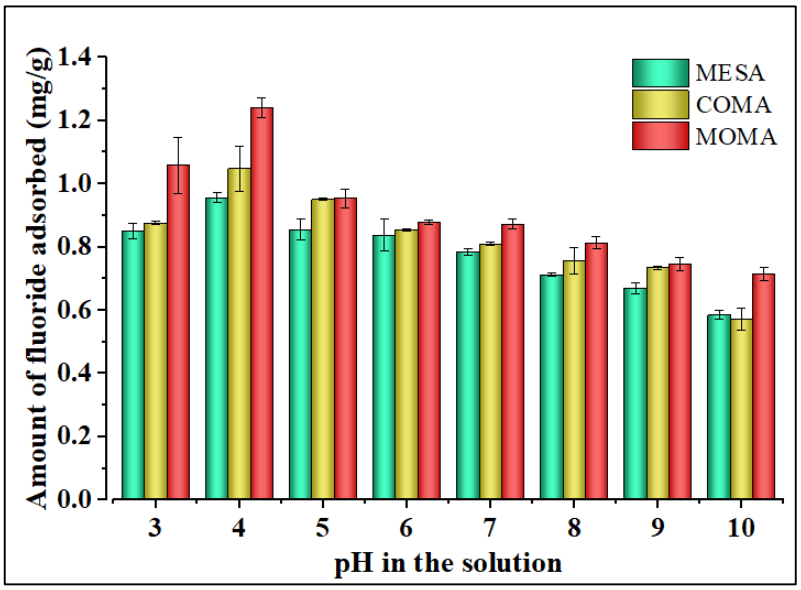

Figure 4.60: Removal of fluoride from potable water changing pH in the solution

The initial fluoride concentration was changed in a range of 1.0–13.0 mg/L using a MOMA dosage of 2.0 g/L. MOMA showed different fluoride adsorption capacities with varying concentrations of fluoride (Figure 4.61). A higher percentage of removal was observed at the 3.0 mg/L fluoride concentration. The percentage of fluoride removal decreased gradually when the fluoride concentration of the solution increased. The fluoride adsorbed increased from 0.40 ± 0.11 to 3.96 ± 0.23 mg/g when the initial fluoride concentrations were increased. Formation of aluminium fluoride (AlF_3) complexes (Illeperuma et al., 2009; Kumar et al., 2011), precipitation of magnesium fluorite (Kanehiraa et al., 2013) and adsorption of fluoride alone are possible fluoride removal processes on the solid-liquid interface. Excluding 10.0 mg/L and 13.0 mg/L, residual concentrations in other fluoride concentration (1.0 mg/L to 7.0 mg/L) were within the limit of permissible level stipulated by the study (0.2 mg/L).

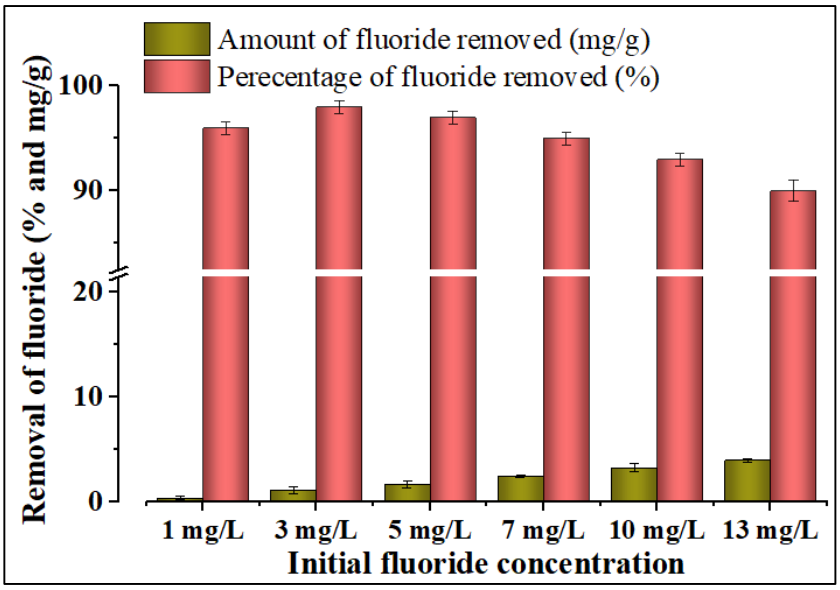

Figure 4.61: Removal of fluoride changing initial fluoride concentration

The initial calcium concentrations have varied within a range of 50–1000 mg/L with 3.0 mg/L of fluoride using 2.0 g/L of MOMA (Figure 4.60). The amount of fluoride adsorbed by MOMA was determined as 0.95 ± 0.11–1.16 ± 0.21 mg/g. Magnesium oxide ion on the surface of MOMA produces magnesium hydroxide ($Mg(OH)_2$ complexes (Islam and Patel, 2007). Replacement of hydroxyl groups (–OH) by fluoride ions might increase their electronegativity and high reactivity (Habuda-Stanić et al., 2014); thus, the removal of fluoride was increased from the solution. The removal of fluoride was observed as effective in the presence of high calcium, which should be less than 750.0 mg/L. The possible synergic effects on CKDu by fluoride in the presence of calcium was proposed by Wasana and co-workers in 2016 when fluoride concentration is less than the WHO maximum level of 1.5 mg/L. Thus, MOMA helps to control the synergic effect of fluoride in the presence of calcium.

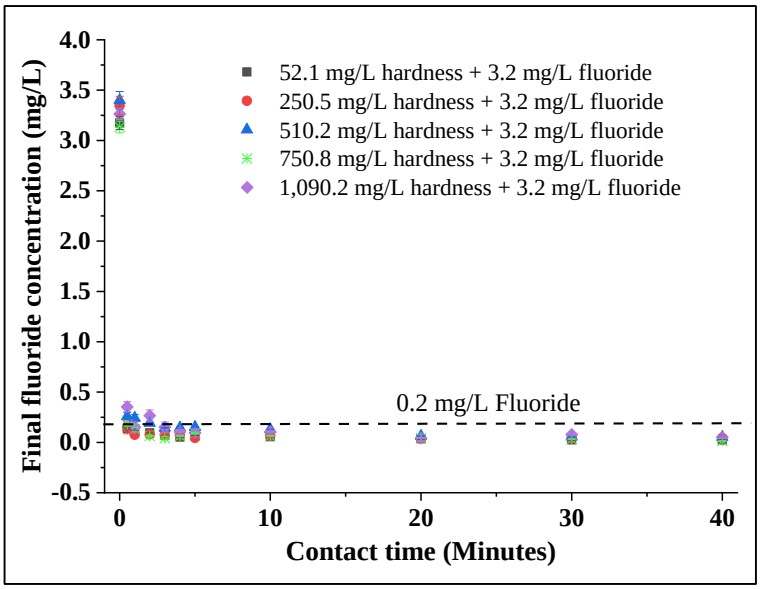

Figure 4.62: Removal of fluoride from potable water changing initial fluoride and hardness concentration

(iii) Adsorption of hardness by Zeolite

The percentages of hardness removal increased (68 ± 2% – 93 ± 1%) with the change of ZEOL dosage from 1.0–8.0 g/L ($t_{0.96}$, $P < 0.05$). The system reached equilibrium at the 4.0 g/L of ZEOL dosage (Figure 4.61). The amount of hardness removed per 1.0 g of ZEOL was decreased (86.0 ± 0.09 mg/g–14.7 ± 0.52 mg/g) gradually while ZEOL dosage was increased as the system reached an equilibrium state. The hardness removal increased linearly with the ZEOL dosage increase in the range of 1.0 to 4.0 g/L. After 4.0 g/L of ZEOL, the hardness removal decreased considerably, indicating no significant difference in hardness removal. The decreased amount of removal was observed due to the unsaturation of active sites during the adsorption process in the different systems by Peng et al. (2018). Hence, the optimum dosage of ZEOL was chosen as 4.0 g/L as hardness removal did not show a significant change after 4.0 g/L. The optimum dosage of ZEOL occupied in each test carried out using ZEOL. EDAX analysis of ZEOL corroborated that ZEOL attributes with different metal oxides on the surface may increase cations' removal in the solution. Hardness in potable water consists of high

content of cations such as calcium and magnesium (Wasana et al., 2016 & Dharma-wardana, 2018), which can be removed effectively from potable water by ZEOL.

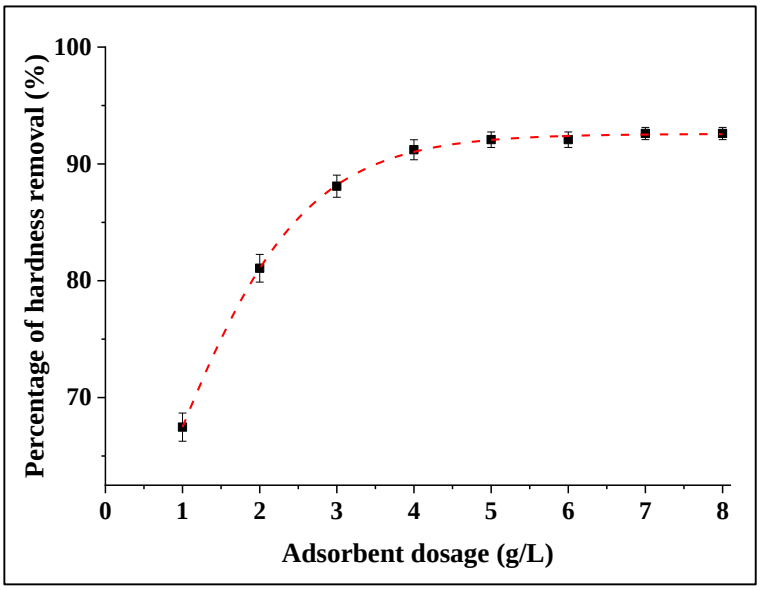

Figure 4.63: Removal of hardness changing the dosage of ZEOL (Hardness concentration - 500.0 mg/L)

The contact time results in removing hardness were presented in Figure 4.62 within the contact time range from 0.5 minutes to 30.0 minutes. The hardness concentration was 500.0 mg/L, the solution pH was 5, and the adsorbent dosage was 4.0 g/L. The removal of hardness was increased initially because of the abundance availability of active adsorption sites. The adsorption capacity gradually increased with the increase of contact time (Percentage of removal 84 ± 1%–95 ± 2%; the amount of adsorbed 28.25 ± 0.21–30.12 ± 0.11 mg/g). After 2 minutes of contact time, the hardness removal rate gradually decreased, and the system reached the point of saturation, indicating 90% of hardness removal (nZVI – 27%, FeON – 43%, GO – 36%, COMA-12%, MOMA – 23%). The hardness removal rate decreased due to limited adsorption sites on the surface (Geethamani et al., 2013). During the batch adsorption studies, a monolayer of adsorbate forms on the surface of the adsorbent. Hence, the rate of removal is controlled by the rate of adsorbate transport from the outer sphere to the adsorbent's inner sphere (from

liquid to the solid interface) (Hall et al., 1966). However, the treated water meets the required drinking water reference value of 120.0 mg/L.

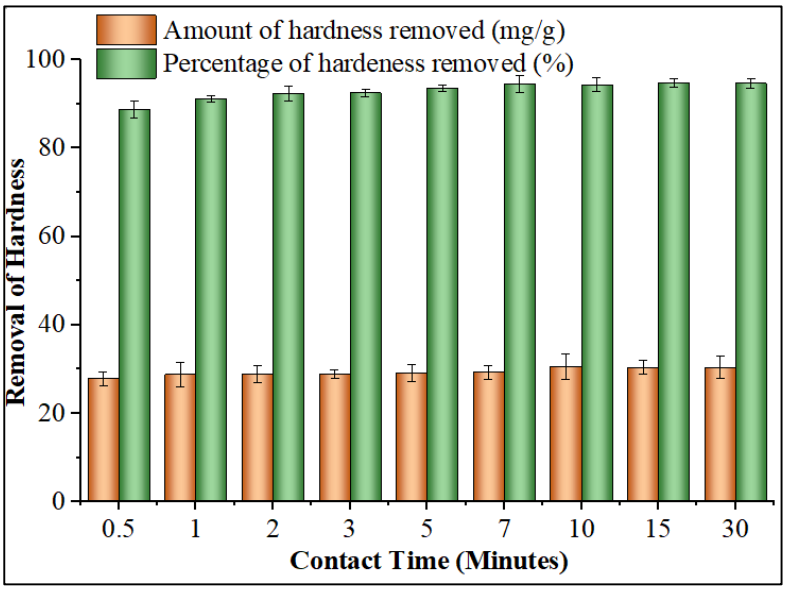

Figure 4.64: Removal of hardness changing contact time (hardness concentration - 500.0 mg/L)

The results of percentages of hardness removal in pH changes with 500.0 mg/L of hardness, 4.0 g/L of ZEOL, 100.0 mL of the solution and 30 minutes of contact time were presented in Figure 4.65. When the pH of the solution was increased from pH 5 to the alkalinity range by adding NaOH dropwise, the precipitation formation in the solution occurred with a colourless cloudy appearance. Hardness removal was increased from 44 ± 1% to 93 ± 2% until the pH of the solution increased from pH 3 to pH 7. The optimum percentage of hardness removal was observed at pH 7. When the pH of the solution was increased further, the percentage of hardness removal was decreased gradually from 77 ± 1% to 53 ± 3% for the pH range in 8–10. The lower removal percentage of hardness was observed at the lower range of pH (acidic) attributed to protonation of ion exchange in functional groups on the surface of ZEOL, or H^+ ion compete with calcium and magnesium ions to occupy on the adsorption sites of the

ZEOL (Aragaw & Ayalew, 2019). In alkaline media, metal hydroxide formation may be the prominent reason for the gradual reduction of hardness removal.

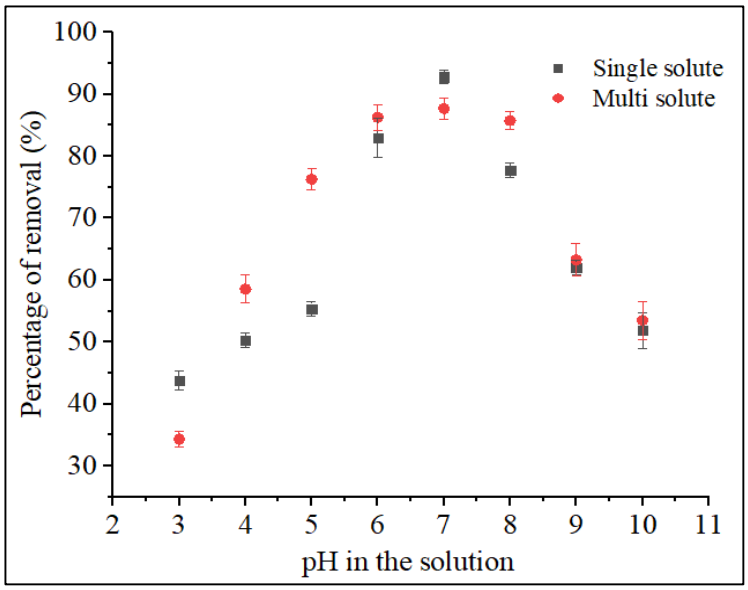

Figure 4.65: Removal of hardness changing pH in the solution (hardness concentration - 500.0 mg/L)

The results in the effects of initial hardness concentration (a range from 50.0 mg/L to 1,000.0 mg/L) were presented in Figure 4.66 with 4.0 g/L ZEOL, 30 minutes' contact time and 100.0 mL of solution. The results showed that the amount of hardness removed was increased (3.06 ± 1.15 mg/g–26.86 ± 1.52 mg/g) with initial hardness concentrations, attributed to the higher content of ions in a unit volume of the solution. However, the percentage of hardness removal was decreased gradually (96 ± 1%–86 ± 2%) when the initial hardness concentration was increased. Initial metal concentration was driven to overcome mass transfer between the solid and liquid phases (Peng et al., 2018). Hardness in solution interacts with adsorption sites on the surface at lower concentrations, facilitating 99 ± 1% hardness removal. With higher hardness concentrations, most calcium and magnesium ions remained in the solution as unadsorbed ions due to the saturation of the adsorption sites, leading to the reduction of hardness removal.

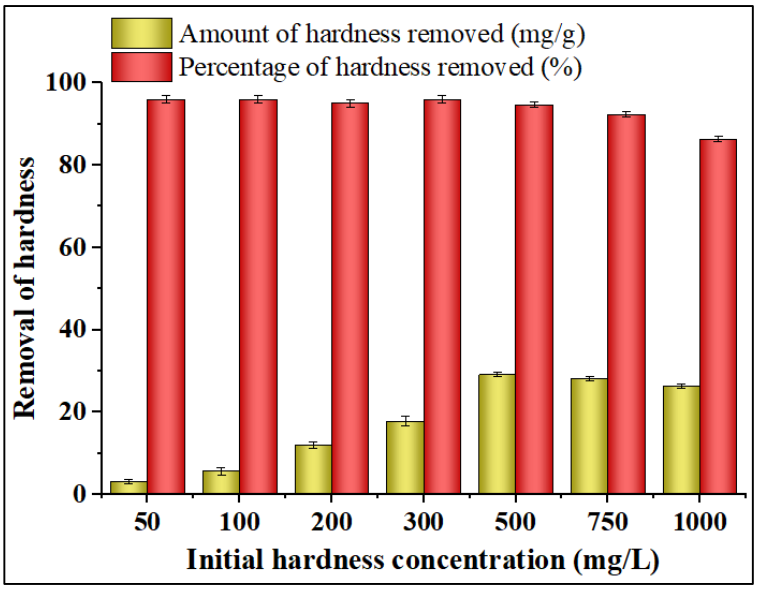

Figure 4.66: Removal of hardness changing the initial hardness concentration

The results in effects of different fluoride concentrations in removing hardness were presented in Figure 4.67 in multi-solute studies with different fluoride concentrations in a range of 1.0 mg/L to 10.0 mg/L and with 508.0 mg/L of hardness in each solution. The percentage of hardness removal was not varied (94 ± 1% –96 ± 2%) with increased fluoride concentration. The fluoride removal rate remained in the range of 41 ± 1% to 64 ± 1% with the fixed hardness concentration. The percentage of hardness removal by ZEOL was observed greater than fluoride removal in the multicomponent system, which attributed to the ZEOL surface consists of different metal oxides. Negatively charged metal oxide and pH 6.5 in the solution may increase calcium and magnesium cations' removal more than anion like fluoride. The results were shown that ZEOL was not a promising adsorbent to remove fluoride and manifested a high capacity to remove hardness in the presence of fluoride. The ZEOL has shown its attributes of selective adsorption of hardness. In a multi-solute system, the competition of the fluoride and hardness for the existing adsorption site can decrease the percentage of removal. Additionally, interactions of fluoride and hardness while transporting from the liquid phase to the surface of ZEOL may be the reason for the reduction in fluoride removal

percentage (Worch, 2012). Therefore, ZEOL was chosen as one of the adsorbents used to remove hardness in a multi-layer column.

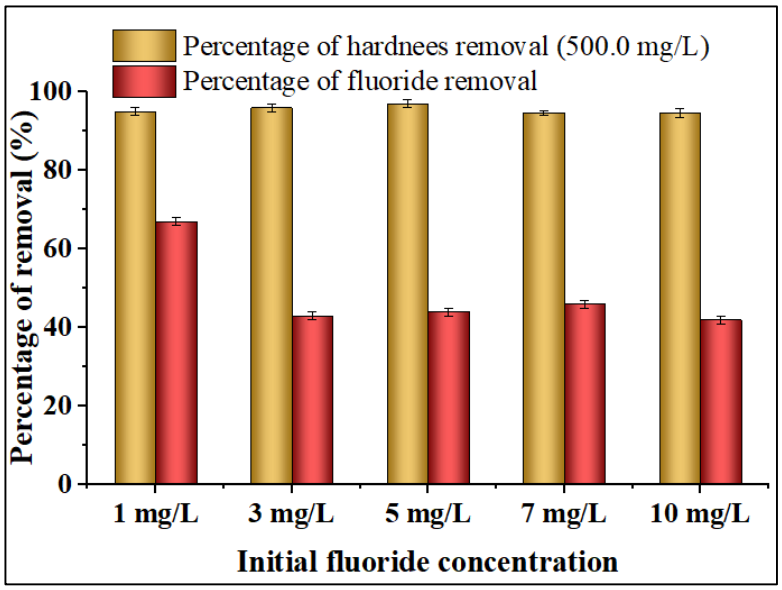

Figure 4.67: Removal of hardness changing the initial fluoride concentration

(iv) Removal of *E. coli* using SONPs and SONPs + GO composite

The results of the removal of *E. coli* using SONPs and SONPs + GO are described in this section. First, the results of SONPs in removing *E. coli* using the inhibition zone method, well-diffusion method, and optical density method were presented. Later, batch adsorption studies were discussed.

(a) Investigation of SONPs distribution pattern through culture media

The results showed that SONPs diffused through the culture media following the shape of an irregular radial distribution pattern. Growth inhibition of *E coli* by the reaction of SONPs occurs following the distribution pattern (Figure 4.66). The distribution pattern of silver oxide particles was observed limited with lower SONPs dosage. The SONPs distribution circle area was expanded substantially when the dosage was increased in a range of 0.125–0.200 g for 96 hours.

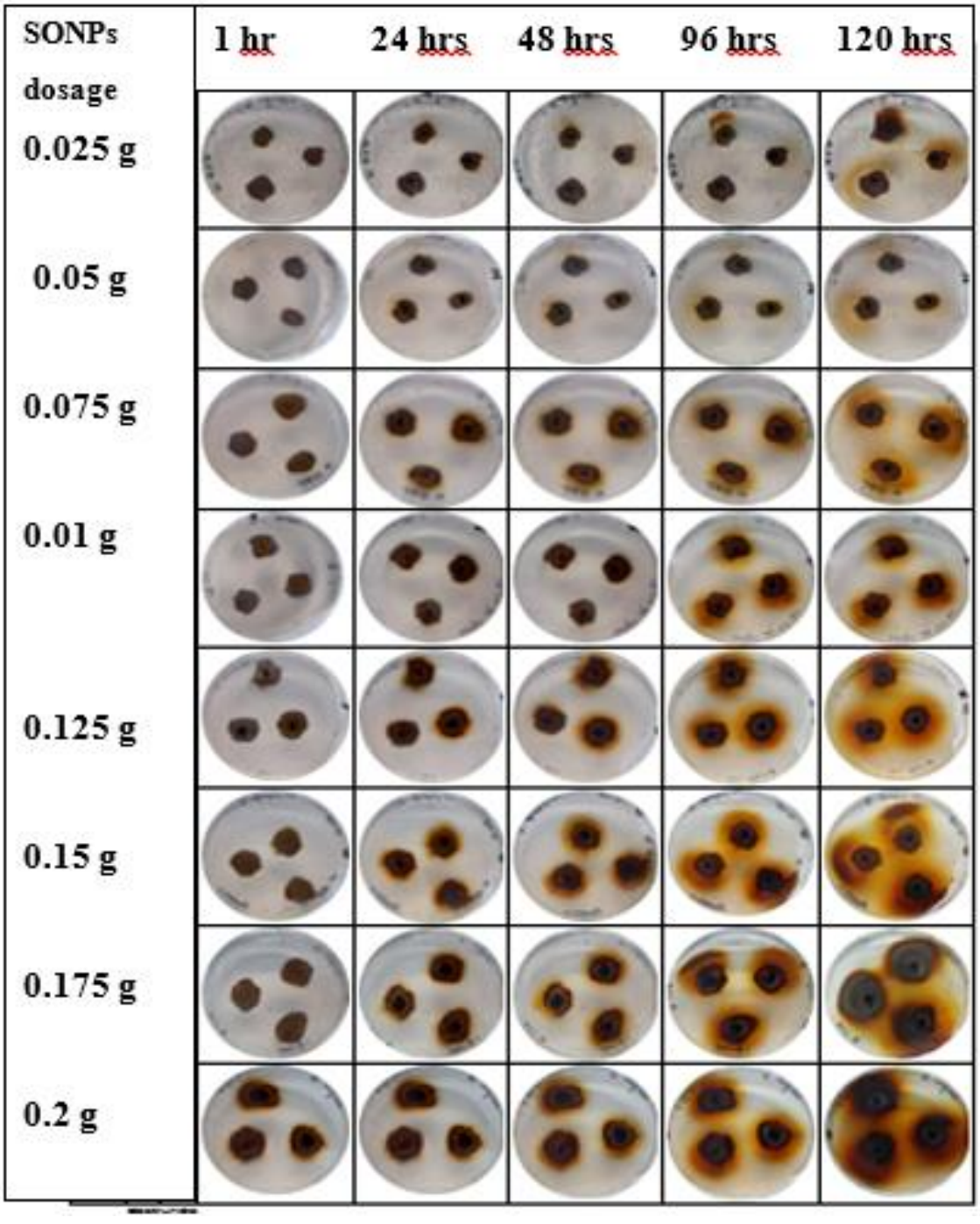

Figure 4.68: Distribution pattern of SONPs through the culture media

The results corroborated that a higher dosage of SONPs inhibits bacteria growth in the area expanded greater than lower dosages. The distribution of SONPs through agar with higher dosages increases bacterial cells' contact with silver particles.

(b) Investigation of a range of suitable SONPs + GO dosage using the inhibition zone method

Figure 4.67 illustrates the formation of the inhibition zone in the presence of SONPs + GO in a range of 0.025 g to 0.2 g. An inhibition zone of *E. coli* bacteria was observed starting to form at 0.025 g of SONPs + GO dosage for 24 hours of contact time (Figure 4.68). The inhibition zone diameter was increased from minimum to maximum as 11.60 ± 3.87–23.86 ± 0.87 mm in the range of SONPs + GO 0.025–0.200 g dosages. The inhibition zone diameter of 18.98 ± 2.27 mm was observed at 0.175 mm for a minimum contact time of 24 hours. These results corroborated that 0.175 g of SONPs + GO disperse substantially through the agar media within 24 hours greater than other dosages. However, the maximum diameter of the inhibition zone appeared at 0.15 mm for 120 hours.

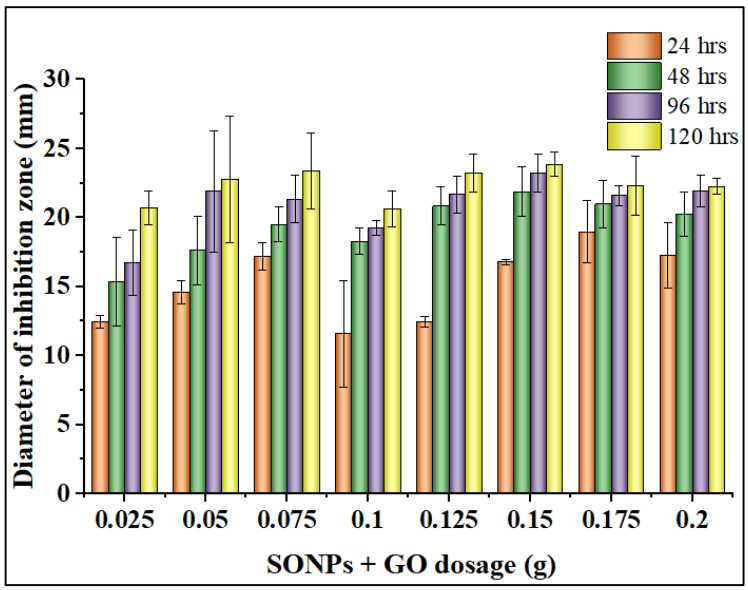

Figure 4.69: Growth inhibition zone diameter of *E. coli* bacteria using an inhibition zone method with a range of SONPs + GO dosage

The paired sample t-test results indicated that mean values in each dosage have a positive correlation and no significant difference between the inhibition zone's diameter ($P > 0.05$). The results indicated that bacterial growth inhibition depends on the initial number of bacterial cells and SONPs + GO dosage. The specific large surface area in SONPs + GO enhances the contact of bacterial cells with the nanoparticles. Large contact areas expect to be eliminating the growth extension of bacterial cells. When nanosilver was in contact with bacterial cells, it has been suggested that nanosilver and bacterial cell interactions produce free radicals, which can damage the cell membrane, make membrane porous, and ultimately lead to cell death (Xiea et al., 2014).

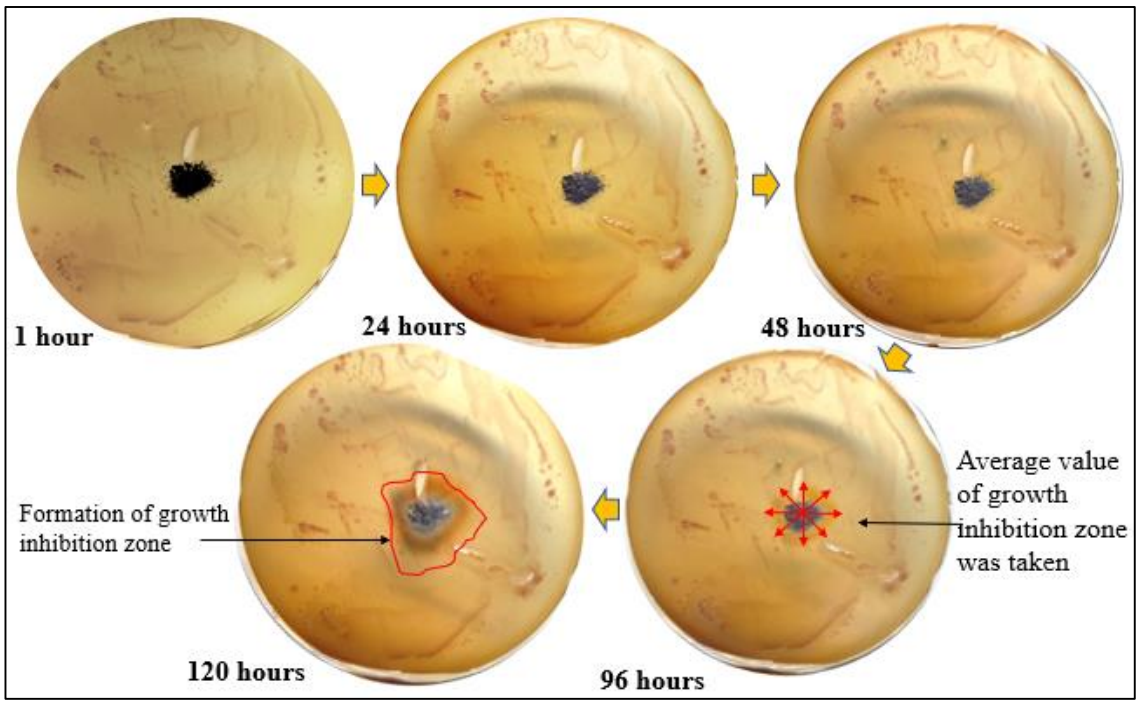

Figure 4.70: Formation of growth inhibition zone of *E coli* bacteria with SONPs + GO

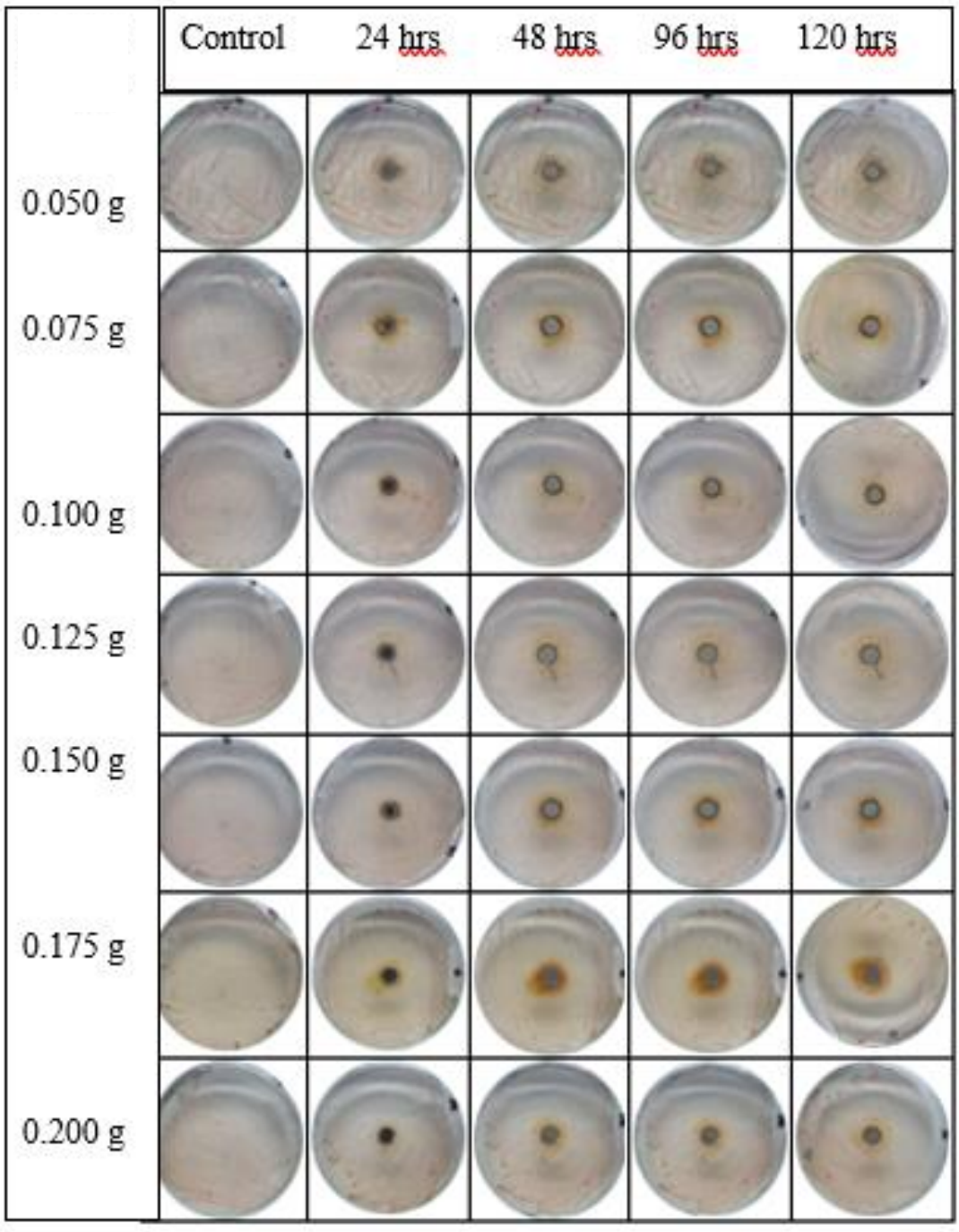

Figure 4.71: Disinfection potential of *E. coli* bacteria by the well-diffusion method with a range of SONPs + GO dosage

(c) Investigation of growth inhibition of *E coli* using the well-diffusion method

The formation of an inhibition zone using the well-diffusion method with a range of SONPs + GO dosage from 0.050 to 0.200 g was depicted in e Figure 4.69.

The formation of the inhibition zone was observed starting at 24 hours of contact time. The formation of a transparent inhibition zone was visible clearly after 48 hours of the incubation period. When the contact time of SONPs + GO was increased with bacterial suspension and a range of SONPs + GO, the dispersion of SONPs + GO was increased through culture media and the disinfection effectiveness of SONPs + GO was increased gradually.

The mean diameter of the inhibition zone for the well-diffusion method varied from minimum to maximum values as 11.70 ± 0.71 to 24.60 ± 0.71 mm (Figure 4.70). The higher inhibition zone diameter was observed with 0.075 g SONPs + GO for each contact time (24, 48, 96 and 120 hours). The results indicated SONPs + GO well-diffused through agar media increases the interaction of silver nanoparticles with bacterial cells and lead to the effective elimination of bacterial cell growth.

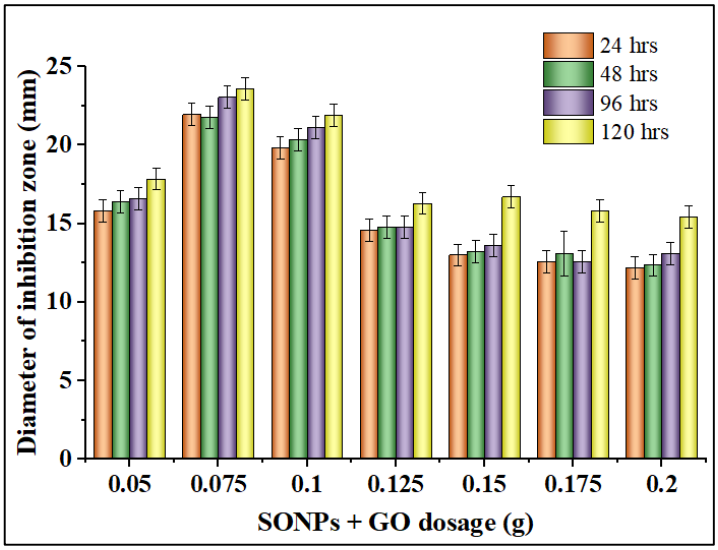

Figure 4.72: Growth inhibition zone diameter of *E. coli* bacteria using a well-diffusion method with a range of SONPs + GO dosage

The attachment of free silver nanoparticles with bacterial cell membrane changes the cell membrane structure, disrupts the production of adenosine triphosphate (ATP) and DNA replication, leading to bacterial cell apoptosis (Choi et al., 2009; Landry et al., 2009). In the presence of SONPs, large quantities of nanoparticles may be attached to the cell membrane resulting accumulation of reactive oxygen species (ROS) and considerable changes in cell membrane leading to inhibition of bacterial cell growth. The results of the paired-sample *t-test* between the diameter of the inhibition zone and contact time indicated a strong positive correlation (0.99) in the mean values of the inhibition zone diameter in the well-diffusion method. The statistical results explained a significant difference between the mean values of inhibition zone diameters in different SONPs dosage ($P < 0.05$).

(d) Investigation of *E. coli* disinfection potential using broth-dilution (Optical density) method

The optical density method results corroborated that different SONPs + GO dosage showed different affinities during the bacterial disinfection process. The control experimental test tubes showed robust bacterial cells changing MacConkey broth culture media's colour from purple to pale yellow (Figure 4.71). The percentage of growth inhibition was observed decreasing with 0.01 g and 0.025 g (Figure 4.72). Due to the low content of silver nanoparticles in the culture media, it may inhibit bacterial growth. The maximum percentage of growth inhibition was observed at 0.075 g of SONPs + GO as 79 ± 20%.

The bacterial cells in the presence of 0.075 g of SONPs + GO were reduced greatly more than the other dosages. The well-dispersion of SONPs through the culture media, contact silver nanoparticles properly with bacterial cells and deposition of bacterial cells died in the bottom of the test tube as sediment appear to be the reasons increasing the percentage of growth inhibition. After SONPs + GO dosage of 0.075 g, the percentage of growth inhibition was observed decreasing. It may be due to the dispersion of the high content of SONPs through the liquid culture media increasing light absorption

across visible ranges of the electromagnetic spectrum. Hence, the percentage of growth inhibition appears decreasing with increasing the dosage of SONPs + GO. The bactericidal effects of the SONPs depend on the dosage of the SONPs + GO and initial bacterial concentration. The results confirmed the SONPs + GO has an excellent potential to react against microorganism in water and act as a disinfection agent.

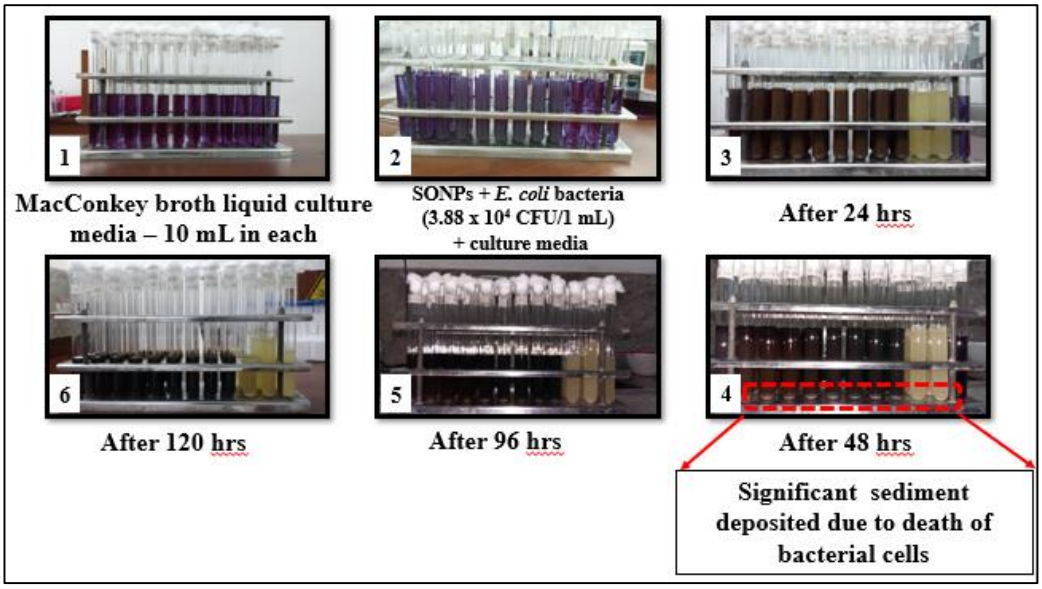

Figure 4.73: Disinfection potential of *E.coli* using broth-dilution (Optical density) method with a range of SONPs + GO dosage

The results of the paired-sample *t-test* indicated that mean values of percentage of growth inhibition are strong, positive correlation and significantly different ($P < 0.05$) for each contact time. The results reject the null hypothesis for means percentages of growth inhibition between contact time are equal ($H_o \neq 1$) and accept the alternative hypothesis ($H_1 = 1$).

However, SONPs are challenging to use as individual material because small SONPs can leach out from the filters. Impregnation of SONPs with GO was practised being avoided the leachability of SONPs from the media. The results of the composite of SONPs and GO in the removal of depicted in Figure 4.73. After impregnating SONPs in GO, the silver particles' leachability was not observed. The composite was washed with

ethanol before storage, removing the loosely bound silver nanoparticles on the GO surface.

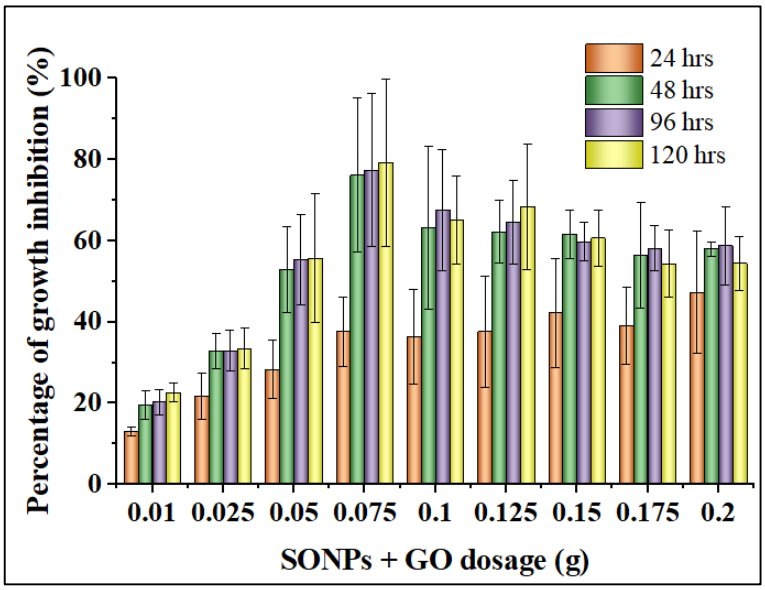

Figure 4.74: Percentage of growth inhibition with broth-dilution (Optical density) method

The results showed that when the SONPs + GO dosages were increased from 0.4 g to 8.0 g for 24 hours, growth inhibition of *E. coli* bacteria was observed decreasing gradually from 0.4 g/L to 4.0 g/L of dosage (12 ± 2 CFU/100 mL to 1 ± 1 CFU/100 mL). Ultimately bacterial cell count becomes zero after 5.2 g/L of SONPs + GO. Before 24 hours of contact time, inhibiting bacterial cells by SONPs + GO was not accomplished as 24 hours was the deterministic factor in removing *E. coli* in potable water. Elimination of bacterial cells was observed effective at the 4.0 g/L of SONPs + GO ($t_{6.74}$, $P < 0.05$), and hence, 4.0 g/L was chosen as the optimum dosage of SONPS + GO composite for fixed-bed column studies. SONPs impregnated on GO was significantly increased the antibacterial activity. The same observation has been observed by Bao et al., 2011 in the removal of *E. coli* and *Streptococcus aureus* using silver nanoparticles/GO composite. Isotherm and kinetic adsorption studies were not conducted because the SONPs + GO composite kill bacteria by damaging cell structure, and not adsorption mechanisms were manifested.

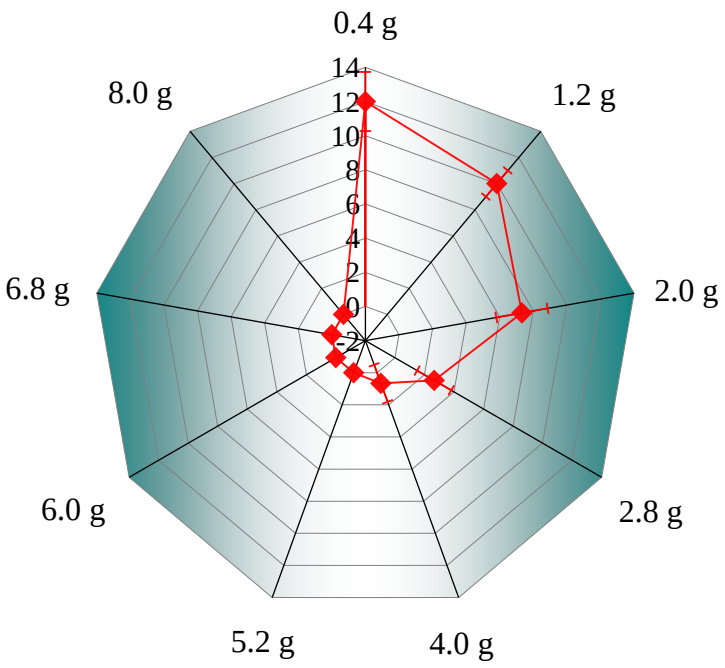

Figure 4.75: Removal effectiveness of *E. coli* bacteria varying dosage of SONPs + GO composite

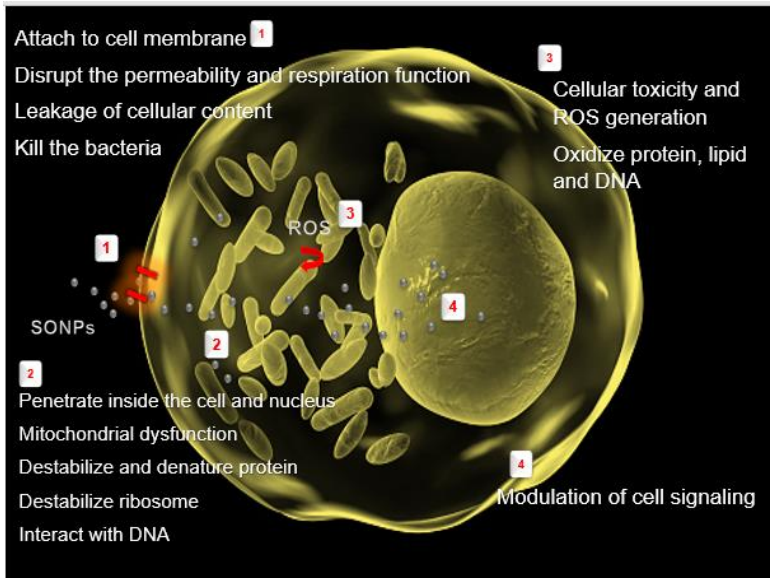

Figure 4.76: Mechanism of how SONPs + GO composite inhibit bacterial growth (Image source: WWW.Gettyimages.com)

Figure 4.74 shows SONPs interactions with bacterial cell walls and how they manifest bacteria's death. SONPs particles increase the damage of cell membrane components and lead to the death of microorganisms due to loss of plasma membrane integrity, which leads to extensive membrane destruction and disruption of bacterial cells. SONPs treated bacterial cells have been shown distinct morphological change, whereas membrane deformation and pore formation along the membrane (Adak et al., 2015). Further, the generation of intracellular reactive oxygen species (ROS) has been facilitated to destroy DNA, RNA, protein, and lipids in the bacterial cell. ROS generates through the damage of the polyunsaturated fatty acid layer in the bacterial cell membrane by lipid peroxidation.

4.4.3. Adsorption isotherms and kinetic models for different adsorbents

The isotherms and kinetic models parameters for fluoride, hardness, and cadmium in removal by different adsorbents are illustrated in Table 4.9. The R^2 values of Langmuir and Freundlich models indicated that experimental data fitted both models. The higher values indicate that adsorption of selected nephrotoxic risk factors follows Langmuir and Freundlich theories. These theories describe monolayer and multilayer adsorption manifest on adsorbent's surface containing homogeneous and heterogenous adsorption sites an infinite number of active adsorption sites. These observations revealed that the initial adsorption process reduces the imbalance of the surface's attractive forces; hence, the later surface free energy of a heterogeneous surface may be formed. The adsorption behaviour describes the monolayer formation followed by multilayer formation (Gawande et al., 2017). The adsorption was prominently occurred by chemisorption and otherwise with the process of physisorption. The equilibrium isotherms and kinetic models parameter for the adsorption of cadmium and calcium by nZVI indicated that R^2 for Langmuir [Figure 4.75(a)] and Freundlich isotherm [Figure 4.75(b)] adsorption models for cadmium (R^2 = 0.99, 0.96) and calcium (R^2 = 0.99, 0.98) show higher values indicating monolayer adsorption onto a surface of nZVI. The maximum monolayer adsorption capacity (Q_m) of nZVI based on the Langmuir model was 8.24 mg/g for cadmium and 24.15 mg/g for calcium. Dimensionless equilibrium

parameters (R_L) were indicated that monolayer adsorption mechanism was most favourable. Freundlich constants (1/n) for the cadmium and calcium were calculated as 0.93 and 0.41, respectively, which indicated adsorption was preferable during the change of solid-liquid phases. Therefore, under single solute experiments, inner-sphere and out-sphere complex formation could be well-preferred for cadmium and calcium.

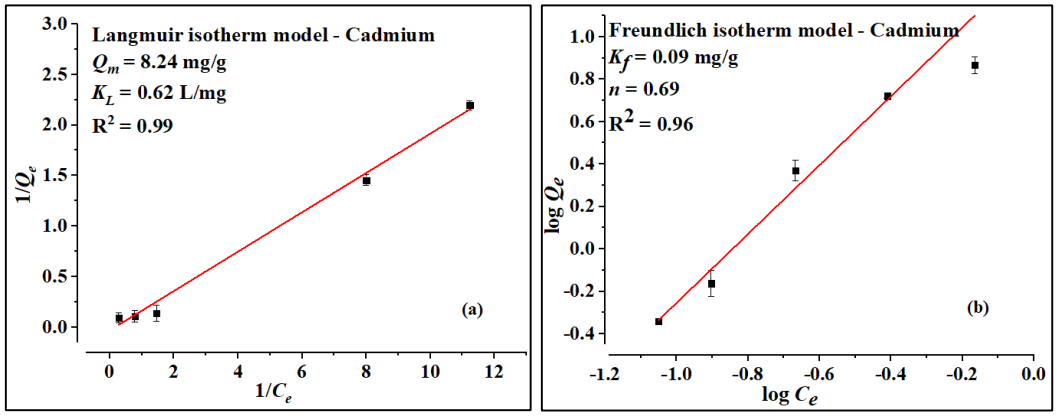

Figure 4.77: Adsorption isotherm models of nZVI for cadmium (a) Langmuir and (b) Freundlich

The surface functional groups determine the adsorption capacity and adsorption selectivity of any adsorbents. The cluster models represent different planes: (i) surface plane (S-plane), which has a fixed number of surface functional groups which are potential to protonation or deprotonation, (ii) inner-sphere plane (IS-Plane) where surface complexes form when there is no water molecule between adsorbed ion and a surface ligand, (iii) outer-sphere plane (OS-plane) forms when there is even one water molecule between a surface functional group and nonspecific adsorption of hydrated cations (protons on the water are directed away from the cation) and hydrated anions (protons on the water of hydration directed towards anions) occurs in the OS-plane, and diffuse plane (d-plane) and hydrated cations, anions and free ions reside in diffuse ions swam area.

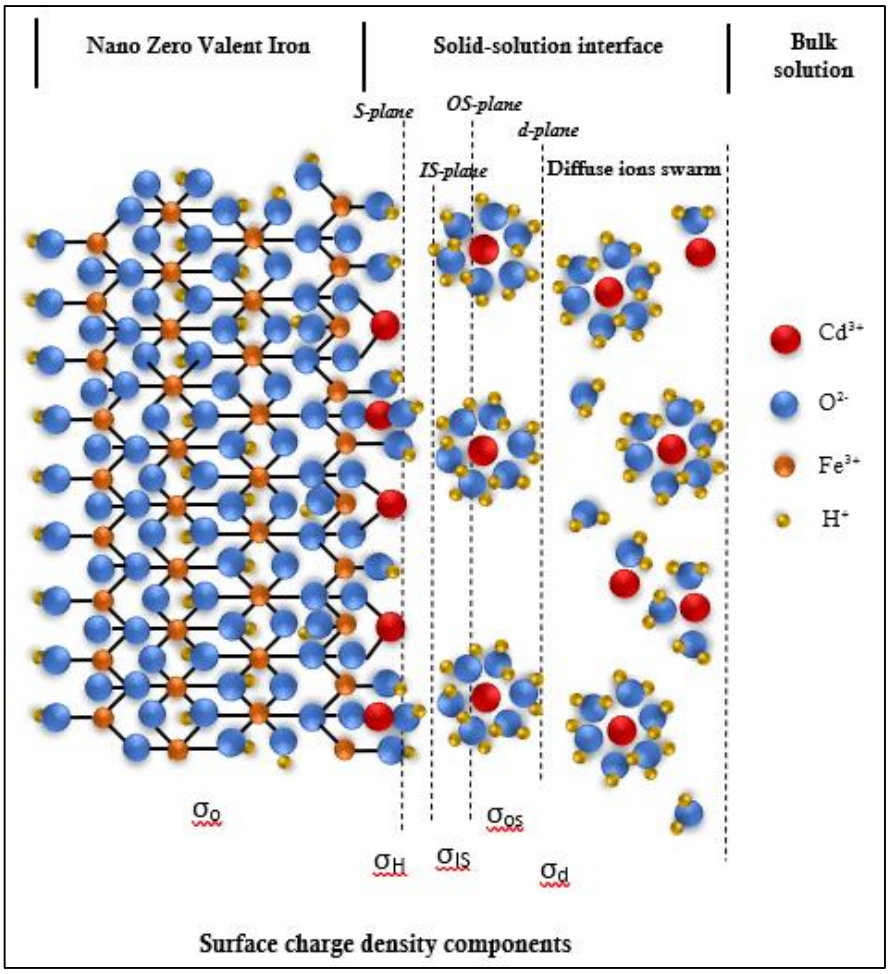

Figure 4.78: Possible adsorption mechanisms of nZVI with cadmium (solution pH 8)

The protonation and deprotonation reaction on surface hydroxyl groups in nZVI can be shown by reactions of; $\equiv FeOH^{o} + H^{+} \rightarrow \equiv FeOH_2^{+}$ and $\equiv FeOH^{o} \rightarrow \equiv FeO + H^{+}$. Surface functional groups are commonly found on nZVI, naming crystalline and amorphous iron oxide, hydroxide, and oxyhydroxide. There are three types of surface hydroxyl groups on nZVI, such as $\equiv FeOH^{-}$, $\equiv Fe_2OH^{o,}$ and $\equiv Fe_3OH^{+}$ and a large amount of cationic charge as an example of Fe^{3+} ion polarise the surface oxygen atoms (Hua et al., 2012). Surface oxygen groups have a high affinity to bind cadmium and calcium in the solution. FT–IR spectrum confirms the possible formation of $\equiv FeOH^{-}$, $\equiv Fe_2OH^{o}$ and $\equiv Fe_3OH^{+}$and $\equiv FeO$ groups on the surface of nZVI after adsorption of water molecules. The formation of Fe–

O surface functional groups that interact with calcium and cadmium ions in the solution generates Fe–O–Ca (Figure 4.76) and Cd bonds (Figure 4.77). Fe–O–Ca bonds represent the active site for fluoride adsorption. It is indicating that surface hydroxyl groups on nZVI playing a significant role in the removal of ions. The schematic diagram indicates monolayer formation, no interaction between adjacent ions following the theories of Langmuir during cadmium and calcium adsorption.

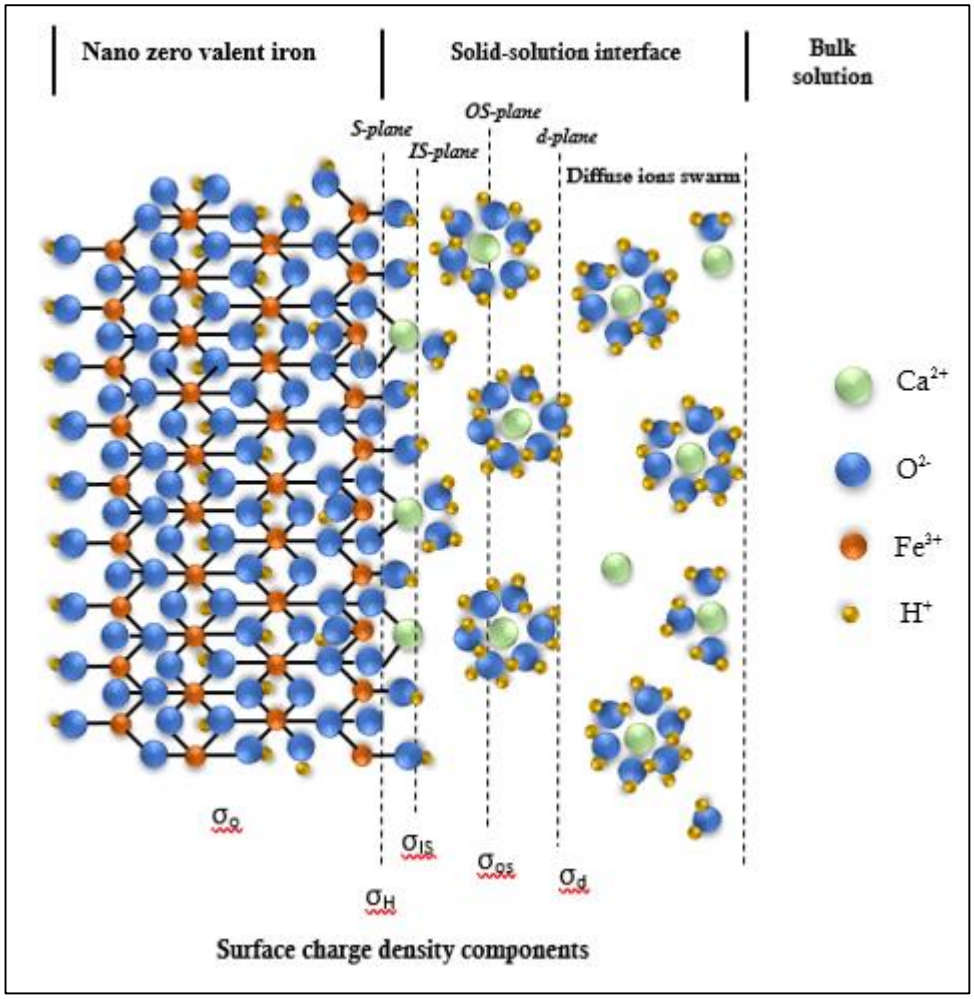

Figure 4.79: Possible adsorption mechanisms of nZVI with calcium(solution pH 8)

The R^2 value for the BET adsorption isotherm [Figure 4.78(a)] of cadmium and calcium were 0.86 and 0.98, which implies the experimental data do not follow the

theory of BET isotherm. The R^2 values of the Dubinin-Radushkevich model [Figure 4.78(b)] were found to be 0.93 and 0.93 for cadmium and calcium, respectively; hence the experimental data were not well-described by the Dubinin-Radushkevich model. The R^2 value of BET, Temkin, and Dubinin-Radushkevich adsorption isotherm models for cadmium and calcium were not best fitted with the experimental data. The equilibrium binding constant, and variation of the adsorption energy calculated for the Temkin model [Figure 4.78(c)] is given in Table 4.9. The R^2 values 0.94 and 0.97 for cadmium and calcium, respectively) of the Temkin model, elucidates the experimental data were not best fitted to the model.

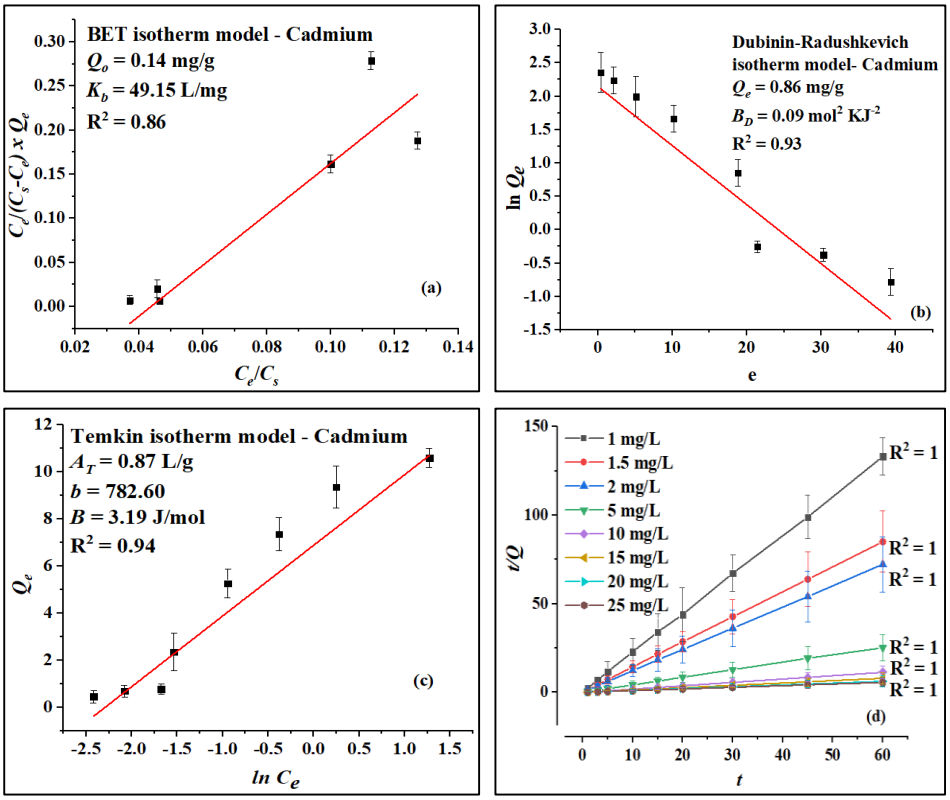

Figure 4.80: Adsorption isotherm and kinetic models of nZVI for cadmium (a) BET, (b) Dubinin-Radushkevich, and (c) Temkin and (d) Pseudo second order

Pseudo-second order kinetic models for cadmium adsorption are given in Figures 4.78 (d). Adsorption kinetics of cadmium and calcium with nZVI is described well by a pseudo-second-order model (Table 4.10). The pseudo-second-order results show that

experimental and calculated Q_e values are approximately equal, and R^2 values reached almost 1.00. The experimental data are best fitted with the pseudo-second-order model greater than the pseudo-first-order model. Hence, the rate-limiting factor of cadmium and calcium adsorption by nZVI is chemisorption, which agrees with covalent bonding by sharing or exchanging electrons among adsorbate adsorbent (Arshadi et al., 2014).

Table 4.12: Equilibrium constants and thermodynamic parameters of single-solute studies

Isotherm model	**Parameters**	**MOMA**	**nZVI**	**ZEOL**
		Fluoride	Cadmium	Hardness
Langmuir	Q_m (mg/g)	18.76	8.24	263.16
	K_L L/mg	0.17	0.62	0.01
	R^2	0.99	0.99	0.99
Freundlich	K_f L/mg	0.38	0.09	0.64
	1/*n*	0.69	0.93	0.74
	R^2	0.98	0.96	0.97
BET	Q_o mg/g	50.78	0.14	0.01
	K_b L/mg	0.06	49.15	40.42
	R^2	0.70	0.86	0.94
Temkin	A_T L/mg	2.88	0.87	63.11
	B J/mol	1.36	3.19	39.67
	R^2	0.87	0.94	0.98
Dubinin-Radushkevich	Q_e mg/g	0.03	0.86	1.61
	E KJ/mol	2.09	2.38	0.04
	B_D mol^2/KJ^2	0.11	0.09	380.45
	R^2	0.87	0.93	0.75

The equilibrium isotherms and kinetic models for the adsorption of fluoride and calcium by MOMA are described below. The R^2 values for Langmuir [Figure 4.79(a)] and Freundlich isotherm [Figure 4.79(b)] adsorption models in the removal of fluoride and calcium indicated higher values as R^2 = 0.99, 0.96 and 0.99, 0.95, respectively.

Table 4.13: Equilibrium constants and thermodynamic parameters for kinetics models in single-solute studies

Pseudo -first order					**Pseudo -second order**			
MOMA								
Fluoride	$Q_{e\ (exp)}$	$Q_{e\ (Cal)}$	K_1	R^2	$Q_{e\ (exp)}$	$Q_{e\ (Cal)}$	K_2	R^2
mg/l	mg/g	mg/g	min^{-1}		mg/g	mg/g	g/min/ mg	
5.00	4.50	0.48	0.003	0.80	2.57	2.98	0.09	0.97
10.00	4.90	0.43	0.016	0.90	4.60	4.83	0.34	0.99
15.00	7.00	0.26	0.017	0.80	6.82	6.96	0.66	1.00
20.00	10.30	0.12	0.030	0.65	10.18	10.44	0.23	0.99
25.00	12.40	2.50	0.002	0.07	10.09	10.09	0.14	0.99
30.00	15.80	3.53	0.001	0.90	12.35	12.53	0.21	1.00
35.00	20.20	4.07	0.001	0.65	16.31	16.64	0.21	1.00
40.00	20.20	4.66	0.013	0.77	19.71	20.04	0.31	1.00
nZVI								
Cadmium	$Q_{e\ (exp)}$	$Q_{e\ (Cal)}$	K_1	R^2	$Q_{e\ (exp)}$	$Q_{e\ (Cal)}$	K_2	R^2
mg/l	mg/g	mg/g	min^{-1}		mg/g	mg/g	g/min/ mg	
1.00	0.44	0.05	1.12	0.09	0.43	0.45	9.14	0.99
1.50	0.69	0.52	0.03	0.15	0.69	0.71	9.73	1.00
2.00	0.81	1.21	0.03	0.39	0.81	0.83	7.45	1.00
5.00	2.34	0.01	0.03	0.19	2.34	2.37	3.78	0.99
10.00	5.25	0.06	0.01	0.32	5.25	5.29	5.85	1.00
15.00	7.36	0.63	0.03	0.17	7.36	7.52	1.11	1.00
20.00	8.91	0.81	0.03	0.19	8.91	9.66	0.19	1.00
25.00	9.75	0.59	0.06	0.29	9.75	10.69	0.14	0.99
ZEOL								
Hardness	$Q_{e\ (exp)}$	$Q_{e\ (Cal)}$	K_1	R^2	$Q_{e\ (exp)}$	$Q_{e\ (Cal)}$	K_2	R^2
mg/l	mg/g	mg/g	min^{-1}		mg/g	mg/g	g/min/ mg	
50.00	3.04	0.17	0.16	0.28	3.04	3.15	2.57	0.99
100.00	5.84	0.77	0.08	0.19	5.84	6.08	1.35	1.00
200.00	12.01	0.75	0.09	0.21	12.00	12.03	4.94	1.00
300.00	17.89	0.16	0.01	0.02	17.89	18.02	5.13	1.00
500.00	29.51	0.16	0.13	0.21	29.51	30.21	0.55	1.00
750.00	28.44	0.35	0.24	0.19	28.44	29.41	0.36	1.00
1000.00	26.86	0.66	0.52	0.14	26.86	28.33	0.24	1.00

The values corroborated that the adsorption process exhibited monolayer adsorption behaviour on the adsorbent's surface, containing a finite number of active adsorption sites. Simultaneously, multilayer formation occurs due to the available heterogeneous surface on the MOMA. The amount of fluoride adsorption at equilibrium (Q_m) of MOMA was calculated as 18.76 mg/g for fluoride based on the Langmuir model (Table 4.9). MOMA has shown higher fluoride adsorption capacity greater than the other adsorbents tested to remove fluoride. The equilibrium parameter (R_L) was between 0.23–0.46 for fluoride, indicating that the monolayer adsorption mechanism was favourable. Freundlich constant (n) obtained for fluoride and calcium was 1.1 and 0.5, respectively, indicating monolayer adsorption for fluoride and calcium is moderately difficult and poor.

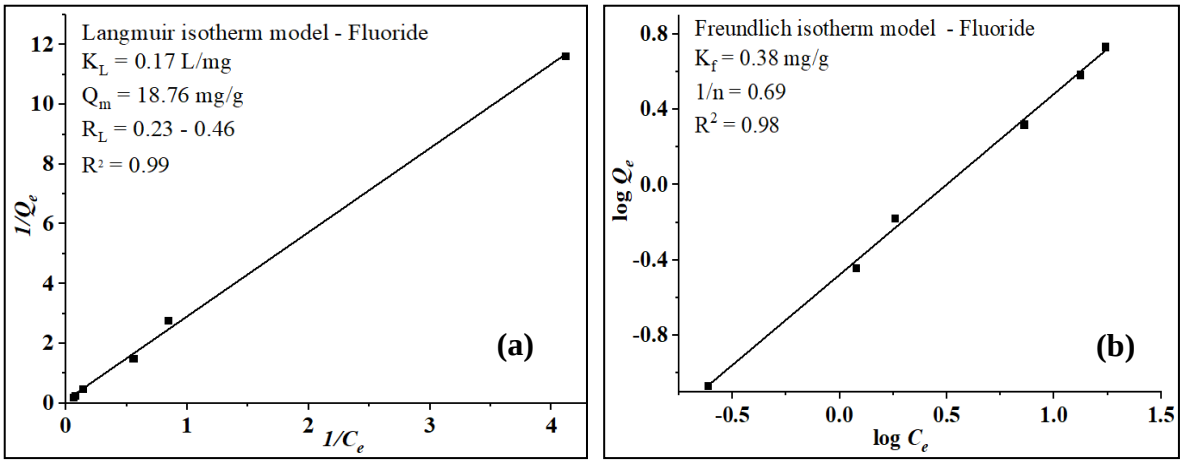

Figure 4.81: Adsorption isotherm models of MOMA for fluoride (a) Langmuir and (b) Freundlich

Multilayer formation with fluoride adsorbed on MOMA's surface can occur due to adsorption sites with heterogeneous surface energy. The protonation and deprotonation reaction on surface hydroxyl groups in MOMA generate reactions of; ≡ Al–OH + H^+ -> ≡ $AlOH^+_2$, ≡$AlOH_2^+$ -> ≡AlOH + H^+, ≡ Al-OH -> ≡ Al–O^- + H^+ as well as MgO on the surface of alumina produce magnesium hydroxide as MgO + H_2O -> Mg $(OH)_2$. Surface functional groups are commonly found on MOMA (Figure 4.80), naming crystalline and

amorphous MgO loaded alumina, aluminol (AlOOH), and magnesium hydroxide. The aluminol functional groups have similar characteristics and reactivity as ≡AlOH located on hydrous aluminium oxides (Adeno et al., 2014). The aluminol groups on the adsorbent surface participate in reactions of protonation, deprotonation, proton exchange, and ligand exchange.

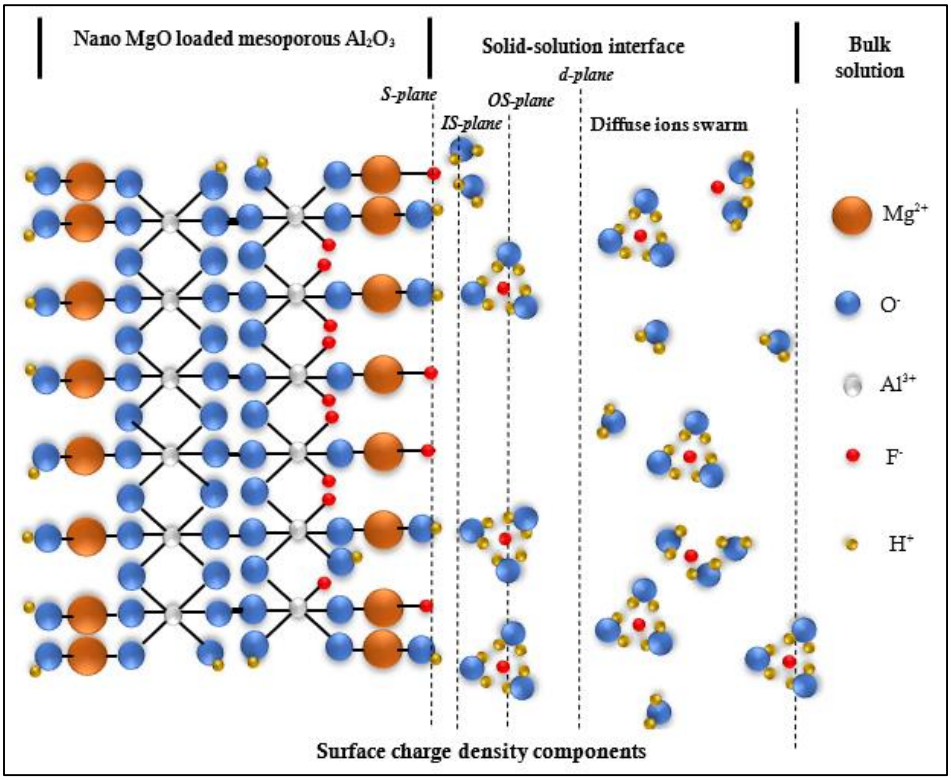

Figure 4.82: Possible adsorption mechanisms of MOMA with fluoride (solution pH 4)

The R^2 value for the BET adsorption isotherm [Figure 4.81(a)] of fluoride and calcium were 0.96 and 0.71, which implies the experiment data follow the BET isotherm assumption of multilayer formation on the MOMA in fluoride and data of calcium adsorption does not follow the theories of multilayer formation. The R^2 values of the Dubinin-Radushkevich model [Figure 4.81(b)] were found to be 0.88 and 0.71 for fluoride and calcium, respectively; hence the experimental data were not well described by the Dubinin-Radushkevich model. All the key parameters relevant to isotherm

analyses are given in Table 4.9. The equilibrium binding constant, and variation of adsorption energy calculated for the Temkin model [Figure 4.81(c)] is given in Table 4.9. The R^2 values (0.87 and 0.79 for fluoride and calcium, respectively) of the Temkin model elucidate that the experimental data were not best fitted to the model.

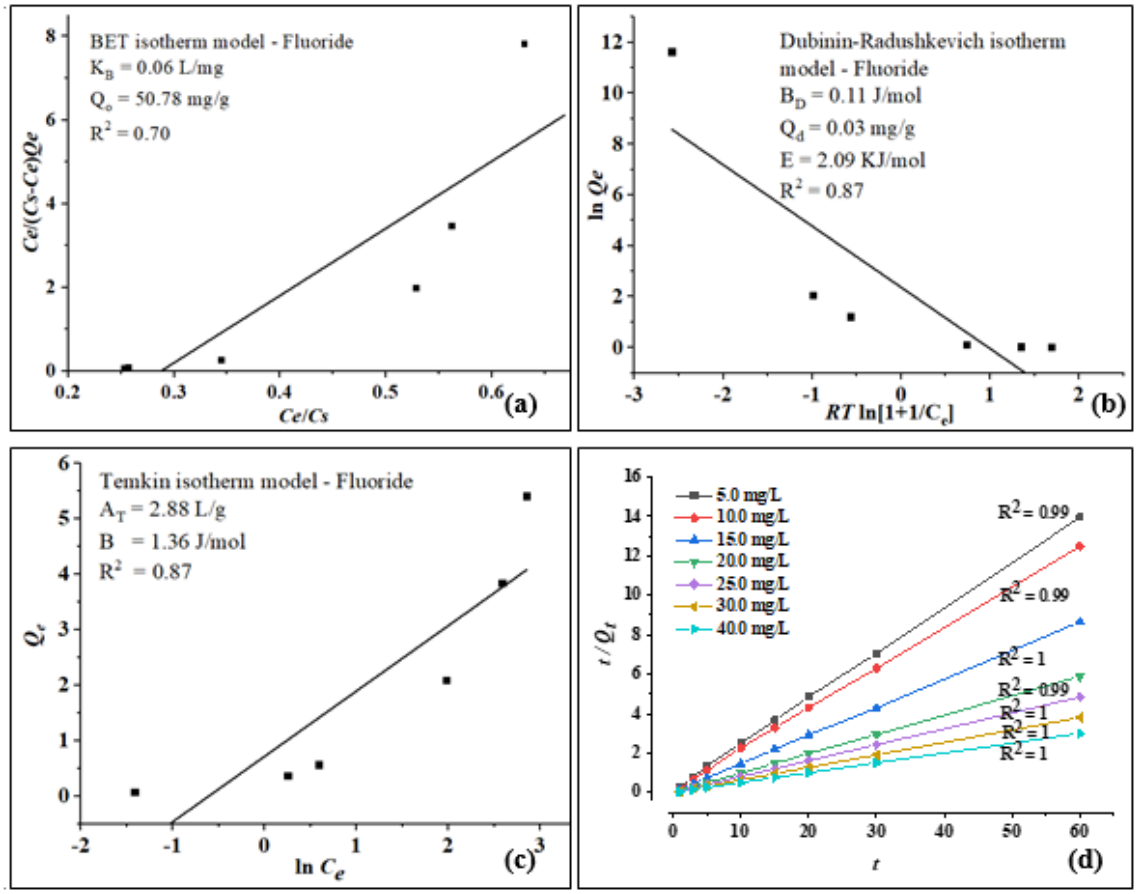

Figure 4.83: Adsorption isotherm and kinetic models of MOMA for fluoride (a) BET, (b) Dubinin-Radushkevich, and (c) Temkin and (d) Pseudo second order

Pseudo 2nd order kinetics model for fluoride adsorption is given in Figures 4.81 (d). Adsorption kinetics of fluoride with MOMA is described well by pseudo 2nd order model greater than pseudo 1st order (Table 4.10). A pseudo-second-order model has been used to describe the adsorption's kinetic behaviour with the chemisorption as a rate-limiting step (Ho and McKay, 1999). The pseudo 2nd order results show that experimental and calculated Q_e values are approximately equal; hence, the rate-limiting

factor of fluoride and calcium adsorption by MOMA is chemisorption.

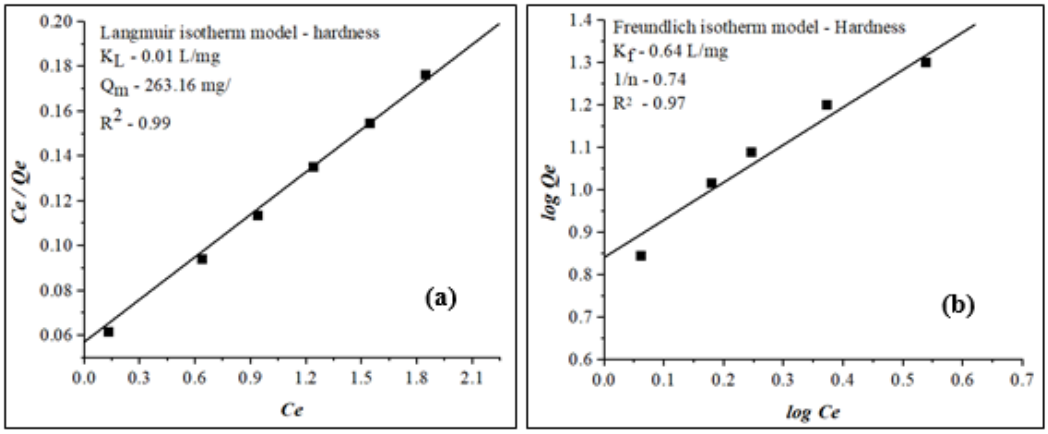

Figure 4.84: Adsorption isotherm models of ZEOL for Hardness (a) Langmuir and (b) Freundlich

The fitting parameter of isotherm and kinetic models of ZEOL were tabulated in Table 4.9 and Table 4.10, respectively. It indicates that the correlation coefficient (R^2) calculated from the Langmuir model (R^2 – 0.99) [Figure 4.82(a)] is higher than the Freundlich model (R^2 – 0.97) [Figure 4.82(b)] for hardness. The results suggest that the adsorption behaviour in the experimental data is appropriately described by the Langmuir model. The Langmuir model describes the adsorption behaviour as a monolayer where adsorption sites are uniformly distributed on the adsorbent's surface, and there is no interaction between the adsorbates. Langmuir model can further describe it is the affinity between adsorbate and adsorbent using separation factor R_L. The values between 0 and 1 indicate the favourable for hardness adsorption.

The R^2 values for BET, DR models are not best fitted with the experimental data. These model values are not described as the adsorption behaviour of ZEOL in the removal of hardness. The experimental data is best fitted with the Temkin model. The Temkin adsorption model describes the heat of adsorption and the adsorbent-adsorbate interaction on surfaces (Samiey & Jonghani, 2015). The equilibrium binding constant,

and variation of adsorption energy calculated for the Temkin model were given in Table 4.9. The positive value of the variation of adsorption energy indicates that the reaction is exothermic.

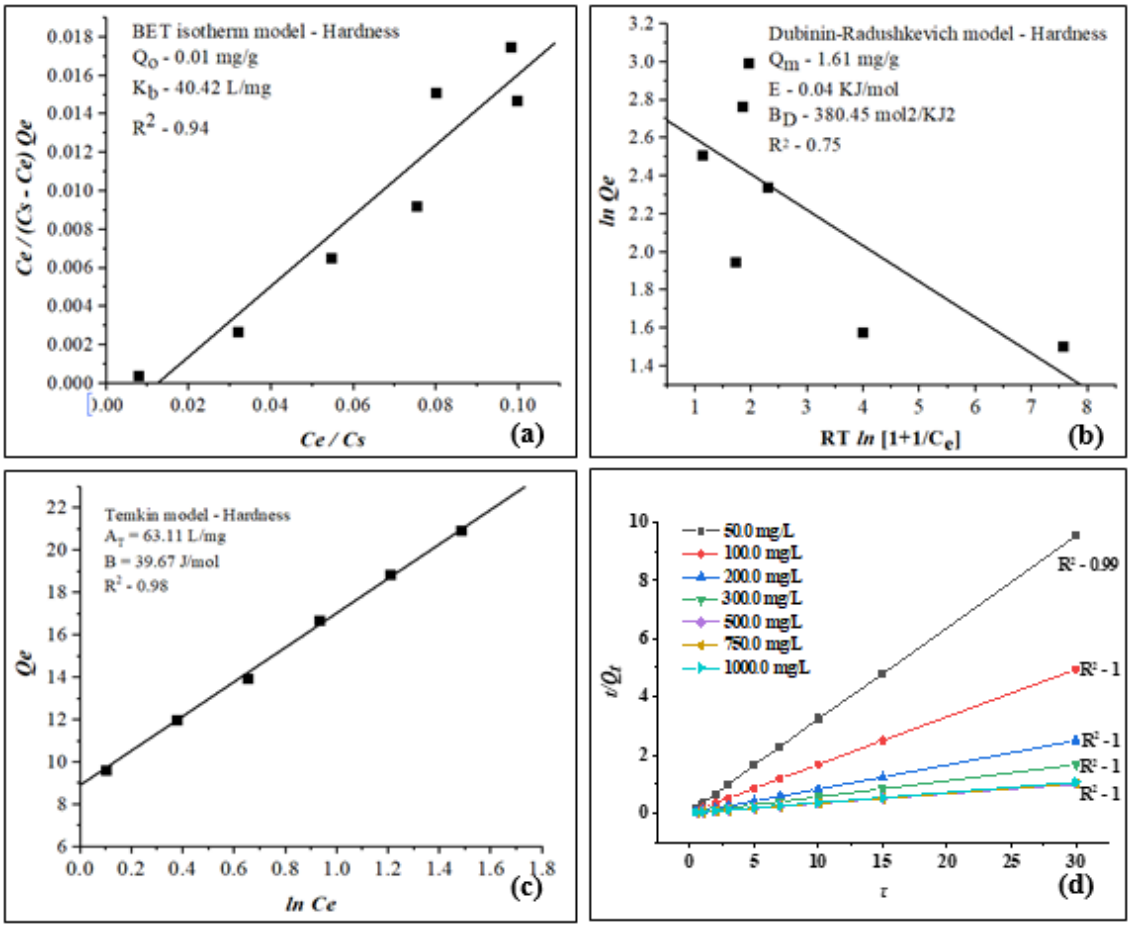

Figure 4.85: Adsorption isotherm and kinetic models of ZEOL for hardness (a) BET, (b) Dubinin-Radushkevich, and (c) Temkin and (d) Pseudo second order

Pseudo 2nd order kinetics model for hardness adsorption is given in Figures 4.83 (d). Adsorption kinetics of hardness with ZEOL are described well by the pseudo 2nd order model greater than the pseudo 1st order (Table 4.10). A pseudo-second-order model has been used to describe the adsorption's kinetic behaviour with the chemisorption as a rate-limiting step (Ho and McKay, 1999). The pseudo 2nd order results show that experimental and calculated Q_e values are approximately equal; hence, the rate-limiting

factor of fluoride and calcium adsorption by ZEOL is chemisorption.

4.4.4. Regeneration studies of MOMA, nZVI, ZEOL and SONPs + GO

The results of desorption and reactivation studies of nZVI, MOMA, ZEOL and SONPs + GO were presented under section 4.4.4, which describe the regeneration potential of these adsorbents selected for multi-layered fixed-bed column studies. Adsorption and desorption studies were corroborated that different eluting agents such as NaOH (pH 10), HCl (pH 4), and EDTA (pH 7) in different pH can use to regenerate the adsorbents for reuse.

The regeneration process of nZVI showed that NaOH was the most effective eluting agent in the nZVI regeneration process. The adsorption efficiency of cadmium (100 ± 1 to 98 ± 2%) during five adsorption-desorption processes with NaOH remained relatively constant (Figure 4.84). The amounts of cadmium adsorbed per unit mass of nZVI during the five NaOH adsorption-desorption processes was varied from 0.001 ± 0.1 to 0.003 ± 0.1 mg/g. nZVI showed less dissociation value of $Fe^{2+/}Fe^{3+}$ as 0.004 mg/L.

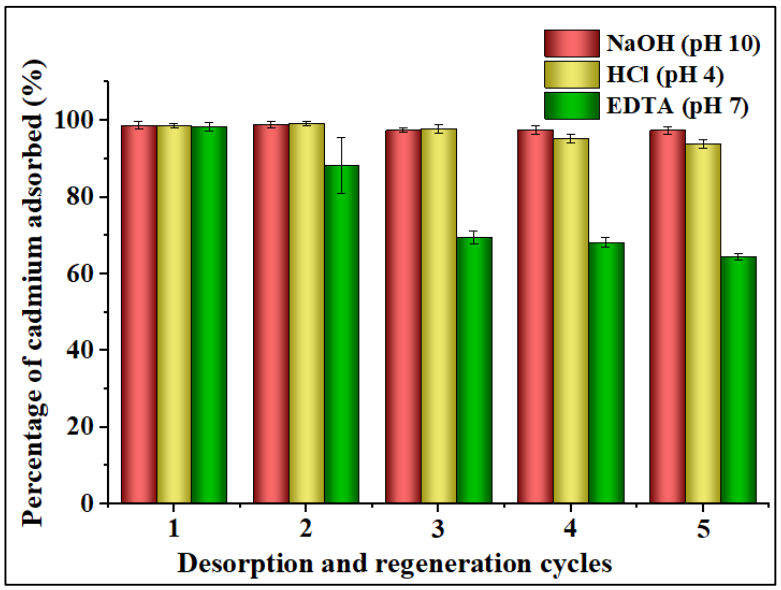

Figure 4.86: Percentage of cadmium adsorption by nZVI with three different eluting agents NaOH, HCl, and EDTA

The adsorption efficiency for cadmium decreased gradually from 99 ± 1 to 93 ± 2% with HCl eluting agent. The amounts of cadmium adsorbed during regeneration cycles were calculated from 0.001 ± 0.01 to 0.002 ± 0.01 mg/g. The adsorption efficiency of cadmium with EDTA was gradually decreased from 98 ± 1 to 64 ± 3%. Amounts of cadmium with EDTA during five adsorption-desorption cycles were calculated from 0.001 ± 0.1 to 0.002 ± 0.1 mg/g. EDTA was found to be dissociated 17.98 mg/L of $Fe^{2+/}Fe^{3+}$ during the adsorption process; the values were considerably high. Both adsorption and desorption were decreased with EDTA during five adsorption-desorption cycles.

The reduction of cadmium adsorption might occurr due to the stronger chelating property of EDTA that made it difficult to reverse the adsorption properties of nZVI. Moreover, the reusability of nZVI eluted from EDTA decreased since EDTA damages the binding site (Kordialik-Bogacka, 2011). The paired sample t-test corroborated that mean values of cadmium adsorption (97.9 ± 0.8%) with NaOH eluting agent is presented a strong, positive correlation with mean values of cadmium adsorption (96.9 ± 2.2%) in different regeneration cycles of HCl. The Null hypothesis is considered to mean values of cadmium adsorption with NaOH are significantly different from other eluting agents $H_o = 1$, alternative hypothesis $H_1 \neq 1$). The mean cadmium adsorption values of NaOH and HCl are not significantly different ($P < 0.05$). Hence, the null hypothesis is rejected. The mean cadmium adsorption values of EDTA (78 ± 15%) are manifested a positive, strong correlation and significantly different ($p < 0.05$) from the mean cadmium adsorption values of NaOH and HCl. The results of nZVI regeneration studies indicated that NaOH and HCl are the most suitable eluting agents to regenerate the nZVI in removing cadmium.

The results of MOMA regeneration studies manifested that EDTA was one of the most effective eluting agents that could be used to regenerate for MOMA. MOMA's adsorption effectiveness was reported as approximately 95% of adsorption of fluoride during five adsorption-desorption cycles with EDTA (Figure 4.85). After the 5^{th} cycle, the percentage of adsorption-desorption decreased drastically. The fluoride adsorbed

amounts during five EDTA adsorption-desorption cycles varied from 0.79 to 1.01 mg/g. The adsorption effectiveness of fluoride was observed gradually decreasing from 96 to 71% with HCl. The results of regeneration studies indicated that NaOH was a less effective eluting agent in the process of MOMA regeneration. MOMA showed less dissociation value of Al^{3+} as 0.001 mg/L, where the concentration values were not exceeded the WHO drinking water guideline values. The paired sample t-test values indicated that the mean values of fluoride adsorption with NaOH show a weak positive correlation with HCl and EDTA values. Mean fluoride adsorption values of NaOH (37 ± 27%) are significantly different ($p < 0.05$) from the mean fluoride adsorption values of HCl and EDTA. The mean fluoride adsorption values of HCl (88 ± 9%) and EDTA (89 ± 9%) are not significantly different from each other, accepting the null hypothesis ($H_o = 1$, $H_1 \neq 1$, and $P > 0.05$). The regeneration studies of MOMA in removal fluoride indicate that HCl and EDTA are the most suitable eluting agents to regenerate MOMA.

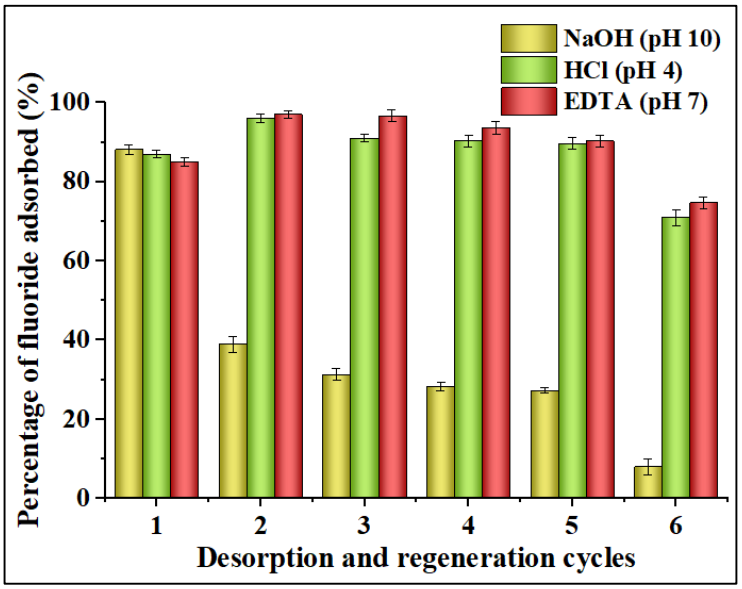

Figure 4.87: Percentage of fluoride adsorption by MOMA with three different eluting agents NaOH, HCl, and EDTA

The results indicated that EDTA was one of the most effective eluting agents in the ZEOL regeneration process. The adsorption efficiency of hardness (90 to 95%) during six adsorption-desorption processes with EDTA remained relatively constant (Figure

4.86). The amounts of hardness adsorbed per unit mass of ZEOL during six EDTA adsorption-desorption processes was varied from 93.08 ± 0.12 to 98.64 ± 0.05 mg/g. Moreover, the capacity of the reusability of ZEOL eluted from EDTA has increased since EDTA damages the surface of the adsorbent (Kordialik-Bogacka, 2011), which lead to open up the new adsorption sites. The adsorption efficiency of hardness removal gradually decreased from 95–80% with HCl eluting agents during the six-consecutive regeneration cycles. Amounts of hardness adsorbed during regeneration cycles were calculated from 98.66 ± 0.01 to 83.04 ± 0.52 mg/g. HCl performed less effectively in the desorption of hardness from the zeolite. The adsorption effectiveness of hardness with NaOH was gradually decreased from 95 to 83%. The degradation of adsorption effectiveness of zeolite with NaOH was showed during six adsorption-desorption cycles. Amounts of hardness with NaOH during five adsorption-desorption cycles were calculated from 98.33 ± 0.11 to 83.58 ± 1.22 mg/g.

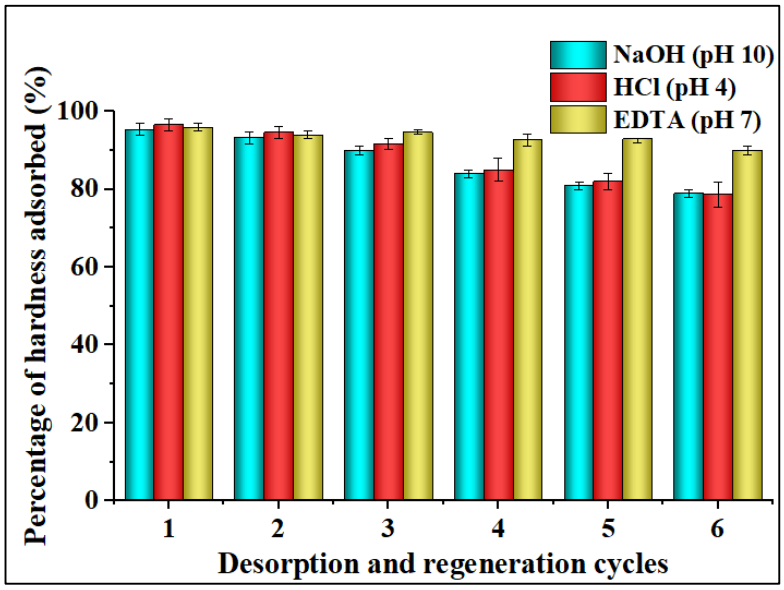

Figure 4.88: Percentage of hardness adsorption by ZEOL with three different eluting agents NaOH, HCl, and EDTA

The results of paired-sample t-test values indicated that the mean values of hardness adsorption with NaOH eluting agent show a strong positive correlation with HCl and

EDTA values ($P < 0.05$). Mean hardness adsorption values of NaOH (87 ± 7%) are significantly different ($p < 0.05$) from the mean hardness adsorption values of HCl and EDTA. The mean hardness adsorption values of HCl (88 ± 7%) and EDTA (93 ± 3%) are not significantly different from each other, accepting the null hypothesis ($H_o = 1$, $H_1 \neq 1$, *and* $P > 0.05$). The regeneration studies of ZEOL in removal hardness indicate that HCl and EDTA are the most suitable eluting agents to regenerate ZEOL.

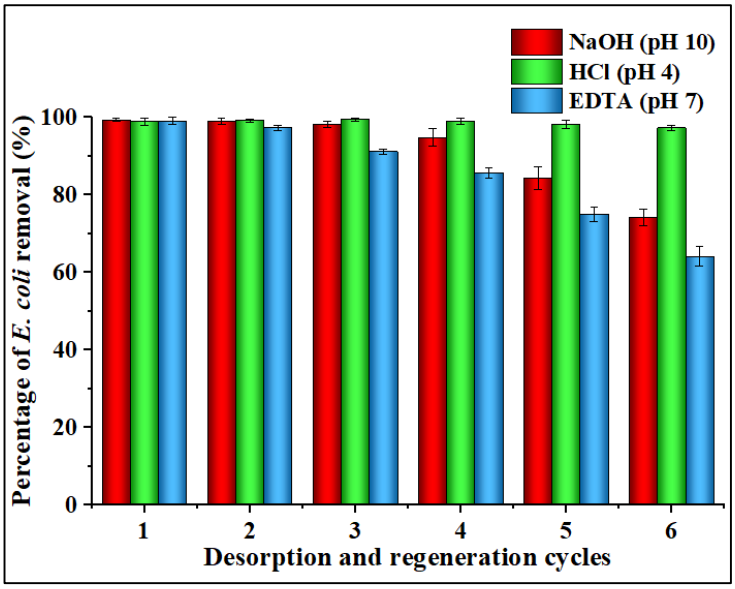

Figure 4.89: Percentage of E. coli removed by SONPs + GO with three different eluting agents NaOH, HCl, and EDTA

The results of regeneration studies of SONPs + GO indicated that HCl was one of the most effective eluting agents. The removal efficiency of *E. coli* (99 to 96%) (Figure 4.87) was decreased during six regeneration cycles. Enhancement of HCl's eluting properties might be improved due to the stronger disinfection properties of Cl^- ion. NaOH (99% – 72%) and EDTA (99% – 63%) showed less effectiveness as eluting agents in regeneration studies of SONPs + GO. The results of paired-sample t-test values indicated that the mean values of *E. coli* removal with NaOH, HCl, and EDTA show a strong positive correlation with each eluting agent. Mean *E. coli* removal values of NaOH (92 ± 10%), HCl (99 ± 1%), and EDTA (85 ± 14%) are significantly difference

from the mean *E. coli* removal values of NaOH, HCl and EDTA ($H_o = 1$, $H_1 \neq 1$, *and* $P > 0.05$). The results of regeneration studies of SONPs + GO in removal *E. coli* indicate that HCl is the most suitable eluting agent to regenerate SONPs + GO. The results indicated that HCl is the most suitable eluting agent to regenerate nZVI, MOMA, ZEOL and SONPs + GO.

4.4.5. Fixed bed column studies to remove nephrotoxic risk factors

The breakthrough curves (BTC) results were determined using experimental data of ZEOL, MOMA, and SONPs + GO in the removal of hardness, fluoride, and *E. coli* in potable water presented in this section. The time of breakthrough reached and the shape of BTC are essential characteristics in column studies to determine the operation, dynamic response of the column and scaling up to commercial use. BTCs of ZEOL, MOMA, and SONPs + GO are presented in the section relevant to different flow rates of 1.0 mg/L, 2.0 mg/L, and 3.0 mg/L and different bed heights. Later, results of adsorption isotherm and kinetics models in fixed bed column studies were discussed. The calculations relevant to the home filter design and the cost of 1.0 L of treated water production were finally described in the section.

4.4.5.1. Selection of materials for fixed-bed column studies in removing hardness, fluoride, and *E. coli*

ZEOL, MOMA, SONPs + GO were selected after series of batch experiments to remove hardness, fluoride, and *E. coli*, respectively. Different materials were tested to determine the maximum adsorption capacity at equilibrium for hardness and fluoride. The adsorption capacity of each material was investigated, changing the physio-chemical properties such as initial concentration, adsorbent dosage, pH and contact time. The highest adsorption capacity was shown by ZEOL (263.10 mg/g) in hardness removal and MOMA (18.76 mg/g) in fluoride removal. Therefore, ZEOL and MOMA were selected to remove fluoride and hardness in the multi-layered filter system. Negatively charged metal oxides in ZEOL facilitate the hardness removal (Ca^{2+} and Mg^{2+} are positively charged). Positively charged Al^{3+} and Mg^{2+} in MOMA shows a higher affinity towards

fluoride ion in the solution. Aluminium and magnesium ions bind more fluoride in the solution more than other materials. Therefore, maximum adsorption capacity at the equilibrium of the MOMA has increased substantially. The summary of the results in adsorption studies is included in Table 4.11.

Table 4.14: Performance of materials selected for removing hardness and fluoride

Constituents	Materials						
	Maximum adsorption capacity (mg/g)						
	ZEOL	MESA	COMA	MOMA	FeON	nZVI	GO
Hardness	263.1	12.78	-	-	9.85	15.77	24.23
Fluoride	4.23	-	17.82	18.76	10.75	-	6.24
Cadmium	-	-	-	-	-	8.24	-

The results of the percentage of growth inhibition, inhibition zone diameter is present in Table 4.12 for *E. coli* removal using GO, SONPs, ZnO, TiO_2 and SONPs + GO. The results show that SONPs + GO performed (% of growth inhibition 99%, inhibition zone diameter 19.98 mm) greater than other materials. Hence, SONPs + GO was chosen for *E. coli* removal in a multi-layered system.

Table 4. 15: Performance of materials selected for removing E. coli

Constituents	Materials									
	Growth inhibition rate (%) (24 hours for 0.5 g)					Inhibition zone diameter (mm) (48 hours for 0.05 g)				
	GO	SONPs	ZnO	TiO_2	SONPs + GO	GO	SONPs	ZnO	TiO_2	SONPs + GO
E. coli	56	94	89	68	99	5.3	14.1	12.67	7.65	19.98

The fixed-bed characteristics were determined by the parameters of bed densities and bed porosities. The results of each parameter illustrate in Table 4.13. Bulk density of materials is an important parameter characterizing mass/volume ratio in a fixed-bed column. It represents the ratio of material mass and the total volume of fixed-bed, including liquid and solid. The bulk densities of ZEOL, MOMA, and SONPs + GO are calculated as 0.45 ± 0.01, 0.36 ± 0.49, and 0.84 ± 0.01. In a batch reactor, materials are dispersed in large volumes of liquid. Hence, the bulk density has the character of a mass concentration of the solid particles. In a fixed-bed column, materials are arranged in the column, and void volume is considerably lower. The void volume is changed during filter operation (Worch, 2012); thus, bulk density changed during backwashing and resettling the materials. Table 4.13: represents the characteristics of the material ZEOL, MOMA, and SONPs + GO.

Table 4.16: Material characteristics of ZEOL, MOMA, and SONPs + GO

Materials	Particle density (g/cm^3)	Material density (g/cm^3)	Bulk density (g/cm^3)	Particle porosity	Bulk porosity	Particle size (nm)	Surface area (m^2/g)
ZEOL	0.71 ± 0.03	1.99 ± 0.43	0.45 ± 0.01	0.63 ± 0.07	0.36 ± 0.03	640.00	756.00 [Vyas et al. (2014)]
MOMA	0.54 ± 0.04	2.89 ± 0.49	0.36 ± 0.05	0.81 ± 0.02	0.34 ± 0.03	15.30	290.00 [Wang et al. (2016)]
SONPs + GO	1.13 ± 0.02	3.57 ± 0.17	0.84 ± 0.01	0.68 ± 0.01	0.26 ± 0.01	1,084.23	1,201.00 [Aboelfetoh et al. (2020)]

(i) Experiment 01 - fixed-bed column studies to remove single-solute using a single layer of ZEOL, MOMA, and SONPs + GO with different flow rates and bed heights

(a) Effect of flow rate on breakthrough curves

Removal of hardness using ZEOL

The effect of flow rate in removing hardness using ZEOL was presented in Figure 4.88 with three different flow rates 1.0 mL/min, 2.0 mL/min, and 3.0 mL/min and bed heights

3.5 cm. The BTCs investigated that the real breakthroughs (C_t/C_o = 0.24) were reached faster with a higher flow rate of 3.0 mL/min within 8 hours, 2.0 mL/min within 16 hours and 1.0 mL/min within 34 hours. Hardness reached its real breakthrough point rapidly when the flow velocity is increased. When the flow rate was increased by 1.0–3.0 mL/min, the flow velocity was increased by 0.45 ± 0.03–1.36 ± 0.09 cm/min. With the higher flow velocity, the effective residence time across the bed was decreased by 7.75 ± 0.53 minutes, 3.88 ± 0.26 minutes, and 2.58 ± 0.18 minutes in flow rates of 1.0, 2.0, and 3.0 mL/min, respectively. Hence, adsorbate cannot find enough time to reach adsorption equilibrium due to the lower column bed utilisation. Then, the ideal breakthrough time of the system decreased drastically in higher flow rates of 2.0 mL/min [Ideal breakthrough time (C_t/C_o = 0.5) 22 hours)] and 3.0 mL/min [Ideal breakthrough time (C_t/C_o = 0.5) 14 hours)] greater than 1.0 mL/min [Ideal breakthrough time (C_t/C_o = 0.5) 48 hours)].

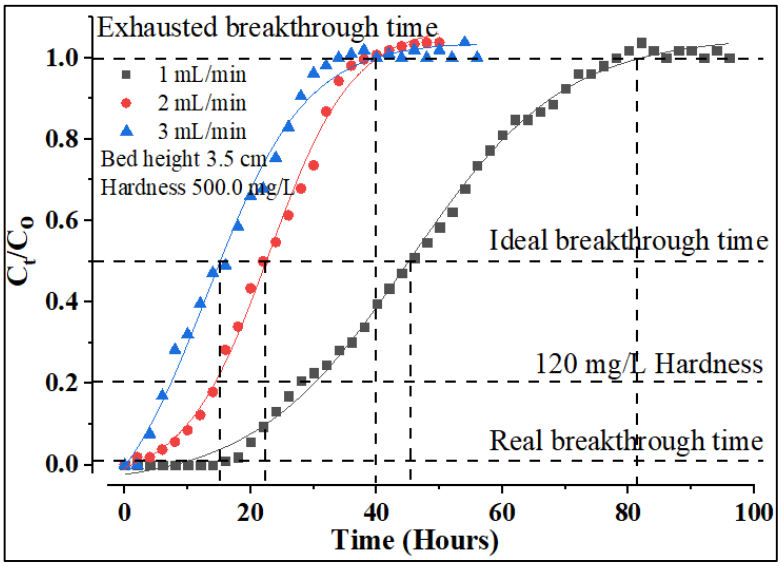

Figure 4.90: Breakthrough curves of ZEOL in the fixed-bed column with different flow rates 1.0 mL/min, 2.0 mL/min, and 3.0 mL/min in bed height 3.5 cm

The specific throughput at the column bed decreased as 210.53 ± 3.82–148.61 ± 2.69 L/Kg when the flow rate increased from 1.0–3.0 mL/min. The total amount of ions sent to the column (m_{Total}) was calculated at C_t/C_o = 0.24 as 68.4 mg, among the amount,

57% of hardness (the total mass of adsorbed (Q_{Total}) 39.6 mg) was removed by the 3.5 cm ZEOL column with 1.0 mL/min flow rate comparison to 2.0 [(m_{Total}) = 70.3 mg, (Q_{Total}) = 36.6 mg, 56%] and 3.0 mL/min [(m_{Total}) = 34.2 mg, (Q_{Total}) = 14.5 mg, 42%] flow rates.

The adsorbent usage rate indicated that the low flow rate uses the lower mass of materials (1.0 mL/min – adsorbent usage rate, which is the rate of 0.91 g/L, and the 2.0 mL/min rate is 3.55 g/L 3.0 mL/min – adsorbent usage rate 5.44 g/L). The heights in the mass transfer zone were calculated as 3.4 cm, 3.46 cm, and 3.27 cm for 1.0, 2.0, and 3.0 mL/min flow rates, respectively. The bed life of the ZEOL was increased with the lower flow rate greater than the higher flow rate in the fixed bed column. The same observations were highlighted by Kavand et al., 2017.

The effect of flow rate in removing hardness using ZEOL was presented in Figure 4.89 with three different flow rates 1.0 mL/min, 2.0 mL/min, and 3.0 mL/min and bed heights 4.5 cm. The BTCs observed that the real breakthrough was reached faster within 20 hours with a higher flow rate of 3.0 mL/min, 2.0 mL/min within 24 hours, and 1.0 mL/min within 42 hours. Hardness reached its real breakthrough point rapidly when the flow velocity is increased. When the flow rate was increased by 1.0–3.0 mL/min, the effective filter velocity gradually increased. The higher flow velocity was decreased the effective residence time across the bed as 9.97 minutes, 4.99 minutes, and 3.32 minutes and empty bed contact time was determined as 27.69 minutes, 13.85 minutes, and 9.23 minutes for flow rates of 1.0, 2.0, and 3.0 mL/min, respectively. Then, the ideal breakthrough time of the system decreased drastically in higher flow rates of 2.0 mL/min [Ideal breakthrough time (C_t/C_o = 0.5) 44 hours)] and 3.0 mL/min [Ideal breakthrough time (C_t/C_o = 0.5) 30.0 hours)] greater than 1.0 mL/min [Ideal breakthrough time (C_t/C_o = 0.5) 62 hours)].

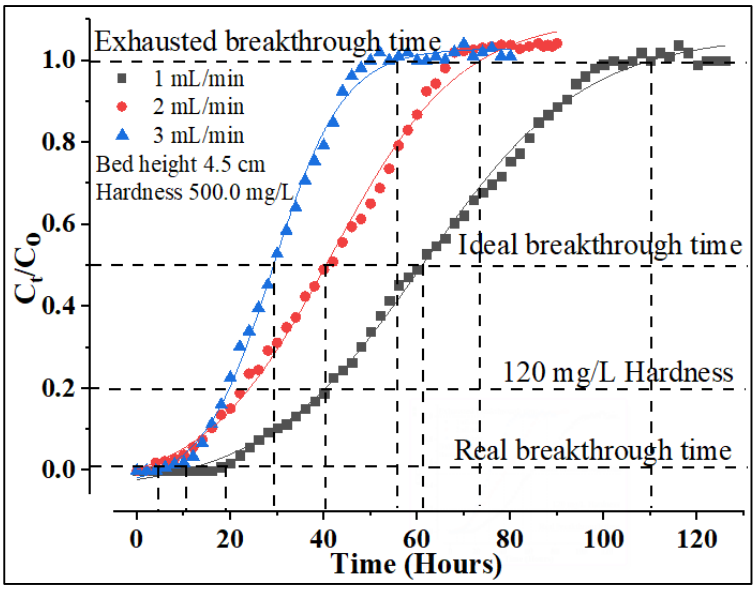

Figure 4.91: Breakthrough curves of ZEOL in the fixed-bed column with different flow rates 1.0 mL/min, 2.0 mL/min, and 3.0 mL/min in bed height 4.5 cm

The total amount of ions sent to the column (m_{Total}) was calculated as 1,399.2 mg, among the amount, 77% of hardness (the total mass of adsorbed (Q_{Total}) 1,082.4 mg) was removed by the 3.5 cm ZEOL column with 1.0 mL/min flow rate comparison to 2.0 [(m_{Total}) = 1,272.0 mg, (Q_{Total}) = 984.0 mg] and 3.0 mL/min [(m_{Total}) = 1,144.2 mg, (Q_{Total}) = 885.6 mg] flow rates. The amount of hardness adsorbed at the equilibrium was calculated as 240.3 mg/g, 209.3 mg/g, 198.4 mg/g for 1.0, 2.0, and 3.0 mL/min flow rates. The adsorbent usage rate was indicated that the low flow rate uses the lower mass of adsorbent (1.0 mL/min – adsorbent usage rate 0.71 g/L, 2.0 mL/min – adsorbent usage rate 1.92 g/L, and 3.0 mL/min – adsorbent usage rate 3.82 g/L). At the same time, they adsorb the elements in the potable water. The bed life of the ZEOL was increased with the lower flow rate and decreased with a higher flow rate in the fixed bed column.

The effect of flow rate in removing hardness using ZEOL was presented in Figure 4.90 with three different flow rates 1.0 mL/min, 2.0 mL/min, and 3.0 mL/min and bed heights 5.5 cm. The BTCs observed that the real breakthrough was reached faster within 32 hours with a higher flow rate of 3.0 mL/min, 28 hours for 2.0 mL/min, and 50 hours

for 1.0 mL/min. When the flow rate was increased by 1.0–3.0 mL/min, the effective filter velocity was increased gradually from 0.45–1.35 cm/min. The higher flow velocity was decreased the effective residence time across the bed as 12.19 minutes, 6.09 minutes, and 4.06 minutes and empty bed contact time was determined as 33.85 minutes, 16.92 minutes, and 11.28 minutes for flow rates of 1.0, 2.0, and 3.0 mL/min, respectively. The ideal breakthrough time of the system decreased drastically in higher flow rates of 2.0 mL/min [Ideal breakthrough time (C_t/C_o = 0.5) 44.0 hours)] and 3.0 mL/min [Ideal breakthrough time (C_t/C_o = 0.5) 52.0 hours)] greater than 1.0 mL/min [Ideal breakthrough time (C_t/C_o = 0.5) 68.0 hours)]. The total amount of ions sent to the column (m_{Total}) was calculated as 1,780.8 mg, among the amount, 77% of hardness (the total mass of adsorbed (Q_{Total}) 1,377.6 mg) was removed by 3.5 cm ZEOL column with 1.0 mL/min flow rate comparison to 2.0 [(m_{Total}) = 1,653.6 mg, (Q_{Total}) = 269.3 mg] and 3.0 mL/min [(m_{Total}) = 1,717.2 mg, (Q_{Total}) = 1,328.4 mg] flow rates.

The removal efficiencies of each ZEOL bed (3.5 cm, 4.5 cm, and 5.5 cm) are substantially the same. The amount of hardness adsorbed at the equilibrium was calculated as 105.96 mg/g, 98.40 mg/g, 102.18 mg/g for 1.0, 2.0, and 3.0 mL/min flow rates. Hardness concentration in the solution, which is filtered through the column bed, changes continuously and hence, the mass transfer process does not operate at a steady-state (Worch, 2012). Therefore, the amount of adsorption at equilibrium indulges in changing with different flow rates. The adsorbent usage rate was indicated that a low flow rate uses less mass of adsorbent (1.0 mL/min – adsorbent usage rate 0.64 g/L, 2.0 mL/min – adsorbent usage rate 1.40 g/L, and 3.0 mL/min – adsorbent usage rate 3.11 g/L). At the same time, they adsorb the elements in the potable water.

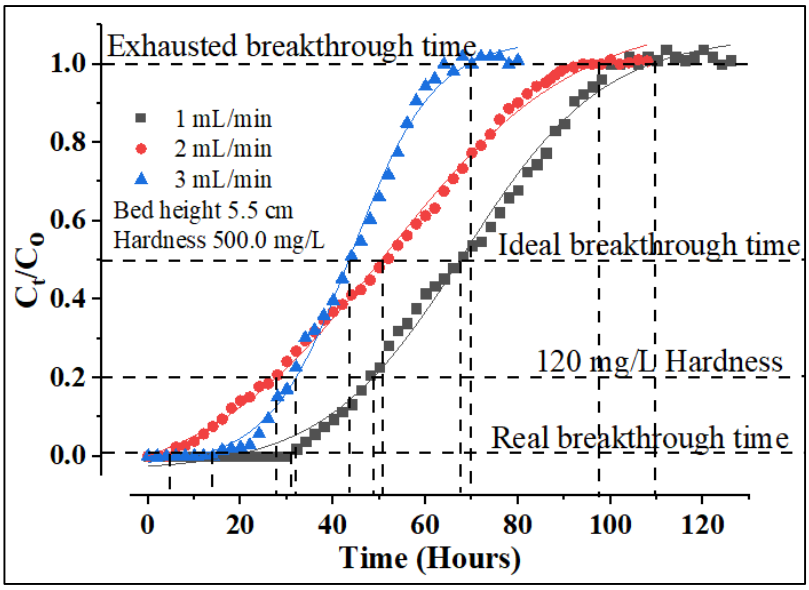

Figure 4.92: Breakthrough curves of ZEOL in the fixed-bed column with different flow rates 1.0 mL/min, 2.0 mL/min, and 3.0 mL/min in bed height 5.5 cm

Removal of fluoride using MOMA – effects of flow rate

The effect of flow rate in removing fluoride using MOMA was presented in Figure 4.91 with three different flow rates 1.0 mL/min, 2.0 mL/min, and 3.0 mL/min and bed heights 1.0 cm. The BTCs observed that the real breakthrough (C_t/C_o = 0.06) was reached faster within 4 hours with a higher flow rate of 3.0 mL/min, 5 hours for 2.0 mL/min, and 6 hours for 1.0 mL/min. The real breakthrough time of each flow rate occurred early since the lower bed height was used for the column bed. MOMA reached its ideal breakthrough point fast when the effective flow velocity increased from 0.6–1.8 cm/min with different flow rates. When the flow rate was increased by 1.0–3.0 mL/min, the linear filter velocity was increased gradually from 0.2 cm/min to 0.6 cm/min. The higher flow velocity was decreased the effective residence time across the bed as 1.67 minutes, 0.83 minutes, and 0.56 minutes and empty bed contact time was determined as 4.91 minutes, 2.45 minutes, and 1.64 minutes for flow rates of 1.0, 2.0, and 3.0 mL/min, respectively. Then, the ideal breakthrough time of the system decreased drastically in higher flow rates of 2.0 mL/min [Ideal breakthrough time (C_t/C_o = 0.5) 20.0 hours)] and

3.0 mL/min [Ideal breakthrough time (C_t/C_o = 0.5) 14.0 hours)] greater than 1.0 mL/min [Ideal breakthrough time (C_t/C_o = 0.5) 22.0 hours)].

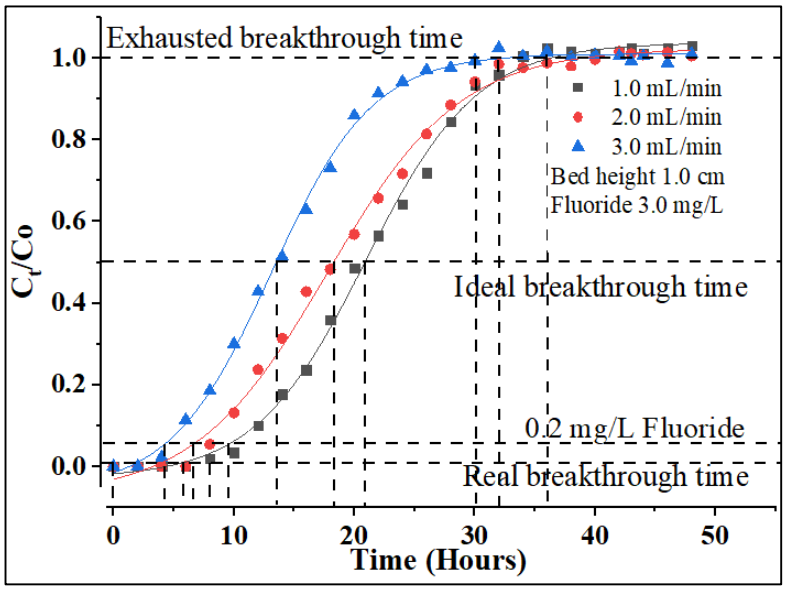

Figure 4.93: Breakthrough curves of MOMA in the fixed-bed column with different flow rates 1 mL/min, 2 mL/min, and 3 mL/min in bed height 1.0 cm

The total mass of fluoride sent to the column was calculated as 9.36 mg, among the mass, 93% of fluoride (the total mass of adsorbed 8.74 mg) was removed by the 1.0 cm MOMA column with 1.0 mL/min flow rate comparison to 2.0 [(m_{Total}) = 12.5 mg, (Q_{Total}) = 11.9 mg] and 3.0 mL/min [(m_{Total}) = 14.0 mg, (Q_{Total}) = 13.3 mg] flow rates. The percentage of fluoride removal was observed to decrease drastically with a higher flow rate. The amount of iron adsorbed at the equilibrium was calculated as 9.2 mg/g, 12.2 mg/g, and 13.8 mg/g for 1.0, 2.0, and 3.0 mL/min flow rates. Bed life is substantially short, with the bed height 1.0 cm. The results corroborated that the column's performance with lower bed height is significantly different when the flow rate was changed. The bed height is the dependable parameter that manipulates the adsorbate's removal process and adsorbent in the liquid-solid interface (Worch, 2012).

The effect of flow rate in removing fluoride using MOMA was presented in Figure 4.92 with three different flow rates 1.0 mL/min, 2.0 mL/min, and 3.0 mL/min and bed

heights 1.5 cm. The BTCs observed that the real breakthrough was reached faster within 6 hours with a higher flow rate of 3.0 mL/min,10 hours for 2.0 mL/min, and 18 hours for 1.0 mL/min. When the flow rate was increased by 1.0–3.0 mL/min, the effective filter velocity was increased gradually (0.59–1.79 cm/min). The higher effective flow velocity was decreased the effective residence time across the bed as 2.50 minutes, 1.25 minutes, and 0.83 minutes and empty bed contact time was determined as 7.36 minutes, 3.68 minutes, and 2.45 minutes for flow rates of 1.0, 2.0, and 3.0 mL/min, respectively. Then, the ideal breakthrough time of the system decreased drastically in higher flow rates of 2.0 mL/min [Ideal breakthrough time (C_t/C_o = 0.5) 28.0 hours)] and 3.0 mL/min [Ideal breakthrough time (C_t/C_o = 0.5) 22.0 hours)] greater than 1.0 mL/min [Ideal breakthrough time (C_t/C_o = 0.5) 38.0 hours)].

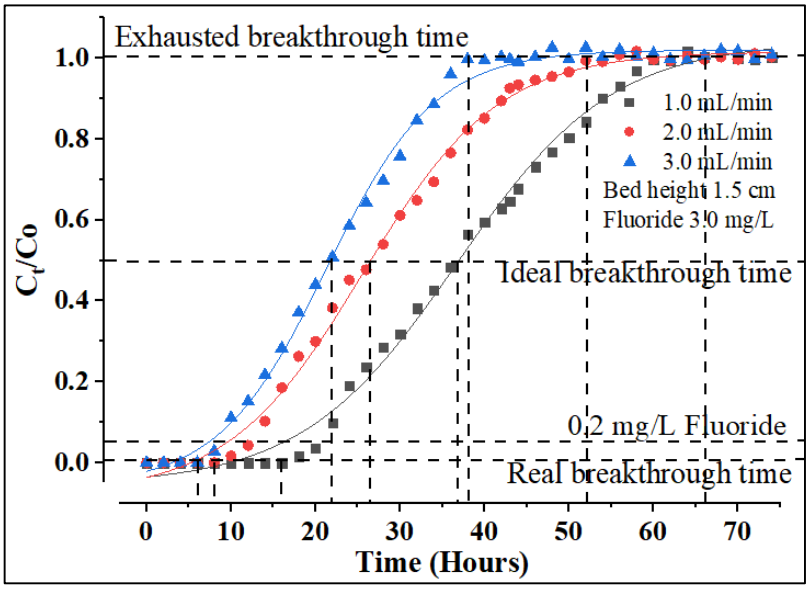

Figure 4.94: Breakthrough curves of MOMA in the fixed-bed column with different flow rates 1.0 mL/min, 2.0 mL/min, and 3.0 mL/min in bed height 1.5 cm

The total amount of fluoride sent to the column (m_{Total}) was calculated as 9.4 mg, among the amount, 93% of fluoride (the total mass of adsorbed (Q_{Total}) 8.7 mg) was removed by 1.5 cm MOMA column with 1.0 mL/min flow rate comparison to 2.0 [(m_{Total}) = 12.5 mg, (Q_{Total}) = 11.9 mg] and 3.0 mL/min [(m_{Total}) = 14.0 mg, (Q_{Total}) =

13.1 mg] flow rates. The amount of iron adsorbed at the equilibrium was calculated as 4.6 mg/g, 6.4 mg/g, and 6.1 mg/g for 1.0, 2.0, and 3.0 mL/min flow rates. Bed life is substantially short with a bed height of 1.5 cm and greater than with a 1.0 cm bed height. The results corroborated that the column's performance with different flow rates is significantly different from the same bed height. The different breakthrough behaviour elaborated that the fix-bed adsorption behaviour depends on equilibrium adsorption (adsorption capacity and adsorption isotherm), adsorption kinetics (diffusion), hydraulic hold-up, and column geometry (Kavand et al., 2017; Inglezakis et al., 2006).

The effect of flow rate in removing fluoride using MOMA was presented in Figure 4.93 with three different flow rates 1.0 mL/min, 2.0 mL/min, and 3.0 mL/min and bed heights 2.0 cm. The BTCs observed that the real breakthrough was reached faster within 12 hours with a higher flow rate of 3.0 mL/min, 16 hours for 2.0 mL/min, and 28 hours for 1.0 mL/min. The real breakthrough time of each flow rate was observed shorter with a lower bed height of 1.0 cm and increase gradually with the higher bed heights of 1.5 cm and 2.0 cm. With higher adsorbent mass in column bed, effective residence time (contact time) increases; accordingly, sweep efficiency increases (Sen et al., 2002). Then, counter ions on the adsorbent surface exposure highly to the flow of solution and hence the adsorption capacity increases (Yaguba et al., 2015). When the flow rate was increased by 1.0–3.0 mL/min, the effective filter velocity was increased gradually (0.59–1.79 cm/min). The higher effective flow velocity was decreased the effective residence time across the bed as 3.34 minutes, 1.67 minutes, and 1.11 minutes and empty bed contact time was determined as 9.81 minutes, 4.91 minutes, and 3.27 minutes for flow rates of 1.0, 2.0, and 3.0 mL/min, respectively.

Then, the ideal breakthrough time of the system decreased drastically in higher flow rates of 2.0 mL/min [Ideal breakthrough time (C_t/C_o = 0.5) 38.0 hours)] and 3.0 mL/min [Ideal breakthrough time (C_t/C_o = 0.5) 24.0 hours)] greater than 1.0 mL/min [Ideal breakthrough time (C_t/C_o = 0.5) 54.0 hours)]. The total amount of fluoride sent to the column (m_{Total}) was calculated as 18.7 mg, among the mass, 98% of fluoride (the total mass of adsorbed (Q_{Total}) 18.4 mg) was removed by 2.0 cm MOMA column with 1.0

mL/min flow rate comparison to 2.0 [(m_{Total}) = 15.6 mg, (Q_{Total}) = 15.3 mg] and 3.0 mL/min [(m_{Total}) = 14.0 mg, (Q_{Total}) = 13.8 mg] flow rates. The percentage of fluoride removal by MOMA was observed, remaining gradual change with different bed heights. The amount of iron adsorbed at the equilibrium was calculated as 6.1 mg/g, 5.12 mg/g, and 4.6 mg/g for 1.0, 2.0, and 3.0 mL/min flow rates.

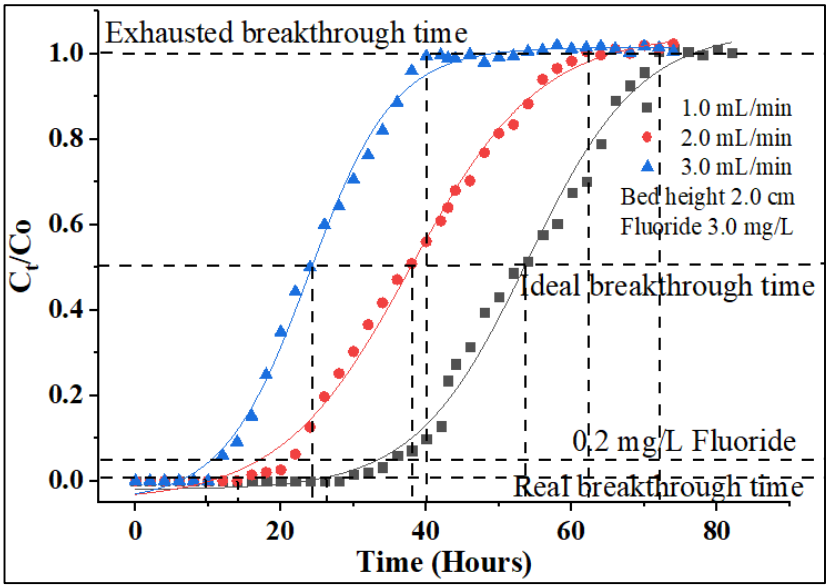

Figure 4.95: Breakthrough curves of MOMA in the fixed-bed column with different flow rates 1.0 mL/min, 2.0 mL/min, and 3.0 mL/min in bed height 2.0 cm

Removal of E. coli using SONPs + GO

The effect of flow rate in removing *E. coli* using SONPs + GO was presented in Figure 4.94 with three different flow rates 1.0 mL/min, 2.0 mL/min, and 3.0 mL/min, bed heights 0.5 cm. The BTCs observed that the real breakthrough (C_t/C_o = 0.001) was reached faster within 14 hours with a higher flow rate of 3.0 mL/min, 80 hours for 2.0 mL/min, and 120 hours for 1.0 mL/min. The real breakthrough time for each flow rate was observed longer, with 1.0 mL/min and 2.0 mL/min compared to 3.0 mL/min. Then, the ideal breakthrough time of the system decreased drastically in higher flow rates of 2.0 mL/min [Ideal breakthrough time (C_t/C_o = 0.5) 142.0 hours)] and 3.0 mL/min [Ideal breakthrough time (C_t/C_o = 0.5) 100.0 hours)] greater than 1.0 mL/min [Ideal

breakthrough time (C_t/C_o = 0.5) 182.0 hours)]. The total time exhausted were observed as 212.0 hours for 1.0 mL/min, 172.0 hours for 2.0 mL/min, and 122.0 hours for 3.0 mL/min. The observations concluded that low bed heights of SONPs + GO could remove *E. coli* in potable water for a longer time with low flow rates. When the system's flow rate was increased by 1.0–3.0 mL/min, the effective filter velocity was increased gradually (0.62, 1.25, and 1.87 cm/min).

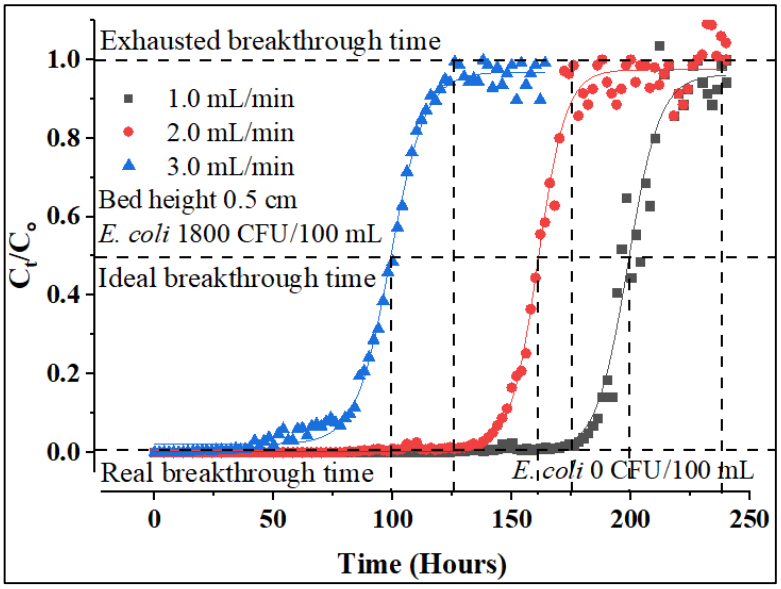

Figure 4.96: Breakthrough curves of SONPs + GO in the fixed-bed column with different flow rates 1.0 mL/min, 2.0 mL/min, and 3.0 mL/min in bed height 0.5 cm

The higher effective flow velocity was decreased the effective residence time across the bed as 0.8 minutes, 0.4 minutes, and 0.3 minutes with the flow rate increased 1.0–3.0 mL/min. The empty bed contact time was determined as 3.08 minutes, 1.54 minutes, and 1.03 minutes for flow rates of 1.0, 2.0, and 3.0 mL/min. The total amount of CFU sent to the column was calculated as 12,960 CFU/100 mL, among the amount, 99% of *E. coli* (the total removal 12,952 CFU/100 mL) was removed by the 0.5 cm SONPs + GO column with 1.0 mL/min flow rate comparison to 2.0 (the total CFU sent 11,664 CFU/100 mL) and 3.0 mL/min (the total CFU sent 4,536 CFU/100 mL) flow rates. The amount of *E. coli* removal at the equilibrium was calculated as 3,238 CFU/100 mL,

2,914 CFU/100 mL, and 1,133 CFU/100 mL for 1.0, 2.0, and 3.0 mL/min flow rates, respectively. The height of the mass transfer zone remains as 0.03 cm in each column bed as the removal of *E. coli* does not occur through adsorption. The results corroborated that the column's performance with different flow rates is significantly different from the same bed height. The effect of flow rate in removing *E. coli* using SONPs + GO was presented in Figure 4.95 with three different flow rates 1.0 mL/min, 2.0 mL/min, and 3.0 mL/min and bed heights 1.0 cm. The BTCs observed that the real breakthrough was reached within 44 hours with a higher flow rate of 3.0 mL/min, 120 hours for 2.0 mL/min, and 160 hours for 1.0 mL/min. The real breakthrough time for each flow rate was observed longer, with 1.0 mL/min and 2.0 mL/min compared to 3.0 mL/min and higher bed height. Then, the ideal breakthrough time of the system reached 224 hours in 1.0 mL/min [Ideal breakthrough time (C_t/C_o = 0.5)] and substantially decreased with higher flow rates of 2.0 mL/min (184.0 hours) and 3.0 mL/min (108.0 hours). The total time exhausted were remarked as 236.0 hours for 1.0 mL/min [Exhausted breakthrough time (C_t/C_o = 0.95), 218.0 hours for 2.0 mL/min, and 144.0 hours for 3.0 mL/min. The results concluded that SONPs + GO could remove *E. coli* in potable water for a longer time with low flow rates and higher bed heights. The longer time taken to reach a breakthrough is beneficial to decrease production and regeneration costs. When the system's flow rate was increased by 1.0–3.0 mL/min, the effective filter velocity was increased gradually. The higher effective flow velocity was decreased the effective residence time across the bed as 1.60 minutes, 0.80 minutes, and 0.53 minutes and the empty bed contact time was observed decreasing as 6.15 minutes, 3.08 minutes, and 2.05 minutes for flow rates of 1.0, 2.0, and 3.0 mL/min, respectively. The total amount of CFU sent to the column was calculated as 17,280 CFU/100 mL, among the amount, 99% of *E. coli* (the total removal 17,270 CFU/100 mL) was removed by the 1.0 cm SONPs + GO column with 1.0 mL/min flow rate comparison to 2.0 (the total CFU sent 18,144 CFU/100 mL) and 3.0 mL/min (the total CFU sent 14,256 CFU/100 mL) flow rates. When the flow rates were increased, the total amount of CFU sent through the column should be increased. However, the total amount of CFU sent to the column and mass of removal were changed irregularly as the unequal dispersion of the *E. coli*

cell in the solution. The amount of *E. coli* removal at the equilibrium was calculated as 2,878 CFU/100 mL, 3,022 CFU/100 mL, and 2,374 CFU/100 mL for 1.0, 2.0, and 3.0 mL/min flow rates, respectively. The bed life of the SONPs + GO was increased with the lower flow rate and with higher bed height greater than the higher flow rate in the fixed bed column.

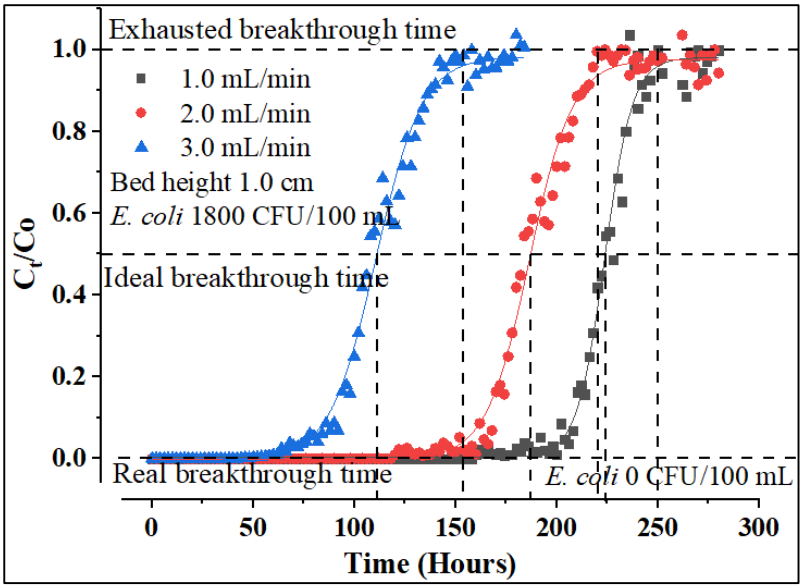

Figure 4.97: Breakthrough curves of SONPs + GO in the fixed-bed column with different flow rates 1.0 mL/min, 2.0 mL/min, and 3.0 mL/min in bed height 1.0 cm

The effect of flow rate in removing *E. coli* using SONPs + GO was presented in Figure 4.96 with three different flow rates 1.0 mL/min, 2.0 mL/min, and 3.0 mL/min, bed heights 1.5 cm. The BTCs observed that the real breakthrough was reached within 70 hours with a higher flow rate of 3.0 mL/min, 80 hours for 2.0 mL/min, and 184 hours for 1.0 mL/min. The real breakthrough time for each flow rate was observed longer, with 1.0 mL/min and 2.0 mL/min compared to 3.0 mL/min and higher bed height. Then, the ideal breakthrough time of the system reached 236 hours in 1.0 mL/min [Ideal breakthrough time (C_t/C_o = 0.5)] and substantially decreased with higher flow rates of 2.0 mL/min (162.0 hours) and 3.0 mL/min (152.0 hours). The total time of the system

exhausted were remarked as 264.0 hours for 1.0 mL/min [Exhausted breakthrough time (C_t/C_o = 0.95), 198.0 hours for 2.0 mL/min, and 188.0 hours for 3.0 mL/min. The results concluded that higher bed heights of SONPs + GO could remove *E. coli* in potable water for a longer time with low flow rates. The higher effective flow velocity with higher flow rates was decreased the effective residence time across the bed as 2.40 minutes, 1.20 minutes, and 0.80 minutes with the flow rate increased 1.0–3.0 mL/min. Empty bed contact time was observed decreasing as 9.23 minutes, 4.62 minutes, and 3.08 minutes for flow rates of 1.0, 2.0, and 3.0 mL/min increased, respectively.

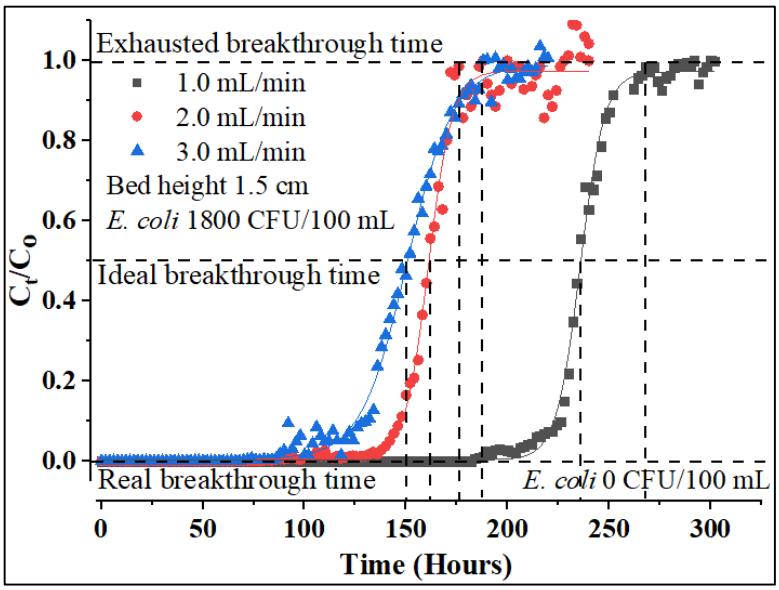

Figure 4.98: Breakthrough curves of SONPs + GO in the fixed-bed column with different flow rates 1.0 mL/min, 2.0 mL/min, and 3.0 mL/min in bed height 1.5 cm

The total amount of CFU sent to the column was calculated as 19,872 CFU/100 mL, among the amount, 99% of *E. coli* (the total removal 19,860 CFU/100 mL) was removed by 1.5 cm SONPs + GO column with 1.0 mL/min flow rate comparison to 2.0 (the total CFU sent 17,280 CFU/100 mL) and 3.0 mL/min (the total CFU sent 16,416 CFU/100 mL) flow rates. When the flow rates were increased, the total amount of CFU sent through the column increased due to specific throughput. The amount of *E. coli* removal

at the equilibrium was calculated as 2,482 CFU/100 mL, 2,158 CFU/100 mL, and 2,050 CFU/100 mL for 1.0, 2.0, and 3.0 mL/min flow rates, respectively.

The results with changing flow rate indicated that the fixed-bed column's overall performance, such as contact time of liquid to a solid phase, mass transfer parameters, and column capacity, was affected when the flow rate is increased. The inverse relationship was observed between the flow rate and the ideal and exhausted breakthrough time of the column bed. The higher flow rate decreases the volume treated by the column and decreases the service time as the occurrence of faster saturation. The breakthrough curve becomes steeper when the flow rate was increased while the breakthrough points and amount of adsorbate adsorbed were decreased (Worch, 2012). The effective resident time of the adsorbate in the column bed was decreased with a higher flow rate. Then, the mass transfer zone quickly reaches the end of the column bed, remarking early saturation.

The short contact time at a higher flow rate decrease the total mass removal of adsorbate by the adsorbent bed. The low flow rate indicates the adsorbate has enough time to contact materials, and hence, the total mass of removal was increased. The same observations have been illustrated by Afroze et al., 2016, Han et al., 2009. The adsorption rate for the low flow rate was high initially, and all available adsorption sites were used effectively since the effluent concentration was zero. The water residence time was considerably high at a slow flow rate than high flow rates (Worch, 2012). The intraparticle mass transfer mechanism controls the adsorbate removal process in the column bed at lower flow rates. The decrease of liquid film resistance at higher flow rates is subject to create external mass transfer resistance at the adsorption (Priya & Radha, 2016). The high flow rates decrease the adsorption capacity with different bed heights; however, the water volume passed through the bed was higher.

(a) Effect of bed height on breakthrough curve

Removal of hardness using ZEOL

The effect of bed height in removing hardness using ZEOL was presented in Figure 4.97 with three different bed heights as 3.5 cm, 4.5 cm, and 5.5 cm with flow rates of 1.0 mL/min. From the BTCs, it was investigated that the real breakthrough (C_t/C_o = 0.23) was reached faster with lower bed height (30.0 hours for 3.5 cm) early comparison to the other two bed heights (42.0 hours for 4.5 cm, and 50.0 hours for 5.5 cm).

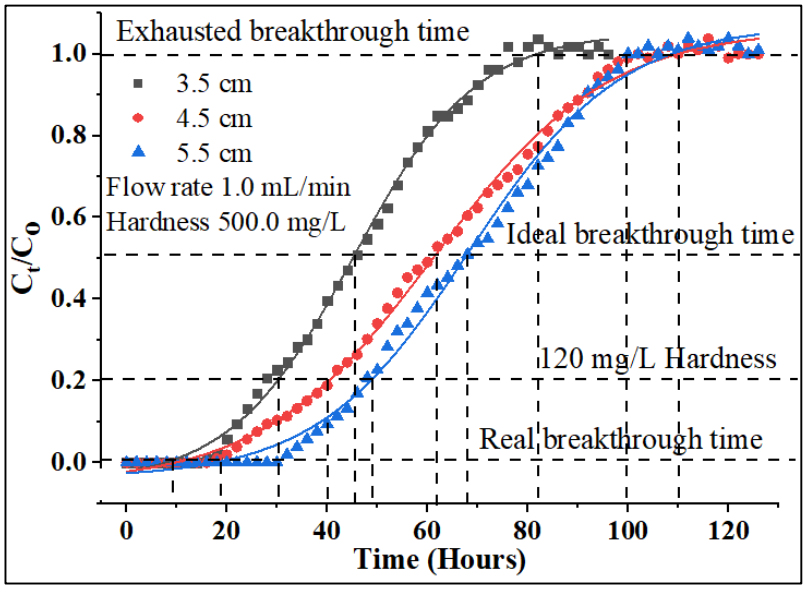

Figure 4.99: Breakthrough curves of ZEOL in the fixed-bed column with different bed heights 3.5 cm, 4.5 cm, and 5.5 cm with a flow rate of 1.0 mL/min

The ideal breakthrough time (C_t/C_o = 0.5) of the system increased considerably with higher bed height greater than lower bed height (Ideal breakthrough time for 3.5 cm – 46.0 hours, for 4.5 cm – 62.0 hours, and for 5.5 cm – 68.0 hours). The total time taken for the system exhausted was observed as 72.0 hours for 3.5 cm [Exhausted breakthrough time (C_t/C_o = 0.95), 96.0 hours for 4.5 cm, and 98.0 hours for 5.5 cm bed heights. The results concluded that a higher bed height of 5.5 cm of ZEOL could remove hardness in potable water for a longer time. The bed life of the ZEOL was increased

with the higher bed heights greater than lower bed heights in the fixed bed column. The results indicated that the breakthrough time of three different bed heights is considerably different from each other, and 5.5 cm of bed height performed best to remove hardness.

The effect of bed height in removing hardness using ZEOL was presented in Figure 4.98 with three different bed heights as 3.5 cm, 4.5 cm, and 5.5 cm with flow rates of 2.0 mL/min. From the BTCs, it was investigated that the real breakthrough (C_t/C_o = 0.23) was reached faster with lower bed height (16.0 hours for 3.5 cm) early comparison to the other two bed heights (24.0 hours for 4.5 cm, and 30.0 hours for 5.5 cm).

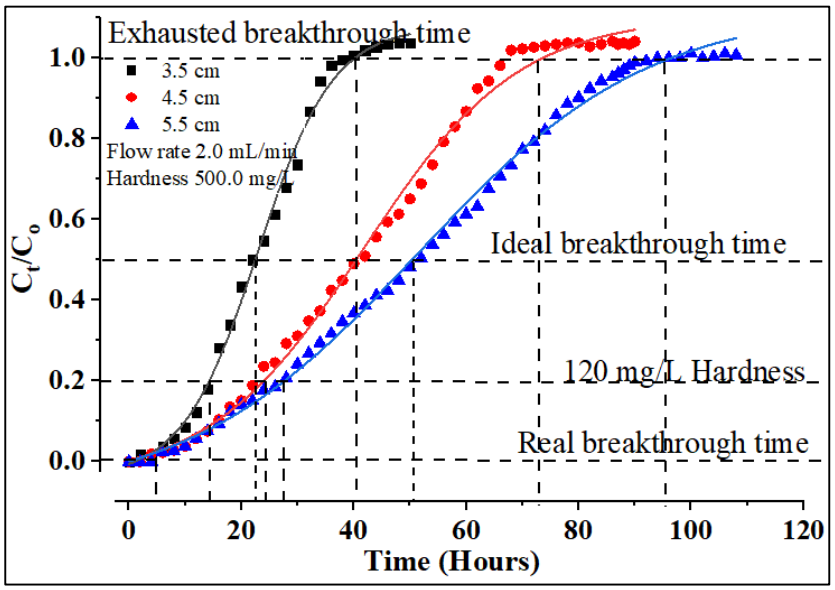

Figure 4.100: Breakthrough curves of ZEOL in the fixed-bed column with different bed heights 3.5 cm, 4.5 cm, and 5.5 cm with a flow rate of 2.0 mL/min

The column reached its real breakthrough point substantially for a shorter time with low bed height. The ideal breakthrough time (C_t/C_o = 0.5) of the system increased considerably with higher bed height greater than lower bed height (Ideal breakthrough time for 3.5 cm – 22.0 hours, for 4.5 cm – 42.0 hours, and for 5.5 cm – 52.0 hours). The total time taken for the system exhausted was observed as 38.0 hours for 3.5 cm [Exhausted breakthrough time (C_t/C_o = 0.95), 66.0 hours for 4.5 cm, and 86.0 hours for 5.5 cm bed heights. The results concluded that the breakthrough time was decreased

with a higher flow rate and lower bed heights of ZEOL. However, when the flow rate increases, the time is taken to reach a real, ideal, and exhausted breakthrough decreases gradually compared to 1.0 mL/min flow rates with different bed heights.

The effect of bed height in removing hardness using ZEOL was presented in Figure 4.99 with three different bed heights as 3.5 cm, 4.5 cm, and 5.5 cm with flow rates of 3.0 mL/min. From the BTCs, it was investigated that the real breakthrough (C_t/C_o = 0.23) was reached faster with lower bed height (8.0 hours for 3.5 cm) early comparison to the other two bed heights (20.0 hours for 4.5 cm, and 32.0 hours for 5.5 cm).

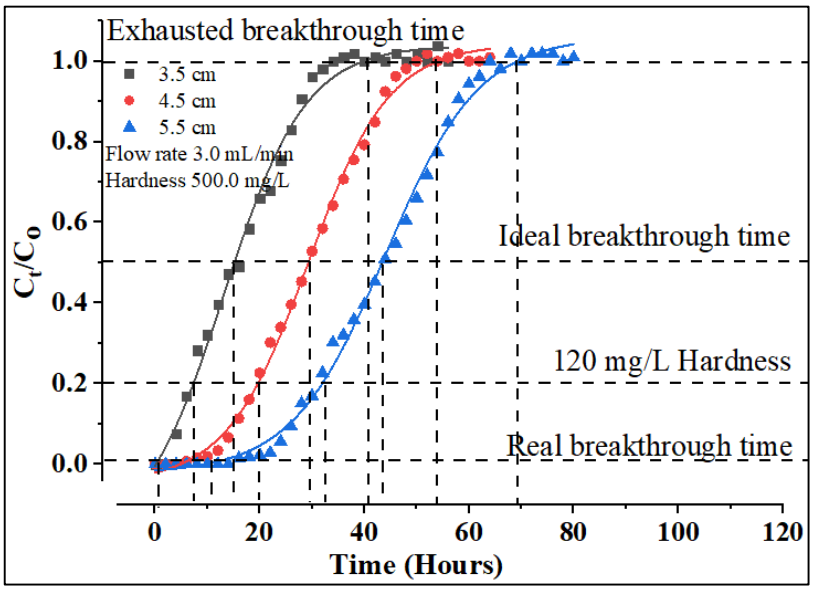

Figure 4.101: Breakthrough curves of ZEOL in the fixed-bed column with different bed heights 3.5 cm, 4.5 cm, and 5.5 cm with a flow rate of 3.0 mL/min

The column reached its real breakthrough point substantially for a shorter time with low bed height. The real breakthrough time of 4.5 cm in 3.0 mL/min flow rate is observed higher than the breakthrough time of 4.5 cm in 2.0 mL/min, maybe due to the formation of channelling through the bed decreased the point of breakthrough. The ideal breakthrough time (C_t/C_o = 0.5) of the system increased considerably with higher bed height greater than lower bed height (Ideal breakthrough time for 3.5 cm – 18.0 hours, for 4.5 cm – 30.0 hours, and for 5.5 cm – 44.0 hours).

The total time taken for the system exhausted was observed as 34.0 hours for 3.5 cm [Exhausted breakthrough time (C_t/C_o = 0.95), 30.0 hours for 4.5 cm, and 44.0 hours for 5.5 cm bed heights. The formation of channelling is shorter than the time taken to reach breakthrough time. The bed life of the ZEOL was increased with the higher bed heights greater than lower bed heights in the fixed bed column. The results collaborated that increase of flow rate with lower bed heights increases the steepness of the BTCs due to speed up the adsorption process, which increase the early occurrence of the breakthrough. Various researchers have highlighted the same observations in a different system (Yagub et al., 2014; Kavand et al., 2017).

Removal of fluoride using MOMA

The effect of bed height in removing fluoride using MOMA was presented in Figure 4.100 with three different bed heights as 1.0 cm, 1.5 cm, and 2.0 cm with flow rates of 1.0 mL/min. From the BTCs, it was investigated that the real breakthrough (C_t/C_o = 0.06) was reached faster with lower bed height (8.0 hours for 1.0 cm) early comparison to the other two bed heights (8.0 hours for 1.5 cm, and 18.0 hours for 2.0 cm). The column reached its real breakthrough point substantially for a shorter time with low bed height. The ideal breakthrough time (C_t/C_o = 0.5) of the system increased considerably with higher bed height greater than lower bed height (Ideal breakthrough time for 1.0 cm – 22.0 hours, for 1.5 cm – 36.0 hours, and for 2.0 cm – 50.0 hours).

The total time taken for the system exhausted was observed as 32.0 hours for 1.0 cm [Exhausted breakthrough time (C_t/C_o = 0.95), 58.0 hours for 1.5 cm, and 70.0 hours for 2.0 cm bed heights. The results concluded that the breakthrough time of the column was decreased with lower bed heights of MOMA. The bed life of the MOMA was increased with the higher bed heights greater than lower bed heights in the fixed bed column. The effect of bed height in removing fluoride using MOMA was presented in Figure 4.101 with three different bed heights as 1.0 cm, 1.5 cm, and 2.0 cm with flow rates of 2.0 mL/min. From the BTCs, it was investigated that the real breakthrough (C_t/C_o = 0.06) was reached faster with lower bed height (8.0 hours for 1.0 cm) early

comparison to the other two bed heights (10.0 hours for 1.5 cm, and 16.0 hours for 2.0 cm). The column reached its real breakthrough point substantially for a shorter time with lower bed height.

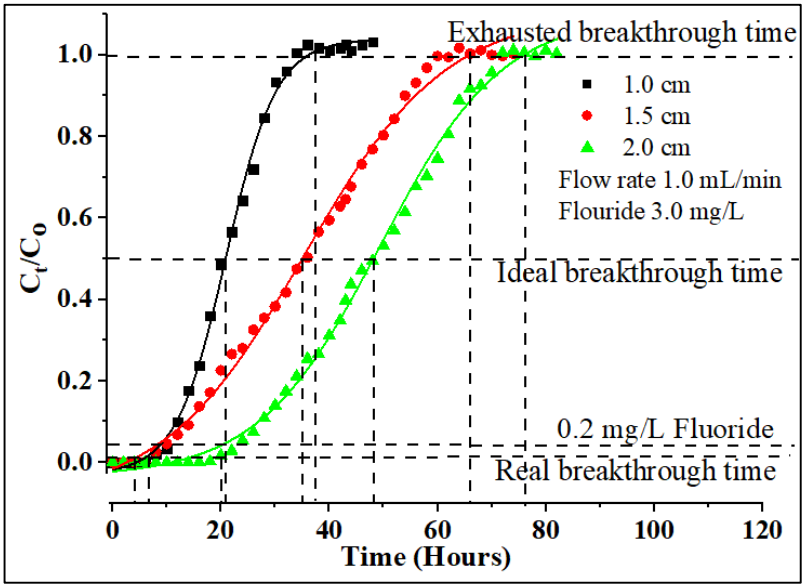

Figure 4.102: Breakthrough curves of MOMA in the fixed-bed column with different bed heights 1.0 cm, 1.5 cm, and 2.0 cm with a flow rate of 1.0 mL/min

The ideal breakthrough time (C_t/C_o = 0.5) of the system increased considerably with higher bed height greater than lower bed height (Ideal breakthrough time for 1.0 cm - 20.0 hours, for 1.5 cm - 28.0 hours, and for 2.0 cm - 38.0 hours). The total time taken for the system exhausted was observed as 40.0 hours for 1.0 cm [Exhausted breakthrough time (C_t/C_o = 0.95), 54.0 hours for 1.5 cm, and 60.0 hours for 2.0 cm bed heights. The results concluded that the breakthrough time of the column was decreased with lower bed heights of MOMA. The effect of bed height in removing fluoride using MOMA was presented in Figure 4.102 with three different bed heights as 1.0 cm, 1.5 cm, and 2.0 cm with flow rates of 3.0 mL/min. From the BTCs, it was investigated that the real breakthrough (C_t/C_o = 0.06) was reached faster with lower bed height (28.0 hours for 1.0 cm) early comparison to the other two bed heights (16.0 hours for 1.5 cm, and 12.0 hours for 2.0 cm).

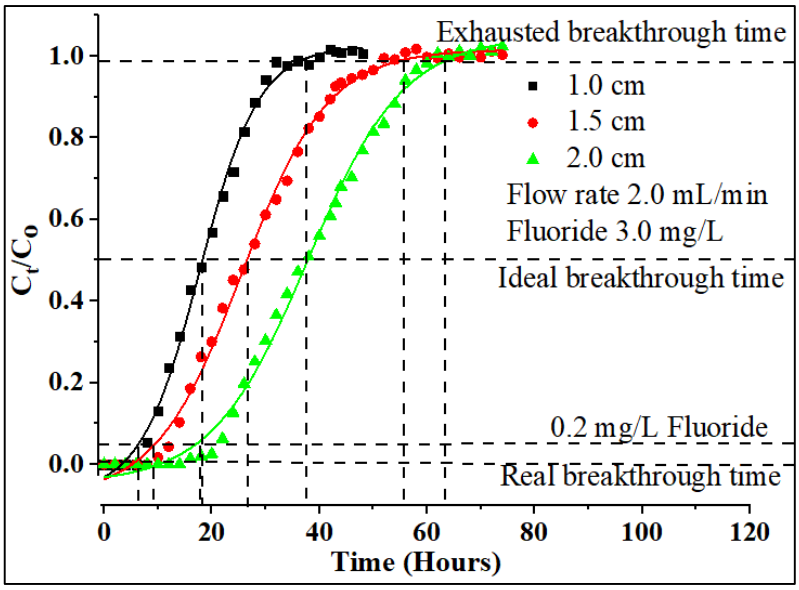

Figure 4.103: Breakthrough curves of MOMA in the fixed-bed column with different bed heights 1.0 cm, 1.5 cm, and 2.0 cm with a flow rate of 2.0 mL/min

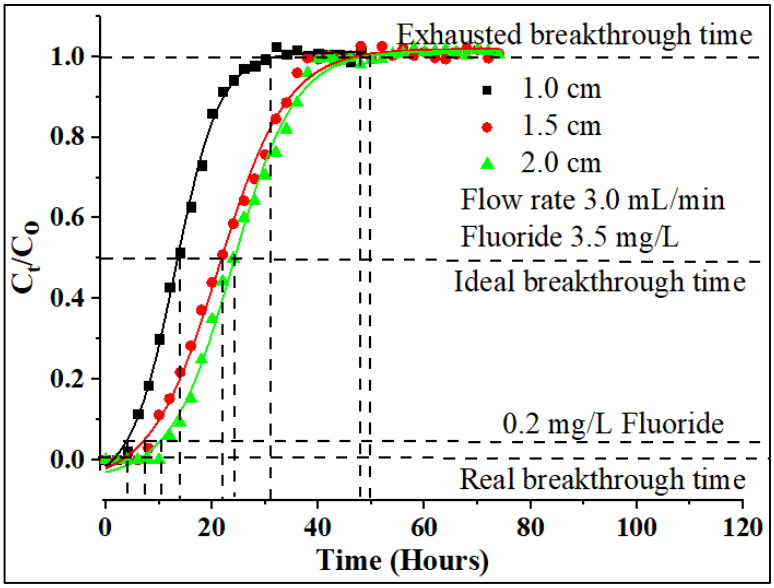

Figure 4.104: Breakthrough curves of MOMA in the fixed-bed column with different bed heights 1.0 cm, 1.5 cm, and 2.0 cm with a flow rate of 3.0 mL/min

The column reached its real breakthrough point substantially for a shorter time with low bed height. The ideal breakthrough time (C_t/C_o = 0.5) of the system increased

considerably with higher bed height greater than lower bed height (Ideal breakthrough time for 54.0 hours in 1.0 cm, for 38.0 hours in 1.5 cm, and for 24.0 hours in 2.0 cm). The total time taken for the system exhausted was observed as 70.0 hours for 1.0 cm [Exhausted breakthrough time (C_t/C_o = 0.95), 62.0 hours for 1.5 cm, and 52.0 hours for 2.0 cm bed heights.

Removal of E. coli using SONPs + GO

The effect of bed height in removing *E. coli* using SONPs + GO was presented in Figure 4.103 with three different bed heights as 0.5 cm, 1.0 cm, and 1.5 cm with flow rates of 1.0 mL/min. From the BTCs, it was investigated that the real breakthrough (C_t/C_o = 0.001) was reached faster with lower bed height (120 hours for 0.5 cm) early comparison to the other two bed heights (160.0 hours for 1.0 cm, and 184.0 hours for 1.5 cm). The column reached its real breakthrough point substantially for a shorter time with low bed height. The ideal breakthrough time (C_t/C_o = 0.5) of the system increased considerably with higher bed height greater than lower bed height (Ideal breakthrough time for 196.0 hours in 0.5 cm, for 224.0 hours in 1.0 cm, and for 236.0 hours in 1.5 cm). The total time taken for the system exhausted was observed as 228.0 hours for 0.5 cm [Exhausted breakthrough time (C_t/C_o = 0.95), 250.0 hours for 1.0 cm, and 292.0 hours for 1.5 cm bed heights.

The effect of bed height in removing *E. coli* using SONPs + GO is presented in Figure 4.104 with three different bed heights as 0.5 cm, 1.0 cm, and 1.5 cm with flow rates of 2.0 mL/min. From the BTCs, it was investigated that the real breakthrough (C_t/C_o = 0.05) was reached faster with lower bed height (80.0 hours for 0.5 cm) early comparison to the other two bed heights (120.0 hours for 1.0 cm, and 150.0 hours for 1.5 cm). The ideal breakthrough time (C_t/C_o = 0.5) of the system increased considerably with higher bed height greater than lower bed height (Ideal breakthrough time for 162.0 hours in 0.5 cm, for 184.0 hours in 1.0 cm, and for 236.0 hours in 1.5 cm).

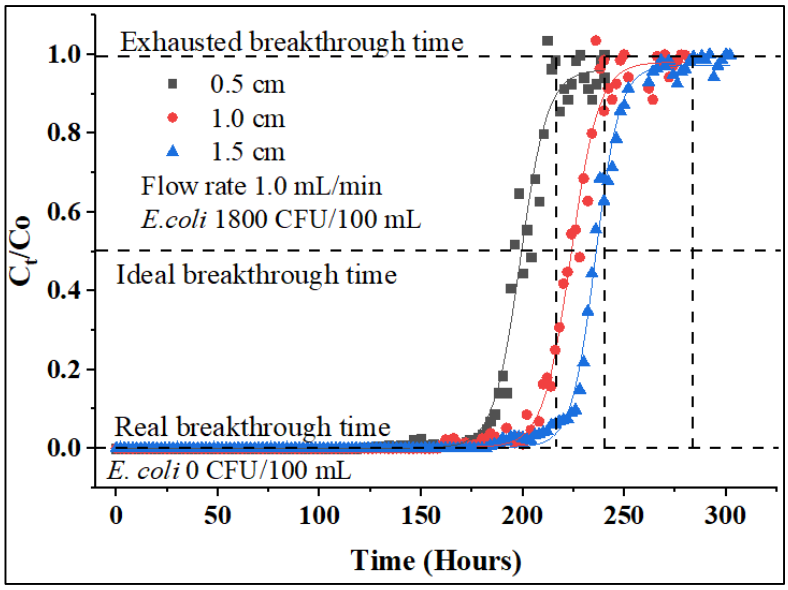

Figure 4.105: Breakthrough curves of SONPs +GO in the fixed-bed column with different bed heights 0.5 cm, 1.0 cm, and 1.5 cm with a flow rate of 1.0 mL/min

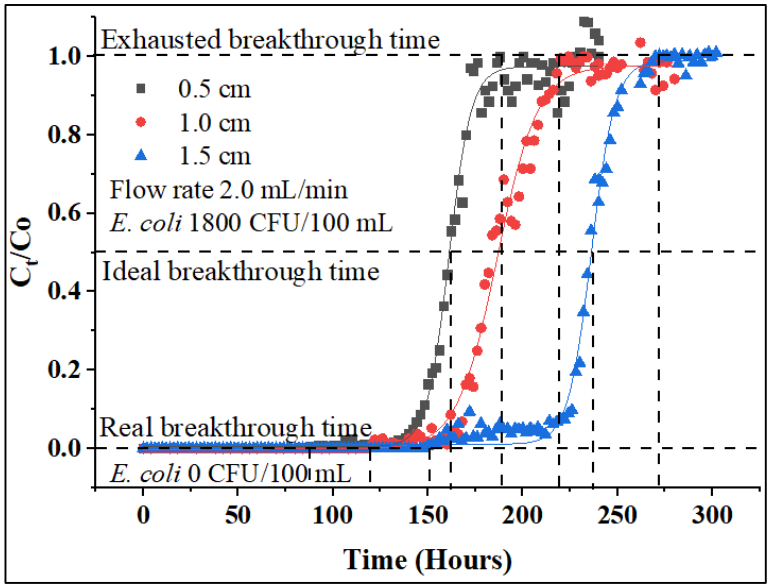

Figure 4.106: Breakthrough curves of SONPs +GO in the fixed-bed column with different bed heights 0.5 cm, 1.0 cm, and 1.5 cm with a flow rate of 2.0 mL/min

The total time taken for the system exhausted were observed as 188.0 hours for 0.5 cm [Exhausted breakthrough time (C_t/C_o = 0.95), 224.0 hours for 1.0 cm, and 270.0

hours for 1.5 cm of bed heights. The breakthrough time was decreased with lower bed heights of SONPs + GO and the time taken to reach breakthrough decrease with increased flow rate with same bed heights compare to the results of 1.0 mL/min flow rate.

The effect of bed height in removing *E. coli* using SONPs + GO is presented in Figure 4.105 with three different bed heights as 0.5 cm, 1.0 cm, and 1.5 cm with flow rates of 3.0 mL/min. From the BTCs, it was investigated that the real breakthrough (C_t/C_o = 0.05) was reached faster with lower bed height (14.0 hours for 0.5 cm) early comparison to the other two bed heights (44 hours for 1.0 cm, and 70.0 hours for 1.5 cm). The real breakthrough time of 0.5 cm SONPs + GO bed with 3.0 mL/min was observed reaching the breakthrough point faster than 1.0 cm and 1.5 cm bed heights. The ideal breakthrough time (C_t/C_o = 0.5) of the system increased considerably with higher bed height greater than lower bed height (Ideal breakthrough time for 102.0 hours in 0.5 cm, for 108.0 hours in 1.0 cm, and for 152.0 hours in 1.5 cm). The total time taken for the system exhausted were observed as 122.0 hours for 0.5 cm [Exhausted breakthrough time (C_t/C_o = 0.95), 142.0 hours for 1.0 cm, and 188.0 hours for 1.5 cm of bed heights. The results indicated that the three different bed heights' breakthrough time is substantially different from each other, and 1.5 cm of bed height was best performed greater than the other two bed heights.

All results of bed heights corroborated that higher bed heights of ZEOL (5.5 cm), MOMA (2.0 cm), and SONPs + GO (1.5 cm) performed best increasing breakthrough time with a lower flow rate of 1.0 mL/min. The higher bed heights increase the fixed bed column's breakthrough time and increase the removal capacity of adsorbents since the loading of ZEOL, MOMA and SONPs + GO was increased. The mass in the material bed seems to be decided by the breakthrough time and the shape of the breakthrough curve. The effective residence time in the fixed-bed column was increased with a higher mass of material loading and simultaneously improve the volumetric sweep efficiency (flooding pattern and mobilities of the solution through bed) (Sen et al., 2002).

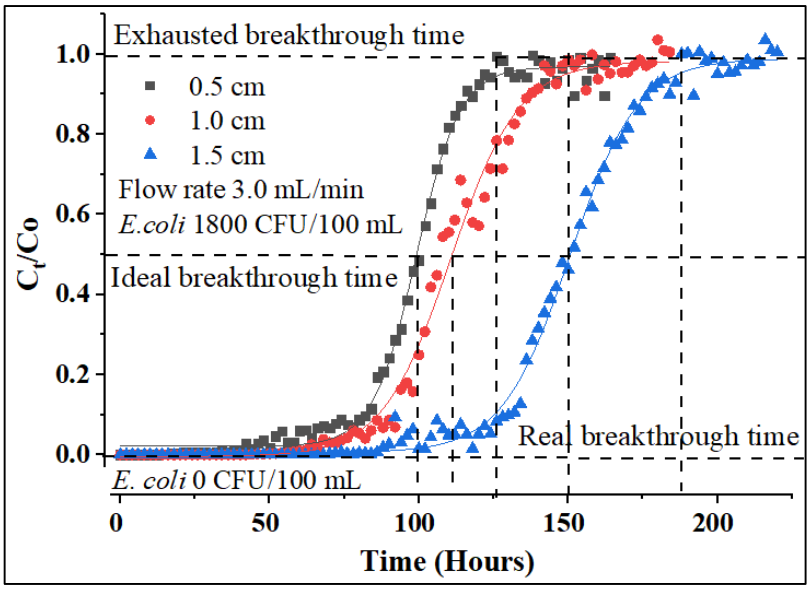

Figure 4.107: Breakthrough curves of SONPs +GO in the fixed-bed column with different bed heights 0.5 cm, 1.0 cm, and 1.5 cm with a flow rate of 3.0 mL/min

Therefore, the total mass of removal was gradually increased with higher bed heights and lower flow rates due to adsorbent surfaces highly exposed to water flow permeated through the material bed. The higher breakthrough time enhances intra-particle diffusion in the material bed, which increases the adsorption capacity (Sadaf and Bhatti, 2014). The removal rate has been observed to increase with higher adsorbent mass due to increased surface area and more adsorption sites. The higher volume of effluent can be treated with a higher mass of materials in the column bed. Hence, the breakthrough time and saturation time of the column were increased. The best-performed bed heights of ZEOL (5.5 cm), MOMA (2.0 cm), and SONPs + GO (1.5 cm), and 1.0 mL/min flow rate were selected to experiment 02.

(ii) Experiment 02 - fixed-bed column studies for multi-solute with a single layer

Comparison of hardness, fluoride, and *E. coli* removal in single-solute and multi-solute systems

The effect of ZEOL in removing hardness in single-solute and multi-solute studies was presented in Figure 4.106, with bed height as 5.5 cm and flow rates of 1.0 mL/min. The BTCs investigated that the real breakthrough (C_t/C_o = 0.05) of ZEOL in removing hardness was reached within 30.0 hours for single-solute and 58.0 hours for multi-solute systems. The real breakthrough time of hardness in the multi-solute system was observed higher than real breakthrough time in the single-solute. When the experimental time was increased further, the gap between the single-solute and multi-solute breakthrough curves was decreased gradually. The reference breakthrough time (C_t/C_o = 0.24) in single-solute and multi-solute was illustrated as 51.0 hours and 59.0 hours, respectively. The ideal breakthrough time (C_t/C_o = 0.50) was observed 72.0 hours in single-solute and 74.0 hours in multi-solute studies.

The total time taken for the system exhausted was observed as 100.0 hours for single-solute [Exhausted breakthrough time (C_t/C_o = 0.95), 86.0, and 105.0 hours for multi-solute studies. Negatively charged different metal oxides (CaO, MgO, Al_2O_3, TiO_2, based on the surface composition of ZEOL indicated in EDAX analysis) in ZEOL give priority to remove Ca^{2+} and Mg^{2+} ions composed in hardness. Thermally transformed Si–O and Al–O from the inert phase to the active phase at a higher temperature in the presence of NaOH increases the removal of hardness in feed solution (Aragaw & Ayalew, 2019). The results concluded that the breakthrough time of the ZEOL column was not shown considerably different in single-solute and multi-solute studies. The adsorption of hardness by ZEOL in multi-solute studies was not interfered by fluoride and *E. coli* in multi-solute solution. ZEOL can be recommended to use in removing hardness in a multi-solute solution.

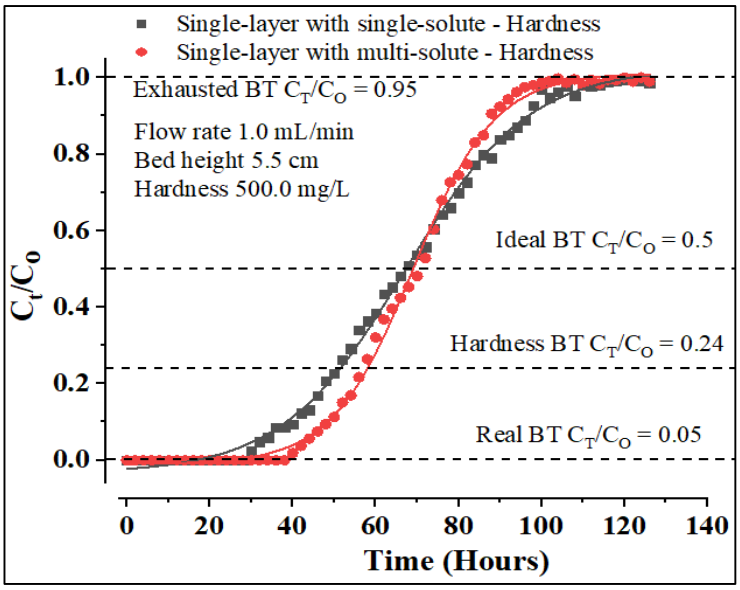

Figure 4.108: Breakthrough curves of ZEOL in the fixed-bed column of single-solute (hardness) and multi-solute (hardness, fluoride, and E. coli) system with bed height 5.5 cm and flow rate 1.0 mL/min

The effect of MOMA in removing fluoride in single-solute and multi-solute systems was presented in Figure 4.107 with a bed height of 2.0 cm and flow rates of 1.0 mL/min. The BTCs investigated that the real breakthrough (C_t/C_o = 0.05) of MOMA in removing fluoride was reached within 28.0 hours for single-solute and 30.0 hours for multi-solute systems. The real breakthrough time indicated that two systems reached their real breakthrough point almost simultaneously, and no higher gap in time was observed.

The reference breakthrough time (C_t/C_o = 0.07) of the MOMA was observed as 32.0 hours for the single-solute and 34.0 hours for the multi-solute systems. The MOMA's ideal breakthrough time (C_t/C_o = 0.50) was observed as 54.0 hours for the single-solute and 58.0 hours for the multi-solute systems. The total time taken for the system exhausted were observed as 76.0 hours for the single-solute and 78.0 hours for the multi-solute systems [Exhausted breakthrough time (C_t/C_o = 0.95).

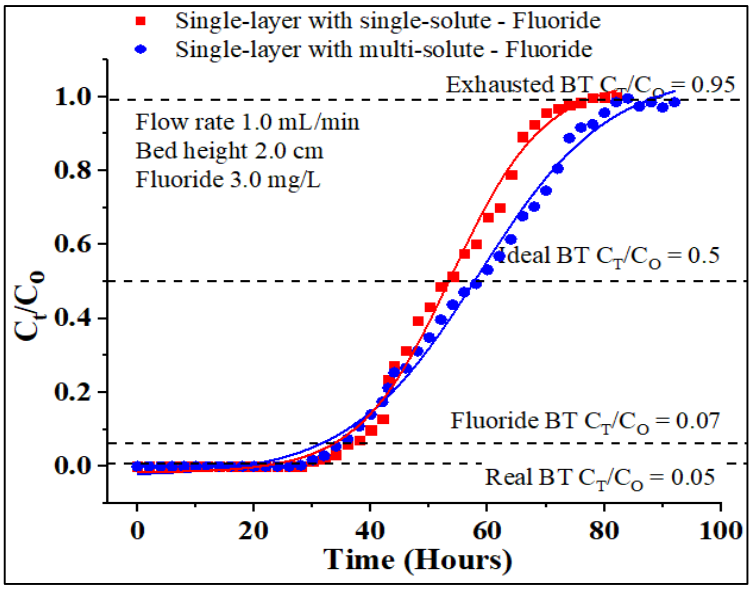

Figure 4.109: Breakthrough curves of MOMA in the fixed-bed column of single-solute (fluoride) and multi-solute (hardness, fluoride, and E. coli) system with bed height 2.0 cm and flow rate 1.0 mL/min

The breakthrough time of MOMA was increased substantially a few hours in removing fluoride in multi-solute solution (with hardness and *E. coli*) compared to fluoride removal in single-solute solution (fluoride alone). The results indicated that the MOMA is selectively removed fluoride in water. Hardness and *E. coli* were not interfered in the removal process of fluoride by MOMA. However, the formation of CaF_2 complexes in the presence of hardness (Chandrajith et al., 2012) can increases fluoride removal slightly.

The effect of SONPs + GO in removing *E. coli* in the single-solute and multi-solute systems were presented in Figure 4.108 with bed heights of 1.5 cm and flow rates of 1.0 mL/min. The BTCs investigated that the real breakthrough (C_t/C_o = 0.05) and reference breakthrough (C_t/C_o = 0.001) of SONPs + GO in removing *E. coli* was reached within 200.0 hours for single-solute and 202.0 hours for multi-solute systems. The real breakthrough time of hardness and fluoride indicated that SONPs + GO did not show higher gap in breakthrough time in single-solute system compared to the multi-solute

system. The ideal breakthrough time (C_t/C_o = 0.50) of the SONPs + GO in removing *E. coli* was observed as 236.0 hours for single-solute and 275.0 hours for multi-solute systems. The higher time difference in the ideal breakthrough time indicated that the multi-solute in the solution influence the *E. coli* removal. Thus, the time taken to reach the ideal breakthrough point was observed increase in the multi-solute system compared to the single-solute system. The total time taken for the system exhausted was observed as 264.0 hours for the single-solute and 352.0 hours for the multi-solute system [Exhausted breakthrough time (C_t/C_o = 0.95)].

The results concluded that the breakthrough time of the SONPs + GO column was increased in removing *E. coli* in multi-solute solution (with hardness and fluoride) compared to *E. coli* removal by SONPs + GO in single-solute solution (*E. coli* alone). The results indicated that the SONPs + GO is selectively removed *E. coli* from water, and hardness and fluoride are interfered in the removal process of *E. coli* by SONPs + GO. Functional groups on the surface of materials such as carboxyl, carbonyl, and epoxy groups contained graphene oxide (MeiJiao et al., 2013). AgO give higher priority to oxidize the bacterial cell in the solution. The formation of CaF_2 in the presence of hardness (Chandrajith et al., 2011) increases the removal of *E. coli* by damaging the cell membrane (Bala et al., 2011). The inhibitory processes prominently with SONPs + GO and mildly CaF_2 increase the time is taken to reach the breakthrough point of *E. coli* in the multi-solute system. The longer breakthrough time decreases the cost of production, and the regeneration increasing the efficacy of SONPs + GO in the multi-layered filter unit.

The results of fixed-bed column studies for multi-solute with single layer indicated that feed solution accompanied with hardness, fluoride, and *E. coli* interfered mildly with the ZEOL, MOMA removal process SONPs + GO. The percentage of removal of hardness (77%), fluoride (94%), and *E. coli* (99%) remained the same while the total mass of adsorbate removal was decreased. The observation in multi-solution interference with a different system in fixed bed studies has been reported by Xu et al., 2012. The results indicated that the removal effectiveness of materials was not changed and

interfered with by other solutes in the multi-solute system. The single-layer with multi-solute studies confirm that further ZEOL, MOMA, and SONPs + GO are promising materials to remove hardness, fluoride, and *E. coli* in potable water. Therefore, a Multi-layered filter system was included ZEOL, MOMA and SONPs + GO in removing hardness, fluoride, and *E. coli*, respectively.

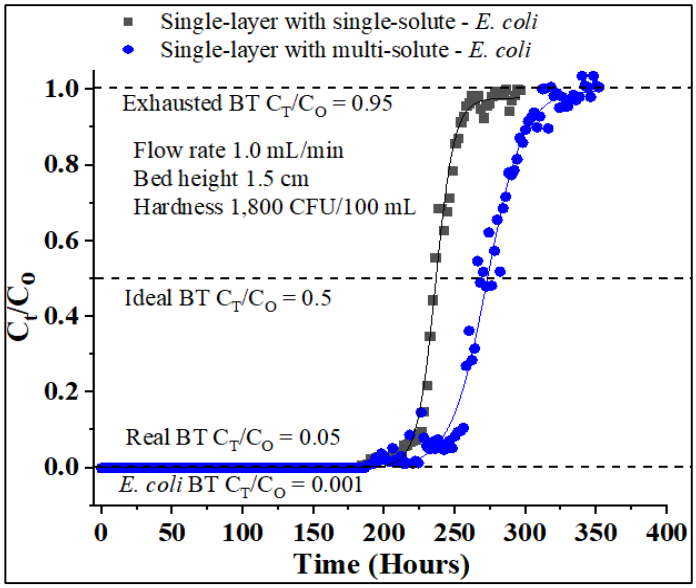

Figure 4.110: Breakthrough curves of MOMA in the fixed-bed column of single-solute (fluoride) and multi-solute (hardness, fluoride, and E. coli) system with bed height 1.5 cm and flow rate 1.0 mL/min

4.4.6. Kinetic models for fixed-bed column operation

(a) The Adam-Bohart model

The results of the Adams-Bohart model for ZEOL in the removal of hardness and MOMA in the removal of fluoride were included in Tables 4.12 and 4.13. Linear curve fitting and non-linear curve fitting were illustrated in Figure 4.109 for fixed-bed column studies of single-layer with single-solute for ZEOL 4.110 for fixed-bed column studies of single-layer with single-solute for MOMA, and Figure 4.111 for fixed-bed column studies of single-layer with multi-solute for ZEOL and MOMA.

Table 4.17: Rate constants and maximum adsorption capacity of Adams–Bohart model for ZEOL for single-layer with multi-solute studies

Flow Rate (mL/min)	Bed height (cm)	K_{AB} (L/mg.min)	N_0 (mg/L)	R^2	Error Analysis (SS)
1.00	3.50	0.000339	54,020	0.90	13.97 ± 0.11
1.00	4.50	0.000034	67,958	0.86	21.63 ± 0.25
1.00	5.50	0.000245	69,589	0.87	17.41 ± 0.05
2.00	3.50	0.000226	39,463	0.88	9.51 ± 0.21
2.00	4.50	0.000226	51,513	0.84	14.81 ± 1.23
2.00	5.50	0.000188	59,160	0.92	21.68 ± 2.60
3.00	3.50	0.000226	33,420	0.90	5.99 ± 0.21
3.00	4.50	0.000245	35,437	0.89	13.46 ± 1.46
3.00	5.50	0.000434	47,078	0.86	8.64 ± 3.12

The adsorption capacity was increased when the bed height was increased. R^2 values were suggested that the experimental data were not best fitted with the Adams-Bohart model and unsuitable to use as an appropriate predictor of the breakthrough curve in this study. It collaborated that experiment data do not follow the theories of the Adam-Bohart model, which describe the rate of adsorption is proportional to the residual concentration in the adsorbent and concentration of adsorbed species. The reason might be due to the model behaving well with the first part of the breakthrough period (Negrea et al., 2020).

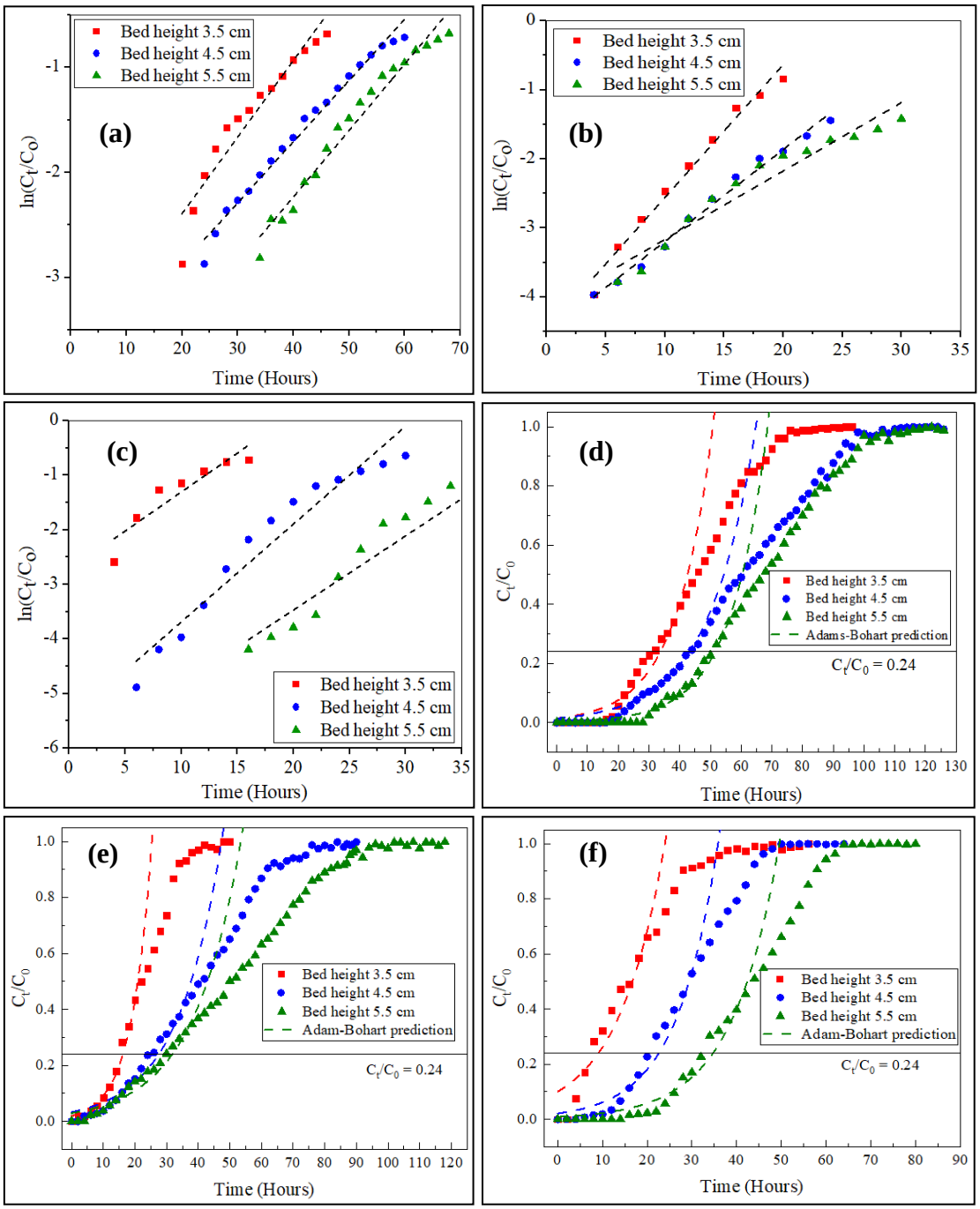

Figure 4.111: Best fitted curves of Adams-Bohart model for fixed bed column studies for single-solute with single-layer, linear curve fitting (a) ZEOL - 1 mL/min, (b) ZEOL - 2 mL/min, (c) ZEOL - 3 mL/min, and non-linear curve fitting (d) ZEOL – 1 mL/min, (e) ZEOL – 2 mL/min, (f) ZEOL – 3 mL/min

Table 4.18: Rate constants and maximum adsorption capacity of Adams–Bohart model for MOMA for single-layer with single-solute studies

Bed height (cm)	Flow Rate (mL/min)	K_{AB} (mL/min .mg)	N_o (mg/L)	R^2	Error Analysis (SS)
1.00	1.00	0.0012	884.00	0.75	1.68 ± 0.17
1.50	1.00	0.0005	1,010.00	0.90	3.32 ± 0.13
2.00	1.00	0.0006	1,723.00	0.83	11.26 ± 0.43
1.00	2.00	0.0009	1,115.00	0.89	2.70 ± 0.18
1.50	2.00	0.0009	1,508.00	0.85	6.77 ± 0.32
2.00	2.00	0.0009	1,511.00	0.91	7.84 ± 0.36
1.00	3.00	0.0009	1,365.00	0.85	4.14 ± 0.34
1.50	3.00	0.0009	1,499.00	0.91	2.63 ± 0.19
2.00	3.00	0.0009	1,594.00	0.92	1.88 ± 0.13

The predicted curves of the Adam-Bohart model for ZEOL and MOMA were compared properly with the experimental data with model values at different experimental conditions (Figure 109 and Figure 110).

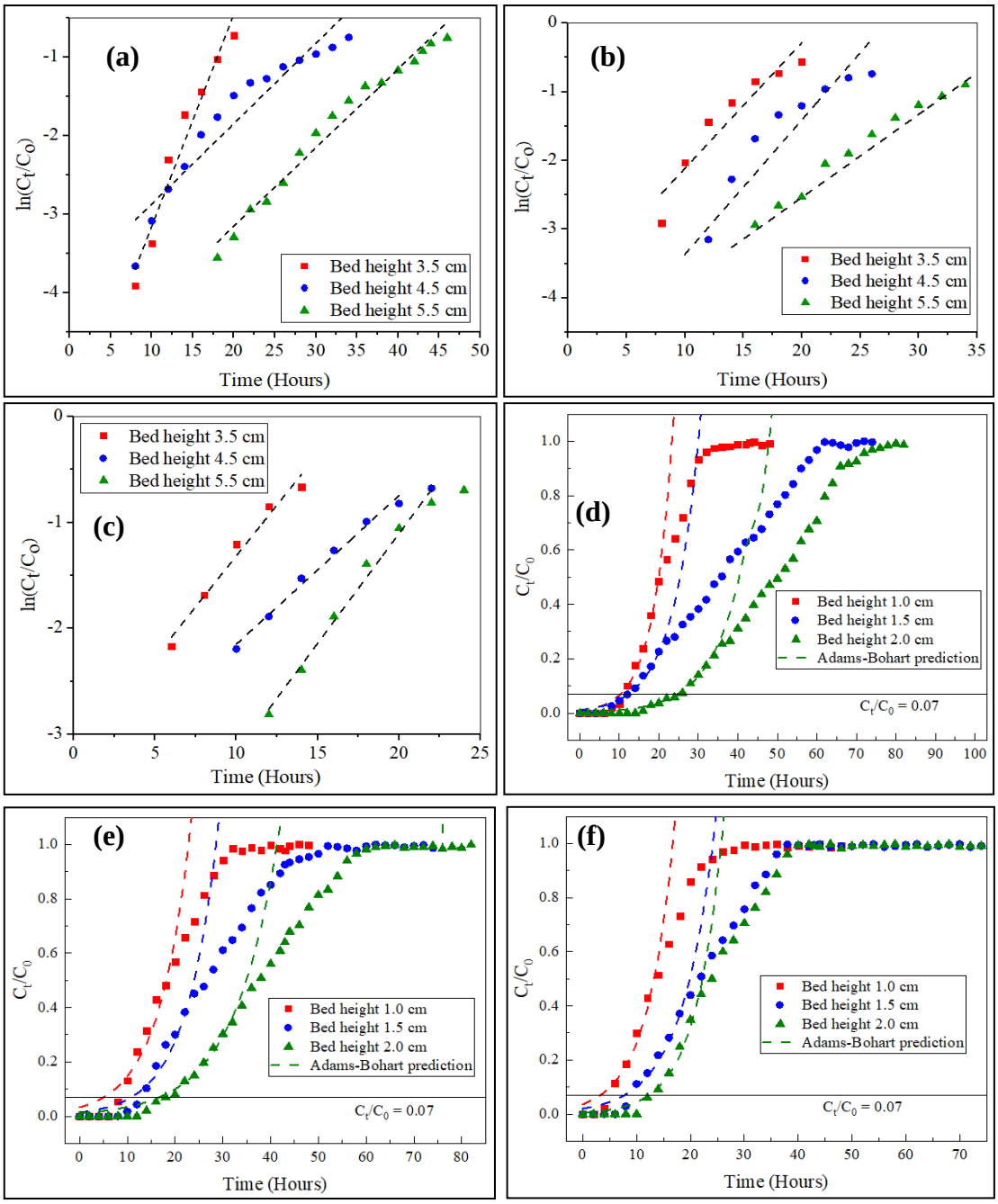

Figure 4.112: Best fitted curves of Adams-Bohart model for fixed-bed column studies for single-solute with single-layer, linear curve fitting (a) MOMA - 1 mL/min, (b) MOMA - 2 mL/min, (c) MOMA - 3 mL/min, and non-linear curve fitting (d) MOMA – 1 mL/min, (e) MOMA – 2 mL/min, (f) MOMA – 3 mL/min

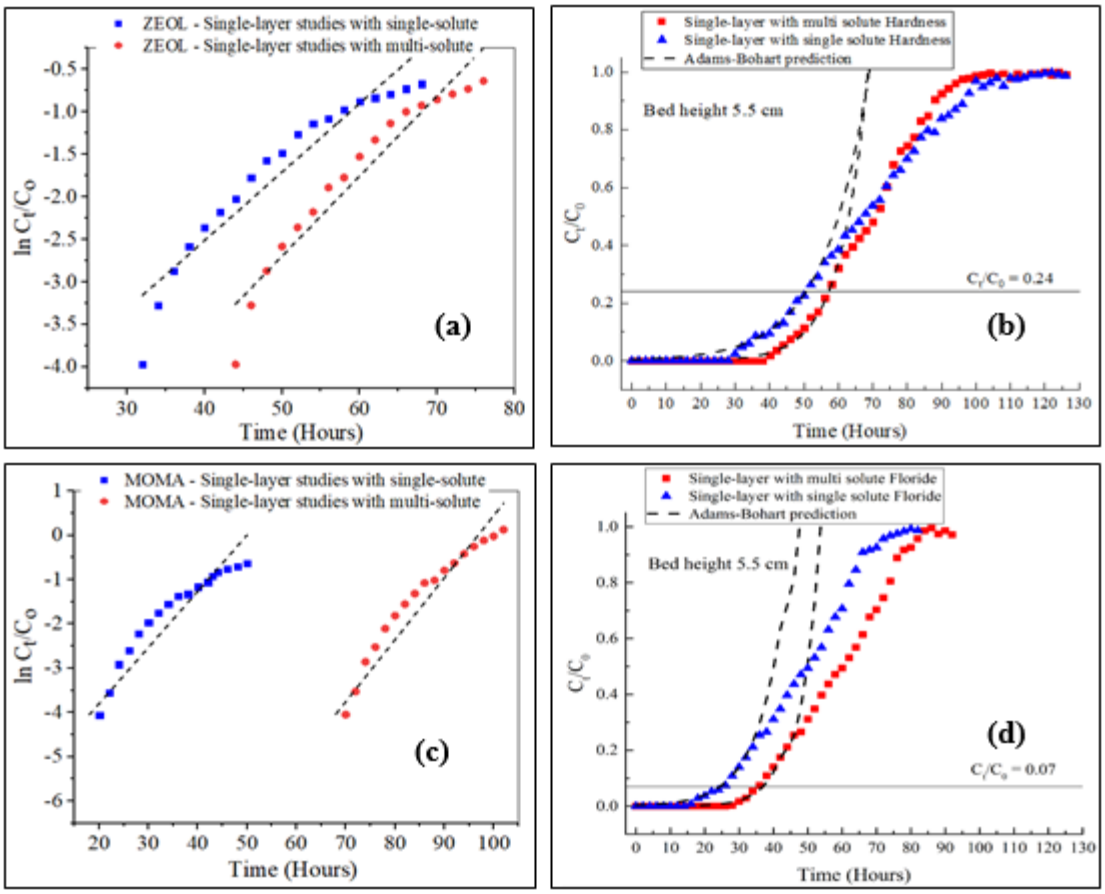

Figure 4.113: Best fitted curves of Adams-Bohart model for fixed-bed column studies for multi-solute with single-layer, linear curve fitting (a) ZEOL - 1 mL/min, 5.5 cm bed height and non-linear curve fitting (b) ZEOL – 1 mL/min, 5.5 cm bed height, linear curve fitting (c) MOMA - 1 mL/min, 2.0 cm bed height and non-linear curve fitting (d) MOMA – 1 mL/min, 2.0 cm bed height

The good agreement was observed in experimental data and predicted data at the initial part of the breakthrough curves. These observations suggested that the Adam-Bohart model is valid for the region until C_t/C_o = 0.5. The higher differences can be observed between experimental data and predicted data after this region (C_t/C_o > 0.5).

The results of the Adam-Bohart model in single-layer with multi-solute studies illustrated that experimental data do not follow the theories of the Adam-Bohart model.

The K_{AB} values in multi-solute studies (hardness – 0.0003 mL/min.mg and fluoride – 0.0008 mL/min.mg) were increased more than single-solute studies (hardness – 0.0002 mL/min.mg and fluoride – 0.0006 mL/min.mg). The N_o values in multi-solute studies (hardness – 69,589.0 mg/L and fluoride – 71,309.0 mg/L) were also increased more than single-solute studies (hardness – 1,723.0 mg/L and fluoride – 3,173.0 mg/L).

The mean sum of square (SS) for error analysis indicated the higher values for hardness (Single-solute - 17.41 ± 0.05 and multi-solute – 15.62 ± 1.24) and fluoride (Single-solute - 11.26 ± 0.43 and multi-solute – 5.68 ± 0.35) removal in single-solute and multi-solute studies for selected bed heights (hardness – 5.5 cm and fluoride – 2.0 cm) and flow rate (1.0 mL/min). The results indicated that K_{AB} and N_O were increased in the single-layer studies with multi-solute studies. In a multi-solute system, the multi-solute competition and their interaction increases the Adams-Bohart rate constant and maximum adsorption capacity per unit volume of the adsorbent column. However, the linear regression coefficient values (R^2) were observed less than 0.95. The observations corroborated that experimental data in the multi-solute system do not follow the Adams-Bohart model's theories.

(b) The Thomas Model

The linear regression results of Thomas model parameters for ZEOL and MOMA have been depicted in Table 4.14 and 4.15 for single-layer studies with single-solute. The R^2 values corroborated that hardness and fluoride adsorption kinetics and isotherms follow the Thomas model's assumption ($R^2 > 0.95$). The Thomas model assumptions described the experimental data follows Langmuir adsorption-desorption kinetics, adsorption rate controlled by surface reaction between adsorbate and unused capacity of adsorbate, and no axial dispersion is considered. Consequently, the Thomas model is valid for presenting and analyzing hardness and fluoride breakthrough results. When the flow rate was increased through the ZEOL bed, it was observed that the K_{TH} value of Thomas's model was increased (0.000003 – 0.000006 L/mg.min). The q_o was gradually increased with the bed height of the ZEOL column was increased (297.01 – 319.27

mg/g) in removing hardness which suggested that increased bed height is subjected to increase the rate of mass transfer in the internal surface of the adsorbent. Similar observations have been observed in removing water contaminants using fixed-bed columns by Pez-Cervantes et al., 2018 and Tovar-Gómez et al., 2013. The error analysis of the Thomas model for ZEOL indicated that the mean sum of the square is small in different experiment sets ranging from 0.01 ± 0.002 to 0.05 ± 0.001.

When the flow rate was increased through the MOMA bed, it was observed that the K_{TH} value of Thomas's model was increased (0.005 – 0.0011 L/mg.min) for 2.0 cm bed height and flow rate from 1.0 – 3.0 mL/min (Table 4.15). The Q_o was gradually increased with the bed height of the MOMA column was increased (14.85 – 19.45 mg/g) in removing fluoride, which suggested that increased bed height is subjected to increase the rate of mass transfer in the higher internal surface of the adsorbent and excess adsorption sites (Cluz-Oliveres et al., 2013; Chu, 2010). The error analysis of the Thomas model for ZEOL indicated that the mean sum of square is small in different experiment sets ranging from 0.76 ± 0.09 to 7.84 ± 0.56.

Table 4.19: Rate constants and adsorption capacity of the Thomas model for ZEOL

Flow Rate (mL/min)	Bed height (cm)	K_{TH} (L/mg.min)	q_e (mg/g)	R^2	Error Analysis (SS)
1.00	3.50	0.000003	297.01	0.99	0.05 ± 0.001
1.00	4.50	0.000002	312.43	0.98	0.05 ± 0.001
1.00	5.50	0.000002	319.27	0.98	0.04 ± 0.001
2.00	3.50	0.000006	286.97	0.99	0.04 ± 0.004
2.00	4.50	0.000003	293.89	0.98	0.05 ± 0.002
2.00	5.50	0.000002	294.66	0.99	0.02 ± 0.009
3.00	3.50	0.000006	298.28	0.98	0.03 ± 0.005
3.00	4.50	0.000005	277.24	0.98	0.01 ± 0.002
3.00	5.50	0.000004	273..04	0.97	0.02 ± 0.002

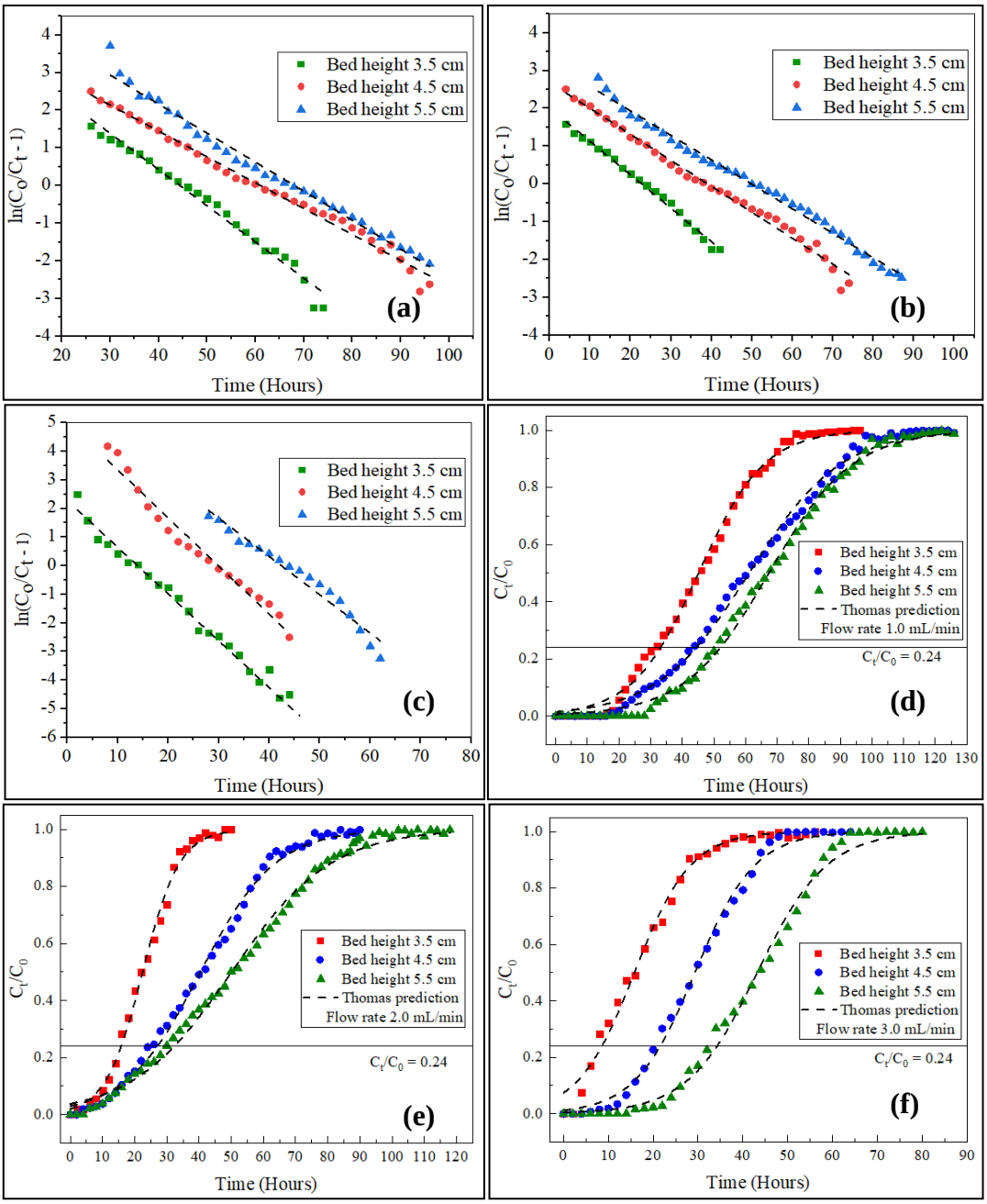

Figure 4.114: Best fitted curves of Thomas model for fixed bed column studies for multi-solute with single-layer, linear curve fitting (a) ZEOL - 1 mL/min, (b) ZEOL - 2 mL/min, (c) ZEOL - 3 mL/min, and non-linear curve fitting (d) ZEOL – 1 mL/min, (e) ZEOL – 2 mL/min, (f) ZEOL – 3 mL/min

Table 4.15: Rate constants and adsorption capacity of the Thomas model for MOMA

Bed height (cm)	Flow Rate (mL/min)	KTH (L/mg.min)	q_e (mg/g)	R^2	**Error Analysis (SS)**
1.00	1.00	0.0012	14.85	0.99	0.76 ± 0.09
1.50	1.00	0.0006	16.75	0.97	2.52 ± 0.10
2.00	1.00	0.0005	19.45	0.98	6.60 ± 0.25
1.00	2.00	0.0011	15.77	0.98	2.94 ± 0.19
1.50	2.00	0.0008	17.76	0.96	4.49 ± 0.21
2.00	2.00	0.0008	18.34	0.97	4.17 ± 0.19
1.00	3.00	0.0014	12.21	0.98	1.43 ± 0.12
1.50	3.00	0.0011	13.57	0.96	7.84 ± 0.56
2.00	3.00	0.0011	17.16	0.98	6.93 ± 0.49

When the bed depth of the fixed-bed column was increased, the calculated values of K_{TH} and q_o were indicated to vary significantly. Thomas model's linear approach generally gives the best correlation results for adsorption of hardness and fluoride during low flow rates. However, linear regression data shows that the Thomas model also provides substantial best fitted for adsorption data with higher flow rates (Table 4.14 and 4.15). The Thomas model results indicated that the higher bed heights and lower flow rates are favourable for removing hardness and fluoride in fixed-bed column studies.

The results of fixed-bed column studies for multi-solute with single-layer (Table 4. 13) indicated that the saturation loading capacity and the linear regression values in experimental data are higher for respective constituents verifying the non-selective removal of adsorbate by the respective adsorbents (q_e of ZEOL for hardness – 286.95 mg/g, R^2 – 0.98, for fluoride – 0.87 mg/g, R^2 – 0.29; q_e of MOMA for hardness – 69.30 mg/g, R^2 – 0.12, for fluoride – 17.59 mg/g, R^2 – 0.98; and q_e of SONPs + GO for hardness – 93.78 mg/g, R^2 – 0.34, for fluoride – 0.66 mg/g, R^2 – 0.59).

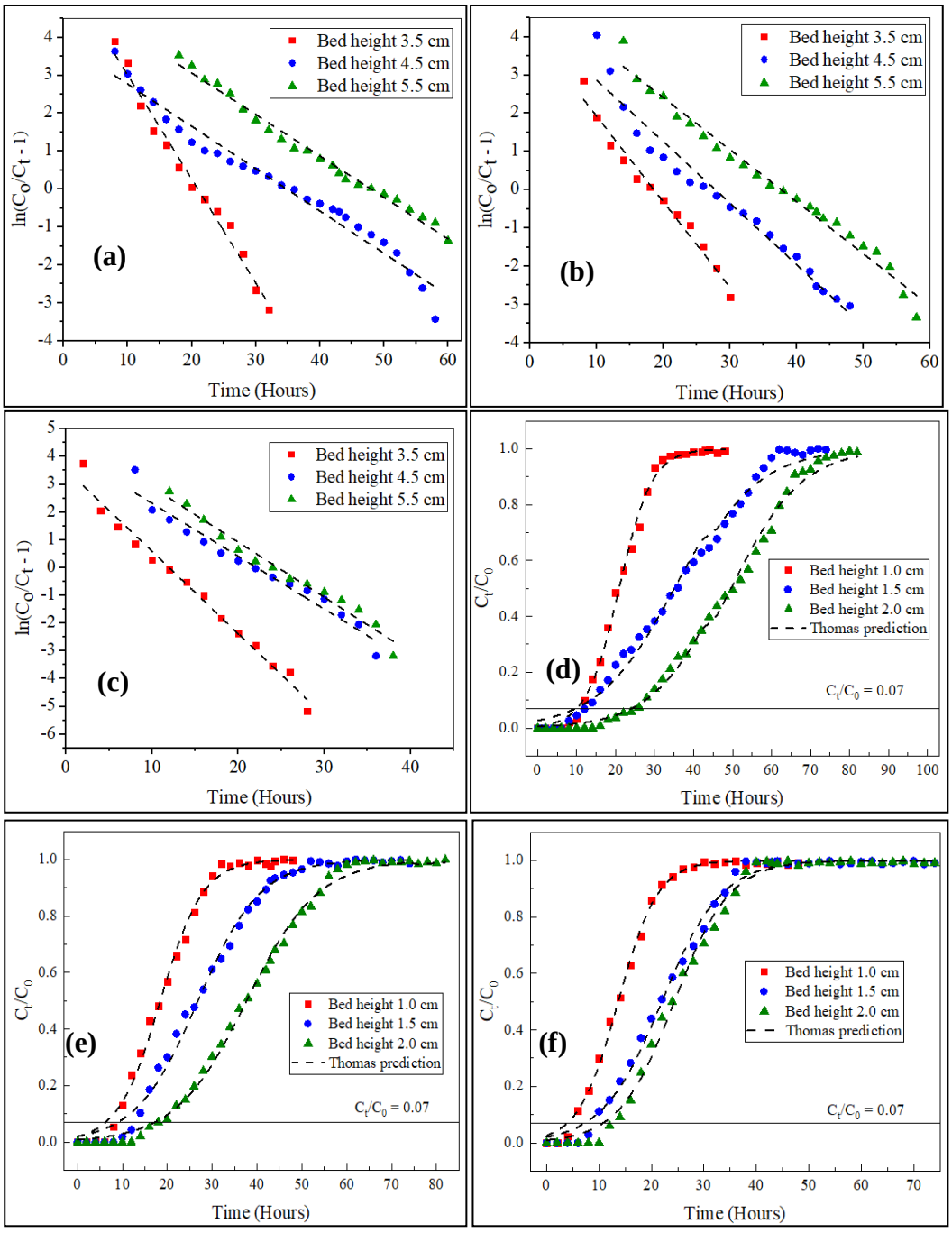

Figure 4.115: Best fitted curves of Thomas model for fixed bed column studies for multi-solute with single-layer, linear curve fitting (a) MOMA - 1 mL/min, (b) MOMA - 2 mL/min, (c) MOMA - 3 mL/min, and non-linear curve fitting (d) MOMA – 1 mL/min, (e) MOMA – 2 mL/min, (f) MOMA – 3 mL/min

Therefore, kinetic of ZEOL and MOMA in fixed column adsorption was followed the theories described by the Thomas model. A similar type of Thomas model for the different systems have been described by Yagub et al., 2015, Kapur and Mondal, 2015.

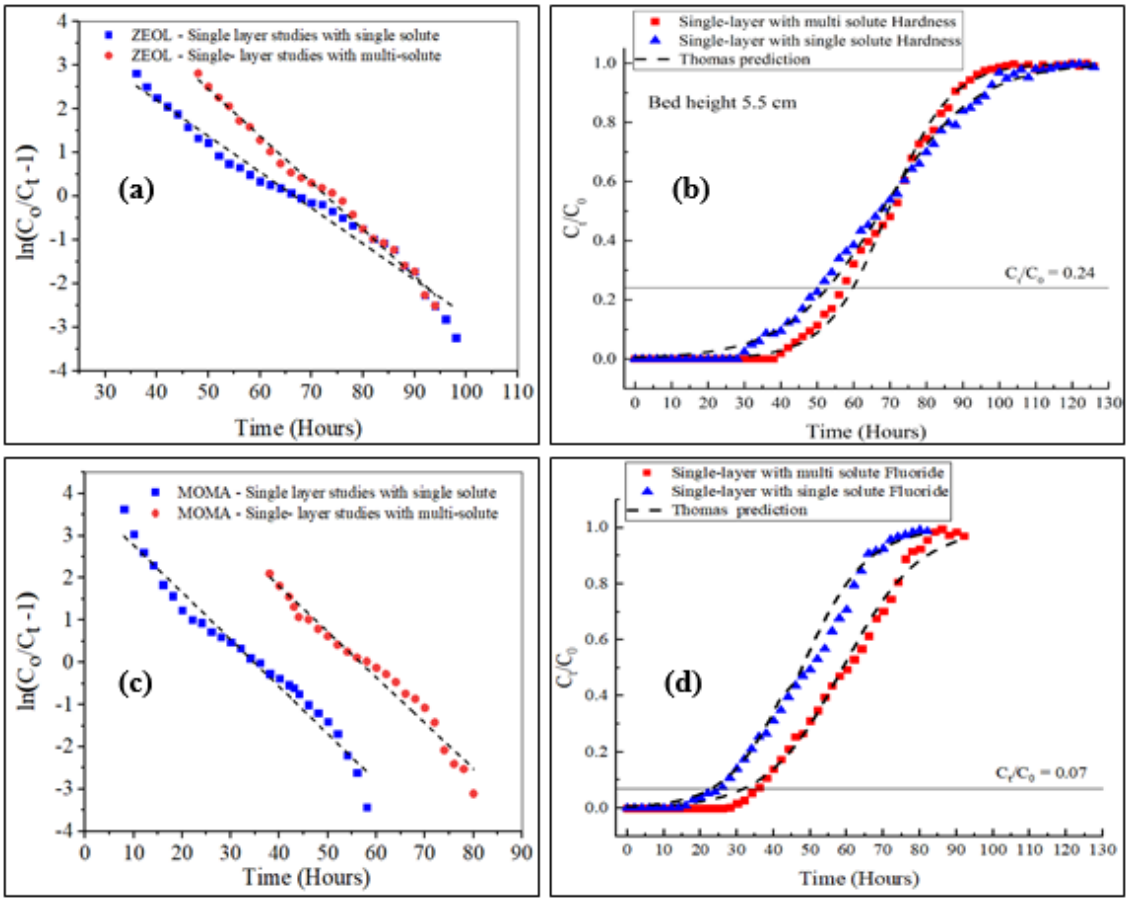

Figure 4.116: Best fitted curves of Thomas model for fixed-bed column studies for multi-solute with single-layer, linear curve fitting (a) ZEOL - 1 mL/min, 5.5 cm bed height and non-linear curve fitting (b) ZEOL – 1 mL/min, 5.5 cm bed height, linear curve fitting (c) MOMA - 1 mL/min, 2.0 cm bed height and non-linear curve fitting (d) MOMA – 1 mL/min, 2.0 cm bed height

The results of the Thomas model in single-layer with multi-solute studies illustrated that experimental data follow the theories of the Thomas model. The K_{TH} values in multi-solute studies (hardness – 0.0028 mL/min.mg and fluoride – 0.0004 mL/min.mg)

were increased more than single-solute studies (hardness – 0.000002 mL/min.mg and fluoride – 0.0005 mL/min.mg). The Q_e values in multi-solute studies (hardness – 286.95 mg/g and fluoride – 17.59 mg/L) were decreased slightly more than single-solute studies (hardness – 319.27 mg/L and fluoride – 19.45 mg/L).

The mean sum of square (SS) for error analysis indicated the lower values for hardness (Single-solute – 0.04 ± 0.001 and multi-solute – 1.29 ± 0.68) and fluoride (Single-solute – 6.60 ± 0.25 and multi-solute – 0.56 ± 0.01) removal in single-solute and multi-solute studies for selected bed heights (hardness – 5.5 cm and fluoride – 2.0 cm) and flow rate (1.0 mL/min). The results indicated that K_{TH} and q_o were increased in the single-layer studies with multi-solute studies. In a multi-solute system, the competition among the multi-solute and their interaction increases the Thomas rate constant and decreases saturation adsorption capacity of the adsorbent per unit mass of the adsorbent in the column. The linear regression coefficient values (R^2) were observed higher than 0.95 indicating experimental data were best fitted with the Thomas model. The observations corroborated that experimental data in a multi-solute system follow the Thomas model's theories.

(c) The Yoon-Nelson model

The linear regression of Yoon-Nelson model parameters for ZEOL, and MOMA, is depicted in Tables 4.16 and 4.17. The R^2 values corroborated that hardness and fluoride adsorption kinetics and isotherms follow the Yoon-Nelson model's assumptions which elaborate "rate of decrease in the probability of adsorption for each adsorbate molecule is proportional to the probability of adsorbate adsorption and the probability of adsorbate breakthrough on the adsorbent". Consequently, the Yoon-Nelson model is valid for presenting and analyzing breakthrough results of hardness, fluoride and is not valid for presenting *E. coli* breakthrough results as the oxidation of bacterial cells is occurred during the removal of *E. coli* by SONPs + GO.

The Yoon-Nelson rate constants (K_{YN}) were varied for the increased bed height (from 3.5 to 5.5 cm) and flow rates. The time required for a 50% breakthrough (τ) was

increased with the increased bed height of ZEOL, MOMA, and SONPs + GO and flow rates. The linear regression data shows that the Yoon-Nelson model provides substantial best fit for adsorption data with higher flow rates (Table 4.16). The Yoon-Nelson model results indicated that the higher bed heights and lower flow rates take a long time to reach a 50% breakthrough in fixed-bed column studies compared to lower bed height and higher flow rates with ZEOL and MOMA. The same pattern was not followed in the removal of *E. coli* using SONPs + GO.

Table 4.20: Rate constants and sorption capacity of the Yoon-Nelson model for ZEOL

Flow Rate (mL/min)	Bed height (cm)	K_{YN} (Min^{-1})	τ (Minutes)	R^2	Error Analysis (SS)
1.00	3.50	0.001	2,346.00	0.99	0.03 ± 0.001
1.00	4.50	0.001	2,458.00	0.99	0.04 ± 0.007
1.00	5.50	0.001	3,776.00	0.98	0.05 ± 0.002
2.00	3.50	0.002	2,223.00	0.99	0.06 ± 0.005
2.00	4.50	0.002	2,469.00	0.98	0.07 ± 0.005
2.00	5.50	0.002	2,823.00	0.99	0.02 ± 0.001
3.00	3.50	0.003	2,215.00	0.98	0.06 ± 0.002
3.00	4.50	0.002	2,276.00	0.97	0.06 ± 0.005
3.00	5.50	0.003	2,474.00	0.98	0.03 ± 0.001

The results of fixed-bed column studies for the mixture of components with ZEOL and MOMA (Table 4.14) indicated that the time to reach 50% breakthrough of adsorbents and the linear regression values in experimental data is higher for hardness, and fluoride, respectively, verifying the selective removal of adsorbate by the respective adsorbents (Q_e of ZEOL for hardness – 4,245 minutes, R^2 – 0.96, for fluoride – 19,500 minutes, R^2 – 0.29; Q_e of MOMA for hardness – 530 minutes, R^2 – 0.78, for fluoride – 3,348 minutes, R^2 – 0.98).

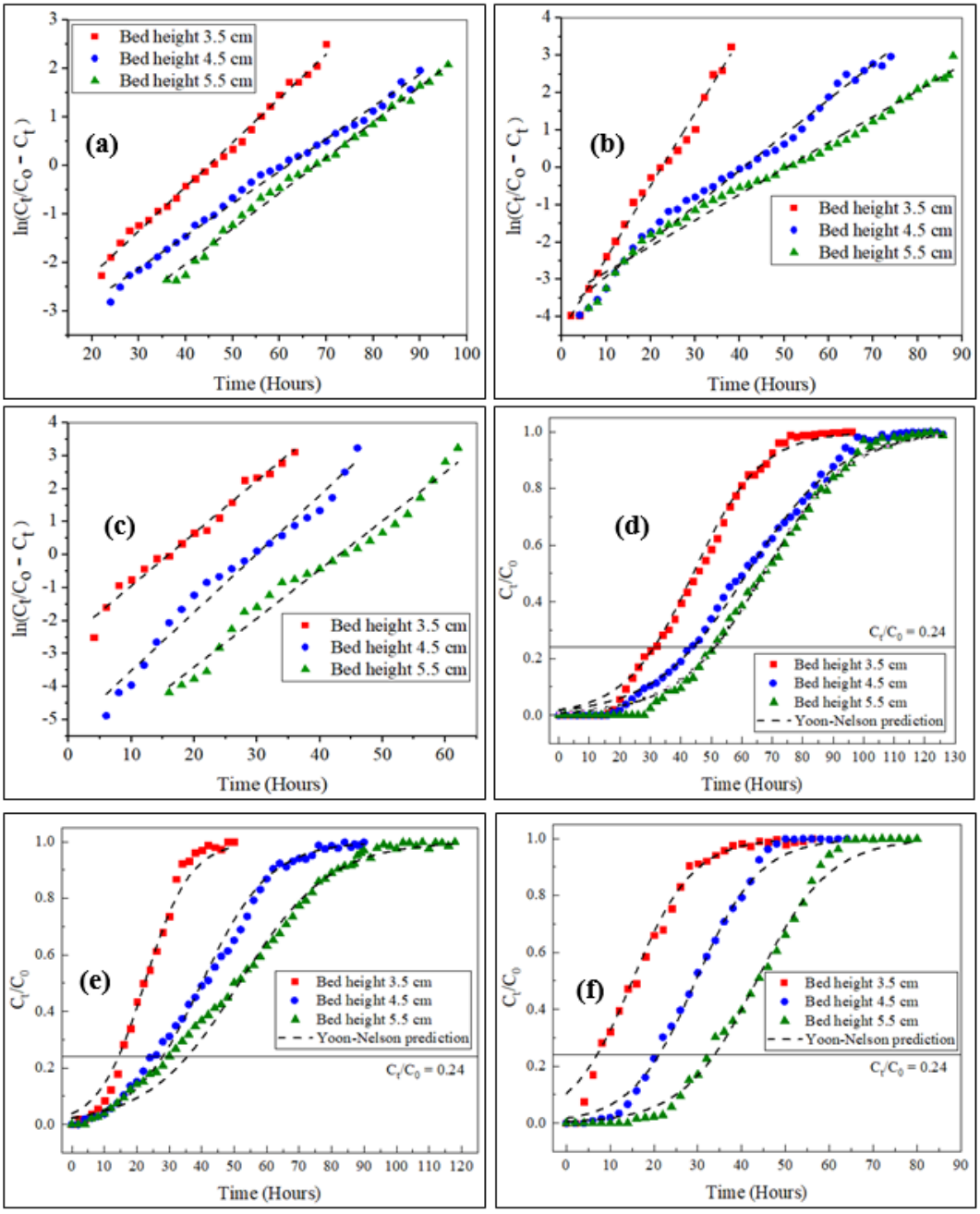

Figure 4.117: Best fitted curves of Yoon-Nelson model for fixed-bed column studies for multi-solute with single-layer, linear curve fitting (a) ZEOL - 1 mL/min, (b) ZEOL - 2 mL/min, (c) ZEOL - 3 mL/min, and non-linear curve fitting (d) ZEOL – 1 mL/min, (e) ZEOL – 2 mL/min, (f) ZEOL – 3 mL/min

The time taken to reach a 50% breakthrough from the Yoon-Nelson model agreed well with the experimental data of ZEOL and MOMA. The high values of linear regression R^2 are further supported. The experimental data of SONPs + GO are not fitted well with the Yoon-Nelson model. The adsorption process was not occurred on the surface of SONPs + GO when *E. coli* bacteria were removed from the water; however, bacterial cells were killed by damaging their cell wall. Therefore, SONPs + GO composite did not follow any kinetics theories.

The results of the Yoon-Nelson model in single-layer with multi-solute studies illustrated that experimental data follow the theories of the Yoon-Nelson model. The K_{YN} values in multi-solute studies (hardness – 0.002 mL/min.mg and fluoride – 0.003 mL/min.mg) were increased more than single-solute studies (hardness – 0.001 mL/min.mg and fluoride – 0.003 mL/min.mg). The values in multi-solute studies (hardness – 4,245 minutes and fluoride – 3,348 minutes) were decreased slightly more than single-solute studies (hardness – 3,776 minutes and fluoride – 2,740 minutes).

Table 4.21: Rate constants and sorption capacity of the Yoon-Nelson model for MOMA

ed height (cm)	Flow Rate (mL/min)	K_{YN} (Min^{-1})	τ (Minutes	R^2	Error Analysis (SS)
1.00	1.00	0.0043	1,586.00	0.98	0.77 ± 0.01
1.50	1.00	0.0020	2,005.00	0.97	0.10 ± 0.01
2.00	1.00	0.0025	2,740.00	0.98	0.25 ± 0.05
1.00	2.00	0.0041	1,085.00	0.97	0.28 ± 0.02
1.50	2.00	0.0036	1,522.00	0.96	0.26 ± 0.01
2.00	2.00	0.0035	2,089.00	0.98	0.28 ± 0.02
1.00	3.00	0.0044	1,402.00	0.98	0.21 ± 0.01
1.50	3.00	0.0035	1,678.00	0.95	0.50 ± 0.01
2.00	3.00	0.0040	1,995.00	0.99	0.54 ± 0.02

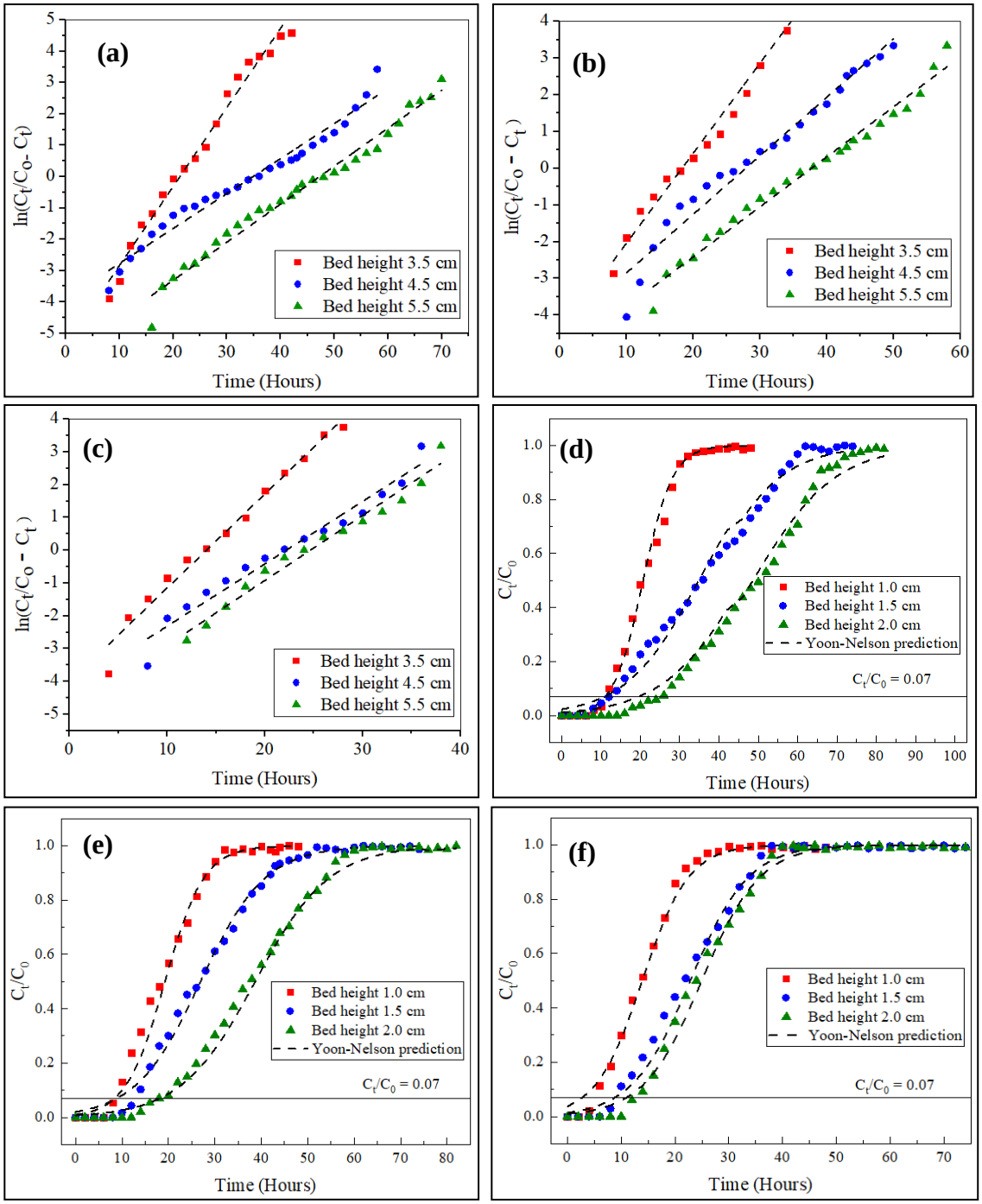

Figure 4.118: Best fitted curves of Yoon-Nelson model for fixed-bed column studies for multi-solute with single-layer, linear curve fitting (a) MOMA - 1 mL/min, (b) MOMA - 2 mL/min, (c) MOMA - 3 mL/min, and non-linear curve fitting (d) MOMA – 1 mL/min, (e) MOMA – 2 mL/min, (f) MOMA – 3 mL/min

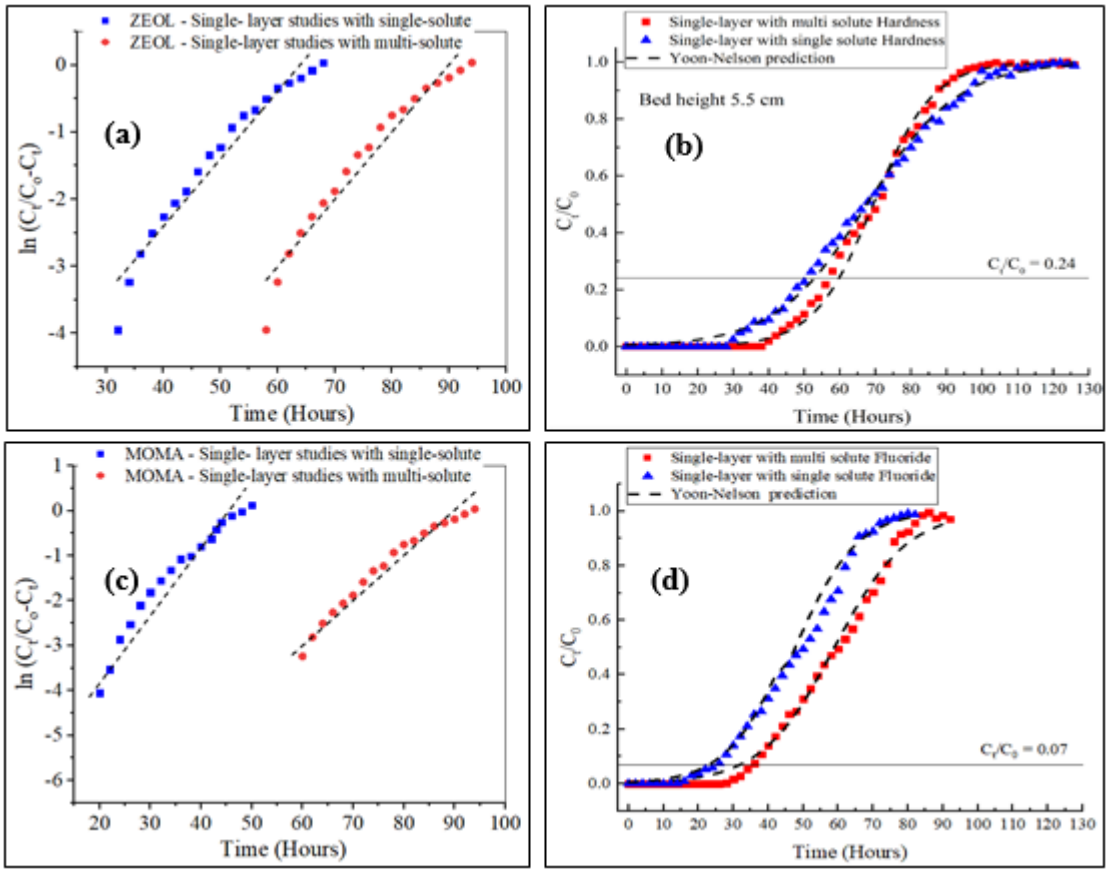

Figure 4.119: Best fitted curves of Yoon-Nelson model for fixed-bed column studies for multi-solute with single-layer, linear curve fitting (a) ZEOL - 1 mL/min, 5.5 cm bed height and non-linear curve fitting (b) ZEOL – 1 mL/min, 5.5 cm bed height, linear curve fitting (c) MOMA - 1 mL/min, 2.0 cm bed height and non-linear curve fitting (d) MOMA – 1 mL/min, 2.0 cm bed height

The mean sum of square (SS) for error analysis indicated the lower values for hardness (Single-solute – 0.05 ± 0.002 and multi-solute – 1.07 ± 0.04) and fluoride (Single-solute – 0.25 ± 0.05 and multi-solute – 0.49 ± 0.01) removal in single-solute and multi-solute studies for selected bed heights (hardness – 5.5 cm and fluoride – 2.0 cm) and flow rate (1.0 mL/min). The results indicated that K_{YN} and τ were increased in the single-layer studies with multi-solute studies. In a multi-solute system, the competition among the multi-solute and their interaction increases the Yoon-Nelson rate constant and

time required for a 50% breakthrough. The linear regression coefficient values (R^2) were observed higher than 0.95 indicating experimental data were best fitted with the Yoon-Nelson model. The observations corroborated that experimental data in a multi-solute system follow the Yoon-Nelson model's theories.

The multi-component system showed similar adsorption behaviour, demonstrated by single column layers in experiment 01 in fixed-bed column studies. The results corroborated that ZEOL, and MOMA, are promising adsorbents to remove hardness and fluoride in potable water. The isotherm and kinetic models of fixed bed adsorption studies justified the non-selective adsorption of hardness and fluoride by ZEOL and MOMA. Their removal effectiveness in removing fluoride and hardness will provide safe potable water for people in CKDu prevalent areas.

(d) Length of the unused bed (LUB) model

The LUB values of the fixed-bed column studies were illustrated in Table 4.15. The larger values of LUB corroborated lower adsorbent bed utilization. The LUB values were calculated as 1.46 cm, 0.57 cm, and 0.23 cm for ZEOL, MOMA, and SONPs + GO, respectively, when the breakthrough points of each material meet maximum allowable concentration (hardness – 120.0 mg/L; C_t/C_o – 0.23, fluoride 0.2 mg/L; C_t/C_o – 0.06, and *E. coli* 0 CFU/100 mL; C_t/C_o – 0.0001). The breakthrough time of ZEOL can be found at 58 hours, while stoichiometric time (t_{st} is the time at $C_t/C_o = 0.5$) at 68 hours considering the symmetric breakthrough curve where film and intraparticle diffusion contribute to the total mass transfer process to the same extent (Worch, 2012). The mass transfer zone (MTZ) velocity of the ZEOL was calculated as 0.08 cm/hour, the stoichiometric height (h_{st}) of the adsorbent bed was 4.04 cm, and LUB 1.46 cm (74% of adsorbent bed has utilized) (Table 4.21).

If the multilayer column provides drinking water for three months, the column should provide service for 25.10 hours without a breakthrough. The height in the ZEOL bed required to remove hardness for three months' service period was calculated as 6.11 cm with the mass of adsorbent 552.60 g. MOMA's LUB value was calculated as 0.57 cm

at the breakthrough time of 24 hours, the stoichiometric time 48 hours, and MTZ transfer velocity as 0.041 cm/hour. The LUB value represented 68% of the adsorbent bed utilised during fluoride removal in the MOMA column. The LUB values of MOMA represent less efficiency of the adsorbent bed utilization. Bed utilization can increase by decreased flow rates and increased bed heights. The value of LUB has been increased with an increased flow rate (Chen et al., 2013).

Table 4.22: Length of unused bed values for the removal of hardness, fluoride, and *E. coli* and adsorber height for the desired engineering breakthrough time

	ZEOL				MOMA				SONPs + GO			
Flow Rate (mL/min)	Bed height (cm)	U_z (cm/hr)	h_{used}(cm)	LUB (cm)	Bed height (cm)	U_z (cm/hr)	h_{used}(cm)	LUB (cm)	Bed height (cm)	U_z (cm/hr)	h_{used}(cm)	LUB (cm)
1	3.5	0.05	1.56	1.94	1.0	0.03	0.25	0.75	0.5	0.002	0.28	0.22
1	4.5	0.05	2.70	1.80	1.5	0.03	0.67	0.83	1.0	0.004	0.68	0.32
1	5.5	0.06	4.18	1.32	2.0	0.03	1.49	0.51	1.5	0.006	1.05	0.45
2	3.5	0.92	2.03	1.47	1.0	0.03	0.27	0.73	0.5	0.003	0.23	0.27
2	4.5	0.06	2.55	1.95	1.5	0.03	0.44	1.06	1.0	0.005	0.55	0.45
2	5.5	0.10	3.27	2.22	2.0	0.03	0.76	1.24	1.5	0.007	0.57	0.93
3	3.5	0.09	0.58	2.92	1.0	0.04	0.23	0.77	0.5	0.004	0.06	0.44
3	4.5	0.10	2.93	2.59	1.5	0.04	0.42	1.08	1.0	0.007	0.31	0.69
3	5.5	0.09	3.90	2.56	2.0	0.05	0.73	1.26	1.5	0.008	0.57	0.93

(Note: υ_z – the MTZ velocity, A_r – cross-sectional area of the adsorber, h_{scaled} – height of the adsorbent bed in scaling process, h_{st} – stochiometric time, T_b – breakthrough time desired)

4.4.7. Batch adsorber versus fixed bed

In batch adsorption studies,

hardness removal capacity of ZEOL at equilibrium was indicated as 29.51 ± 0.23 mg/g (93%) with 508.0 mg/L of hardness, 4.0 g/L of ZEOL dosage, and 30 minutes of contact time. The residual concentration was reached 32.3 ± 0.2 mg/L, which meets the drinking water reference value of 120.0 mg/L considered in the study. The optimum pH in removing hardness was observed as pH 7, where the percentage of removal observed 93 ± 1%. Treated water reaches the pH value of 6.8, which meets the required drinking water pH value of 6.5–8.5. The adsorption isotherm and kinetic data of ZEOL implied that experimental data were best fitted with the Langmuir model (Q_o – 263.16 mg/g, R^2 – 0.99) pseudo-second-order model (Q_{cal} – 30.21 mg/g, R^2 – 0.99) following the monolayer adsorption and chemisorption, respectively.

Fluoride removal capacity of MOMA at equilibrium was indicated as 1.16 ± 0.05 mg/g (96%) with 3.0 mg/L of fluoride, 2.0 g/L of MOMA dosage, and 40 minutes of contact time. The residual concentration was reached 0.12 ± 0.1 mg/L, which meet the drinking water reference value of 0.2 mg/L considered in the study. The optimum pH of the MOMA in removing hardness was observed as pH 4, where the percentage of removal was observed at 98 ± 2%. Treated water reaches the pH value of 7.2, which meets the required drinking water pH value of 6.5–8.5. MOMA's adsorption isotherm and kinetic data implied that experimental data were best fitted with the Langmuir model (Q_o – 18.76 mg/g, R^2 – 0.99) pseudo-second-order model (Q_{cal} – 1.21 mg/g, R^2 – 0.99) following the monolayer adsorption and chemisorption, respectively.

E. coli removal capacity by SONPs + GO at equilibrium was indicated as 1 CFU/100 mL (99%) with 1,800.0 CFU/100 mL of *E. coli*, 4.0 g/L SONPs + GO dosage, and 24 hours contact time. The residual concentration was reached 0 CFU/100 mL, which meet the drinking water guideline value.

In fixed-bed adsorption studies,

Hardness removal capacity by ZEOL at breakthrough point (C_t/C_o = 0.2, hardness concentration at outlet 120.0 mg/L) was indicated 319.27 mg/g (77%) with 500.0 mg/L of hardness, 5.5 cm of ZEOL height, and 1,800 minutes of real breakthrough time in fixed-bed column studies for single-layer with single-solute (Experiment 01, flow rate 1.0 mL/min, bed height 5.5 cm). Treated water reaches a pH value of 7.2, which meets the required drinking water pH value of 6.5–8.5. The adsorption isotherm and kinetic data of ZEOL implied that experimental data were best fitted with the Thomas model (saturation capacity of ZEOL, Q_e – 288.18 mg/g, R^2 – 0.98). The ZEOL saturation adsorption capacity is approximately equal to the Langmuir model's adsorption capacity in the batch adsorption study.

Fluoride removal capacity of MOMA at breakthrough point (C_t/C_o = 0.05, hardness concentration at outlet 0.2 mg/L) was indicated as 18.16 mg/g (95%) with 3.0 mg/L of fluoride, 3.0 g of MOMA dosage, and 1,320 minutes of real breakthrough time in fixed-bed column studies for single-layer with single-solute (Experiment 01, flow rate 1.0 mL/min, bed height 2.0 cm). Treated water reaches a pH value of 6.8, which meets the required drinking water pH value of 6.5–8.5. MOMA's adsorption isotherm and kinetic data implied that experimental data were best fitted with the Thomas model (saturation capacity of MOMA, Q_e – 19.66 mg/g, R^2 – 0.98 the multi-layer unit). The MOMA saturation adsorption capacity is approximately equal to the Langmuir model's adsorption capacity in the batch adsorption study.

E. coli removal capacity of SONPs + GO at breakthrough point (C_t/C_o = 0.001, was determined as 1 CFU/100 mL (99% removal with 1,800 CFU/100 mL), 8.0 g of SONPs + GO dosage. The real breakthrough time in fixed-bed column studies was investigated as 7,200 minutes for single-layer with single-solute (Experiment 01, flow rate 1.0 mL/min, bed height 1.5 cm). Treated water reaches a pH value of 7.4, which meets the required drinking water pH value of 6.5–8.5. The adsorption isotherm and kinetic data of SONPs + GO implied that experimental data were not best fitted with the Thomas model (saturation capacity of SONPs + GO, Q_e – 3,267 CFU/100 mL, R^2 – 0.95).

The most crucial difference between the fixed bed and batch adsorbers was observed as the adsorption capacity for the exact adsorption dosage. In batch adsorber, residual concentration is lower than the initial concentration. In contrast, in fixed bed adsorber, the adsorbate solution feeds continuously to the adsorbent bed, and the adsorbent bed exposes to initial concentration throughout the experiment. In batch adsorption study, adsorbent loading remains in equilibrium with residual adsorbate concentration, and in fixed-bed adsorption, adsorbent loading is in equilibrium with the initial concentration. Moreover, the batch adsorption process needs to be stopped at the desired contact time, and the fixed-bed column study needs to be stopped at the breakthrough time. The batch adsorption study data cannot scale up the process accurately, while the fixed-bed column study data can be used effectively to scaling up the process. In comparison to batch adsorption studies, fixed-bed column studies are more complex.

4.4.8. Calculations for home filter design and cost of production for 1.0 L treated water

The measurements required to design a home filter were calculated based on the results of a multi-layered multi-solute system taken from the LUB model (Appendix VI). The calculation was commenced considering all adsorption process parameters in full-scaled adsorber are same as in the laboratory column. Assumptions were made as a family in CKDu prevalent area consists of 5 members. One person consumes water approximately 2.0 L/day as a daily water requirement (WHO, 2017). The total daily water requirement of a family with five members was calculated as 10.0 L. The treated water is considered supplying for three months to a family (total volume of treated water requirement 10.0 L X 30 days X 3). The height of the ZEOL, MOMA, and SONPs + GO in-home filter design were calculated as 29.09 cm, 18.86 cm, and 6.48 cm, respectively. The volumetric flow rate was calculated as 600.0 cm^3/min. By considering the different materials' heights, the series of cartridges (ZEOL, MOMA, and SONPs + GO) connections were recommended for the home filter unit (Figure 4.119) (Table 4.22).

Table 4.23: Calculations for home filter design

Materials	Mass of materials (Kg) required for scaling up	Column height (cm)	Designed bed volume (cm^3)	Volumetric flow rate (mL/min)	Diameter of the column (cm)
ZEOL	2.63	29.09	5,852.0	600.00	16.00
MOMA	1.37	18.86	3,794.0	600.00	16.00
SONPs + GO	1.09	6.48	1,304.0	600.00	16.00

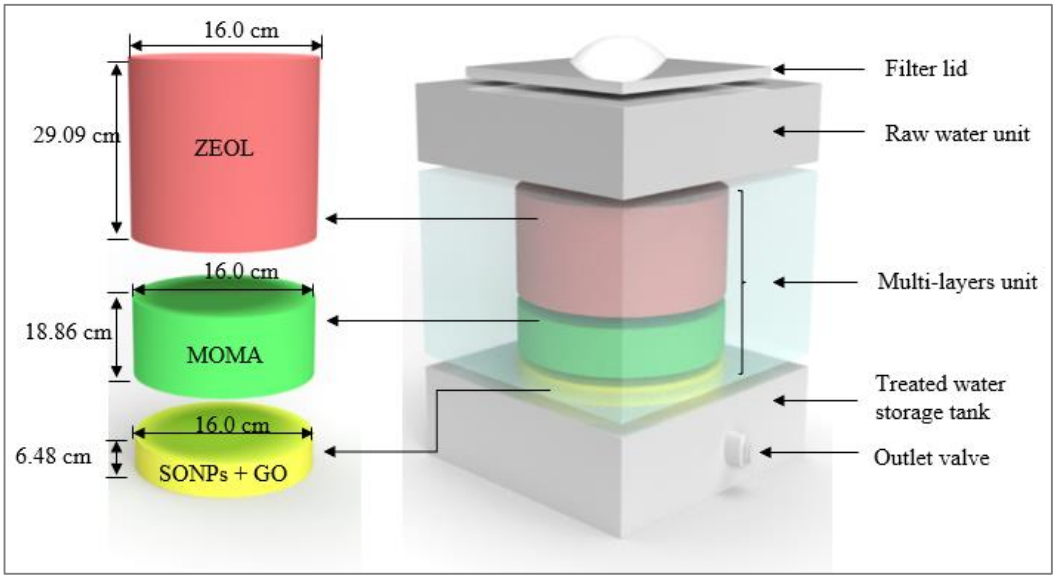

Figure 4.120: The conceptual design of the home filter unit

Results of cost calculation showed that the cost for 1.0 L of treated water production was approximately Rs. 8.80 and total cost for 10.0 L of water (daily consumption of a family) were estimated approximately as Rs. 88.00 (APPENDIX VII). If a family with five household members consumes water for three months, the cost of treated water production was calculated as Rs. 7,920.00 (monthly cost Rs. 2,640.00). After the filter unit's fabrication using the multi-layers system, it is recommended to calculate the home

filter unit's total cost. The home filter unit's economic feasibility is a prerequisite to conducting with households in CKDu prevalent areas to identify the affordability of the filter unit.

4.4.9. Key findings of the objective 04

- XRD, ESEM-EDAX analysis confirmed that nZVI, MOMA, SONPs + GO, and ZEOL were successfully synthesized in the laboratory. The size of the MOMA, SONPs, and nZVI are in nano-levels and FT–IR analysis confirms surface of the materials consists of oxides and hydroxyl functional groups (nZVI: 2θ–44–45º, size – 30.5 nm, spherical with a chain like structure, Fe–62.7 %, O–31.5 %; MOMA: 2θ–11.1º, size–15.3 nm, high porosity, a rough surface with a honey comb like structure, Al–55.4 %, O–44.6 %; GO: 2θ–10–11º, high porosity, a smooth surface with a thin layered structure, C–59.5 %, O–30.3 %; SONPs: 2θ–28.2º, size–64.2 cm, small spherical shapes with a smooth surface, Ag–89.97 %, O–10.03 %; SONPs + GO: flakes with a cluttered appearance, typical wrinkled loose sponge like structure with a large surface, C–24.32 %, Ag–62.00 % and O–13.69 %; ZEOL: consist of fauzabits, NaP_1, Chabazite, spherical shape highly porous with a rough surface, Si–25.90 %, O–45.80 %, Al–12.30 %, Na–6.50 %, Fe–3.60 %, Ca–2.80 %, Ti–1.60 %, K–0.90 % and Mg–0.60 %).
- The optimum dosage of nZVI in removing cadmium and calcium was 4.0 g/L for single and multi-solute batch studies. The percentage of cadmium removal was calculated as more than 91% in the presence of calcium. The optimum pH for batch adsorber of nZVI was indicated as pH 8 (pH_{zpc}), where a higher percentage of cadmium removal was observed (99%). The calcium removal percentage was calculated as 40% implying nZVI gives priority for cadmium adsorption.
- The optimum adsorbent dosage of the MOMA was indicated as 2.0 g/L in the removal of fluoride. The optimum pH of the system was observed as the 4 (pH_{zpc}). More than 98% of fluoride removal was observed with MOMA, where the treated water meets the required drinking water reference value of 0.2 mg/L.

The selective removal of fluoride by MOMA was observed in the presence of hardness.

- ZEOL has indicated the optimum adsorbent dosage as 4.0 g/L showing 93% hardness removal in single-solute studies. The optimum pH value of the system was observed as pH 7 (pH_{zpc}). In the presence of fluoride, the percentage of hardness removal was observed at 96%, which indicated fluoride does not interfere with the adsorption capacity of ZEOL in the removal of hardness. ZEOL has an attribute of selective removal of hardness. The treated water meets the required drinking water reference values of 120.0 mg/L.
- SONPs + GO indicated the optimum removal dosage as 4.0 g/L showing 99% *E. coli* removal after 24 hours with the concentration of 1800 CFU/100 mL and pH 6.5. The treated water meets the required drinking water reference values of 0 CFU/100 mL.
- The adsorption data of nZVI, MOMA, and ZEOL indicated that data best fits the Langmuir model's theories following monolayer adsorption as prominent adsorption behaviour. The adsorption capacity and linear regression values of nZVI, MOMA, and ZEOL at the equilibrium were calculated as Q_e -8.24 mg/g and R^2 - 0.99; Q_e - 18.76 mg/g, R^2 - 0.99; and Q_e - 263.16 mg/g, R^2 -0.99, respectively. The experimental data in nZVI, MOMA, and ZEOL follow the pseudo-second-order model, indicating the rate-limiting factor as chemisorption.
- The regeneration and desorption studies innZVI, MOMA, ZEOL and SONPs + GO indicated that HCl is the most suitable eluting agent (nZVI - 99%, five regeneration cycles; MOMA - 96%, six regeneration cycles; ZEOL–88%, six regeneration cycles; and SONPs + GO–99%, five regeneration cycles).
- The overall performance of the fixed-bed column was affected when the flow rate and bed heights were changed. The best performance for ZEOL (96% of hardness removal) was observed with 1.0 mL/min flow rate and 5.5 cm bed height; for MOMA (96% of fluoride removal) with 1.0 mL/min flow rate and 2.0.cm bed height; and SONPs + GO (99% of hardness removal) with 1.0 mL/min flow rate and 1.5 cm bed heights.

- In the fixed-bed column with a mixture of components, the breakthrough time of the ZEOL column was increased in removing of hardness (real BCT–44.0 hours, ideal BCT–76.0 hours, and exhausted BCT–100.0 hours) in multi-solute solution (with fluoride and *E. coli*) comparing to hardness removal by ZEOL (real BCT–34.0 hours, ideal BCT–68.0 hours, and exhausted BCT–98.0 hours) with the single-solute solution (hardness alone). The results indicated that the ZEOL is selectively removed the hardness in water, and fluoride and *E. coli* is less interfered in the removal process of hardness by ZEOL.
- In the fixed-bed column with a mixture of components, the breakthrough time of the MOMA column was increased in removing of fluoride (real BCT–28.0 hours, ideal BCT–58.0 hours, and exhausted BCT–80.0 hours) in multi-solute solution (with hardness and E. coli) comparing to fluoride removal by MOMA (real BCT–18.0 hours, ideal BCT–50.0 hours, and exhausted BCT–70.0 hours) with the single-solute solution (fluoride alone). The results indicated that the MOMA is selectively removed fluoride in water, and hardness and *E. coli* are less interfered in the fluoride removal process.
- In the fixed-bed column with multi-solute, the breakthrough time of the SONPs + GO was increased in the removal of *E. coli* compared to *E. coli* removal in single-solute solution (real BCT–196.0 hours, ideal BCT–278.0 hours, and exhausted BCT–320.0 hours) (with hardness and fluoride) (real BCT–184.0 hours, ideal BCT–236.0 hours, and exhausted BCT–292.0 hours).
- In a multi-layer unit, the breakthrough time of ZEOL was increased substantially greater than the breakthrough time in removing hardness alone (34.0, 68.0, and 98.0 hours, respectively) and hardness in a multi-solute system (44.0, 76.0, and 100.0 hours, respectively). MOMA's breakthrough time was increased substantially higher than the breakthrough time in removing fluoride alone (18.0, 50.0, and 70.0 hours, respectively) (Fluoride in the multi-solute system (28.0, 58.0, and 80.0 hours, respectively). The breakthrough time of SONPs + GO increased substantially higher than the breakthrough time in removing *E. coli*

alone (184.0, 236.0, and 292.0 hours, respectively) and *E. coli* in a multi-solute system (196.0, 278.0, and 320.0 hours, respectively).

- The linear regression values (R^2) were suggested that the experimental data were not best fitted with the Adams-Bohart model. The model is not suitable for use as an appropriate predictor of the breakthrough curve in fixed-bed column studies for individual elements and multi-solute multi-layer studies.
- In the Thomas model, the saturation loading capacity of adsorbents and the linear regression values in experimental data are higher for respective elements verifying the selective removal of adsorbate by the respective adsorbents (Q_e of ZEOL for hardness–287.53 mg/g, R^2–0.98, for fluoride–0.87 mg/g, R^2–0.29; q_e of MOMA for hardness–69.30 mg/g, R^2–0.12, for fluoride–17.59 mg/g, R^2–0.98). Therefore, ZEOL and MOMA's kinetic in fixed column adsorption was followed the Thomas model theories described.
- In the Yoon-Nelson model, the time to reach 50% breakthrough and linear regression values in experimental data are higher for hardness, fluoride, and *E. coli*. The results verify the non-selective removal of adsorbate by the respective adsorbents (τ of ZEOL for hardness – 4,245 minutes, R^2 – 0.96, for fluoride – 19,500 minutes, R^2 – 0.29; τ of MOMA for hardness – 530 minutes, R^2 – 0.78, for fluoride – 3,348 minutes, R^2 – 0.98).
- The LUB values were calculated as 1.45 cm, 1.00 cm, and 0.33 cm for ZEOL, MOMA, and SONPs + GO. When the breakthrough points of each material were considered, maximum allowable concentration considered in the study (hardness – 120 mg/L; C_t/C_o – 0.23, fluoride 0.2 mg/L; C_t/C_o – 0.06, and *E. coli* 0 CFU/100 mL; C_t/C_o – 0.0001). If the multi-layer column provides drinking water for three months, the column should provide service for 25.01 hours without a breakthrough. The height of the ZEOL bed required to remove hardness for three months of service period was calculated as 29.09 cm with the mass of adsorbent 2.63 Kg, 18.86 cm adsorbent bed height including the mass of 1.37 Kg of MOMA, and 6.48 cm with the mass of 1.09 Kg of SONPs + GO.

- The cost of 1.0 L of treated water production was approximately Rs. 8.80 and total cost for 10.0 L of water (daily consumption of a family) were estimated approximately as Rs. 88.00. If a family with five household members consumes water for three months, the cost of treated water production was calculated as Rs. 7,920.00 (monthly cost Rs. 2,640.00).

4.4.10. Limitation of the study

- Analytical instruments required to analyze nanomaterials' particle size, the surface area of particles, and instruments that control the oxygen-free environment were not found with available facilities in the laboratory during the laboratory experiments. The outside service provider did not conduct the sample analysis due to the high analytical cost per sample.
- The study's primary limitation was found to control the growth retardation of *E. coli* bacteria in a single and multi-solute solution during the fixed bed column experiment. The growth retardation was avoided keeping the sample under 4 ºC in the refrigerator. The nutrition source (Dextrose - monosaccharides) was introduced into the solution every three days and measured *E. coli* cell count using the MPN method.
- Many samples per day were received for analysis as the sampling time desired was 2 hours in fixed bed column studies. The accuracy of the sampling analysis was improved by storing the sample in the refrigerator under 4 ºC.

CHAPTER 5

5. CONCLUSION AND RECOMMENDATIONS

5.1. Conclusion of the study

- Fluoride, hardness, and cadmium values in potable water exceed the drinking water guideline values. The minimum and maximum hardness values in water samples analysed were investigated as 111.73 ± 1.41 mg/L as $CaCO_3$ and 680.33 ± 1.53 mg/L as $CaCO_3$. The minimum and maximum hardness values in literature have been reported as 10.00 ± 0.1 mg/L as $CaCO_3$ and 1921.00 ± 2.5 mg/L as $CaCO_3$. The minimum and maximum fluoride values in water samples analysed were examined as 0.72 ± 0.03 mg/L and 2.84 ± 0.05 mg/L. In literature, the minimum and maximum fluoride values have been reported as 0.18 ± 0.01 mg/L and 13.70 ± 1.2 mg/L. The minimum and maximum cadmium values in water samples analysed were examined as < 0.025 ± 0.01 and 0.0065 ± 0.01 mg/L. The minimum and maximum cadmium values have been reported as < 0.00027 ± 0.01 mg/L and 0.034 ± 0.001 mg/L in the literature. The concentration values implied that potable water consumption by people in CKDu affected areas is vulnerable to adverse health effects, most likely with renal damage.
- The concentration levels of fluoride, hardness and cadmium ions fluctuate in the same well within a concise period (four weeks), illustrating an irregular distribution pattern of concentrations even in the nearest CKDu prevalent villages. The excess or deficiency of fluoride, hardness, and cadmium levels in different places of CKDu prevalence and non-prevalence areas depend on agricultural practices, geochemical composition of groundwater, and mineralogical composition aquifer, seasonal variation of rainfall pattern, and excessive evaporation.
- Available drinking water guideline values are not suitable for providing safe potable water for people in CKDu prevalent areas. Considering their water-related health hazards, the WHO drinking water guideline values were not

derived for hardness (calcium and magnesium). Drinking water-related nephrotoxic health hazards outbreaks in several countries, and the number of affected people increases daily. Hardness in potable water brings synergic effects in combination with fluoride and cadmium. However, these factors are not concerned attentively by any national or international audience when the drinking water standards were derived.

- WHO does not provide the health concern value for hardness in drinking water. The minimum and maximum Sri Lankan drinking water guideline values have been given for calcium and magnesium 100.0–240.0 mg/L and 30.0–150.0 mg/L, for hardness 250.0–600.0 mg/L, respectively. The minimum amount of 250.0 mg/L could be classified as "very hard" according to the general guideline of hard water classification derived by the USGS. In non-CKDu prevalent areas, potable water hardness values were often reported below the level of 120.0 mg/L. The hardness concentrations reported in the CKDu prevalent area water were above the limit of 120.0 mg/L moderately hard water. The past studies postulated that lower levels of hardness in potable water do not bring CKDu; meantime, lower levels of hardness bring non-nephrotoxic health hazards. The hardness distribution pattern in CKDu non-prevalent areas emphasized that the treated water hardness concentration in CKDu prevalent areas should be less than 120.0 mg/L (moderately hard water). Therefore, the hardness level should maintain as 120.0 mg/L in the treated water.
- The fluoride values in CKDu non-prevalent areas show that the distribution pattern of fluoride concentrations was investigated below 1.0 mg/L. Fluoride values reported in the literature and analyzed in the study were scattered around 0.2 mg/L in CKDu non-affected areas. When people consume spring water with fluoride concentrations of about 0.18 mg/L, it has been reported that people are not affected by CKDu. The provision of potable water with a fluoride level of around 0.2 mg/L control the occurrence of CKDu. The nephrotoxic risk factors should remove from potable water to meet hardness of 120.0 mg/L, fluoride of 0.2 mg/L, and cadmium of 0.003 mg/L based on the drinking water standards.

- Different potable water treatment techniques such as reverse osmosis, two-layer, and seven-layer filter units have been introduced in CKDu prevalent areas to solve the potable water issue. The reverse osmosis unit removes most of the ions in water, retaining beneficial ions less in hardness 4.0–20.0 mg/L, high in fluoride 0.29–5.5 mg/L for human intake. The other two filters (two-layer and seven-layer filter units) do not remove fluoride and hardness effectively and added more ions into treated water due to the leachability in some minerals in media. Treated water by these filters does not meet the required drinking water guideline values. Therefore, a new water treatment technology needs to be developed to provide safe drinking water.
- The percentage of hardness as $CaCO_3$ (dry season 28.00 ± 14.78 mg/L; wet season 8.00 ± 0.00 mg/L) fluoride (dry season 0.45 ± 0.14 mg/L; wet season 0.39 ± 0.03 mg/L), calcium (dry season 2.47 ± 1.32 mg/L; wet season mean 0.88 ± 0.32 mg/L), and magnesium (dry season 2.80 ± 3.22 mg/L; wet season mean 0.90 ± 1.00 mg/L) removal observed greater than 80% for each element in potable water treatment using commercial RO units. The deficient concentrations of elements remained in the treated water. However, essential elements required for good health remain in a low concentration in RO treated water. Exposure to low macro and microelements for the long run due to RO treated water consumption brings non-carcinogenic health hazards to people in CKDu prevalent areas.
- The health risk assessment study with RO treated water corroborated that 1–9 age category indicates higher vulnerability for the non-carcinogenic health effects greater than other age categories. The mean HQ values of fluoride (female - F = 1.727, $P > 0.05$; male - F = 1.607, $P > 0.05$) and cadmium (female - F = 0.322, $P > 0.05$; male - F = 0.159, $P > 0.05$), calcium (female - F = 23.739, $P < 0.05$; male - F = 16.181, $P < 0.05$) and magnesium (female - F = 9.460, $P < 0.05$; male - F = 9.419, $P < 0.05$) corroborated that people exposed higher concentrations values are most vulnerable for non-carcinogenic health hazards. If

people exposure to low concentration of nephrotoxic constituents for one year, people are vulnerable for adverse health effects.

- Hazards quotient values of different age categories did not exceed value one (1>HQ) for a short duration of water consumption. Children (Age category 1-9 years) are highly vulnerable to non-carcinogenic health hazards, and their HQ value exceeded one (HQ>1) within a short period before other age categories. HI mean values with high concentrations elaborated that multicomponent concentration combinations have adverse health effects on females in 1–9 and 10–19 years of age categories and males after age 20. Both male and female reach vulnerable condition for non-carcinogenic health hazard within two weeks for higher concentration. The results concluded that long-run consumption of RO water brings non-carcinogenic health effects on people. Hence, people in age category 30-60 years can be victims of CKDu further. Hence, the development of new water treatment units is of utmost importance to provide safe potable water.
- XRD, ESEM-EDAX analysis confirmed that nZVI (30.5 nm), MOMA (15.3 nm), SONPs + GO (64.2 nm), and ZEOL synthesized in the laboratory are at the nano level. Engineered adsorbent materials are easily synthesized in laboratory with available facilities.
- The cadmium removal by nZVI (91%) with 4.0 g/L of dosage, 98% fluoride by MOMA with 2.0 g/L of dosage, 93% hardness by ZEOL with 4.0 g/L of dosage, and 99% *E. coli* by SONPs + GO with 4.0 g/L of dosage corroborate that the selected materials for multilayer column effectively remove cadmium, fluoride, hardness, and *E. coli* in potable water.
- The adsorption isotherms and kinetics data nZVI, MOMA, and ZEOL indicated that data best fits the Langmuir model theories following monolayer adsorption as prominent adsorption behaviour. The adsorption capacity and linear regression values of nZVI, MOMA, and ZEOL at the equilibrium were calculated as Q_e - 8.24 mg/g and R^2 - 0.99; Q_e - 18.76 mg/g, R^2 - 0.99; and Q_e - 263.16 mg/g, R^2 - 0.99, respectively. The experimental data of nZVI, MOMA, and ZEOL follow

the pseudo-second-order model, indicating the rate-limiting factor as chemisorption.

- The regeneration and desorption studies of nZVI, MOMA, ZEOL and SONPs + GO indicated that HCl is the most suitable eluting agent to regenerate materials (nZVI - 99%, 5 regeneration cycles; MOMA- 96%, 6 regeneration cycles; ZEOL – 88%, 6 regeneration cycles; and SONPs + GO – 99%, 5 regeneration cycles). The selected materials can regenerate, which is elaborating that Use of those materials decrease the cost of material production.
- The fixed-bed column study indicated that the fixed-bed column's overall performance is affected when the flow rate and bed heights were changed. The best performance for ZEOL (96% of hardness removal) was observed with 1.0 mL/min flow rate and 5.5 cm bed height; for MOMA (96% of fluoride removal) with 1.0 mL/min flow rate and 2.0.cm bed height; and SONPs + GO (99% of hardness removal) with 1.0 mL/min flow rate and 1.5 cm bed heights. The flow rate and bed height are the deterministic parameters which the performance of the adsorber depended.
- In the fixed-bed column with a mixture of components, the breakthrough time of the ZEOL column was increased in the removal of hardness (real BCT – 44.0 hours, ideal BCT – 76.0 hours, and exhausted BCT – 100.0 hours) in multi-solute solution (with fluoride and *E. coli*) comparing to hardness removal by ZEOL (real BCT – 34.0 hours, ideal BCT – 68.0 hours, and exhausted BCT – 98.0 hours) with the single-solute solution (hardness alone). The breakthrough time of the MOMA column was increased in the removal of fluoride (real BCT – 28.0 hours, ideal BCT – 58.0 hours, and exhausted BCT – 80.0 hours) in multi-solute solution (with hardness and E. coli) comparing to fluoride removal by MOMA (real BCT – 18.0 hours, ideal BCT – 50.0 hours, and exhausted BCT – 70.0 hours) with the single-solute solution (fluoride alone). The breakthrough time of the SONPs + GO column was increased in the removal of *E. coli* (real BCT – 196.0 hours, ideal BCT – 278.0 hours, and exhausted BCT – 320.0 hours) in multi-solute solution (with hardness and fluoride) comparing to *E. coli* removal

by SONPs + GO (real BCT – 184.0 hours, ideal BCT – 236.0 hours, and exhausted BCT – 292.0 hours) with the single-solute solution (*E. coli* alone). The results corroborated that ZEOL, MOMA, and SONPs + GO remove hardness, fluoride, and *E. coli* non-selectively.

- In the Thomas model, the saturation loading capacity of adsorbents and the linear regression values in experimental data are higher for respective elements verifying the selective removal of adsorbate by the respective adsorbents (Q_e of ZEOL for hardness – 287.53 mg/g, R^2 – 0.98, for fluoride – 0.87 mg/g, R^2 – 0.29; Q_e of MOMA for hardness – 69.30 mg/g, R^2 – 0.12, for fluoride – 17.59 mg/g, R^2 – 0.98). ZEOL and MOMA's kinetic in fixed column adsorption was followed the Thomas model theories described.
- In the Yoon-Nelson model, the time to reach 50% breakthrough and linear regression values in experimental data are higher for hardness, fluoride, and *E. coli*. The results verify the non-selective removal of adsorbate by the respective adsorbents (τ of ZEOL for hardness – 4,245 minutes, R^2 – 0.96, for fluoride – 19,500 minutes, R^2 – 0.29; τ of MOMA for hardness – 530 minutes, R^2 – 0.78, for fluoride – 3,348 minutes, R^2 – 0.98).
- The LUB values were calculated as 1.45 cm, 1.00 cm, and 0.33 cm for ZEOL, MOMA, and SONPs + GO when the breakthrough points of each material were considered maximum allowable concentration considered in the study (hardness – 120 mg/L; C_t/C_o – 0.23, fluoride 0.2 mg/L; C_t/C_o – 0.06, and *E. coli* 0 CFU/100 mL; C_t/C_o – 0.0001). If the multi-layer column provides drinking water for three months, the column should provide service for 25.10 hours without a breakthrough. The height of the ZEOL bed required to remove hardness for three months of service period was calculated as 29.09 cm with the mass of adsorbent 2.63 Kg, 18.86 cm adsorbent bed height including the mass of 1.37 Kg of MOMA, and 6.48 cm with the mass of 1.09 Kg of SONPs + GO. LUB model can use to scale-up the fixed-bed column studies data into home water filter unit.
- The cost of 1.0 L of treated water production was approximately Rs. 8.80 and total cost for 10.0 L of water (daily consumption of a family) were estimated

approximately as Rs. 88.00. If a family with five household members consumes water for three months, the cost of treated water production was calculated as Rs. 7,920.00 (monthly cost Rs. 2,640.00).

- The modified fly ash (Zeolite) (ZEOL), MgO loaded alumina (MOMA), silver oxide nanoparticle + graphene oxide composite (SONPs + GO) proposes as the best combination of materials to remove hardness, fluoride, and faecal coliform in the potable water. Their removal capacities, removal effectiveness, consistency in water treatment, feasibility in the multi-solute mixture, less leachability potential, regeneration properties, and affordable cost were manifested as the best combination of materials is most suited for ground and surface water treatment in CKDu prevalent areas.

5.2. Recommendations of the study

- The data published about concentration levels of nephrotoxic risk factors is lacking in country-wise CKDu and non-CKDu areas. The broad picture of the nephrotoxic risk factor can be acquired when the data related to concentrations in all CKDu and non-CKDu areas are available in one platform. All researchers should have free access to the data set to research CKDu prevalent areas.
- The provision of potable water with nephrotoxic risk factors in low concentration is recommended to ensure community health and safety in CKDu prevalent areas (where people who consumed water from natural springs are not affected by the CKDu). The study emphasizes the need to immediately revise drinking water guideline values for hardness (calcium and magnesium) to ensure water safety.
- The in-depth studies are recommended to establish the drinking water guideline values for the hardness of 120.0 mg/L and fluoride of 0.2 mg/L for prevalent CKDu areas.
- Hardness (calcium and magnesium), fluoride, and cadmium have been found to be nephrotoxic risk factors, leading to damaged nephrons in kidneys. However, WHO and other institutes such as USEPA and the European Union do not derive guideline values for nephrotoxic risk factors in potable water. Hence, it is

necessary to derive nephrotoxic drinking water standards for fluoride, hardness, cadmium, and other nephrotoxic elements in water to protect the community.

- A series of experiment was suggested in term of identifying interaction of fluoride and hardness at nephrotoxic reference level with other constituents in water.
- Most countries have not been revised drinking water standards for long years. However, industrialization, popularisation, and inappropriate livelihood increase ground and surface water sources contamination within a short period. Therefore, it is brought forward as a proposal to revisit drinking water guideline values once every three years to ensure water safety and protect the community's health.
- Consumption of water treated by domestic filter units can increase the severity of CKDu, makes healthy people vulnerable to CKDu, and increases non-nephrotoxic health hazards. Therefore, it is a prerequisite to investigate the vulnerability of non-CKDu affected people to nephrotoxic and non-nephrotoxic health hazards. A detailed study is recommended to further investigate the nephrotoxic and non-nephrotoxic health hazards due to domestic filters' consumption of treated water.
- The recommendation would be proposed to find the nephrotoxic reference values of daily intake for different nephrotoxic water constituents.
- Consumption of RO-treated water, in the long run, increases the vulnerability of people in different age categories to nephrotoxic and non-nephrotoxic health hazards. The health concerned issue has been given less attention by authorized parties such as government and non-governmental organizations active in the water sector in Sri Lanka. Therefore, it is a prerequisite to providing safe potable water to people in CKDu prevalent areas to protect community health by introducing a reliable drinking water treatment unit that effectively removes nephrotoxic risk factors from ground and surface water.
- Therefore, the fabrication of a multi-layer water treatment unit using the best combination of adsorbent materials is recommended to provide safe, clean potable water for the community in CKDu prevalent areas. Providing safe and

clean water will ensure community health controlling nephrotoxic and non-nephrotoxic health hazards and increase the community's living standards by lessening the suffocation.

- The use of local low-cost materials (e.g., clay) is recommended to develop the filter unit further, hopefully decreasing the unit cost of production. After fabrication, performance evaluation of filter unit is recommended to determine their removal efficacy of hardness, fluoride, and faecal coliform with time, the durability of the multi-layered unit, O & M issues, limitations, and any unforeseen conditions for long-term sustainability.

5.3. Future studies needed

- A database, including concentrations of all nephrotoxic risk factors in all CKDu prevalence and non-prevalence areas, needs to be evaluated considering the monsoonal variations and geological formations.
- The detailed study on hypotheses proposed for CKDu needs to be studied. The in-depth study on non-nephrotoxic health hazard considering the agnostic effect of the combination of nephrotoxic risk factors and their lower and higher concentrations need to be conducted.
- Nephrotoxic drinking water standards need to be promulgated after launching an in-depth study about water quality parameters of potable water consumed by people in CKDu prevalent areas.
- Full-scale dose assessment of nephrotoxic reference values needs to be conducting considering the interaction with other water constituents.
- A solution needs to find treating RO reject water before releasing it into the environment, reuse reject water for toilet flushing or improve technology to minimize reject water production. These solutions will decrease contamination of soil and groundwater further by RO reject water.
- The in-depth study needs to investigate how different filter units introduced in CKDu prevalent and non-prevalent areas perform to ensure water safety.

- The study needs to investigate the removal effectiveness of the commercial RO unit used at present, removing all ions and compounds in water, including hydrogeochemical properties, heavy metals, and agrochemicals.
- A detailed study about the characterization of RO feed, treated, and rejected water, including all RO units established in Sri Lanka, should evaluate to ensure people's water safety consumed RO treated water for the long run.
- A treatment solution should further investigate the RO reject water, further avoiding contamination of soil and water sources from nephrotoxic risk factors.
- People exposed to higher concentrations values of nephrotoxic risk factors are most vulnerable to non-carcinogenic health hazards. Therefore, potable water quality protection and monitoring measures should be incorporated into CKDu affected areas, and new water treatment technologies should introduce to provide safe drinking water to people.
- The removal of different nephrotoxic risk factors (agrochemical and heavy metals) needs to be studied using the multi-layered unit.
- ZEOL needs to be improved further to use as an adsorbent to remove heavy metals in water and incorporated them into the multi-layered unit.
- Once the optimum combination of materials in the form of a multi-layer filter is fabricated, replication by at least 30 numbers needs to be done for verifications at the CKDu prevalent areas.
- Performance of these units needs to be evaluated in terms of removal efficiency of nephrotoxic elements and compounds with time, the durability of the filter cartridges, O & M issues, limitations, unforeseen conditions experienced, etc. Once such drawbacks are identified, the filter unit developed would be further modified for long-term sustenance.
- The home filter unit needs to be fabricated using the best combination of the multi-layer unit. Besides, the extra layer of activated carbon needs to be included in the conceptual design further to increase the taste and colour of the treated water.

REFERENCES

Abdelhalim, A. O., Galal, A., Hussein, M. Z., & Sayed, I. E. (2016). Graphene Functionalization by 1,6-Diaminohexane and Silver Nanoparticles for Water Disinfection. *J. Nanomater.*, 1485280, 7.

Aboelfetoh, E. F., Gemeay, A. H., & El-Sharkawy, R. G. (2020). Effective disposal of methylene blue using green immobilized silver nanoparticles on graphene oxide and reduced graphene oxide sheets through one-pot synthesis. *Environ Monit Assess*, 192:355.

Abraham, G., Agarwal, S. K., Gowrishankar, S., & Vijayan, M. (2019). Chronic Kidney Disease of Unknown Etiology: Hotspots in India and Other Asian Countries. *J. Sem Nephrol*, 39(3):272-277.

Adak, D., Sarkar, M., Mait, M., Tamang, A., Mandal, S., & Chattopadhyay, B. (2015). Anti-microbial efficiency of nano silver-silica modified geopolymer mortar for. *RSC Advances*, 1-28.

Adeno, F., Mulugeta, E., Zewge, F. & Chebude, Y. (2014). Adsorptive removal of fluoride from water nano scale aluminum oxidehydroxide (AlOOH). *Bull. Chem. Soc. Ethiop.*, 215–227.

Afroze, S., Sen, T. K. & Ang, H. M. (2016). Adsorption performance of continuous fixed bed column for the removal of methylene blue (MB) dye using Eucalyptus sheathiana bark biomass. *Res Chem Intermed*, 42, 2343–2364.

Akl, M. A., Aly, H. F., Soliman, H. M., Abd-Elrahman, A. M., & Abd-Elhamid, A. I. (2013). Preparation and characterization of silica nanoparticles by wet mechanical attrition of white and yellow sand. *J Nanomed. Nanotechnol*, 4(183), 1–14.

Allender, P. S. et al., (1996). "Dietary calcium and blood pressure: a meta-analysis of randomized clinical trials". *Ann Intern Med*., IX(124), 825-31.

Al-Khaldi, F. A., Abu-Sharkh, B., Abulkibash, A. M. & Atieh, M. A. (2015). Cadmium removal by activated carbon, carbon nanotubes, carbon nanofibers, and carbon fly ash: a comparative study. *Desalin Water Treat*, 53(5), 1417–1429.

Alemua, S., Mulugeta, E., Zewgea, F., & Chandravanshia, B. S. (2014). Water defluoridation by aluminium oxide–manganese. *Environ. Technol.,* 1893-1903.

Ambepitiya, I. J. (2015). Cadmium in drinking water sources in Sri Lanka and applicability of low-cost adsorbents for cadmium removal. Delft: UNESCO-IHE Institute for Water Education.

Anuradha, C. D., Kanno, S. Hirano, S. (2001). Oxidative damage to mitochondria is a preliminary step to caspase-3 activation in fluoride-induced apoptosis in HL- 60 cells. *Free Radic. Biol. Med*., 31, 367–373.

Ansari, M. A., Khan, H. M., Khan, A. A., Cameotra, S. S., Saquib, Q., & Musarrat, J. (2014). Interaction of Al2O3 nanoparticles with Escherichia coli and their cell envelope biomolecules. *J. Appl. Microbiol*, doi:10.1111/jam.12423

APHA. (1999). Standard Methods for the Examination of Water and Wastewater. American Public Health Association, American Water Works Association, Water Environment Federation.

Aragaw, T. A. & Ayalew, A. A. (2019). Removal of water hardness using zeolite synthesized from Ethiopian kaolin by hydrothermal method. *Water Pract Tech*, 14(1), 145–159.

Arigony, A. L. V., De Oliveira, I. M., Machado, M., Bordin, D. L., Bergter, L., Prá, D., & Henriques, J. A. P. (2013). The influence of micronutrients in cell culture: A reflection on viability and genomic stability. *BioMed Research International*, 2013. https://doi.org/10.1155/2013/597282.

Arshadi, M., Amiri, M. J., Mousavi, S. (2014). Kinetic, equilibrium and thermodynamic investigations of Ni (II), Cd (II), Cu (II) and Co (II) adsorption on barley straw ash. *Water resour. Ind*., 6, 1–17.

Ashbolt, N. J. (2004). Microbial contamination of drinking water and disease outcomes in developing regions. *Toxicol.*, I-III(198), 229–238.

Assefa, B. (2006). Defluoridation of Ethiopian Rift Valley Region water using reverse osmosis membranes. *JEEA*, 6.

Athuraliya, N. T., Abeysekera, T. D., Amerasinghe, P. H., Kumarasiri, R., Bandara, P., Karunaratne, U., Jones, A. L. (2011). Uncertain etiologies of proteinuric-chronic kidney disease in rural Sri Lanka. *Kidney Int.*, 80, 1212–1221.

Ayob, A., Abdullah, A. Z. (2012). Characterisation of Polymer-Stabilized Nano Zero-valent Iron Particle by Ultrasonic Irradiation-assisted Method. *J. Polym. Mater.* 29, 167–179.

Ayoob, S. & Gupta, A.K., (2006). "Fluoride in Drinking Water: A Review on the Status and Stress Effects". Critical Reviews in Environmental Science and Technology, DOI:10.1080/10643380600678112, VI (36), 433-87.

Azouaoua, N., Sadaoui, Z., Djaafri, A. & Mokaddema, H. (2010). Adsorption of cadmium from aqueous solution onto untreated coffee grounds:Equilibrium. kinetics and thermodynamics. *J Hazard Mater*, 184, 126–134.

Azzam, A., El-Wakeelb, S., Mostafaa, B. & El-Shahatc, M. F. (2016). Removal of Pb, Cd, Cu and Ni from aqueous solution using nano scale zero valent iron particles. *J Environ Chem Eng*, IV, 2196–2206.

Bala, T., Armstrong, G., Laffir, F., & Thornton, R. (2011). Titania–silver and alumina–silver composite nanoparticles: Novel, versatile synthesis, reaction mechanism and potential antimicrobial application. *J. Colloid Interface Sci*., 395–403.

Balasooriya, S., Munasinghe, H., A. T. Herath, A. T., Diyabalanage, S., Ileperuma, O. A., Manthrithilake, H., Chandrajith, R. (2019). Possible links between groundwater geochemistry and chronic kidney disease of unknown etiology (CKDu): an investigation from the Ginnoruwa region in Sri Lanka. *Expo Health*, 1–12.

Baldisserotto, B., Chowdhury, M. J., & Wood, C. M. (2005). Effects of dietary calcium and cadmium on cadmium accumulation, calcium and cadmium uptake from the water, and their interactions in juvenile rainbow trout. *Aquat Toxicol*, 99-117

Bandarage, A. (2013). Political Economy of Epidemic Kidney Disease in Sri Lanka. *SAGE J*, 3-4.

Bandara, N. J. G. J. (2003). Water and wastewater issue in Sri Lanka. *Water Sci. Technol*., XII(47), 3025–312.

Bandara, R. M. C. J., Bandara, B. M. R., Abeykoon, D. M. B., Wickramasinghe, A., Wijesundara, D. S. Karunaratne, V. & Karunaratne, N. (2011). Proceedings of the Peradeniya University Research Sessions, Sri Lanka. 16(24), 156.

Barbier, O., Arreola-Mendoza, L., Razo, D. L. M. (2010). Molecular mechanisms of fluoride toxicity. *Chemico-Biolog. Interac*. 188, 319–333.

Barroso-Bogeat, A., Alexandre-Franco, M., Fernández-González, C. & Gómez-Serrano, V. (2016). Activated carbon surface chemistry: Changes upon impregnation with Al(III), Fe(III) and Zn(II)-metal oxide catalyst precursors from NO3− aqueous solutions. *Arab. J. Chem*., In press.

Bartram, J., & Pedley, S. (1996). Microbiological Analysis. In Water Quality Monitoring - A Practical Guide to the Design and Implementation of Freshwater Quality Studies and Monitoring Programmes (pp. 1–27). Geneva: United Nations Environment Programme and the World Health Organization.

Batuman, V. (2006). Fifty years of Balkan endemic nephropathy: daunting questions, elusive answers. *Kidney International*, New York, 69, 644–646.

Belkada, F. D., Kitous, O., Drouiche, N., Aoudj, S., Bouchelaghem, O., Abdi, N., Mameri, N. (2018). Electrodialysis for fluoride and nitrate removal from synthesized photovoltaic industry wastewater. *Sep Purif. Technol*., 108–115.

Benjwal, P., Kumar, M., Chamolia, P., & Kar, K. K. (2015). Enhanced photocatalytic degradation of methylene blue and adsorption of arsenic (III) by reduced graphene oxide (rGO)–metal oxide (TiO2/Fe3O4) based nanocomposites. *RSC Adv*, 5, 73249.

Bernstein, D. S., Sadowsky, N., Hegsted, D. M., Guri, C. D., Stare, E. J., (1966). Prevalence of osteoporosis in high- and low-fluoride areas in North Dakota. *JAMA*, 198:499–504.

Bhatnagar, A., Kumar, E., Sillanpaa, M. (2011). Fluoride removal from water by adsorption - a review. *Chem Eng J*. 171:811–840.

BNDWQS. (2009). Bangladesh National Drinking Water Quality Survey of 2009. Bangladesh: Bangladesh Bureau of Statistics, Planning Division, Ministry of Planning.

Bo¨hmer, H., Mu¨ller, H. & Resch, K.L., (2000). "Calcium supplementation with calcium rich mineral waters: a systematic review and meta-analysis of its bioavailability". *Osteoporosis Int*, (11), pp.938–43.

Baldisserotto, B., Chowdhury, M. J., & Wood, C. M. (2005). Effects of dietary calcium and cadmium on cadmium accumulation, calcium and cadmium uptake from the water, and their interactions in juvenile rainbow trout. *Aquat Toxicol*, 99-117

Boparai, H. K., Joseph, M., & O'Carroll, D. M. (2013). Cadmium (Cd^{2+}) removal by nano zerovalent iron: surface analysis, effects of solution chemistry and surface complexation modelling. *Environ Sci Pollut Res.*, 20 (9), 6210–6221.

Borzou, A., Kalbasi, M., Hoodaji, M., Abdouss, M., & Mohammadi, A. (2014). Isotherm investigation of the adsorption of cadmium onto modified poly(ethylene terephthalate) fiber. *Euro J of Exp Bio*, 4(2), 136–142.

Bovend'Eerdt, T. J., Botell, R. E., & Wade, D. T. (2009). Writing SMART rehabilitation goals and achieving goal attainment scaling: a practical guide. *Clin. Rehabil*., 352–361.

Braghetta, A., DiGiano, F. A., Ball, W. P. (1997). Nanofiltration of natural organic matter: pH and ionic strength effects. *J. Environ. Eng.* 123, 628–641.

Braeken, L., Ramaekers, R., Zhang, Y., Maes, G., Van Der Bruggen, B., Vandecasteele, C. (2005). Influence of hydrophobicity on retention in nanofiltration of aqueous solutions containing organic compounds. *J. of Membrane Sci.* 252 (1–2), 195–203.

Borke, J. L., Whiteford, G. M. (1999). Chronic fluoride ingestion decreases 45Ca uptake by rat kidney membranes. *J Nutr*. 129,1209–1231.

Brunauer, S., Emmett, P.H., Teller, E. (1938). Adsorption of gases in multi molecular layers. *J Am Chem Soc*. 60, 309–319.

Brooks, A. S., Rozenwald, M. N., Geohring, L., Lion, L. W., & Steenhuis, T. S. (2000). Phosphorus removal by wollastonite: A constructed wetland substrate. *Ecol Eng*, 15, 121–132.

Bykkam, S., Rao, K. V., Chakra, C. H., Thunugunta, T. (2013), Synthesis and characterization of graphene oxide and its antimicrobial activity against klebseilla and Staphylococus. *Int J Adv Biotechnol Res*, 4(1), 142–146.

Cadotte, E., Petersen, R. J., Larson, R. E., Erickson, E. E. (1980). New Thin-Film Composite Seawater Reverse-Osmosis Membrane. *Desalination*, 32, 25–31.

Carolin, C. F., Kumar, P. S., Saravanan, A., Oshiba, G. J., Naushad, M. (2017). Efficient Techniques for the Removal of Toxic Heavy Metals from Aquatic Environment: A Review. *J. Environ. Chem. Eng*., 5(3), 2782–2799.

Cama, J., Ayora, C., Querol, X., & Gonor, J. (2005). Dissolution kinetics of synthetic zeolite NaP1and its implication to zeolite treatment of contaminated water. *Environ Sci Technol*, 39:4871–4877.

Camacho, L. M., Torres, A., Saha, D., Deng, S. (2010). Adsorption equilibrium and kinetics of fluoride on sol-gel-derived activated alumina adsorbents. *J. Colloid Interface Sci*., 349, 307–313.

Chandra, A.K., Sengupta, P., Goswami, H. & Sarkar, M., (2013). Effects of dietary magnesium on testicular histology, steroidogenesis, spermatogenesis and oxidative stress markers in adult rats. *Indian J Exp Biol*. , I(51), 37-47.

Chandrajith, R., Nanayakkara, S., Itai, K., Aturaliya, T. N., Dissanayake, C. B., Abeysekera, T., Harada, K., Watanabe, T., Koizumi, A. (2011a). Chronic kidney diseases of uncertain etiology (CKDue) in Sri Lanka: geographic distribution and environmental implications. *Environ Geochem Health*, 33(3), 267–278.

Chandrajith, R., Dissanayake, C. B., Ariyarathna, T., Herath, H. M., & Padmasiri, J. P. (2011b). Dose-dependent Na and Ca in fluoride-rich drinking water –Another major cause of chronic renal failure in tropical arid regions. *Sci. Total Environ*., 409, 671–675.

Chandrajith, R., Padmasiri, J. P., Dissanayake, C. B. & Prematilaka, K. M. (2012). Spatial distribution of fluoride in groundwater of Sri Lanka, *J. Natn. Sci. Foundation Sri Lanka*, 40(4), 303–309.

Chang, Y., Chang, P., Lee, Y., Lee, T., Lai, Y., & Chen, S. (2014). Morphological and structural evolution of mesoporous calcium aluminate nanocomposites by microwave-assisted synthesis. *Micropor Mesopor Mat*, 134–142.

Chavkin, S. (2012). As kidney disease kills thousands across continents, scientist scramble for answers, Mystery in the field. USA: The Center for Public Intregrity.

Childress, A. E., & Elimelech, M., (1996). Effect of solution chemistry on the surface charge of polymeric reverse osmosis and nanofiltration membranes. *J. Membr. Sci.* 119, 253–268.

Chekli, L., Bayatsarmadi, B., Sekine, B. R., Sarkar, B., Shen, A. M., Scheckel, K. G., Skinner, W., Naidu, R., Shon, H. K., Lombi, E., Donner, E. (2016). Analytical characterisation of nanoscale zero-valent iron: A methodological review. *Analytica Chimica Acta*. 903, 13–35.

Chemistry Learning, Free Online Education Resource. *(2009, March 5). Retrieved from www.chemistrylearning.com: http://www.chemistrylearning.com/adsorption.*

Chen, S., Yue, Q., Gao, B., Li, Q. X., & Fu, K. (2012). Adsorption of hexavalent chromium from aqueous solution by modified corn stalk: A fixed-bed column study. *Bioresour. Technol*, 113, 114–120.

Chen, H., Zhang, H., & Yan, Y. (2013). Adsorption dynamics of toluene in structured fixed bed with ZSM-5 membrane/PSSF composites. *Chem. Eng. J.* , 336-344.

Chen, Z., Liu, T., Tang, J., Zheng, Z., Wang, H., Shao, Q., & Feng, T. (2018). Characteristics and mechanisms of cadmium adsorption from aqueous solution using lotus seedpod-derived biochar at two pyrolytic temperatures. *Environ Sci Pollut R*, 25(12), 11854–11866.

Choi, O., Clevenger, T. E., Deng, B., Surampalli, R. Y., Ross, L. J., & Hu, Z. (2009). Role of sulfide and ligand strength in controlling nanosilver toxicity. *Water Res*., 1879–1886.

Comstock, G.W. (1971). “Fatal Arteriosclerotic heart disease, water hardness at water socioeconomic characteristics”. *Ame. J. of Epidemiology*, I(94), pp.1-10.

Conidi, C., Castro-Muñoz, R., & Cassano, A. (2020). Membrane-Based Operations in the Fruit Juice Processing Industry: A Review. Beverages, 6(1), 18–29.

Collons, J. J. (1967). The LUB/equilibrium section concept for fixed-bed adsorption. *Chem Eng Progs, 31-35.*

Coronell, O., Marinas, B. J., & Cahill, D. G. (2011). Depth heterogeneity of fully aromatic polyamide active layers in reverse osmosis and nanofiltration membranes. *Environ Sci Technol*, 45, 4513–4520.

Correa-Rotter, R., Wesseling, C., & Johnson, R. J. (2014). CKD of Unknown Origin in Central America: The Case for a Mesoamerican Nephropathy. *Am J Kidney Dis*., 63(3): 506–520

Cooray, T., Wei, Y., Zhong, H., Zheng, L., Weragoda, S. K., & Weerasooriya, R. (2019). Assessment of Groundwater Quality in CKDu Affected Areas of Sri Lanka: Implication for Drinking Water Treatment. *Int. J. Environ. Res. Public Health*, 16, 1698.

Cruza, R. & Flores, J. V. (2017). Reduction of Coliforms presents in domestic residual waters by Air-Ozone Micro-Nanobubbles In Carhuaz city, Peru. *J. Nanotechnol*., 1, 9–17.

Cundy, A. B., Hopkinson, L., Whitby, R. L. (2008). Use of iron-based technologies in contaminated land and groundwater remediation: a review. *Sci. Total Environ*., 400: 42–51.

CSE, (2012). Environmental contamination and its association with Chronic Kidney Disease of Unknown Etiology in North Central Region of Sri Lanka. Centre for Science and environment, New Delhi, India.

Crawford, R. J., Harding, I. H., Mainwaring, D. E. (1993). Adsorption and co-precipitation of single heavy metals ions onto the hydrated oxides of iron and chromium. *Langmuir*. 9, 3050–3056.

Da Conceição, V. M., Ugri, M. C. B. A., Silveira, C., et al. (2015). Removal of Excess Fluoride from Groundwater Using Natural Coagulant Moringa oleifera Lam and Microfiltration. *Can J Chem Eng*. 93:37–45.

Dayananda, D., Sarva, V. R., Prasad, S. V., Arunachalam, J. G. (2014). Preparation of CaO loaded mesoporous Al_2O_3: Efficient adsorbent for fluoride removal from water. *Chem Eng J*, 248, 430–439.

Das, M. R., Sarma, R. K., Saikia, R., Vinayak S., Kale, V. S., Manjusha V., Shelke, M. V. & Sengupta, P. (2011). Synthesis of silver nanoparticles in an aqueous suspension of graphene oxide sheets and its antimicrobial activity. *Colloid Surf B: Biointerfaces*, 83, 16–22.

Dayananda, D., Sarva, V. R., Prasad, S. V., & Arunachalam, J. G. (2014). Preparation of CaO loaded mesoporous Al_2O_3: Efficient adsorbent for fluoride removal from water. *Chem Eng J*, 248, 430–439.

Devaraj, P., Kumari, P., Aarti, C. & Renganathan, A. (2013). Synthesis and Characterization of Silver Nanoparticles Using Cannonball Leaves and Their Cytotoxic Activity against MCF-7 Cell Line. *J. Nanotechnol*., 2013, 598328.

Devi, R., Umlong, L. M., Raul, P. K., Das, B., Banerjee, S., & Singh, L. (2014). Defluoridation of water using nano-magnesium oxide. *J Exp Nanosci*, 9(5), 512–524.

Dewagea, N. B., Liyanagea, A. S., Pittman, C. U. & Mohanb, D. (2018). Fast nitrate and fluoride adsorption and magnetic separation from water on α-Fe2O3 and Fe3O4 dispersed on Douglas fir biochar. *Bioresour. Technol*., 263, 258–265.

Dharmagunawardana, H. A. (2009). Fluoride problem in the groundwater of Sri Lanka. *Economic Review*. 35(3–4), 46–48.

Dharmawardana, M. W., Amarasiri, S. L., Dharmawardene, N. & Panabokke, C. R. (2014). Chronic Kidney Disease of Unknown etiology and Ground water ionicity; study base on Sri Lanka. *Environ Geochem Health*, 37(2), 221–31.

Dharma-wardana, M. W. C. (2018). Chronic Kidney Disease of Unknown aetiology (CKDu) and multiple-ion interactions in drinking water. *Environ Geochem Health*, 40(2), 705.

Dissanayake, C. B. (2005). Water quality in the dry zone of Sri Lanka-some interesting health aspects. *J. Nat. Sci. Found*. Sri Lanka, 161-165.

Diawara, C. K., Diop, S. N., Diallo, M. A., & M. A. Farcy, M. A. (2011). Determination Performance of nanofiltration (NF) and low pressure reverse osmosis (LPRM) membranes in the removal of fluorine and salinity from brackish drinking water, *J Water Resour Prot*, 3, 912-917.

Dissanayake, C. B., & Chandrajith, R. (2017). Groundwater fluoride as a geochemical marker in the etiology of chronic kidney disease of unknown origin in Sri Lanka. *Ceylon J. Sci*. 46.

Dissanayake, C. B., & Chandrajith, R. (2019). Fluoride and hardness in groundwater of tropical regions - review of recent evidence indicating tissue calcification and calcium phosphate nanoparticle formation in kidney tubules. *Ceylon J. Sci*., 48(3), 197–207.

Dubinin, M. M. (1960). The potential theory of adsorption of gases and vapours for adsorbents with energetically non uniform surfaces. *Chem Rev*. 60, 235–241.

Do, D. D. (1998). Adsorption Analysis: Equilibrium and Kinetics. London: Imperial College Press.

Dong, H., Zhaoa, F., Zenga, G., Tanga, L., Fana, C., Zhanga, L, Zenga, Y., Hea, Q., Xiea, Y., & Wu, Y. (2016). Aging study on carboxymethyl cellulose-coated zero-valent iron nanoparticles in water: Chemical transformation and structural evolution. *J Hazard Mater*, 312, 234–242.

Elliott H. A. & Huang C. P. 1979 The effect of complex formation on the adsorption characteristics of heavy metals. *Environ. Int.* 2(3), 145–155.

Elhefnawy, O. & Elabd, A. A. (2017). Natural silica sand modified by calcium oxide as a new adsorbent for uranyl ions removal from aqueous solutions. *Radiochim. acta*, 105(10), 821-830.

Elkhatib, E., Mahdy, A., Sherif, F. & Elshemy, W. (2016). Competitive Adsorption of Cadmium (II) from Aqueous Solutions onto Nanoparticles of Water Treatment Residual. *J. Nanomat*., 2016, 10.

Elledge, M. F., Redmon, J. H., Levine, K. E., Wickremasinghe, R. J., Wanigasariya, K. P., & Peiris-John, R. J. (2014). ChronicKidney Disease of Unknown Etiology in Sri Lanka: Quest for Understanding and Global Implications, Triangle Park, NC, USA,: RTI Brief Research; RTI Press.

Ene-Iordache, B., Perico, N., Bikbov, B., Carminati, S., Remuzzi, A., Perna, A., Islam, N., Bravo, R.F., Aleckovic-Halilovic, M., Zou, H., Zhang, L., Gouda, Z., Tchokhonelidze, I., Abraham, G., Mahdavi-Mazdeh, M., Gallieni, M., Codreanu, I., Togtokh, A., Sharma, S.K., Koirala, P., Uprety, S., Ulasi, I. & Remuzzi, G. (2016). Chronic kidney disease and cardiovascular risk in six regions of the world (ISN-KDDC): A cross-sectional study. *Lancet Glob Health*, 4(5), e307–e319.

Ergun, E., Tor, A., Cengeloglu, Y., et al. (2008). Electrodialytic removal of fluoride from water: Effects of process parameters and accompanying anions. *Sep Purif Technol*. 64:147–153.

Essington, M. E. (2005). Soil and water chemistry an integrative approach. Washington: Taylor & Francis.

EPA. (2002). Method 1604: Total Coliforms and Escherichia coli in Water by Membrane Filtration Using a Simultaneous Detection Technique (MI Medium). Pennsylvania Avenue, NW, Washington, DC 20460: U.S. Environmental Protection Agency.

Fabrizi, L., (2014). "Demiwater and health. Health risks from drinking of demineralised water, Water treatment solution", Lenntech.

Fang, Z., Chen, J., Qiu, X., Qiu, X., Cheng, W., & Zhu, L. (2011). Effective removal of antibiotic metronidazole from water by nanoscale zero-valent iron particles, *Desalination*, 268: 60–67.

Fernando, M. S., Wimalasiri, A. K., Ratnayake, S. P., Jayasinghe, J. M., William, G. R., Dissanayake, D. P., De Silva, R. M. (2019). Improved nanocomposite of montmorillonite and hydroxyapatite for defluoridation of water. *RSC Adv*, 35588–35598.

Franus, W., Wdowin, M. & Franus, M. (2014). Synthesis and characterization of zeolites prepared from industrial fly ash. *J Environ Monit Assess*, IX(186), 5721–5729.

Freundlich, H. M. F. (1906). Over the adsorption in solution. J Phys Chem. 57, 385–471.

Fu, R., Yang, Y., Xu, Z., Zhang, X., Guo, X., & Bi, B. (2015). The removal of Chromium (VI) and lead (II) from groundwater using sepiolite-supported nanoscale zero-valent iron (S-NZVI). *Chemosphere*, 138, 726–734.

Galvan-Ruiz, M., Hernandez, J., Banos, L., Noriega-Montes, J., & Rodríguez-García, M. E. (2009). Characterisation of calcium carbonate, calcium oxide, calcium hydroxide as starting point to the improvement of lime for their use in construction. *J Mater Civ Eng*, 21, 625–708.

Gaurav, Y., Devendra, P. & Kumar, P. (2014). Assessment of Ground Water Quality and its Impact on Health of people around Rewa City, MP, India. *Int. Res. J. Environment Sci*, III (7), 70–72.

Gawande, S. M., Belwalkar, N. S., & Mane, A. A. (2017). Adsorption and its Isotherm – Theory. *IJSER*, 312–316.

Gedam, V. V., Patil, J. L., Kagne, S., Sirsam, R. S., & Labhasetwar, P. (2012). Performance evaluation of polyamide reverse osmosis membrane for removal of contaminants in ground water collected from Chandrapur district, *J. Membrane Sci. Techno.*, 2 (3), 1 – 5.

Geethamani, C. K., Ramesh, S. T., Gandhimathi, R., & Nidheesh, P. V. (2013). Fluoride sorption by treated fly ash: kinetic and isotherm studies. *J Mater Cycles Waste Manag*, 381–392.

Gifford, F. J., Gifford, R. M., Eddleston, M., & Dhaun, N. (2017). Endemic Nephropathy Around the World. *Kidney Int Rep*., 282–292.

Gong, K., Hu, Q., Xiao, Y., Cheng, X., Liu, H., Wang, N., Qiu, B., & Guo, Z. (2018). Triple Layered Core-Shell ZVI@Carbon@Polyaniline Composites Enhanced Electron Utilization in Cr (VI) Reduction, *J. Mater. Chem. A, 6,* 11119–11128.

González-Quiroz, M., Pearce, N., Caplin, B., & Nitsch, D. (2018). What do epidemiological studies tell us about chronic kidney disease of undetermined cause in Meso-America? A systematic review and meta-analysis. *Clin. Kidney J.*, 496–506.

Gorry, C. (2014). CKDu Ravages the Salvadoran Countryside, *MEDICC Review*. 16(2), 5–8.

Goud, R. V., Kumar, B. L., Abhilash, N., Prasad, P. R., & Saradhi, B. V. (2015). Comparision studies on Adsorbants for removal of Hardness from Water by using newly Prepared Zeolite. *IJAPBS*, 4(2), 342–354.

Gropper, S. & Smith, J., (2012). Water and electrolytes. In Advanced Nutrition and Human Metabolism. 6th ed. USA: Wadsworth, Cengage Learning. 608.

Gutiérrez-Amavizca, B. E., Orozco-Castellanos, R., Ortíz-Orozco, R., Padilla-Gutiérrez, J., Valle, Y., Gutiérrez-Gutiérrez, N., Figuera, L. E. (2013). Contribution of GSTM1, GSTT1, and MTHFR polymorphisms to end-stage renal disease of unknown etiology in Mexicans. *Indian J Nephrol.*, 23(6), 438–443.

Habuda-Stanić, M., Ravančić, M. E. & Flanagan, A. (2014). A Review on adsorption of fluoride from aqueous solution. *Materials*, 7, 6317–6366.

Hady, H. A. E. (2012). Syntheses and antimicrobial activity of some new thiohydantoin and thiazole derivatives. *Der Pharma Chemica*, 4(6), 2202–2207.

Hall, K. R., Eagleton, L. C., Aerivos, A., & Vemeclen, T. (1966). Pore- and solid-diffusion kinetics in fixed-bed adsorption under constant constant pattern. *Ind Eng Chem Fund*, 212–223.

Han, R., Wang, Y., Zhao, X., Wang, Y., Xie, F., & Cheng, J. T. (2009). Adsorption of methylene blue by phoenix tree leaf powder in a fixed-bed column: experiments and prediction of breakthrough curves. *Desalination*, 284–297.

Heiri, C., Wolf, A., Rohrer, L., & Bugmann, H. (2009). Forty years of natural dynamics in Swiss beech forests: Structure, composition, and the influence of former management. *Ecological Applications*, 19, 1920–1934.

Herath, H. M., Kawakami, T., & Tafu, M. (2018). The Extremely High Adsorption Capacity of Fluoride by Chicken Bone Char (CBC) in Defluoridation of Drinking

Water in Relation to Its Finer Particle Size for Better Human Health. *Healthcare*, 6, 123.

Ho, Y.S., & McKay, G. (1999). Pseudo-second order model for sorption processes. *Process Biochem*. 34, 451–465.

Hoyos-Sánchez, M. C., Córdoba-Pacheco, A. C., Rodríguez-Herrera, F. R. & Uribe-Kaffure, R. (2017). Removal of Cd (II) from Aqueous Media by Adsorption onto Chemically and Thermally Treated Rice Husk. *J. Chem*., 5763832.

Hua, M., Zhang, S., Pan, B., Zhang, W., Lv, L., & Zhang, Q. (2012). Heavy metal removal from waste/wastewater by nano sized metal oxides: A review. *J. Hazard. Mater*., 211, 317–331.

Ileperuma, O. A., Dharmagunawardhane, H. A. & Herath, K. P. R. P. (2009). Dissolution of aluminium from sub-standard utensils under high fluoride stress: a possible risk factor for chronic renal failure in the North-Central Province. *J. Natn. Sci. Foundation Sri Lanka*, 219–222.

Imtiaz, A., Farrukh, M., Khaleeq-ur-rahman, M. & Adnan, R. (2013). Micelle-Assisted synthesis of Al2O3·CaO nanocatalyst: Optical properties and their applications in photodegradation of 2,4,6-Trinitrophenol. *Sci. World J*., 2013, 641420.

Inglezakis, V., & Inglezakis, V. (2006). Adsorption, ion exchange and catalysis: Design of operations and environmental applications. *Elsevier*, 3, 243–307.

Islam, M. & Patel, R. (2007). Evaluation of removal efficiency of fluoride from aqueous solution using quick lime. *J. Hazard. Mater.*, I-II(143), 303–310.

Iwami, O. et al., (1994). Motor neuron disease on the Kii Peninsula of Japan: excess manganese intake from food coupled with low magnesium in drinking water as a risk factor. *Sci. Total Environ*., (149), 121-35.

Jabeen, H., Kemp, K. C., & Chandra, V. (2013). Synthesis of nano zerovalent iron nanoparticles– Graphene composite for the treatment of lead-contaminated water, *J Environ Manage*, 130, 429e435.

Jacqmin, H., Letenneur, L., Barberger-Gateau, P. & Dartigues, J. (1994). Components of drinking water and risk of cognitive impairment in the elderly. *Am. J. Epidemiol*, 48–57.

Jadhav, S. V., Gadipelly, C. R., Marathe, K. V., et al. (2014). Treatment of fluoride concentrates from membrane unit using salt solutions. *J Water Process Eng.* 2:31–36.

Jaishankar, M., Tseten, T., Anbalagan, N., Mathew, B. B., & Beeregowda, K. N. (2014). Toxicity, mechanism and health effects of some heavy metals. *Interdiscip Toxicol*, II(7), 60–72.

Jain, S. J., & Snoeyink, V. L. (1973). Adsorption from bi-solute systems on active carbon. *J Water Pollut Control Fed*., 45, 2463–2479.

Jalalia S. A. & Allafchian, A. R. (2015). Assessment of antibacterial properties of novel silver nanocomposite. *J Taiwan Ins Chem E*., 1–8.

Janković, S., Bukvić, D., Marinković, J., Janković, J., Marić, I., & Djukanović, L. (2013). Trends in Incidence and Prevalence of Balkan Endemic Nephropathy in the Three Most Affected Villages in Serbia Over a 36-Year Period. *Ren. Fail*., 35(4), 509–513.

Jarup, L. (2003). Hazards of heavy metal contamination. *Br. Med. Bull*., 68, 167–182.

Jacqmin, H., Letenneur, L., Barberger-Gateau, P. & Dartigues, J., 1994. Components of drinking water and risk of cognitive impairment in the elderly. *Am. J. Epidemiol*, 48-57.

Jayasekara, K. B., Dissanayake, D. M., Sivakanesan, R., Ranasinghe, A., Karunarathna, R. H., Waligamage, G., & Kumara, G. M. (2015). Epidemiology of Chronic

Kidney Disease, With Special Emphasis on Chronic Kidney Disease of Uncertain Etiology, in the North Central Region of Sri Lanka. *Int. J. Epidemiol*., 275-280.

Jayasinghe, S. (2014). Chronic Kidney Disease of Unknown Etiology Should Be Renamed Chronic Agrochemical Nephropathy. *MEDICC Rev*., 16(2), 72–74.

Jayasumana, C., Gajanayaka, R. & Siribaddana, S. (2014). Importance of arsenic and pesticides in epidemic chronic kidney disease in Sri Lanka. *BMC Nephrol*, 15, 124.

Jayasumana, C., Gunatilake, S. & Senanayake, P. (2015). Glyphosate, hard water, and nephrotoxic metals: Are they the culprits behind the epidemic of Chronic Kidney Disease of Unknown Etiology in Sri Lanka? *J. Environ. Res. Public Health*, II (11), 2125–2147.

Jayathilake, N., Mendis, S. & Maheepala, P. M. F. C. N. R. P. T. (2013). Chronic kidney disease of uncertain aetiology: prevalence and causative factors in a developing country. *BMC Nephrol*, 14, 180.

Jayarathna, L., Bandara, A., Ng, W.J., Weerasooriya, R. (2015). Fluoride adsorption on $\gamma - Fe_2O_3$ nanoparticles. *J Environ Health Sci Eng.* 13, 54.

Jayaweera, M., Sudasinghe, M., Gunawardana, B., Peiris, A., & Manathunge, J. (2019). Use of CaO Loaded Mesoporous Alumina for Defluoridation of Potable Groundwater Containing Elevated Calcium Levels. *Environ*, 66.

Jinadasa, K. B., Weerasooriya, S. W., & Dissanayake, C. B. (1988). A rapid method for defluoridation of fluoride rich drinking water at village level. *Environ. Sci.,* 305–312.

Jo, M., Soto, L., Arocho, M., St John, J., & Hwang, S. (2015). Optimum mix design of fly ash geopolymer paste and its use in pervious concrete for removal of fecal coliforms and phosphorus in water. *Constr Build Mater*, 93, 1097–1104.

Judd, E. & Calhoun, D. A. (2015). Management of hypertension in CKD: Beyond the guidelines, *Adv Chronic Kidney Dis.* 22(2), 116–22.

Kakavandi, B., Jafari, A. J., Kalantary, R. R., Nasseri, S., Ameri, A., Esrafily, A. (2013). Synthesis and properties of Fe_3O_4-activated carbon magnetic nanoparticles for removal of aniline from aqueous solution: equilibrium, kinetic and thermodynamic studies. *Iranian J Environ Health Sci Eng.*, 10, 19.

Kanehiraa, S., Kanamori, S., Nagashima, K., Saeki, T., Visbal, H., Fukui, T., & Hirao, K. (2013). Controllable hydrogen release via aluminum powder corrosion in calcium hydroxide solutions. *JAsCerS*, 296–303.

Kannan, D. & Mani, N. (2014). Removal of hardness (Ca^{2+}, Mg^{2+}) and alkalinity from ground water by low cost adsorbent using phyllanthus emblica wood. *IJCPA*, 1(4), 208–212.

Kansara, N., Bhati, L., Narang, M., & Vaishnavi, R. (2016). Wastewater treatment by ion exchange method: a review of past and recent researches. *Environ. Sci.,* 143–150.

Kapur, M., & Mondal, M. K. (2015). Design and model parameters estimation for fixed–bed column adsorption of Cu(II) and Ni(II) ions using magnetized saw dust. *Desalin water treat.,* 1–12.

Karthikeyan, M. & Elango, K. (2008). Removal of fluoride from aqueous solution using graphite: A kinetic and thermodynamic study. *Indian J. Chem. Technol.*, 15, 525–532.

Katalo, R., Okuda, T., Nghiem, L. D., & Fujioka, T. (2018). Moringa oleifera coagulation as pretreatment prior to microfiltration for membrane fouling mitigation. *Environ. Sci. Water Res. Technol*., 1604–1611.

Katarzyna, I., 2009. Selection of Sorbent for Removing Pesticides during Water Treatment. *J. Hazard. Mater*, Issue 169, 953.

Kavand, M., Fakoor, E., Mahzoon, S., & Soleimani, M. (2017). An improved Film-Pore-Surface Diffusion Model in the fixed-bed column adsorption for heavy metal ions: Single and multi-component systems. *Process Saf Environ Prot*. 330–342.

Kesting, R. E. (1990). The 4 Tiers of Structure in integrally skinned phase inversion membranes and their relevance to various separation regimes. *J. Appl. Polym. Sci*., 41, 2739–2752.

Kiran, B. & Kaushik, A. (2008). Cyanobacterial biosorption of Cr(VI): application of two parameter and Bohart Adams models for batch and column studies. *Chem Eng J.*, 144(3), 391–399.

Ku, Y., & Chiou, H. M., (2002) The adsorption of fluoride ion from aqueous solution by activated alumina. *Water Air Soil Pollut*. 133, 349–361.

Kumanan, M., Sathya, G., Nandakumar, V. & Berchmans, I. J. (2016). Extraction of potash from k-feldspar mineral by acid and molten salt leaching processes. *Int J Min Met Mater*., 1–10.

Kumar, E., Bhatnagar, A., Kumar, U. & Sillanpa, M. (2011). Defluoridation from aqueous solutions by nano-alumina: characterization and sorption studies. *J. Hazard. Mater*, 186, 1042–1049.

Kumar, R. P., Dongre, A., Muruganandham, R., Deshmukh, P., & Rajagovindan, D. (2019). Prevalence of Chronic Kidney Disease and Its Determinants in Rural Pondicherry, India-A Community Based Cross-Sectional Study. *Open Urol Nephrol J*, 14–22.

Koc J., Sidoruk M., Rochwerger A. (2009). Calcium ion migration in agricultural and afforested lake catchments. *Ecol. Chem. Eng* A 16, 3: 201-212.

Kordialik-Bogacka, E., (2001). Surface properties of yeast cells during heavy metal biosorption, *Cent Eur J Chem*, 9(2):348–351.

Kohri, K., Kodama, M., Ishikawa, Y., Katayama, Y., Takada, M., Katoh, Y., Kurita, T. (1989). Magnesium-to-calcium ratio in tap water, and its relationship to geological features and the incidence of calcium-containing urinary stones. *J Urol*, 142(5), 1272–1275.

Konale, R. A., Mahale, N. K., & Ingle, S. T. (2020). Nano-zeolite-graphene oxide composite for calcium hardness removal: isotherm and kinetic study. *Water Pract. Technol*., 15 (4): 1011–1031.

Kozisek, F., (2005). "Health Risks from Drinking demineralized water". National Institute of Public Health, Czech Republic, 1-16.

Landry, B. K., Nadworny, P. L., Maham, Y., Burrell, J. C., & Burrell, R. E. (2009). The kinetics of thermal instability in nanocrystalline silver and the effect of heat treatment on the antibacterial activity of nanocrystalline silver dressings. *Biomaterials*, 6929–6939.

Lagergren, S. (1898). About the theory of so-called adsorption of soluble substances. *Kungliga Svenska Vetenskapsakademiens Handlingar*. 24, 1–39.

Langmuir, I. (1918). The adsorption of gases on plane surfaces of glass, mica and platinum. *J Am Chem Soc*. 40, 1361–1403.

Laux, T. S., Bert, P. J., Ruiz, B. G., González, M., Unruh, M., Aragon, A., & Lacourt, T. C. (2012). Nicaragua revisited: evidence of lower prevalence of chronic kidney disease in a high-altitude, coffee-growing village. *J Nephrol*., 25(4), 533–540.

Lavrenko, V. A., Podchernyaeva, I. A., Shchur, D. V., Zolotarenko, A. D., & Zolotarenko, A. D. (2017). Features of physical and chemical adsorption during interaction of polycrystalline and nanocrystalline materials with gases. *Powder Metall Met Ceram*., 23–33.

Le, N. L. & Nunes, S. P. (2016). Materials and membrane technologies for water and energy sustainability. *Sustainable Mater. Technol*., 7, 1–28.

Lehmann, M. & Zouboulis, A. I. M. K. A. (2001). Modeling the sorption of metals from aqueous solutions on goethite fixed bed. *Environ pollut*, 113(2), 121–128.

Lesbani, A., Sitompul, S., Mohadi, R. & Hidayati, N. (2016). Characterization and utilisation of Calcium Oxide (CaO) thermally decomposed from fish bones as a catalyst in the production of biodiesel from waste cooking oil. *Makara J. Technol*, 20, 121–126.

Levine, K. E., Redmon, J. H., Elledge, M. F., Wanigasuriya, K. P., K., S., Munoz, B., Wickremasinghe, R. (2016). Quest to identify geochemical risk factors associated with chronic kidney disease of unknown etiology (CKDu) in an endemic region of Sri Lanka—a multimedia laboratory analysis of biological, food, and environmental samples. *Environ Monit Assess*, 188 (10), 548.

Lin, C. L., Lee, C. F., Chiu, W. Y. (2005). Preparation and properties of poly (acrylic acid) oligomer stabilized superparamagnetic ferrofluid. *J Colloid Interface Sci*. 291, 411–20.

Lin, L., Lin, Y., Li, C., Wu, D., & Kong, H. (2016). Synthesis of zeolite/hydrous metal oxide composites from coal fly ash as efficient adsorbents for removal of methylene blue from water. *Int. J Miner. Process.*148, 32–40.

Liu, A., Liu, J., Zhang, W. (2005). Transformation and composition evolution of nanoscale zero-valent iron (nZVI) synthesised by borohydride reduction in static water, *Chemosphere*, 119, 1068–1074.

Liu, H., Zhang, J., Ngo, H. H., Guo, W., Wu, H., Guo, Z., Cheng, C., and Zhang, C., (2015). Effect on physical and chemical characteristics of activated carbon on adsorption of trimethoprim: Mechanism study, *RSC Adv.*, Royal Society of Chremistry. 28, 335-348.

Liu, J., Liu, A. Zhang, W. (2016). The influence of polyelectrolyte modification on nanoscale zero-valent iron (nZVI): Aggregation, sedimentation, and reactivity with Ni (II) in water, *Chem Eng J*, 303, 268–274.

Liang, B.M., Sharp, R.E. & Baskin, T.I., (1997). “Regulation of Growth Anisotropy in Well-Watered and Water-Stressed Maize Roots”. *Plant Physiol*., (115), pp.101-11.

Loryuenyong, V., Totepvimarn, K., Eimburanapravat, P., Boonchompoo, W. Achanai Buasri, A. (2013). Preparation and Characterization of Reduced Graphene Oxide Sheets via Water-Based Exfoliation and Reduction Methods, *Adv. Mater. Sci. Eng*., 923403.

Lounici, H., Belhocine, D., Grib, H., Drouiche, M., Pauss, A., & Mameri, N. (2004). Fluoride removal with electro-activated alumina. *Desalination*, 287–293.

Lovre, D., Sulay Shah, S., Sihota, A. & Fonseca, V. A. (2018). Managing Diabetes and cardiovascular risk in chronic kidney disease patients. *Endocrinol Metab Clin North Am*., 47(1), 237–257.

Lukchis, G. M. (1973). Adsorption systems. Pt. 1: Design by mass transfer zone concept. Chem Eng New York, 111-116.

Lv, D., Liu, Y., Zhou, J., Yang, K., Lou, Z., Baig, S. A., Xu, X. (2018). Application of EDTA-functionalized bamboo activated carbon (BAC) for Pb(II) and Cu(II) removal from aqueous solutions, *Appl. Surf. Sci.* 428, 648–658.

Ma, L., Wei, Q., Chen, Y. & Song, Q. (2018). Removal of cadmium from aqueous solutions using industrial coal fly ash-nZV. *Royal society open science*, 5, 171051.

Mahagamage, M. G., & Manage, P. M. (2017). Water quality and microbial contamination statust of Madawachchiya, Padaviya and Kebathigollawa areas in Anuradhapura district. Proceeding of the national aquatic resources research and development agency (NARA) p. 45. Sri Lanka: NARA.

Mahagamage, M. G. Y. L., & Manage, P. M. (2019). Water quality and microbial contamination status of Madawachchiya, Padaviya and Kebithigollewa areas in Anuradhapura District, Sri Lanka. *J. Water Land Dev*., 42(1), 1–11.

Mallick, A., Mohaptra, B. C., & Sarangi, N. (2010). Bioaccumulation of sodium, potassium, calcium and magnesium in Rohu, Labeo rohita (Ham.) fry. *Curr. World Environ.*, 111-116.

MeiJiao, L. Jing, L. XuYu, Y. Changan, Z. Jia, Y. Hao, H. & XianBao, W. 2013 Applications of graphene-based materials in environmental protection and detection. Chinese Science Bulletin 58, 2698–2710.

Mohapatra, M., Anand, S., Mishra, B. K., Giles, D. E. Singh, P. (2009). Review of fluoride removal from drinking water, *J. Environ. Manage*. 91, 67–77.

Melles, Z. & Kiss, S., 1992. Influence of the magnesium content of drinking water and of magnesium therapy on the occurrence of preeclampsia, http://www.pelicanwater.com

Mohapatra, M., Mohapatra, L., Singh, P., Anand, S., Mishra, B. K. (2010). A comparative study on Pb (II), Cd (II), Cu (II), Co (II) adsorption from single and binary aqueous solutions on additive assisted nano-structured goethite, *Int. J. Eng. Sci. Technol*. 2, 89–103.

Majewska-Nowak, K., Grzegorzek, M., & Kabsch-Korbutowicz, M. (2015). Removal of fluoride ions by batch electrodialysis. *Environ Prot Eng*, 67–81.

Marinković, D. M., Stanković, M. V., Veličković, A. V., Avramović, J. M., Cakić, M. D., & Veljković, V. B. (2015). The synthesis of CaO loaded onto Al2O3 from calcium acetate and its application in transesterification of the sunflower oil. *Adv Technol*, 26–32.

Melles, Z. & Kiss, S. (1992). Influence of the magnesium content of drinking water and of magnesium therapy on the occurrence of preeclampsia. *Magnes Res*., 5(4), 277–286.

Mishra, M. K. (2016). Fourier Transform Infrared Spectrophotometry studies of chromium trioxide-phthalic acid complexes. *Chem. Sci. Trans*, 5(3), 770–774.

Miyake, Y. et al., (2004). "Ecological association of water hardness with prevalence of childhood atopic dermatitis in a Japanese urban area". *Environ Res.,* I(94), pp.33-37.

Mohseni-Bandpi, A., Kakavandi, B., Kalantary, R. R., Azari, A., Keramati, A. (2015). Development of a novel magnetite-chitosan composite for the removal of fluoride from drinking water: Adsorption modelling and optimization. *RSC Adv*. 5, 73279–73289.

Mohri, T., Hisanaga, A. & Ishinishi, N. (1990). Arsenic intake and excretion by Japanese adults: a 7-day duplicate diet study. *Food Chem Toxicol*, 521–529.

Mohsin, M., Safdar, S., Asghar, F. & Jamal, F., (2013). Assessment of Drinking Water Quality and its Impact on Residents Health in Bahawalpur City. *Int. J. of Hum and Soci. Sci.,* III (15), 114–128.

Moreno-Piraj´an, J. C., Rangel, D., Amaya, B., Vargas, E. M., & Giraldo, L. (2008). Design and Construction of Equipment to Make Adsorption at Pilot Plant Scale of Heavy Metals. *Verlag der Zeitschrift fu¨r Naturforschung*, 454-461.

Morel, F. M., & Hering, J. G. (1993). Principles and Applications of Aquatic Chemistry. Wiley.

Moustafa, M. T. (2017). Removal of pathogenic bacteria from waste water using silver nanoparticles synthesized by two fungal species. *Wat. Sci*., 31, 164–176.

Mu¨ller, C. M., Pejcic, B., Esteban, L., Piane, C. D., Raven, M., & Mizaikoff, B. (2014). Infrared attenuated total reflectance spectroscopy: an innovative strategy for analyzing mineral components in energy relevant systems. *Sci. Rep*., 4, 6764.

Naik, B., Prasad, V. S. & Ghosh, N. N. (2010). Development of a simple aqueous solution based chemical method for synthesis of mesoporous c-alumina powders with disordered pore structure. *J Porous Mater*, 115–121.

Naddy, R. B., Stubblefield, W. A., May, J. R., Tucker, S. A., Hockett, J. R. (2002). The effect of calcium and magnesium ratios on the toxicity of copper to five aquatic species in freshwater, *Environ Toxicol Chem*. 21(2):347-52.

Nanayakkara, S., Senevirathna, S. T. M. L. D., Karunaratne, U., Chandrajith, R., Harada, K. H., Hitomi, T., Watanabe, T., Abeysekera, T., Aturaliya, T. N. C. & Koizumi, A. (2012a). Evidence of tubular damage in the very early stage of chronic kidney disease of uncertain etiology in the North Central Province of Sri Lanka: A cross-sectional study. *Environ Health Prev Med.* 17(2), 109–117.

Nghiem, L. D. Schafer A. I., & Elimelech, M. (2004). Removal of natural hormones by nanofiltration membranes: measurement, modelling and mechanisms, *Environ. Sci. Technol*., 38(19), 1888–1896.

Noble, A., Amerasinghe, P., Manthrithilake, H., & Arasalingam, S. (2014). Review of literature on chronic kidney disease of unknown etiology (CKDu) in Sri Lanka. 158, IWMI.

NDWQSN. (2005). National drinking water quality standards. Nepal: Ministry of Physical Planning and Works.

NSDWQ. (2008). National Standards for Drinking Water Quality. Government of Pakistan: Pakistan Environmental Protection Agency, Ministry of Environment.

NSPRC. (2006). Standards of drinking water quality. China: Ministry of Health.

NSW. (2008). Dialysis Water Pre-treatment for In-Centre and Satellite Haemodialysis Units in NSW: A Set of Guidelines. Sidney: Renal Services Network, Liverpool Hospital

Obregón-Valencia, D. & Sun-Kou, M. R. (2014). Comparative cadmium adsorption study on activated carbon prepared from aguaje (Mauritia flexuosa) and olive fruit stones (Olea europaea L.). *J. Environ. Chem. Eng*., 2, 2280–2288.

Orantes, C. M., Herrera, R., Almaguer, M., Brizuela, E. G., Núñez, L., Alvarado, N. P., Orellana, P. (2014). Epidemiology of chronic kidney disease in adults of Salvadoran agricultural communities. *MEDICC Rev*., 16(2):23-30.

Paranagama, D., 2014. Chronic kidney disease of unknown origin in Sri Lanka and its relation to drinking water supplies. PhD Thesis.

Paulchamy B., Arthi, G., & Lignesh, B. D. (2015). Simple Approach to Stepwise Synthesis of Graphene Oxide Nanomaterial. *J. Nanomed. Nanotechnol*., 6 (1), 253.

Panmand, R. P., Patil, R. H., Kale, B. B., Nikam, L. K., Kulkarni, M. V., Thombre, D. K., & Gosavib, S. W. (2014). Self assembly of nanostructured hexagonal cobalt dendrites: an efficient anti-coliform agent. *RSC Adv*., 4(9), 4586–4595.

Patnaik, S., Mishra, P. C., Nayak, R. N., Giri, A. K. (2015). Removal of fluoride from aqueous solution using chitosan-iron complex. *J Anal Bioanal Tech*. 7, 326.

Patterson, P., (1939). The Scherrer Formula for X-Ray Particle Size Determination. *Phys. Rev*, 56, 978.

Peng, S., Wang, R., Yang, L., He, L. H., & Liu, X. (2018). Biosorption of copper, zinc, cadmium and chromium ions from aqueous solution by natural foxtail millet shell. *Ecotoxicol. Environ. Saf*., 61–69.

Perera, B. T., Rajapaksha, R. H., Arachchige, R. C., & Kottegoda, I. R. (2020). Cost-effective and non-toxic method to modify clay to increase the hardness adsorption capacity of clay. *Int. J. Chem. Sci*., 22–27.

Peraza, S., Wesseling, C., Aragon, A., Leiva, R., García-Trabanino, R. A., Torres, C., Hogstedt, C. (2012). Decreased kidney function among agricultural workers in El Salvador. *Am J Kidney Dis*., 59(4), 531-540.

Petala, E., Dimos, K., Douvalis, A., Bakas, T., Tucek, J., Zboril, R., & Karakassides, M. A. (2013). Nanoscale zero-valent iron supported on mesoporous silica: Characterization and reactivity for Cr(VI) removal from aqueous solution. *J Hazard Mater*. 261, 295–306.

Pez-Cervantes, J. L., Sa´nchez-Machado, D. I., Sa´nchez-Duarte, R. G. & Correa-Murrieta, M. A. (2018). Study of a fixed-bed column in the adsorption of an azo dye from an aqueous medium using a chitosan–glutaraldehyde biosorbent. *Adsorpt Sci Technol*, 36(1-2), 215–232.

Pitawala, L., Nanayakkara, W. H., & Nanayakkara, K. G. (2020). Utilization of coal fly ash in the adsorptive removal of fluoride from contaminated groundwater. *Mater. Sci. Eng*., 849 012025

Popkin, B.M., D'Anci, K. E. & Rosenberg, I. H., (2010). Water, *Hydration and Health. Nutr Rev*, VIII (68), 439–458.

Prathibha, C., Sharma, B., Chunduri, L. A., Aditha, S. K., Rattan, T., & Venkataramaniah, K. (2015). Nano Calcium-Aluminum Mixed Oxide: A Novel and Effective Material for Defluoridation of Drinking Water. *Sep. Sci. Technol*., 1915–1924.

Priya, S. S. & Radha, K. (2015). Fixed-bed column dynamics of tetracycline hydrochloride using commercial grade activated carbon: comparison of linear and nonlinear mathematical modeling studies. *Desalin Water Treat*., 57(40), 18964–18980.

Querol, X., Moreno, N., Umana, J. C., Alstuey, A., Hernandez, E., Lopez-solar, A., & Plana, F. (2002). Synthesis of zeolites from coal fly ash: An overview. *Int. J. Coal Geol*., 50, 413–423.

Querol, X., Moreno, N., Alastuey, A., Juan, R., Andres, J. M., Lopez-solar, A., & Valero, A. (2007). Synthesis of high ion exchange zeolites from coal fly ash. *Geol. Acta.*, 49–57.

Qiu, X., Fang, Z., Liang, B., Gu, F., & Xu, Z. (2011). Degradation of decabromodiphenyl ether by nano zero-valent iron immobilized in mesoporous silica microspheres. *J Hazard Mater*. 193, 70–81.

Radjenovic, J., Petrovic, M., Ventura, F., Barcelo, D., (2008)., Rejection of pharmaceuticals in nanofiltration and reverse osmosis membrane drinking water treatment, *water research,* 42: 3601-3610.

Radke, C. J., Prausnitz, J. M. (1972). Thermodynamics of multi-solute adsorption from dilute liquid solutions. *Am Inst Chem J.*, 18: 761–768.

Raul, P., Umlong, I. M., Purkait, M. K. (2012). Removal of Fluoride from Water Using Iron Oxide-Hydroxide Nanoparticles. *J Nanosci Nanotechnol*. 12, 3922–3930.

Ranasinghe, J., & Nanayakkara, N. (2018). Utilization of fly ash as an adsorbent material for removing major pollutants in sri lankan ground water. The 9th International Conference on Sustainable Built Environment (pp. 23-29). Kandy, Sri Lanka: ICSBE2018-423

Rango, T., Jeuland, M., Manthrithilake, H., McCornick, P. (2015). Nephrotoxic contaminants in drinking water and urine, and chronic kidney disease in rural Sri Lanka, *Sci Total Environ*. 518–519, 574–585.

Reddy B. R., Priya D. N., Park K. H. (2006). Separation and recovery of cadmium (II), cobalt (II) and nickel (II) from sulphate leach liquors of spent Ni–Cd batteries using phosphorus-based extractants. *Sep. Puri. Technol*., 50(2), 161–166.

Rivera-Garza, M., Olguín, M., García-Sosa, I., Alcántara, D., & Rodríguez-Fuentes, G. (2000). Silver supported on natural Mexican zeolite as an antibacterial material. *Micropor Mesopor Mat*, 39, 431–444.

Road Development Authority, Environmental and Social Development Division, (2014). Rehabilitation and improvement of 5 km to 24 km section of Vavuniya – Kebithigollewa – Horowpathana (A029) road. Initial Environmental Examination (IEE) Report. Colombo: Road Development Authority, Ministry of Highways, Ports and Shipping.

Robshaw, T., & Dawson, R. B. (2019). Towards the implementation of an ion-exchange system for recovery of fluoride commodity chemicals. Kinetic and dynamic studies. *Chem. Eng. J.*, 367

Rolence-China, C. R. (2016). Adsorption studies on water hardness removal by using cachewnut shell activated carbon as an adsorbent. *Afr. J. Sci. Res.*, 5(4), 78–81.

Roncal-Jimenez, C., Lanaspa, M. A., Jensen, T., & Sanchez-Lozada, L. G. (2015). Mechanisms by Which Dehydration May Lead to Chronic Kidney Disease. *Ann Nutr Metab*, 10–13.

Sabolić, I. (2006). Common mechanisms in nephropathy induced by toxic metals. *Nephron Physiol*., 104(3), 107–114.

Sadaf, S., Bhatti, H. N. (2014). Evaluation of peanut husk as a novel, low cost biosorbent for the removal of indosol orange RSN dye from aqueous solutions: Batch and fixed bed studies, *Clean Technol. Environ. Policy*, 16, 527–544.

Sadiq, M., Chowdhury, B., Chandrasekaran, N., & Mukherjee, A. (2009). Antimicrobial sensitivity of Escherichia coli to alumina nanoparticles. *Nanomedicine: NBM*, 282–286.

Samiey, B. & Jonaghani, A. S. (2015). A New Approach for Analysis of Adsorption from Liquid Phase: A Critical Review. *J. Pollut Eff. Cont*., 3(2), 1–9.

Sauerheber, R. (2013). Physiologic Conditions Affect Toxicity of Ingested Industrial Fluoride. *J Environ Res Public Health*, ID 439490.

Seiferth, O., Wolter, K., Dillmann, B., Klivenyi, G., J., F., Scarano, D., & Zecchina, A. (1999). IR investigations of CO_2 adsorption on chromia surfaces: Cr_2O_3 (0001)/Cr (110) versus polycrystalline a-Cr_2O_3. *Surf. Sci*., 421, 176–190.

Sen, T., Mahajan, S. & Khilar, K. (2002). Colloid-associated contaminant transport in porous media: 1. Experimental studies. *AIChE*, 48, 2366–2374.

Sengupta, P. (2013). Potential Health Impacts of Hard Water. *Int J Prev Med*, 866–75.

Sengupta, P., Sarkar, M. & Chandra, A., (2010). "Effect of consumption of excess hard water salts on male gonadal status in adult albino rats". Abstract of national conference by vidyasagar university, 277.

Sengupta, P., Sarkar, M. & Chandra, A., (2011). "Hard water intake and its consequence on male reproductive physiology". 18th West Bengal State Science and Technology Congress, 113-14.

Sepehr, M. N., Zarrabi, M., Kazemian, H., Amrane, A., Yaghmaian, K., & Ghaffari, H. R. (2013). Removal of hardness agents, calcium and magnesium, by natural and alkaline modified pumice stones in single and binary systems. *Appl Surf Sci*, 274, 295–305.

Sevonkaev, I. & Matijević, E. (2009). Formation of magnesium fluoride particles of different morphologies. *Langmuir*, 25(18), 10534–10543.

Shah, Dawood, M. & Iqbal., M. (2010). Diazinon-induced Oxidative Stress and Renal Dysfunction in Rats. *Food Chem Toxicol*, 3345–3353.

Sharma, G., & Jeewanandam, P. (2013). Synthesis of self-assembled prismatic iron oxide nanoparticles by a novel thermal decomposition route. *RSC Adv*. 3, 189–200.

Shen, J. & Schäfer, A. (2014). Removal of Fluoride and uranium by Nanofiltration and reverse osmosis: A review. *Chemisorption*, 117, 679–691.

Sheneshen, E. S., Fathy, M., El-Naggar, I. M., Ahmed, S. A., Shehata, N., & Shehata, A. M. (2018). Effective Solutions of Hardness by Using Adsorption Technique on Kaolinite Smectite Adsorbent from Aqueous Solution. *Int. J. Chem. Sci*., 16(1), 235–246.

Shimelis, B., Zewge, F., & Chandravanshi, B. S. (2006). Removal of excess fluoride from water by aluminum hydroxide, *Bull. Chem. Soc. Ethiopia*, 20, 17–34.

Shukla, S., Jadaun, A., Arora, V., Sinha, R. K., Biyani, N., & Jain, V. K. (2015). In vitro toxicity assessment of chitosan oligosaccharide coated iron oxide nanoparticles. *Toxicol Rep*., 2, 27–39.

Sowers, M., Whitford, G. M. & Clark, M. K. J. M. L. (2005). "Elevated serum fluoride concentrations in women are not related to fractures and bone mineral density". *J. Nutr*, (135), 2247-52.

Singh, P., Saharan, V. & George, S. (2018). Studies on performance characteristics of calcium and magnesium amended alumina for defluoridation of drinking water. *J. Environ. Chem. Eng*., 6, 1364–1377.

Singh, R., Kumar, M., Khajuria, H., Ladol, J., & Sheikh, H. N. (2018). Hydrothermal synthesis of magnetic Fe3O4–nitrogen-doped graphene hybrid composite and its application as photocatalyst in degradation of methyl orange and methylene blue dyes in presence of copper (II) ions. *Chem Pap*., 72(5), 1181–1192.

Smith, A. H., Hopenhayn-Rich, C., Bates, M. N., Goeden, H. M., Hertz-Picciotto, I., Duggan, H. M., & Smith, M. T. (1992). Cancer risks from arsenic in drinking water. *Environ Health Perspect*., 259–267.

Sivakumar, S. R., Ravisankar, R., Raghu, Y., Chandrasekaran, A., & Chandramohan, J. (2012). FTIR spectroscopic studies on coastal sediment samples from Cuddalore District, Tamilnadu, India. *IJACS*, 1, 40–46.

Song, Y., Dong, B., Gao, N., & Deng, Y. (2015). Comparative Evaluation of Aluminum Sulfate and Ferric Sulfate-Induced Coagulations as Pretreatment of Microfiltration for Treatment of Surface Water. *Int J Environ Res Public Health*, 6700–6709.

Sontheimer, H., Crittenden, J. C. & Summers, R. S. (1988). Activated carbon for water treatment, S1: Karlsruhe: DVGW-Forschungsstelle, Engler-Bunte-Institut, Universitat Karlsruhe.

Souza, M. A., Johann, S., Lima, L. A., Campos, F. F., Mendes, I. C., Beraldo, H., & Zani, C. L. (2013). The antimicrobial activity of lapachol and its thiosemicarbazone and semicarbazone derivatives. *Mem Inst Oswaldo Cruz*, 108(3), 342–351.

Strochkova, L. S. & Zhavoronkov, A. A., (1983). Fluoride as an activator of enzymatic systems. *Fluoride*, 16(3), 181-186.

Sudasinghe, M. I., Rathnayake, N., Jayaweera, M. W., Manathunga, J. M. A., Gunawardana, W. B. Herath, H. M. P. C. K. (2014) The effects of consuming Reverse Osmosis purified water in CKDu affected areas: An application to Anuradhapuara, proceeding of the International Forestry and Environmental Symposium 2014, Department of Forestry and Environmental Science, University of Sri Jayawardanapura, Nugegoda, Sri Lanka. pp 45.

Sudasinghe, M., Jayaweera, M., Gunawardana, B., Manatunge, J., & Madhusanka, G. (2019). Defluoridation of calcium-rich groundwater using iron oxide nanoparticles. *Water Pract Tech*, 665.

Sujana, M. G., Thakur, R. S., & Rao, S. B. (1998). Removal of fluoride from aqueous solution by using alum sludge, *J. Colloid Interface Sci*., 206, 94–101.

Sullivan, J. B. and Krieger, G. R. (2001). Clinical environmental health and toxic exposure, Lippincott Williams & Wilkin publishers, 17.

Sun, Y. P., Li, X., Cao, J., Zhang, W., & Wang, H. P. (2006). Characterisation of zero-valent iron nanoparticles, *Adv. Colloid Interface Sci*., 120, 47–56.

Sun, Y., Fang, Q., Dong, J., & Cheng, X. X. (2011). Removal of fluoride from drinking water by natural stilbite zeolite modified. *Desalination*, 121-12.

Tansel, B., Sager, J., Rector, T., Garland, J., Strayer, R.F., Levine, L., Roberts, M., Hummerick, M., Bauer, J. (2006). Significance of hydrated radius and hydration shells on ionic permeability during nanofiltration in dead end and cross flow modes. *Sep. Purif. Technol*. 51, 40–47.

Tchobanoglous, G., Burton, F. L. & Stensel, H. D., (2003). Wastewater Engineering Treatment and Reuse. 4th ed. New Delhi: McGraw Hill Education (India) Private Limited.

Tempkin, M. I., & Pyzhev, V. (1940). Kinetics of ammonia synthesis on promoted iron catalyst. *Acta Phys Chim Sin*. 12, 327–356.

Thakur, S., & Karak, N. (2015). Alternative methods and nature-based reagents for the reduction of graphene oxide: A review. *Carbon*, 224-242.

Thuy, D. P., Anh, V. N. & Bruggen, V. B., (2012). Evaluation of Two Low-Cost–High-Performance Adsorbent Materials in the Waste-to-Product Approach for the Removal of Pesticides from drinking water. Clean – Soil, Air, Water, III (40), 246-253.

Tovar-Gómez, R., Moreno-Virgen, M. R., Dena-Aguilar, J. A., Hernández-Montoya, V., Bonilla-Petriciolet, A., & Montes-Morán, M. A. (2013). Modeling of fixed-bed adsorption of fluoride on bone char using a hybrid neural network approach. *Chem. Eng. Technol*., 1098-1109.

UNEP/WHO. (1996). Water Quality Monitoring - A Practical Guide to the Design and Implementation of Freshwater Quality Studies and Monitoring Programmes, Ed:

Bartram, J and Ballance, R. Geneva: United Nations Environment Programme and the World Health Organization.

USEPA. (1991). Water-quality criteria, standards, or recommended limits for selected properties and constituents. United State: Environmental Protection Agency.

USEPA. (1992). Guidelines for Exposure Assessment, Washington: United State Environmental Protection Agency.

USEPA (2018). National primary drinking water regulations, United States: United States Environmental Protection Agency.

USGS. (2012). Water Hardness and Alkalinity, USA: United State Geological Survey.

Valko, M., Morris, H. & Cronin, M. (2005). Metals, toxicity and oxidative stress. *Curr Med Chem*, XII(10), 1161–1208.

Van Elsas, J. D., Semenov, A. V., Costa, R., & Trevors, J. T. (2011). Survival of Escherichia coli in the environment: Fundamental and public health aspects. *ISME J.*, 5(2), 173–183.

Van Dam RA, Hogan AC, McCullough CD, Houston MA, Humphrey CL, Harford AJ. (2010). "Aquatic toxicity of magnesium sulfate, and the influence of calcium, in very low ionic concentration water", *Environ Toxicol Chem*. 2010 Feb;29(2):410-21. doi: 10.1002/etc.56.

Viswanathan, N., Meenakshi, S. (2009). Role of metal ion incorporation in ion exchange resin on the selectivity of fluoride. *J Hazard Mater*. 162:920–930.

Vyas, R. K., Kumar, S., & Kumar, S. (2004). Determination of micropore volume and surface area of zeolite molecular sieves by D-R and D-A equations: A comparative study. *Indian J. Chem. Technol*., 704-709.

Wanasinghe, W. C., Gunarathna, M. H., Herath, H. M., & Jayasinghe, G. Y. (2018). Drinking Water Quality on Chronic Kidney Disease of Unknown Aetiology (CKDu) in Ulagalla Cascade, Sri Lanka. *Sabaragamuwa Univ. J.*, 17–27.

Wang, Q., Kanel, S. R., Park, H., Ryu, A., & Choi, H. (2009). Controllable synthesis, characterisation, and magnetic properties of nanoscale zerovalent iron with specific high Brunauer–Emmett–Teller surface area, *J Nanopart Res*. 11, 749–755.

Wang, K., Zhao, J., Li, H., Zhang, X., & Shi, H. (2016). Removal of Cadmium (II) from aqueous solution by granular activated carbon supported magnesium hydroxide. *J Taiwan Inst Chem E*, 61, 287–291.

Wang, L., Zhang, Y., Sun, N., Sun, W., Hu, Y., & Tang, H. (2019). Precipitation Methods Using Calcium-Containing Ores for Fluoride Removal in Wastewater. *Minerals*, 511–520.

Warnakulasuriya, K.A.A.S., Balasuriya, S., Perera, P.A.J. & Peiris, L.C.L., (1992). Determining optimal levels of fluoride in drinking water hot, dry climates—A case study in Sri Lanka. *Community Dent Oral Epidemiol*, (2), 364–67.

Wasana, H. M. S., Aluthpatabendi, D., Kularatne, W. M. T. D., Wijekoon, P., Weerasooriya, R., & Bandara, J. (2016). Drinking water quality and chronic kidney disease of unknown etiology (CKDu): synergic effects of fluoride, cadmium, and hardness of water. *Environ Geochem Health*. 38, 157–168.

Wasana, H. M., Perera, D. G., Gunawardena, P. S., Fernando, P. S., & Bandara, J. (2017). WHO water quality standards Vs Synergic effect(s) of fluoride, heavy metals, and hardness in drinking water on kidney tissues. *Sci. Rep.*, 7:42516

Weaver, V. M., Fadrowski, J. J., & Jaar, B. G. (2015). Global dimensions of chronic kidney disease of unknown etiology (CKDu): a modern era environmental and/or occupational nephropathy? *BMC Nephrol* , 16, 145.

Weber, T. W., & Chakravorti, R. K. (1974). Pore and solid diffusion models for fixed bed adsorbers. *AIChE J.*, 20, 228–238.

Weragoda, S. K., & Kawakami, T. (2017). Evaluation of Groundwater Quality in 14 Districts in Sri Lanka:A Collaboration Research Between Sri Lanka and Japan. In F. Kurisu, A. L. Ramanathan, A. A. Kazmi, & M. Kumar, Trends in Asian Water Environmental Science (pp. 151-160). India: Springer International Publishing.

Wickramarathna, S., Balasooriya, S., Diyabalanage, S., & Chandrajith, R. (2017). Tracing environmental aetiological factors of chronic kidney diseases in the dry zone of Sri Lanka—A hydrogeochemical and isotope approach. *J. Trace Elem. Med. Biol.*, 44(June), 298–306.

Wijerathne, C., Weragoda, S. K. & Kawakami, T. (2014). A review of chronic kidney disease due to unknown etiology and groundwater quality in dry zone in Sri Lanka. International conference on advances in Applied Science and Environmental Engineering, Malaysia.

Williams, S., (2012). Health Effects of Drinking Distilled Water, Living Healthy, Every Topic Every angle, http://www.livinghealthy360.com/index.php/health-effects-of-drinking-distilled-water-6157/, Accessed: 1st of October 2014.

Wimalawansa S. J. (2014). Escalating chronic kidney diseases of multi-factorial origin in Sri Lanka: causes, solutions, and recommendations. *Environ Health Prev Med* 19(6):375–394

Wimalawansa, S. J. (2020). Molecular and cellular toxicity of fluoride in mystery, tubulointerstitial chronic kidney disease: a systematic review. In Reviews in Environmental Science and Biotechnology (19). https://doi.org/10.1007/s11157-019-09521-0.

WHO, (1986). “Health impact of acidic deposition. Science of the total environment”, World Health Organization.

WHO, (2003). “pH in Drinking-water”. Background document for development of WHO Guidelines for Drinking-water Quality.

WHO, (2004). “Guidelines for Drinking-Water Quality. Geneva”: World Health Organization (WHO).

WHO, 2009. Calcium and magnesium in drinking-water: public health significance, Geneva: WHO, ISBN 978 92 4 156355 0.

WHO, 2012. Investigation and evaluation of Chronic Kidney Disease of uncertain aetiology in Sri Lanka, Geneva: World Health Organization.

WHO, 2017. Guidelines for drinking water quality: 4th edition incorporating the 1st addendum. World Health Organization, Geneva, CC BY-NC-SA 3.0 IGO.

Worch, E., 2012. Adsorption Technology in water treatment fundamentals, processes and modelling. Germany: Walter de Gruyter GmbH & Co. KG, Berlin/Boston.

Wu, S., Sun, A., & Zhai, F. (2011). Fe_3O_4 magnetic nanoparticles synthesis from tailings by ultrasonic chemical co-precipitation. *Mater Lett.* 65, 1882–1884.

Wu, L., Liao, L., Lv, G., Qin, F., He, Y., & Wang, X. (2013). Micro-electrolysis of Cr (VI) in the nanoscale zero-valent iron loaded activated carbon, *J Hazard Mater*, 254– 255, 277– 283.

Wu, S., Kong, L., & Liu, J. (2016). Removal of mercury and fluoride from aqueous solutions by three-dimensional reduced-graphene oxide aerogel. *Res Chem Intermed*, 42(5), 4513–4530.

Xiea, W., Vua, K., Yangb, G., Tawfiqa, K., & Chena, G. (2014). Escherichia coli growth and transport in the presence of nanosilver under variable growth conditions. *Environ. Technol*., 2306-2313.

Xu, P., Drewes, J. E., Bellona, C., Amy, G., Kim, T. U., Adam, M., & Heberer, T. (2005). Rejection of emerging organic micropollutants in nanofiltration-reverse osmosis membrane applications. *Water Environ Res*, 77(1), 40–48.

Xu, J., Yang, H., Fu, W., Du, K., Sui, Y., Chen, J., Zeng, Y., Li, M., & Zou, G. (2007). Preparation and magnetic properties of magnetite nanoparticles by sol-gel method. *J Magn Magn Mater*. 309, 307–311.

Xu, X., Li, Q., Cui, H., Pang, J., An, H., Wang, W., & Zhai, J. (2012). Column-mode fluoride removal from aqueous solution by magnesia-loaded fly ash cenospheres. *Environ. Technol*., 33:12, 1409-1415.

Xu, C., Yang, W., Liu, W., Sun, H., Jiao, C., & Lin, A. (2018). Performance and mechanism of Cr (VI) removal by zero–valent iron loaded onto expanded graphite. *J Environ Sci*. 67, 14–22.

Yaguba, M. T., Sena, T. K., Afrozea, S., & M., A. H. (2015). Fixed-bed dynamic column adsorption study of methylene blue (MB) onto pinecone. *Desalin Water Treat*, 1–14.

Yang, C. (1998). Calcium and magnesium in drinking water and risk of death from cerebrovascular disease. *Stroke*, 411–14.

Yang, C. et al., 2002. Association of very low birth weight with calcium levels in drinking *Water*. *Environ. Research, Section A*, 189-194.

Yang, Y., Lin, X., Huang, H., Feng, D., Ba, Y., Cheng, X., & Cui, L. (2015). Sodium fluoride induces apoptosis through reactive oxygen species-mediated endoplasmic reticulum stress pathway in Sertoli cells. *J Environ Sci*, 81–89.

Yin, K., Irene, Lo, I. M. C., Dong, H., Rao, P., & Mak, M. S. H. (2012). Lab-scale simulation of the fate and transport of nano zero-valent iron in subsurface environments: Aggregation, sedimentation, and contaminant desorption, *J Hazard Mater*, 227– 228, 118–125.

Yoon, Y. H. & Nelson, J. H. (1984). Application of gas adsorption kinetics. I:A theoretical model for respirator cartridge service life. *Am. Ind. Hyg. Assoc. J*., 45, 509–516.

Zhang, Y, Zheng, R., Zhao, J. Ma, F., Zhang, Y., & Meng, Q. (2014). Characterization of H3PO4-Treated Rice Husk Adsorbent and Adsorption of Copper (II) from Aqueous Solution, *BioMed Res Int*, 8, 496878.

Zhang, X., Fan, L., & Roddick, F. A. (2015). Effect of feedwater pre-406 treatment using UV oxidation for mitigating the fouling of a ceramic MF membrane caused by soluble algal organic matter. *J Membrane Sci*, 683–689.

Zhang, C., Li, Y., Wang, T., Jiang, Y., & Wang, H. (2017). Adsorption of drinking water fluoride on a micron-sized magnetic Fe_3O_4@Fe-Ti composite adsorbent. *Appl Surf Sci*, 363, 507–515.

"2540 SOLIDS (2017)", Standard Methods For the Examination of Water and Wastewater, DOI: 10.2105/SMWW.2882.030.

"2320 ALKALINITY (2017)", Standard Methods For the Examination of Water and Wastewater, DOI: 10.2105/SMWW.2882.023.

APPENDIX I

	Household Survey - Use of domestic water purification systems								
	Socio- economic information								
.	Name:								
.	Address:								
	GPS coordinate								
.	Sex:	a) Male		bFe male					
.	Age:	<20 yrs		21-30		31-40			
		41-50		51-60		61-70			
		71-80		81<yrs					
.	Education:	< Grade 5		Gr. 6-8		Gr.9-11			
		Gr.12-13		Higher education					
.	Occupation	a) Government		b) Private			c) Housewife		
		d) Farming		e) Schooling			f) Unemployed		
.	Household Income:	a) Rs. 10,000 - 20,000			b) Rs. 21,000 - 30,000			c) Rs. 31,000-40,000	
		d)Rs. 41,000 - 50,000			e) Rs. 51,000 - 60,000			f) Rs. 61,000-70,000	
		g) Rs. 71,000 - 80,000			h) Rs. 81,000 - 90,000			i) Rs. 90,000<	
	No. of household members								
		a) 1- 3		b) 4 - 6		c) 7 - 9		d) 9<	
.	Is there any household member suffering with Chronic Kidney Disease (CKDu)?								
		a) Yes		b) No					
10	If yes, number of household members suffer with CKDu								

.									
11.	How many years do they suffer with CKDu?								
		<1yrs		1-2yrs		2-3 yrs		3-4yrs	4-5yrs
		5yrs<							
	Water consumption pattern								
12	What is your drinking water source?								
		a) Dug well			b) Tube well			c) Agro well	
		d) Reservoir			e) Water stream			f) Piped born water	
13	Do you purify drinking water before consuming?					a) Yes		b) No	
14	If yes, which types of method do you use to purify water?								
		a) Water filter			b) Cloth filtering			c) Boiling water	
		d) RO							
15. If you currently use RO water, what kinds of filter unit did you use earlier?									
16	If use water filter in Q14, what is the brand name? (Check product's manual)								
17	What is supplier of the water filter?								
18	What is the cost of the water filter?								
		a) < Rs. 5,000			b) Rs. 5,001 - 8,000			c) Rs. 9,001-12,000	
		d) Rs.12,001 - 17,000			e) Rs. 17,001 - 25,000			f) Rs. 25,001 - 35,000	
		g) Rs. 35,001<							
19	What is the filter technique used in the water filter?								
		a) Media Filtration			b) RO			c) Ozonation	
		d) Nano filtration			e) Softening			f) UV sterilization	
		g) De-mineralization			h) Cartridge filtration				
20	Specification of the water filter								

	a) Model No.					h) Handling			
	b) Capacity of the filter (l/day)						Easy		Complex
	c) Initial water flow								
	d) Height (cm)						Yes		No
	e) Width (cm)					j) Is filter need electricity supply?			
	f) Replacement duration						Yes		No
	g) Weight (with full of water)								
21.	How many times do you fill in the water filter?								
		a) Day		b) Week					
22.	Is one service per day enough to meet the demand of household water consumption/day?								
		a) Yes		b) No					
23.	If no, what do you practice meeting extra demand?								
		a) Use raw water			b) Buy purified water				
		c) Use boiled water							
24.	How many years do you consume treated water?								
		a) <1 yrs		b) 2 yrs		c) 3 yrs		4 4 years	
		d) 5 yrs		e) 8 yrs		f) 10 yrs		g 10yrs<	
25.	What improvements do you expect in the water filter?								
26.	How many times do you drink water per day?								
		a) 1		b) 2 - 3		c) 4 - 5		6 - 7	
27.	What amount of water do you drink at a service?								
		a) Liter		Glass		Bottle		Other	
28.	Is there any positive improvement in kidney disease after drinking treated water?								
		a) Yes		No					
29.	If yes, what kind of improvement do you find in disease? (Check								

	health record book)								
		a) Improve body weight				b) Increase glomerular filtration rate			
		c) Reduce Joint's pains				d) Other			
30.	Would you like to drink filtered water?								
		a) Yes		b) No					
31.	If no, what are reasons for dislike;								
		a) Taste is not good							
		b) Like to drink raw water							
		c) Lazy to fill water filter							
		d) Other							
32.	Which types of attributes do you expect, if you are going to buy a new water filter?								
33.	How much could you spend to buy a new water filter?								
		a) Rs< 2,000			b) Rs. 2,001 - 5,000			c) Rs. 5,001 - 8,000	
		d) Rs. 8,001 - 11,000			e) Rs. 11,001 - 14,000			f) Rs. 14,001-17,000	
		g) Rs. 17,001 - 20,000			h) Rs. 20,001 - 25,000			i) Rs. 25,000<	
34.	Do you expect any government support to purchase a well perform water filter?								
		a) Yes		b) No					
35.	If yes, which type of support do you need?								
		a) Donation of water filter				b) Subsidized price			
		c) Only reliable technology				c) Other			

APPENDIX II

Checklist for performance evaluation of water purification system

Model No.	
Supplier	
Initial Price Rs.	
Recurring cost Rs.	
Capacity (L/day)	
Weight with full of water (kg)	
Height (cm)	
Width (cm)	
Depth (cm)	
Top chamber capacity (L)	

Bottom chamber capacity (L) | |

Materials use to produce technology _____

_____

Exporting country | |

Filter technique	a) Media Filtration		b) Ultra Filtration	
	c) De-mineralizing		d) UV sterilization	
	e) Nano filtration		f) Cartridge filtration	
	g) Softening		h) Reverse Osmosis	
	i) Electro deionization		j) Ozonation	

Filter materials	a) Sand		b) Activated carbon		
	c) Silver nano		d) Ion nano		
	e) Mineral stones		f) Mineral sand		
	g)Ironic exchange resin		h) Far infared ball		
	i) Ceramic		Clay		k) Rice husk
	l) Microfiber		thers		

Duration of filter media

Operational water quality parameters	Raw water	Filtrate
1. Hardness		
2. Fluoride		
3. Calcium		
4. Magnesium		
5. Aluminum		
6. Cadmium		
7. Arsenic		
8. pH		
9. Dissolve Oxygen		
10. Coliform, *E. coli*		

Is it easy to maintain for everyone?) Yes b) No

Does its breakdown easily? Yes b) No

Is filter easy to use?

a) Very easy		b)		c)	

		Easy		Acceptable	
d) Difficult		e) Very difficult			

Removal efficiency of the filter

a) Very poor	
b) Poor	
c) Marginal	
d) Good	
e) Very good	

Can filter media reuse?

a) No reuse	
b) In same scale	
c) In different scale	

Does filter contribute to control the disease?

a) Negative improvement	
b) No improvement	
c) Low positive improvement	
d) Moderate positive improvement	

e) High positive improvement	

Does filter media have any effects on environment/health?

a) Negative impact		List down
b) No impact		
c) Low positive impact		
d) Moderate positive impact		
e) High positive impact		

Does filter meet requirement of CKDu affected/ non affected people?

a) Poor fit to the requirement	
b) Insufficient fit to the requirement	
c) More or less meet requirement	
d) Meet requirement	
e) Exceeds requirement	

APPENDIX III

Questionnaire for Socio-economic Evaluation of CKDu Subjects

A) General Information of Chief Occupant

1) Name _____

2) Address _____

_____

_____

3) Age _____

4) Job _____

5) Ownership of the land a) Private ☐ b) Government ☐ c) Other _____

6) Extent of the land 1/4 acres _____

_____

7) Income

(i) Main source of income: _____ (ii) Amount (per season/month):

(ii) Secondary Sources of income: _____ (ii) Amount (per season/month):

_____

_____

_____

(iii) Below poverty line or Above: _____

(Poverty line for A'pura: Rs. 3,808 per person per month)

(Average monthly income for NC Province: Rs. 35,000)

8) Number of persons in the house

a) Grand fathers	☐	b) Grand mothers	☐	c) Mother	☐	d) Father	☐
a)1. Age	☐	b)1. Age	☐	c)1. Age	☐	d)1. Age	☐
a)2. No. of years	☐	b)2. No. of years	☐	c)2. No. of years	☐	d)2. No. of years	☐
e) Spouse	☐	f) Other relatives	☐	g) Children	☐	h) Grand	☐

						children	
	e)1. Age		f)1. Age		g)1. Age	h)1. Age	
	e)2. No. of years		f)2. No. of years		g)2. No. of years	h)2. No. of years	
	i) Others						
	i)1.Age						
	i)2. No. of years						
9) Number of persons affected	a) Grand fathers		b) Grand mothers		c) Mother	d) Father	
	a)1. Age		b)1. Age		c)1. Age	d)1. Age	
	a)2. No. of years		b)2. No. of years		c)2. No. of years	d)2. No. of years	
	e) Spouse		f) Other relatives		g) Children	h) Grand children	
	e)1. Age		f)1. Age		g)1. Age	h)1. Age	
	e)2. No. of years		f)2. No. of years		g)2. No. of years	h)2. No. of years	
	i) Others						
	i)1.Age						
	i)2. No. of years						
10) Number of persons not affected	a) Grand fathers		b) Grand mothers		c) Mother	d) Father	
	a) Age		b) Age		c) Age	d) Age	
	e) Spouse		f) Other relatives		g) Children	h) Grand children	
	e) Age		f) Age		g) Age	h) Age	
	i) Others						
	i) Age						

11) Number of deaths	a) Grand fathers		b) Grand mothers		c) Mother		d) Father	
	a)1. Age		b)1. Age		c)1. Age		d)1. Age	
	a)2. Year		b)2. Year		c)2. Year		d)2. Year	
	e) Spouse		f) Other relatives		g) Children		h) Grand children	
	e)1. Age		f)1. Age		g)1. Age		h)1. Age	
	e)2. Year		f)2. Year		g)2. Year		h)2. Year	
	i) Others							
	i)1.Age							
	i)2. Year							

B) General information of interviewee

12) Name _____

13) Relationship to chief occupant

a) Cheif occupant		a) Grand fathers		b) Grand mothers		c) Mother		d) Father	
e) Spouse		f) Other relatives		g) Children		h) Grand children		i) Others	

14) Date of birth

15) Sex a) Male b) Female

16) Nationality

a) Sinhala		b) SL Tamil		c) Indian Tamil		d) Muslim		e) Burger	
f) Maley		g) Other							

17) Religion

a) Buddhist		b) Hindu		c) Islam		d) Roman Catholic		e) Other	

18) Education a) <Grade 5 ☐ b) Grade 8 ☐ c) O/L ☐ d) A/L ☐ e) Higher ☐

19) District in which the interviewee was born _____

20) No. of years of stay in the present address _____

21) During that period did you stay in other places? a) Yes ☐ b) No ☐

22) If yes, the places where the interviewee stayed at with duration

_____

_____

23) Are you employed now? a) Yes ☐ b) No ☐

24) If yes, present employment

a) Farmers	☐	b) Gvt. employ.	☐	c) Veg. seller	☐	d) Labour	☐	e) V/F Picker	☐
years	☐	years	☐	years	☐	years	☐	years	☐
f) Own business	☐	g) Private	☐	h) Fruit seller	☐	i) Food process	☐	j) Unemployee	☐
years	☐	years	☐	years	☐	years	☐	years	☐

k) Other _____

25) Income from present employment

(i) Main source of income: _____ (ii) Amount (per season/month):

(ii) Secondary Sources of income: _____ (ii) Amount (per season/month):

_____

_____

26) Past employment

a) Farmers	☐	b) Gvt. employ.	☐	c) Veg. seller	☐	d) Labour	☐	e) V/F Picker	☐
years	☐	years	☐	years	☐	years	☐	years	☐
f) Own business	☐	g) Private	☐	h) Fruit seller	☐	i) Food process	☐	j) Other	☐
years	☐	years	☐	years	☐	years	☐	years	☐

_____

27) Income from past employment

(i) Main source of income: _____ (ii) Amount (per season/month): _____

(ii) Secondary Sources of income: _____ (ii) Amount (per season/month): _____

_____

28) If not a regular farmer, do you engage in any other agricultural activities?

a) Yes ☐ b) No ☐

29) If yes, type of activities engaged _____

_____

30) No. of years of such practices _____

C) Health related information

31) When did you get yourself diagnosed by the medical practitioner? _____

32) How? _____

_____

33) Early symptoms before the diagnosis

a)	Appetite loss	☐
b)	Fatigue/ weakness	☐
c)	Numbness	☐
d)	Panting	☐
e)	Anemia	☐
f)	Fever	☐
g)	Headaches	☐
h)	Itching	☐
g)	Nausea	☐
j)	Weight loss	☐

k)	Bowel Irritation	
l)	Irregular bowel movements	
m)	Joint pain	
n)	Irrigular habits of urination	
0)	Burning sensation while urination	
p)	Swelling	
q)	Lazyness	
r)	Passing blood	
s)	Other(specify)	

34) Signs & symptoms after the diagnosis

a)	Appetite loss	
b)	Fatigue/ weakness	
c)	Numbness	
d)	Panting	
e)	Anemia	
f)	Fever	
g)	Headaches	
h)	Itching	
g)	Nausea	
j)	Weight loss	
k)	Bowel Irritation	
l)	Irregular bowel movements	
m)	Joint pain	
n)	Irrigular habits of urination	
0)	Burning sensation while urination	
p)	Swelling	
q)	Lazyness	
r)	Passing blood	

s) Other(specify) _____

35) What signs and symtoms you encourage to meet doctor?

a) Appetite loss ☐
b) Fatigue/ weakness ☐
c) Numbness ☐
d) Panting ☐
e) Anemia ☐
f) Fever ☐
g) Headaches ☐
h) Itching ☐
g) Nausea ☐
j) Weight loss ☐
k) Bowel Irritation ☐
l) Irregular bowel movements ☐
m) Joint pain ☐
n) Irrigular habits of urination ☐
0) Burning sensation while urination ☐
p) Swelling ☐
q) Lazyness ☐
r) Passing blood ☐
s) Other(specify) _____

36) Did you have any kidney problem when you were born? a) Yes ☐ b) No ☐

37) If yes, what were the problems? _____

38) Have you been suffering from the following?

a) <u>Diabetic</u> ☐

b)	Hyphertension	
c)	Inflammation	
d)	Swelling of organs	
e)	High Cholesterol	
f)	Clogging and hardening of the arteries and veins	
g)	stones in the kidney	
h)	Cancer	
i)	Leptospirosis	
j)	Malaria	
k)	Other (Specify)	

39) Have you been taking medicine for the following?

Hypetension		For how long	
Diabetic		For how long	
High Cholesterol		For how long	
Any other as pain killers		For how long	

Any comments

40) Do you have any kith & kins with kidney disease? a) Yes b) No

41) Relationship with kith & kins

42) What are treatments you took at early stages

a) Western

b) Ayurvedic

a) Arishta b) Kasaya c) Guli d) Others

c) Other ☐ _____

43)What are treatment you take at present

a) Western ☐ _____

b) Ayurvedic ☐ _____

a) Arishta ☐ b) Kasaya ☐ c) Guli ☐ d) Others ☐

c) Other ☐ _____

44) If different answer in 42 & 43, why did you change the treatment methods

_____

45) Types of activities you practice to feel comfortable

_____

_____

46) a. After treatment, do you have any improvement

_____

46) b. What is the present condition of the illness

_____

_____

D) Food habits

47) Cooking utensils (Present)

a) Aluminium ☐ b) Clay pots ☐ c) Stainless steel ☐ d) Plastic ☐

e) Other (Specify) _____

_____

_____

*Past _____

_____

48) Places of food preparation (Present)

a) At home ☐ b) Outdoor ☐ c) Field cottage ☐ d) Other ☐

_____

_____

*Past _____

_____ _____ _____

49) Methods of preparation (Present)		a) Boiling	☐	b) Heating	☐	c) Raw	☐	d) Half cook ☐
		e) Fully cook	☐					
	*Past							
50) Staple foods								
After Diagnosis								
Breakfast	a) Rice & curries	☐	b) Cassava	☐	c) Sweet potato	☐	d) Indiginous yams ☐	e) Jack fruit ☐
	f) Bread fruit	☐	g) Noodles	☐	h) Products made of Wheat flour		☐	i) Grains ☐
	j) Maize	☐	k) Rice flour	☐	k) Products made of Kurakkan flour	☐	☐	l)Legumes /Pulses ☐
	Other							
	Source							
Lunch	a) Rice & curries	☐	b) Cassava	☐	c) Sweet potato	☐	d) Indiginous yams ☐	e) Jack fruit ☐
	f) Bread fruit	☐	g) Noodles	☐	h) Products made of Wheat flour		☐	i) Grains ☐
	j) Maize	☐	k) Rice flour	☐	k) Products made of Kurakkan flour	☐	☐	l)Legumes /Pulses ☐
	Other							
	Source							
Dinner	a) Rice & curries	☐	b) Cassava	☐	c) Sweet potato	☐	d) Indiginous yams ☐	e) Jack fruit ☐
	f) Bread fruit	☐	g) Noodles	☐	h) Products made of Wheat flour		☐	i) Grains ☐
	j) Maize	☐	k) Rice flour	☐	k) Products made of Kurakkan flour	☐	☐	l)Legumes /Pulses ☐
	Other							
	Source							

Before Diagnosis

Breakfast	a) Rice & curries		b) Cassava		c) Sweet potato		d) Indiginous yams		e) Jack fruit		
	f) Bread fruit		g) Noodles		h) Products made of Wheat flour				i) Grains		
	j) Maize		k) Rice flour		k) Products made of Kurakkan flour				l)Legumes /Pulses		
	Other										
	Source										
Lunch	a) Rice & curries		b) Cassava		c) Sweet potato		d) Indiginous yams		e) Jack fruit		
	f) Bread fruit		g) Noodles		h) Products made of Wheat flour				i) Grains		
	j) Maize		k) Rice flour		k) Products made of Kurakkan flour				l)Legumes /Pulses		
	Other										
	Source										
Dinner	a) Rice & curries		b) Cassava		c) Sweet potato		d) Indiginous yams		e) Jack fruit		
	f) Bread fruit		g) Noodles		h) Products made of Wheat flour				i) Grains		
	j) Maize		k) Rice flour		k) Products made of Kurakkan flour				l)Legumes /Pulses		
	Other										
	Source										

51) Types of fruits

Source

52) Types of vegetable often use

Source

53) Types of green leaves

Source

54) Types of Meat consumed

Source

55) Types of fish

i) Inland fish

Source

ii) Sea fish

Source

56) Other foods

Source

57) Types of diary products

Source

58) Types of Junk/instant foods

59) Types of fried foods

60) Did you follow diaetary restrictions at present?

a) Protein diets ☐ b) Salted diets ☐ c) Fluid intake ☐ d) Potasium diets ☐

e) Phosphorous diet ☐ f) Low Sugar ☐ g) Other ☐

61) Did you take advices from authorities about food habits

62) If yes, what were they?

E) Types of liquids and water uses

63) Extent of water consumption

a) Plenty ☐ b) Adequate ☐ c) Non Adequate ☐

64) Drinking water source

a) Garden well	☐	b) Common well	☐	c) Agro-well	☐	d)Tubewell	☐
e) Pipe-borne	☐	f) Water Bowser	☐	g) Streams	☐	h) Canals	☐
i) Irrigation Canals	☐	j) Tanks (wewa)	☐	k) Bottled water	☐		

*Past

65) Nature of the water being consumed

a) Raw water ☐

b) Treated water (Common) ☐

c) Treated water (Individual) ☐

*Past

66) Water quality for drinking

a) Hardness (Kiwul)	☐	b) Fluoride (Teeth discolouration)	☐	c) Colour	☐
d) Odour	☐	e) Taste	☐	f) Turbidity	☐

67) Level of treatment at the household level

a) No treatment ☐ b) Boiled ☐ c) Chlorination ☐

d) Filter ☐

*Past

68) Types of beverage

a) Belimal ☐ c)Ranawara ☐ d) Polpala ☐ e) Tea ☐

f) Other ☐

69) Method of water storage

a) Aluminium pots ☐ b) Brass pots ☐ c) Clay pots ☐ d) Plastic (HDPE) ☐

70) Cooking water source

a) Garden well ☐ b) Common well ☐ c) Agro-well ☐ d)Tubewell ☐

e) Pipe-borne ☐ f) Water Bowser ☐ g) Streams ☐ h) Canals ☐

i) Irrigation Canals ☐ j) Tanks (wewa) ☐ k) Bottled water ☐

*Past

71) nature of the water being consumed

a) Raw water ☐

b) Treated water (Common) ☐

c) Treated water (Individual) ☐

*Past

72) Water quality for cooking

a) Hardness (Kiwul) ☐ b) Fluoride (Teeth discolouration) ☐ c) Colour ☐

d) Odour ☐ e) Taste ☐ f) Turbidity ☐

73) Level of treatment at the household level
a) No treatment ☐ b) Boiled ☐
c) Chlorination ☐ d) Filter ☐

74) Bathing/cleaning water source
a) Garden well ☐ b) Common well ☐ c) Agro-well ☐ d)Tubewell ☐
e) Pipedborn ☐ f) Water Bowser ☐ g) Streams ☐ h) Canals ☐
i) Irrigation Canals ☐ j) Tanks (wewa) ☐ k) Bottled water ☐

75) Nature of the water being consumed
a) Raw water ☐
b) Treated water (Common) ☐
c) Treated water (Individual) ☐

*Past

76) Water quality for bathing/cleaning
a) Hardness(Kiwul) ☐ b) Fluoride (Teeth discolouration) ☐ c) Colour ☐
d) Odour ☐ e) Taste ☐ f) Turbidity ☐

77) Level of treatment at the household level
a) No treatment ☐ b) Boiled ☐
c) Chlorination ☐ d) Filter ☐

80) Obstacles to access clean water

81) Suggestions to improve water quality

82) What are the available water treatment technologies? i) Reverse Osmosis ☐ ii) Filters ☐ iii)Others ☐

83) Type of model a) Commercial ☐ b) Domestic ☐

84) Cost of 1litre of water

85) The benificial uses for which the above-mentioned treated water is used

F) General Habits

86) Types of chewing products a) Betel ☐ b) Aricanut ☐ c) Lime (Hunu) ☐ d) Tobacco ☐ e) Babul ☐ f) Other

87.1) How often

87.2) How long

88) Smoking a) Yes ☐ b) No ☐

88.1) If yes a) Cigar ☐ b) Beedi ☐ c) Cigarette ☐ d) Ganja ☐ e) Kerala ☐

f) tobacco powder ☐ g) drugs ☐ h) Other ☐ Ganja ☐

88.2) How often _____

88.3) How long _____

89) Alcohol a) Yes ☐ b) No ☐

89.1) If yes a) Beer ☐ b) Kasippu ☐ c) Arrack ☐ d) Coconut toddy ☐

e) Other _____

89.2) How often _____

89.3) How long _____

G) Livelihood habits

90) Occupation

a) Farmers	☐	b) Gvt. employ.	☐	c) Veg. seller	☐	d) Labour	☐	e) V/F Picker	☐
years	☐	years	☐	years	☐	years	☐	years	☐
f) Own business	☐	g) Private	☐	h) Fruit seller	☐	i) Food process	☐	j) Other	☐
years	☐	years	☐	years	☐	years	☐	years	☐

91)a. Types of fertilizers a) Compost ☐ b) Manure made of crop residues ☐ ☐ Artificial ☐

91) b. Types of Artificial Fertilizers a) Agstar ☐ b) Urea ☐ c) TSP ☐ d)MOP ☐

e) Zinc Sulphate ☐ f) NPK ☐ g) Other ☐

_____

_____

92). Types of pesticides a) Roundup ☐ b) Nominee ☐ c) Micasa ☐ d) ☐

e) Ridomil ☐ f) Admire ☐ g) Other ☐ Proponex ☐

93) Frequency and rate of pesticide/Fertilizer application?

Name	Application method	Frequency	Rate/ha	Quantity (ml)

94) Any precautionary measures taken

a) Rubber gloves ☐

b) Shirts ☐ a) Long sleeves ☐ b)Sleeveless ☐

c) Mask ☐

d) Long pants over boots ☐

e) Rubber Boots ☐

f) Bathing after applying pesticides ☐

g) Wash hand and face ☐

h) Eat, drink, or smoking when handling pesticide, a) Yes ☐ b) No ☐

I) Avoid windy days ☐

j) Others ☐

95) If No, reasons for avoiding safety precaution measures

96) Where do you store pesticides?

- a) Store pesticides together with food, drinks or feed ☐
- b) Keep pesticides to reach for children ☐
- c) No lock the cabinet or room keeping pesticide ☐
- d) Check the pesticide store regularly ☐
- e) Other ☐

97) How do you transport pesticides?

- a) Transport pesticide with safe container ☐
- b) When transport pesticide, beware to avoid spillage ☐
- c) Pesticide keep separately with other goods ☐
- d) Other (Specify)

98) Disposal methods of empty Pesticide bottles

99) How do you clean the spray tank?

H) Leisure time activities

100) How do you spend your leisure time?

- a) Visiting public place ☐
- b) Cultivation activities at Home Garden ☐
- c) Meeting friends ☐
- d) Relaxing ☐

101) Sports/ Games _____

_____

102) Water contact activities _____

I) Injuries

103)Types of injuries a) Snake bites ☐ b) Dog bites ☐ c) Rat bites ☐ d) Cat bites ☐ e) Other ☐

_____

104) Treatment methods _____

_____

APPENDIX IV

	Well	Reservoir	Irrigation	Agro well	Spring	Pipe borne	Tube well	Drinking vessels	Dry zone	Wet zone	Reference	WHO	SL
Cadmium (mg/l)	–	$3*10^{-2}$ - $6*10^{-2}$	_	_	_	_	_	_	_	_	Wanigasuriya et al., 2011	0.003	0.003
	–	$3*10^{-2}$ - $6*10^{-2}$	_	_	_	_	_	_	_	_	Bandara et al., 2010a		
	$2.05*10^{-4}$– 0.187	$8*10^{-5}$– $2.9*10^{-2}$	_	$0.272*10^{-2}$– 0.039	_	$8.8*10^{-4}$– $1.04*10^{-2}$	$1.7*10^{-3}$– $3.4*10^{-2}$	_	_	_	Bandara et al., 2010b		
	$<2.7*10^{-6}$- $6*10^{-6}$	$< 7*10^{-7}$- $7*10^{-6}$	_	_	_	_		$<2.7*10^{-6}$ - $3.1*10^{-5}$	_	_	Chandrajith et al., 2010		
	_	_	_	_	_	_	_	_	$< 2*10^{-7}$ - $7*10^{-7}$	$< 2*10^{-7}$- $5*10^{-7}$	Chandrajith et al., 2012b		
	_	_	_	_	_	_	_	_	_	_	CSE, 2012		
	$5*10^{-3}$	_	_	_	_	_	_	_	_	_	Dharmawardana et al., 2014		
	_	_	_	_	$2.96*10^{-4}$ - $705*10^{-4}$		_	_	_	_	Wasana et al., 2015		
	$4*10^{-5}$	_	$1*10^{-5} \pm 1*10^{-5}$	_	$1*10^{-6}$ - $3*10^{-5}$	$1*10^{-5} \pm 1*10^{-5}$	$5*10^{-5}$	_	_	_	Rango et al., 2015		
Aluminum (mg/l)	$1.53*10^{-3}$- 0.152	$3.17*10^{-3}$- $7.33*10^{-2}$	_	_	_	_	_	$3.03*10^{-3}$ - 0.191	_	_	Chandrajith et al., 2010		
	_	_	_	_	_	_	_	_	_	_	CSE, 2012		
	0.2	_	_	_	_	_	_	_	_	_	Dharmawardana et al., 2014		
	_	_	_	_	$4.918*10^{-2}$ - $7.954*10^{-2}$	_	_	_	_	_	Wasana et al., 2015		
	$4.1*10^{-3}$ - $8*10^{-2}$	_	$1.68*10^{-2} \pm 4.77*10^{-3}$	_	$1.16*10^{-3}$ - $2.7*10^{-2}$	$2.21*10^{-2} \pm 2.46*10^{-2}$	$2.62*10^{-2}$	_	_	_	Rango et al., 2015		
	_	_	_	_	_	_	_	_	_	_			
	_	_	_	_	_	_	_	_	_	_			
Arsenic (mg/l)	$<1.5*10^{-4}$- $8.27*10^{-4}$	$1.66*10^{-4}$- $3.58*10^{-4}$	_	_	_	_	_	$<1.5*10^{-4}$ - $9.22*10^{-4}$	_	_	Chandrajith et al., 2010		0.01 - 0.05
	$8.8*10^{-2}$ - $7.4*10^{-2}$	_	_	_	_	_	_	_	_	_	Kawakami et al. 2012		
	$1.02*10^{-3}$ - 0.101	_	_	_	_	_	_	_	_	_	Fonseka et al. 2012		
	_	_	_	_	_	_	_	_	_	_	CSE, 2012		
	$1*10^{-2}$	_	_	_	_	_	_	_	_	_	Dharmawardana et al., 2014		

	_	_	_	_	ND	_	_	$1.8*10^{-5}$ - $1.61*10^{-3}$	_	_	Wasana et al., 2015		
	$8.6*10^{-4}$	_	ND	_	ND	$1.5*10^{-4} \pm 2.6*10^{-4}$	$6.2*10^{-4}$	_	_	_	Rango et al., 2015		
	$1*10^{-3}$ - $6.6*10^{-2}$	_	_	_	_	_	_	_	_	_	Weragoda & Kawakami, 2017		
Fluoride (mg/l)	0.05-5.9	0.2 - 0.87	_	_	_	_	0.18-5.2	_	_	_	Van der Hoek et al., 2003	1.5	1 - 1.5
	$1.18*10^{-3}$-$5.3*10^{-3}$	_	_	_	_	_	_	_	_	_	Chandrajith et al., 2010		
	_	_	_	_	_	_	_	_	<0.02 - 13.7	<0.02 - 9	Chandrajith et al. 2012a		
	0.8	0.7	_	_	0.4	_	1	_	_	_	CSE, 2012		
	0.21 - 7.03	_	_	_	_	_	_	_	_	_	Charuni et al., 2014		
	2	_	_	_	_	_	_	_	_	_	Dharmawardana et al., 2014		
		_	_	_	0.061-0.069	_	_	_	_	_	Wasana et al., 2015		
	$9.5*10^{-2}$ - 4.3	_	0.26 ± 0.01	_	0.19	0.71 ± 0.52	0.49 - 1.78	_	_	_	Rango et al., 2015		
	0.1 - 7	_	_	_	_	_	_	_	_	_	Weragoda & Kawakami, 2017		
Calcium (mg/l)	256	_	_	_	_	_	_	_	_	_	Chandrajith et al. 2011b	200	75 - 200
	_	_	_	_	_	_	_	_	9.1 - 18.9	6.1 - 9.9	Chandrajith et al. 2012a		
	86.1	86.1	_	_	16	_	61.6	_	_	_	CSE, 2012		
	200	_	_	_	_	_		_	_	_	Dharmawardana et al., 2014		
	8.3 - 104	_	23.6 ± 1.73	_	0.35 - 10	47.6 ± 31.7	21.6 - 92.3	_	_	_	Rango et al., 2015		
	_	_	_	_	_	_	_	_	_	_			
Magnesium (mg/l)	1280	_	_	_	_	_	_	_	_	_	Chandrajith et al 2011b		
	_	_	_	_	_	_	_	_	9 - 23.3	8.5 - 45.1	Chandrajith et al. 2012a	150	30 - 100
	13.5	13.5	_	_	13	_	22.4	_	_	_	CSE, 2012		
	150	_	_	_	_	_		_	_	_	Dharmawardana et al., 2014		
	2 - 81	_	11 ± 0.34	_	0.24 - 4.8	37.3 ± 40.5	10.5 - 40.3	_	_	_	Rango et al., 2015		
Hardness (mg/l)	1921	_	_	_	_	_	_	_	_	_	Chandrajith et al. 2011b	500	300 - 600
	10-820	_	_	_	_	_	_	_	_	_	Fonseka et al. 2012		
	258.3	192.5	_	_	93.3	_	246	_	_	_	CSE, 2012		

	1733.3	_	_	_	_	_	_	_	_	_	Charuni et al., 2014		
	_	_	_	_	16.52 - 26.86	_	_	_	_	_	Wasana et al., 2015		
	68.5 - 411	_	114 ± 0.64	_	7.5 - 63.6	241 ± 190	162 - 405	_	_	_	Rango et al., 2015		

APPENDIX V

Summary of the questionnaire results

Characteristics	% of data	Characteristics	% of data
Gender of the head of the family unit		**Signs & symptoms after the diagnosis**	
Male	25 (100%)	Appetite loss	38%
Female	0 (0%)	Fatigue/ weakness	52%
Total number of family members	73	Numbness	14%
Male	47%	Panting	38%
Female	53%	Anemia	5%
Age distribution of the sample		Fever	19%
1 -- 9	16%	Headaches	19%
9 – 18	32%	Itching	10%
20 – 50	16%	Nausea	10%
50 - 70	20%	Weight loss	14%
70 -90	12%	Bowel Irritation	9%
90 ≤	4%	Irregular bowel movements	0%
Number of occupants in the family unit	12%	Joint pain	52%
3 >	12%	Irregular habits of urination	14%
3	80%	Burning sensation during urination	19%
4 – 5	8%	Swelling	24%
Occupation of the head of the family		Laziness	29%
Farmer	84%	Passing blood	0%
Govt. servant.	4%	**People affected by non-communicable diseses**	
Mill owner	8%	Diabetic	24%

Forces	6%	Hyphertension	18%
CKDu affected people in the sample	34%	Inflammation	57%
Male	60%	Swelling of organs	4%
Female	4%	High Cholesterol	4%
Age distribution of CKDu affected people		Clogging and hardening of the arteries and veins	4%
1 -- 9	0%	stones in the kidney	9%
9 – 18	4%	Cancer	0%
20 – 50	25%	Leptospirosis	4%
50 - 70	54%	Malaria	2%
70 -90	14%	**Food habits**	
90 ≤	4%	Cooking utensils	
Source of drinking water		Aluminum pots	43%
Common well (CW)	9%	Clay pots	76%
Garden well (GW)	10%	Stainless steel	19%
Central reverse osmosis plant (CRO)	64%	Plastic	4%
Tube well	9%	**Observed improvements after RO filtration**	
Domestic RO water	8%	Improvement in taste	92%
Nature of water consumption		Improvement in taste + odour + colour	8%
Adequacy of water for drinking		**Daily filtered volume with the RO unit**	
Plenty	52%	0 – 5 L	28%
Adequate	44%	5 – 10 L	24%
Non-adequate	4%	10 – 15 L	4%
Drinking water aquired sources		15 <	44%
Garden well	24%	**Time is taken for the RO unit to clog**	
Common well	29%	0 – 1 year	44%
Tube well	10%	1 – 2 years	48%

Pipe-borne	14%	2 < years	8%
Tanks (wewa)	24%	**Replacement component during maintenance**	
Characteristics of water source		Carbon/sediment filter	36%
Hardness taste	68%	RO membrane	16%
Colour	4%	Carbon/ sediment filter + Motor	8%
Hardness + colour	8%	Carbon/ sediment filter + RO membrane	12%
Hardness + Dental fluorosis	8%	Storage tank	4%
Hardness + Odour + colour	4%	Disinfection unit	8%
		Disinfection unit + RO membrane	8%
		Motor	4%

APPENDIX VI

The calculation for home filter design

The measurements required to design a home filter were calculated based on the results of multi-layered with multi-solute system taken from the LUB model. Assumptions were made as a family in CKDu prevalent area consists of 5 members. One person consumes water approximately 2.0 L/day as daily water requirement (WHO, 2017). The total daily water requirement of a family with five members was calculated as 10.0 L. The treated water is considered supplying for three months to a family (total volume of treated water requirement 10.0 L X 30 days X 3). The home filter design was conducted considering the mass transfer zone velocity/per unit area of materials in the lab experimental column is equal to the mass transfer velocity/ per unit area of the material in the home filter unit

Volumetric flow rate required to obtain 200.0 mL of water for 20 seconds.

= 200 mL ÷ 20 X 60 minute

= **600.0 mL/minute**

Volume of water required to treat for three months

= 10,000.0 mL X 30 X 3

= 900,000.00 mL

LUB = Z/ TS (Ts-Tb),

ZEOL calculation

Ts = 44 hours, Tb = 31 hours, Q = 3.0 mL/min, Z = 5.5 cm, Tb scale = 25.01 hours

= 5.5/44 X (44-31)

= 0.125 X 13

= 1.625 cm

Mass transfer zone velocity Vz = Z/ Ts

= 5.5/44

= 0.125 cm/hr

Bed height of scale up filter = Vz X Tb scale

= 0.125 X 25.01

= 3.126 cm

Total bed height including LUB = Zscale + LUB

= 3.126 + 1.625 cm

= 4.75 cm

Then, the bed volume of ZEOL

$= \pi r^2$ X Z

= 22/7 X 1.4 cm X 1.4 cm X 4.75 cm

= **29.26 cm^3**

If the bed volume is 29.26 cm^3 for 3.0 mL/min, the bed volume for 600.0 mL/min;

= 29.26 cm^3 X 200

= **5,852.0 cm^3**

The diameter of the cartridge is assumed as 16.0 cm and then radius of the cartridge is 8.0 cm

Then, the cross-sectional area of home filter unit $= \pi r^2$

$= 22/7 \text{ X } 8.0 \text{ cm X } 8.0 \text{ cm}$

$= 201.14 \text{ cm}^2$

The height of the home filter unit for ZEOL $\pi r^2 \text{ X } Z = 5{,}852.0$

$Z = 5{,}852.0 / 201.14$

$=$ **29.09 cm**

Mass of ZEOL required to treat potable water for 3 months,

(bulk density of ZEOL = 0.45 g/cm^3)

d (Bulk density) = *m* (Mass of material) ÷ *V* (Volume of column bed)

$m = d \text{ X } V$

$= 0.45 \text{ g/cm}^3 \text{ X } 5{,}852.0 \text{ cm}^3$

$= 2{,}633.40 \text{ g}$

$=$ **2.63 Kg**

MOMA calculation

Ts = 24 hours, Tb = 12 hours, Q = 3.0 mL/min, Z = 2.0 cm, Tb scale = 25.01 hours

$= 2.0/24 \text{ X } (24\text{-}12)$

$= 0.083 \text{ X } 12$

$= 1.0 \text{ cm}$

Mass transfer zone velocity $Vz = Z/ Ts$

= 2.0/24

= 0.083 cm/hr

Bed height of scale up filter = Vz X Tb scale

= 0.083 X 25.01

= 2.08 cm

Total bed height including LUB = Zscale + LUB

= 2.08 + 1.0 cm

= 3.08 cm

Then, the bed volume of MOMA

$= \pi r^2$ X Z

= 22/7 X 1.4 cm X 1.4 cm X 3.084 cm

= **18.97 cm^3**

If the bed volume is 29.26 cm^3 for 3.0 mL/min, the bed volume for 600.0 mL/min;

= 18.97 cm^3 X 200

= **3,794.0 cm^3**

The diameter of the cartridge is assumed as 16.0 cm and then radius of the cartridge is 8.0 cm

Then, the cross-sectional area of home filter unit $= \pi r^2$

= 22/7 X 8.0 cm X 8.0 cm

$= 201.14\ cm^2$

The height of the home filter unit for MOMA $\pi r^2 \text{ X } Z = 3{,}794.0$

$Z = 3{,}794.0 / 201.14$

$= \mathbf{18.86\ cm}$

Mass of MOMA required to treat potable water for 3 months,

(bulk density of MOMA = 0.36 g/cm^3)

d (Bulk density) = *m* (Mass of material) ÷ *V* (Volume of column bed)

$m = d \text{ X } V$

$= 0.36\ g/cm^3 \text{ X } 3{,}794.0\ cm^3$

$= 1{,}365.84\ g$

$= \mathbf{1.37\ Kg}$

SONPs + GO calculation

Ts = 152 hours, Tb = 70 hours, Q = 3.0 mL/min, Z = 1.5 cm, Tb scale = 25.01 hours

$= 1.5/152 \text{ X } (152 - 70)$

$= 0.0098 \text{ X } 82$

$= 0.81\ cm$

Mass transfer zone velocity $Vz = Z / Ts$

$= 1.5/152$

$= 0.0098\ cm/hr$

Bed height of scale up filter = Vz X Tb scale

= 0.0098 X 25.01

= 0.25 cm

Total bed height including LUB = Zscale + LUB

= 0.25 + 0.81 cm

= 1.06 cm

Then, the bed volume of SONPs + GO

= πr^2 X Z

= 22/7 X 1.4 cm X 1.4 cm X 1.06 cm

= **6.52 cm^3**

If the bed volume is 29.26 cm^3 for 3.0 mL/min, the bed volume for 600.0 mL/min;

= 6.52 cm^3 X 200

= **1,304.0 cm^3**

The diameter of the cartridge is assumed as 16.0 cm and then radius of the cartridge is 8.0 cm

Then, the cross-sectional area of home filter unit = πr^2

= 22/7 X 8.0 cm X 8.0 cm

= 201.14 cm^2

The height of the home filter unit for SONPs + GO πr^2 X Z = 1,304.0

$$Z = 1{,}304.0 / 201.14$$

$$= \mathbf{6.48\ cm}$$

Mass of SONPs + GO required to treat potable water for 3 months,

(bulk density of SONPs + GO = 0.84 g/cm^3)

$$d \text{ (Bulk density)} = m \text{ (Mass of material)} \div V \text{ (Volume of column bed)}$$

$$m = d \text{ X } V$$

$$= 0.84 \text{ g/cm}^3 \text{ X } 1{,}304.0 \text{ cm}^3$$

$$= 1{,}095.36\text{g}$$

$$= \mathbf{1.09\ Kg}$$

The mass of the ZEOL, MOMA and SONPs + GO in-home filter design were calculated as 2.63 Kg, 1.37 Kg, and 1.09 Kg, respectively to treat the potable water for 3 months. By considering the different columns' heights, the home filter unit will be fabricated as the series of cartridges (ZEOL, MOMA and SONPs + GO).

APPENDIX VII

The calculation for the cost of 1.0 L of water production

Cost calculation of ZEOL, MOMA, and SONPs + GO was estimated to determine the approximate value for 1.0 L of treated water production. The total cost required to treat water for one year was calculated as summarised below.

Cost for 1 L of treated water production using ZEOL

Specific throughput of ZEOL = 469.49 L/kg

Cost for production of 1kg of ZEOL production = Rs. 120.00/kg

Number of regeneration cycles = 5

Cost for 1kg of ZEOL with five regeneration cycles = Rs. 120.00/5

= Rs. 24.00

Cost for production of 1 L of treated water = Rs 24.00/469.49

= Rs. 0.05/L

Cost for production of 8 L of treated water = Rs. 0.05 χ 8.0 L

= Rs. 0.40

Cost for production of 8 L/day of treated water for 6 months

= Rs. 0.40 x 180 days

= Rs. 72.00

Cost for 1 L of treated water production using MOMA

Specific throughput of MOMA = 415.79 L/kg

Cost for production of 1kg of MOMA production = Rs. 6,541.00/kg

Number of regeneration cycles = 5

Cost for 1kg of MOMA with five regeneration cycles = Rs. 6,541.00/5

= Rs. 1308.20

Cost for production of 1 L of treated water = Rs 1,308.20/415.79

= Rs. 3.15/L

Cost for production of 8 L of treated water = Rs. 3.15 χ 8.0 L

= Rs. 25.20

Cost for production of 8 L/day of treated water for 6 months

= Rs. 25.20 x 180 days

= Rs. 4,536.00

Cost for 1 L of treated water production using SONPs + GO

Specific throughput of SONPs + GO = 1,457.44 L/kg

Cost for production of 1kg of SONPs + GO production = Rs. 27,774.00/kg

Number of regeneration cycles = 5

Cost for 1kg of SONPs + GO with five regeneration cycles = Rs. 27,774.00/5

= Rs. 5,554.80

Cost for production of 1 L of treated water

=Rs 5,554.80/1457.44

= Rs. 3.81/L

Cost for production of 8 L of treated water = Rs. 3.81 χ 8.0 L

= Rs. 30.48

Cost for production of 8 L/day of treated water for 6 months

= Rs. 30.48 x 180 days

= Rs. 5,486.40